Geometrical and combinatorial generalizations of the associahedron

Thibault Manneville

Thèse de doctorat
de l'Université Paris-Saclay
préparée à l'École polytechnique

ÉCOLE DOCTORALE N° 580
STIC – Sciences et technologies de
l'information et de la communication

Spécialité de doctorat : Mathématiques et informatique

par

M. Thibault Manneville

Généralisations géométriques et combinatoires de l'associaèdre

Thèse présentée et soutenue à l'École polytechnique, le 6 juillet 2017,

Composition du jury :

M.	Frédéric Chapoton	Directeur de recherches CNRS & Université de Strasbourg	(Rapporteur)
M.	Florent Hivert	Professeur Université Paris-Sud	(Président du jury)
M.	Christophe Hohlweg	Professeur Université du Québec à Montréal	(Examinateur)
Mme	Sophie Morier-Genoud	Maître de conférences Université Pierre et Marie Curie	(Examinatrice)
M.	Lionel Pournin	Professeur Université Paris-13	(Examinateur)
M.	Francisco Santos Leal	Professeur Université de Cantabrie	(Examinateur)
M.	Vincent Pilaud	Chargé de recherches CNRS & École polytechnique	(Co-Directeur de thèse)
M.	Gilles Schaeffer	Directeur de recherche CNRS & École polytechnique	(Directeur de thèse)

Rapporteur non présent à la soutenance :

M.	Nathan Reading	Professeur associé Université de l'État de Caroline du Nord	(Rapporteur)

Remerciements

Je tiens à remercier du fond du cœur mes directeurs de thèse *Vincent Pilaud* et *Gilles Schaeffer*. L'un comme l'autre ont été de précieux guides le long de ce chemin sinueux et parfois angoissant de la thèse. *Gilles* m'a très avantageusement suivi et conseillé, que ce soit dans mes choix scientifiques ou plus stratégiques, et je lui exprime ici toute ma gratitude. Je suis également très honoré d'avoir pu l'assister pendant son cours à l'École polytechnique, à l'occasion duquel il m'a beaucoup appris. Quant à *Vincent*, je lui dois les thématiques que j'aime tant, trois années extrêmement agréables de formation à la recherche et des moments de complicité scientifique inoubliables. La première impression que j'ai eue en le rencontrant à Berlin s'est largement confirmée par la facilité avec laquelle nous avons travaillé ensemble et l'amitié que nous partageons désormais. Je lui suis redevable bien au-delà du "simple" accomplissement scientifique que représente ce manuscrit et j'espère avoir été digne du temps, de l'intérêt et de l'énergie qu'il m'a si généreusement accordés.

Frédéric Chapoton est l'instigateur d'une part importante de cette thèse. J'ai eu le plaisir privilégié de partager avec lui des conversations très intéressantes lors de nos diverses rencontres en conférence et je l'en remercie.

Je suis également très reconnaissant à *Nathan Reading* d'avoir lui aussi donné de son temps pour relire et commenter mon travail.

C'est un honneur pour moi que l'un et l'autre aient accepté d'être mes rapporteurs. Tous deux me firent nombre de remarques et corrections fort à propos.

Je remercie les membres de mon jury d'avoir bravé moult contraintes de calendrier pour me permettre de soutenir. Parmi eux *Paco Santos*, qui m'a accueilli avec une hospitalité sans égale à Santander, et avec qui je suis extrêmement fier d'avoir eu une collaboration aussi fructueuse à cette occasion. Je dois de plus à *Paco* une séance particulièrement efficace de remise en selle alors que je commençais à m'enliser dans le futur chapitre 10 de cette thèse. *Lionel Pournin* s'est allègrement joint à lui dans cette tâche et c'est un ravissement pour moi qu'il ait également accepté de faire partie de mon jury. Son enthousiasme communicatif a égayé et, je l'espère, égaiera encore nos travaux ensemble. J'adresse enfin mes plus chaleureux remerciements à *Florent Hivert*, dont j'admire l'émerveillement face à la beauté de la combinatoire et l'osmose magique par laquelle il diffuse son immense culture scientifique autour de lui, à *Christophe Hohlweg*, dont je ne saurais oublier les retours toujours très encourageants sur mon travail et l'accueil à Montréal, et à *Sophie Morier-Genoud*, avec qui j'ai eu le plaisir d'échanger à l'occasion d'une rencontre au LIX, d'avoir eux aussi accepté de participer à mon jury.

J'ai également une pensée pour mes co-auteurs. Outre ceux que j'ai déjà cités, je suis heureux d'avoir collaboré avec *Cesar Ceballos* et *Jean-Philippe Labbé*, dont j'ai beaucoup apprécié le contact agréable et enrichissant lors de nos diverses rencontres. Je ne saurais de plus oublier mon tout premier co-auteur, *Stefan Felsner*, qui a instillé en moi le goût de la recherche lors de mon stage de master. Son invitation à revenir à Berlin pour exposer mes travaux lors de ma thèse m'a fait très plaisir.

Je remercie celles et ceux qui ont participé de près ou de loin à mon enrichissement mathématique lors d'échanges aussi agréables que formateurs. Eu égard à cette description fuligineuse des personnes concernées, je ne saurais prétendre en faire la liste complète sans impardonnable oubli. Néanmoins je tiens à avoir un mot particulier à l'attention de *Jérémie Bettinelli* et *Jean-Christophe Novelli* pour leurs profitables conseils avant ma présentation à FPSAC notamment, d'*Éric Fusy* pour son intérêt sincère lors de nos conversations sur mes travaux, d'*Alexander Garver* et *Thomas McConville* pour les discussions sur nos travaux respectifs, de *Yann Palu* et *Pierre-Guy Plamondon* pour leur disponibilité lors du groupe de travail d'algèbres amassées et leur bonne humeur, de *Viviane Pons* pour sa passion pour le treillis de Tamari et son aide précieuse dans

Merci enfin à mes amis parisiens, d'adoption ou de souche, de l'ENS ou d'ailleurs, qui ont largement contribué à mon épanouissement par les diverses festivités qui nous ont réunis. Un grand merci à *Benoît*, que je mentionne ici à seule fin qu'il reste content, à *David*, à quelques pas de qui j'ai vécu plus d'un an sans le savoir, à *Diego*, algébriste à la vision monochromatique dont j'ai finalement battu la thèse de deux pages à force d'assauts logorrhéiques dans mes remerciements, à *Florent*, certes prêt mais à jamais à la rue au bad, à *Florian*, à qui je souhaite bien du succès du côté obscur de la Force, à *Guillaume*, dont les exotiques performances laitières restent pour moi un mystère, à *Jean-Luc*, «dans» son arbre fiché, à *Jhih-Huang*, qui m'excusera peut-être un jour d'avoir jeté sa mixture qui traînait mollement sur la table de Montrouge, à *Kathleen*, qui pour être lorraine a toute sa place ici, à *Maxime*, sectaire nain bleu aimant martyriser les pauvres géologues, à *Maxime*, dont le rire communicatif et si caractéristique résiste toujours aux analyses de fréquence, à *Médéric*, dont je saurai un jour (promis) écrire sans faute et sans réfléchir le nom de la compagne, à *Miguel*, dont les vidéos insolites laissent alternativement hilare et dubitatif, à *Nicolas*, à qui je souhaite au plus vite de compléter son inscription en master, à *Nicolas* et *Virginie*, amis escrimeurs amateurs de défaites sévères, à *Vincent*, précieux allié dans mon ambition de profiter moi aussi du système, à *Weikun*, à qui je suis navré de n'avoir rien à reprocher, et à *Yichao*, dont les expériences culinaires à base de vide d'avocat trouveront toujours mon plus total soutien.

Enfin, je me dois de me parer à nouveau de mon masque de gravité pour remercier comme de juste ma famille, dont je me désole de voir chaque membre aussi peu souvent. J'espère que ma mamie, mes oncles et tantes, mes cousins et cousines comprendront en lisant ce manuscrit pourquoi j'étais à ce point occupé. Je leur réaffirme à tous ma plus tendre affection.

Je remercie pour finir *Bernadette* et *François*, mô môman et mon pôpa, amateurs invétérés de mes «beaux dessins», *Mariore*, ma 'tite sœur que j'ai réussi à garder à l'œil près de moi jusqu'à présent et dont la complicité m'est si nécessaire, et bien sûr *Aude*, ma chérie que j'aime fort. Leur amour et leur soutien rendent presque facile chaque pas de plus à franchir.

Enfin bref et pour faire court, à tous un grand merci !

Résumé

L'associaèdre se situe à l'interface de plusieurs domaines mathématiques. Combinatoirement, il s'agit du complexe simplicial des dissections d'un polygone convexe (ensembles de diagonales ne se croisant pas deux à deux). Géométriquement, il s'agit d'un polytope dont les sommets et les arêtes encodent le graphe dual du complexe des dissections. Enfin l'associaèdre décrit la structure combinatoire qui définit la présentation par générateurs et relations de certaines algèbres, dites « amassées ». Du fait de son omniprésence, de nouvelles familles généralisant cet objet sont régulièrement découvertes. Cependant elles n'ont souvent que de faibles interactions. Leurs études respectives présentent de notre point de vue deux enjeux majeurs : chercher à les relier en se basant sur les propriétés connues de l'associaèdre ; et chercher pour chacune des cadres combinatoire, géométrique et algébrique dans le même esprit.

Dans cette thèse, nous traitons le lien entre combinatoire et géométrie pour certaines de ces généralisations : les associaèdres de graphes, les complexes de sous-mots et les complexes d'accordéons. Nous suivons un fil rouge consistant à adapter, à ces trois familles, une méthode de construction des associaèdres comme éventails (ensembles de cônes polyédraux), dite méthode des d-vecteurs et issue de la théorie des algèbres amassées. De manière plus large, notre problématique principale consiste à réaliser, c'est-à-dire plonger géométriquement dans un espace vectoriel, des complexes abstraits. Nous obtenons trois familles de nouvelles réalisations, ainsi qu'une quatrième encore conjecturale dont les premières instances constituent déjà des avancées significatives.

Enfin, en sus des résultats géométriques, nous démontrons des propriétés combinatoires spécifiques à chaque complexe simplicial abordé.

Abstract

The associahedron is at the interface between several mathematical fields. Combinatorially, it is the simplicial complex of dissections of a convex polygon (sets of mutually noncrossing diagonals). Geometrically, it is a polytope whose vertices and edges encode the dual graph of the complex of dissections. Finally the associahedron describes the combinatorial structure defining a presentation by generators and relations of certain algebras, called "cluster algebras". Because of its ubiquity, we regularly come up with new families generalizing this object. However there often are only few interactions between them. From our perspective, there are two main issues when studying them: looking for relations on the basis of known properties of the associahedron; and, for each, looking for combinatorial, geometric and algebraic frameworks in the same spirit.

In this thesis, we deal with the link between combinatorics and geometry for some of these generalizations: graph associahedra, subword complexes and accordion complexes. We follow a guidelight consisting in adapting, to these three families, a method for constructing associahedra as fans (sets of polyhedral cones), called the d-vector method and coming from cluster algebra theory. More generally, our main concern is to realize, that is geometrically embed in a vector space, abstract complexes. We obtain three new families of generalizations, and a fourth conjectural one whose first instances already constitute significant advances.

Finally in addition to the geometric results, we prove combinatorial properties specific to each encountered simplicial complex.

Contents

PART I

INTRODUCTION AND PRELIMINARIES

Cette thèse de A à Z

1.1 Présentation de l'associaèdre

Les associaèdres apparaissent dans de multiples domaines des mathématiques. Leur étude, ainsi que celle de leurs nombreuses généralisations, constitue en soi un champ de recherche, à l'interface entre la combinatoire, la géométrie et l'algèbre. Cette thèse se concentre sur les deux premiers aspects, tout en tirant certaines de ses inspirations du dernier. Commençons par motiver notre travail sur la base de différentes formes mathématiques que peuvent prendre les associaèdres.

1.1.1 Arbres binaires et leur graphe de rotation

Les associaèdres sont des objets naturels pour décrire le comportement de structures de données appelées *arbres binaires de recherche* (voir par exemple [Knu98, section 6.2] pour une présentation détaillée et des motivations algorithmiques).

Un *arbre binaire* T sur un ensemble S est une structure récursive définie par :
- soit $T = \varnothing$ est l'arbre vide, sans *nœud*,
- soit T est un triplet (L, r, R), où $r \in S$ est la *racine* de T, dont le *fils gauche* L (resp. *droit* R) est un arbre binaire. Les *nœuds* de T sont r et les nœuds de ses fils.

On note couramment un arbre binaire $T = (L, r, R)$ sur S de la façon suivante :

$$T = \begin{array}{c} r \\ L \nearrow \nwarrow R \end{array}.$$

Quand S n'est pas spécifié, on note génériquement les nœuds $\bullet$. La figure 1.1 (gauche) représente tous les arbres binaires à 3 noeuds. La *hauteur* $h(T)$ d'un arbre binaire T est récursivement définie par

$$h(\varnothing) = -1 \qquad \text{et} \qquad h\left(\begin{array}{c} \bullet \\ L \nearrow \nwarrow R \end{array} \right) = \max(h(L), h(R)) + 1.$$

Lorsque les nœuds d'un arbre binaire T sont des nombres tels que tout nœud est strictement supérieur (resp. inférieur) aux nœuds de son fils gauche (resp. droit), on dit que T est un *arbre binaire de recherche*. Cette propriété permet en effet de réaliser efficacement recherches et insertions dans les arbres binaires lorsqu'ils sont *équilibrés*,
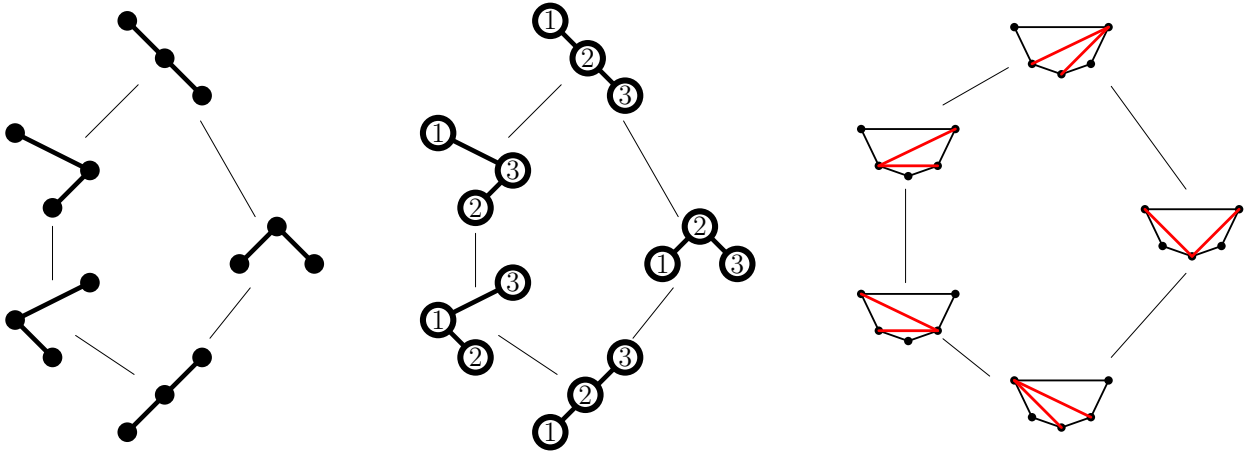
FIGURE 1.1 – Les arbres binaires à 3 nœuds (gauche, avec $\mathrm{T}_{\max}^2$ en haut), les arbres binaires de recherches sur $\{1, 2, 3\}$ (centre) et les triangulations d'un hexagone (droite). Les arêtes entre deux arbres (resp. triangulations), orientées vers le haut, correspondent aux rotations droites (flips augmentant la pente), de sorte que chaque dessin donne une interprétation combinatoire du treillis de Tamari $\mathcal{T}(3)$. Sans orientation, ils représentent le graphe de rotation (resp. de flip) $\mathcal{F}(2)$, ici un cycle à 5 sommets.

c'est-à-dire quand la différence de hauteurs entre les fils de tout nœud est d'au plus 1. Afin de toujours travailler avec des arbres équilibrés, même après l'insertion ou la suppression d'un élément, les algorithmes d'équilibrage utilisent la *rotation droite* ρ_r et la *rotation gauche* ρ_ℓ définies de la façon suivante :

$$\rho_r \left(\begin{array}{c} x_2 \\ x_1 \quad \mathrm{T}_3 \\ \mathrm{T}_1 \quad \mathrm{T}_2 \end{array} \right) := \begin{array}{c} x_1 \\ \mathrm{T}_1 \quad x_2 \\ \mathrm{T}_2 \quad \mathrm{T}_3 \end{array} \qquad \text{et} \qquad \rho_\ell \left(\begin{array}{c} x_1 \\ \mathrm{T}_1 \quad x_2 \\ \mathrm{T}_2 \quad \mathrm{T}_3 \end{array} \right) := \begin{array}{c} x_2 \\ x_1 \quad \mathrm{T}_3 \\ \mathrm{T}_1 \quad \mathrm{T}_2 \end{array} .$$

Observons que la définition récursive des arbres binaires (de recherche) induit naturellement une rotation droite (resp. gauche) à chaque nœud de tout arbre binaire dont le fils droit (resp. gauche) est non vide. La figure 1.1 (gauche et centre) illustre ces opérations. Elles permettent de définir le *graphe de rotation* $\mathcal{F}(n)$ dont les sommets sont les arbres binaires avec $n + 1$ nœuds et dont les arêtes contiennent les paires d'arbres binaires obtenus l'un à partir de l'autre par une rotation (voir la figure 1.1 gauche et centre). Ce graphe est le premier objet que l'on peut appeler un *associaèdre*. De nombreuses études ont porté sur les propriétés géodésiques de ce graphe. Remarquons d'abord qu'il est connexe. En effet on peut appliquer une rotation droite à tout nœud d'un arbre binaire dont le fils gauche n'est pas vide. Comme il n'y a qu'un seul arbre binaire $\mathrm{T}_{\max}^n$ dont tous les nœuds ont un fils gauche vide (l'arbre du haut de la figure 1.1 gauche), on peut obtenir n'importe quel arbre binaire à partir d'un autre en lui appliquant successivement une suite de rotations droites puis de rotations gauches. On peut même raffiner cette preuve pour obtenir la borne supérieure de $2n$ sur le diamètre de $\mathcal{F}(n)$. Pour cela, on définit la *branche droite* d'un arbre binaire T comme l'arbre vide si T est vide, et comme l'arbre contenant sa racine et la branche droite de son fils droit sinon. Remarquons qu'à un arbre binaire T différent de $\mathrm{T}_{\max}^n$, on peut non seulement appliquer une rotation droite, mais on peut même le faire en un nœud de la branche droite de T, de sorte que le nouvel arbre obtenu à partir de T a un nœud de plus sur sa branche droite. Ainsi tout arbre binaire peut être transformé en $\mathrm{T}_{\max}^n$ en au plus n rotations droites, ce qui donne la borne $2n$ sur le diamètre de $\mathcal{F}(n)$. Contrairement à la borne supérieure, il est très difficile d'évaluer précisément les distances

dans $\mathcal{F}(n)$, et si la question épineuse du diamètre exact de $\mathcal{F}(n)$ a récemment été résolue [STT88, Pou14], calculer efficacement la distance de rotation entre arbres binaires reste un problème ouvert. Enfin, l'étude des associaèdres est aussi liée à la recherche d'éventuelles structures de données nouvelles inspirées des arbres binaires (comme les *arbres cambriens* [CP17] par exemple).

1.1.2 Triangulations et graphe des flips

Le nombre d'arbres binaires avec n nœuds est le n-ème *nombre de Catalan* $C_n := \frac{1}{n+1}\binom{2n}{n}$ [OEI10, A000108]. Ces nombres sont omniprésents en combinatoire et comptent énormément d'objets[1] (voir par exemple [Sta01, chapitre 6]). Les *triangulations* de polygones convexes forment une famille de Catalan et sont en pratique le modèle combinatoire que nous privilégions pour travailler sur les associaèdres. Étant donné un polygone $\mathcal{P}$ à $n+3$ côtés, une *triangulation* de $\mathcal{P}$ est un ensemble de diagonales de $\mathcal{P}$ qui ne se croisent pas deux à deux, et maximal pour cette propriété (voir la figure 1.2 gauche). Ce nom vient du fait qu'une triangulation peut de façon équivalente être vue comme une subdivision de $\mathcal{P}$ en triangles sans création de nouveau sommet. Notons que la définition ne dépend pas de la géométrie de $\mathcal{P}$ puisque les croisements entre diagonales sont déterminés par l'ordre cyclique sur leurs sommets. C'est pourquoi nous représentons généralement $\mathcal{P}$ soit comme un polygone régulier, soit dans la configuration de la figure 1.2, c'est-à-dire avec un grand côté horizontal et une chaîne convexe en dessous de ce côté. Dans cette configuration, une bijection simple entre les triangulations de $\mathcal{P}$ et les arbres binaires consiste à associer à toute triangulation son *arbre dual*, comme illustré par la figure 1.2. Cette bijection induit de plus une correspondance entre la rotation dans les arbres binaires et l'opération de *flip* dans les triangulations : soit T une triangulation et $\delta \in$ T, enlever δ de T crée un quadrilatère dans T. Ce quadrilatère a exactement deux diagonales, à savoir δ et une autre δ'. On peut donc remplacer δ par δ' dans T pour obtenir une nouvelle triangulation T' $:= ($T $\cup \{\delta'\}) \smallsetminus \{\delta\}$ (voir la figure 1.2 droite). On dit que T' est obtenue à partir de T en *flippant* δ. La bijection de la figure 1.2 fait correspondre les rotations droites (resp. gauches) aux *flips augmentant* (resp. *diminuant*) *la pente*, c'est-à-dire tels que la diagonale introduite a une pente supérieure (resp. inférieure) à celle de la diagonale enlevée. Le *graphe des flips* de $\mathcal{P}$ est le graphe dont les sommets sont les triangulations de $\mathcal{P}$ et dont les arêtes correspondent aux flips. Ce graphe est isomorphe au graphe $\mathcal{F}(n)$ sur les arbres binaires (voir la figure 1.2 droite) et est donc aussi un modèle combinatoire de l'associaèdre.

L'associaèdre présente la propriété combinatoire importante suivante : en orientant les arêtes du graphe des flips $\mathcal{F}(n)$ dans la direction de l'accroissement de pente (ou
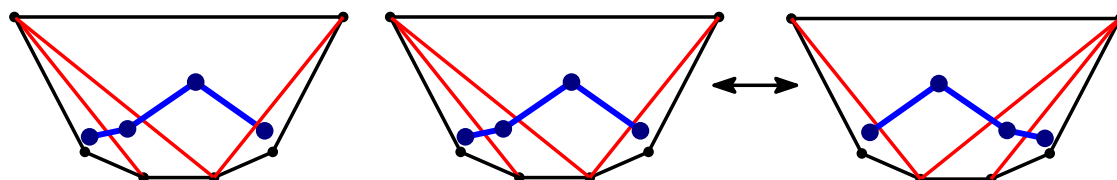
FIGURE 1.2 – Une bijection entre les arbres binaires à $n+1$ nœuds (en bleu) et les triangulations d'un $(n+3)$-gone (en rouge), illustrée pour $n = 3$ (gauche). Quand le polygone $\mathcal{P}$ est dessiné dans cette configuration, avec un grand côté horizontal e, l'arbre binaire associé à une triangulation est son arbre dual, enraciné au triangle qui contient e. Cette bijection fait correspondre les rotations droites (resp. gauche) dans les arbres binaires avec les flips augmentant (resp. diminuant) la pente (droite).

---

[1]Selon R. Stanley, il y a actuellement 207 interprétations combinatoires de ces nombres.
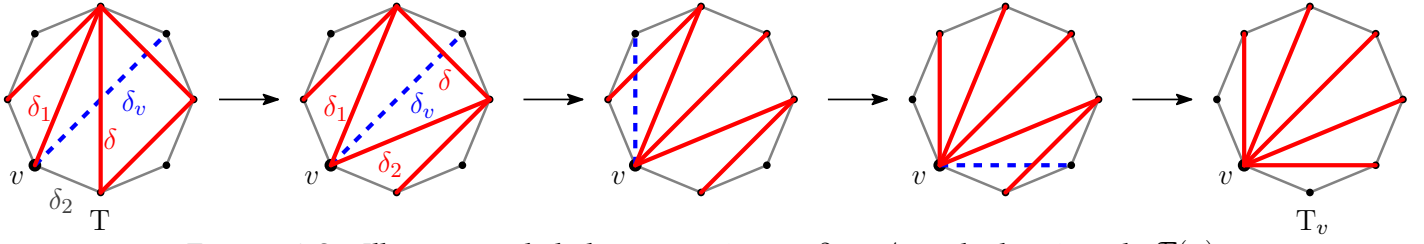
FIGURE 1.3 – Illustration de la borne supérieure $2n - 4$ sur le diamètre de $\mathcal{F}(n)$.

de façon équivalente, dans la direction donnée par les rotations droites), on obtient un graphe dirigé acyclique, qui se trouve être le diagramme de Hasse d'un *treillis*, appelé le *treillis de Tamari* $\mathcal{T}(n + 1)$ (voir [Tam51] et la figure 1.1). Ce treillis est lui aussi au centre d'études variées et a été généralisé dans diverses directions. Enfin, à part être une famille de Catalan, les triangulations de polygones convexes sont aussi les premiers exemples de triangulations de configurations de points dans le plan (voir [DRS10] et les références qui s'y trouvent), ce qui explique aussi pour partie l'intérêt qu'elles suscitent. Comme nous l'avons dit, les triangulations sont un modèle complémentaire aux arbres binaires pour étudier l'associaèdre. Illustrons cela en montrant que la borne $2n$ sur le diamètre du graphe $\mathcal{F}(n)$ que nous avons prouvée dans la section 1.1.1 peut être améliorée à $2n - 4$ pour $n \geq 10$ (voir la figure 1.3), qui est en fait la valeur exacte du diamètre du graphe des flips $\mathcal{F}(n)$ dans ce cas [Pou14].

Preuve (borne supérieure $2n - 4$ sur le diamètre de $\mathcal{F}(n)$). Soit $\mathcal{P}$ un $(n+3)$-gone et v un sommet de $\mathcal{P}$, on note T_v la triangulation de $\mathcal{P}$ contenant les n diagonales de $\mathcal{P}$ incidentes à v. Soit T une triangulation de $\mathcal{P}$ ne contenant pas une diagonale δ_v incidente à v. Alors δ_v se trouve entre deux diagonales (potentiellement des côtés de $\mathcal{P}$) de T incidentes à v, que nous notons δ_1 et δ_2. Ces deux diagonales appartiennent à un même triangle de T, dont nous appelons la troisième diagonale δ. Comme δ_1 et δ_2 ne sont pas consécutives dans T_v, la diagonale δ est *interne* (n'est pas un côté de $\mathcal{P}$) et peut donc être flippée dans T en une nouvelle diagonale, incidente à v. On conclut par une récurrence immédiate que si T contient $\deg_v(\mathrm{T})$ diagonales incidentes à v, alors $n - \deg_v(\mathrm{T})$ flips suffisent pour la transformer en la triangulation T_v. En particulier la distance de flip entre T et une autre triangulation T' vaut au plus $2n - (\deg_v(\mathrm{T}) + \deg_v(\mathrm{T}'))$. Enfin les diagonales de $\mathrm{T} \cup \mathrm{T}'$ (comptées avec répétitions) ont au total $4n$ extrémités (comptées avec répétitions), de sorte qu'en moyenne un sommet de $\mathcal{P}$ est incident à $\frac{4n}{n+3} = 4 - \frac{12}{n+3}$ diagonales de $\mathrm{T} \cup \mathrm{T}'$. Cette moyenne est strictement supérieure à 3 pour $n \geq 10$ et il existe donc un sommet v de $\mathcal{P}$ pour lequel $\deg_v(\mathrm{T}) + \deg_v(\mathrm{T}') \geq 4$.   ∎

1.1.3   Polytopes

Pour la partie géométrique de cette thèse, on s'intéresse en premier lieu aux *polytopes*. Rappelons qu'un *polytope* est l'enveloppe convexe d'un nombre fini de points dans $\mathbb{R}^d$ (voir le chapitre 3, en particulier la section 3.2.1). Les polytopes sont, entre autres choses, des exemples de *polyèdres*, qui sont les domaines de définition des problèmes d'optimisation linéaire (voir [GM07]). En particulier tout un pan de la recherche dans ce domaine a pour objet le diamètre combinatoire des polytopes, en lien avec la conjecture dite « de Hirsch polynomiale », qui affirme que le diamètre du graphe d'un polytope est borné par un polynôme en son nombre de facettes (voir [San13] pour un panorama détaillé sur ce sujet). Cependant la combinatoire des polytopes fait ressortir de nombreux problèmes difficiles (NP-durs), ce qui rend d'autant plus appréciable d'avoir à notre disposition des familles de polytopes dont la combinatoire se décrit facilement. Dans cet esprit, un exemple classique est le *permutaèdre de dimension n* Perm(n) (ou simplement *n-permutaèdre*), que l'on définit comme l'enveloppe convexe des permutations de $[n + 1] := \{1, 2, \ldots, n + 1\}$, vues comme vecteurs dans $\mathbb{R}^{n+1}$ (voir figure 1.4).
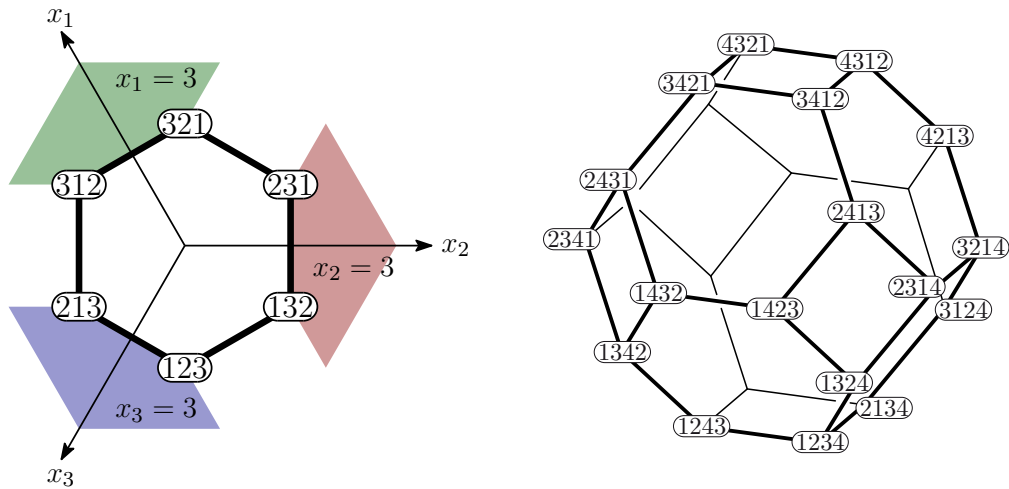
FIGURE 1.4 – Le 2-permutaèdre plongé dans $\mathbb{R}^3$ (gauche) et le 3-permutaèdre (droite).

Formellement, en notant $\mathfrak{S}_{n+1}$ le groupe symétrique des permutations de $[n+1]$, on a

$$\mathsf{Perm}(n) := \mathrm{conv}\left((\sigma(i))_{i\in[n+1]} \,\middle|\, \sigma \in \mathfrak{S}_{n+1} \right).$$

Les associaèdres sont un autre exemple de tels polytopes. En effet si nous avons décrit les associaèdres par la donnée combinatoire des graphes des flips (ou de rotation), le terme *associaèdre* désigne plus fréquemment le polytope qui leur est associé.

Théorème A ([Hai84, Lee89, GKZ08, BFS90, SS93, SS97, RSS03, Lod04, HL07, CSZ15]). *Pour tout entier n, il existe un polytope de dimension n dont le graphe est isomorphe au graphe des flips $\mathcal{F}(n)$. Un tel polytope est appelé un n-associaèdre.*

Nous revenons sur quelques preuves du théorème A dans la section 1.2.2. Les figures 1.5 et 1.6 illustrent différentes réalisations du 3-associaèdre. Comme nous l'avons vu, avoir des polytopes décrits par des graphes des flips est pratique du point de vue de la géométrie. Il se trouve qu'en retour, la géométrie de ces polytopes peut nous aider à trouver des propriétés combinatoires qui ne sont pas faciles à prouver directement. Par exemple D. Sleator, R. Tarjan et W. Thurston [STT88] ont utilisé des polytopes hyperboliques dans leur étude du diamètre combinatoire de l'associaèdre. Un exemple plus récent est donné dans la section 9.4 de cette thèse, où certaines propriétés des *complexes d'accordéon* sont obtenues sur la base de leur *réalisations polytopales*. Cette notion de « réalisation » est la raison pour laquelle nous travaillons conjointement sur des aspects combinatoires et géométriques. De façon informelle, une réalisation géométrique d'une structure combinatoire S est un objet plongé dans un espace vectoriel, qui peut être entièrement défini par une information finie encodée par S. D'une certaine manière, c'est une façon de plonger fidèlement une structure abstraite dans un

| [Lod04, HL07] | [HL07] | [CFZ02, HL07, CSZ15] | [CSZ15] |
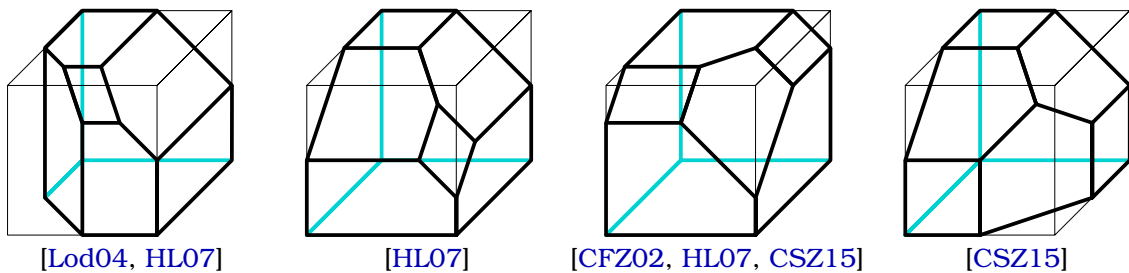
FIGURE 1.5 – Exemples de 3-associaèdres. Figure de [CSZ15], avec permission.

cadre géométrique. Le théorème A illustre la réalisation d'un graphe par un polytope, mais ce ne sont pas les seuls types de réalisations que nous allons considérer. Dans cette thèse, on s'intéresse principalement à la réalisation de *complexes simpliciaux* (c'est aussi le cas dans le théorème A). De plus les réalisations que nous donnons sont souvent des *éventails*, à savoir nous encodons des complexes simpliciaux par des cônes polyédraux s'intersectant proprement. L'objectif de cette thèse se résume donc ainsi.

> **But :** d'une part nous essayons de mieux comprendre des objets abstraits de la famille des associaèdres ; d'autre part nous travaillons avec ces objets dans le but d'obtenir de nouvelles constructions de polytopes et d'éventails non triviaux.

Nous réservons la présentation formelle des complexes simpliciaux, polytopes et éventails pour le chapitre 3, où nous donnons les pré-requis nécessaires à la lecture de ce manuscrit. Décrivons à présent le contexte mathématique dans lequel il s'inscrit.

1.2   État de l'art

La première apparition de la structure combinatoire de l'associaèdre est le treillis de Tamari (voir la section 1.1.2) dans la thèse de D. Tamari [Tam51]. Il fut ensuite étudié en tant que complexe simplicial (voir la section 3.1) par J. Stasheff [Sta63] dans le but d'étudier des propriétés d'homotopie des H-espaces, notamment pour leur rapport avec les théories d'associativité. Au niveau de la géométrie, la première réalisation de l'associaèdre comme polytope convexe est due à M. Haiman [Hai84] et C. Lee [Lee89]. Comme nous l'avons expliqué, l'associaèdre a engendré un courant de recherche florissant dans différentes directions, que l'on peut plus ou moins répartir entre « combinatoire », « géométrie » et « algèbre ». Nous présentons d'abord quelques propriétés remarquables de l'associaèdre dans chacun de ces mondes, en soulignant certaines interactions, avant d'en venir à la construction des d-vecteurs, qui est au cœur de cette thèse.

1.2.1   Combinatoire

Comme nous l'avons déjà relevé dans la section 1.1.2, les arbres binaires et les triangulations forment des familles de Catalan et décrivent le treillis de Tamari $\mathcal{T}(n+1)$. Les
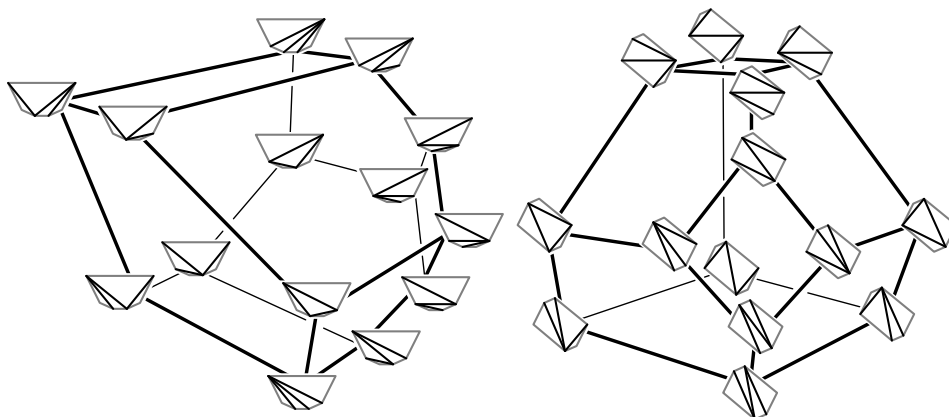
FIGURE 1.6 – Deux 3-associaèdres de C. Hohlweg et C. Lange [HL07] (voir aussi la figure 1.5 gauche et centre gauche). Les treillis cambriens correspondants sont obtenus en les orientant du bas vers le haut. Celui de gauche est initialement dû à S. Shnider et S. Sternberg [SS93, SS97] et J.-L. Loday [Lod04]. Figure de [LP13], avec permission.

propriétés algébriques et combinatoires de ce dernier ont été très largement étudiées et généralisées. L'une des raisons à cela est son lien fort avec l'*ordre faible* sur les permutations. Rappelons que $\mathfrak{S}_{n+1}$ est le groupe symétrique des permutations de $[n+1]$. L'*ensemble des inversions* d'une permutation $\sigma \in \mathfrak{S}_{n+1}$ est l'ensemble des paires (i, j) d'entiers tels que $i < j$ et $\sigma(i) > \sigma(j)$. L'*ordre faible* est la relation d'ordre $\preccurlyeq$ sur les permutations définie par

$$\forall \sigma, \sigma' \in \mathfrak{S}_{n+1}, \ \sigma \preccurlyeq \sigma' \Longleftrightarrow \mathrm{inv}(\sigma) \subseteq \mathrm{inv}(\sigma').$$

Cet ordre est un treillis aux multiples propriétés combinatoires. Par exemple ses chaînes maximales encodent les factorisations minimales de la permutation $[n+1, \ldots, 1]$ en produit de transpositions simples. Dans [BW97, section 9] A. Björner et M. Wachs ont observé que restreindre l'ordre faible aux permutations évitant le motif (132) en donnait un *sous-treillis*, isomorphe au treillis de Tamari. N. Reading [Rea06] a ensuite généralisé le treillis de Tamari en définissant les *treillis cambriens*, dont il a aussi montré qu'ils sont des *treillis quotients* de l'ordre faible. Un treillis cambrien (de type A) est décrit par une suite de $n+1$ signes $\varepsilon \in \{+, -\}^{n+1}$ (appelée *signature*) de la façon suivante : à partir de ε, on construit un *polygone cambrien* $\mathcal{P}_{\varepsilon}$ obtenu en plaçant deux sommets étiquetés 0 et $n+2$ sur l'axe horizontal puis en plaçant les autres sommets par ordre croissant d'abscisse entre 0 et $n+2$, au-dessus ou en-dessous de la droite passant par 0 et $n+2$ selon le signe correspondant dans ε. Le treillis cambrien déterminé par ε est alors l'ordre partiel dont le diagramme de Hasse est le graphe des flips de $\mathcal{P}_{\varepsilon}$, où les arêtes sont orientées selon les flips augmentant la pente. En particulier le treillis de Tamari $\mathcal{T}(n+1)$ est le treillis cambrien correspondant à la signature $(-)_{i \in [n+1]}$. La figure 1.6 représente le treillis de Tamari et un autre treillis cambrien. Nous n'étudions pas directement les treillis cambriens dans cette thèse, mais ils sont naturellement visibles sur les objets qui nous intéressent.

1.2.2 Géométrie

Les polytopes que nous considérons sont décrits par des structures combinatoires, dont certaines propriétés sont « lisibles géométriquement ». Par exemple, en orientant le graphe du permutaèdre $\mathsf{Perm}(n)$ (plongé dans $\mathbb{R}^{n+1}$ comme dans la section 1.1.3) dans la direction donnée par le vecteur $(n+1, n, \ldots, 1) - (1, 2, \ldots, n+1)$, on obtient le diagramme de Hasse de l'ordre faible. Comme nous l'avons vu dans le théorème A, une kyrielle de réalisations polytopales de l'associaèdre furent découvertes par à peu près autant d'auteurs [Hai84, Lee89, GKZ08, BFS90, SS93, SS97, RSS03, Lod04, HL07, CSZ15]. Parmi elles on distingue trois familles principales.

Les polytopes secondaires. Les polytopes secondaires de configurations de points ont été introduits par I. Gelfand, M. Kapranov et A. Zelevinsky dans [GKZ08]. L'associaèdre apparaît dans ce cadre comme le polytope secondaire d'un ensemble de points du plan en position convexe. Comme deux configurations différentes génèrent deux polytopes différents, cela permet d'obtenir une famille très nombreuse de réalisations. Néanmoins les associaèdres ne sont certainement pas centraux dans cette théorie, étant donné qu'ils en constituent l'exemple « le plus facile ».

Les associaèdres par signatures. S. Shnider et S. Sternberg ont construit dans [SS93, SS97] une réalisation de l'associaèdre obtenue en oubliant certaines inégalités définissant le permutaèdre $\mathsf{Perm}(n)$. J.-L. Loday donna dans [Lod04] une interprétation des coordonnées des sommets de cette réalisation basée sur des calculs simples sur les arbres binaires. Entre autres propriétés, cet associaèdre, que nous appelons associaèdre de Loday, peut être orienté dans la même direction linéaire que le permutaèdre de sorte que l'orientation induite sur son graphe en fait le

diagramme de Hasse du treillis de Tamari. Prouvant une conjecture de N. Reading [Rea06], C. Hohlweg et C. Lange [HL07] obtinrent par la suite approximativement 2^n réalisations différentes du n-associaèdre, dont l'associaèdre de Loday, construites à partir du permutaèdre de façon similaire à ce dernier. La méthode de C. Hohlweg et C. Lange utilise les triangulations des polygones cambriens (voir la section 1.2.1). En effet leurs réalisations sont spécialement adaptées afin que les diagrammes de Hasse des treillis cambriens (de type A) s'obtiennent en choisissant une bonne orientation linéaire dans leurs espaces ambiants respectifs (voir la figure 1.6). Enfin la description combinatoire des sommets de ces réalisations donnée dans [HL07] fut ensuite réinterprétée par C. Lange et V. Pilaud [LP13] sur les arbres duaux des triangulations des polygones cambriens.

Les d-**associaèdres.** La dernière famille de réalisations fut découverte dans le contexte des *algèbres amassées* par F. Chapoton, S. Fomin et A. Zelevinsky [CFZ02]. Dans cet article, une réalisation est donnée pour chaque *associaèdre généralisé* en utilisant des *degrés de compatibilité*, qui sont aussi les *vecteurs dénominateur* (voir [FZ03b, CP15]) dans l'algèbre amassée correspondante. F. Santos a ensuite étendu cette méthode dans le cas du type A, dans un article publié avec C. Ceballos et G. Ziegler [CSZ15, Section 5], afin d'obtenir environ $C_n = \frac{1}{n+1}\binom{2n}{n}$ réalisations différentes du n-associaèdre classique.

Le même article de C. Ceballos, F. Santos et G. Ziegler [CSZ15] fournit par ailleurs un aperçu précis sur les méthodes précédemment décrites. Nous nous concentrerons sur la dernière, qui est pour ainsi dire le fil rouge de la partie géométrique de cette thèse. Elle s'appuie sur les algèbres amassées, que nous présentons maintenant.

1.2.3   Algèbre

Les permutations et les arbres apparaissent également dans des contextes algébriques, en indexant notamment les bases d'algèbres de Hopf combinatoires [LR98, HNT05, Cha00, CP17]. Ces algèbres n'étant que peu reliées à notre étude, nous passons directement aux algèbres amassées. Elles furent introduites par S. Fomin et A. Zelevinsky dans une série d'articles communs [FZ03b, FZ02, FZ03a, FZ07] et un article avec A. Berenstein [BFZ05]. Dès lors, diverses applications leur ont été trouvées, notamment en théorie des systèmes dynamiques discrets, en géométrie tropicale, en théorie de Teichmüller et en géométrie de Poisson (voir [FZ04] pour un tour d'horizon).

Comme nous n'avons pas besoin de la définition précise (et lourde) des algèbres amassées, nous nous contentons de donner quelques idées informelles suffisantes à la compréhension de ce qui suit. En particulier nous ne considérons que des algèbres sur le corps $\mathbb{Q}$ des nombres rationnels. Une *algèbre amassée* est une algèbre commutative $\mathcal{A}$ donnée par une présentation par générateurs et relations définie combinatoirement : les générateurs de $\mathcal{A}$ sont appelés les *variables d'amas*. Elles sont regroupées en *amas* non disjoints, tous de cardinal identique (le *rang* de $\mathcal{A}$). À chaque amas on associe une *matrice d'échange*[2], avec laquelle il forme une *graine*. Les matrices d'échange encodent un processus involutif appelé *mutation*, qui relie les amas de la façon suivante : étant donné une graine $\mathbf{s} = (X, \mathbf{B})$ constituée d'un amas $X = (x_1, \ldots, x_n)$ et d'une matrice d'échange $\mathbf{B}$, et un entier $i \in [n]$, la mutation de $\mathbf{s}$ en x_i transforme la graine $\mathbf{s}$ en une nouvelle graine $\mathbf{s}' = (X', \mathbf{B}')$ où

- l'amas $X' = (x'_1, \ldots, x'_n)$ satisfait $x'_j = x_j$ pour tout $j \neq i$, et les variables x_i et x'_i, qui sont *échangées* au cours de la mutation, sont liées par une relation algébrique de la forme $x_i x'_i = M^+ + M^-$ dans $\mathcal{A}$, où M^+ et M^- sont des monômes premiers entre eux en les variables x_j (pour $j \neq i$) déterminés par $\mathbf{B}$;
- la matrice $\mathbf{B}'$ est une nouvelle matrice d'échange aussi déterminée par $\mathbf{B}$.

---

[2]Une matrice d'entiers avec une propriété un peu moins forte que l'antisymétrie.
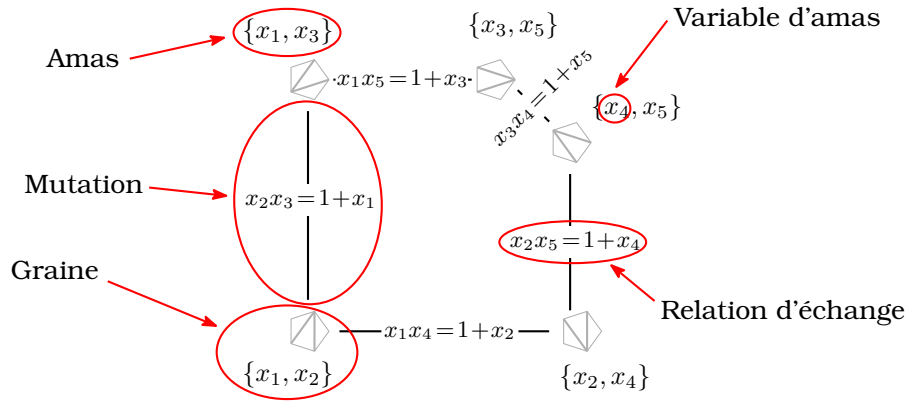
FIGURE 1.7 – Le graphe de mutation d'une algèbre amassée de type A et de rang 2, et l'illustration du vocabulaire des algèbres amassées. Ici les données combinatoires qui encodent les mutations sont les triangulations d'un pentagone. Ce graphe de mutation est isomorphe au graphe des flips $\mathcal{F}(2)$.

La raison d'être des matrices d'échange est de coder le processus de mutation. Elles sont donc remplaçables par n'importe quelle autre structure combinatoire remplissant le même rôle. Certaines mutations se décrivent par exemple en termes de *carquois* (multigraphes dirigés, voir par exemple [Kel13, section 3]), ou par des objets plus spécifiques (triangulations de surfaces épointées, triangulations centralement symétriques ...).

Les relations $x_i x_i' = M^+ + M^-$ sont les *relations d'échange* et définissent la présentation de $\mathcal{A}$. Le *graphe d'échange* (ou *graphe de mutation*) de $\mathcal{A}$ est le graphe dont les sommets sont les graines de $\mathcal{A}$ et dans lequel deux graines sont adjacentes si une mutation transforme l'une en l'autre. Il est important de préciser que les graines sont considérées à permutation et ré-étiquetage de leurs variables près, de sorte qu'il faut penser aux amas comme à des ensembles non ordonnés. Si les éléments d'un amas sont généralement donnés avec un ordre, c'est parce qu'ils indexent les lignes et colonnes de la matrice d'échange associée. La figure 1.7 illustre les définitions précédentes.

Observons que la donnée d'une seule graine suffit à déterminer toute son algèbre amassée. Les algèbres amassées sont de fait généralement introduites par une première description du processus de mutation, après quoi l'on considère la sous-algèbre du corps $\mathbb{Q}(x_1^\circ, \ldots, x_n^\circ)$ (des fonctions rationnelles sur $\mathbb{Q}$ en n variables) engendrée par l'ensemble des variables d'amas contenues dans toutes les graines obtenues à partir d'une *graine initiale* $s^\circ = (X^\circ, \mathbf{B}^\circ)$ (ayant pour *amas initial* $X^\circ = (x_1^\circ, \ldots, x_n^\circ)$) par des mutations successives. Le développement des variables d'amas de la figure 1.7 en fractions rationnelles d'un amas initial fixé sont donnés dans la figure 1.8, qui illustre également la première propriété cruciale des algèbres amassées.

Théorème B (Phénomène de Laurent, [FZ02, théorème 3.1]). *Pour tout amas initial* $X^\circ = (x_1^\circ, \ldots, x_n^\circ)$ *d'une algèbre amassée* $\mathcal{A}$ *et toute variable d'amas* x *de* $\mathcal{A}$*, le développement de* x *comme fraction rationnelle en les variables* $(x_1^\circ, \ldots, x_n^\circ)$ *est un polynôme de Laurent*[3].

Parmi les algèbres amassées, on s'intéresse en particulier à celles dont le graphe de mutation est fini. Ce sont les *algèbres amassées de type fini*, décrite de façon équivalente comme les algèbres amassées avec un nombre fini de variables d'amas. Ce résultat est un sous-produit de la classification exacte des algèbres amassées de type fini.

---

[3]C'est-à-dire une fraction rationnelle dont le dénominateur est un monôme en $(x_1^\circ, \ldots, x_n^\circ)$.

$$\{x_1, x_3\} \qquad\qquad \{x_3, x_5\}$$
$$\{x_1^\circ, \tfrac{1+x_1^\circ}{x_2^\circ}\} \qquad \{\tfrac{1+x_1^\circ}{x_2^\circ}, \tfrac{1+x_1^\circ+x_2^\circ}{x_1^\circ x_2^\circ}\}$$

$$x_1 x_5 = 1 + x_3$$

$$x_3 x_4 = 1 + x_5$$

$$\{\tfrac{1+x_2^\circ}{x_1^\circ}, \tfrac{1+x_1^\circ+x_2^\circ}{x_1^\circ x_2^\circ}\}$$
$$\{x_4, x_5\}$$

$$x_2 x_3 = 1 + x_1$$

$$x_2 x_5 = 1 + x_4$$

$$x_1 x_4 = 1 + x_2$$

$$\{x_1^\circ, x_2^\circ\} \qquad\qquad \{x_2^\circ, \tfrac{1+x_2^\circ}{x_1^\circ}\}$$
$$\{x_1, x_2\} \qquad\qquad \{x_2, x_4\}$$
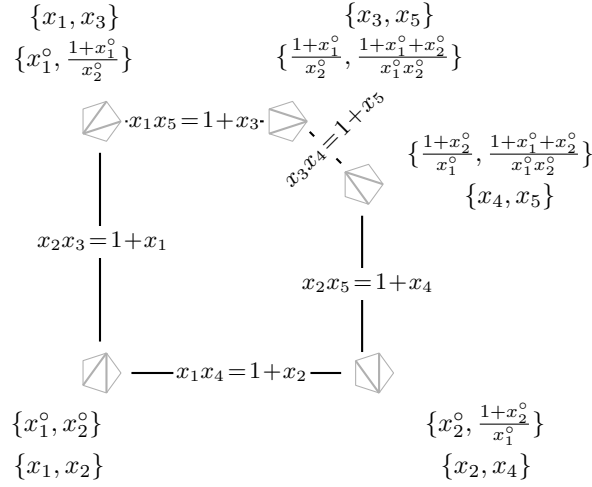
FIGURE 1.8 – Le développement des variables d'amas de la figure 1.7 en les variables de l'amas initial (x_1, x_2). Toutes ces fractions rationnelles sont des polynômes de Laurent en (x_1, x_2) (voir le théorème B).

Théorème C (Classification des types finis, [FZ03a, théorèmes 1.7 et 1.8]). *Les algèbres amassées de type fini sont classifiées par les systèmes de racines cristallographiques[4]. En particulier le graphe de mutation des algèbres amassées de type A_n est isomorphe au graphe des flips $\mathcal{F}(n)$.*

Les variables d'amas d'une algèbre amassée $\mathcal{A}$ sont combinatoirement liées par le graphe de mutation de $\mathcal{A}$, qui est le *graphe dual* du *complexe d'amas* de $\mathcal{A}$, défini comme le complexe simplicial dont les facettes sont les amas de $\mathcal{A}$.

Exemple. Le complexe amassé de type A et de rang n est le *complexe des dissections* d'un polygone convexe $\mathcal{P}$ à $n+3$ sommets, c'est-à-dire le complexe dont les faces sont les *dissections* (ensembles de diagonales ne se croisant pas deux à deux) de $\mathcal{P}$. Le graphe dual de ce complexe est le graphe $\mathcal{F}(n)$. Il se trouve que tous les complexes amassés de type fini non exceptionnels ont une interprétation semblable à celle en type A, à savoir en termes de configurations géométriques d'arcs ne se croisant pas dans le plan (voir [FZ03a, CP15]). Ainsi qu'expliqué dans la section 6.3.3, les amas de type B sont par exemple encodés par les triangulations centralement symétriques d'un polygone centralement symétrique.

L'une des propriétés pour lesquelles nous nous intéressons aux algèbres amassées de type fini est que leur structure est entièrement décrite par la combinatoire de leurs complexes d'amas. Les algèbres amassées de type fini sont donc en quelque sorte des « réalisations algébriques » de leurs complexes d'amas.

Théorème D ([FZ03a, théorème 1.12]). *Les algèbres amassées de type fini (sans coefficient) sont caractérisées par leurs complexes d'amas. Autrement dit deux algèbres amassées de type fini (sans coefficient) sont isomorphes si et seulement si leurs complexes d'amas le sont.*

---

[4]Dans toute le manuscrit, nous n'utilisons jamais la théorie de Coxeter mais nous mentionnons régulièrement les différents « type » des systèmes de racines. Notre travail traite essentiellement le type A mais nous faisons parfois des remarques ou comparaisons avec les autres types. Cependant tous les résultats sont formulés afin qu'aucun pré-requis sur ce sujet ne soit nécessaire à leur compréhension. Nous renvoyons donc le lecteur intéressé aux manuels classiques [Hum90, BB05].

Enfin, en plus de ces propriétés algébriques, les complexes d'amas ont le bon goût d'avoir des réalisations comme polytopes convexes.

Théorème E (Associaèdres généralisés, [CFZ02, théorème 1.4],[HLT11, Ste13],[PS15a, corollaire 6.10])**.** *Tout complexe d'amas de type fini admet une réalisation polytopale, appelée l'associaèdre généralisé du même type. Dans ce contexte, l'associaèdre classique est l'associaèdre généralisé de type A.*

Admettre des réalisations comme polytope est en fait une propriété plus forte, pour un complexe simplicial, que d'admettre des réalisations par éventail. Ainsi le théorème E implique que les complexes amassés de type fini admettent aussi des réalisations par éventails. Néanmoins les réalisations par polytopes sont généralement obtenues en deux étapes, à savoir d'abord la construction d'une réalisation par éventail, que l'on montre seulement ensuite être l'*éventail normal* d'un polytope. C'est le cas pour la réalisation des associaèdres généralisés par F. Chapoton, S. Fomin et A. Zelevinsky [CFZ02], qui se fonde sur la construction d'un éventail proposée par S. Fomin et A. Zelevinsky [FZ03b]. La preuve de C. Hohlweg, C. Lange et H. Thomas [HLT11] est une extension de la construction des associaèdres par signatures, présentée dans la section 1.2.2, aux complexes d'amas de type fini. Elle repose sur les mêmes motivations, à savoir les articles de N. Reading et D. Speyer [Rea06, RS09], dans lequel des réalisations des complexes amassés de type fini par les *éventails cambriens* sont déjà construites. Les polytopes construits dans [HLT11] ont pour éventails normaux ces éventails cambriens. Les réalisations de S. Stella [Ste13] et de V. Pilaud et C. Stump [PS15a] sont essentiellement les mêmes que celles de [HLT11] mais elles apportent de nouvelles perspectives sur les complexes d'amas. En particulier S. Stella [Ste13] fait le lien entre les éventails cambriens et les *éventails d'amas* et V. Pilaud et C. Stump [PS15a] généralisent les *polytopes de briques* introduits par V. Pilaud et F. Santos [PS12].

Les théorèmes D et E décrivent ce que nous appelons un « triptyque combinatoire-géométrie-algèbre » en ce sens qu'un même objet peut être indifféremment pensé dans ces trois mondes. En particulier quand nous travaillons avec des généralisations de l'associaèdre, l'une de nos principales quêtes consiste à chercher d'autres triptyques semblables à celui-ci, avec autant de propriétés analogues à celles des complexes d'amas, des associaèdres généralisés et des algèbres amassées que possible.

1.2.4 La construction des d-vecteurs

Nous venons de souligner que la plupart des réalisations polytopales de complexes simpliciaux commencent par la construction d'un éventail approprié. Cela dit trouver de nouvelles réalisations par éventail, même pour des complexes notoirement polytopaux, n'est pas seulement appréciable en tant que première étape, mais aussi parce que deux polytopes sont en général considérés comme « essentiellement différents » quand leurs éventails normaux ne sont pas linéairement isomorphes (voir la section 3.2). Pour ce qui est des complexes d'amas de type fini, il existe deux constructions majeures issues de la théorie des algèbres amassées. L'éventail réalisé dans [FZ03b] (dont la preuve qu'il est polytopal est donnée dans [CFZ02]) se situe à l'intersection des deux familles de réalisations résultant de ces constructions. Nous avons en fait déjà donné une idée de ces constructions dans la section 1.2.2. D'une part les associaèdres par signature sont en effet expliqués en termes de g-vecteurs par S. Stella [Ste13]. Nous présentons ces vecteurs en type A dans le chapitre 9. D'autre part les réalisations de F. Santos [CSZ15, section 5] étendent la construction par les **d**-vecteurs, que nous présentons maintenant.

Étant donné une algèbre amassée $\mathcal{A}$ et un amas initial $X^\circ = (x_1^\circ, \ldots, x_n^\circ)$ de $\mathcal{A}$, le phénomène de Laurent (théorème B) permet d'associer à chaque variable d'amas x son *vecteur dénominateur* par rapport à X°

$$\mathbf{d}(X^\circ, x) := [(x_1^\circ \,\|\, x), \ldots, (x_n^\circ \,\|\, x)],$$

$\{x_1, x_3\}$ $\{x_3, x_5\}$
$\{(-1, 0), (0, 1)\}$ $\{(0, 1), (1, 1)\}$

$\cdot x_1 x_5 = 1 + x_3 \cdot$ $x_3 x_4 = 1 + x_5$

                                                          $\{(1, 0), (1, 1)\}$
                                                          $\{x_4, x_5\}$

$x_2 x_3 = 1 + x_1$

                                             $x_2 x_5 = 1 + x_4$

$\{(-1, 0), (0, -1)\}$ $x_1 x_4 = 1 + x_2$ $\{(0, -1), (1, 0)\}$
$\{x_1, x_2\}$ $\{x_2, x_4\}$
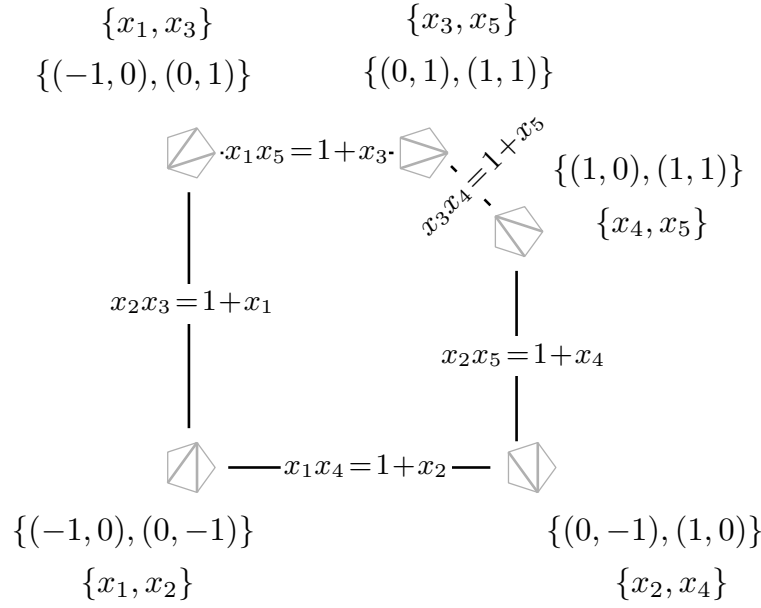
FIGURE 1.9 – Les **d**-vecteurs des variables d'amas du graphe de mutation de la figure 1.7 par rapport à l'amas initial $(x_1, x_2) = (x_1^\circ, x_2^\circ)$. La première (resp. deuxième) coordonnée de chaque **d**-vecteur correspond au degré de compatibilité avec x_1° (resp. x_2°). Les **d**-vecteurs sont groupés par amas. Les valeurs de leurs entrées sont obtenues à partir des développements explicites de la figure 1.8 ou bien directement des croisements entre les diagonales correspondantes dans les triangulations associées aux amas.

aussi appelé son **d**-*vecteur*, où $(x_i^\circ \,\|\, x)$ est l'exposant de la variable d'amas initiale x_i° dans le développement de x comme polynôme de Laurent en les variables de X° (cette notation n'est pas ambiguë par la proposition G 1). Il se trouve que cette quantité, initialement définie comme un *degré de compatibilité* de façon algébrique par S. Fomin et A. Zelevinsky [FZ03b], a une interprétation combinatoire en termes de croisements dans les modèles géométriques pour les complexes d'amas des types finis non exceptionnels [FZ03b, CP15]. Dans le cas de l'associaèdre classique, les variables d'amas sont représentées par les diagonales d'un polygone convexe $\mathcal{P}$ et le degré de compatibilité peut être directement lu dans ce cadre : étant donné deux diagonales δ et δ' de $\mathcal{P}$, on a $(\delta \,\|\, \delta') = (\delta' \,\|\, \delta) = -1$ si $\delta = \delta'$, $(\delta \,\|\, \delta') = (\delta' \,\|\, \delta) = 0$ si δ et δ' ne se croisent pas, et $(\delta \,\|\, \delta') = (\delta' \,\|\, \delta) = 1$ sinon. Ainsi à partir de toute triangulation initiale T° de $\mathcal{P}$, on peut associer à chaque diagonale de $\mathcal{P}$ un vecteur à coordonnées dans $\{-1, 0, 1\}$, dont les entrées sont indicées par les diagonales de T°.

Théorème F ([CSZ15, théorème 5.1]). *Pour toute triangulation initiale T° de $\mathcal{P}$, les vecteurs dans $\{\mathbf{d}(\mathrm{T}^\circ, \delta) \,|\, \delta$ diagonale de $\mathcal{P}\}$ sont les rayons d'un éventail simplicial complet réalisant le complexe des dissections de $\mathcal{P}$. Dans la terminologie des algèbres amassées, cela signifie qu'en type A, les vecteurs dénominateur associés à toute graine initiale supportent une réalisation du complexe d'amas par un éventail simplicial complet.*

Nous reprenons l'exemple des figures 1.7 et 1.8 pour illustrer le théorème F. Dans la figure 1.9, nous donnons les vecteurs dénominateur des variables d'amas par rapport à l'amas initial choisi dans la figure 1.8, tandis que la figure 1.10 illustre l'éventail obtenu à partir de ces vecteurs. En sus du théorème F, il a été prouvé que les **d**-vecteurs supportent un éventail simplicial complet réalisant le complexe d'amas en tous types pour l'*amas initial biparti* par S. Fomin et A. Zelevinsky [FZ03a], en tous types pour tout *amas initial acyclique* par S. Stella [Ste13], et pour tout amas initial en types A, B
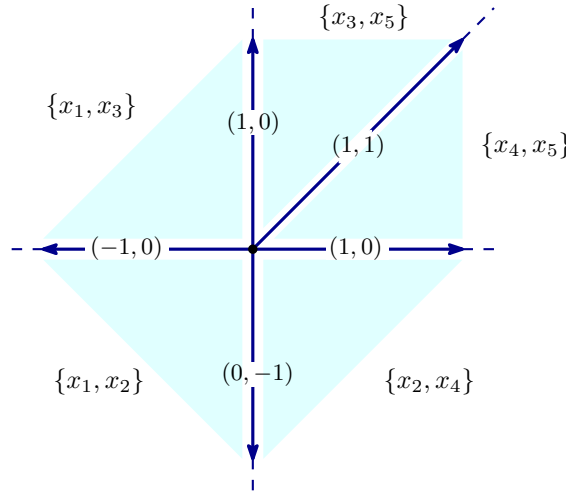
FIGURE 1.10 – L'éventail réalisant l'associaèdre de type A_2 obtenu à partir des **d**-vecteurs de la figure 1.9. On associe à chaque amas le cône engendré par les **d**-vecteurs de ses variables d'amas. Chaque rayon **r** de cet éventail est l'intersection de deux cônes correspondant à deux amas qui eux-mêmes s'intersectent en une variable, dont le **d**-vecteur engendre **r**.

et C dans le chapitre 6 de cette thèse. Nous nous attendons à ce que cette propriété soit vraie dans toute algèbre amassée de type fini.

Comme nous l'avons vu, la construction des **d**-vecteurs repose sur une notion de degré de compatibilité $(\,\|\,)$, qui satisfait des propriétés générales directement héritées de la structure des algèbres amassées.

Proposition G (corollaire immédiat de [FZ03b, section 3.5]). *Dans toute algèbre amassée de type A, B, C ou D, le degré de compatibilité satisfait les propriétés suivantes.*
1. *La fonction $(\,\|\,)$ est à valeurs entières et est définie sur les couples de variables d'amas de $\mathcal{A}$, autrement dit l'entrée $(x_i^\circ \,\|\, x)$ du **d**-vecteur d'une variable d'amas x par rapport à un amas initial $X^\circ = (x_1^\circ, \ldots, x_n^\circ)$ ne dépend que de x_i°, et non de tout l'amas X°. De façon équivalente, l'exposant de x_i° dans le dénominateur de x est toujours le même quand x est développée en les variables d'un amas initial contenant x_i°.*
2. *Pour toute variable d'amas x de $\mathcal{A}$, on a $(x \,\|\, x) = -1$ et $(x \,\|\, x') \geq 0$ pour toute variable d'amas x' de $\mathcal{A}$ différente de x.*
3. *Deux variables d'amas distinctes x et x' de $\mathcal{A}$ sont compatibles (appartiennent à un même amas) si et seulement si $(x \,\|\, x') = (x' \,\|\, x) = 0$.*
4. *Deux variables d'amas distinctes x et x' de $\mathcal{A}$ sont échangeables (sont échangées par une mutation) si et seulement si $(x \,\|\, x') = (x' \,\|\, x) = 1$.*

Remarque. Notre description du degré de compatibilité sur les diagonales d'un polygone et la proposition G impliquent qu'en type A, deux variables d'amas sont toujours soit compatibles, soit échangeables. Ce point est clair si l'on part de l'interprétation combinatoire des variables d'amas en termes de diagonales. En effet si deux diagonales δ, δ' d'un polygone $\mathcal{P}$ ne se croisent pas, alors elles appartiennent à une certaine triangulation de $\mathcal{P}$, et donc les variables d'amas correspondantes appartiennent à un amas commun. Si au contraire δ et δ' se croisent, alors leurs sommets définissent un quadrilatère Q dans $\mathcal{P}$, dont les quatre côtés (soit des diagonales internes, soit des côtés de $\mathcal{P}$) ne croisent ni δ, ni δ'. Ainsi une triangulation contenant ce quadrilatère contient nécessairement soit δ, soit δ', et flipper l'une introduit l'autre. Cela implique que des diagonales incompatibles sont échangeables.

Même si elle s'inscrit dans un contexte algébrique, la méthode des d-vecteurs a une interprétation combinatoire claire. En particulier lorsque nous traitons de généralisations combinatoires de l'associaèdre, nous essayons systématiquement de nous en inspirer pour construire des réalisations par éventails. Nous espérons bien sûr en tirer un moyen de passer de la combinatoire à la géométrie, mais aussi à de potentielles structures algébriques avec des propriétés analogues à celles des algèbres amassées. En d'autres termes cette approche par les d-vecteurs, même sans qu'il ne s'agisse plus de vecteurs dénominateur, est une stratégie générale dans notre quête de nouveaux triptyques combinatoire-géométrie-algèbre.

1.3   Contribution de cette thèse

En tant que cas particulier de familles plus larges, l'associaèdre admet naturellement de nombreuses généralisations, souvent définies en premier lieu combinatoirement.

Cette thèse propose des avancées dans la compréhension combinatoire et géométrique de trois familles de sphères simpliciales. En particulier nous appliquons avec succès la stratégie des d-vecteurs décrite précédemment, avec l'espoir que ses inspirations de nature algébrique puissent également aboutir à des progrès à ce niveau. Nous obtenons aussi d'autres propriétés combinatoires spécifiques à chaque famille, qui vont au-delà du strict nécessaire à l'implémentation de la méthode des d-vecteurs. Enfin nous donnons des réalisations par éventail supplémentaires, basées sur d'autres techniques.

1.3.1   Matériel de la thèse

Cette thèse s'appuie sur trois articles publiés ou acceptés pour publication :

[**Man17a**] Fan realizations for some 2-associahedra, Thibault Manneville, à paraître dans *Experiment. Math.*, 2017.

[**MP15**] Graph properties of graph associahedra, Thibault Manneville and Vincent Pilaud, *Sém Lothar. Combin.*, 73 :B73d, 2015.

[**MP17a**] Compatibility fans for graphical nested complexes, Thibault Manneville and Vincent Pilaud, *J. Combin. Theory Ser. A*, 150 : 36–107, 2017.

et deux prépublications :

[**Man17b**] The serpent nest conjecture on accordion complexes, Thibault Manneville, prépublication `arXiv:1704.01534`, 2017.

[**MP17b**] Geometric realizations of accordion complexes, Thibault Manneville and Vincent Pilaud, prépublication `arXiv:1703.09953`, 2017.

1.3.2   Plan et aperçu des résultats

Dans le chapitre 3, nous donnons les définitions et pré-requis sur les complexes simpliciaux et leurs liens avec la géométrie polyédrale nécessaires tout au long du manuscrit. Le reste de la thèse est séparé en deux parties indépendantes, que nous suivons pour présenter nos contributions principales. La partie II concerne une famille de complexes simpliciaux indexés par les graphes simples, et nous présentons dans la partie III des résultats sur deux familles que nous rassemblons pour des raisons expliquées alors. Les deux parties s'organisent selon le même schéma global :

1. un chapitre introductif (le chapitre 4, puis le chapitre 7 et les sections 8.1 et 8.2) dans lequel nous donnons des définitions et des éléments de contexte sur les complexes dont il est question ;
2. un chapitre traitant des aspects combinatoires spécifiques à ces complexes (des propriétés graphiques dans le chapitre 5 et des résultats énumératifs dans le chapitre 8) ;
3. un ou deux chapitres dédiés à des réalisations géométriques, par des éventails ou des polytopes. Deux d'entre elles étendent la construction des d-vecteurs (le chapitre 6 et la section 9.3), deux autres s'appuient sur des idées différentes (la section 9.2 et le chapitre 10).

Un appendice au chapitre 5 complète enfin les deux parties. Nous ne donnons ici que les idées nécessaires pour résumer nos résultats et gardons les présentations détaillées de chaque famille de complexes pour les chapitres correspondants.

1.3.2.1 Associaèdres de graphes et nestoèdres

Les *associaèdres de graphes* sont des complexes simpliciaux indexés par les graphes simples introduits par M. Carr et S. Devadoss [CD06]. Étant donné un graphe G, le *complexe emboîté* $\mathcal{N}(\mathrm{G})$ de G est le complexe simplicial dont les sommets sont les *tubes* (sous-graphes connexes) de G et dont les faces sont les *tubages* de G (les ensembles de tubes de G qui, deux à deux, soit sont emboîtés, soit n'ont pas de sommets adjacents dans G). M. Carr et S. Devadoss ont donné une réalisation polytopale pour chacun d'entre eux, retrouvée par la suite de différentes façons par plusieurs auteurs. L'associaèdre est un cas particulier de cette famille (obtenu quand G est un chemin). Nous présentons ces complexes en détail au chapitre 4.

Propriétés combinatoires. Dans le chapitre 5, nous étudions des propriétés graphiques des graphes duaux $\mathcal{F}(\mathrm{G})$ des complexes emboîtés $\mathcal{N}(\mathrm{G})$, avec des extensions aux complexes emboîtés plus généraux définis par A. Postnikov [Pos09]. Nos premiers résultats concernent des propriétés géodésiques de ces graphes, qui généralisent des faits déjà connus sur le graphe des flips $\mathcal{F}(n)$ défini dans la section 1.1.2. Notons $\delta(\mathcal{F}(\mathrm{G}))$ le diamètre du graphe $\mathcal{F}(\mathrm{G})$. Notre motivation initiale est la preuve récente de la valeur exacte du diamètre des associaèdres par L. Pournin [Pou14].

Théorème H ([STT88, Pou14]). *Le diamètre du graphe des flips $\mathcal{F}(n)$ est $2n-4$ pour $n \geq 9$.*

Notre premier résultat décrit un phénomène de structure relativement clair du point de vue géométrique, étant donné la construction proposée par M. Carr et S. Devadoss.

Théorème I (théorème 5.4, généralisé par le théorème 5.9). *Le diamètre $\delta(\mathcal{F}(.))$ est une fonction croissante, c'est-à-dire si $\mathrm{G} \subseteq \mathrm{G}'$, alors $\delta(\mathcal{F}(\mathrm{G})) \leq \delta(\mathcal{F}(\mathrm{G}'))$.*

Pour obtenir des bornes sur les diamètres des associaèdres de graphes, nous utilisons la *non-leaving-face property* **NLFP**. Un complexe simplicial a cette propriété si, dans tout chemin dual entre deux de ses facettes, les sommets communs à ces facettes ne disparaissent à aucun moment. L'associaèdre est un exemple de complexe satisfaisant cette propriété.

Théorème J ([STT88]). *Dans un plus court chemin de flips entre deux triangulations, aucune diagonale commune à ces triangulations n'est flippée.*

Les associaèdres de graphe ne satisfont pas tous **NLFP**. Nous donnons un contre-exemple dans la section 5.3.3. Toutefois nous obtenons le résultat plus faible suivant, où l'on considère tout tubage de G comme l'ordre d'inclusion sur ses tubes.

Proposition K (proposition 5.14 (i)). *Soit* T, T' *deux tubages maximaux sur* G *et* $\mathsf{T} = \mathsf{T}_0, \mathsf{T}_1, \ldots, \mathsf{T}_k = \mathsf{T}'$ *un plus court chemin dual dans* $\mathcal{N}(\mathrm{G})$ *entre* T *et* T'. *Tout tubage* T_i *(*$i \in [k]$*) contient le plus grand idéal supérieur commun à* T *et* T'.

À partir des théorèmes H et I, de la proposition K et d'arguments plus géométriques, nous obtenons les bornes, asymptotiquement exactes, suivantes sur le diamètre du graphe dual de tout associaèdre de graphe.

Théorème L (théorème 5.16). *Pour tout graphe* G *connexe avec* $n+1$ *sommets et* e *arêtes,*

$$\max(2n - 18, e) \le \delta(\mathcal{F}(\mathrm{G})) \le \binom{n+1}{2}.$$

Une part importante de nos preuves utilisent des « réductions combinatoires » qui ne sont pas toujours nécessaires mais simplifient la présentation. De plus le fait de bien comprendre ces réductions indique aussi que nous parvenons à isoler la complexité « réelle » des objets que nous manipulons. En particulier nous nous intéressons souvent à la façon dont les complexes simpliciaux peuvent se décomposer en *jointures* de complexes plus petits. Pour les associaèdres de graphes, et en fait pour n'importe quel complexe emboîté général, nous donnons une description complète des décompositions de ce type, qui implique en particulier que les associaèdres de graphes ont un comportement « rigide » à cet égard.

Théorème M (corollaire immédiat de la proposition 5.23). *Pour tout graphe* G, *le complexe emboîté* $\mathcal{N}(\mathrm{G})$ *se décompose en une jointure de complexes simpliciaux plus petits* $\mathcal{C}_1 * \cdots * \mathcal{C}_k$ *si et seulement si* G *a* k *composantes connexes* $\mathrm{G}_1, \ldots, \mathrm{G}_k$ *telles que* $\mathcal{C}_i$ *est isomorphe à* $\mathcal{N}(\mathrm{G}_i)$ *pour tout* $i \in [k]$.

Enfin nous montrons dans l'appendice A qu'essentiellement tous les associaèdres de graphes sont hamiltoniens. Ce résultat étend la même propriété déjà connue pour des sous-familles spécifiques des associaèdres de graphes, dont les associaèdres classiques.

Théorème N (théorèmes 5.1 et A.1). *Pour tout graphe* G *ayant au moins deux arêtes, le graphe* $\mathcal{F}(\mathrm{G})$ *est hamiltonien.*

Réalisations par éventails utilisant des d-vecteurs. Au niveau géométrique, nous décrivons au chapitre 6 l'extension suivante de la construction par les $\mathbf{d}$-vecteurs aux associaèdres de graphes.

Étant donné deux tubes t, t' d'un graphe simple G, on définit le *degré de compatibilité* $(\mathsf{t} \,\|\, \mathsf{t}')$ de t par rapport à t' comme étant $(\mathsf{t} \,\|\, \mathsf{t}') = -1$ si $\mathsf{t} = \mathsf{t}'$, $(\mathsf{t} \,\|\, \mathsf{t}') = 0$ si $\mathsf{t} \ne \mathsf{t}'$ sont *compatibles* (emboîtés ou d'union non connexe), et $(\mathsf{t} \,\|\, \mathsf{t}') = |\{\text{voisins de } \mathsf{t} \text{ dans } \mathsf{t}' \smallsetminus \mathsf{t}\}|$ sinon. Comme le degré de compatibilité dans les algèbres amassées (voir la proposition G), il satisfait $(\mathsf{t} \,\|\, \mathsf{t}') \ge 0$ pour tous tubes t, t' distincts de G, avec égalité si et seulement si t et t' sont compatibles, et $(\mathsf{t} \,\|\, \mathsf{t}') = 1 = (\mathsf{t}' \,\|\, \mathsf{t})$ si et seulement si t et t' sont échangeables. Comme dans la section 1.2.4, nous définissons le *vecteur de compatibilité* $\mathbf{d}(\mathsf{T}^\circ, \mathsf{t}) := [(\mathsf{t}_1^\circ \,\|\, \mathsf{t}), \ldots, (\mathsf{t}_n^\circ \,\|\, \mathsf{t})]$ d'un tube t par rapport à un tubage maximal initial $\mathsf{T}^\circ := \{\mathsf{t}_1^\circ, \ldots, \mathsf{t}_n^\circ\}$.

Remarquons que notre degré est asymétrique, ce qui induit une notion naturelle de dualité. On définit donc le *vecteur de compatibilité dual* $\mathbf{d}^*(\mathsf{t}, \mathsf{T}^\circ) := [(\mathsf{t} \,\|\, \mathsf{t}_1^\circ), \ldots, (\mathsf{t} \,\|\, \mathsf{t}_n^\circ)]$ de t par rapport T°. Pour distinguer clairement avec les vecteurs de compatibilité duaux, nous appelons souvent $\mathbf{d}(\mathsf{T}^\circ, \mathsf{t})$ le vecteur de compatibilité *primal*. Bien qu'il n'y ait plus de dénominateur dans ce contexte, nous gardons la lettre $\mathbf{d}$ pour degré et pour coller à la notation des algèbres amassées. En effet nos degrés de compatibilité pour les chemins et cycles coïncident avec ceux définis dans [FZ03b] pour les types A, B, et C. Les degrés de compatibilité entre variables d'amas de type A correspondent aux degrés

de compatibilité (primaux et duaux) sur les tubes des chemins, tandis que les degrés de compatibilité entre variables d'amas de type C (resp. B) correspondent aux degrés de compatibilité primaux (resp. duaux) entre les tubes des cycles.

Notre résultat principal est la réalisation par éventail de compatibilité suivante, analogue à celle de F. Santos dans [CSZ15, section 5].

Théorème O (théorèmes 6.10 et 6.14, étendus par le théorème 6.53). *Pour tout graphe* G, *les vecteurs de compatibilité primaux (resp. duaux) des tubes de* G *par rapport à tout tubage maximal initial* T° *sur* G *supportent un éventail simplicial complet* $\mathcal{D}(G, T^\circ)$ *réalisant le complexe emboîté* $\mathcal{N}(G)$ *de* G.

Nous étudions également le nombre d'éventails de compatibilité distincts que nous obtenons. Suivant [CSZ15], nous considérons comme équivalents deux éventails de compatibilité $\mathcal{D}(G, T^\circ)$ et $\mathcal{D}(G', T'^\circ)$ si un isomorphisme linéaire envoie l'un sur l'autre (voir la section 3.2.2). Un tel isomorphisme linéaire induit un isomorphisme entre les complexes emboîtés de G et G'. En plus de ceux induits par les isomorphismes de graphes entre G et G', nous montrons dans la section 6.4.2 un isomorphisme de complexes emboîtés non trivial sur toute *araignée* (ensemble de chemins tous reliés par une extrémité à une même clique). Nous montrons que cet isomorphisme est essentiellement le seul isomorphisme non trivial entre des complexes emboîtés de graphes.

Théorème P (théorème 6.37). *Tous les isomorphismes de complexes emboîtés sont induits par des isomorphismes de graphes* $G \to G'$, *sauf si l'une des composantes connexes de* G *est une araignée.*

Corollaire Q (corollaire 6.40 étendu par le corollaire 6.41). *Si aucune composante connexe de* G *n'est un chemin, alors le nombre de classes d'isomorphisme linéaires des éventails de compatibilité de* G *est le nombre d'orbites des tubages maximaux de* G *sous l'action du groupe d'automorphisme de* G.

L'étape suivante serait de montrer que tous ces éventails simpliciaux sont les éventails normaux de polytopes. Cette question reste ouverte, sauf pour quelques graphes particuliers : en plus des graphes à au plus 4 sommets, nous résolvons le cas des chemins et des cycles, avec une preuve similaire à celle proposée dans [CSZ15].

Théorème R (théorème 6.46). *Tous les éventails de compatibilité primaux et duaux des chemins et des cycles sont polytopaux. En particulier, la construction par les* $\mathbf{d}$-*vecteurs donne bien une réalisation polytopale du complexe amassé pour toute graine initiale en types* A, B *et* C.

1.3.2.2 Complexes de sous-mots et complexes d'accordéons

Comme nous l'expliquons au chapitre 7, nous nous intéressons avant tout aux *complexes de sous-mots* [KM04]. Notre étude des complexes d'accordéons est motivée par des liens intrigants que nous développons dans la section 8.4. Il se trouve malgré cela que nous obtenons finalement plus de résultats sur les complexes d'accordéons (chapitres 8 et 9) que sur les complexes de sous-mots (chapitre 10).

Étant donné une dissection D d'un polygone convexe $\mathcal{P}$, on définit le *complexe d'accordéons* $\mathcal{AC}(D)$ de D comme le complexe simplicial dont les faces sont les dissections de $\mathcal{P}$ contenant uniquement certaines diagonales autorisées par D, appelées les *diagonales* D-*accordéon*. De façon informelle, ces diagonales sont celles qui croisent un ensemble connexe de diagonales (où l'on inclut les côtés de $\mathcal{P}$) de D, lorsque celle-ci est tournée d'un très petit angle puis superposée sur $\mathcal{P}$. Nous présentons en détail les complexes d'accordéons dans les sections 8.1 et 8.2.

Propriétés combinatoires des complexes d'accordéons.   Dans son article [Cha16],
F. Chapoton propose trois problèmes, qui incluent la réalisation des complexes d'accor-
déons par des polytopes (que nous abordons au paragraphe suivant) et des questions
énumératives. La principale d'entre elles concerne l'existence d'une bijection entre les
facettes du complexe d'accordéons $\mathcal{AC}(\mathrm{Q})$ d'une quadrangulation Q et des objets appe-
lés *nids de serpents* de Q. Cette question se généralise naturellement à n'importe quelle
dissection, en utilisant la définition de *nids de serpents propre* comme des ensembles
de chemins duaux dans l'arbre dual de D qui ne croisent aucune cellule de D par des
diagonales non incidentes et de sorte que, deux à deux, ils ne terminent pas dans une
même cellule en y entrant par le même côté. Les nids de serpents sont alors définis
comme les classes d'équivalence des nids de serpents propres qui induisent le même
schéma local au voisinage de chaque diagonale de D. Nous exhibons une bijection, ba-
sée sur des décompositions « à la Catalan » des dissections D-accordéon maximales,
répondant ainsi par l'affirmative à la question de F. Chapoton.

Théorème S (théorème 8.15). *Pour toute dissection* D*, il y a autant de facettes dans le
complexe d'accordéons* $\mathcal{AC}(\mathrm{D})$ *que de nids de serpents de* D*.*

Pour prouver le théorème S, nous décrivons les *coques* dans les complexes d'ac-
cordéons et obtenons par là même une description des décompositions en jointures
analogue au théorème M.

Proposition T (proposition 8.6). *Étant donné une dissection* D*, le complexe d'accor-
déons* $\mathcal{AC}(\mathrm{D})$ *se décompose en jointure de complexes simpliciaux plus petits si et seule-
ment si* D *contient un* pont *(cellule avec au moins* 2 *côtés de* $\mathcal{P}$ *non consécutifs). Les termes
de la décomposition de* $\mathcal{AC}(\mathrm{D})$ *sont alors eux-mêmes des complexes d'accordéons.*

F. Chapoton définit aussi le F-triangle d'une quadrangulation Q dans [Cha16], dont
la définition s'étend aussi à des dissections arbitraires. Ce triangle de nombres est un
raffinement du f-*vecteur* du complexe d'accordéons $\mathcal{AC}(\mathrm{D})$. À savoir le terme indicé
par deux entiers k et r dans le F-triangle d'une dissection D est le nombre de dissec-
tions D-accordéon avec k diagonales parmi lesquelles exactement r appartiennent à D.
F. Chapoton conjecture que l'opération de *twist* sur les dissections, qui consiste à appli-
quer une symétrie axiale à l'une des parties obtenues en coupant une dissection le long
d'une de ses diagonales avant de la recoller à l'autre partie, préserve cette statistique.
Nous démontrons cette conjecture.

Théorème U (théorème 8.19). *Si une dissection* D' *est obtenue à partir d'une dissection* D
par une opération de twist, alors les F*-triangles de* D *et de* D' *sont égaux.*

Réalisations des complexes d'accordéons par des éventails et des polytopes.   Dans
le chapitre 9, nous donnons des réalisations géométriques des complexes d'accor-
déons $\mathcal{AC}(\mathrm{D})$ en adaptant les méthodes classiques des algèbres amassées, dont la
construction par les $\mathbf{d}$-vecteurs. En reprenant la même interprétation du degré de com-
patibilité entre les diagonales en type A, nous produisons des réalisations par éven-
tails, qui étendent la construction de l'associaèdre par les $\mathbf{d}$-vecteurs (quand D est une
triangulation). Pour cela nous définissons le *degré de compatibilité* entre deux diago-
nales D-accordéon δ et δ' comme la quantité $(\delta \,\|\, \delta') = -1$ si $\delta = \delta'$, $(\delta \,\|\, \delta') = 0$ si δ
et δ' ne se croisent pas et $(\delta \,\|\, \delta') = 1$ sinon. Avec ce degré on définit une fois de plus
des $\mathbf{d}$-vecteurs, pour lesquels nous obtenons le résultat suivant.

Théorème V (théorème 9.33). *À part si* D *contient une cellule intérieure paire, les* $\mathbf{d}$*-
vecteurs des diagonales* D*-accordéon par rapport à la facette particulière* D *du complexe
d'accordéons* $\mathcal{AC}(\mathrm{D})$ *supportent un éventail simplicial complet* $\mathcal{F}^{\mathbf{d}}(\mathrm{D})$ *réalisant* $\mathcal{AC}(\mathrm{D})$*.*

En plus de ce résultat, nous donnons un contre-exemple pour toute dissection de référence D contenant une cellule intérieure paire. Le théorème V ne fournit pas une réalisation pour chaque facette du complexe $\mathcal{AC}(D)$, mais nous suspectons cette propriété pour les dissections dont il est question. Nous adaptons également la construction des associaèdres généralisés par les g-vecteurs au contexte des complexes d'accordéons, ce qui nous permet de trouver des réalisations comme éventails de tous les complexes d'accordéons, sans restriction. Une fois de plus, nous n'obtenons pas une réalisation pour chaque facette du complexe mais nous montrons que notre second éventail est polytopal, répondant ainsi positivement à la question géométrique de F. Chapoton [Cha16].

Théorème W (théorème 9.19). *Pour toute dissection* D*, il existe un polytope simple réalisant le complexe d'accordéons* $\mathcal{AC}(D)$*. On appelle ce polytope l'*accordéoèdre *de* D *et on le note* $\mathsf{Acco}(D)$*.*

Les polytopes du théorème W sont obtenus en oubliant les inégalités définissant un certain *zonotope* défini à partir de vecteurs analogues aux c-*vecteurs* des algèbres amassées. Après nos résultats géométriques, nous donnons une interprétation combinatoire de ces c-vecteurs. En utilisant le fait que les complexes d'accordéons sont des sous-complexes des associaèdres, nous utilisons la cohérence des signes de g-vecteurs pour obtenir une construction purement géométrique des *accordéoèdres*.

Théorème X (théorème 9.40). *Si une dissection* D *de* $\mathcal{P}$ *est contenue dans une autre dissection* D′ *de* $\mathcal{P}$*, alors on peut obtenir un polytope réalisant le complexe d'accordéons* $\mathcal{AC}(D)$ *en projetant l'accordéoèdre* $\mathsf{Acco}(D')$ *sur un sous-espace de coordonnées. En particulier tout complexe d'accordéons peut être réalisé en projetant un associaèdre classique obtenu par la construction des* g-*vecteurs.*

Notre construction par les g-vecteurs garde une mémoire des symétries de la dissection de référence D, nous permettant de décrire des objets de type B/C. Même si D peut avoir de nombreuses symétries, on ne peut plonger que les types B/C, ce qui est courant sur ce genre de structures.

Théorème Y (proposition 9.28). *Pour toute dissection centralement symétrique* D*, il existe un polytope simple réalisant le complexe des dissections* D-*accordéon centralement symétriques.*

Réalisations par éventails de certains complexes de sous-mots. Comme nous n'avons pas besoin de la définition des complexes de sous-mots pour décrire notre dernier résultat, nous renvoyons le lecteur au chapitre 7. L'important ici est que l'on conjecture depuis une dizaine d'années que ces complexes ont des réalisations polytopales, et que très peu de progrès en ce sens ont été faits depuis leur apparition. Dans le chapitre 10, nous décrivons des réalisations par éventails de certains complexes de sous-mots et donnons des candidats pour la famille des 2-*associaèdres*. Cette famille se décrit de la façon suivante. Étant donné des entiers n et k, le k-*associaèdre* simplicial $\mathbf{\Delta}_{k,n}$ est le complexe simplicial dont les faces sont les k-*dissections* d'un $n + 2k + 1$-gone $\mathcal{P}$, c'est-à-dire les ensembles de diagonales de $\mathcal{P}$ dans lesquels il n'existe pas $k + 1$ diagonales se croisant deux à deux. Ces complexes forment une *famille universelle* parmi les complexes de sous-mots, ce qui signifie que leur trouver des réalisations géométriques revient à trouver des réalisations géométriques pour tous les complexes de sous-mots de type A. Le chapitre 10 décrit une tentative en vue d'obtenir de telles réalisations, basée sur des mouvements combinatoires locaux à l'intérieur des complexes de sous-mots. Nous obtenons des éventails réalisant des 2-associaèdres jamais réalisés auparavant.

Théorème Z (théorème 10.2). *Tous les* 2-*associaèdres* $\mathbf{\Delta}_{2,n}$ *pour* $n \in [8]$ *ont des réalisations par éventails.*

Le théorème Z est un résultat purement expérimental vérifié par ordinateur. Les rayons utilisés pour construire nos éventails sont décrits par un schéma de coordonnées pour tout $n \in \mathbb{N}$, qui pourrait tout à fait s'avérer valide pour tous les 2-associaèdres. Nous avons deviné ce schéma après des étapes heuristiques successives, la dernière faisant intervenir un aléa visant à perturber avantageusement des rayons candidats dégénérés. Les autres étapes correspondent à la traduction intuitive de transformations combinatoires sur les complexes de sous-mots qui induisent, entre autres choses, des *subdivisions stellaires* (voir la section 3.1) et *subdivisions stellaires inverses* d'arêtes. Dans notre travail, ces opérations apparaissent véritablement comme des outils uniquement dans ce dernier chapitre 10. Cependant nous les avons rencontrées dans tous les contextes que nous avons mentionnés.

1.3.3   Subdivisions stellaires d'arêtes

Même si nous ne prouvons pas de résultat spécial en utilisant les subdivisions stellaires, cette thèse suggère de regarder plus avant la classe des complexes simpliciaux pouvant être obtenus par des suites de jointures et de subdivisions stellaires d'arêtes, à partir de bords de 1-simplexes. Ces complexes sont entre autres des *complexes de cliques*, réalisables par des polytopes (voir lemme 10.4) dont les *duaux polaires* sont généralement appelés *cubes 2-tronqués*. Comme nous l'expliquons dans la section 3.2.3, être un complexe de cliques est une propriété nécessaire pour envisager une construction s'appuyant sur de notre stratégie des d-vecteurs. La classe des cubes 2-tronqués inclut les associaèdres de graphes, et conjecturalement les complexes de sous-mots de type A qui sont en plus des complexes de cliques. Elle a déjà été étudiée dans des travaux sur les complexes de cliques en général [LN16] ou en topologie torique [BP15, sections 1.5 et 1.6] par exemple. Tout au long de cette thèse, nous avons essayé de définir des opérations combinatoires sur les différentes structures sous-jacentes aux complexes que nous étudiions, ayant pour effets topologiques des subdivisions stellaires. Comme nous l'avons dit, ce genre de transformation existe déjà dans les complexes de sous-mots [Gor14]. Nous mentionnons en section 8.4 deux transformations relativement naturelles sur certaines dissections, qui induisent des subdivisions stellaires d'arêtes sur leurs complexes d'accordéons. Pour le moment notre intérêt pour ces opérations tient surtout au potentiel cadre unificateur qu'elles pourraient nous fournir. Nous les mentionnons comme l'une des perspectives ouvertes par cette thèse.

This thesis from A to Z

2.1 Presentation of the associahedron

Associahedra relevantly appear in multiple mathematical areas. Their study, so as this of their many generalizations, is therefore a field of research by itself, at the interface between combinatorics, geometry and algebra. This thesis focuses on the first two aspects, with inspirations from the third one. We begin with some motivations based on several mathematical interpretations of associahedra.

2.1.1 Binary trees and rotation graph

Associahedra are natural objects to describe the behavior of data structures called *binary search trees* (see for instance [Knu98, Section 6.2] for a detailed presentation and algorithmic motivations).

Given a set S, a *binary tree* T on S is a structure recursively defined as follows:
- either $\mathrm{T} = \varnothing$ is the empty tree, with no *node*,
- or T is a triple $(\mathrm{L}, r, \mathrm{R})$, where $r \in S$ is the *root* of T, whose *left* (resp. *right*) *child* L (resp. R) is itself a binary tree on S. The *nodes* of T are r and the nodes of L and R.

The usual notation for a binary tree $\mathrm{T} = (\mathrm{L}, r, \mathrm{R})$ on S is

$$\mathrm{T} = \underset{\mathrm{L} \quad \mathrm{R}}{\overset{r}{\diagup \diagdown}} \, .$$

When S is unspecified, we generically denote nodes by $\bullet$. Figure 2.1 (left) represents all binary trees with 3 nodes. The *height* $h(\mathrm{T})$ of a binary tree T is recursively defined by

$$h(\varnothing) = -1 \qquad \text{and} \qquad h\left(\underset{\mathrm{L} \quad \mathrm{R}}{\overset{\bullet}{\diagup \diagdown}} \right) = \max(h(\mathrm{L}), h(\mathrm{R})) + 1.$$

When the nodes of a binary tree T are integers such that any node is greater (resp. smaller) than all nodes of its left (resp. right) child, the tree T is called a *binary search tree*. This property indeed allows efficient search and insertion operations in binary trees that are *balanced*, that is in which the difference of height between the two children of any node is at most 1. In order to keep binary search trees balanced while
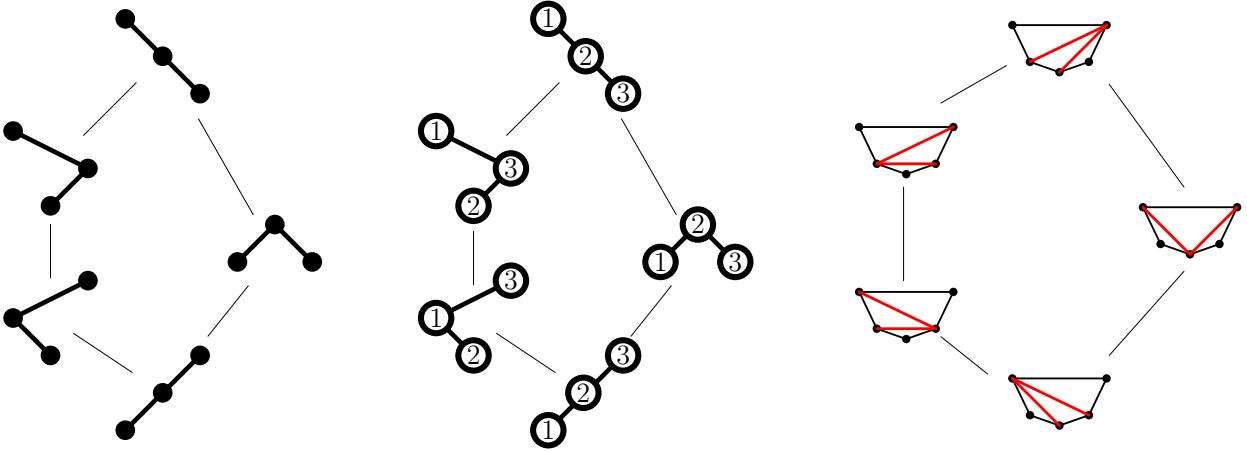
Figure 2.1 – All binary trees with 3 nodes (left, with $\mathrm{T}^2_{\max}$ at the top), all binary search trees with three nodes in $\{1, 2, 3\}$ (middle) and all triangulations of a hexagon (right). Lines between binary (search) trees (resp. triangulations), oriented upwards, correspond to right rotations (resp. slope increasing flips), so that each picture is a combinatorial representation of the Tamari lattice $\mathcal{T}(3)$. Without the orientation, they also represent the rotation (resp. flip) graph $\mathcal{F}(2)$, that is a cycle with 5 vertices.

manipulating them (for instance inserting or deleting elements), balancing algorithms use the *right* (resp. *left*) *rotation* operation ρ_r (resp. ρ_ℓ), defined as follows.

$$\rho_r \left(\begin{matrix} & & x_2 \\ & x_1 & \ \ \mathrm{T}_3 \\ \mathrm{T}_1 & \ \mathrm{T}_2 \end{matrix} \right) := \begin{matrix} x_1 \\ \mathrm{T}_1 \ \ \ x_2 \\ \ \ \ \mathrm{T}_2 \ \ \mathrm{T}_3 \end{matrix} \qquad \text{and} \qquad \rho_\ell \left(\begin{matrix} x_1 \\ \mathrm{T}_1 \ \ \ x_2 \\ \ \ \ \mathrm{T}_2 \ \ \mathrm{T}_3 \end{matrix} \right) := \begin{matrix} & & x_2 \\ & x_1 & \ \ \mathrm{T}_3 \\ \mathrm{T}_1 & \ \mathrm{T}_2 \end{matrix} \ .$$

Moreover, the recursive definition of binary trees naturally induces a right (resp. left) rotation at each node with nonempty right (resp. left) child in any binary tree. Figure 2.1 (left and middle) illustrates these operations. From them one can define the *rotation graph* $\mathcal{F}(n)$ whose vertices are binary trees with $(n+1)$ nodes and whose edges connect two binary trees related by a rotation (see Figure 2.1 left and middle). This graph is the first object that can be called an *associahedron*. For the previous reasons, numerous studies focused on geodesic properties of the graph $\mathcal{F}(n)$. First it is connected. Indeed, in a binary tree, one can apply a right rotation to any node with nonempty left child. As there is only one binary tree $\mathrm{T}^n_{\max}$ all of whose nodes have empty left children (see the top tree in Figure 2.1 left), any two binary trees are reachable from each other by successively applying a sequence of right rotations and a sequence of left rotations. This analysis can be refined to derive the upper bound $2n$ for the diameter of $\mathcal{F}(n)$. For this recursively define the *right branch* of a binary tree T as the empty tree if $\mathrm{T} = \varnothing$ and as the tree formed by its root and the right branch of its right child otherwise. Now remark that if a binary tree T is different from $\mathrm{T}^n_{\max}$, then it is not only possible to apply a right rotation to T, but such rotation can moreover be done at a node on the right branch of T, so that the new tree obtained from T has one node more on its right branch. Any binary tree can thus be transformed into $\mathrm{T}^n_{\max}$ in at most n right rotations, which proves the bound $2n$ for the diameter of $\mathcal{F}(n)$. Contrarily to upper bounds, giving precise evaluations for the distances in $\mathcal{F}(n)$ is very challenging, and if the hard question of finding the exact diameter of $\mathcal{F}(n)$ was recently settled [STT88, Pou14], it remains an open problem to efficiently compute the rotation distance between any two binary trees. Finally a last computer science purpose linked to associahedra is to look for potential new data structures, inspired from binary trees (as *Cambrian trees* [CP17] for instance).

2.1.2 Triangulations and flip graphs

The number of binary trees with n nodes is the n-th *Catalan number* $C_n := \frac{1}{n+1}\binom{2n}{n}$ [OEI10, A000108]. These numbers are ubiquitous in combinatorics and count many other objects[1] (see for instance [Sta01, Chapter 6]). The *triangulations* of convex polygons are such a Catalan family, and are in practice the main combinatorial model used to deal with associahedra. Given a convex polygon $\mathcal{P}$ with $n+3$ vertices, a *triangulation* of $\mathcal{P}$ is an inclusion maximal set of pairwise noncrossing diagonals of $\mathcal{P}$ (see Figure 2.2 left). The name comes from the fact that a triangulation of $\mathcal{P}$ can equivalently be though of as a subdivision of $\mathcal{P}$ into triangles without creating any new vertex. Notice that the formal definition does not rely on the geometry of $\mathcal{P}$ since crossings between diagonals have a combinatorial translation in term of cyclic order on their vertices. Therefore, we generally represent $\mathcal{P}$ either as a regular polygon or in the configuration of Figure 2.2, that is with a long horizontal boundary edge and a convex chain under it. In this last configuration, taking the *dual tree* of a triangulation provides a simple bijection between triangulations of $\mathcal{P}$ and binary trees with $n+1$ nodes, as illustrated in Figure 2.2. This bijection moreover induces a correspondence between rotations on binary tree and the natural *flip* operations on triangulation. Consider a triangulation T and a diagonal $\delta \in$ T. Removing δ from T creates a quadrilateral in T, which has exactly two diagonals, namely δ and another one δ'. On can then replace δ by δ' to obtain a new triangulation $T' := (T \cup \{\delta'\}) \setminus \{\delta\}$ (see Figure 2.2 right). We say that T' is obtained from T by *flipping* δ. Under the bijection of Figure 2.2, right (resp. left) rotations correspond to *slope increasing* (resp. *decreasing*) *flips*, that is where the introduced diagonal has a greater (resp. smaller) slope than the removed one. The *flip graph* of $\mathcal{P}$ is the graph whose vertices are the triangulations of $\mathcal{P}$ and whose edges correspond to flips between them. This graph is isomorphic to the graph $\mathcal{F}(n)$ on binary trees (see Figure 2.2 right) and so is also a combinatorial model for the associahedron.

At the combinatorial level, the associahedron has the interesting following property. The edges of the flip graph $\mathcal{F}(n)$ can be oriented in the directions given by slope increasing flips (or equivalently right rotations for binary trees), namely if a diagonal δ of a triangulation T is flipped into a diagonal δ' of greater slope, then the edge of $\mathcal{F}(n)$ between the triangulations T and $T' = T \cup \{\delta'\} \setminus \{\delta\}$ is oriented from T to T'. The resulting directed graph is acyclic, and it is in fact the Hasse diagram of a *lattice*, called the *Tamari lattice* $\mathcal{T}(n+1)$ (see [Tam51] and Figure 2.1), at the center of many studies and also generalized in several directions. Moreover, apart from being a relevant Catalan family, triangulations of convex polygons are also the very first example of triangulations
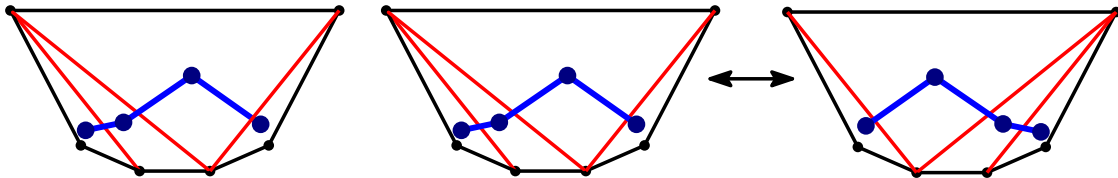
Figure 2.2 – A bijection between binary trees with $n+1$ nodes (in blue) and triangulations of a $(n+3)$-gon (in red), illustrated for $n = 3$ (left). When the polygon $\mathcal{P}$ is drawn in this configuration, with a long horizontal boundary edge e, the binary tree associated to a triangulation is just the dual tree of this triangulation, rooted at the triangle containing e. This bijection makes right (resp. left) rotations on binary trees correspond to slope increasing (resp. decreasing) flips on triangulations (right).

---

[1]According to R. Stanley, there are currently 207 different combinatorial interpretations for them.
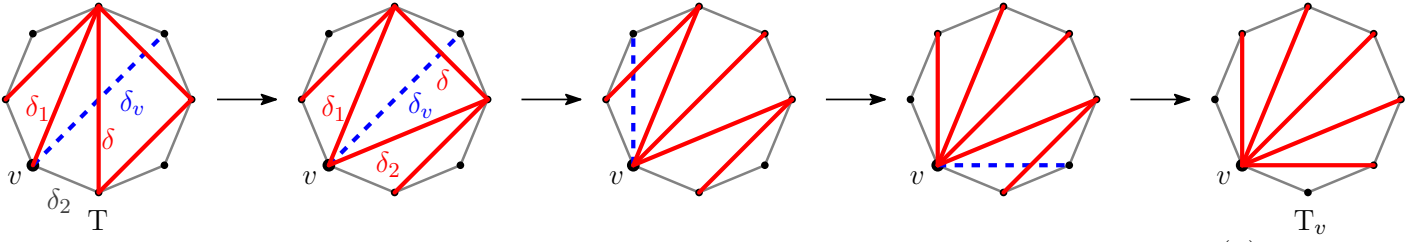
Figure 2.3 – Illustration of the proof of the upper bound $2n - 4$ on the diameter of $\mathcal{F}(n)$.

of points configurations in the plane (see [DRS10] and references therein), explaining why the focus naturally comes to them. Finally triangulations are a convenient complementary model in addition to binary trees for studying the associahedron. To illustrate that, let us refine the bound $2n$ on the diameter of $\mathcal{F}(n)$ proved in Section 2.1.1 to $2n-4$ for $n \geq 10$ (see Figure 2.3 for an illustration of this proof), which is in fact the exact value of the diameter of the flip graph $\mathcal{F}(n)$ in this case [Pou14].

Proof (upper bound $2n - 4$ on the diameter of $\mathcal{F}(n)$). Consider an $(n + 3)$-gon $\mathcal{P}$, a vertex v of $\mathcal{P}$ and let T_v be the triangulation of $\mathcal{P}$ consisting of the n diagonals of $\mathcal{P}$ incident to v. Let T be a triangulation of $\mathcal{P}$ that does not contain a diagonal δ_v incident to v. Then δ_v lies between two consecutive diagonals (either *internal diagonals* or boundary edges) of T incident to v, that we denote δ_1 and δ_2. These diagonals belong to a common triangle of T, whose third diagonal we denote δ. As δ_1 and δ_2 are not consecutive in T_v, the diagonal δ is internal and can therefore be flipped in T, to obtain a new diagonal, which is incident to v. A straightforward induction thus shows that if T contains $\deg_v(\mathrm{T})$ diagonals incident to v, then it can be transformed into T_v in $n - \deg_v(\mathrm{T})$ flips. In particular the flip distance between T and any other triangulation T' is at most $2n - (\deg_v(\mathrm{T}) + \deg_v(\mathrm{T}'))$. Finally observe that the diagonals in $\mathrm{T} \cup \mathrm{T}'$ (with repetitions) have in total $4n$ extremities (with repetitions). So in average a vertex of $\mathcal{P}$ is incident to $\frac{4n}{n+3} = 4 - \frac{12}{n+3}$ diagonals of $\mathrm{T} \cup \mathrm{T}'$. In particular if $n \geq 10$, this average value is strictly greater than 3, and there is a vertex v of $\mathcal{P}$ for which $\deg_v(\mathrm{T}) + \deg_v(\mathrm{T}') \geq 4$. ∎

2.1.3 Polytopes

For the geometric part of this thesis, we are primarily interested in *polytopes*. We recall that a *polytope* is the convex hull of finitely many points in $\mathbb{R}^d$ (see Chapter 3, in particular Section 3.2.1 for more details). Among other things, polytopes are bounded *polyhedra*, that are the feasibility domains of linear optimization problems (see [GM07]). In particular a whole field of research on polytopes concerns their combinatorial diameter, in relation with the so called polynomial Hirsch conjecture, asserting that the diameter of the graph of a polytope is polynomial in its number of facets (see [San13] for a rich survey on these topics). Yet dealing with the combinatorics of polytope is hard in general, and it is valuable to have families of examples whose combinatorial structure is easily described. A very classical polytope in this spirit is the *n-dimensional permutahedron* Perm(n) (or *n-permutahedron*), defined as the convex hull of all the permutations of $[n + 1] := \{1, 2, \ldots, n + 1\}$ seen as vectors in $\mathbb{R}^{n+1}$ (see Figure 2.4). Formally if we denote by $\mathfrak{S}_{n+1}$ the symmetric group of permutations of $[n + 1]$, we have

$$\mathsf{Perm}(n) := \mathrm{conv}\left((\sigma(i))_{i \in [n+1]} \mid \sigma \in \mathfrak{S}_{n+1}\right).$$

Associahedra are another instance of such polytopes. Indeed, if we previously described associahedra with the combinatorial data of flip (or rotation) graphs, the term *associahedron* more usually refers to the corresponding polytope.

Theorem A ([Hai84, Lee89, GKZ08, BFS90, SS93, SS97, RSS03, Lod04, HL07, CSZ15])**.** *For any integer n, there exists an n-dimensional polytope whose graph is isomorphic to the flip graph $\mathcal{F}(n)$. Such a polytope is called an n-associahedron.*
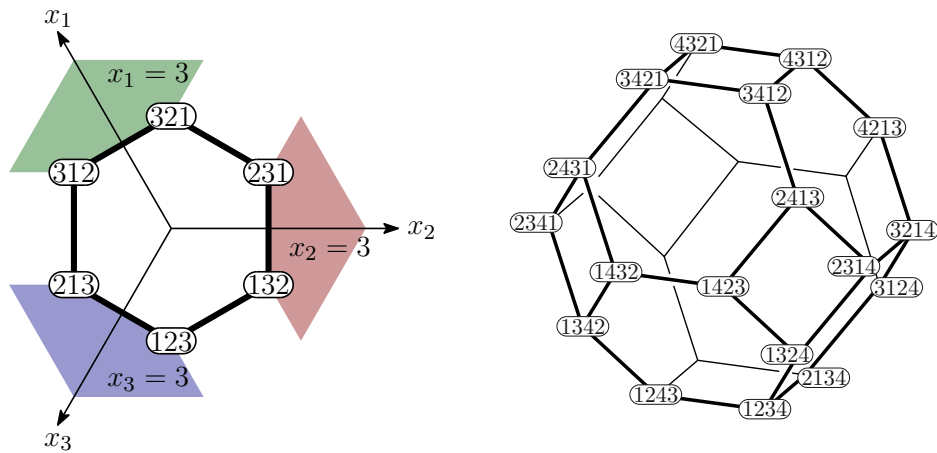
Figure 2.4 – The 2-permutahedron embedded in $\mathbb{R}^3$ (left) and the 3-permutahedron (right).

We discuss some proofs of Theorem A in Section 2.2.2. Figures 2.5 and 2.6 illustrate some realizations by different authors for the 3-associahedron. As we explained, having polytopes described by flip graphs is convenient for geometric purposes. In turn the geometry of such polytopes can sometimes provide us with combinatorial results that are hard to prove directly. For instance D. Sleator, R. Tarjan and W. Thurston [STT88] used arguments of hyperbolic polytopes in their attempt to determine the combinatorial diameter of associahedra. A more recent example of this fact is Section 9.4 of this thesis, where some properties of *accordion complexes* are derived directly from their *polytopal realizations*. This notion of "realization" is the reason why we jointly study combinatorial and geometric properties. Informally, a geometric realization of a combinatorial structure S is any object in a vector space that is fully describable by a finite information encoded by S. In some sense it is a way to faithfully embed an abstract structure in a geometric setting. Theorem A illustrates the realization of a graph by a polytope but they are not the only kind of objects we are interested in. In this thesis, we are indeed more concerned with realizing *simplicial complexes* (which in fact is also the case in Theorem A). Moreover the realizations that we give are mainly *fan realizations*, that is we encode simplicial complexes by sets of cones intersecting properly. The main goal of this thesis can thus be summed up as follows.

Goal: on the one hand we try to provide a better understanding of some abstract relatives of the associahedron; on the other hand we work with them into obtaining new constructions of rich and relevant instances of polytopes and fans.

We keep the formal presentation of simplicial complexes, fans and polytopes for Chapter 3, where we give the general preliminaries needed along the manuscript, and now go to the description of the mathematical context in which our work takes place.

[Lod04, HL07]   [HL07]   [CFZ02, HL07, CSZ15]   [CSZ15]
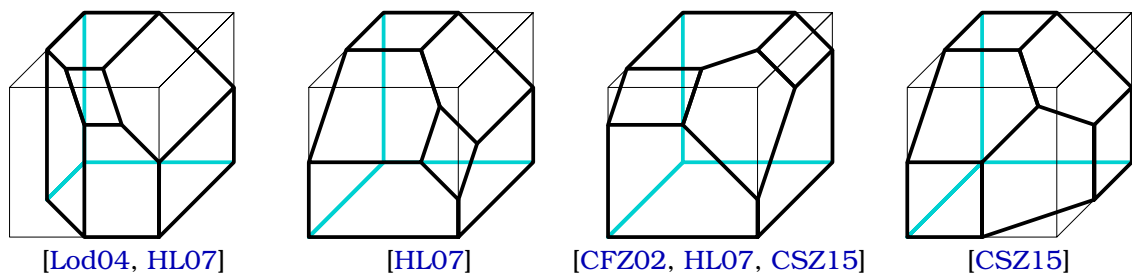
Figure 2.5 – Examples of 3-associahedra. Figure from [CSZ15], with permission.

2.2 State of the art

The combinatorial structure of the associahedron first appeared as the Tamari lattice (see Section 2.1.2) in early work of D. Tamari [Tam51]. It was then studied as a simplicial complex (see Section 3.1) by J. Stasheff [Sta63], in order to study homotopy properties of H-spaces, in connection with associativity theories. At the geometric level, the first realizations of the associahedron as a convex polytope are due to M. Haiman [Hai84] and C. Lee [Lee89]. As we previously mentioned, the associahedron motivated a flourishing trend of research in various fields, that can more or less be distributed between "combinatorics", "geometry" and "algebra". We first present a few remarkable properties of the associahedron in each world and describe some connections before detailing the **d**-vector construction, which is at the heart of this thesis.

2.2.1 Combinatorics

As we pointed out in Section 2.1.2, binary trees and triangulations are relevant in Catalan combinatorics and encode the Tamari lattice $\mathcal{T}(n+1)$. The algebraic and combinatorial properties of the latter was extensively studied and generalized. One of the reasons is its deep connection with the *weak order* on permutations. We recall that $\mathfrak{S}_{n+1}$ is the symmetric group of permutations of $[n+1]$. The *inversion set* $\mathrm{inv}(\sigma)$ of a permutation $\sigma \in \mathfrak{S}_{n+1}$ is the set of pairs (i,j) satisfying $i < j$ and $\sigma(j) < \sigma(i)$. The *weak order* is the order relation $\preccurlyeq$ on permutations defined by

$$\forall \, \sigma, \sigma' \in \mathfrak{S}_{n+1}, \ \sigma \preccurlyeq \sigma' \Longleftrightarrow \mathrm{inv}(\sigma) \subseteq \mathrm{inv}(\sigma').$$

This order on permutations is a lattice with many combinatorial properties. For instance its maximal chains encode the minimal factorizations of the permutation $[n+1,\ldots,1]$ into products of simple transpositions. In [BW97, Section 9] A. Björner and M. Wachs observed that restricting the weak order to (132)-avoiding permutations yields a *sublattice* of the weak order, that is isomorphic to the Tamari lattice. N. Reading [Rea06] extended the Tamari lattice to *Cambrian lattices* and moreover showed that they were *quotient lattices* of the weak order. A (type A) Cambrian lattice can be described by a sequence of $n+1$ signs $\varepsilon \in \{+,-\}^{n+1}$ (called a *signature*) as follows. The signature ε determines a *Cambrian polygon* $\mathcal{P}_\varepsilon$ obtained by drawing two vertices labeled 0 and $n+2$ on the horizontal axis and then draw the other vertices in abscissa
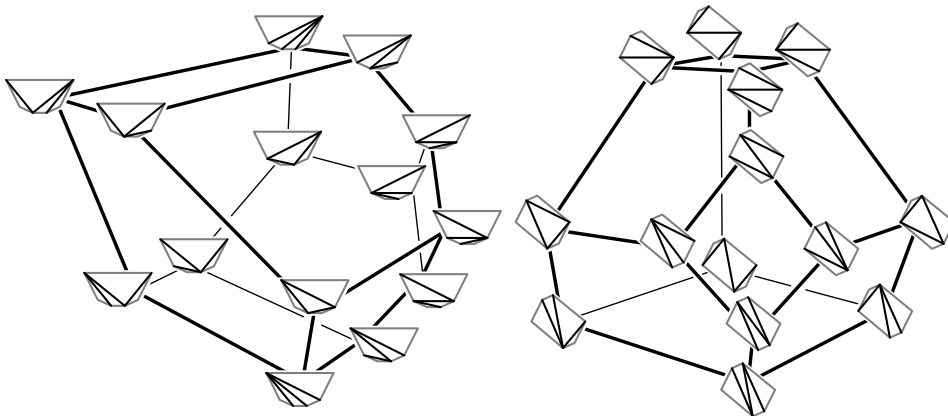
Figure 2.6 – Two 3-associahedra by C. Hohlweg and C. Lange [HL07] (see also Figure 2.5 left and middle left). The corresponding Cambrian lattices are obtained by orienting them from bottom to top. The left one is initially due to S. Shnider and S. Sternberg [SS93, SS97] and J.-L. Loday [Lod04]. Figure from [LP13], with permission.

increasing order between 0 and $n + 2$ either above or under the line determined by 0 and $n + 2$, depending on the corresponding sign in ε. The Cambrian lattice determined by ε is then the flip graph of $\mathcal{P}_\varepsilon$, oriented by slope increasing flips. In particular the Tamari lattice $\mathcal{T}(n + 1)$ is the Cambrian lattice obtained from the signature $(-)_{i \in [n+1]}$. Figure 2.6 illustrates the Tamari lattice and another Cambrian lattice, when the two graphs are oriented from bottom to top. We do not study Cambrian lattices directly in this thesis, but they are naturally encoded in the geometric objects that we deal with.

2.2.2 Geometry

The polytopes that we are interested in are described by combinatorial structures, some of whose properties are "readable" directly from the geometry. As an instance, the graph of the permutahedron $\mathrm{Perm}(n)$ (embedded in $\mathbb{R}^{n+1}$ as in Section 2.1.3), when oriented in the direction given by the vector $(n + 1, n, \ldots, 1) - (1, 2, \ldots, n + 1)$, is the Hasse diagram of the weak order. As mentioned in Theorem A, many authors provided polytopal realizations for the associahedron [Hai84, Lee89, GKZ08, BFS90, SS93, SS97, RSS03, Lod04, HL07, CSZ15], resulting in three main families.

Secondary polytopes. Secondary polytopes of point configurations were introduced by I. Gelfand, M. Kapranov and A. Zelevinsky in [GKZ08]. The associahedron appears as the secondary polytope of points in convex position in the plane. As different configurations give rise to different polytopes, it provides us with an important family of realizations. Associahedra are yet not the central object of this theory and somehow constitute the "easiest" examples to deal with from this perspective.

Associahedra *via* signatures. S. Shnider and S. Sternberg produced in [SS93, SS97] a realization of the associahedron, obtained by forgetting some inequalities defining the permutahedron $\mathrm{Perm}(n)$. J.-L. Loday gave in [Lod04] an interpretation for the coordinates of the vertices of this realization, based on simple computations on binary trees. Among other properties, this associahedron, that we refer to as the Loday associahedron, can be oriented in the same linear direction as the permutahedron so that the induced orientation on its graphs makes it isomorphic to the Hasse diagram of the Tamari lattice. Motivated by N. Reading's work on Cambrian lattices [Rea06], C. Hohlweg and C. Lange [HL07] obtained about 2^n different realizations of the n-associahedron, including Loday's, constructed from the permutahedron $\mathrm{Perm}(n)$ similarly to the latter. The method of C. Hohlweg and C. Lange is based on triangulations of Cambrian polygons (see Section 2.2.1). Their realizations are indeed designed into satisfying the specific property that suitable linear orientations of their ambient space induce orientations of their graphs providing the Hasse diagrams of all (type A) Cambrian lattices (see Figure 2.6). They also gave a combinatorial description of the vertices of their realizations, that was later reinterpreted by C. Lange and V. Pilaud [LP13] in terms of the dual trees of the triangulations of Cambrian polygons.

d-associahedra. The last family of realizations was discovered in the broader context of *cluster algebras* by F. Chapoton, S. Fomin and A. Zelevinsky [CFZ02]. In this paper, one realization for each *generalized associahedron* was given, using *compatibility degrees*, which are also the *denominator vectors* (see [FZ03b, CP15]) of the corresponding cluster algebra. F. Santos then extended this method in the type A case, in a paper published with C. Ceballos and G. Ziegler [CSZ15, Section 5], to obtain about $C_n = \frac{1}{n+1}\binom{2n}{n}$ different realizations of the classical n-associahedron.

The same paper by C. Ceballos, F. Santos and G. Ziegler [CSZ15] provides a precise survey on these methods so that we do not give more details here. We only focus on the last one, that is so to say the "guidelight" of the geometric part of this thesis. As mentioned, it relies on cluster algebra results, which we discuss in the next section.

2.2.3 Algebra

Permutations and (binary) trees also appear in more algebraic contexts as they index bases of combinatorial Hopf algebras [LR98, HNT05, Cha00, CP17]. But Hopf algebras do not carry a lot of underlying motivations for this thesis, and we skip their presentation and go directly to cluster algebras. They were introduced by S. Fomin and A. Zelevinsky in a series of papers [FZ03b, FZ02, FZ03a, FZ07] and in a paper with A. Berenstein [BFZ05]. Since then, cluster algebras happened to have applications in diverse areas, including discrete dynamical systems, quiver representations, tropical geometry, Teichmüller theory and Poisson geometry (see [FZ04] for a survey).

We do not need the (heavy) precise definition of cluster algebras, and thus only give the informal ideas necessary for our purposes. For simplicity, we restrict ourself to algebras over the field $\mathbb{Q}$ of rational numbers. A *cluster algebra* is a commutative algebra $\mathcal{A}$ defined by a combinatorially controlled presentation by generators and relations: the generators of $\mathcal{A}$ are called the *cluster variables*. They are grouped into overlapping *clusters* of same cardinality (the *rank* of $\mathcal{A}$), to each of which is associated an *exchange matrix*[2], with which it forms a *seed*. The exchange matrices encode an involutory *mutation* process relating the clusters to each other as follows. Given a seed $\mathbf{s} = (X, \mathbf{B})$ consisting in a cluster $X = (x_1, \ldots, x_n)$ and an exchange matrix $\mathbf{B}$, and an integer $i \in [n]$, the mutation of $\mathbf{s}$ at x_i transforms the seed $\mathbf{s}$ into a new seed $\mathbf{s}' = (X', \mathbf{B}')$ where

- the cluster $X' = (x'_1, \ldots, x'_n)$ satisfies $x'_j = x_j$ for any $j \neq i$, and the variables x_i and x'_i, that are *exchanged* by the mutation, are related by an algebraic relation of the form $x_i x'_i = M^+ + M^-$ in $\mathcal{A}$, where M^+ and M^- are relatively prime monomials in the variables x_j (for $j \neq i$) determined by $\mathbf{B}$;
- the matrix $\mathbf{B}'$ is a new exchange matrix also obtained from the data of $\mathbf{B}$.

The point of exchange matrices is to encode the mutation process. They can therefore be replaced by any relevant combinatorial structure suitably playing that role. Some mutations can for instance be described in terms of *quivers* (directed multigraphs, see for instance [Kel13, Section 3]), or even more specific objects in well-behaved cases (triangulations of punctured surfaces, centrally symmetric triangulations...).

The relations $x_i x'_i = M^+ + M^-$ are the *exchange relations* and define the presentation of $\mathcal{A}$. The *exchange* (or *mutation*) *graph* of $\mathcal{A}$ is the graph whose vertices are the seeds of $\mathcal{A}$ and where seeds are adjacent if they are related by a mutation. It is important to
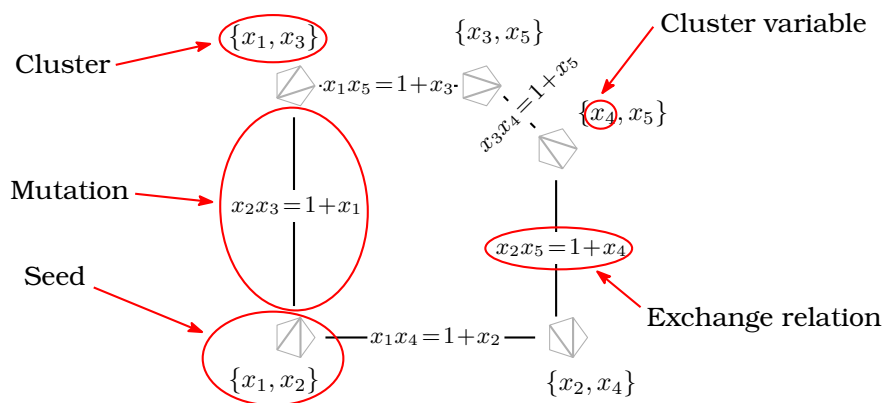
Figure 2.7 – The mutation graph of a the type A cluster algebras of rank 2 and several cluster algebra terminologies illustrated on it. Here the combinatorial data encoding the mutations are the triangulations of a pentagon. This mutation graph is therefore isomorphic to the flip graph $\mathcal{F}(2)$.

---

[2]Exchange matrices are integer matrices slightly more general than skew symmetric matrices.

$$\{x_1, x_3\} \qquad \{x_3, x_5\}$$
$$\{x_1^\circ, \tfrac{1+x_1^\circ}{x_2^\circ}\} \qquad \{\tfrac{1+x_1^\circ}{x_2^\circ}, \tfrac{1+x_1^\circ+x_2^\circ}{x_1^\circ x_2^\circ}\}$$

$$\cdot x_1 x_5 = 1 + x_3 \cdot \qquad x_3 x_4 = 1 + x_5$$

$$\{\tfrac{1+x_2^\circ}{x_1^\circ}, \tfrac{1+x_1^\circ+x_2^\circ}{x_1^\circ x_2^\circ}\}$$
$$\{x_4, x_5\}$$

$$x_2 x_3 = 1 + x_1$$

$$x_2 x_5 = 1 + x_4$$

$$x_1 x_4 = 1 + x_2$$

$$\{x_1^\circ, x_2^\circ\} \qquad \{x_2^\circ, \tfrac{1+x_2^\circ}{x_1^\circ}\}$$
$$\{x_1, x_2\} \qquad \{x_2, x_4\}$$
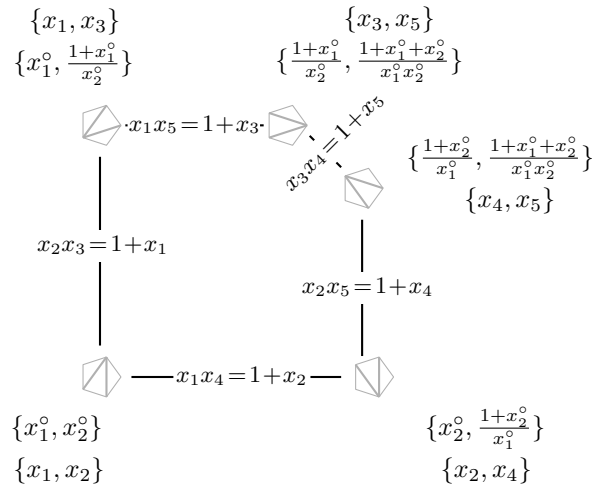
Figure 2.8 – The expansions of all cluster variables in the mutation graph of Figure 2.7 in the variables of the initial cluster (x_1, x_2). All these expansions are Laurent polynomials in (x_1, x_2) (see Theorem B).

precise that seeds are meant up to permutation and relabeling of cluster variables, so that the clusters should be though of as sets (and not tuples) of cluster variables. In fact the elements of a cluster are usually given with an order because they index the entries of the corresponding exchange matrix. Figure 2.7 illustrates these definitions.

Observe that the data of one seed is enough to determine the whole cluster algebra. Cluster algebras are thus generally introduced by describing the mutation process and then considering the subalgebra of the field $\mathbb{Q}(x_1^\circ, \dots, x_n^\circ)$ (of rational function over $\mathbb{Q}$ in n variables) generated by all the cluster variables in the seeds obtainable from an *initial seed* $s^\circ = (X^\circ, \mathbf{B}^\circ)$ (with *initial cluster* $X^\circ = (x_1^\circ, \dots, x_n^\circ)$) by sequences of mutations. The expansion of the cluster variables of Figure 2.7 in some initial cluster are given in Figure 2.8, which also illustrates the very first crucial property of cluster algebras.

Theorem B (Laurent phenomenon, [FZ02, Theorem 3.1])**.** *Given any initial cluster $X^\circ = (x_1^\circ, \dots, x_n^\circ)$ of a cluster algebra $\mathcal{A}$ and any cluster variable x of $\mathcal{A}$, the expansion of x as a rational function in the initial variables $(x_1^\circ, \dots, x_n^\circ)$ is a Laurent polynomial*[3]*.*

Among cluster algebras, we are particularly interested in those having a finite mutation graph. Such algebras are called *finite type cluster algebras* and are equivalently those cluster algebras with a finite number of cluster variables. In fact this result is a byproduct of the exact classification of finite type cluster algebras.

Theorem C (Finite type classification, [FZ03a, Theorems 1.7 and 1.8])**.** *Finite type cluster algebras are classified by crystallographic root systems*[4]*. In particular the mutation graph of cluster algebras of type A_n is isomorphic to the flip graph $\mathcal{F}(n)$.*

The cluster variables of a cluster algebra $\mathcal{A}$ are combinatorially related by the mutation graph of $\mathcal{A}$. It is the *dual graph* of the *cluster complex* of $\mathcal{A}$, namely the simplicial complex whose facets are the clusters of $\mathcal{A}$.

---

[3]That is a rational function whose denominator is a monomial in $(x_1^\circ, \dots, x_n^\circ)$.

[4]In the whole thesis, we never use Coxeter theory but often mention the different "types" of Coxeter and crystallographic root systems. Our setting mostly includes type A objects, but we sometimes make remarks on or comparisons with other types. However all our results are formulated in order to require no background on this topic, and we therefore only refer the interested reader to the classical textbooks [Hum90, BB05].

Example. For instance the type A cluster complex of rank n is the *dissection complex* of a convex polygon $\mathcal{P}$ with $n + 3$ vertices, namely the simplicial complex whose faces are the *dissections* (sets of pairwise noncrossing diagonals) of $\mathcal{P}$. The dual graph of this complex is the flip graph $\mathcal{F}(n)$. In fact all nonexceptional finite type cluster complexes have interpretations similar to that in type A, that is in terms of geometric configurations of noncrossing arcs in the plane (see [FZ03a, CP15]). As explained in Section 6.3.3, type B clusters are for example encoded by the centrally symmetric triangulations of a centrally symmetric polygon.

One of the properties making finite type cluster algebras interesting is that their structure is fully described by the combinatorics of the cluster complex. Finite type cluster algebras thus are somehow "algebraic realizations" of their cluster complex.

Theorem D ([FZ03a, Theorem 1.12]). *Finite type (coefficient-free) cluster algebras are characterized by their cluster complexes. Equivalently, isomorphic finite type (coefficient-free) cluster algebras have isomorphic cluster complexes.*

Finally, completing these algebraic properties, cluster complexes are particularly nice from our perspective as they admit geometric realizations as polytopes.

Theorem E (Generalized associahedra, [CFZ02, Theorem 1.4],[HLT11, Ste13],[PS15a, Corollary 6.10]). *Any finite type cluster complex has a polytopal realization, called a* generalized associahedron *of the corresponding type. In this setting the classical associaedron is the type A generalized associahedron.*

For a simplicial complex, being realizable as a polytope is in fact stronger than as a fan, and so formally Theorem E implies that cluster complexes also admit fan realizations. Yet polytopal realizations are often obtained in two steps, namely one first constructs a fan realization and only then shows that this fan is the *normal fan* of a polytope. This is the case for the realization of generalized associahedra by F. Chapoton, S. Fomin and A. Zelevinsky [CFZ02], based on the fan construction proposed by S. Fomin and A. Zelevinsky [FZ03b]. The proof by C. Hohlweg, C. Lange and H. Thomas [HLT11] is an extension of the construction of associahedra *via* signatures presented in Section 2.2.2 to all finite type cluster complexes. It relies on the same motivations, namely the articles of N. Reading and D. Speyer [Rea06, RS09], where in particular realizations of finite type cluster complexes by *Cambrian fans* are already given. The polytopes in [HLT11] are designed especially into having these fans as normal fans. The realizations by S. Stella [Ste13] and by V. Pilaud and C. Stump [PS15a] are essentially the same as in [HLT11] but bring new perspectives on cluster complexes. In particular S. Stella [Ste13] relates Cambrian fans to *cluster fans* and V. Pilaud and C. Stump [PS15a] generalize the *brick polytopes* and the settings introduced by V. Pilaud and F. Santos [PS12].

Theorems D and E describe what we call a "triad combinatorics–geometry–algebra" in the sense that a same object can equivalently be thought of in these three different worlds. In particular when dealing with generalizations of the associahedron, one of our main issues consists in finding analogs of this triad, that mimic as much as possible the nice properties of cluster complexes, generalized associahedra and cluster algebras.

2.2.4 The d-vector construction

As we just underlined, most polytopal realizations of simplicial complexes start by the construction of a suitable fan. But providing new fan realizations of complexes, even known to have polytopal ones, is not only valuable as a "first step", but also because two polytopes are generally considered to be "essentially different" when their normal fans are not linearly isomorphic (see Section 3.2). Concerning finite type cluster complexes,

there are two main constructions arising from cluster algebra theory. The fan realized in [FZ03b] (shown to be polytopal in [CFZ02]) somehow represents the intersection of the two resulting families of realizations. In fact we already gave their flavor in Section 2.2.2. On the one hand associahedra *via* signatures are indeed explained in terms of g-vectors by S. Stella in [Ste13]. We present these vectors for the type A in Chapter 9, in relation with its content. On the other hand the realizations by F. Santos in [CSZ15, Section 5] extends to the **d**-vector construction, that we explain now.

Given a finite type cluster algebra $\mathcal{A}$ and an initial cluster $X^\circ = (x_1^\circ, \ldots, x_n^\circ)$ of $\mathcal{A}$, the Laurent phenomenon (Theorem B) allows us to associate to each cluster variable x its *denominator vector* with respect to X°

$$\mathbf{d}(X^\circ, x) := [(x_1^\circ \,\|\, x), \ldots, (x_n^\circ \,\|\, x)],$$

also called its **d**-*vector*, where $(x_i^\circ \,\|\, x)$ is the exponent of the initial cluster variable x_i° in the expansion of x as a Laurent polynomial in X° (the notation is not ambiguous by Proposition G 1). It turns out that this quantity, initially defined as a *compatibility degree* in algebraic terms by S. Fomin and A. Zelevinsly [FZ03b], has a combinatorial interpretation in term of crossings in the different geometric models for nonexceptional finite type cluster complexes [FZ03b, CP15]. In the case of the classical associahedron, cluster variables are represented by the diagonals of a convex polygon $\mathcal{P}$ so that the compatibility degree can be read directly in this setting: for two diagonals δ, δ' of $\mathcal{P}$, we have $(\delta \,\|\, \delta') = (\delta' \,\|\, \delta) = -1$ if $\delta = \delta'$, $(\delta \,\|\, \delta') = (\delta' \,\|\, \delta) = 0$ if δ and δ' do not cross, and $(\delta \,\|\, \delta') = (\delta' \,\|\, \delta) = 1$ otherwise. So any initial triangulation T° of $\mathcal{P}$ provides us with a vector with coordinates in $\{-1, 0, 1\}$ associated to each diagonal of $\mathcal{P}$, whose entries correspond to the diagonals of T°.

Theorem F ([CSZ15, Theorem 5.1]). *For any initial triangulation T° of $\mathcal{P}$, the vectors in $\{\mathbf{d}(\mathrm{T}^\circ, \delta) \,|\, \delta \text{ diagonal of } \mathcal{P}\}$ are the rays of a complete simplicial fan realizing the complex of dissections of $\mathcal{P}$. In cluster algebra terms, it means that the denominator vectors associated to any initial seed in type A support a complete simplicial fan realizing the corresponding cluster complex.*

We continue the example of Figures 2.7 and 2.8 to illustrate Theorem F. In Figure 2.9, we give the denominator vectors of all cluster variables with respect to the initial cluster chosen in Figure 2.8, and we show in Figure 2.10 the fan obtained from these vectors. Besides Theorem F, it is proved by S. Fomin and A. Zelevinsky [FZ03a] that the **d**-vectors support a complete simplicial fan realizing the cluster complex for the *bipartite initial cluster* in all types, by S. Stella [Ste13] for all *acyclic initial clusters* in all types, and for any initial cluster in types A, B and C in Chapter 6. We expect this property to hold for any initial cluster, acyclic or not, of any finite type cluster algebra.

As we saw, the **d**-vector construction relies on a notion of compatibility degree $(\,\|\,)$, which fulfills general properties directly inherited from the cluster algebra structure.

Proposition G (direct corollary of [FZ03b, Section 3.5]). *In any type A, B, C or D cluster algebra $\mathcal{A}$, the compatibility degree $(\,\|\,)$ satisfies the following properties.*

1. *The function $(\,\|\,)$ is an integer function defined on couples of cluster variables of $\mathcal{A}$, that is the entry $(x_i^\circ \,\|\, x)$ of the **d**-vector of a cluster variable x with respect to an initial cluster $X^\circ = (x_1^\circ, \ldots, x_n^\circ)$ does only depend on x_i°, and not on the whole cluster X°. Equivalently, the exponent of x_i° in the denominator x is always the same when x is expanded in any initial cluster containing x_i°.*
2. *For any cluster variable x of $\mathcal{A}$, we have that $(x \,\|\, x) = -1$ and $(x \,\|\, x') \geq 0$ for any cluster variable x' of $\mathcal{A}$ different from x.*
3. *Two distinct cluster variables x and x' of $\mathcal{A}$ are compatible (that is they belong to a common cluster) if and only if $(x \,\|\, x') = (x' \,\|\, x) = 0$.*
4. *Two distinct cluster variables x and x' of $\mathcal{A}$ are exchangeable (that is they are exchanged along a mutation) if and only if $(x \,\|\, x') = (x' \,\|\, x) = 1$.*

$$\{x_1, x_3\} \qquad \qquad \{x_3, x_5\}$$
$$\{(-1, 0), (0, 1)\} \qquad \{(0, 1), (1, 1)\}$$

$\cdot x_1 x_5 = 1 + x_3 \cdot$

$x_3 x_4 = 1 + x_5$

$\{(1, 0), (1, 1)\}$

$\{x_4, x_5\}$

$x_2 x_3 = 1 + x_1$

$x_2 x_5 = 1 + x_4$

$x_1 x_4 = 1 + x_2$

$$\{(-1, 0), (0, -1)\} \qquad\qquad \{(0, -1), (1, 0)\}$$
$$\{x_1, x_2\} \qquad\qquad\qquad \{x_2, x_4\}$$
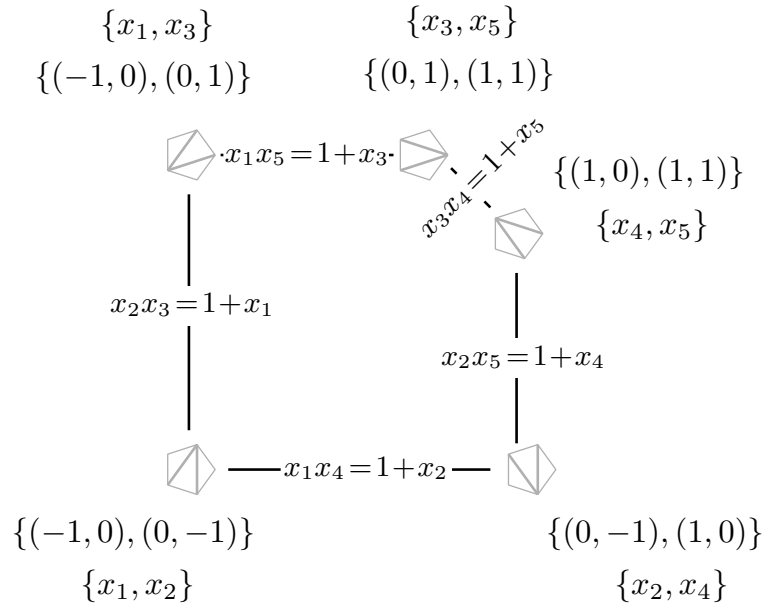
Figure 2.9 – The **d**-vectors of all cluster variables in the mutation graph of Figure 2.7 with respect to the initial cluster $(x_1, x_2) = (x_1^\circ, x_2^\circ)$. The first (resp. second) coordinate of each **d**-vector corresponds to the compatibility degree with x_1° (resp. x_2°). The **d**-vectors are grouped accordingly to the clusters. The values of their entries are obtained either by considering the explicit expansions of Figure 2.8 or directly the crossings between the corresponding diagonals in the triangulations indexing each cluster.

$\{x_3, x_5\}$

$\{x_1, x_3\}$

$(1, 0)$

$(1, 1)$

$\{x_4, x_5\}$

$(-1, 0)$ $(1, 0)$

$\{x_1, x_2\}$ $(0, -1)$ $\{x_2, x_4\}$
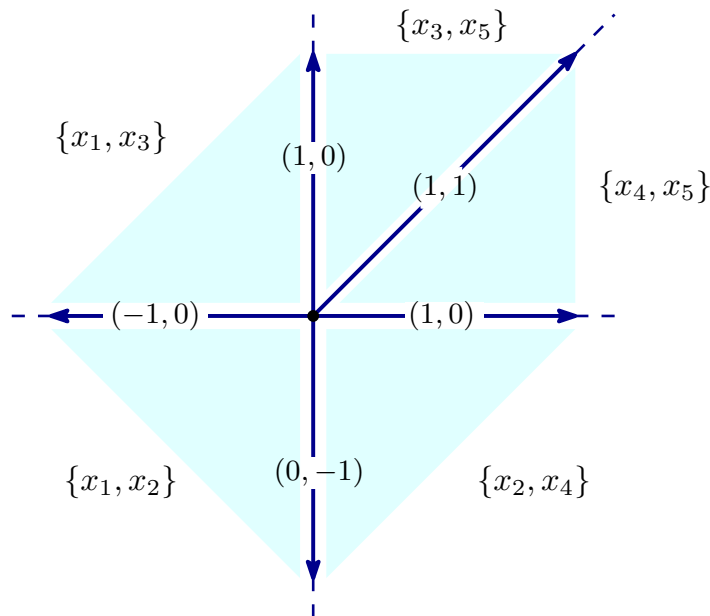
Figure 2.10 – The fan realizing the type A_2 associahedron obtained from the **d**-vectors of Figure 2.9. Each cluster is associated to the cone generated by the **d**-vectors of its cluster variables. Each ray **r** of this fan is the intersection of 2 cones corresponding to 2 clusters themselves intersecting in only one variable, whose **d**-vector generates **r**.

Remark. From our description of the compatibility degree on the diagonals of a polygon and from Proposition G, it follows that any two cluster variables in type A are always either compatible or exchangeable. This is clear from the interpretation of cluster variables in terms of diagonals. Indeed if two diagonals δ, δ' of a polygon $\mathcal{P}$ do not cross, then they belong by definition to a certain triangulation of $\mathcal{P}$, meaning that the corresponding cluster variables belong to a common cluster. If on the contrary δ and δ' cross, then their vertices define a quadrilateral Q in $\mathcal{P}$, whose four edges (either diagonals or boundary edges of $\mathcal{P}$) do not cross either δ nor δ'. Then any triangulation containing this quadrilateral has to contain either δ or δ' and flipping the present one introduces the other. This implies that noncompatible diagonals are exchangeable.

Even if stated in an algebraic context, the **d**-vector method turns out to have a clear combinatorial interpretation. In particular, when dealing with combinatorial relatives of associahedra, we try to systematically inspire from it to construct fan realizations. The expected outcome is of course a way from combinatorics to geometry, but also maybe to algebraic structures with analog properties as those of cluster algebras. In other terms this **d**-vector approach, even when there is no denominator involved any more, is a general strategy for us to look for new triads combinatorics–geometry–algebra.

2.3 Contribution of the thesis

As a special instance of broader families, the associahedron naturally admits generalizations in many directions, that are often first defined at the combinatorial level.

This thesis provides progresses in the combinatorial and geometric understanding of three families of simplicial spheres. In particular we follow with substantial successes the **d**-vector strategy exposed earlier with the hope that its algebraic inspiration can lead to advances also at that level. We also derive combinatorial properties specific to each families, that go beyond those that are necessary to implement the **d**-vector method. Finally we provide additional new fan realizations using alternative techniques.

2.3.1 Material of the thesis

The thesis relies on three articles either published or accepted for publication:

[Man17a] Fan realizations for some 2-associahedra, Thibault Manneville, to appear in *Experiment. Math.*, 2017.

[MP15] Graph properties of graph associahedra, Thibault Manneville and Vincent Pilaud, *Sém Lothar. Combin.*, 73:B73d, 2015.

[MP17a] Compatibility fans for graphical nested complexes, Thibault Manneville and Vincent Pilaud, *J. Combin. Theory Ser. A*, 150 : 36–107, 2017.

and two preprint articles:

[Man17b] The serpent nest conjecture on accordion complexes, Thibault Manneville, preprint `arXiv:1704.01534`, 2017.

[MP17b] Geometric realizations of accordion complexes, Thibault Manneville and Vincent Pilaud, preprint `arXiv:1703.09953`, 2017.

2.3.2 Outline

In Chapter 3, we give the definitions and background on simplicial complexes and their relations to polyhedral geometry needed all along the manuscript. The rest of the thesis is separated into two independent parts, that we follow to present our main contributions. Part II deals with a family of simplicial complexes indexed by simple graphs, and we present in Part III results on two families that we put together for reasons explained there. Both parts are organized according to the same global scheme:

1. an introductory chapter (Chapter 4 and Chapter 7 together with Sections 8.1 and 8.2) that provides the definitions and pieces of context for the currently considered complexes;
2. a chapter dealing with some specific combinatorial aspects of these complexes (graphical properties in Chapter 5 and enumerative results in Chapter 8);
3. one or two chapters dedicated to geometric realizations as fans or polytopes. Two of them extend the d-vector construction (Chapter 6 and Section 9.3), and two others are based on different ideas (Section 9.2 and Chapter 10).

An appendix to Chapter 5 follows the two parts. We keep the individual presentation of each family of complexes that we study for the corresponding chapters and just give here the ideas necessary to sum up our results.

2.3.2.1 Graph associahedra and nestohedra

Graph associahedra are simplicial complexes indexed by simple graphs that were introduced by M. Carr and S. Devadoss [CD06]. Given a graph G, one defines the *nested complex* $\mathcal{N}(G)$ of G as the simplicial complex whose vertices are the *tubes* (connected subgraphs) of G and whose faces are the *tubings* (sets of tubes of G that are pairwise either nested or that do not have vertices adjacent in G) on G. M. Carr and S. Devadoss described one polytopal realization for each of them, then recovered in several ways by many other authors. The associahedron is a special instance of this family, when G is specified to be a path. We present these complexes and the related literature in more detail in Chapter 4.

Combinatorial properties.   In Chapter 5 we study properties of the dual graphs $\mathcal{F}(G)$ of nested complexes $\mathcal{N}(G)$, with some extensions to general nested complexes defined by A. Postnikov [Pos09]. Our first results concern geodesic properties for these graphs, extending known results for the flip graph $\mathcal{F}(n)$ defined in Section 2.1.2. We denote by $\delta(\mathcal{F}(G))$ the diameter of $\mathcal{F}(G)$. Our initial motivation is the recent proof by L. Pournin of the exact value of the diameter of the n-associahedron for all values of n [Pou14].

Theorem H ([STT88, Pou14]). *The diameter of the flip graph $\mathcal{F}(n)$ is $2n - 4$ for $n \geq 9$.*

Our first result combinatorially describes a structural phenomenon that is relatively clear from the geometric perspective, given the construction of M. Carr and S. Devadoss.

Theorem I (Theorem 5.4, generalized by Theorem 5.9). *The diameter $\delta(\mathcal{F}(.))$ is a non-decreasing function, that is if $G \subseteq G'$, then $\delta(\mathcal{F}(G)) \leq \delta(\mathcal{F}(G'))$.*

To come up with bounds on the diameters of graph associahedra, we use what we call the *nonleaving-face property* **NLFP**. A simplicial complex has this property if in any dual path between two of its facets, the common vertices of the extremities of this path never disappear. The associahedron is an instance of complex having this property.

Theorem J ([STT88]). *In a shortest sequence of flips between two triangulations, none of their common diagonals is flipped.*

Graph associahedra do not necessarily satisfy **NLFP** and we give a counterexample in Section 5.3.3. However we obtain the following weaker result, where tubings on G are seen as the inclusion posets on their tubes.

Proposition K (Proposition 5.14 (i))**.** *Let* T, T' *be two maximal tubings on* G *and* $\mathsf{T} = \mathsf{T}_0, \mathsf{T}_1, \ldots, \mathsf{T}_k = \mathsf{T}'$ *be a shortest dual path in* $\mathcal{N}(\mathrm{G})$ *between* T *and* T'. *Then any tubing* T_i $(i \in [k])$ *contains all tubes of the maximal common upper ideal of* T *and* T'.

Combining Theorems H and I and Proposition K, together with more geometric arguments, we obtain the following asymptotically tight bounds on the diameter of the dual graph of any graph associahedron.

Theorem L (Theorem 5.16)**.** *For any connected graph* G *with* $n+1$ *vertices and* e *edges, we have*

$$\max(2n - 18, e) \leq \delta(\mathcal{F}(\mathrm{G})) \leq \binom{n+1}{2}.$$

A significant proportion of our proofs uses "combinatorial reductions" that are not always necessary but simplify the presentation. Moreover understanding such reductions is also an hint that we isolate the "true" complexity of the objects that we manipulate. In particular we are often interested in how simplicial complexes decompose into *joins* of smaller ones. For graph associahedra, and in fact general nested complexes, we obtain a complete description of such decompositions, implying in particular that graph associahedra behave "rigidly" from this point of view.

Theorem M (direct corollary of Proposition 5.23)**.** *For any graph* G*, the nested complex* $\mathcal{N}(\mathrm{G})$ *decomposes as a join of smaller simplicial complexes* $\mathcal{C}_1 * \cdots * \mathcal{C}_k$ *if and only if* G *has* k *connected components* $\mathrm{G}_1, \ldots, \mathrm{G}_k$ *such that* $\mathcal{C}_i$ *is isomorphic to* $\mathcal{N}(\mathrm{G}_i)$ *for all* $i \in [k]$.

Finally we show in Appendix A that essentially all graph associahedra contain a Hamiltonian cycle. This result extends the corresponding property, that was already known for specific subfamilies of graph associahedra, including classical associahedra.

Theorem N (Theorems 5.1 and A.1)**.** *For any graph* G *with at least two edges, the graph* $\mathcal{F}(\mathrm{G})$ *is Hamiltonian.*

Fan realizations using d**-vectors.** On the geometric side, we describe in Chapter 6 the following extension of the **d**-vector construction to all graph associahedra.

Given two tubes t, t' of a simple graph G, we define the *compatibility degree* $(\mathsf{t} \,\|\, \mathsf{t}')$ of t with respect to t' to be $(\mathsf{t} \,\|\, \mathsf{t}') = -1$ if $\mathsf{t} = \mathsf{t}'$, $(\mathsf{t} \,\|\, \mathsf{t}') = 0$ if $\mathsf{t} \neq \mathsf{t}'$ are *compatible* (nested or with disconnected union), and $(\mathsf{t} \,\|\, \mathsf{t}') = |\{\text{neighbors of } \mathsf{t} \text{ in } \mathsf{t}' \smallsetminus \mathsf{t}\}|$ otherwise. Similar to the compatibility degree for cluster algebras (see Proposition G), it satisfies $(\mathsf{t} \,\|\, \mathsf{t}') \geq 0$ for any distinct tubes t, t' of G, with equality if and only if t and t' are compatible, and $(\mathsf{t} \,\|\, \mathsf{t}') = 1 = (\mathsf{t}' \,\|\, \mathsf{t})$ if and only if t and t' are exchangeable. As in Section 2.2.4, we define the *compatibility vector* $\mathbf{d}(\mathsf{T}^\circ, \mathsf{t}) := [(\mathsf{t}_1^\circ \,\|\, \mathsf{t}), \ldots, (\mathsf{t}_n^\circ \,\|\, \mathsf{t})]$ of a tube t with respect to an initial maximal tubing $\mathsf{T}^\circ := \{\mathsf{t}_1^\circ, \ldots, \mathsf{t}_n^\circ\}$.

Notice that our degree is asymmetric, which yields a natural notion of duality. We define the *dual compatibility vector* $\mathbf{d}^*(\mathsf{t}, \mathsf{T}^\circ) := [(\mathsf{t} \,\|\, \mathsf{t}_1^\circ), \ldots, (\mathsf{t} \,\|\, \mathsf{t}_n^\circ)]$ of t with respect to T°. To make the distinction clear from the dual compatibility vector, we often call $\mathbf{d}(\mathsf{T}^\circ, \mathsf{t})$ the *primal* compatibility vector. Although there is no notion of denominator anymore, we still use the letter $\mathbf{d}$ to stand for compatibility **d**egree, and to match with the cluster algebra notations. Indeed, our compatibility degrees for paths and cycles coincide with the compatibility degrees of [FZ03b] in types A, B, and C. Compatibility degrees on type A cluster variables correspond to compatibility (and dual compatibility) degrees on

tubes of paths while compatibility degrees in type C (resp. B) cluster variables correspond to primal (resp. dual) compatibility degrees on tubes of cycles.

Our main result is the following analog of the compatibility fan for path associahedra constructed by F. Santos in [CSZ15, Section 5].

Theorem O (Theorems 6.10 and 6.14, extended by Theorem 6.53). *For any graph* G, *the primal (resp. dual) compatibility vectors of all tubes of* G *with respect to any initial maximal tubing* T° *on* G *support a complete simplicial fan* $\mathcal{D}(G, T^\circ)$ *realizing* $\mathcal{N}(G)$.

We also study the number of distinct compatibility fans that we obtain. As in [CSZ15], we consider that two compatibility fans $\mathcal{D}(G, T^\circ)$ and $\mathcal{D}(G', T'^\circ)$ are equivalent if they differ by a linear isomorphism (see Section 3.2.2). Such a linear isomorphism induces an isomorphism between the nested complexes of G and G'. Besides those induced by graph isomorphisms between G and G', we exhibit in Section 6.4.2 a nontrivial nested complex isomorphism on any *spider* (a set of paths attached by one endpoint to a clique). We show that it essentially is the only nontrivial nested complex isomorphism.

Theorem P (Theorem 6.37). *All nested complex isomorphisms are induced by graph isomorphisms* $G \to G'$, *except if one of the connected components of* G *is a spider.*

Corollary Q (Corollary 6.40, extended by Corollary 6.41). *If no connected components of* G *is a path, then the number of linear isomorphism classes of compatibility fans of* G *is the number of orbits of maximal tubings on* G *under graph automorphisms of* G.

The next step would be to realize all these complete simplicial fans as normal fans of convex polytopes. This question remains open, except for some particular graphs: besides all graphs with at most 4 vertices, we settle the case of paths and cycles following a similar proof as in [CSZ15].

Theorem R (Theorem 6.46). *All compatibility and dual compatibility fans of paths and cycles are polytopal. In particular the* **d**-*vector construction provides polytopal realizations of finite type cluster complexes from any initial seed in types* A, B *and* C.

2.3.2.2   Subword complexes and accordion complexes

As explained in Chapter 7, we are primarily interested in *subword complexes* [KM04]. Our study of accordion complexes [GM16] is motivated by intriguing relations that we develop in Section 8.4. It nevertheless turns out that we obtain more results concerning accordion complexes (Chapters 8 and 9) than subword complexes (Chapter 10).

Given a dissection D of a convex polygon $\mathcal{P}$, the *accordion complex* $\mathcal{AC}(D)$ of D is the simplicial complex whose faces are the dissections of $\mathcal{P}$ containing only certain diagonals determined by D, called the D-*accordion diagonals*. Informally, these diagonals are those that cross a connected set of diagonals (including boundary edges) of D, when D is rotated by a very small angle and superimposed on $\mathcal{P}$. The detailed presentation of accordion complexes is done in Sections 8.1 and 8.2.

Combinatorial properties of accordion complexes.   F. Chapoton raised in [Cha16] three challenges, including realizing accordion complexes as polytopes (that we discuss in the next paragraph) and enumerative questions. The main one consists in asking for a bijection between the facets of the accordion complex $\mathcal{AC}(Q)$ of any quadrangulation Q and objects called the *serpent nests* of Q. The question can be generalized to arbitrary dissections using the definition of *proper serpent nests* as sets of dual paths in the dual tree of D that do not cross any cell of D by nonincident diagonals and such that no two of them end up in the same cell by the same diagonal. Serpent nests can then be defined as the equivalence classes of proper serpent nests inducing the same local pattern at each diagonal of D. We exhibit a bijection, based on Catalan-like decompositions of D-accordion maximal dissections, giving a positive answer to F. Chapoton's question.

Theorem S (Theorem 8.15). *For any dissection* D, *there are as many facets in the accordion complex* $\mathcal{AC}(D)$ *as serpent nests of* D.

To prove Theorem S, we describe the *links* in accordion complexes and derive in addition the description of their decompositions into joins analog to this in Theorem M.

Proposition T (Proposition 8.6). *Given a dissection* D, *the accordion complex* $\mathcal{AC}(D)$ *decomposes into joins of smaller simplicial complexes if and only if* D *contains a* bridge *(a cell containing at least* 2 *nonconsecutive boundary edges of* $\mathcal{P}$*). In this case the terms of the decomposition of* $\mathcal{AC}(D)$ *are themselves accordion complexes.*

Finally F. Chapoton also defined the F-triangle of a quadrangulation Q in [Cha16], whose definition can also be extended to arbitrary dissections. This triangle of numbers is a refinement of the f-*vector* of the accordion complex $\mathcal{AC}(D)$. Namely the term indexed by integers k and r in the F-triangle of a dissection D is the number of D-accordion dissections with k diagonals among which exactly r belong to D. F. Chapoton conjectures that the *twist* operation on dissections, consisting in applying a mirror symmetry to one of the two part obtained by cutting a dissection along a diagonal before gluing them back together, preserves this statistic. We prove this conjecture.

Theorem U (Theorem 8.19). *If a dissection* D' *is obtained from a dissection* D *by a twist operation, then the* F-*triangles of* D *and* D' *are equal.*

Fan and polytopal realizations of accordion complexes. In Chapter 9, we give geometric realizations for accordion complexes $\mathcal{AC}(D)$ based on classical constructions of cluster algebras, including the $\mathbf{d}$-vector construction. Following the very same interpretation of the compatibility degree on diagonals in type A, we provide fan realizations, extending the $\mathbf{d}$-vector construction of the associahedron (when D is a triangulation). Namely we define the *compatibility degree* of two D-accordion diagonals δ and δ' to be the quantity $(\delta \,\|\, \delta') = -1$ if $\delta = \delta'$, $(\delta \,\|\, \delta') = 0$ if δ and δ' do not cross and $(\delta \,\|\, \delta') = 1$ otherwise. This degree gives rise to $\mathbf{d}$-vectors, for which we obtain the following result.

Theorem V (Theorem 9.33). *Except if* D *contains an even interior cell, the* $\mathbf{d}$-*vectors of* D-*accordion diagonals with respect to the distinguished facet* D *of the accordion complex* $\mathcal{AC}(D)$ *support a complete simplicial fan* $\mathcal{F}^{\mathbf{d}}(D)$ *realizing* $\mathcal{AC}(D)$.

In addition to this result, we provide a counterexample for any reference dissection D containing an even interior cell. Theorem V does not give us a realization for each facet of the complex $\mathcal{AC}(D)$, but we expect this property to be true for the same dissections. We also adapt the other classical construction of generalized associahedra by g-vectors to the setting of accordion complex, which allows us to realize any accordion complex $\mathcal{AC}(D)$ as a fan, without any restriction. Again we do not obtain one realization for each facet of the complex, but we show that our second fan realization is polytopal, giving a positive answer to the geometric question of F. Chapoton [Cha16].

Theorem W (Theorem 9.19). *For any dissection* D, *there is a simple polytope realizing the accordion complex* $\mathcal{AC}(D)$. *It is called the* accordeohedron *of* D *and denoted by* Acco(D).

The polytopes of Theorem W are obtained by forgetting inequalities in a *zonotope* defined from vectors analog to the $\mathbf{c}$-*vectors* of cluster algebras. After our geometric results, we also provide a combinatorial interpretation of these $\mathbf{c}$-vectors. Using that accordion complexes are in fact subcomplexes of the associahedron, we use the sign coherence of the g-vectors to obtain a purely geometric construction of *accordiohedra*.

Theorem X (Theorem 9.40). *If a dissection* D *is included in another dissection* D', *then a polytope realizing the accordion complex* $\mathcal{AC}(D)$ *can be obtained from* Acco(D') *by a projection on a coordinate subspace. In particular any accordion complex can be realized by projecting a classical associahedron obtained from the* g-*vector construction.*

Our g-vector construction keeps track of the symmetries of the reference dissection D, allowing to derive type B/C objects. Even if D can exhibit many symmetries, we can only embed type B/C, which is commonly the case with cluster-like structures.

Theorem Y (Proposition 9.28). *For any centrally symmetric dissection D, there exists a simple polytope realizing the complex of centrally symmetric D-accordion dissections.*

Fan realizations of some subword complexes. As we do not need the precise definition of subword complexes to present our last result, we refer the reader to Chapter 7. The important fact for now is that polytopal realizations are conjectured for about a decade for them, and that very few progresses have been done in this direction since they were introduced. In Chapter 10, we provide fan realizations for some instances of subword complexes and give conjectural ones for the whole subfamily of 2-*associahedra*. This family can be described as follows. Given integers n and k, the simplicial k-*associahedron* $\mathbf{\Delta}_{k,n}$ is the simplicial complex whose vertices are the diagonals of a convex $(n+2k+1)$-gon $\mathcal{P}$ and whose faces are the k-*dissections* of $\mathcal{P}$, namely the sets of diagonals of $\mathcal{P}$ such that no $k+1$ of them pairwise cross each other. These complexes form a *universal family* among subword complexes, meaning that providing geometric realizations for all of them would result in geometric realizations for all type A subword complexes. Chapter 10 describes a tentative approach towards such realizations, based on local combinatorial moves inside subword complexes. We obtain fans realizing 2-associahedra for which no geometric realizations were known before.

Theorem Z (Theorem 10.2). *All 2-associahedra $\mathbf{\Delta}_{2,n}$ for $n \in [8]$ have fan realizations.*

Theorem Z is a purely experimental result and was checked computationally. The rays used to construct our fans are described by a coordinate pattern for any $n \in \mathbb{N}$, that potentially could as well be valid for all 2-associahedra. We guessed this pattern after successive heuristic steps, the last of which relies on a randomization in order to suitably perturb degenerate sets of candidate rays. The other steps correspond to intuitive translations of combinatorial transformations on subword complexes that induce, among other things, *stellar subdivisions* (see Section 3.1) and *reverse stellar subdivisions* of edges. In our work, these operations really appear as a tool only in this last Chapter 10. However, we encountered them in all the other contexts mentioned before.

2.3.3 Stellar subdivisions of edges

Even if we do not prove any special result using stellar subdivisions, this thesis suggests to have a deeper look at the class of simplicial complexes obtainable by successive operations of join and stellar subdivision of edges, starting from boundaries of 1-simplexes. All complexes of this class are *flag* and realizable as polytopes (see Lemma 10.4) whose *polar duals* are usually called 2-*truncated cubes*. As explained in Section 3.2.3, the notion of flagness is a necessary property of any complex for which a $\mathbf{d}$-vector-like construction can be defined. The class of 2-truncated cubes includes graph associahedra and conjecturally flag type A subword complexes. It already motivated some works on general flag simplicial complexes [LN16] or in the context of toric topology [BP15, Sections 1.5 and 1.6] for instance. Throughout this thesis, we tried to define relevant combinatorial operations on the different underlying data of the complexes that we studied, whose topological effects are stellar subdivisions. As we mentioned, this kind of moves already exists for subword complexes [Gor14]. We also mention in Section 8.4 two relatively natural transformations on some dissections, inducing stellar subdivisions of edges on their accordion complexes. For now our interest for these operations mostly comes from the potentially unifying framework they could provide us with. We only mention them as a perspective opened by this work.

3

General preliminaries and notations

In this chapter, we formally define some notions used in Chapter 2 and fix a few notations. We use the classical associahedron as running example to illustrate them. We assume the reader to be familiar with basic graph theory (see [Ber58, Die10] for a complete presentation). In all the thesis, the term "maximal" is, without more precision, meant with respect to the inclusion order. We detail preliminary notions on simplicial complexes in Section 3.1 and give some basics on polyhedral geometry in Section 3.2.

3.1 Simplicial complexes

Simplicial complexes are our main combinatorial structures. We give the definitions that are relevant in our context and refer the reader to [Sta13, online Chapter 13], [Sta97, pages 307–311] and [Hat02, Chapter 0 and Section 2.1] for a detailed introduction.

Given a finite set V, a *(abstract) simplicial complex* (or simply a *complex*) on V is a subset $\mathcal{C}$ of the power set of V closed under taking subsets: $\mathcal{C} \subseteq 2^V$ and $f \subseteq g \in \mathcal{C} \Rightarrow f \in \mathcal{C}$. Usually one requires $\mathcal{C}$ to contain all singletons. The elements of V, and by extension the corresponding singletons, are the *vertices* of $\mathcal{C}$. The pairs in $\mathcal{C}$ are the *edges* of $\mathcal{C}$ and form together with the vertices a graph called the *1-skeleton* of $\mathcal{C}$. The elements of $\mathcal{C}$ are its *faces*, the inclusion maximal of which are called *facets*. We will always describe any explicit complex by its list of facets, which is equivalent to the whole data. We will moreover denote a complex whose single facet is an edge $\{x, y\}$ directly by xy, and we will use the notation x both for the vertex x and for the singleton $\{x\}$. If $\mathcal{C} = 2^V$, then $\mathcal{C}$ is called a *simplex*. In particular any face of a simplicial complex is the unique facet of a simplex, therefore the faces of $\mathcal{C}$ are also called the simplices of $\mathcal{C}$. The *dimension* of a face $f \in \mathcal{C}$ is the quantity $\dim(f) := |f| - 1$ while the dimension of $\mathcal{C}$ is $\dim(\mathcal{C}) := \max_{f \in \mathcal{C}} \dim(f)$. The complex $\mathcal{C}$ is *pure* if all its facets have the same dimension $d \geq 0$, in which case $\mathcal{C}$ is also called a d-complex. The faces of dimension $(d-1)$ of a d-complex are called its *ridges*. The *facet adjacency graph* (or *dual graph*) of a pure simplicial complex $\mathcal{C}$ is the graph whose vertices are the facets of $\mathcal{C}$, with two facets belonging to a common edge (or being *adjacent*) if their intersection is a ridge of $\mathcal{C}$. Two simplicial complexes are *isomorphic* if there is a bijection between their vertices inducing a bijection between their faces.
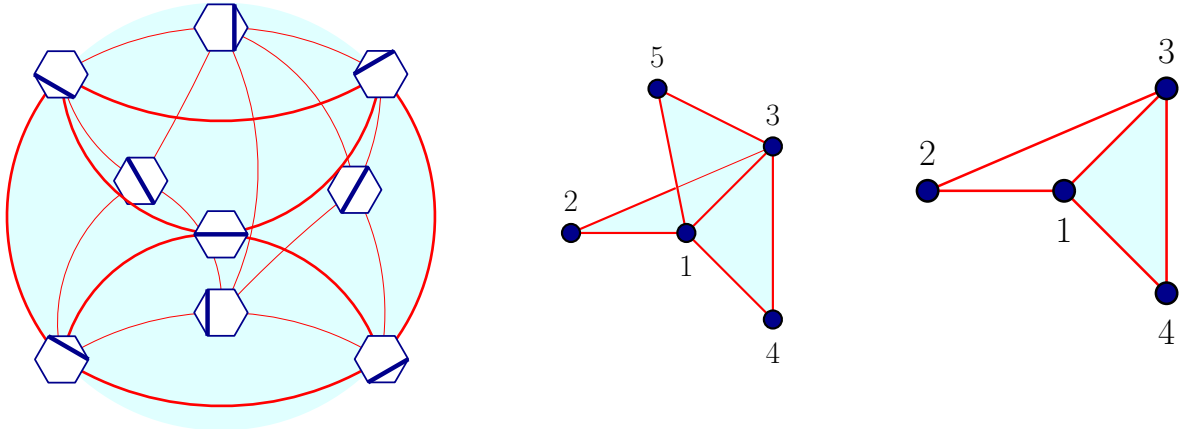
Figure 3.1 – The topological realizations of the simplicial 3-associahedron embedded on a sphere, whose vertices are the diagonals of a hexagon (left), of the complex on $[5]$ with facets $\{\{1,2,3\},\{1,3,4\},\{1,3,5\}\}$ (middle) and of the complex on $[4]$ with facets $\{\{1,2\},\{2,3\},\{1,3,4\}\}$ (right). The 3-associahedron is a 2-dimensional sphere.

Example 3.1. The *simplicial n-associahedron*[1] is the simplicial complex whose vertices are the internal diagonals of a convex polygon $\mathcal{P}$ with $n+3$ vertices, and whose faces are the sets of pairwise noncrossing internal diagonals. It is pure of dimension $(n-1)$ since its facets are the triangulations of $\mathcal{P}$, that all have cardinality n. Its dual graph is isomorphic to the flip graph $\mathcal{F}(n)$ defined in Section 2.1.2.

An abstract simplicial complex $\mathcal{C}$ can equivalently be dealt with as a topological space *via* its *topological realization* $\mathcal{T}op(\mathcal{C})$ defined as follows. Identifying the vertex set of $\mathcal{C}$ to $[n]$, and denoting $\mathbf{e}_1,\ldots,\mathbf{e}_n$ the canonical basis of $\mathbb{R}^n$, we have

$$\mathcal{T}op(\mathcal{C}) := \bigcup_{f\in\mathcal{C}} \operatorname{conv}\{\mathbf{e}_i \mid i\in f\},$$

where conv denotes the convex hull operator. The topological realization is meant up to homeomorphism. Informally it is a simple way to represent simplicial complexes, as collections of *topological simplexes* glued to each other along faces. We again refer to [Sta13, online Chapter 13] for details. Figure 3.1 illustrates the topological realizations of a simplicial 3-associahedron and other examples.

A simplicial complex $\mathcal{C}$ is a *pseudo-manifold* (without boundary) if it is pure and *thin*, that is any ridge of $\mathcal{C}$ is contained in exactly two facets of $\mathcal{C}$.

Example 3.2.   • The simplicial associahedron is a pseudo-manifold. Indeed its ridges are the sets of diagonals obtained by deleting a diagonal in a triangulation. There are then exactly two ways to extend a ridge to obtain a triangulation of $\mathcal{P}$. This property allows to define the flip operation on triangulations (see Section 2.1.2).
   • The complex of Figure 3.1 (middle) is pure but is not a pseudo-manifold since its ridge $\{1,3\}$ is contained in three facets.

Finally a complex is a *simplicial sphere* (or simply a *sphere*) if its topological realization is homeomorphic to the n-dimensional sphere. In this case the complex itself is of dimension n. Any sphere is a pseudo-manifold (see Figure 3.1 left).

A *nonface* of a complex $\mathcal{C}$ is an element in $2^{\mathrm{V}} \smallsetminus \mathcal{C}$. The complex $\mathcal{C}$ is *flag* if all its inclusion minimal nonfaces are pairs. In this case $\mathcal{C}$ is also called a *clique complex*, because its faces are exactly the cliques of its 1-skeleton.

---

[1]Where n stands for the dimension of the corresponding polytope (See Section 3.2.1).
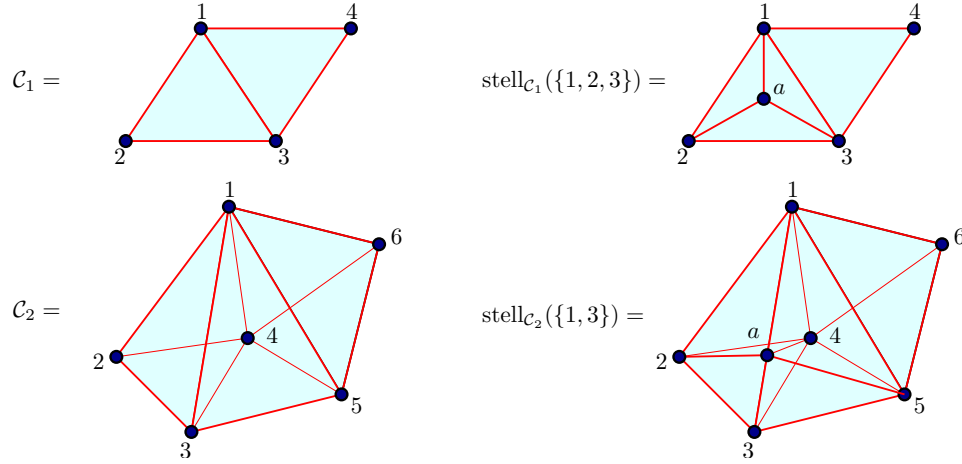
Figure 3.2 – A 2-complex $\mathcal{C}_1 = \{\{1,2,3\},\{1,3,4\}\}$ (top left) and the stellar subdivision of the facet $\{1,2,3\}$ in it (top right), and a 3-complex $\mathcal{C}_2 = \{\{1,2,3,4\},\{1,3,4,5\},\{1,4,5,6\}\}$ (bottom left) and the stellar subdivision of the edge $\{1,3\}$ in it (bottom right).

Example 3.3.
- The simplicial associahedron is flag since it is the clique complex of the graph whose vertices are the diagonals of $\mathcal{P}$ with two diagonals being adjacent if they do not cross. It can be checked in Figure 3.1 (left) that all triangles formed by any three edges of the 2-associahedron also belong to the associahedron.
- The complexes represented in Figures 3.1 (right) and 3.2 (top right) are not flag. In both cases, the triangle $\{1,2,3\}$ is a minimal nonface.

Given two complexes $\mathcal{C}_1$ and $\mathcal{C}_2$, the *join* of $\mathcal{C}_1$ and $\mathcal{C}_2$ is the complex

$$\mathcal{C}_1 * \mathcal{C}_2 := \{f \sqcup f' \mid f \in \mathcal{C}_1, f' \in \mathcal{C}_2\}$$

where $\mathcal{C}_1$ and $\mathcal{C}_2$ are considered with disjoint vertex sets and "$\sqcup$" is the disjoint union. The dual graph of $\mathcal{C}_1 * \mathcal{C}_2$ is then the Cartesian product of the dual graphs of $\mathcal{C}_1$ and $\mathcal{C}_2$.

Given a face f of a simplicial complex $\mathcal{C}$, the *star* $\mathrm{st}_{\mathcal{C}}(f)$, the *link* $\mathrm{lk}_{\mathcal{C}}(f)$ and the *deletion* $\mathrm{del}_{\mathcal{C}}(f)$ of f in $\mathcal{C}$ are the complexes respectively defined by

$$\mathrm{st}_{\mathcal{C}}(f) := \{f' \in \mathcal{C} \mid f \cup f' \in \mathcal{C}\},$$
$$\mathrm{lk}_{\mathcal{C}}(f) := \{f' \in \mathcal{C} \mid f \cap f' = \varnothing \text{ and } f \cup f' \in \mathcal{C}\},$$
$$\mathrm{del}_{\mathcal{C}}(f) := \{f' \in \mathcal{C} \mid f \not\subseteq f'\}.$$

Most combinatorial properties of simplicial complexes that we consider are closed under joins and links, as for instance being a pseudo-manifold or a sphere.

Example 3.4.
- Given an $(n+3)$-gon $\mathcal{P}$ and a diagonal δ of $\mathcal{P}$, the link of δ in the simplicial n-associahedron defined by $\mathcal{P}$ is the join of the two associahedra defined by the two polygons into which $\mathcal{P}$ is split by δ.
- The link of the edge $\{1,3\}$ in the complex of Figure 3.1 (middle) is $\{\{2\},\{4\},\{5\}\}$ and the link of the vertex 1 in the complex of Figure 3.1 (right) is $\{\{2\},\{3,4\}\}$.

For a complex $\mathcal{C}$ and a face f of $\mathcal{C}$, the *stellar subdivision* of f in $\mathcal{C}$ is the complex

$$\mathrm{stell}_{\mathcal{C}}(f) := \mathrm{del}_{\mathcal{C}}(f) \cup \{f' \cup \{a\} \mid f \not\subseteq f' \in \mathrm{st}_{\mathcal{C}}(f)\} = \mathrm{del}_{\mathcal{C} \cup \mathrm{st}_{\mathcal{C}}(f) * \{a\}}(f)$$

where $a \notin \mathrm{V}$ is a new vertex, called *subdivision vertex*. Intuitively the stellar subdivision corresponds to "putting a vertex in the middle of the face f" and adding the faces necessary to preserve the topology of the complex (see Figure 3.2 for examples). We really need stellar subdivisions only in Chapter 10, but we conclude this section with them as they repeatedly appears while dealing with the objects in this thesis (see Section 2.3.3).

3.2　Polyhedral geometry

We now give the notions of polyhedral geometry needed in the thesis and their relations to abstract simplicial complexes. For a complete presentation on *polytopes* and *fans*, we refer the reader to [Zie95], [Mat01, Chapters 1 and 5] and [DRS10, Section 2.1.1].

3.2.1　Polytopes

We denote the convex hull of a set $\mathbf{S}$ of points in $\mathbb{R}^d$ by $\mathrm{conv}(\mathbf{S})$. A *polytope* is the convex hull of a finite set of points in $\mathbb{R}^d$. Equivalently a polytope $\mathbf{P}$ is a bounded intersection of finitely many closed affine half-spaces in $\mathbb{R}^d$. The *dimension* of $\mathbf{P}$ is the dimension of its affine hull in $\mathbb{R}^d$, and we abbreviate "polytope of dimension d" to d-polytope. A *supporting hyperplane* of $\mathbf{P}$ is an affine hyperplane that does not separate any two points of $\mathbf{P}$. A *face* of $\mathbf{P}$ is the intersection of $\mathbf{P}$ with one of its supporting hyperplanes. By convention $\mathbf{P}$ itself is also considered as a face. The faces of a polytope are themselves polytopes and we again abbreviate "face of dimension d" to d-face. The 0-faces (resp. 1-faces, resp 1-codimensional faces) of $\mathbf{P}$ are its *vertices* (resp. *edges*, resp. *facets*). The *graph* (or 1-*skeleton*) of $\mathbf{P}$ is the graph whose vertices are the vertices of $\mathbf{P}$ and whose edges are the pairs of vertices of $\mathbf{P}$ belonging to a common edge of $\mathbf{P}$. A *geometric simplex* is the convex hull of affinely independent points in $\mathbb{R}^d$ and a polytope is *simplicial* if all its faces, except maybe itself, are simplices. The nonmaximal faces of a simplicial polytope $\mathbf{P}$, seen as the sets of their vertices, form a simplicial complex called the *boundary complex* of $\mathbf{P}$. A complex $\mathcal{C}$ is *polytopal* (or has a *polytopal realization*) if there is a simplicial polytope whose boundary complex is isomorphic to $\mathcal{C}$.

Example 3.5.　　• 2-polytopes are exactly convex planar polygons and are simplicial.
- The octahedron (see Figure 3.3 left) is a 3-dimensional simplicial polytope.
- For any $n \in \mathbb{N}$, the simplicial n-associahedron has polytopal realizations generically called *geometric simplicial n-associahedron*. Figure 3.3 (middle right) illustrates a polytopal realization of the simplicial 3-associahedron.

The faces of a polytope are naturally ordered by inclusion, forming the *face lattice* of the polytope. We refer to [Sta97, Sections 3.1 to 3.5] for background on posets and lattices, and to [Zie95, Chapter 2] for more details on the face lattice. Given a polytope $\mathbf{P}$, there is a polytope $\mathbf{P}^\diamond$ called the *polar dual* of $\mathbf{P}$, whose face lattice is dual to the face lattice of $\mathbf{P}$ (see Figure 3.3). The polar dual of a simplicial polytope is called *simple*. The polar duality is an involution, that is $(\mathbf{P}^\diamond)^\diamond = \mathbf{P}$, so that from a combinatorial point of view, dealing with simplicial or simple polytopes is equivalent. For reasons explained in Section 3.2.2, we prefer to work with simple polytopes. When $\mathbf{P}$ is simplicial, the graph of $\mathbf{P}^\diamond$ is isomorphic to the dual graph of the boundary complex of $\mathbf{P}$. In particular the graph of the polar dual of the geometric simplicial associahedron is isomorphic to the
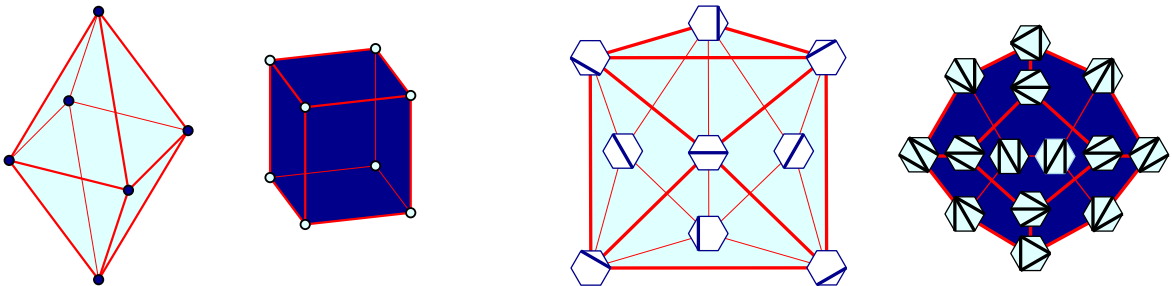
Figure 3.3 – From left to right: the octahedron and its polar dual (the cube), and a geometric simplicial 3-associahedron $\mathsf{Asso}(3)$ and its polar dual.

flip graph $\mathcal{F}(n)$ defined in Section 2.1.2 (see Figures 2.6 and 3.3 right). We abuse notations and still denote by $\mathsf{Asso}(n)$ any simple polytope whose graph is isomorphic to $\mathcal{F}(n)$. The following result implies that the flip graph $\mathcal{F}(n)$ already carries all the combinatorial data of the associahedron $\mathsf{Asso}(n)$. This explains why we primarily considered this flip graph itself as the associahedron.

Theorem 3.6 ([BM87, Kal88])**.** *Two simple polytopes with isomorphic graphs have isomorphic face lattices. Equivalently two polytopal simplicial complexes with isomorphic dual graphs are isomorphic.*

3.2.2 Fans

We now present *fans*, that are in practice the main geometric objects of this thesis. The definitions are very similar to those presented in Section 3.2.1. The notions of fans and polytopes can indeed be treated in a common setting (see [Zie95]). However there are important differences, in particular concerning simplicial complex realizations, that we are interested in. We therefore choose a separate presentation.

We denote by $\mathbb{R}_{\geq 0}\mathbf{V}$ (resp. $\mathbb{R}_{>0}\mathbf{V}$) the positive (resp. strictly positive) span of a set $\mathbf{V}$ of vectors in $\mathbb{R}^d$, namely the set of all linear combinations of elements of $\mathbf{V}$ with positive (resp. strictly positive) coefficients. A *polyhedral cone* (or just a *cone*) is the positive span of a finite set of vectors in $\mathbb{R}^d$. Equivalently a cone is the intersection of finitely many closed linear halfspaces. The *dimension* of a cone is the dimension of its linear span. The *faces* of a cone are its intersections with its *supporting hyperplanes*, that is the linear hyperplanes that do not strictly separate two of its elements. Faces of a cone still are cones and the 1-dimensional faces of a cone are its *rays*. A cone is *simplicial* if it is generated by independent vectors. A simplicial cone is generated by its rays and any subset of its rays generates one of its faces.

A *(polyhedral) fan* is a set of cones closed by taking faces and such that any two of them intersect in a common face. The maximal faces of the fan are its *facets*. A fan is *simplicial* if all its cones are, and it is *complete* if the union of its cones covers the whole space $\mathbb{R}^d$. A simplicial fan $\mathcal{F}$ naturally defines a simplicial complex $\mathcal{C}_{\mathcal{F}}$ whose vertices are the rays of $\mathcal{F}$ and whose faces are the subsets of rays generating the cones of $\mathcal{F}$. A simplicial complex $\mathcal{C}$ is then *realizable as a fan* if there exists a simplicial fan $\mathcal{F}$ such that $\mathcal{C}$ is isomorphic to $\mathcal{C}_{\mathcal{F}}$. The fan $\mathcal{F}$ is then called a *fan realization* of the complex $\mathcal{C}$. Figure 3.4 illustrates these notions.
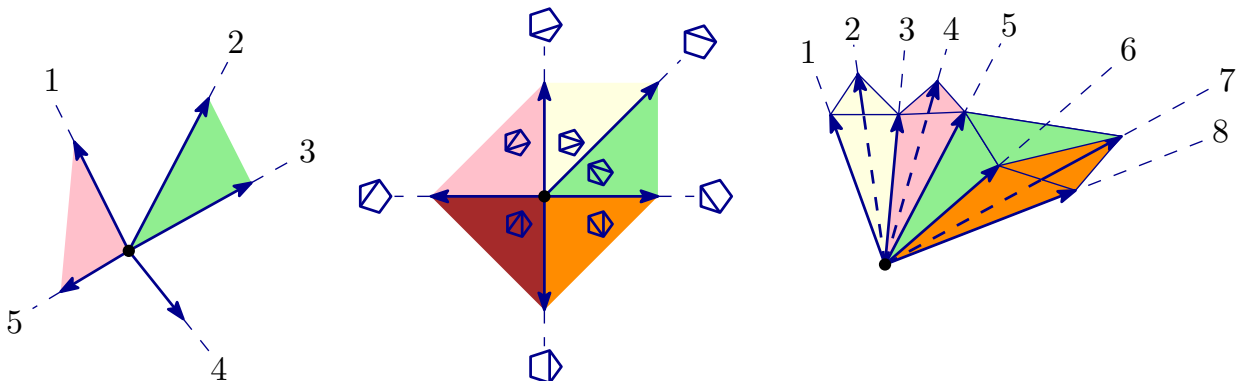
Figure 3.4 – A simplicial fan in dimension 2 whose associated complex has facets $\{\{4\}, \{1, 5\}, \{2, 3\}\}$ (left), a complete simplicial fan in dimension 2 realizing the simplicial 2-associahedron (middle) and a simplicial fan in dimension 3 whose associated complex has facets $\{\{1, 2, 3\}, \{3, 4, 5\}, \{5, 6, 7\}, \{6, 7, 8\}\}$ (right).

A simplicial complex realizable by a complete simplicial fan is a sphere. Indeed the intersection of the corresponding fan with the standard sphere in $\mathbb{R}^d$ provides a topological realization of this complex. In particular a fan realizing a 1-codimensional simplicial sphere is always complete. However simplicial spheres need not have fan realizations in general (see for instance [Ewa96, Theorems 5.5 and 5.7]). To realize a simplicial sphere as a complete simplicial fan, it suffices to find suitable coordinates for generators of the rays corresponding to its vertices. These vectors then *support* (that is, are the rays of) a complete simplicial fan realizing the complex if and only if a certain condition on adjacent facets is satisfied.

Proposition 3.7 (see *e.g.* [DRS10, Corollary 4.5.20])**.** *For a simplicial sphere $\mathcal{C}$ with vertex set V and a set of vectors $\mathbf{V} := (\mathbf{v}_x)_{x \in V}$ of $\mathbb{R}^d$, the set of cones $\{\mathbb{R}_{\geq 0} \mathbf{V}_f \mid f \in \mathcal{C}\}$, where $\mathbf{V}_f := \{\mathbf{v}_x \mid x \in f\}$, forms a complete simplicial fan if and only if*

1. *there exists a facet F of $\mathcal{C}$ such that $\mathbf{V}_F$ is a basis of $\mathbb{R}^d$ and such that the open cones $\mathbb{R}_{>0} \mathbf{V}_F$ and $\mathbb{R}_{>0} \mathbf{V}_{F'}$ are disjoint for any facet F' of $\mathcal{C}$ distinct from F;*

2. *for adjacent facets F, F' of $\mathcal{C}$ with $F \smallsetminus \{x\} = F' \smallsetminus \{x'\}$, there is a linear dependence*

$$\alpha \, \mathbf{v}_x + \alpha' \, \mathbf{v}_{x'} + \sum_{y \in F \cap F'} \beta_y \, \mathbf{v}_y = 0$$

   on $\mathbf{V}_{F \cup F'}$ in which the coefficients α and α' have the same sign (different from 0). When these conditions hold, this linear dependence is unique up to rescaling.

In [DRS10, Corollary 4.5.20], Condition 1 is a special case of "property (IPP)" and Condition 2 is a special case of "property (ICoP)". Moreover the result stays true when stated with Condition 1 holding for any facet. Proposition 3.7 is our main geometric tool. All fan realizations in this thesis rely on it. Since our concern is only about realizing spheres, by "fan realization" we mean from now on that the corresponding fan is complete. Simplicial spheres realizable as fans are also called *geodesic spheres*.

Proposition 3.8. *If $\mathcal{C}$ is a geodesic sphere, then so is the link $\mathrm{lk}_{\mathcal{C}}(f)$ of any face $f \in \mathcal{C}$.*

Proof. We already said that link of spheres are themselves spheres in Section 3.1, so we only check here the conditions of Proposition 3.7 to prove that $\mathrm{lk}_{\mathcal{C}}(f)$ has a fan realization. Let V be the vertex set of $\mathcal{C}$ and let $\{\mathbf{v}_x \mid x \in V\}$ be a set of vectors in $\mathbb{R}^d$ generating the rays of a fan realization of $\mathcal{C}$. These vectors then satisfy the conditions of Proposition 3.7. Let $\mathbf{V}$ be the orthogonal complement in $\mathbb{R}^d$ of the space spanned by $\{\mathbf{v}_x \mid x \in f\}$ and $\mathbf{p} : \mathbb{R}^d \to \mathbf{V}$ denote the orthogonal projection from $\mathbb{R}^d$ to $\mathbf{V}$. Consider the set of vectors $\{\mathbf{p}(\mathbf{v}_x) \mid x \in \mathrm{lk}_{\mathcal{C}}(f)\}$ of $\mathbf{V}$. These vectors clearly satisfy Condition 2 of Proposition 3.7, since the corresponding linear dependence are obtained by applying $\mathbf{p}$ to these between the vectors $\{\mathbf{v}_x \mid x \in V\}$. For Condition 1, consider a facet F of $\mathrm{lk}_{\mathcal{C}}(f)$. By definition of the link, the set $F \cup f$ is a facet of $\mathcal{C}$. In particular the set $\{\mathbf{v}_x \mid x \in F \cup f\}$ is a basis of $\mathbb{R}^d$ since it spans a simplicial cone of full dimension. This implies that the set $\{\mathbf{p}(\mathbf{v}_x) \mid x \in F\}$ is a basis of $\mathbf{V}$. Now suppose, for sake of contradiction, that another facet F' of $\mathrm{lk}_{\mathcal{C}}(f)$ is such that the open cones $\mathbb{R}_{>0}\{\mathbf{p}(\mathbf{v}_x) \mid x \in F\}$ and $\mathbb{R}_{>0}\{\mathbf{p}(\mathbf{v}_y) \mid y \in F'\}$ are not disjoint, so that there are strictly positive coefficients $\{\alpha_x \mid x \in F\}$ and $\{\beta_y \mid y \in F'\}$ such that

$$\sum_{x \in F} \alpha_x \mathbf{p}(\mathbf{v}_x) = \sum_{y \in F'} \beta_y \mathbf{p}(\mathbf{v}_y). \tag{3.1}$$

As a vector in $\mathbb{R}^d$, we can then expand the left hand side of Equation (3.1) in the basis $\{\mathbf{v}_x \mid x \in F \cup f\}$ and its right hand side in the basis $\{\mathbf{v}_y \mid y \in F' \cup f\}$ to obtain

$$\sum_{x \in F} \alpha'_x \mathbf{v}_x + \sum_{z \in f} \delta_z \mathbf{v}_z = \sum_{y \in F'} \beta'_y \mathbf{v}_y + \sum_{z \in f} \gamma_z \mathbf{v}_z. \tag{3.2}$$

Applying the projection $\mathbf{p}$ to both sides of Equation (3.2) yields back Equation (3.1), so that $\alpha'_x = \alpha_x > 0$ for any $x \in F$ and $\beta'_y = \beta_y > 0$ for any $y \in F'$, since $\{\mathbf{p}(\mathbf{v}_x) \,|\, x \in F\}$ and $\{\mathbf{p}(\mathbf{v}_y) \,|\, y \in F'\}$ are both bases of $\mathbf{V}$. Partitioning $f := f_1 \sqcup f_2$ according to the sign of the coefficients $\lambda_z := \delta_z - \gamma_z$ in Equation (3.2), we finally obtain a linear dependence with positive coefficient of the form

$$\sum_{x \in F} \alpha_x \mathbf{v}_x + \sum_{z \in f_1} \lambda_z \mathbf{v}_z = \sum_{y \in F'} \beta_y \mathbf{v}_y + \sum_{z \in f_2} \lambda_z \mathbf{v}_z.$$

This contradicts that the cones associated to the faces $F \cup f_1$ and $F' \cup f_2$ in the fan realization of $\mathcal{C}$ intersect in a common face and concludes the proof. ∎

3.2.3 Flagness condition for the d-vector construction

As explained in Section 2.2.4, one of our main goals is to extend the $\mathbf{d}$-vector construction of the associahedron to other classes of simplicial spheres. We recall that this construction is based on a compatibility degree $(.\,\|\,.)$ on the diagonals of a polygon. We look for extensions relying on the same principle and require, for cluster algebra motivations, that our new "compatibility" degrees fulfill Condition 3 of Proposition G, namely "nonequal vertices x and y belong to a common facet if and only if $(x \,\|\, y) = (y \,\|\, x) = 0$". Let us now briefly explain why this can only be achieved for spheres that are flag.

Assume that there is some compatibility degree $(.\,\|\,.) : \mathrm{V} \times \mathrm{V} \to \mathbb{Z}$ on the vertices of a simplicial sphere $\mathcal{C}$ fulfilling Condition 3 of Proposition G. As in Section 2.2.4, given any initial facet $F^\circ = \{x_1^\circ, \ldots, x_n^\circ\}$ of $\mathcal{C}$ and any vertex x of $\mathcal{C}$, define the $\mathbf{d}$-vector of x with respect to F° as the vector $\mathbf{d}(F^\circ, x) := [(x_1^\circ \,\|\, x), \ldots, (x_n^\circ \,\|\, x)]$ in $\mathbb{R}^{F^\circ}$. Suppose that for any facet F° of $\mathcal{C}$, the corresponding $\mathbf{d}$-vectors support a complete simplicial fan realizing $\mathcal{C}$ and assume, for sake of contradiction, that $\mathcal{C}$ is not flag. It means that there is a minimal nonface $\bar{f} \in 2^{\mathrm{V}} \smallsetminus \mathcal{C}$ containing at least three vertices. Let us choose a distinguished vertex x in $\bar{f}$. Since $\bar{f}$ is a minimal nonface, there exists a facet F of $\mathcal{C}$ containing $\bar{f} \smallsetminus \{x\}$. We take the same notations as in the proof of Proposition 3.8, where the face f is specified to $\bar{f} \smallsetminus \{x\}$, the ambient space is $\mathbb{R}^F$ and the vectors $\{\mathbf{v}_y \,|\, y \in \mathrm{V}\}$ are the $\mathbf{d}$-vectors with respect to F. By Condition 3 of Proposition G, all $\mathbf{d}$-vectors of vertices in $\mathrm{lk}_{\mathcal{C}}(f)$ already lie in $\mathbf{V}$. In particular the orthogonal projection $\mathbf{p} : \mathbb{R}^F \to \mathbf{V}$ defined in the proof of Proposition 3.8 is the identity function on these vectors, so that the set of cones $\{\mathbf{d}(F, r) \,|\, r$ vertex of $\mathrm{lk}_{\mathcal{C}}(f)\}$ is a complete simplicial fan in $\mathbf{V}$. This implies in particular that any vector in $\mathbf{V}$ is a positive linear combination of the $\mathbf{d}$-vectors of the vertices of a face in $\mathrm{lk}_{\mathcal{C}}(f)$. Now for any vertex y in f, the vertices x and y belong to a face of $\mathcal{C}$, since $\bar{f}$ is a minimal nonface. Therefore there must hold $(y \,\|\, x) = 0$ for any $y \in f$ by Condition 3 of Proposition G, so that $\mathbf{d}(F, x)$ belongs to $\mathbf{V}$. Thus there exists a face $f' \in \mathrm{lk}_{\mathcal{C}}(f) \subseteq \mathcal{C}$ such that the intersection of the cones $\mathbb{R}_{\geq 0}\{\mathbf{d}(F, y) \,|\, y \in f'\}$ and $\mathbb{R}_{\geq 0}\mathbf{d}(F, x)$ is $\mathbb{R}_{\geq 0}\mathbf{d}(F, x)$, which is not a face of $\mathbb{R}_{\geq 0}\{\mathbf{d}(F, y) \,|\, y \in f'\}$. This contradicts that the $\mathbf{d}$-vectors with respect to F support a complete simplicial fan realizing $\mathcal{C}$. ∎

3.2.4 The normal fan of a polytope

Given a d-polytope $\mathbf{P}$ in $\mathbb{R}^d$ and a face $\mathbf{F}$ of $\mathbf{P}$, the *normal cone* of $\mathbf{F}$ is the cone $\mathcal{N}_{\mathbf{P}}^{\diamond}(\mathbf{F})$ in the dual space $(\mathbb{R}^d)^*$ of $\mathbb{R}^d$ defined by

$$\mathcal{N}_{\mathbf{P}}^{\diamond}(\mathbf{F}) := \{\phi \in (\mathbb{R}^d)^* \,|\, \mathbf{F} = \mathrm{Argmax}_{\mathbf{P}}(\phi)\},$$

where Argmax denotes the argument of the maxima operator. In words, the cone $\mathcal{N}_{\mathbf{P}}^{\diamond}(\mathbf{F})$ is the set of linear functional whose restriction to $\mathbf{P}$ is maximized exactly at $\mathbf{F}$. If $\mathbf{P}$ contains the origin of $\mathbb{R}^d$ in its interior, it is interpreted as the sets of outgoing normal
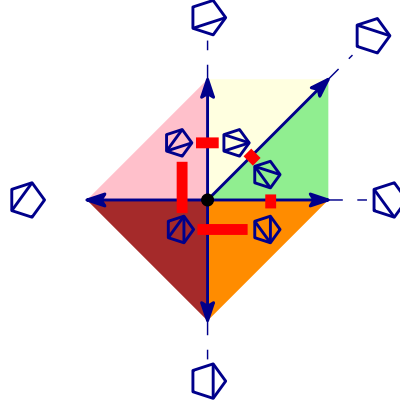
Figure 3.5 – The polar dual of a 2-associahedron (vertices are blue triangulations and edges appear red) and its normal fan.

directions to $\mathbf{F}$ in $\mathbb{R}^d$, hence the name. The *normal fan* $\mathcal{F}^\diamond(\mathbf{P})$ of $\mathbf{P}$ is defined by

$$\mathcal{F}^\diamond(\mathbf{P}) := \{\mathcal{N}_{\mathbf{P}}^\diamond(\mathbf{F}) \,|\, \mathbf{F} \text{ face of } \mathbf{P}\}.$$

Figure 3.5 illustrates the normal fan of a simple 2-associahedron.

The normal fan of a polytope $\mathbf{P}$ is always complete and the inclusion order on its faces is reverse to this on the faces of $\mathbf{P}$. Moreover, if $\mathbf{P}$ is simple, then its normal fan is simplicial. Since the polar dual $\mathbf{P}^\diamond$ of $\mathbf{P}$ also have a face lattice reverse to this of $\mathbf{P}$, both $\mathcal{F}_{\mathbf{P}}^\diamond$ and $\mathbf{P}^\diamond$ realize the same simplicial complex. In particular any simplicial complex realizable as a polytope is also realizable as a complete simplicial fan. Again the converse is not true (see for instance [DRS10, Section 7.1]). All proofs that some fans are the normal fans of some polytopes rely on the following characterization, in connection to regular triangulations of vector configurations and to the theory of secondary polytopes [GKZ08] (see also [DRS10]). Equivalent formulations appear *e.g.* in [CFZ02, Lemma 2.1], [Zel06, Proposition 6.3], [HLT11, Theorem 4.1], or [CSZ15, Lemma 5.4]. We follow the presentation of [CSZ15, Lemma 5.4] which fits our previous notations.

Proposition 3.9. *Let $\mathcal{F}$ be a complete simplicial fan in $\mathbb{R}^d$ and let $\mathbf{R}$ denote a set of vectors generating its rays. Then the following are equivalent:*
  1. *$\mathcal{F}$ is the normal fan of a simple polytope in $(\mathbb{R}^d)^*$;*
  2. *There exists a map $\omega : \mathbf{R} \to \mathbb{R}_{>0}$ such that for any two maximal adjacent cones $\mathbb{R}_{\geq 0}\mathbf{S}$ and $\mathbb{R}_{\geq 0}\mathbf{S}'$ of $\mathcal{F}$ with $\mathbf{S}, \mathbf{S}' \subseteq \mathbf{R}$ and $\mathbf{S} \smallsetminus \{\mathbf{s}\} = \mathbf{S}' \smallsetminus \{\mathbf{s}'\}$, we have*

$$\alpha\,\omega(\mathbf{s}) + \alpha'\,\omega(\mathbf{s}') + \sum_{\mathbf{r} \in \mathbf{S} \cap \mathbf{S}'} \beta_{\mathbf{r}}\,\omega(\mathbf{r}) > 0, \qquad where \qquad \alpha\,\mathbf{s} + \alpha'\,\mathbf{s}' + \sum_{\mathbf{r} \in \mathbf{S} \cap \mathbf{S}'} \beta_{\mathbf{r}}\,\mathbf{r} = 0$$

  is the unique (up to rescaling) linear dependence between the vectors in $\mathbf{S} \cup \mathbf{S}'$ with $\alpha, \alpha' > 0$.

Under these conditions, $\mathcal{F}$ is the normal fan of the polytope defined by

$$\left\{ \phi \in (\mathbb{R}^d)^* \,\middle|\, \phi(\mathbf{r}) \leq \omega(\mathbf{r}) \text{ for all } \mathbf{r} \in \mathbf{R} \right\}.$$

The map ω of Proposition 3.9 is called a *height function*. Following [CSZ15], we consider that two polytopes are *normally equivalent* if there is a linear isomorphism sending the normal fan of the first one to the normal fan of the second one. The reason of this choice is clear from the similar formulations of Propositions 3.7 and 3.9. Indeed if two simplicial fans $\mathcal{F}$ and $\mathcal{F}'$ are linearly isomorphic, then any valid height function for $\mathcal{F}'$ provided by Proposition 3.9 is also valid for $\mathcal{F}$, because the linear dependences of Proposition 3.7 between the rays of $\mathcal{F}$ and of $\mathcal{F}'$ are the same. So when caring about geometric realizations, it is natural first to try to construct many fans before looking for the corresponding polytopes, and then classify polytopes up to normal equivalence.

Part II

Graph associahedra and nestohedra

4

Context and motivations

4.1 Introduction

In this first part, we deal with the family of *nestohedra* (called *nested polytopes* in [Zel06]) introduced by A. Postnikov [Pos09] and E.M. Feichtner and D. Kozlov [FK04]. We are interested in these polytopes first because permutahedra and associahedra appear as particular instances of nestohedra. Secondly we want to formalize and deepen the idea that the boundary complexes of nestohedra behave analogously to finite type cluster complexes, according to previous remarks of A. Zelevinsky.

> A. Zelevinsky [Zel06]: "Our aim is to bring into focus the striking similarity between nested complexes and associated fans and polytopes on one side, and cluster complexes and generalized associahedra [...] on the other side."

Nestohedra include the class of *graph associahedra* defined by M. Carr and S. L. Devadoss [CD06], which naturally generalize the classical associahedra. Most results that follow concern this particular family, as it really seems to constitute a shadow of finite type cluster complexes among nestohedra.

> A. Zelevinsky [Zel06]: "For them an analogy with cluster complexes becomes sharper: in particular, the corresponding nested complex is a clique complex."

In this first chapter, we define nestohedra and graph associahedra, and give a few motivations for studying them. In particular we briefly discuss Laurent Phenomenon algebras, introduced by T. Lam and P. Pylyavskyy [LP16a, LP16b]. These algebras play the same role for a class of nestohedra (including graph associahedra) as this played by cluster algebras for generalized associahedra.

Chapter 5 gathers the results of [MP15] on combinatorial properties of the 1-skeleton of graph associahedra, with some extensions to general nestohedra. Namely we give structural properties and bounds on its diameter, and some of its geodesics. Chapter 5 also contains the characterization of nested complexes that decompose as joins of other simplicial complexes, which is not in [MP15].

Finally we describe in Chapter 6 a $\mathbf{d}$-vector-like construction of fans realizing graph associahedra presented in [MP17a]. These realizations are meaningful since for instance they recover the $\mathbf{d}$-vector construction of generalized associahedra of types A and B/C. Moreover we classify all isomorphisms of graphical nested complexes, which in return allows us to classify our realizations up to *geometric* (normal) equivalence.

4.2   Definition of nestohedra and first properties

In [Pos09], A. Postnikov defines *generalized permutahedra* as the polytopes obtained from the classical permutahedron $\mathrm{Perm}(n) = \mathrm{conv}((\sigma(1), \ldots, \sigma(n+1)) | \sigma \in \mathfrak{S}_{n+1})$ by relaxing the constant terms in the inequalities defining its facets. Informally, a generalized permutahedron is a polytope obtained by moving facets of $\mathrm{Perm}(n)$ along their normal rays. We will concentrate on the subclass of generalized permutahedra called *nestohedra*. A polytope in this class can be described by a combinatorial data called a *building set*. According to E.M. Feichtner and D. Kozlov [FK04], this notion first appeared in works of W. E. Fulton and R. MacPherson [FM94] and C. De Concini and C. Procesi [DP95], but with definitions depending upon geometric objects. The purely combinatorial definitions of building sets and their nested complexes were independently introduced by A. Postnikov [Pos09] and E.M. Feichtner and D. Kozlov [FK04]. We refer to [CD06, FS05, Pos09, Zel06] for more details and motivations on building sets and related structures. We mostly follow the presentation of A. Postnikov [Pos09].

Definition 4.1. Let V be a finite set. A *building set* on the *ground set* V is a set $B \subseteq 2^V$ of subsets of V satisfying the two following conditions.

(B1) If $b, b' \in B$ and $b \cap b' \neq \varnothing$, then $b \cup b' \in B$, and

(B2) the set B contains all singletons $\{v\}$ for $v \in V$.

For instance, if G is a simple graph with vertex set V, then the subsets of V inducing the connected subgraphs of G form a (*graphical*) building set. We describe these particular building sets in more detail in Section 4.3. We denote by $B_{\max}$ the set of inclusion maximal elements of B. The building set B is *connected* if $B_{\max}$ is a singleton, in which case $B_{\max} = \{V\}$. A B-*nested set* (or a *nested set on* B) on B is a subset N of B such that

(N1) for any $n, n' \in N$, either $n \subseteq n'$ or $n' \subseteq n$ or $n \cap n' = \varnothing$, and

(N2) for any $k > 1$ pairwise disjoint sets $n_1, \ldots, n_k \in N$, the union $n_1 \cup \ldots \cup n_k$ is not in B.

Definition 4.2. The B-*nested complex* is the $(|V| - |B_{\max}|)$-dimensional simplicial complex $\mathcal{N}(B)$ of all nested sets on B containing only elements in $B \smallsetminus B_{\max}$.

For a building set B and an element $b \in B$, the *restriction of* B *to* b is the building set

$$B_{|b} := \left\{ b' \mid b' \in B, b' \subseteq b \right\}.$$

Observe that for a nonconnected building set B, the nested complex $\mathcal{N}(B)$ is the join of the nested complexes $B_{|b_{\max}}$ of all restrictions of elements $b_{\max} \in B_{\max}$. Conversely for building sets $B_1, \ldots, B_k$ on disjoint ground sets $V_1, \ldots, V_k$, the *disjoint union* of $B_1, \ldots, B_k$ is the building set $B_1 \sqcup \cdots \sqcup B_k$ on the ground set $V_1 \sqcup \cdots \sqcup V_k$.

Examples 4.3. Relevant examples of nested complexes include
- simplexes, that are nested complexes corresponding to building sets of minimal size, namely building sets of the form $\{\{v\} \mid v \in V\} \cup \{V\}$,
- the classical permutahedron $\mathrm{Perm}(n)$, which corresponds to the nested complex of the building set of maximal size, namely the building set $2^{[n+1]}$,
- the classical associahedron $\mathrm{Asso}(n)$ is the nested complex of the building set consisting in all intervals of $[n+1]$.

The permutahedron and the associahedron have in fact a little more structure as they appear to be *graph associahedra* (see Figure 4.2 in Section 4.3). These two examples are treated in more detail in Section 6.3.

Nested complexes are relevant to many extends, one of which being that they admit beautiful and meaningful geometric realizations as polytopes.

Theorem 4.4 ([FS05, Pos09, Zel06])**.** *For any building set* B*, the nested complex* $\mathcal{N}(\mathsf{B})$ *is realizable as the boundary complex of a convex polytope, called a* nestohedron*, and generically denoted by* Nest(B)*.*

Let us briefly describe the construction of A. Postnikov [Pos09] in order to to highlight a relevant fact on nested complexes. Let B be a building set on $[n + 1]$ for an integer n. Let $\triangle_{[n+1]}$ denote the standard simplex of $\mathbb{R}^{n+1}$ and $\triangle_I$ denote the face of $\triangle_{[n+1]}$ corresponding to a subset $I \subsetneq [n + 1]$. Let Nest(B) denote the Minkowski sum of all simplexes $\triangle_{\mathsf{b}}$ for all $\mathsf{b} \in \mathsf{B}$, that is

$$\mathsf{Nest}(\mathsf{B}) := \sum_{\mathsf{b} \in \mathsf{B}} \triangle_{\mathsf{b}}.$$

Then Nest(B) is a simple polytope whose polar dual realizes the nested complex $\mathcal{N}(\mathsf{B})$ (see Figure 4.4 for an illustration). We come back to this construction in Section 6.1.1.

Proposition 4.5 (*e.g.* [FK04, Theorem 3.4][FM04, Theorem 4.2])**.** *Any nested complex can be obtained by successive stellar subdivisions of a simplex.*

Proof. (Sketch). Let **P** be the Minkowski sum of $\triangle_{[n+1]}$ and some of its faces, and I be a proper subset of $[n + 1]$. Suppose that the affine hull of $\triangle_{[n+1] \smallsetminus I}$ is directed by the same vector space as this directing the affine hull of a face **F** of **P**. One can then show that the Minkowski sum of **P** and $\triangle_I$ is combinatorially isomorphic to the polytope obtained by truncating the face **F** of **P**. Now for simple polytopes, face truncations correspond to stellar subdivisions of the corresponding dual face in the dual of their boundary complex. Since connected nested complexes are the dual complexes of polytopes constructed as Minkowski sums of $\triangle_{[n+1]}$ and of some faces of it, and since the Minkowski sum is commutative, we can show the result for connected nested complexes by induction on the number of summands, starting with higher dimensional ones (see [CD06, Lemma 2.15] for details on this method). As nonconnected nested complexes are joins of connected nested complexes, we are done. ■

4.3 Graph associahedra

We now present a rich family of nested complexes, namely the class of *graphical nested complexes* (or *graph associahedra*). They were introduced by M. Carr and S. Devadoss in [CD06] in connection to C. De Concini and C. Procesi's wonderful arrangements [DP95]. To study these complexes, we introduce a more specific terminology, following the presentation of [CD06]. Given a simple graph G with vertex set V, we denote by $\kappa(\mathrm{G})$ the set of connected components of G, and by $\mathrm{G}[U]$ the subgraph of G induced by a subset U of V.

A *tube* of G is a nonempty subset t of vertices of G inducing a connected subgraph $\mathrm{G}[\mathsf{t}]$ of G. The inclusion maximal tubes of G are its connected components, whose set we denote by $\kappa(\mathrm{G})$; all other tubes are called *proper*. The set of all tubes of G is denoted $\mathsf{B}(\mathrm{G})$. It is clearly a building set, called the *graphical building set* of G. Two tubes t, t' of G are *compatible* if they are either *nested*, that is $\mathsf{t} \subseteq \mathsf{t}'$ or $\mathsf{t}' \subseteq \mathsf{t}$ (Conditions N1), or disjoint and nonadjacent, that is $\mathsf{t} \cup \mathsf{t}'$ is not a tube of G (Condition N2). A *tubing* on G is a set T of pairwise compatible proper tubes of G. The collection of all tubings on G then coincides with the nested complex of the graphical building set $\mathsf{B}(\mathrm{G})$, called the *nested complex* of G and denoted by $\mathcal{N}(\mathrm{G})$. We say that a nested complex is *graphical* if the underlying building set is a graphical building set. We already know by Theorem 4.4 that the complex $\mathcal{N}(\mathrm{G})$ is isomorphic to the dual boundary complex of a simple convex polytope. This result was already proved for graphical nested complexes by M. Carr and S. Devadoss [CD06]. In this case this polytope is also called the *graph associahedron* of G, and is denoted by Asso(G).
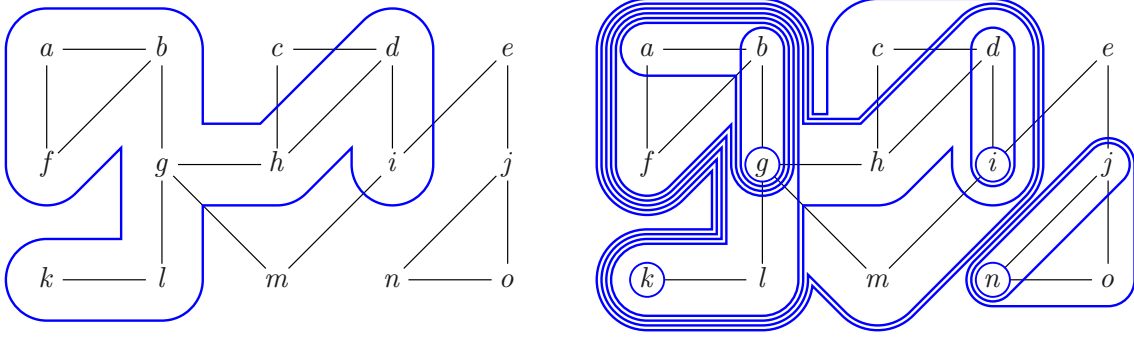
Figure 4.1 – A tube t_{ex}° of G_{ex} (left) and a maximal tubing T_{ex}° on G_{ex} (right).

Example 4.6. We illustrate the previous notions with an example (see Figure 4.1), that we follow here and in Chapter 6. We have represented a graph G_{ex} on the left with a tube $t_{ex}^{\circ} := \{a, b, d, f, g, h, i, k, l\}$, and a maximal tubing T_{ex}° on G_{ex} on the right.

Example 4.7 (Classical polytopes). For certain families of graphs, graph associahedra specialize to classical polytopes (see Figure 4.2):

  (i) the path associahedron $\mathsf{Asso}(P_{n+1})$ coincides with the n-associahedron,

 (ii) the cycle associahedron $\mathsf{Asso}(O_{n+1})$ coincides with the n-cyclohedron,

(iii) the complete graph associahedron $\mathsf{Asso}(K_{n+1})$ coincides with the n-permutahedron.

A more detailed treatment of these specific families of graph associahedra is done in Sections 6.3.2, 6.3.3 and 6.3.4 respectively.

Remark 4.8. Note that $B(G)_{\max} = \kappa(G)$ so that the building set $B(G)$ is connected if and only if G is. In particular if G has connected components G_i for $i \in [k]$, then the graph associahedron $\mathsf{Asso}(G)$ is isomorphic to the Cartesian product $\mathsf{Asso}(G_1) \times \cdots \times \mathsf{Asso}(G_k)$.

Let $n = |V| - |\kappa(G)|$. The nested complex $\mathcal{N}(G)$ is an $(n-1)$-dimensional sphere, and so a pseudo-manifold in particular. This induces a *flip* operation, described in Proposition 5.2: in any maximal tubing T on G, any tube t can be replaced by a unique other tube t' of G such that $T \cup \{t'\} \smallsetminus \{t\}$ is still a maximal tubing on G. A *flip* is a pair of distinct maximal tubings T, T' on G such that $T \smallsetminus \{t\} = T' \smallsetminus \{t'\}$ for some tubes $t \in T$ and $t' \in T'$. The dual graph of $\mathcal{N}(G)$ is the *flip graph* of G, denoted by $\mathcal{F}(G)$, whose vertices are maximal tubings on G and whose edges are flips between them.

Example 4.9. Figure 4.3 illustrates the flip between two maximal tubings T_{ex} and T'_{ex} on G_{ex}. The flipped tubes $t_{ex} = \{a, b, c, d, f, g, h, k, l, m\}$ and $t'_{ex} = \{c, d, e, h, i, m\}$ are dashed red, the *forced tubes* (see Section 6.2.1) are green.

We saw in Section 2.2.4 that we are interested in giving many nonequivalent geometric realizations of nested complexes using **d**-vector-like constructions (which is done in Chapter 6). As explained in Section 3.2.2, such a strategy cannot be successfully applied to nonflag complexes. Graph associahedra are defined as clique complexes of a certain compatibility relation, and so are flag by definition. But graphical nested complexes are far from being the only flag nested complexes, even up to isomorphism.

Example 4.10. Consider the path P_4 with ground set $\{1, 2, 3, 4\}$. The nested complex $\mathcal{N}(B_{ex})$ of the building set $B_{ex} = B(P_4) \cup \{1, 2, 4\}$ is flag, connected and it has one more facet than the associahedron $\mathsf{Asso}(4)$. From the realization of $\mathsf{Nest}(B_{ex})$ presented in Figure 4.4 and the explicit description of all 3-dimensional connected graph associahedra given in Appendix A (Figure A.10), we obtain that $\mathcal{N}(B_{ex})$ is not isomorphic to a graphical nested complex. A quick way to check it consists in observing that no graph associahedron has the same number of facets as $\mathsf{Nest}(B_{ex})$.
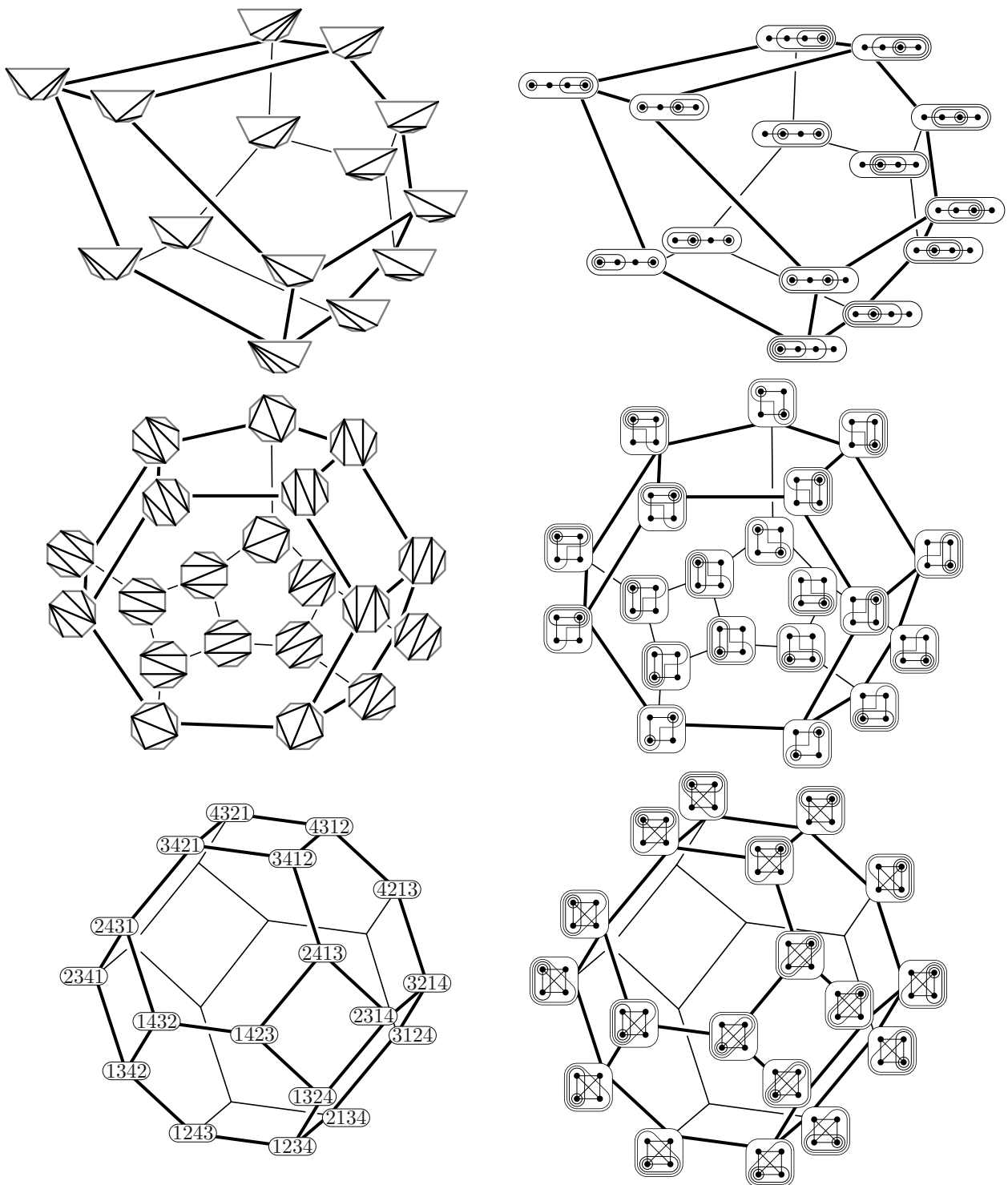
Figure 4.2 – The classical associahedron (top left) is the path associahedron (top right), the cyclohedron (middle left) is the cycle associahedron (middle right) and the permutahedron (bottom left) is the complete graph associahedron (bottom right).
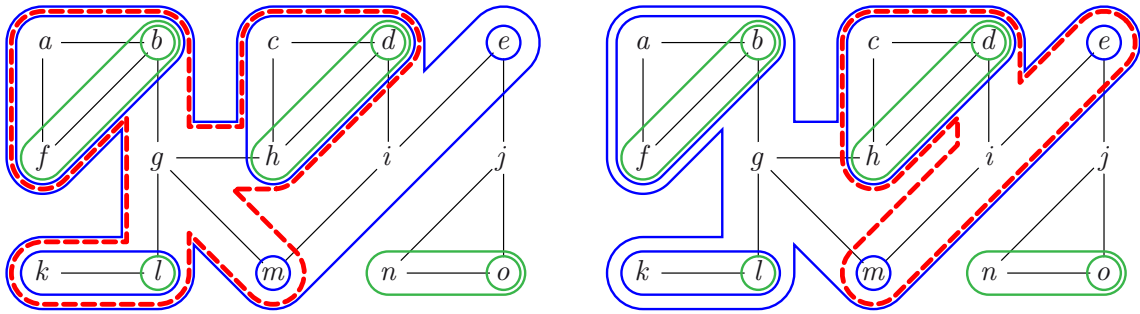
Figure 4.3 – The flip between two maximal tubings $\mathsf{T}_{\mathbf{ex}}$ and $\mathsf{T}'_{\mathbf{ex}}$ on $\mathsf{G}_{\mathbf{ex}}$.
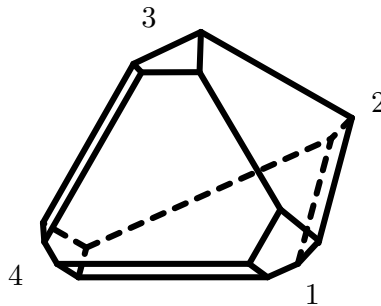
Figure 4.4 – The nestohedron $\mathsf{Nest}(\mathsf{B}_{\mathbf{ex}})$ is not isomorphic to a graph associahedron.

Example 4.10 can be generalized to any connected graph G containing a vertex $v \in \mathrm{V}$ such that $\mathrm{G}[\mathrm{V} \smallsetminus v]$ is not connected: for such graph, the set $\mathsf{B} = \{\mathrm{V} \smallsetminus \{v\}\} \cup \mathsf{B}(\mathrm{G})$ is a building set, and $\mathcal{N}(\mathsf{B})$ can clearly be obtained from $\mathcal{N}(\mathrm{G})$ by applying a stellar subdivision on the face containing the tubes inducing the connected components of $\mathrm{G}[\mathrm{V} \smallsetminus v]$. If v disconnects G into exactly two connected components, then the stellar subdivision is applied to an edge of $\mathcal{N}(\mathrm{G})$, which preserves flagness. In this case $\mathcal{N}(\mathsf{B})$ is flag and contains exactly one vertex more than $\mathcal{N}(\mathrm{G})$. Observe that $\mathcal{N}(\mathrm{G})$ is a natural subcomplex of $\mathcal{N}(\mathsf{B})$. We can then check that $\mathcal{N}(\mathsf{B})$ is not isomorphic to a graphical nested complex. Indeed the description of isomorphisms between graphical nested complexes given in Section 6.4.2 implies that a connected graph G' such that $\mathcal{N}(\mathsf{B}) \cong \mathcal{N}(\mathrm{G}')$ would contain a strict subgraph isomorphic to G, and thus that $|\mathsf{B}(\mathrm{G}')| > |\mathsf{B}|$, a contradiction.

The only study concerning flag nested complexes that we are aware of is a paper of V. Volodin [Vol10], where flag nestohedra are realized by successive truncations of 2-codimensional faces of a cube. Dealing with general flag nested complexes is not easy and it is a challenging question to provide relevant and useful characterizations for them. However we still understand them more than nonflag nested complexes, that only admit a single (up to equivalence) known polytopal realization each, as explained in Section 6.1.1. A family of nonflag nested complexes is presented in Section 4.4.2.

4.4   Laurent phenomenon algebras

In Chapters 5 and 6, we will respectively be concerned with combinatorial and geometric considerations on graphical nested complexes. Following the very same triad motivation as before, we conclude this chapter with some more algebraic motivations. Recently T. Lam and P. Pylyavskyy [LP16a, LP16b] defined *Laurent Phenomenon algebras* (or *LP-algebras*), in order to generalized cluster algebras. The definition of LP-algebras is similar to that of cluster algebras, namely a LP-algebra is an algebra generated by a

set of variables grouped into clusters, that are the vertices of an exchange graph, the edges of which are still called mutations. The difference is that mutations are not any more encoded by mutation matrices, rather by *exchange polynomials* attached to each variable in each cluster[1]. The precise definitions related to clusters and the mutation process are technical and since we will not use them, we simply refer to [LP16a] for the detailed presentation of LP-algebras. LP-algebras exhibits many common properties with cluster algebras, among which two particularly interest us.

Theorem 4.11 (Laurent Phenomenon [LP16a, Theorem 5.1])**.** *Let $\mathcal{A}$ be a LP-algebra and let X° be any initial seed of $\mathcal{A}$. Any cluster variable of $\mathcal{A}$ is a Laurent polynomial in the variables contained in X°.*

In particular, there is a natural notion of **d**-vectors associated to any initial seed of a LP-algebra, just as in cluster algebras. For now very few is known about these vectors for general LP-algebras. The second property that we are interested in is the possibility, as in cluster algebras, to freeze a cluster variable [LP16a, Section 3.5]. Namely all seeds that can be obtained by mutations from an initial one $X^\circ = \{(x_1, P_1), \ldots, (x_m, P_m)\}$ without mutating the variable x_1 are the vertices of a graph isomorphic to the mutation graph of a new LP-algebra. But it does not mean that the class of cluster complexes of LP-algebras is closed under links. Even if it is reasonable to believe it, it is not known so far that links are connected in such cluster complexes.

As for cluster algebras, we focus our interest on mutation graphs of LP-algebras that are finite. Until now, we are not aware of any characterization of such complexes. From the point of view presented in this thesis, LP-algebras are interesting to many extends.

4.4.1 Unification

As we just mentioned, we expect finite cluster complexes of LP-algebras to be closed under links. Since all classes of complexes that we consider in this thesis have this same property, it allows to hope of defining related LP-algebra structures in order to unify them in a natural common framework. We have seen in Proposition 4.5 that nested complexes can be obtained from a simplex by successive stellar subdivisions of faces, a property that is either known or conjectured for almost all combinatorial structures studied in this thesis. This raises the following question.

Question 4.12. For a cluster complex $\mathcal{C}$ of a LP-algebra and a face F of $\mathcal{C}$, is the stellar subdivision $\mathrm{stell}_{\mathcal{C}}(F)$ isomorphic to the cluster complex of a LP-algebra?

Question 4.12 seems to be hard in general. Indeed even if stellar subdivisions are local operations, building a LP-algebra with a prescribed cluster complex requires a strong control on all its seeds. As we recently studied LP-algebras of rank 2 both theoretically and computationally, it seemed that the answer to Question 4.12 is negative, or "at least for sufficiently generic LP-algebras". For them it is possible to show that the only finite cluster complexes of dimension 1 are the triangle, the square, the pentagon, the hexagon and the octagon. Yet nongeneric examples give rise to other cluster complexes with much more than 8 seeds.

4.4.2 Some nested complexes are cluster complexes

There are some hints towards a classification of finite cluster complexes of LP-algebras. One of them is that graph associahedra appear as instances of finite cluster complexes of some LP-algebras. In [LP16b], T. Lam and P. Pylyavskyy study in more detail *linear LP-algebras*, that is those LP-algebras in one of whose clusters, all polynomials attached to cluster variables are of degree 1. They show the following result.

---

[1]That is the exchange polynomial attached to a variable depends on the cluster in which this variable is considered and it is updated along mutations.

Theorem 4.13 ([LP16b, Theorem 1.1]). *Let $\mathcal{A}$ be a LP-algebra such that all exchange polynomials in a given cluster X have degree 1, nonconstant coefficients in $\{0, 1\}$, and algebraically independent constant coefficients. The cluster complex of $\mathcal{A}$ is finite.*

T. Lam and P. Pylyavskyy are even able to describe the cluster complexes of such LP-algebras. Some cluster complexes of linear LP-algebras are the *design graphical nested complexes* that are defined and studied in Section 6.4.4. The only relevant fact for our current concern is that graphical nested complexes are (connected) links of them, so that they also are the cluster complexes of some LP-algebras. Nevertheless one should again be careful with this statement as, contrarily to cluster algebras, it does not mean that they fully describe a unique LP-algebra structure [LP16b, Section 6.2].

In fact, any nested complex has a "design" version, but once more we do not need it for technical purposes so that we skip the proper definition. The cluster complexes of linear LP-algebras that are not design graphical nested complexes however still are design nested complexes of some building sets, namely those consisting of strongly connected components of a certain directed graph. We mention them for completeness and in order to present the only class of nonflag nested complexes encountered in this thesis. For a directed graph G on a vertex set V, we keep denoting by $B(G)$ the building set consisting in the subsets of V inducing strongly connected components of G. Notice that undirected graphs are naturally identified to some instances of this class by replacing each of their undirected edge by a pair of opposite directed edges. Suppose that G contains a directed cycle $v_1 \to \cdots \to v_k \to v_1$ of length at least 3, then the nested complex $\mathcal{N}(G)$ is not flag. Indeed the set $\{v_1, \ldots, v_k\}$ belongs to $B(G)$ but none of its proper subsets of cardinality at least 2 does, meaning that the simplex $\{\{v_1\}, \ldots, \{v_k\}\}$ is a minimal nonface of $\mathcal{N}(G)$. In fact the following straightforward characterization of nonflag "digraphical" nested complexes holds.

Lemma 4.14. *Let G be a simple digraph. Let $\mathcal{M}(G)$ be the graph whose vertices are the strongly connected induced subgraphs of G and where $t_1 \to t_2$ is an edge if $t_1 \cap t_2 = \varnothing$ and there is an edge in G from a vertex in t_1 to a vertex in t_2. Then $\mathcal{N}(G)$ is flag if and only if $\mathcal{M}(G)$ does not contain any induced directed cycle of length at least 3.*

Proof (Sketch). The proof follows the same lines as before, replacing v_i's by t_i's in a directed induced cycle of $\mathcal{M}(G)$ for the "if" part. For the "only if" part, one derives easily from the direct translation of having a minimal nonface in $\mathcal{N}(G)$ that no t in such a nonface can have indegree nor outdegree at least 2 in $\mathcal{M}(G)$.   ■

Question 4.15. Are all nested complexes the cluster complexes of some LP-algebras?

4.4.3   Towards a d-vector construction

To conclude this chapter, recall the existence of **d**-vectors, implied by the Laurent phenomenon (Theorem 4.11). Preliminary computations indicate that these vectors do not behave as comfortably as in finite type cluster algebras. In particular their entries do depend on the whole initial seed, and not separately from each initial variable. Even worse, their entries cannot encode compatibility of cluster variables in flag cluster complexes. Indeed, even in this case, if an initial variable x° and another cluster variable x belong to a common cluster, the exponent of x° in x need not be 0, depending on the initial cluster X°. However our experiments suggest that for linear LP-algebras, the **d**-vectors still support a complete simplicial fan realizing the cluster complex.

Question 4.16. For which LP-algebras $\mathcal{A}$ with finite cluster complex, and for which initial clusters X°, do the **d**-vectors calculated with respect to X° support a complete simplicial fan realizing the cluster complex of $\mathcal{A}$?

<div style="text-align: right; font-weight: bold; font-size: 3em;">5</div>

Graph properties of graph associahedra

5.1 Introduction

5.1.1 Motivations

In this chapter, we consider graph properties, namely the diameter, decomposition in Cartesian products and Hamiltonicity, of the flip graphs of nested complexes. For the n-permutahedron, the diameter of the *transposition graph* is the number $\binom{n+1}{2}$ of inversions of the longest permutation of $[n+1]$. Moreover, H. Steinhaus [Ste64], S. Johnson [Joh63], and H. Trotter [Tro62] independently designed an algorithm to construct a Hamiltonian cycle of this graph. On the other hand, the diameter of the associahedron motivated intensive research and relevant approaches, involving volumetric arguments in hyperbolic geometry [STT88] and combinatorial properties of Thompson's groups [Deh10]. Recently, L. Pournin gave a purely combinatorial proof that the diameter of the n-associahedron is precisely $2n - 4$ as soon as $n \geq 9$ [Pou14]. Moreover J. Lucas [Luc87] proved that its graph is Hamiltonian, after which F. Hurtado and M. Noy [HN99] obtained a simpler proof of this result, using a hierarchy of triangulations organizing all triangulations of convex polygons into an infinite generating tree.

5.1.2 Overview

Motivated by the examples of the associahedron and the permutahedron, we prove in this chapter structural properties, bounds of the diameter and some geodesic properties of the flip graphs of graph associahedra and nested complexes. Based on an inductive decomposition of graph associahedra, we also show the following statement.

Theorem 5.1. *For a graph* G *with at least two edges, the flip graph* $\mathcal{F}(\mathrm{G})$ *is Hamiltonian.*

If the strategy of the proof of Theorem 5.1 is quite elegant, its actual formalization has to go through heavy case analyses. Therefore we delay the section devoted to it to Appendix A. In Section 5.2, we give additional preliminaries on graph associahedra. In Section 5.3, we study diameter and geodesic properties of the flip graphs of graph associahedra, with some extensions to general nested complexes. Finally we characterize in Section 5.4 those nested complexes that decompose into joins of other simplicial complexes.

5.2   Preliminaries

5.2.1   Proper and nonproper tubes

Until now, we did not pay that much attention about the distinction between *proper* and *nonproper* elements of building sets that we encountered. These notions will however be very helpful in order to clarify the presentation of Section 5.3.

We consider a simple graph G with vertex set V and κ connected components. A tube is *proper* if it does not induce a connected component of G. A tubing is *proper* if it contains only proper tubes and *loaded* if it contains $B(G)_{max}$. Since inclusion maximal tubes are compatible with all tubes, we can transform any tubing T into a proper tubing $T \setminus B(G)_{max}$ or into a loaded tubing $T \cup B(G)_{max}$, and we switch along the chapter to whichever version better suits the current purpose. Observe by the way that maximal tubings are automatically loaded. Figure 5.1 illustrates these notions on a graph with 9 vertices.
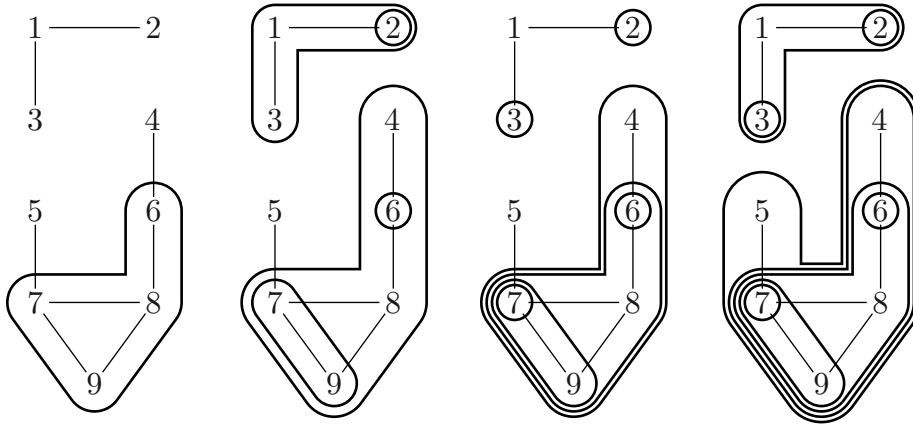
Figure 5.1 – from left to right: a proper tube, a tubing, a maximal proper tubing, and a maximal (loaded) tubing.

With this terminology the nested complex $\mathcal{N}(G)$ is the set of all proper tubings on G, and the flip graph $\mathcal{F}(G)$ is the graph whose vertices are the maximal proper tubings on G and whose edges connect maximal proper tubings related by a flip. We refer to Figures 4.3 and 5.2 for illustrations, and to Section 5.2.3 for a description of flips in tubings. To avoid confusion, we always use the term *edge* for the edges of the graph G, and the term *flip* for the edges of the flip graph $\mathcal{F}(G)$. To simplify the presentation, it is sometimes more convenient to consider the *loaded flip graph*, obtained from $\mathcal{F}(G)$ by loading all its vertices with $B(G)_{max}$, and that we abusively still denote by $\mathcal{F}(G)$. Note that only proper tubes can be flipped in each maximal tubing on the loaded flip graph.

5.2.2   Spines

Spines provide convenient representations of the tubings on G. For a tubing T on G and a tube t of $T \cup \kappa(G)$, we define $\lambda(t, T) := t \setminus \bigcup_{t' \in T, t' \subsetneq t} t'$. The sets $\lambda(t, T)$ for $t \in T \cup \kappa(G)$ form a partition of the vertex set of G. When T is a maximal tubing, each set $\lambda(t, T)$ contains a unique vertex of G that we call the *root* of t in T. The *spine* S of T is the Hasse diagram of the inclusion poset on $T \cup B(G)_{max}$, where the node corresponding to a tube $t \in T \cup B(G)_{max}$ is labeled by $\lambda(t, T)$ (see Figure 5.2 for an illustration). Spines are called $B(G)$-forests in [Pos09] and can be defined in full generality for nested complexes.

For a tubing T on a graph G, with associated spine S, the compatibility condition on the tubes of T implies that S is a rooted forest, where roots correspond to elements

of $B(G)_{max}$. The tubes of $T \cup B(G)_{max}$ are the descendants sets $\mathrm{desc}(s, S)$ of the nodes s of the forest S, where $\mathrm{desc}(s, S)$ denotes the union of the labels of the descendants of s in S, including s itself. The tubing $T \cup B(G)_{max}$ is maximal if and only if all labels are singletons, and we then identify nodes with their labels (see again Figure 5.2).

Let $T, \bar{T}$ be tubings on G with corresponding spines $S, \bar{S}$. Then $\bar{T} \subseteq T$ if and only if $\bar{S}$ is obtained from S by edge contractions. We say that S *refines* $\bar{S}$, that $\bar{S}$ *coarsens* S, and we write $\bar{S} \prec S$. Given any node s of S, we denote by S_s the *subspine* of S induced by all descendants of s in S, including s itself.

5.2.3 Flips

As already mentioned, the nested complex $\mathcal{N}(G)$ is a sphere, which induces a natural flip operation on maximal proper tubings on G: for any maximal proper tubing T on G and any tube $t \in T$, there is a unique proper tube $t' \notin T$ of G such that $T' := T \triangle \{t, t'\}$ is again a proper tubing on G. We denote this flip by $T \leftrightarrow T'$. The flip operation is then described by the following proposition, whose proof is left to the reader.

Proposition 5.2. *Let t be a tube in a maximal tubing T on G, and let $\bar{t}$ be the inclusion minimal tube of $T \cup \kappa(G)$ which strictly contains t. Then the unique tube t' such that $T' = T \triangle \{t, t'\}$ is again a maximal tubing on G is the connected component of $G[\bar{t} \smallsetminus \lambda(t, T)]$ containing $\lambda(\bar{t}, T)$.*

Remark 5.3. For the same reasons as for graph associahedra, there is a notion of flips on maximal elements of any nested complex, that can be described exactly as in Proposition 5.2. Again we choose to state Proposition 5.2 only for graph associahedra since we will not need it in other contexts.

This description of flips translates to spines as follows. The flip between the tubings T and T' corresponds to a rotation between the corresponding spines S and S'. This operation is local: it only perturbs the nodes v and v' and their children. More precisely, v is a child of v' in S, and becomes the parent of v' in S'. Moreover, the children of v in S contained in t' become children of v' in S'. All other nodes keep their parents. Figure 5.2 illustrates a flip both on tubings and spines.
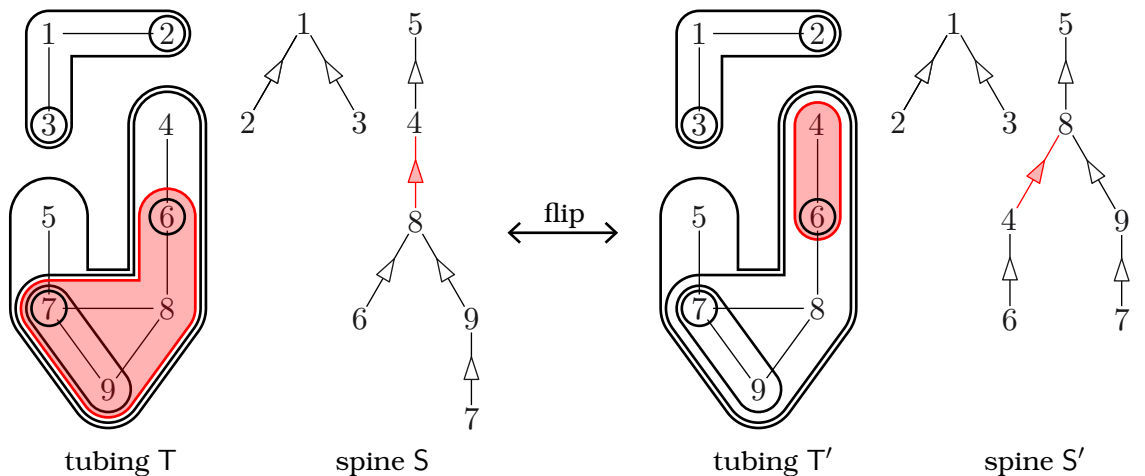
Figure 5.2 – The flip of a proper tube (shaded, red) in a maximal tubing seen both on the tubings and on the corresponding spines.

5.3 Diameter

Let $\delta(\mathcal{F}(\mathrm{G}))$ denote the diameter of the flip graph $\mathcal{F}(\mathrm{G})$. For example, for the complete graph K_{n+1}, the diameter of the n-dimensional permutahedron is $\delta(\mathcal{F}(K_{n+1})) = \binom{n+1}{2}$, while for the path P_{n+1}, the diameter of the classical n-dimensional associahedron is $\delta(\mathcal{F}(\mathrm{P}_{n+1})) = 2n - 4$ for $n > 9$, by results of [STT88, Pou14]. We discuss in this section properties of the diameter $\delta(\mathcal{F}(\mathrm{G}))$ and of the geodesics in the flip graph $\mathcal{F}(\mathrm{G})$. The results of Section 5.3.1 are extended to nestohedra in Section 5.3.2. We prefer to present the ideas first on graph associahedra as they prepare the intuition for the more technical proofs on nestohedra.

5.3.1 Nondecreasing diameters

Our first purpose is to show that $\delta(\mathcal{F}(\cdot))$ is nondecreasing.

Theorem 5.4. $\delta(\mathcal{F}(\bar{\mathrm{G}})) \leq \delta(\mathcal{F}(\mathrm{G}))$ *for any two graphs* $\mathrm{G}, \bar{\mathrm{G}}$ *such that* $\bar{\mathrm{G}} \subseteq \mathrm{G}$.

Remark 5.5. We could prove this statement by a geometric argument. Indeed, in the same spirit as this of Proposition 4.5, one could show that the graph associahedron $\mathsf{Asso}(\mathrm{G})$ can be obtained from the graph associahedron $\mathsf{Asso}(\bar{\mathrm{G}})$ by successive face truncations. Geometrically, this operation replaces the truncated face $\mathbf{F}$ by its Cartesian product with a simplex of codimension $\dim(\mathbf{F}) + 1$. Therefore, a path in the graph of $\mathsf{Asso}(\mathrm{G})$ naturally projects to a shorter path in the graph of $\mathsf{Asso}(\bar{\mathrm{G}})$. Even if the geometric formulation is much more intuitive, our proof is a purely combinatorial translation of it, which has the advantage to help formalizing the argument.

Observe first that deleting an isolated vertex in G does not change the nested complex $\mathcal{N}(\mathrm{G})$. We can thus assume that the graphs G and $\bar{\mathrm{G}}$ have the same vertex set and that $\bar{\mathrm{G}} = \mathrm{G} \smallsetminus \{(u,v)\}$ is obtained by deleting a single edge (u,v) from G. We define below a map Ω from tubings on G to tubings on $\bar{\mathrm{G}}$ which induces a surjection from the flip graph $\mathcal{F}(\mathrm{G})$ onto the flip graph $\mathcal{F}(\bar{\mathrm{G}})$. For consistency, we use t and T for tubes and tubings of G and $\bar{\mathsf{t}}$ and $\bar{\mathsf{T}}$ for tubes and tubings of $\bar{\mathrm{G}}$.

Given a tube t of G (proper or not), define $\Omega(\mathsf{t})$ to be the coarsest partition of t into tubes of $\bar{\mathrm{G}}$. In other words, $\Omega(\mathsf{t}) = \{\mathsf{t}\}$ if (u,v) is not an isthmus of $\mathrm{G}[\mathsf{t}]$, and otherwise $\Omega(\mathsf{t}) = \{\bar{\mathsf{t}}_u, \bar{\mathsf{t}}_v\}$ where $\bar{\mathsf{t}}_u$ and $\bar{\mathsf{t}}_v$ are the vertex sets of the connected components of $\bar{\mathrm{G}}[\mathsf{t}]$ containing u and v respectively. For a set of tubes T of G, define $\Omega(\mathsf{T}) := \bigcup_{\mathsf{t} \in \mathsf{T}} \Omega(\mathsf{t})$. See Figure 5.3 for an illustration.

Lemma 5.6. *For any tubing* T *on* G, *the set* $\Omega(\mathsf{T})$ *is a tubing on* $\bar{\mathrm{G}}$ *and* $|\mathsf{T}| \leq |\Omega(\mathsf{T})|$.

Proof. It is immediate to see that Ω sends tubings on G to tubings on $\bar{\mathrm{G}}$. We prove by induction on $|\mathsf{T}|$ that $|\mathsf{T}| \leq |\Omega(\mathsf{T})|$. Consider a nonempty tubing T, and let t be an inclusion maximal tube of T. By induction hypothesis, $|\mathsf{T} \smallsetminus \{\mathsf{t}\}| \leq |\Omega(\mathsf{T} \smallsetminus \{\mathsf{t}\})|$. We now distinguish two cases:

(i) If (u,v) is an isthmus of $\mathrm{G}[\mathsf{t}]$, then $\Omega(\mathsf{t}) = \{\bar{\mathsf{t}}_u, \bar{\mathsf{t}}_v\} \not\subseteq \Omega(\mathsf{T} \smallsetminus \{\mathsf{t}\})$. Indeed, since $\bar{\mathsf{t}}_u$ and $\bar{\mathsf{t}}_v$ are adjacent in G, two tubes of T whose images by Ω produce $\bar{\mathsf{t}}_u$ and $\bar{\mathsf{t}}_v$ must be nested. Therefore, one of them contains both $\bar{\mathsf{t}}_u$ and $\bar{\mathsf{t}}_v$, and thus equals $\mathsf{t} = \bar{\mathsf{t}}_u \cup \bar{\mathsf{t}}_v$ by maximality of t in T.

(ii) If (u,v) is not an isthmus of $\mathrm{G}[\mathsf{t}]$, then $\Omega(\mathsf{t}) = \{\mathsf{t}\} \not\subseteq \Omega(\mathsf{T} \smallsetminus \{\mathsf{t}\})$. Indeed, if $\mathsf{t}' \in \mathsf{T}$ is such that $\mathsf{t} \in \Omega(\mathsf{t}')$, then $\mathsf{t} \subseteq \mathsf{t}'$ and thus $\mathsf{t} = \mathsf{t}'$ by maximality of t in T.

We conclude that $|\Omega(\mathsf{T})| \geq |\Omega(\mathsf{T} \smallsetminus \{\mathsf{t}\})| + 1 \geq |\mathsf{T} \smallsetminus \{\mathsf{t}\}| + 1 = |\mathsf{T}|$.   ∎
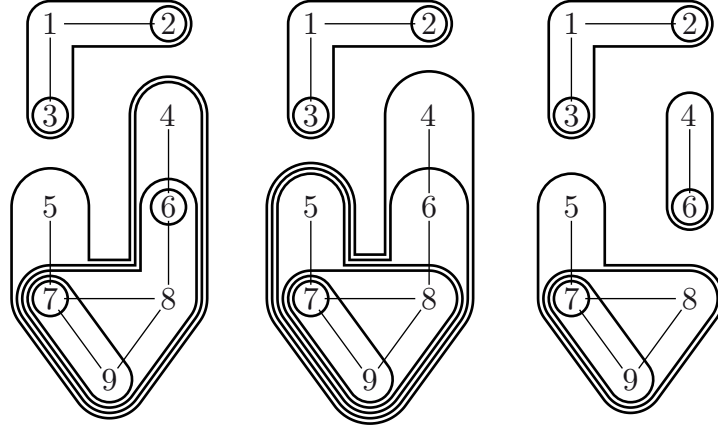
Figure 5.3 – Two maximal tubings (left and middle) with the same image by the map Ω (right). The middle tubing is the preimage of the rightmost tubing obtained by the process decribed in the proof of Corollary 5.7 with $u = 6$ and $v = 8$.

Corollary 5.7. *The map Ω induces a graph surjection from the loaded flip graph $\mathcal{F}(G)$ onto the loaded flip graph $\mathcal{F}(\bar{G})$, i.e. a surjective map from maximal tubings on G to maximal tubings on $\bar{G}$ such that adjacent tubings on G are sent to identical or adjacent tubings on $\bar{G}$.*

Proof. Let $\bar{\mathsf{T}}$ be a tubing on $\bar{G}$. If all tubes of $\bar{\mathsf{T}}$ containing u also contain v (or the opposite), then $\bar{\mathsf{T}}$ is a tubing on G and $\Omega(\bar{\mathsf{T}}) = \bar{\mathsf{T}}$. Otherwise, let $\bar{\mathsf{T}}_u$ denote the set of tubes of $\bar{\mathsf{T}}$ containing u but not v and $\bar{\mathsf{t}}_v$ denote the maximal tube containing v but not u. Then $(\bar{\mathsf{T}} \smallsetminus \bar{\mathsf{T}}_u) \cup \left\{ \bar{\mathsf{t}}_u \cup \bar{\mathsf{t}}_v \,\middle|\, \bar{\mathsf{t}}_u \in \bar{\mathsf{T}}_u \right\}$ is a tubing on G whose image by Ω is $\bar{\mathsf{T}}$. See Figure 5.3 for an illustration. The map Ω is thus surjective from tubings on G to tubings on $\bar{G}$. Moreover, any preimage $\mathsf{T}_\circ$ of a maximal tubing $\bar{\mathsf{T}}$ can be completed into a maximal tubing T with $\Omega(\mathsf{T}) \supseteq \Omega(\mathsf{T}_\circ) = \bar{\mathsf{T}}$, and thus satisfying $\Omega(\mathsf{T}) = \bar{\mathsf{T}}$ by maximality of $\bar{\mathsf{T}}$.

Remember that two distinct maximal tubings on G are adjacent if and only if they share precisely $|V| - 1$ common tubes. Consider two adjacent maximal tubings T, T' on G, so that $|\mathsf{T} \cap \mathsf{T}'| = |V| - 1$. Since $\Omega(\mathsf{T} \cap \mathsf{T}') \subseteq \Omega(\mathsf{T}) \cap \Omega(\mathsf{T}')$ and $|\Omega(\mathsf{T} \cap \mathsf{T}')| \geq |\mathsf{T} \cap \mathsf{T}'|$ by Lemma 5.6, we have $|\Omega(\mathsf{T}) \cap \Omega(\mathsf{T}')| \geq |\mathsf{T} \cap \mathsf{T}'| = |V| - 1$. The tubings $\Omega(\mathsf{T}), \Omega(\mathsf{T}')$ are thus adjacent if $|\Omega(\mathsf{T}) \cap \Omega(\mathsf{T}')| = |\mathsf{T} \cap \mathsf{T}'|$ and equal if $|\Omega(\mathsf{T}) \cap \Omega(\mathsf{T}')| > |\mathsf{T} \cap \mathsf{T}'|$. ∎

Remark 5.8. We can in fact precisely describe the preimage $\Omega^{-1}(\bar{\mathsf{T}})$ of a maximal tubing $\bar{\mathsf{T}}$ on $\bar{G}$ as follows. As in the previous proof, let $\bar{\mathsf{T}}_u$ denote the chain of tubes of $\bar{\mathsf{T}}$ containing u but not v and similarly $\bar{\mathsf{T}}_v$ denote the chain of tubes of $\bar{\mathsf{T}}$ containing v but not u. Any linear extension L of these two chains defines a preimage of $\bar{\mathsf{T}}$ where the tubes of $\bar{\mathsf{T}}_u \cup \bar{\mathsf{T}}_v$ are replaced by the tubes $\bigcup \{ \mathsf{t}' \in \mathsf{L} \mid \mathsf{t}' \leq_\mathsf{L} \mathsf{t} \}$ for $\mathsf{t} \in \mathsf{L}$. In terms of spines, this translates to shuffling the two chains corresponding to $\bar{\mathsf{T}}_u$ and $\bar{\mathsf{T}}_v$. Details are left to the reader.

Proof of Theorem 5.4. Consider two maximal tubings $\bar{\mathsf{T}}, \bar{\mathsf{T}}'$ on $\bar{G}$. Let T, T' be maximal loaded tubings on G such that $\Omega(\mathsf{T}) = \bar{\mathsf{T}}$ and $\Omega(\mathsf{T}') = \bar{\mathsf{T}}'$ (surjectivity of Ω), and $\mathsf{T} = \mathsf{T}_0, \ldots, \mathsf{T}_\ell = \mathsf{T}'$ be a geodesic between them ($\ell \leq \delta(\mathcal{F}(G))$). Deleting repetitions in the sequence $\bar{\mathsf{T}} = \Omega(\mathsf{T}_0), \ldots, \Omega(\mathsf{T}_\ell) = \bar{\mathsf{T}}'$ yields a path from $\bar{\mathsf{T}}$ to $\bar{\mathsf{T}}'$ (Corollary 5.7) of length at most $\ell \leq \delta(\mathcal{F}(G))$. So $\delta(\mathcal{F}(G)) \geq \delta(\mathcal{F}(\bar{G}))$. ∎

5.3.2　Extension to nestohedra

The results of the previous section can be extended to the nested complex on an arbitrary building set. Although the proofs are more abstract and technical, the ideas behind are essentially the same.

For any building set B we call *proper* the elements of $B \smallsetminus B_{\max}$, where $B_{\max}$ again denotes the set of inclusion maximal elements of B.

As before, a B-nested set N is *proper* if $N \cap B_{\max} = \varnothing$ and *loaded* if $B_{\max} \subseteq N$. The nested complex $\mathcal{N}(B)$ is, with this terminology the set of all proper nested sets on B. We denote by $\delta(\mathcal{F}(B))$ the diameter of the dual graph $\mathcal{F}(B)$ of $\mathsf{Nest}(B)$. As previously, it is more convenient to regard the vertices of $\mathcal{F}(B)$ as maximal loaded nested sets.

The *spine* of a nested set N is the Hasse diagram of the inclusion poset of $N \cup B_{\max}$. Spines are called B-forests in [Pos09]. The definitions and properties of Section 5.2.2 extend to general building sets, see [Pos09] for details.

We shall now prove the following generalization of Theorem 5.4.

Theorem 5.9. $\delta(\mathcal{F}(\bar{B})) \leq \delta(\mathcal{F}(B))$ *for any two building sets* $B, \bar{B}$ *on* V *such that* $\bar{B} \subseteq B$.

The proof follows the same line as that of Theorem 5.4. We first define a map Ω which transforms elements of B to subsets of $\bar{B}$ as follows: for $b \in B$ (proper or not), define $\Omega(b)$ as the coarsest partition of b into elements of $\bar{B}$. Observe that $\Omega(b)$ is well-defined since $\bar{B}$ is a building set, and that the elements of $\Omega(b)$ are precisely the inclusion maximal elements of $\bar{B}$ contained in b. For a nested set N on B, we define $\Omega(N) := \bigcup_{n \in N} \Omega(n)$. The following statement is similar to Lemma 5.6.

Lemma 5.10. *For any* $N \in \mathcal{N}(B)$, *the image* $\Omega(N)$ *belongs to* $\mathcal{N}(\bar{B})$ *and* $|N| \leq |\Omega(N)|$.

Proof. Consider a nested set N on B. To prove that $\Omega(N)$ is a nested set on $\bar{B}$, we start with condition (N1). Let $\bar{n}, \bar{n}' \in \Omega(N)$ and let $n, n' \in N$ such that $\bar{n} \in \Omega(n)$ and $\bar{n}' \in \Omega(n')$. Since N is nested, we can distinguish two cases:

- Assume that n and n' are disjoint. Then $\bar{n} \cap \bar{n}' = \varnothing$ since $\bar{n} \subseteq n$ and $\bar{n}' \subseteq n'$.

- Assume that n and n' are nested, *e.g.* $n \subseteq n'$. If $\bar{n} \cap \bar{n}' \neq \varnothing$, then $\bar{n} \cup \bar{n}'$ is in $\bar{B}$ and is a subset of n'. By maximality of $\bar{n}'$ in n', we obtain $\bar{n} \cup \bar{n}' = \bar{n}'$, and thus $\bar{n} \subseteq \bar{n}'$.

To prove Condition (N2), consider pairwise disjoint elements $\bar{n}_1, \ldots, \bar{n}_k \in \Omega(N)$ with respective preimages $n_1, \ldots, n_k \in N$, that is $\bar{n}_i \in \Omega(n_i)$ for all $i \in [k]$. We assume, for sake of contradiction, that $\bar{n} := \bar{n}_1 \cup \cdots \cup \bar{n}_k \in \bar{B}$ and we prove that $n := n_1 \cup \cdots \cup n_k \in B$. Indeed, $\bar{n}, n_1, \ldots, n_k$ all belong to B and $\bar{n} \cap n_i \neq \varnothing$ (it contains $\bar{n}_i$) so that $\bar{n} \cup n$ also belongs to B by multiple applications of Property (B1) of building sets. Moreover, $\bar{n} \subseteq n$ so that $n = \bar{n} \cup n \in B$. Finally, we conclude distinguishing two cases:

- If there is $i \in [k]$ such that n_i contains all n_j, then n_i contains all $\bar{n}_j$ and thus $\bar{n}$. This contradicts the maximality of $\bar{n}_i$ in n_i since $\bar{n}_i \subsetneq \bar{n} \in \bar{B}$.

- Otherwise, merging intersecting elements allows us to assume that $n_1, \ldots, n_k$ are pairwise disjoint and $n := n_1 \cup \cdots \cup n_k \in B$ contradicts Condition (N2) for N.

This concludes the proof that $\Omega(N)$ is a nested set on $\bar{B}$.

We now prove that $|N| \leq |\Omega(N)|$ by induction on $|N|$. Consider a nonempty nested set N and let $n_\circ$ be an inclusion maximal element of N. By induction hypothesis, $|N \smallsetminus \{n_\circ\}| \leq |\Omega(N \smallsetminus \{n_\circ\})|$. Let $\Omega(n_\circ) = \{\bar{n}_1, \ldots, \bar{n}_k\}$. Consider $n_1, \ldots, n_k \in N$ such that $\bar{n}_i \in \Omega(n_i)$, and let $n := n_1 \cup \cdots \cup n_k$. As $n_\circ, n_1, \ldots, n_k$ all belong to B and $n_\circ \cap n_i \neq \varnothing$ (it contains $\bar{n}_i$), we have $n_\circ \cup n \in B$ by multiple applications of Property (B1) of building sets. Moreover, $n_\circ \subseteq n$ so that $n = n_\circ \cup n \in B$. It follows by Condition (N2) on N that

there is $i \in [k]$ such that n_i contains all n_j, and thus $\mathsf{n}_\circ \subseteq \mathsf{n}_i$. We obtain that $\mathsf{n}_\circ = \mathsf{n}_i$ by maximality of $\mathsf{n}_\circ$. We conclude that $\mathsf{n}_\circ$ is the only element of N such that $\bar{\mathsf{n}}_i \in \Omega(\mathsf{n}_\circ)$, so that $|\Omega(\mathsf{N})| \geq |\Omega(\mathsf{N} \smallsetminus \{\mathsf{n}_\circ\})| + 1 \geq |\mathsf{N} \smallsetminus \{\mathsf{n}_\circ\}| + 1 = |\mathsf{N}|$. ∎

Corollary 5.11. *The map Ω induces a graph surjection from the loaded flip graph $\mathcal{F}(\mathsf{B})$ onto the loaded flip graph $\mathcal{F}(\bar{\mathsf{B}})$, i.e. a surjective map from maximal nested sets on B to maximal nested sets on $\bar{\mathsf{B}}$ such that adjacent nested sets on B are sent to identical or adjacent nested sets on $\bar{\mathsf{B}}$.*

Proof. To prove the surjectivity, consider a nested set $\bar{\mathsf{N}}$ on $\bar{\mathsf{B}}$. The elements of $\bar{\mathsf{N}}$ all belong to B and satisfy Condition (N1) for nested sets. It remains to transform the elements in $\bar{\mathsf{N}}$ which violate Condition (N2). If there is no such violation, then $\bar{\mathsf{N}}$ is a nested set on B and $\Omega(\bar{\mathsf{N}}) = \bar{\mathsf{N}}$. Otherwise, consider pairwise disjoint elements $\bar{\mathsf{n}}_1, \ldots, \bar{\mathsf{n}}_k$ of $\bar{\mathsf{N}}$ such that $\mathsf{n} := \bar{\mathsf{n}}_1 \cup \cdots \cup \bar{\mathsf{n}}_k$ is in B and is maximal for this property. Consider the subset $\bar{\mathsf{N}}' := (\bar{\mathsf{N}} \smallsetminus \{\bar{\mathsf{n}}_1\}) \cup \{\mathsf{n}\}$ of B. Observe that:

- $\bar{\mathsf{N}}'$ still satisfies Condition (N1). Indeed, if $\bar{\mathsf{n}} \in \bar{\mathsf{N}}$ is such that $\mathsf{n} \cap \bar{\mathsf{n}} \neq \varnothing$, then $\bar{\mathsf{n}}$ intersects at least one element $\bar{\mathsf{n}}_i$. Since $\bar{\mathsf{N}}$ is nested, $\bar{\mathsf{n}} \subseteq \bar{\mathsf{n}}_i$ or $\bar{\mathsf{n}}_i \subseteq \bar{\mathsf{n}}$. In the former case, $\bar{\mathsf{n}} \subseteq \mathsf{n}$ and we are done. In the latter case, $\bar{\mathsf{n}}$ and the elements $\bar{\mathsf{n}}_j$ disjoint from $\bar{\mathsf{n}}$ would contradict the maximality of n.

- $\bar{\mathsf{N}}'$ still satisfies $\Omega(\bar{\mathsf{N}}') = \bar{\mathsf{N}}$. Indeed, $\bar{\mathsf{n}}_1 \in \Omega(\mathsf{n})$ since $\Omega(\mathsf{n}) = \{\bar{\mathsf{n}}_1, \ldots, \bar{\mathsf{n}}_k\}$. For the latter equality, observe that $\{\bar{\mathsf{n}}_1, \ldots, \bar{\mathsf{n}}_k\}$ is a partition of n into elements of $\bar{\mathsf{B}}$ and that a coarser partition would contradict Condition (N2) on $\bar{\mathsf{N}}$.

- n cannot be partitioned into two or more elements of $\bar{\mathsf{N}}'$. Such a partition would refine the partition $\Omega(\mathsf{n})$, and would thus contradict again Condition (N2) on $\bar{\mathsf{N}}$. Therefore, $\bar{\mathsf{N}}'$ has strictly less violations of Condition (N2) than $\bar{\mathsf{N}}$.

- All violations of Condition (N2) in $\bar{\mathsf{N}}'$ only involve elements of $\bar{\mathsf{B}}$. Indeed, pairwise disjoint elements $\bar{\mathsf{n}}'_1, \ldots, \bar{\mathsf{n}}'_\ell \in \bar{\mathsf{N}}'$ disjoint from n and such that $\mathsf{n} \cup \bar{\mathsf{n}}'_1 \cup \cdots \cup \bar{\mathsf{n}}'_\ell \in \mathsf{B}$ would contradict the maximality of n.

These four points enable us to decrease the number of violations of Condition (N2) until we reach a nested set N on B which still satisfies $\Omega(\mathsf{N}) = \bar{\mathsf{N}}$.

The second part of the proof is identical to that of Corollary 5.7. ∎

From Corollary 5.11, the proof of Theorem 5.9 is identical to that of Theorem 5.4.

5.3.3 Geodesic properties

In this section, we focus on properties of the geodesics in the graphs of nestohedra. We consider three properties for a face F of a polytope $\mathbf{P}$:

NLFP F has the *non-leaving-face property* in $\mathbf{P}$ if F contains all geodesics connecting two vertices of F in the graph of $\mathbf{P}$.

SNLFP F has the *strong non-leaving-face property* in $\mathbf{P}$ if any path connecting two vertices v, w of F in the graph of $\mathbf{P}$ and leaving the face F has at least two more steps than a geodesic between v and w.

EFP F has the *entering-face property* in $\mathbf{P}$ if for any vertices u, v, w of $\mathbf{P}$ such that $u \notin F$, $v, w \in F$, and u and v are neighbors in the graph of $\mathbf{P}$, there exists a geodesic connecting u and w whose first edge is the edge from u to v.
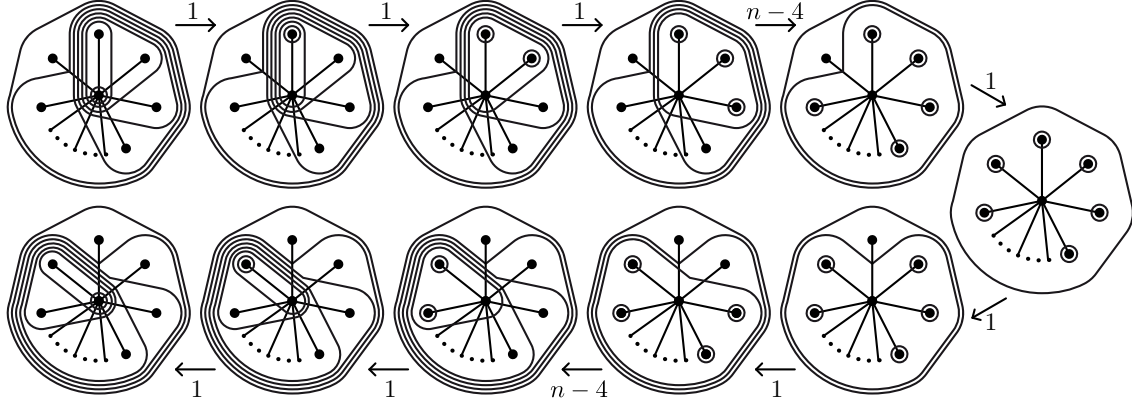
Figure 5.4 – A geodesic (of length $2n$) between two maximal tubings of the star that flips their common tube (the central vertex).

For a face F of a polytope $\mathbf{P}$, we have EFP $\iff$ SNLFP $\Rightarrow$ NLFP. However, the reverse of the last implication is wrong: all faces of a simplex have the NLFP (all vertices are at distance 1), but not the SNLFP. Alternative counterexamples with no simplicial face already exist in dimension 3. Among classical polytopes the n-dimensional cube, permutahedron, associahedron, and cyclohedron all satisfy the EFP. The NLFP is further discussed in [CP16].

Contrarily to the classical associahedron, not all faces of a graph associahedron have the NLFP. A counterexample is given by the star with n branches: Figure 5.4 shows a path of length $2n$ between two maximal tubings T, T', while the minimal face containing T and T' is an $(n-1)$-dimensional permutahedron (see the face description in [CD06, Theorem 2.9]) and the graph distance between T and T' in this face is $\binom{n}{2}$. It turns out however that the following faces of the graph associahedra, and more generally of nestohedra, always have the SNLFP.

Lemma 5.12. *We call* upper ideal face *of the nestohedron* $\mathrm{Nest}(\mathsf{B})$ *a face corresponding to a loaded nested set* $\mathsf{N}^{\uparrow}$ *that satisfies the following equivalent properties:*

(i) *any element of* B *not in* $\mathsf{N}^{\uparrow}$ *but compatible with* $\mathsf{N}^{\uparrow}$ *is contained in an inclusion minimal element of* $\mathsf{N}^{\uparrow}$,

(ii) *the set* $\lambda(\mathsf{n}, \mathsf{N}^{\uparrow}) := \mathsf{n} \smallsetminus \bigcup \left\{ \mathsf{n}' \in \mathsf{N}^{\uparrow} \,\middle|\, \mathsf{n}' \subsetneq \mathsf{n} \right\}$ *is a singleton for any inclusion nonminimal element* n *of* $\mathsf{N}^{\uparrow}$,

(iii) *the forest obtained by deleting all leaves of the spine* $\mathsf{S}^{\uparrow}$ *of* $\mathsf{N}^{\uparrow}$ *forms an upper ideal of any spine refining* $\mathsf{S}^{\uparrow}$.

Proof. We first prove that (i)⇒(ii). Assume that $\mathsf{n} \in \mathsf{N}^{\uparrow}$ is not inclusion minimal and that $\lambda(\mathsf{n}, \mathsf{N}^{\uparrow})$ contains two distinct elements $v, w \in \mathsf{V}$. One can then check that the maximal element of B contained in n and containing v but not w is compatible with $\mathsf{N}^{\uparrow}$, but not contained in an inclusion minimal element of $\mathsf{N}^{\uparrow}$. This proves that (i)⇒(ii).

Conversely, assume (ii) and consider $\mathsf{b} \in \mathsf{B}$ not in $\mathsf{N}^{\uparrow}$ but compatible with $\mathsf{N}^{\uparrow}$. Since $\mathsf{N}^{\uparrow}$ is loaded, there exists $\mathsf{n} \in \mathsf{N}^{\uparrow}$ strictly containing b and minimal for this property. Since b is compatible with $\mathsf{N}^{\uparrow}$, we obtain that $\lambda(\mathsf{n}, \mathsf{N}^{\uparrow})$ contains at least one element from b and one from $\mathsf{n} \smallsetminus \mathsf{b}$, and is thus not a singleton. It follows by (ii) that n is an inclusion minimal element of $\mathsf{N}^{\uparrow}$, and it contains b.

The equivalence (ii) $\iff$ (iii) follows directly from the definition of the spines and their labelings, and the fact that a nonsingleton node in a spine can be split in a refining spine. ∎

Proposition 5.13. *Any upper ideal face of the nestohedron* $\mathsf{Nest}(\mathsf{B})$ *satisfies* SNLFP.

Proof. Consider an upper ideal face F of $\mathsf{Nest}(\mathsf{B})$ corresponding to the loaded nested set $\mathsf{N}^\uparrow$. We consider the building set $\bar{\mathsf{B}} \subseteq \mathsf{B}$ on V consisting of all elements of B (weakly) contained in an inclusion minimal element of $\mathsf{N}^\uparrow$ together with all singletons $\{v\}$ for elements $v \in V$ not contained in any inclusion minimal element of $\mathsf{N}^\uparrow$. The reader is invited to check that $\bar{\mathsf{B}}$ is indeed a building set on V. It follows from Lemma 5.12 that

- $\lambda(\mathsf{n}, \mathsf{N}^\uparrow) = \mathsf{n}$ if n is an inclusion minimal element of $\mathsf{N}^\uparrow$,

- $\lambda(\mathsf{n}, \mathsf{N}^\uparrow) = \{v\}$ with v contained in no inclusion minimal element of $\mathsf{N}^\uparrow$ otherwise,

and thus that the map $\lambda(\cdot, \mathsf{N}^\uparrow)$ is a bijection from $\mathsf{N}^\uparrow$ to $\bar{\mathsf{B}}_{\max}$.

Consider the surjection Ω from the maximal nested sets on B to the maximal nested sets on $\bar{\mathsf{B}}$ as defined in the previous section: $\Omega(\mathsf{N}) = \bigcup_{\mathsf{n} \in \mathsf{N}} \Omega(\mathsf{n})$ where $\Omega(\mathsf{n})$ is the coarsest partition of n into elements of $\bar{\mathsf{B}}$. Following [STT88, CP16], we consider the *normalization* $\Omega^\star$ on maximal nested sets on B defined by $\Omega^\star(\mathsf{N}) := \big(\Omega(\mathsf{N}) \smallsetminus \bar{\mathsf{B}}_{\max}\big) \cup \mathsf{N}^\uparrow$. We claim that $\Omega^\star(\mathsf{N})$ is a maximal nested set on B:

- it is nested since both $\Omega(\mathsf{N}) \smallsetminus \bar{\mathsf{B}}_{\max}$ and $\mathsf{N}^\uparrow$ are themselves nested, and all elements of $\Omega(\mathsf{N}) \smallsetminus \bar{\mathsf{B}}_{\max}$ are contained in a minimal element of $\mathsf{N}^\uparrow$.

- it is maximal since $\Omega(\mathsf{N})$ also is (Corollary 5.11) and $|\Omega^\star(\mathsf{N})| = |\Omega(\mathsf{N})|$ for $\lambda(\cdot, \mathsf{N}^\uparrow)$ is a bijection from $\mathsf{N}^\uparrow$ to $\bar{\mathsf{B}}_{\max}$, and $\bar{\mathsf{B}}_{\max} \subseteq \Omega(\mathsf{N})$ while $\big(\Omega(\mathsf{N}) \smallsetminus \bar{\mathsf{B}}_{\max}\big) \cap \mathsf{N}^\uparrow = \varnothing$.

It follows that the map $\Omega^\star$ combinatorially projects the nestohedron $\mathsf{Nest}(\mathsf{B})$ onto its face F.

Let $\mathsf{N}_0, \ldots, \mathsf{N}_\ell$ be a path in the loaded flip graph $\mathcal{F}(\mathsf{B})$ whose endpoints $\mathsf{N}_0, \mathsf{N}_\ell$ lie in the face F, but which leaves the face F. In other words, $\mathsf{N}^\uparrow \subseteq \mathsf{N}_0, \mathsf{N}_\ell$ and there are $0 \leq i < j \leq \ell$ such that $\mathsf{N}^\uparrow \subseteq \mathsf{N}_i, \mathsf{N}_j$ while $\mathsf{N}^\uparrow \not\subseteq \mathsf{N}_{i+1}, \mathsf{N}_{j-1}$. We claim that

$$\Omega^\star(\mathsf{N}_0) = \mathsf{N}_0, \quad \Omega^\star(\mathsf{N}_\ell) = \mathsf{N}_\ell, \quad \Omega^\star(\mathsf{N}_i) = \mathsf{N}_i = \Omega^\star(\mathsf{N}_{i+1}) \quad \text{and} \quad \Omega^\star(\mathsf{N}_{j-1}) = \mathsf{N}_j = \Omega^\star(\mathsf{N}_j),$$

so that the path $\mathsf{N}_0 = \Omega^\star(\mathsf{N}_0), \ldots, \Omega^\star(\mathsf{N}_\ell) = \mathsf{N}_\ell$ from N_0 to N_ℓ in F has length at most $\ell - 2$ after deletion of repetitions.

To prove our claim, consider a loaded nested set N on B containing a maximal proper nested set $\bar{\mathsf{N}}$ on $\bar{\mathsf{B}}$. Then $\Omega(\mathsf{N}) \supseteq \Omega(\bar{\mathsf{N}}) = \bar{\mathsf{N}}$ so that $\Omega(\mathsf{N}) = \bar{\mathsf{N}} \cup \bar{\mathsf{B}}_{\max}$ by maximality of $\bar{\mathsf{N}}$. This shows $\Omega^\star(\mathsf{N}) = \bar{\mathsf{N}} \cup \mathsf{N}^\uparrow$. In particular, if $\mathsf{N} = \bar{\mathsf{N}} \cup \mathsf{N}^\uparrow$, then $\Omega^\star(\mathsf{N}) = \mathsf{N}$. Moreover, if N' is adjacent to $\mathsf{N} = \bar{\mathsf{N}} \cup \mathsf{N}^\uparrow$ and does not contain $\mathsf{N}^\uparrow$, then N' contains $\bar{\mathsf{N}}$ and $\Omega^\star(\mathsf{N}') = \mathsf{N}$. This shows the claim and concludes the proof. ∎

Proposition 5.13 specializes in particular to the non-leaving-face and entering face properties for the upper set faces of graph associahedra.

Proposition 5.14. *(i) If* T *and* T' *are two maximal tubings on* G, *then any maximal tubing on a geodesic between* T *and* T' *in the flip graph* $\mathcal{F}(G)$ *contains any common upper set to the inclusion posets of* T *and* T'.

(ii) If T, T' *and* T'' *are three maximal tubings on* G *such that* $\mathsf{T} \smallsetminus \{\mathsf{t}\} = \mathsf{T}' \smallsetminus \{\mathsf{t}'\}$ *and* t' *belongs to the maximal common upper set to the inclusion poset of* T' *and* T'', *then there is a geodesic between* T *and* T'' *starting by the flip from* T *to* T'.

Proof. Using Proposition 5.13, it is enough to show that the maximal common upper set $\mathsf{T}^\uparrow$ to the inclusion posets of T and T' defines an upper ideal face of $\mathsf{Asso}(G)$. For this, we use the characterization (ii) of Lemma 5.12. Consider an inclusion nonminimal tube t of $\mathsf{T}^\uparrow$. Let t' be a maximal tube of $\mathsf{T}^\uparrow$ such that $\mathsf{t}' \subsetneq \mathsf{t}$. Then t' has a unique neighbor v in $G[\mathsf{t}]$ and all connected components of $G[\mathsf{t} \smallsetminus \{v\}]$ are both in T and T', thus in $\mathsf{T}^\uparrow$. Thus $\lambda(\mathsf{t}, \mathsf{T}^\uparrow) = \{v\}$. ∎

Remark 5.15. For an arbitrary building set B, the maximal common upper set $\mathsf{N}^\uparrow$ to the inclusion poset of two maximal nested sets N, N' is not always an upper ideal face of $\mathsf{Nest}(\mathsf{B})$. A minimal example is the building set $\mathsf{B} = \{\{1\}, \{2\}, \{3\}, \{1,2,3\}\}$ and the nested sets $\mathsf{N} = \{\{1\}, \{2\}, \{1,2,3\}\}$ and $\mathsf{N}' = \{\{2\}, \{3\}, \{1,2,3\}\}$. Their maximal common upper set $\mathsf{N}^\uparrow = \{\{2\}, \{1,2,3\}\}$ is not an upper ideal face of $\mathsf{Nest}(\mathsf{B})$ since $\lambda(\{1,2,3\}, \mathsf{N}^\uparrow) = \{1,3\}$ is not a singleton. Moreover, the face corresponding to $\mathsf{N}^\uparrow$ does not satisfy SNLFP.

5.3.4   Diameter bounds

Using Theorem 5.4 and Proposition 5.14, the lower bound on the diameter of the associahedron [Pou14], the classical construction of graph associahedra of [CD06, Pos09] and the diameter of graphical zonotopes, we obtain the inequalities on the diameter $\delta(\mathcal{F}(G))$ of $\mathcal{F}(G)$.

Theorem 5.16. *For any connected graph G with $n + 1$ vertices and e edges, the diameter $\delta(\mathcal{F}(G))$ of the flip graph $\mathcal{F}(G)$ is bounded by*

$$\max(e, 2n - 18) \leq \delta(\mathcal{F}(G)) \leq \binom{n+1}{2}.$$

Proof. For the upper bound, we use that the diameter is nondecreasing (Theorem 5.4) and that the n-dimensional permutahedron has diameter $\binom{n+1}{2}$, the maximal number of inversions in a permutation of $\mathfrak{S}_{n+1}$.

The lower bound consists in two parts. For the first part, we know that the normal fan of the graph associahedron $\mathsf{Asso}(G)$ refines the normal fan of the graphical zonotope of G (see *e.g.* [Zie95, Lect. 7] for a reference on zonotopes). Indeed, the graph associahedron of G can be constructed as a Minkowski sum of the faces of the standard simplex corresponding to tubes of G ([CD06, Pos09]) while the graphical zonotope of G is the Minkowski sum of the faces of the standard simplex corresponding only to edges of G. Since the diameter of the graphical zonotope of G is the number e of edges of G, we obtain that the diameter $\delta(\mathcal{F}(G))$ is at least e. For the second part of the lower bound, we use again Theorem 5.4 to restrict the argument to trees. Let T be a tree on $n + 1$ vertices. We first discard some basic cases:

  (i) If T has precisely two leaves, then T is a path and the graph associahedron $\mathsf{Asso}(\mathsf{T})$ is the classical n-dimensional associahedron, whose diameter is known to be larger than $2n - 4$ by L. Pournin's result [Pou14].

 (ii) If T has precisely 3 leaves, then it consists in 3 paths attached by a 3-valent node v, see Figure 5.5 (left). Let w be a neighbor of v and $\mathsf{P}_1, \mathsf{P}_2$ denote the connected components of $\mathsf{T} \smallsetminus w$. Observe that P_1 and P_2 are both paths and denote by $p_1 + 1$ and $p_2 + 1$ their respective lengths. Let $\mathsf{T}'_1, \mathsf{T}''_1$ (resp. $\mathsf{T}'_2, \mathsf{T}''_2$) be a diametral pair of maximal tubings on P_1 (resp. on P_2), and consider the maximal tubings $\mathsf{T}' = \mathsf{T}'_1 \cup \mathsf{T}'_2 \cup \{\mathsf{P}_1, \mathsf{P}_2\}$ and $\mathsf{T}'' = \mathsf{T}''_1 \cup \mathsf{T}''_2 \cup \{\mathsf{P}_1, \mathsf{P}_2\}$ on the tree T. Finally, denote by T the maximal tubing on T obtained by flipping P_1 in T'. Since $\{\mathsf{P}_1, \mathsf{P}_2\}$ is a common upper set to the inclusion posets of T' and T'', Proposition 5.14 (ii)
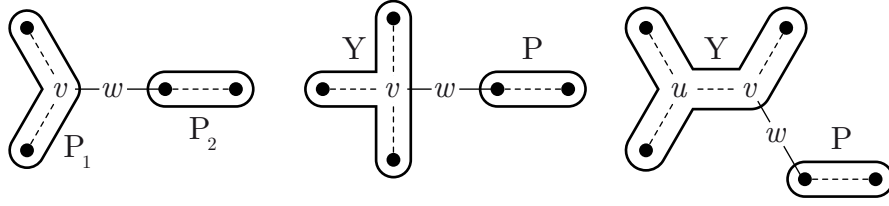
Figure 5.5 – Decompositions of trees with 3 or 4 leaves.

ensures that there exists a geodesic from T to T'' that starts by the flip from T to T'. Moreover, Proposition 5.14 (i) ensures that the distance between T' and T'' is realized by a path staying in the face of $\mathsf{Asso}(\mathsf{T})$ corresponding to $\{\mathsf{P}_1, \mathsf{P}_2\}$, which is the product of a classical p_1-dimensional associahedron by a classical p_2-dimensional associahedron. We conclude that

$$\delta(\mathcal{F}(\mathsf{T})) \geq 1 + \delta(\mathcal{F}(\mathsf{P}_1)) + \delta(\mathcal{F}(\mathsf{P}_2)) \geq 1 + (2p_1 - 4) + (2p_2 - 4) = 2(p_1 + p_2 + 2) - 11 = 2n - 11.$$

(iii) If T has precisely 4 leaves, it either contains a single 4-valent node v or precisely two 3-valent nodes u, v, see Figure 5.5 (middle and right). Define w to be a neighbor of v, not located in the path between u and v in the latter situation. Then w disconnects T into a path P on $p + 1$ nodes and a tree Y with $y + 1$ nodes and precisely 3 leaves. A similar argument as in (ii) shows that

$$\delta(\mathcal{F}(\mathsf{T})) \geq 1 + \delta(\mathcal{F}(\mathsf{P})) + \delta(\mathcal{F}(\mathsf{Y})) \geq 1 + (2p - 4) + (2y - 11) = 2(p + y + 2) - 18 = 2n - 18.$$

We can now assume that the tree T has $k \geq 5$ leaves $l_1, \ldots, l_k$. Let $\bar{\mathsf{V}} = \mathsf{V} \smallsetminus \{l_1, \ldots, l_k\}$ and $\bar{\mathsf{T}} = \mathsf{T}[\bar{\mathsf{V}}]$ denote the tree obtained by deleting the leaves of T. By induction hypothesis, there exist two maximal tubings $\bar{\mathsf{T}}$ and $\bar{\mathsf{T}}'$ on $\bar{\mathsf{T}}$ at distance at least $2(n - k) - 18$. Define $\mathsf{t}_i := \mathsf{V} \smallsetminus \{l_1, \ldots, l_i\}$ for $i \in [k]$, and $\mathsf{t}'_j := \mathsf{V} \smallsetminus \{l_j, \ldots, l_k\}$ for $j \in [k]$. Consider the maximal tubings $\mathsf{T} := \bar{\mathsf{T}} \cup \{\mathsf{t}_1, \ldots, \mathsf{t}_k\}$ and $\mathsf{T}' := \bar{\mathsf{T}}' \cup \{\mathsf{t}'_1, \ldots, \mathsf{t}'_k\}$ on T. We claim that the distance between these tubings is at least $2n - 18$. To see it, consider the surjection Ω from the tubings on T onto that of $\bar{\mathsf{T}} \sqcup \{l_1, \ldots, l_k\}$ as defined in Section 5.3.1. It sends a path $\mathsf{T} = \mathsf{T}_0, \ldots, \mathsf{T}_\ell = \mathsf{T}'$ in the flip graph $\mathcal{F}(\mathsf{T})$ to a path

$$\bar{\mathsf{T}} \cup \{\{l_1\}, \ldots, \{l_k\}\} = \Omega(\mathsf{T}_0), \ldots, \Omega(\mathsf{T}_\ell) = \bar{\mathsf{T}}' \cup \{\{l_1\}, \ldots, \{l_k\}\}$$

in the flip graph $\mathcal{F}(\bar{\mathsf{T}} \sqcup \{l_1, \ldots, l_k\})$ with repeated entries. Since $\bar{\mathsf{T}}$ and $\bar{\mathsf{T}}'$ are at distance at least $2(n - k) - 18$ in the flip graph $\mathcal{F}(\bar{\mathsf{T}})$, this path has at least $2(n - k) - 18$ nontrivial steps, so we must show that it has at least $2k$ repetitions. These repetitions appear whenever we flip a tube t_i or t'_j. Indeed, we observe that the image $\Omega(\mathsf{t})$ of any tube $\mathsf{t} \in \{\mathsf{t}_i \mid i \in [k]\} \cup \left\{\mathsf{t}'_j \mid j \in [k]\right\}$ is composed by $\bar{\mathsf{V}}$ together with single leaves of T. Since all these tubes are connected components of $\bar{\mathsf{T}}$, we have $\Omega(\mathsf{T} \smallsetminus \{\mathsf{t}\}) = \Omega(\mathsf{T})$ for any maximal loaded tubing T containing t. To conclude, we distinguish three cases:

(i) If the tube $\mathsf{t}_k = \bar{\mathsf{V}} = \mathsf{t}'_1$ is never flipped along the path $\mathsf{T} = \mathsf{T}_0, \ldots, \mathsf{T}_\ell = \mathsf{T}'$, then we need at least $\binom{k}{2}$ flips to transform $\{\mathsf{t}_1, \ldots, \mathsf{t}_k\}$ into $\{\mathsf{t}'_1, \ldots, \mathsf{t}'_k\}$. This can be seen for example from the description of the link of t_k in $\mathcal{N}(\mathsf{T})$ in [CD06, Theorem 2.9]. Finally, we use that $\binom{k}{2} \geq 2k$ since $k \geq 5$.

(ii) Otherwise, we need to flip all $\{\mathsf{t}_1, \ldots, \mathsf{t}_k\}$ and then back all $\{\mathsf{t}'_1, \ldots, \mathsf{t}'_k\}$. If no flip of a tube t_i produces a tube t'_j, we need at least $2k$ flips which produces repetitions in $\Omega(\mathsf{T}_0), \ldots, \Omega(\mathsf{T}_\ell)$.

(iii) Finally, assume that we flip precisely once all tubes in $\{t_1, \ldots, t_k\}$ and then back all tubes in $\{t'_1, \ldots, t'_k\}$, and that a tube t_i is flipped into a tube t'_j. According to the description of flips, we have $i = k - 1$ and $j = 2$. If $p \in [\ell]$ denotes the position such that $T_p \smallsetminus \{t_{k-1}\} = T_{p+1} \smallsetminus \{t'_2\}$, we moreover know that $t_{k-1} \in T_q$ for $q \le p$, that $t'_2 \in T_q$ for $q > p$, and that $\bar{V} \in T_p \cap T_{p+1}$. Applying the non-leaving-face property either to the upper set $\{t_{k-1}, t_k\}$ in $\mathsf{Asso}(G[t_{k-1}])$ or to the upper set $\{t'_1, t'_2\}$ in $\mathsf{Asso}(G[t'_2])$, we conclude that it would shorten the path $T_0, \ldots, T_\ell$ to avoid the flip of $t_k = \bar{V} = t'_1$, which brings us back to Situation (i). ∎

Remark 5.17. We note that although asymptotically optimal, our lower bound $2n - 18$ is certainly not sharp. We expect the correct lower bound to be the bound $2n - 4$ for the associahedron. Better upper bound can also be worked out for certain families of graphs. For example, L. Pournin investigates the cyclohedra (cycle associahedra) in [Pou17]. As far as trees are concerned, we understand better stars and their subdivisions. The diameter $\delta(\mathcal{F}(K_{1,n}))$ for the star $K_{1,n}$ is exactly $2n$ (for $n \ge 5$), see Figure 5.4. In fact, the diameter of the graph associahedron of any starlike tree (subdivision of a star) on $n + 1$ vertices is bounded by $2n$. To see it, we observe that any tubing is at distance at most n from the tubing $T_\circ$ consisting in all tubes adjacent to the central vertex. Indeed, we can always flip a tube in a tubing distinct from $T_\circ$ to create a new tube adjacent to the central vertex. This argument is not valid for nonstarlike trees.

Remark 5.18. The lower bound in Theorem 5.16 shows that the diameter $\delta(\mathcal{F}(G))$ is at least the number of edges of G. In view of Theorem 5.9, it is tempting to guess that the diameter $\delta(\mathcal{F}(G))$ is of the same order as the number of edges of G. Adapting arguments from Remark 5.17, we can show that the diameter of any tree associahedron $\delta(\mathcal{F}(T))$ is of order at most $n \log n$. In any case, the following question remains open.

Question 5.19. Is there a family of trees T_n on n nodes such that $\delta(\mathcal{F}(T_n))$ is of order $n \log n$? Even more specifically, consider the family of trees illustrated in Figure 5.6: $T_1 = K_{1,3}$ (tripod) and T_{k+1} is obtained by grafting two leaves to each leaf of T_k. What is the order of the diameter $\delta(\mathcal{F}(T_k))$?

T_1 $\qquad$ T_2 $\qquad$ T_3 $\qquad$ T_4 $\qquad$ T_5
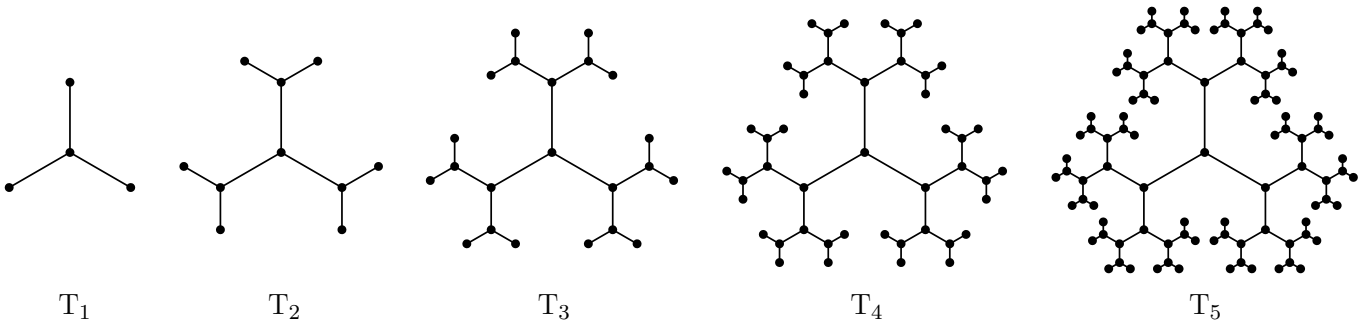
Figure 5.6 – The family of trees T_k: the tree T_1 is the tripod and T_{k+1} is obtained from T_k by connecting two new nodes to each leaf of T_k.

Remark 5.20. We ask Question 5.19 for the specific family $(T_k)_{k \in \mathbb{N}}$ of trees because we expect this family to achieve asymptotically the bound $n \log n$ that we previously mentioned. Yet proving it seems hard. Indeed we saw that the proof of Theorem 5.16 highly relies on L. Pournin's bound on the diameter of the associahedron. Finding an alternative way to prove sharp lower bounds on the diameter of some tree associahedra would on the contrary lead to new approaches to recover this very challenging result.

Remark 5.21. The upper bound $\delta(\mathcal{F}(\mathsf{B})) \leq \binom{n+1}{2}$ holds for an arbitrary building set B by Theorem 5.4 and the fact that the permutahedron is the nestohedron on the complete building set. In contrast, the lower bound is not valid for arbitrary connected building sets. For example, the nestohedron on the trivial connected building set

$$\{\{1\}, \ldots, \{n+1\}, \{1, \ldots, n+1\}\}$$

is the n-dimensional simplex, whose diameter is 1.

5.4 Decomposition of nested complexes into joins

We conclude this chapter with a characterization of all nested complexes that decompose as joins of smaller simplicial complexes. For a *connected* building set B, one could expect that the corresponding nested complex $\mathcal{N}(\mathsf{B})$ have no immediate decomposition into joins of other nested complexes. Yet the following construction, attributed to N. Erokhovets by V. Volodin in [Vol10, see Lemma 2 and Corollary 2 in the arXiv version], shows that any product of nested complexes is isomorphic to the nested complex of a connected building set. Let $\mathsf{B}_\circ$ be a building set on a ground set $\mathsf{V}_\circ = \{v_1, \ldots, v_{n+1}\}$ and $\mathsf{B}_1, \ldots, \mathsf{B}_{n+1}$ be $n+1$ connected building sets on respective disjoint ground sets $\mathsf{V}_1, \ldots, \mathsf{V}_{n+1}$. The *composition of* $\mathsf{B}_\circ$ *with* $\mathsf{B}_1, \ldots, \mathsf{B}_{n+1}$ is the set

$$\mathsf{B}_\circ(\mathsf{B}_1, \ldots, \mathsf{B}_{n+1}) := \mathsf{B}_1 \cup \cdots \cup \mathsf{B}_{n+1} \cup \left\{ \bigsqcup_{v_i \in \mathsf{b}} \mathsf{V}_i \; \middle| \; \mathsf{b} \in \mathsf{B}_\circ \right\}.$$

Observe that there are in fact $(n+1)!$ possible compositions of $\mathsf{B}_\circ$ with $\mathsf{B}_1, \ldots, \mathsf{B}_{n+1}$, corresponding to all possible ways to label the elements of $\mathsf{V}_\circ$. It is straightforward to check that the set $\mathsf{B}_\circ(\mathsf{B}_1, \ldots, \mathsf{B}_{n+1})$ satisfies the conditions of Definition 4.1, so that it is a building set on the ground set $\mathsf{V}_1 \sqcup \cdots \sqcup \mathsf{V}_{n+1}$. It is moreover clear from Definition 4.2 that the nested complex $\mathcal{N}(\mathsf{B}_\circ(\mathsf{B}_1, \ldots, \mathsf{B}_{n+1}))$ is isomorphic to the nested complex $\mathcal{N}(\mathsf{B}_\circ \sqcup \mathsf{B}_1 \sqcup \cdots \sqcup \mathsf{B}_{n+1}) \cong \mathcal{N}(\mathsf{B}_\circ) * \mathcal{N}(\mathsf{B}_1) * \cdots * \mathcal{N}(\mathsf{B}_{n+1})$.

Proposition 5.22 (attributed to N. Erokhovets in [Vol10])**.** *Any nested complex is isomorphic to the nested complex of some connected building set.*

Proof (Sketch). Assume that B is not connected and contains no inclusion maximal singleton, and let $\mathsf{b}_{\max}^1, \ldots, \mathsf{b}_{\max}^k$ be the elements of $\mathsf{B}_{\max}$. If $\ell = |\mathsf{b}_{\max}^1| \geq 2$, then using the composition of $\mathsf{B}_{|\mathsf{b}_{\max}^1}$ with other elements of $\mathsf{B}_{\max}$ (and potentially adding isolated singletons), we can construct a building set B' such that $|\mathsf{B}'_{\max}| < |\mathsf{B}_{\max}|$ and $\mathcal{N}(\mathsf{B}) \cong \mathcal{N}(\mathsf{B}')$. Since isolated singletons in B do not influence $\mathcal{N}(\mathsf{B})$, we conclude by induction. ∎

A building set B is *trivial* if it consists in a disjoint union of singletons, and it is *indecomposable* if the nested complex $\mathcal{N}(\mathsf{B})$ is not isomorphic to a join of at least two nontrivial simplicial complexes. Observe that an indecomposable building set B need not be connected. Indeed the disjoint union of an indecomposable building set and of a trivial building set is indecomposable but not connected. The following statement shows that the notion of indecomposability is the relevant one concerning potential decompositions of nested complexes into join of smaller simplicial complexes.

Proposition 5.23. *A building set B is indecomposable if and only if it is not of the form $\mathsf{B}_1 \sqcup \cdots \sqcup \mathsf{B}_{[n+1]}$ or $\mathsf{B}_\circ(\mathsf{B}_1, \ldots, \mathsf{B}_{[n+1]})$ for building sets $\mathsf{B}_\circ, \mathsf{B}_1, \ldots, \mathsf{B}_k$ with disjoint ground sets, such that at least two of them are nontrivial.*

Proof. The "only if" part directly follows from the properties of the composition of building sets. Let B be a building set with ground set V such that $\mathsf{B}_{\max}$ contains no singleton. We can assume that $|\mathsf{B}_{\max}| = 1$ since otherwise B is already a disjoint union of nontrivial building sets. We define the set

$$\bar{V} := \left\{ \mathsf{b} \in \mathsf{B} \smallsetminus \mathsf{B}_{\max} \mid \forall \mathsf{b}' \in \mathsf{B}, \mathsf{b} \cap \mathsf{b}' = \varnothing \text{ or } \mathsf{b} \subseteq \mathsf{b}' \text{ or } \mathsf{b}' \subseteq \mathsf{b} \right\}$$

that somehow constitutes the "real combinatorial ground set" of the building set B. Observe that $\bar{V}$ contains all singletons. Consider the set $\hat{V} = \{\mathsf{b}_1, \ldots, \mathsf{b}_k\}$ of inclusion maximal elements of $\bar{V}$. It is immediate that the set $\hat{\mathsf{B}}$ defined by

$$\hat{\mathsf{B}} := \left\{ \{\mathsf{b}_{i_1}, \ldots, \mathsf{b}_{i_p}\} \mid \forall j \in [p], \mathsf{b}_{i_j} \in \hat{V} \text{ and } \left(\bigcup_{j \in [p]} \mathsf{b}_{i_j} \right) \in \mathsf{B} \right\}$$

is a building set with ground set $\hat{V}$ and that $\mathsf{B} = \hat{\mathsf{B}}(\mathsf{B}_{|\mathsf{b}_1}, \ldots, \mathsf{B}_{|\mathsf{b}_k})$. Therefore B is a composition of at least two nontrivial building sets if $\bar{V}$ contains other elements than singletons. Assume that B is not indecomposable. Then B can be partitioned into two parts B_1 and B_2 which are the respective vertex sets of two simplicial complexes $\mathcal{C}_1$ and $\mathcal{C}_2$ such that $\mathcal{N}(\mathsf{B}) \cong \mathcal{C}_1 * \mathcal{C}_2$. Since the class of nested complexes is closed by links (see for instance [Zel06, Proposition 3.2]), the complexes $\mathcal{C}_1$ and $\mathcal{C}_2$ are isomorphic to some nontrivial nested complexes. Therefore both parts $\mathsf{B}_1, \mathsf{B}_2$ of B contain other elements than singletons. We can assume that V (the only element in $\mathsf{B}_{\max}$) is contained in B_1. Let now $\mathsf{b}_2^{\max}$ be an inclusion maximal element in B_2. Since $\mathcal{N}(\mathsf{B})$ is the join of $\mathcal{C}_1$ and $\mathcal{C}_2$, for any element $\mathsf{b}_1 \in \mathsf{B}_1$, the set $\{\mathsf{b}_2^{\max}, \mathsf{b}_1\}$ is a B-nested set, in particular $\mathsf{b}_1 \subseteq \mathsf{b}_2^{\max}$ or $\mathsf{b}_2^{\max} \subseteq \mathsf{b}_1$ or $\mathsf{b}_1 \cap \mathsf{b}_2^{\max} = \varnothing$. As we chose $\mathsf{b}_2^{\max}$ to be inclusion maximal in B_2, this property holds for any element in $\mathsf{B} = \mathsf{B}_1 \sqcup \mathsf{B}_2$. Since $V \in \mathsf{B}_1 \not\supseteq \mathsf{b}_2^{\max}$, we have that $\mathsf{b}_2^{\max} \notin \mathsf{B}_{\max}$ and so that $\mathsf{b}_2^{\max} \in \bar{V}$. The building set B is thus a composition of building sets as the set $\bar{V}$ does not only contain singletons. So any nonindecomposable building set that is not a disjoint union of nontrivial building sets is a composition of nontrivial building sets, which concludes the proof for the "if" part. ∎

Remark 5.24. After Proposition 5.23, the natural question to ask is whether there is a relevant description of isomorphisms between two given nested complexes. This is not an easy question, mainly because of our lack of rich combinatorial models to describe nested complexes in general. However, this question is settled for graphical nested complexes in Section 6.4.2 (see Theorem 6.37), where in particular *nontrivial* isomorphisms (not induced by permutations of the ground set) are exhibited.

<div style="text-align: right;">

6

</div>

Compatibility fans for graphical nested complexes

6.1 Introduction

6.1.1 Motivations

In this chapter, we consider more geometric questions related to graphical nested complexes. Although we will not use them in the remaining of this chapter, we briefly survey some constructions of *nested fans* and graph associahedron in more detail than in Chapter 4. A nested fan is constructed implicitly in [CD06] for graph associahedra, and explicitly in [Pos09, FS05, Zel06] for arbitrary nested complexes. Let $(\mathbf{e}_v)_{v \in V}$ be the canonical basis of $\mathbb{R}^V$, let $\mathbb{H} := \left\{ \mathbf{x} \in \mathbb{R}^V \mid \forall W \in \kappa(G), \sum_{w \in W} x_w = 0 \right\}$ and $\pi : \mathbb{R}^V \to \mathbb{H}$ denote the orthogonal projection on $\mathbb{H}$. Let $\mathbf{g}(\mathsf{t}) := \pi\left(\sum_{v \in \mathsf{t}} \mathbf{e}_v \right)$ denote the projection of the characteristic vector of a tube t of G, and define $\mathbf{g}(\mathsf{T}) := \{ \mathbf{g}(\mathsf{t}) \mid \mathsf{t} \in \mathsf{T} \}$ for a tubing T on G. These vectors support a complete simplicial fan realization of the nested complex:

Theorem 6.1 ([CD06, Pos09, FS05, Zel06])**.** *For any graph* G, *the collection of cones*

$$\mathcal{G}(G) := \{ \mathbb{R}_{\geq 0} \, \mathbf{g}(\mathsf{T}) \mid \mathsf{T} \text{ tubing on } G \}$$

is a complete simplicial fan of $\mathbb{H}$, *called the* nested fan *of* G, *realizing the nested complex* $\mathcal{N}(G)$.

The normal fan of the graph associahedra and nestohedra of [CD06, Dev09, Pos09, FS05, Zel06] coarsens the type A Coxeter arrangement: its rays are the characteristic vectors of the tubes, and its cones are generated by characteristic vectors of compatible tubes. In particular it makes sense to consider it as an analogue of the **g**-vector fans of type A cluster algebras.

Remark 6.2. The cones of $\mathcal{G}(G)$ can be encoded by spines (see Section 5.2.2): the cone $\mathbb{R}_{\geq 0} \, \mathbf{g}(\mathsf{T})$ is the *braid cone* of the spine S of T and is polar to the *incidence cone* of S:

$$\mathbb{R}_{\geq 0} \, \mathbf{g}(\mathsf{T}) = \{ \mathbf{x} \in \mathbb{H} \mid x_v \leq x_w \text{ for all } v \to w \in \mathsf{S} \} = \left(\mathbb{R}_{\geq 0} \, \{ \mathbf{e}_v - \mathbf{e}_w \mid v \to w \in \mathsf{S} \} \right)^\diamond$$

As we saw in Chapter 4, it is proved in [CD06, Dev09, Pos09, FS05, Zel06] that the nested fan comes from a polytope.

Theorem 6.3 ([CD06, Dev09, Pos09, FS05, Zel06])**.** *For any graph* G*, the nested fan* $\mathcal{G}(G)$ *is the normal fan of the graph associahedron* $\mathrm{Asso}(G)$*.*

It is remarkable that these different papers all obtain the same geometric realization (they all have the same normal fan) with relatively different constructions. Originally, M. Carr and S. Devadoss constructed $\mathrm{Asso}(G)$ by iterative truncations of faces of the standard simplex [CD06]. S. Devadoss then gave explicit integer coordinates for the facets in [Dev09]. A. Postnikov [Pos09] and independently E. M. Feichtner and B. Sturmfels [FS05] constructed nestohedra by Minkowski sums of faces of the standard simplex (see Section 4.2). Finally, A. Zelevinsky [Zel06] realized the nested fan using a characterization of all possible facet inequality descriptions.

Alternative realizations of graph associahedra with different normal fans are obtained by successive truncations of faces of the cube in [Vol10, DFRS15]. In this chapter, we present a construction directly inspired from combinatorial and geometric properties of finite type cluster algebras and generalized associahedra, that we adapt to derive numerous and meaningful new fan realizations of graph associahedra. As we previously mentioned A. Zelevinsky [Zel06] already underlined the closed connection between nested complexes and cluster complexes. We use ideas from cluster algebras to obtain results on graphical nested complexes, which in turn provide us with relevant properties of the geometry of finite type cluster algebras.

6.1.2   Overview

The chapter is organized as follows. In Section 6.2, we define the compatibility degree between two tubes of a graph, review its combinatorial properties, and state our geometric results on compatibility and dual compatibility fans.

We study various examples in Section 6.3. After an exhaustive description of the compatibility fans of all graphs with at most 4 vertices, we study four families of graphs: paths, cycles, complete graphs, and stars. The first two families connect our construction to S. Fomin and A. Zelevinsky's $\mathbf{d}$-vector fans for type A, B, and C cluster complexes.

Section 6.4 discusses various further topics. We first study the behavior of the compatibility fans with respect to products and links. We then describe all nested complex isomorphisms in order to show that most compatibility fans are not linearly isomorphic. We also discuss the question of the realization of our compatibility fans as normal fans of convex polytopes. We extend our construction to design nested complexes [DHV11]. Finally, we discuss the connection of this chapter to LP-algebras [LP16a, LP16b].

Finally, we have chosen to gather all proofs of our results in Section 6.5 with the hope that the properties and examples of compatibility fans treated in Sections 6.3 and 6.4 help the reader's intuition.

6.2   Compatibility degrees, vectors, and fans

6.2.1   Complementary terminology

We first introduce two notions on tubes and tubings of graphs that we will need later. We say that two distinct tubes t, t' of a graph G are *exchangeable* if there exist two adjacent maximal tubings T, T' on G such that $T \smallsetminus \{t\} = T' \smallsetminus \{t'\}$. Note that several such pairs $\{T, T'\}$ are possible, but they all contain certain tubes. We call *forced tubes* of the exchangeable pair $\{t, t'\}$ any tube which belongs to any adjacent maximal tubings T, T' such that $T \smallsetminus \{t\} = T' \smallsetminus \{t'\}$. These tubes are easy to describe: they are precisely the tube $\bar{t} := t \cup t'$ and the connected components of $\bar{t} \smallsetminus (\lambda(t, T) \cup \lambda(t', T'))$.

Here we will follow the same example graph G_{ex} of Examples 4.6. To avoid back and forth references with Chapter 4, we gather Figures 4.1 and 4.3 in Figure 6.1.
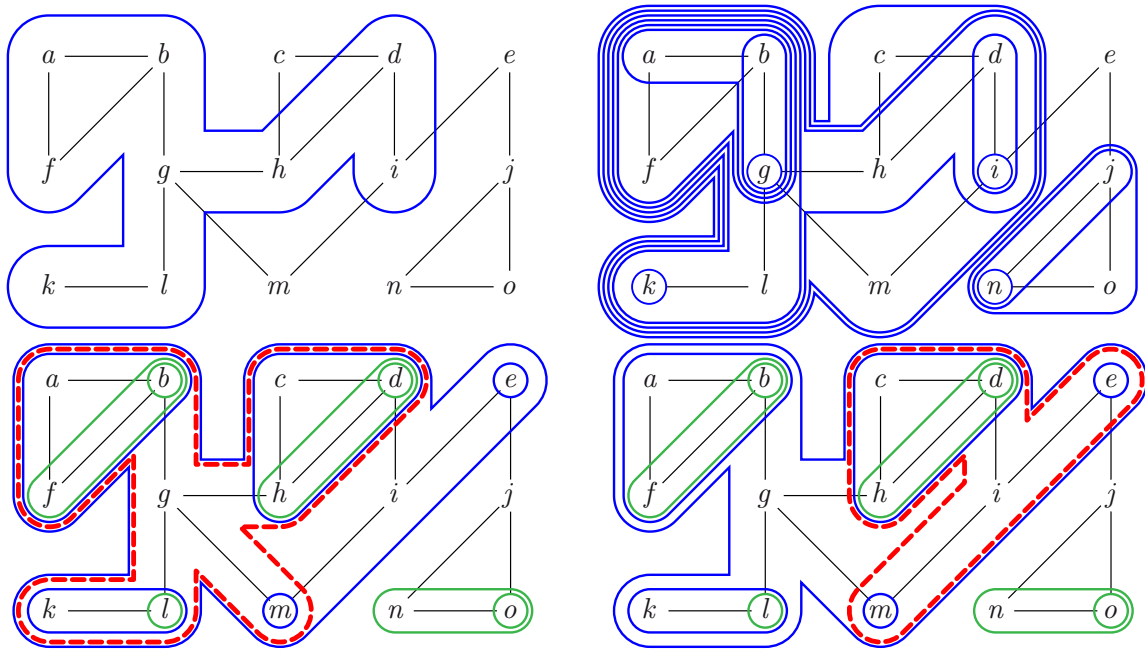
Figure 6.1 – A tube t_{ex}° of G_{ex} (top left), a maximal tubing T_{ex}° on G_{ex} (top right) and the flip between two maximal tubings T_{ex} and T_{ex}' on G_{ex} (bottom).

Example 6.4. Figure 6.1 (bottom) illustrates the flip between two maximal tubings T_{ex} and T_{ex}' on G_{ex}. The exchangeable tubes $t_{ex} = \{a, b, c, d, f, g, h, k, l, m\}$ (with root g) and $t_{ex}' = \{c, d, e, h, i, m\}$ (with root i) that are flipped are dashed red, while the forced tubes of the exchangeable pair $\{t_{ex}, t_{ex}'\}$ are blue.

6.2.2 Compatibility degree

Motivated by the compatibility degrees in finite type cluster algebras, we introduce an analogous notion on tubes of graphical nested complexes.

Definition 6.5. For two tubes t, t' of G, the *compatibility degree* of t with t' is

$$(t \parallel t') = \begin{cases} -1 & \text{if } t = t', \\ |\{\text{neighbors of } t \text{ in } t' \smallsetminus t\}| & \text{if } t \not\subseteq t', \\ 0 & \text{otherwise.} \end{cases}$$

Example 6.6. On the graph G_{ex} of Example 6.4, the compatibility degrees of the red tubes t_{ex}, t_{ex}' and of the blue tube $\bar{t}_{ex} = t_{ex} \cup t_{ex}'$ of Figure 6.1 (bottom) with the tube t_{ex}° of Figure 6.1 (top left) are given by

$$\begin{array}{lll} (t_{ex} \parallel t_{ex}^\circ) = |\{i\}| = 1, & (t_{ex}' \parallel t_{ex}^\circ) = |\{g\}| = 1, & (\bar{t}_{ex} \parallel t_{ex}^\circ) = 0, \\ (t_{ex}^\circ \parallel t_{ex}) = |\{c, m\}| = 2, & (t_{ex}^\circ \parallel t_{ex}') = |\{c, e, m\}| = 3, & (t_{ex}^\circ \parallel \bar{t}_{ex}) = 0. \end{array}$$

Note that the last 0 is forced by the last line of the definition since $t_{ex}^\circ \subsetneq \bar{t}_{ex}$.

We will see in Sections 6.3.2 and 6.3.3 that our compatibility degree on tubes of paths (resp. cycles) corresponds to the compatibility degree on cluster variables in type A (resp. B/C) cluster algebras defined in [FZ03b]. The compatibility degree in cluster algebras encodes compatibility and exchangeability between cluster variables. The analogous result for the graphical compatibility degree is given by the following proposition, proved in Section 6.5.1.

Proposition 6.7. *For any two tubes* t, t' *of* G,

- $(t \parallel t') < 0 \iff (t' \parallel t) < 0 \iff t = t'$,
- $(t \parallel t') = 0 \iff (t' \parallel t) = 0 \iff t$ *and* t' *are compatible, and*
- $(t \parallel t') = 1 = (t' \parallel t) \iff t$ *and* t' *are exchangeable.*

Remark 6.8. It can happen that $(t \parallel t') = 1$ while $(t' \parallel t) \neq 1$, in which case t and t' are not exchangeable. This situation appears as soon as G contains a cycle or a trivalent vertex. See *e.g.* Example 6.6.

Proposition 6.7 should be understood as follows: the compatibility degree between two tubes measures how much they are incompatible. It is natural to use this measure to construct fan realizations of the nested complex: intuitively, pairs of tubes with low compatibility degrees should correspond to rays close to each other. We make this idea precise in the next section.

6.2.3   Compatibility fans

We consider the compatibility vectors with respect to an arbitrary initial maximal tubing T°. Remember that any maximal tubing on G has precisely $n := |V| - |\kappa(G)|$ tubes.

Definition 6.9. Let $T^\circ := \{t_1^\circ, \dots, t_n^\circ\}$ be any initial maximal tubing on G. The *compatibility vector* of a tube t of G with respect to T° is the vector $\mathbf{d}(T^\circ, t) := [(t_1^\circ \parallel t), \dots, (t_n^\circ \parallel t)]$. The *compatibility matrix* of a tubing $T := \{t_1, \dots, t_m\}$ on G with respect to T° is the matrix $\mathbf{d}(T^\circ, T) := [(t_i^\circ \parallel t_j)]_{i \in [n], j \in [m]}$.

Remember that we denote by $\mathbb{R}_{\geq 0} \mathbf{M}$ the polyhedral cone generated by the column vectors of a matrix $\mathbf{M}$. Note that the compatibility vectors of the initial tubes are given by the negative of the basis vectors, while all other compatibility vectors lie in the positive orthant: $\mathbf{d}(T^\circ, T^\circ) = -\mathbf{I}_n$ and $\mathbf{d}(T^\circ, t)$ has nonnegative entries for $t \notin T^\circ$. Our main result asserts that these compatibility vectors support a complete simplicial fan realization of the graphical nested complex.

Theorem 6.10. *For any graph* G *and any maximal tubing* T° *on* G, *the collection of cones*

$$\mathcal{D}(G, T^\circ) := \{\mathbb{R}_{\geq 0} \, \mathbf{d}(T^\circ, T) \mid T \text{ tubing on } G\}$$

is a complete simplicial fan which realizes the nested complex $\mathcal{N}(G)$. *We call it the* compatibility fan *of* G *with respect to* T°.

We prove this statement in Section 6.5.3. The proof relies on the characterization of complete simplicial fans presented in Proposition 3.7. Unfortunately, we are not able to compute the linear dependence between the compatibility vectors involved in an arbitrary flip. To illustrate the difficulty, we show in the following example that these linear dependences may be complicated. In particular, they do not always involve only the forced tubes of the flip.

Example 6.11. Consider the initial maximal tubing T_{ex}° of the graph G_{ex} of Figure 6.1 (top right) and the flip $T_{ex} \smallsetminus \{t_{ex}\} = T'_{ex} \smallsetminus \{t'_{ex}\}$ illustrated in Figure 6.1 (bottom). The linear dependence between the compatibility vectors of the tubes of $T_{ex} \cup T'_{ex}$ with respect to T_{ex}° is

$$2 \, \mathbf{d}(T_{ex}^\circ, t_{ex}) + \mathbf{d}(T_{ex}^\circ, t'_{ex}) - \mathbf{d}(T_{ex}^\circ, \{d\}) - \mathbf{d}(T_{ex}^\circ, \{e\})$$
$$- 3 \, \mathbf{d}(T_{ex}^\circ, \{m\}) + 4 \, \mathbf{d}(T_{ex}^\circ, \{k, l\}) - 3 \, \mathbf{d}(T_{ex}^\circ, \{c, d, h\}) = 0.$$

Observe that the tube $\{d\}$ is involved in this linear dependence although it is not a forced tube of the exchangeable pair $\{t_{ex}, t'_{ex}\}$.

Theorem 6.10 has the following nonobvious consequences.

Corollary 6.12. *For any initial tubing* T° *on* G,
- *the compatibility vector map* $\mathsf{t} \mapsto \mathbf{d}(\mathsf{T}^\circ, \mathsf{t})$ *is injective:* $\mathbf{d}(\mathsf{T}^\circ, \mathsf{t}) = \mathbf{d}(\mathsf{T}^\circ, \mathsf{t}') \;\Rightarrow\; \mathsf{t} = \mathsf{t}'$.
- *the compatibility matrix* $\mathbf{d}(\mathsf{T}^\circ, \mathsf{T})$ *of any maximal tubing* T *on* G *has full rank.*

6.2.4 Dual compatibility fan

It is also interesting to consider the following dual notion of compatibility vectors, where the roles of t and $\mathsf{t}_1^\circ, \ldots, \mathsf{t}_n^\circ$ are reversed. The results are similar, and the motivation for this dual definition will become clear in Section 6.3.3.

Definition 6.13. Let $\mathsf{T}^\circ := \{\mathsf{t}_1^\circ, \ldots, \mathsf{t}_n^\circ\}$ be an arbitrary initial maximal tubing on G. The *dual compatibility vector* of a tube t of G with respect to the tubing T° is the integer vector $\mathbf{d}^*(\mathsf{t}, \mathsf{T}^\circ) := [(\mathsf{t} \,\|\, \mathsf{t}_1^\circ), \ldots, (\mathsf{t} \,\|\, \mathsf{t}_n^\circ)]$. The *dual compatibility matrix* of a tubing $\mathsf{T} := \{\mathsf{t}_1, \ldots, \mathsf{t}_m\}$ on G with respect to T° is the matrix $\mathbf{d}^*(\mathsf{T}, \mathsf{T}^\circ) := [(\mathsf{t}_j \,\|\, \mathsf{t}_i^\circ)]_{i \in [n], j \in [m]}$.

The following statement is the analogue of Theorem 6.10.

Theorem 6.14. *For any graph* G *and any maximal tubing* T° *on* G, *the collection of cones*

$$\mathcal{D}^*(\mathrm{G}, \mathsf{T}^\circ) := \{\mathbb{R}_{\geq 0}\, \mathbf{d}^*(\mathsf{T}, \mathsf{T}^\circ) \mid \mathsf{T}\ tubing\ on\ \mathrm{G}\}$$

is a complete simplicial fan which realizes the nested complex $\mathcal{N}(\mathrm{G})$. *We call it the* dual compatibility fan *of* G *with respect to* T°.

The proof of this statement appears in Section 6.5.4. It is a direct application of Theorem 6.10 using duality between compatibility and dual compatibility matrices.

Example 6.15. Consider the initial maximal tubing $\mathsf{T}_{\mathrm{ex}}^\circ$ on the graph G_{ex} of Figure 6.1 (top right) and the flip $\mathsf{T}_{\mathrm{ex}} \smallsetminus \{\mathsf{t}_{\mathrm{ex}}\} = \mathsf{T}_{\mathrm{ex}}' \smallsetminus \{\mathsf{t}_{\mathrm{ex}}'\}$ illustrated in Figure 6.1 (bottom). The linear dependence between the dual compatibility vectors of the tubes of $\mathsf{T}_{\mathrm{ex}} \cup \mathsf{T}_{\mathrm{ex}}'$ with respect to $\mathsf{T}_{\mathrm{ex}}^\circ$ is

$$2\, \mathbf{d}^*(\mathsf{t}_{\mathrm{ex}}, \mathsf{T}_{\mathrm{ex}}^\circ) + \mathbf{d}^*(\mathsf{t}_{\mathrm{ex}}', \mathsf{T}_{\mathrm{ex}}^\circ) - \mathbf{d}^*(\{e\}, \mathsf{T}_{\mathrm{ex}}^\circ) - \mathbf{d}^*(\{c, d, h\}, \mathsf{T}_{\mathrm{ex}}^\circ) = 0.$$

6.3 Examples for specific graphs

In this section, we provide examples of compatibility fans for particular families of graphs. We start with graphs with few vertices to illustrate the variety of compatibility fans. We then describe compatibility fans for paths, cycles, complete graphs and stars using alternative combinatorial models (triangulations, lattice paths, ...). For paths and cycles, we give an explicit connection to the compatibility degree in cluster algebras of types A, B, and C. The examples of this section shall help the intuition for further properties studied in Section 6.4 and for the proofs gathered in Section 6.5.

6.3.1 Graphs with few vertices

In view of Proposition 6.31 below, we restrict to connected graphs. The only connected graphs with 3 vertices are the 3-path and the triangle, whose compatibility fans are represented in Figure 6.2. The other possible choices for the initial tubing in these pictures would produce the same fans: it is clear for the triangle as all maximal tubings are obtained from one another by graph isomorphisms; for the path, it is an illustration of the nontrivial isomorphisms between compatibility fans studied in Section 6.4.2.

The first interesting compatibility fans appear in dimension 3 for connected graphs on 4 vertices. All possibilities up to linear transformations are represented in Figure 6.4. Instead of representing cones in the 3-dimensional space, we intersect the
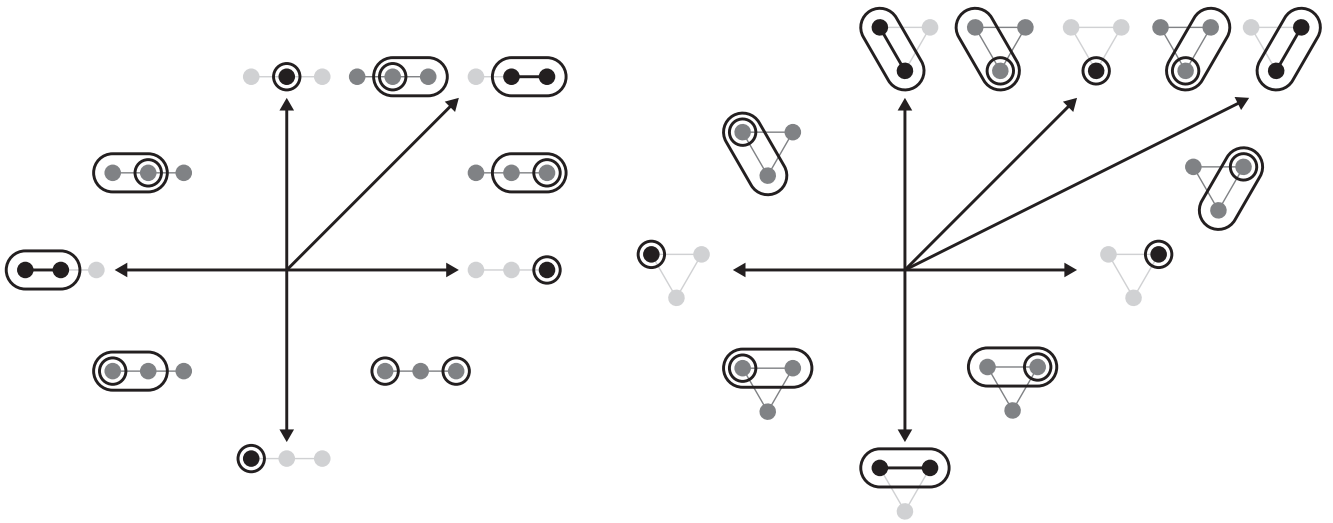
Figure 6.2 – Compatibility fans of the 3-path (left) and of the triangle (right).

compatibility vectors with the unit sphere, make a stereographic projection of the resulting points on the sphere (the pole of the projection is the point of the sphere in direction $-\mathbf{e}_1 - \mathbf{e}_2 - \mathbf{e}_3$), and draw the cones on the resulting planar points. Under this projection, the three external vertices correspond to the tubes of the initial tubing, and the external face corresponds to the initial tubing. For the sake of readability, we do not label the remaining vertices of the projection. Their labels can be reconstructed from the initial tubes by flips. For example, the tubes corresponding to the vertices of the top pictures of Figure 6.4 are given in Figure 6.3.

The pictures become more complicated in dimension 4. To illustrate them, we have represented in Figure 6.5 the stereographic projection of the compatibility fan for an arbitrary maximal tubing on the path, cycle, complete graph, and star on 5 vertices.
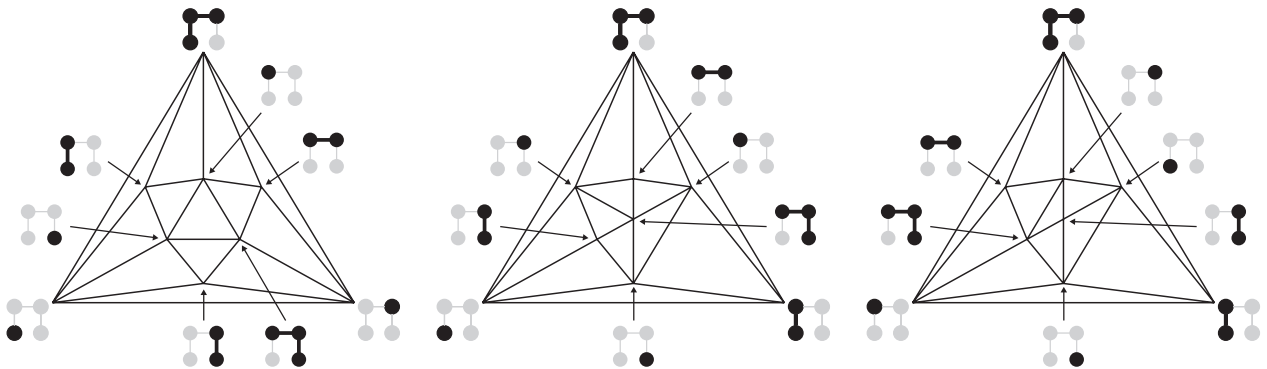
Figure 6.3 – All tubes in the top pictures of Figure 6.4.
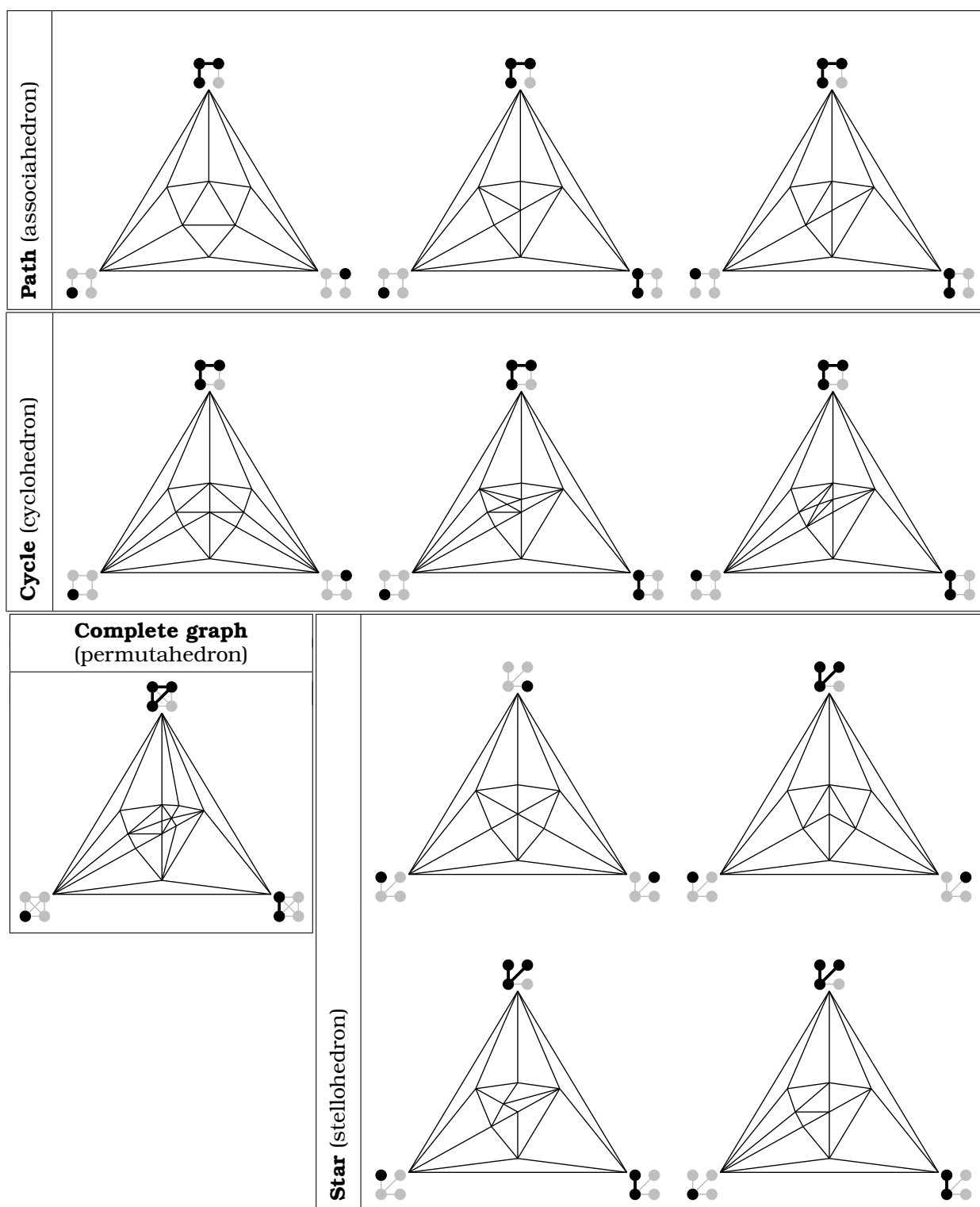
Figure 6.4 – All possible compatibility fans up to linear isomorphism, for all connected graphs on 4 vertices (see also the end of the picture on page 84 for the two remaining graphs). Instead of representing the cones in the 3-dimensional space, we intersect the compatibility vectors with the unit sphere, make a stereographic projection of the resulting points on the sphere (the pole of the projection is the point of the sphere in direction $-\mathbf{e}_1 - \mathbf{e}_2 - \mathbf{e}_3$), and draw the cones on the resulting planar points.
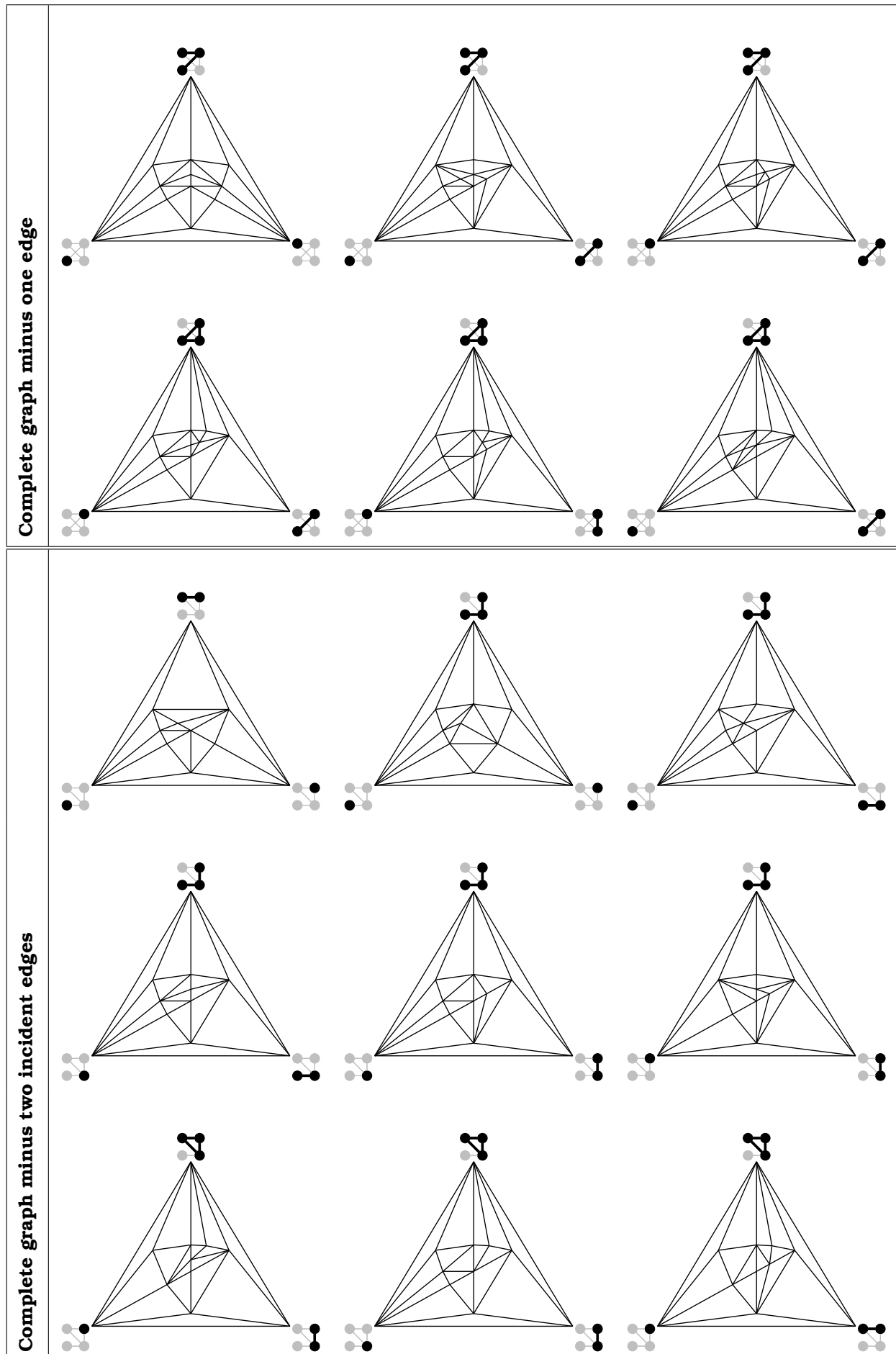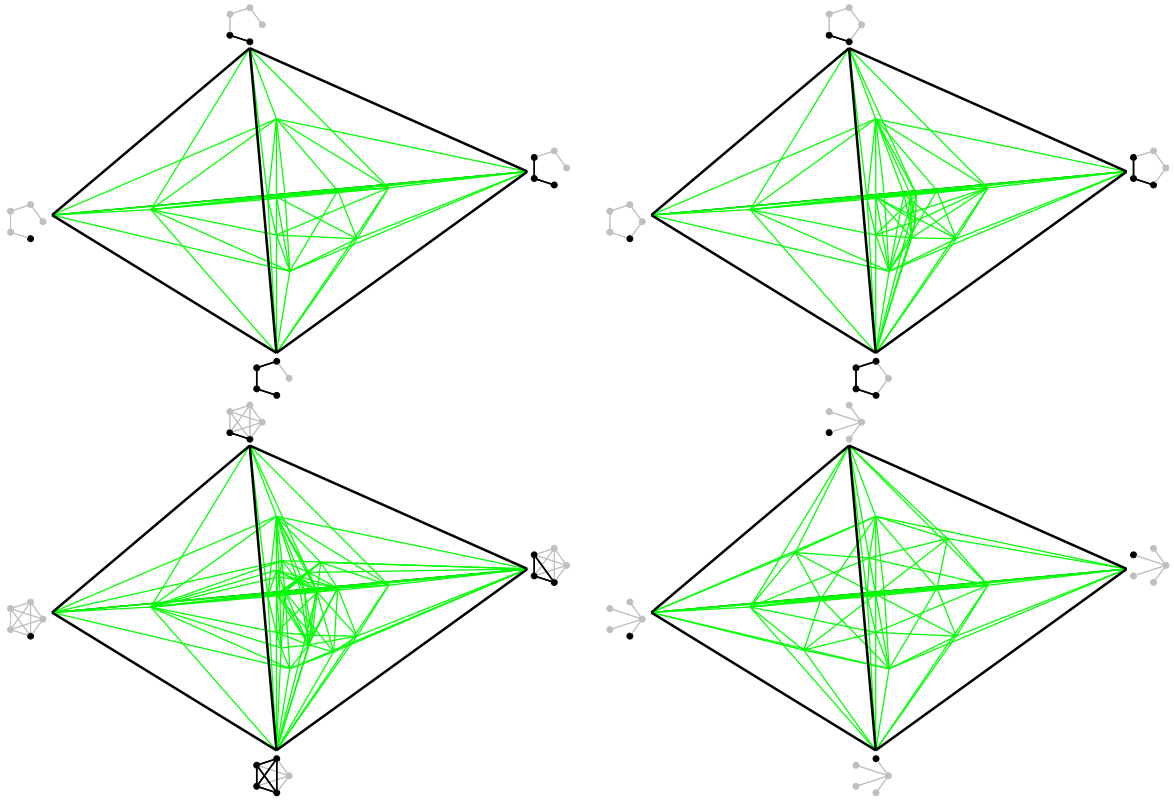
Figure 6.5 – Stereographic projection of the compatibility fan for particular initial maximal tubings on the path, cycle, complete graph, and star on 5 vertices.

6.3.2 Paths

We now consider the nested complex $\mathcal{N}(\mathrm{P}_{n+1})$ and the compatibility fan $\mathcal{D}(\mathrm{P}_{n+1}, \mathsf{T}^\circ)$ for the path P_{n+1} on $n+1$ vertices. As already mentioned in the Chapter 4, the nested complex $\mathcal{N}(\mathrm{P}_{n+1})$ is isomorphic to the n-dimensional *simplicial associahedron*, *i.e.* the simplicial complex of sets of pairwise noncrossing diagonals of an $(n+3)$-gon. It is convenient to present the correspondence as follows. Consider an $(n + 3)$-gon Q_{n+3} with vertices labeled from left to right by $0, 1, \ldots, n + 2$ and such that all vertices $1, \ldots, n+1$ are located strictly below the boundary edge $[0, n + 2]$. We can therefore identify the path P_{n+1} with the path $1, \ldots, n + 1$ on the boundary of Q_{n+3}. We then associate to a diagonal δ of Q_{n+3} the tube t_δ of P_{n+1} whose vertices are located strictly below δ, see Figures 6.6 and 4.2 (top). Finally, we associate to a set Δ of pairwise noncrossing internal diagonals of Q_{n+3} the set of tubes $\mathsf{T}_\Delta := \{\mathsf{t}_\delta \mid \delta \in \Delta\}$, see Figure 4.2 (top). The reader can check that the map $\Delta \mapsto \mathsf{T}_\Delta$ defines an isomorphism between the simplicial associahedron and the nested complex $\mathcal{N}(\mathrm{P}_{n+1})$: two diagonals δ, δ' of Q_{n+3} are noncrossing if and only if the corresponding tubes $\mathsf{t}_\delta, \mathsf{t}_{\delta'}$ of P_{n+1} are compatible.

It follows by classical results on the associahedron that the path P_{n+1} has:

- $\dfrac{n(n + 3)}{2}$ proper tubes [OEI10, A000096] (internal diagonals of the $(n + 3)$-gon),

- $\dfrac{1}{n + 2}\dbinom{2n + 2}{n + 1}$ maximal tubings [OEI10, A000108] (triangulations of the $(n + 3)$-gon),
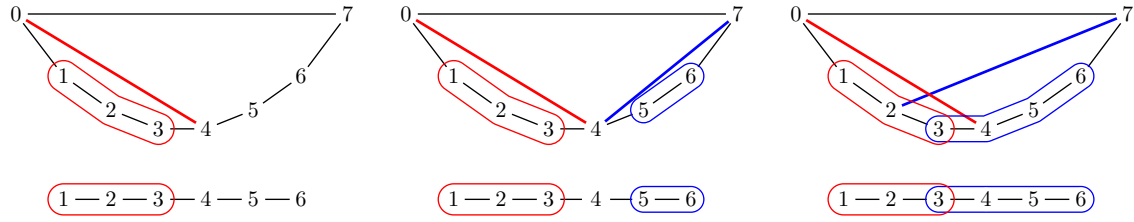
Figure 6.6 – Isomorphism between the simplicial associahedron and the nested complex of a path: diagonals are sent to tubes (left), preserving the compatibility (middle) and incompatibility (right). See also Figure 4.2 (top).

- $\dfrac{1}{k+1}\dbinom{n}{k}\dbinom{n+k+2}{k}$ tubings with k tubes [OEI10, A033282] (dissections of the $(n+3)$-gon into k parts).

The following statement, whose proof is left to the reader, describes the behavior of the map $\delta \mapsto t_\delta$ with respect to compatibility degrees.

Proposition 6.16. *For any two diagonals δ, δ' of Q_{n+3}, the compatibility degree of the corresponding tubes t_δ and $t_{\delta'}$ of P_{n+1} is given by*

$$(t_\delta \,\|\, t_{\delta'}) = \begin{cases} -1 & \textit{if } \delta = \delta', \\ 0 & \textit{if } \delta \neq \delta' \textit{ do not cross,} \\ 1 & \textit{if } \delta \neq \delta' \textit{ cross.} \end{cases}$$

In other words, our compatibility degree between tubes of P_{n+1} coincides with the compatibility degree between type A cluster variables defined by S. Fomin and A. Zelevinsky in [FZ03b], and our graphical compatibility fan coincides with the type A compatibility fan defined for the bipartite initial cluster in [FZ03a] and for any initial cluster in [CSZ15, Section 5]. We thus obtain an alternative proof of F. Santos' result [CSZ15, Section 5].

Corollary 6.17. *For type A cluster algebras, the denominator vectors (or compatibility vectors) of all cluster variables with respect to any initial cluster support a complete simplicial fan which realizes the cluster complex.*

Remark 6.18 (Dual compatibility fan)**.** The compatibility fan $\mathcal{D}(P_{n+1}, T^\circ)$ and the dual compatibility fan $\mathcal{D}^*(P_{n+1}, T^\circ)$ coincide since the compatibility degree is symmetric for tubes of P_{n+1}.

Remark 6.19 (Linear dependences)**.** In the case of the path P_{n+1}, the linear dependences are explicitly described in [CSZ15]. They are derived from the case of the octagon by edge contraction in the interpretation in terms of triangulations. They can only involve the two flipped tubes and the forced tubes, and the coefficients are either 1 or 2 for the flipped tubes and -1 or 0 for the forced tubes. See Section 6.5.6 for more details.

Remark 6.20. The compatibility degree for tubes of a path takes values in $\{-1, 0, 1\}$. It is tempting to construct compatibility fans for graphical nestohedra using the naive compatibility degree defined by $(t \,\|\, t') = -1$ if $t = t'$, $(t \,\|\, t') = 0$ if $t \neq t'$ are compatible, and $(t \,\|\, t') = 1$ if $t \neq t'$ are incompatible. This naive approach works for the paths but fails for any other connected graph since two distinct tubes would get the same compatibility vectors. See Figure 6.7 for examples on the triangle and on the tripod.
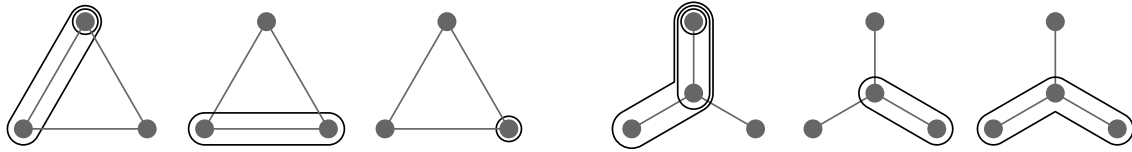
Figure 6.7 – Counter-examples to the naive definition of compatibility degrees: both on the triangle and on the tripod, all tubes of the initial maximal tubing on the left are incompatible with the two distinct tubes on the right.

6.3.3 Cycles

We now consider the nested complex $\mathcal{N}(O_{n+1})$ and the compatibility fan $\mathcal{D}(O_{n+1}, T^\circ)$ for the cycle O_{n+1} on $n+1$ vertices. As already mentioned in the Chapter 4, the nested complex $\mathcal{N}(O_{n+1})$ is isomorphic to the n-dimensional *simplicial cyclohedron*, *i.e.* the simplicial complex of sets of pairwise noncrossings pairs of centrally symmetric internal diagonals (including duplicated long diagonals) of a regular $(2n+2)$-gon R_{2n+2}. The explicit correspondence works as follows. We label the vertices of R_{2n+2} cyclically with two copies of $[n+1]$. We then associate

- to a duplicated long diagonal δ with vertices labeled by i the tube $\mathsf{t}_\delta := [n+1] \smallsetminus \{i\}$ of O_{n+1},

- to a pair of centrally symmetric diagonals $\{\delta, \bar{\delta}\}$ the tube t_δ of O_{n+1} which consists of the labels of the vertices of R_{2n+2} separated from the center of R_{2n+2} by δ and $\bar{\delta}$.

Finally, we associate to a set Δ of pairwise noncrossing pairs of centrally symmetric internal diagonals of R_{2n+2} the set of tubes $T_\Delta := \{\mathsf{t}_\delta \mid \delta \in \Delta\}$. See Figures 6.8 and 4.2 (middle). The reader can check that the map $\Delta \mapsto T_\Delta$ defines an isomorphism between the simplicial cyclohedron and the nested complex $\mathcal{N}(O_{n+1})$: two pairs of centrally symmetric diagonals (or duplicated long diagonals) $\{\delta, \bar{\delta}\}$ and $\{\delta', \bar{\delta}'\}$ of R_{2n+2} are noncrossing if and only if the corresponding tubes t_δ and $\mathsf{t}_{\delta'}$ of O_{n+1} are compatible.
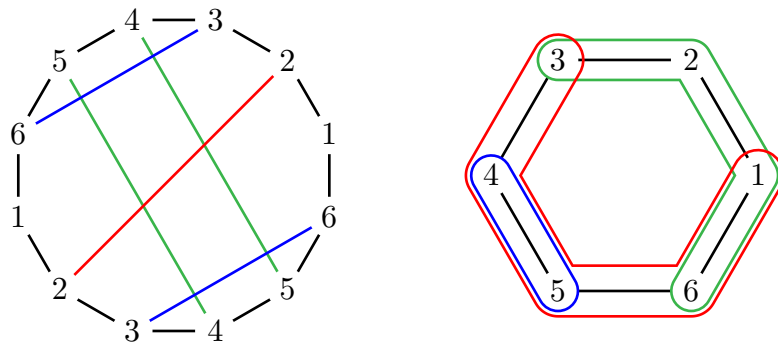
Figure 6.8 – Isomorphism between the simplicial cyclohedron and the nested complex of a cycle: centrally symmetric pairs of diagonals are sent to tubes, preserving the compatibility and incompatibility. See also Figure 4.2 (middle).

It follows by classical results on the cyclohedron that the cycle O_{n+1} has:

- $n(n+1)$ proper tubes [OEI10, A002378] (centrally symmetric pairs of diagonals),

- $\dbinom{2n}{n}$ maximal tubings [OEI10, A000984] (centrally symmetric triangulations),

- $\binom{n}{k}\binom{n+k}{k}$ tubings with k tubes [OEI10, A063007] (centrally symmetric dissecti-
ons).

The following statement, whose proof is left to the reader, describes the behavior of the map $\{\delta, \bar{\delta}\} \mapsto t_\delta$ with respect to compatibility degrees.

Proposition 6.21. *For any two pairs of centrally symmetric diagonals (or duplicated long diagonals) $\{\delta, \bar{\delta}\}$ and $\{\delta', \bar{\delta}'\}$ of R_{2n+2}, the compatibility degree $(t_\delta \,\|\, t_{\delta'})$ of the corresponding tubes t_δ and $t_{\delta'}$ of O_{n+1} is the number of crossings between the two diagonals δ and $\bar{\delta}$ and the diagonal δ'.*

In other words, our compatibility degree (resp. dual compatibility degree) between tubes of O_{n+1} coincides with the compatibility degree between type C (resp. type B) cluster variables defined by S. Fomin and A. Zelevinsky in [FZ03b]. Moreover, our graphical compatibility fan (resp. dual compatibility fan) coincides with the type C (resp. type B) compatibility fan defined for an acyclic initial cluster in [FZ03a]. This extends for any arbitrary initial cluster to the following corollary.

Corollary 6.22. *For type B and C cluster algebras, the denominator vectors (or compatibility vectors) of all cluster variables with respect to any initial cluster support a complete simplicial fan which realizes the cluster complex.*

Remark 6.23 (Dual compatibility fan). Since the compatibility degree is not symmetric for tubes of O_{n+1}, the compatibility fan $\mathcal{D}(O_{n+1}, T^\circ)$ and the dual compatibility fan $\mathcal{D}^*(O_{n+1}, T^\circ)$ do not coincide. Figures 6.9 and 6.10 show both fans for different initial tubings on the cycles O_3 and O_4.
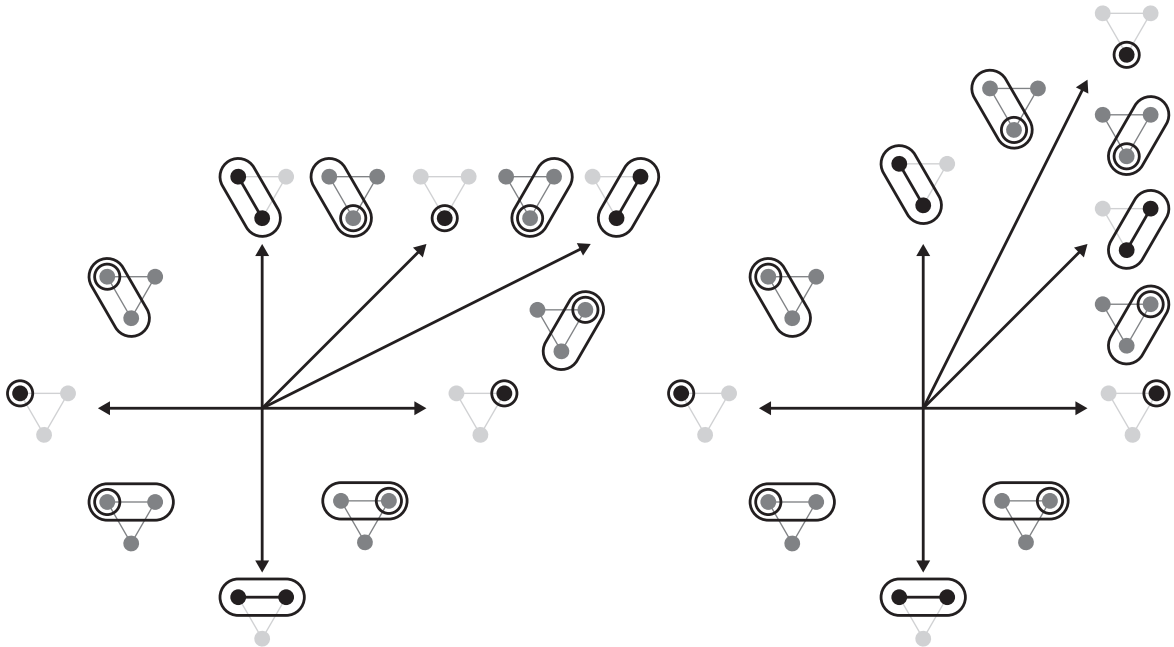
Figure 6.9 – Compatibility (left) and dual compatibility (right) fans for the triangle.

Remark 6.24 (Linear dependences). As for paths, only finitely many linear dependences occur for all cycles O_{n+1}, both on compatibility vectors as on dual compatibility vectors. Indeed, with the interpretation of the maximal tubings in terms of centrally
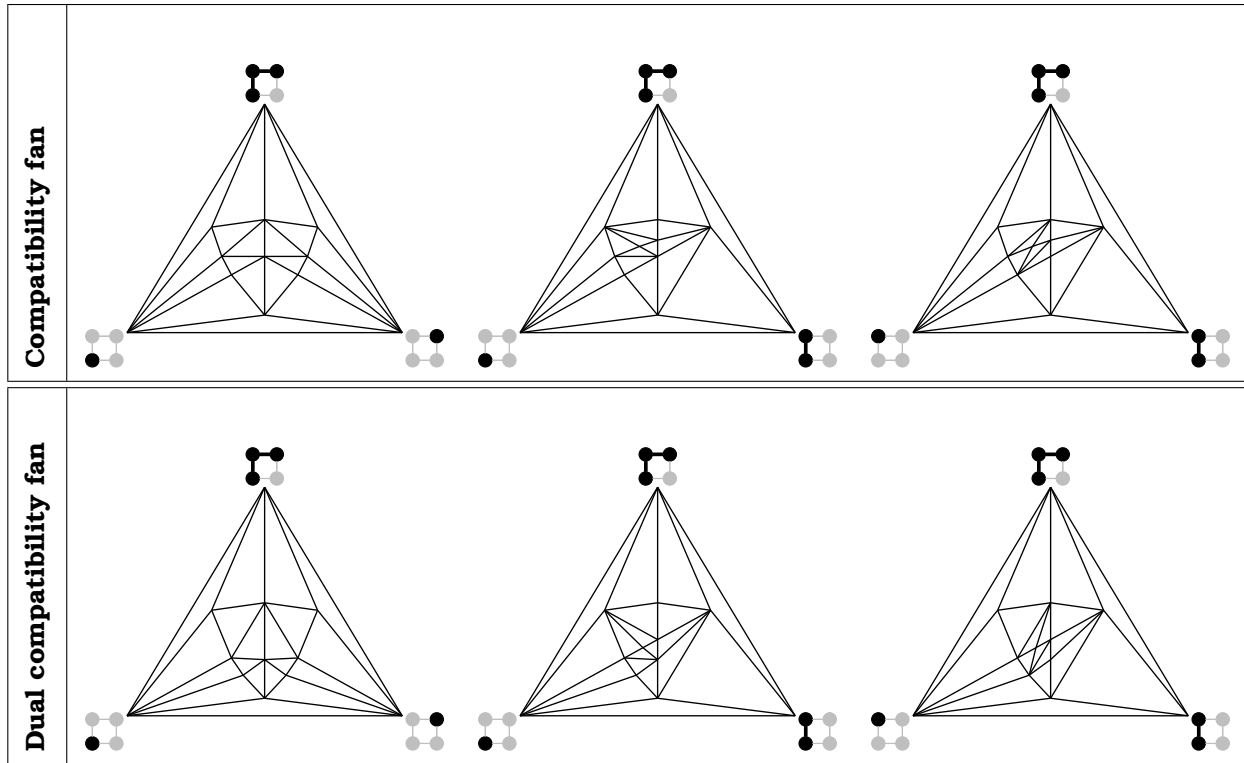
Figure 6.10 – Compatibility (top) and dual compatibility (bottom) fans for the cycle on 4 vertices with respect to different initial tubings.

symmetric triangulations, the same kind of arguments as in [CSZ15] ensure that all these dependences can be inferred by checking the cycle O_8 on 8 vertices. As for the path, these linear dependences only involve flipped and forced tubes, and the coefficients of the flipped tubes may only be 1 or 2 and these of the forces tubes may only be $0, -1$ or -2. See Section 6.5.6 for more details.

It is easy to find an example of a maximal tubing on the tripod such that one of the linear dependences obtained with respect to this maximal tubing does not only involve forced tubes. It implies in particular that the paths and cycles are the only graphs that have this property. It is then tempting to ask whether it is a coincidence that these graphs also are the only ones whose corresponding associahedra also are generalized associahedra.

6.3.4 Complete graphs

We now consider the nested complex $\mathcal{N}(K_{n+1})$ and the compatibility fan $\mathcal{D}(K_{n+1}, T^{\circ})$ for the complete graph K_{n+1} on $n+1$ vertices. As already mentioned in Chapter 4, the nested complex $\mathcal{N}(K_{n+1})$ is isomorphic to the n-dimensional *simplicial permutahedron*, *i.e.* the simplicial complex of collections of pairwise nested subsets of $[n+1]$. See Figure 4.2 (bottom).

It follows by classical results on the permutahedron that the complete graph K_{n+1} has:

- $2^n - 2$ proper tubes [OEI10, A000918] (proper subsets of $[n]$),

- $n!$ maximal tubings [OEI10, A000142] (permutations of $[n]$),

- $k!\,S(n,k)$ tubings with k tubes, where $S(n,k)$ is the Stirling number of second kind (*i.e.* the number of ways to partition a set of n elements into k nonempty subsets) [OEI10, A008277].

For two tubes t, t' of K_{n+1}, the compatibility degree of t with t' is $(t \,\|\, t') = -1$ if $t = t'$, $(t \,\|\, t') = 0$ if t and t' are distinct and nested, and $(t \,\|\, t') = |t' \smallsetminus t|$ otherwise. This connects the compatibility vector $\mathbf{d}(T^\circ, t)$ to an alternative combinatorial model for the permutahedron in terms of lattice paths. Since all maximal tubings are equivalent, we can assume that $T^\circ = \{[i] \mid i \in [n]\}$. For any tube t of K_{n+1}, we consider the lattice paths $\phi(t)$ and $\psi(t)$ whose horizontal steps above abscissa $[i, i+1]$ lie at height $|t \smallsetminus [i]|$ and $([i] \,\|\, t)$ respectively. These lattice paths are illustrated in Figure 6.11, where $\phi(t)$ is the plain path while $\psi(t)$ is dotted until it meets $\phi(t)$. The proof of the following statement is left to the reader.

Proposition 6.25.   *(i) For any tube t of K_{n+1}, the lattice path $\phi(t)$ decreases from $(0, |t|)$ to $(n+1, 0)$ with vertical steps of height 0 or 1.*

  (ii) ϕ is surjective on the decreasing paths ending at $(n+1, 0)$ with vertical steps of height 0 or 1.

 (iii) For any tubes t, t' of K_{n+1}, we have $t \subseteq t'$ if and only if $\phi(t')$ decreases when $\phi(t)$ decreases. In particular, the paths $\phi(t)$ and $\phi(t')$ are then noncrossing.

 (iv) For a tubing T on K_{n+1}, the map

$$\sigma(T) : i \longmapsto |\{t \in T \mid \phi(t) \text{ has a descent at abscissa } i\}| + 1$$

  is a surjection from $[n+1]$ to $[|T|+1]$, and therefore $\pi(T) := \bigsqcup_{j \in [|T|+1]} \sigma^{-1}(j)$ is an ordered partition of $[n+1]$ into $|T|+1$ parts. The map $T \mapsto \pi(T)$ defines an isomorphism form the nested complex $\mathcal{N}(K_{n+1})$ to the refinement poset of ordered partitions.

 (v) For a tube t of K_{n+1} not in T°, the path $\psi(t)$ is obtained from the path $\phi(t)$ by replacing the initial down stairs by an horizontal path at height 0. See Figure 6.11, where $\psi(t)$ is dotted until it meets $\phi(t)$.
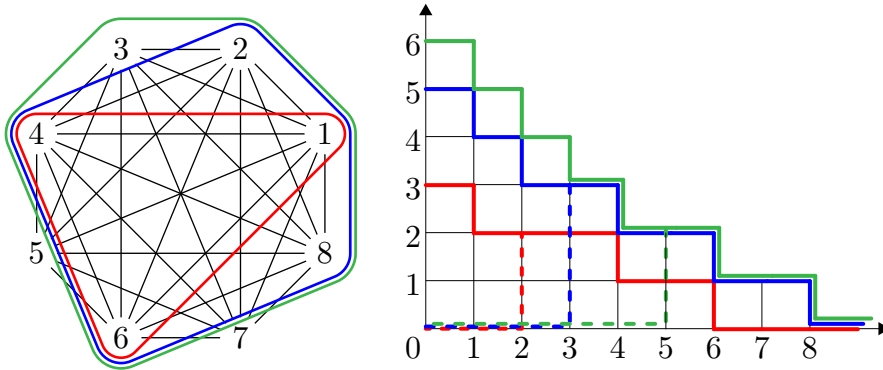
Figure 6.11 – The tubing $\{146, 12468, 123468\}$ corresponds to three noncrossing decreasing lattice paths, and to the ordered partition $57|3|28|146$.

Remark 6.26 (Dual compatibility fan). As discussed in Section 6.4.2 below, the complementation $t \mapsto V \smallsetminus t$ defines an automorphism of the nested complex $\mathcal{N}(K_{n+1})$, which dualizes the compatibility degree: $(t \,\|\, t') = (V \smallsetminus t' \,\|\, V \smallsetminus t)$ for any tubes t, t' of K_{n+1}. Therefore, the dual compatibility fans are compatibility fans: for any maximal tubing T° on K_{n+1},

$$\mathcal{D}^*(K_{n+1}, T^\circ) = \mathcal{D}(K_{n+1}, \{V \smallsetminus t^\circ \mid t^\circ \in T^\circ\}).$$

Remark 6.27 (Linear dependences). For the complete graph, the linear dependences between compatibility vectors of tubes involved in a flip can already be complicated. However, the coefficients (α, α') of the flipped tubes in these dependences can only take the following values:

$$(k, k) \text{ with } k > 0, \qquad \text{or} \qquad (k, kp) \text{ with } k, p > 0, \qquad \text{or} \qquad (kp + p, kp) \text{ with } k, p > 0.$$

6.3.5 Stars

We finally consider the nested complex $\mathcal{N}(X_{n+1})$ and the compatibility fan $\mathcal{D}(X_{n+1}, T^\circ)$ for the star X_{n+1} with $n + 1$ vertices, *i.e.* the tree with n leaves $\ell_1, \ldots, \ell_n$ all connected to a central vertex denoted $*$. The graph associahedron $\mathsf{Asso}(X_{n+1})$ is called *stellohedron*. We have represented in Figure 6.12 two realizations of the 3-dimensional stellohedron.

One easily checks that the star X_{n+1} has:

- $2^n + n - 1$ proper tubes [OEI10, A052944] (distinguish tubes containing $*$ or not),

- $n! \sum_{i=0}^{n} \dfrac{1}{i!}$ maximal tubings [OEI10, A000522] (consider the smallest tube containing $*$),

- $\sum_{i \in [k]} \binom{n}{k-i} (i-1)! \big(i\, S(n-k+i, i) + S(n-k+i, i-1) \big)$ tubings with k tubes, where
  $S(m, p)$ denotes the Stirling number of second kind (*i.e.* the number of ways to partition a set of m elements into p nonempty subsets) [OEI10, A008277] (to see it, sum over the number i of tubes containing $*$), and

- $4\, n! \sum_{\sum n_i = n} \dfrac{1}{\prod n_i} - 1 = \sum_{i \geq 1} (i+1)^n / 2^i$ tubings in total (including the empty tubing).
  This is the number of chains in the boolean lattice on an n-element set [OEI10, A007047] (an immediate bijection is given by the spines of the tubings).

We consider the initial maximal tubing $T^\circ := \{\{\ell_1\}, \ldots, \{\ell_n\}\}$ whose tubes are the n leaves of X_{n+1}. The other $2^n - 1$ tubes of X_{n+1} are the tubes containing the central
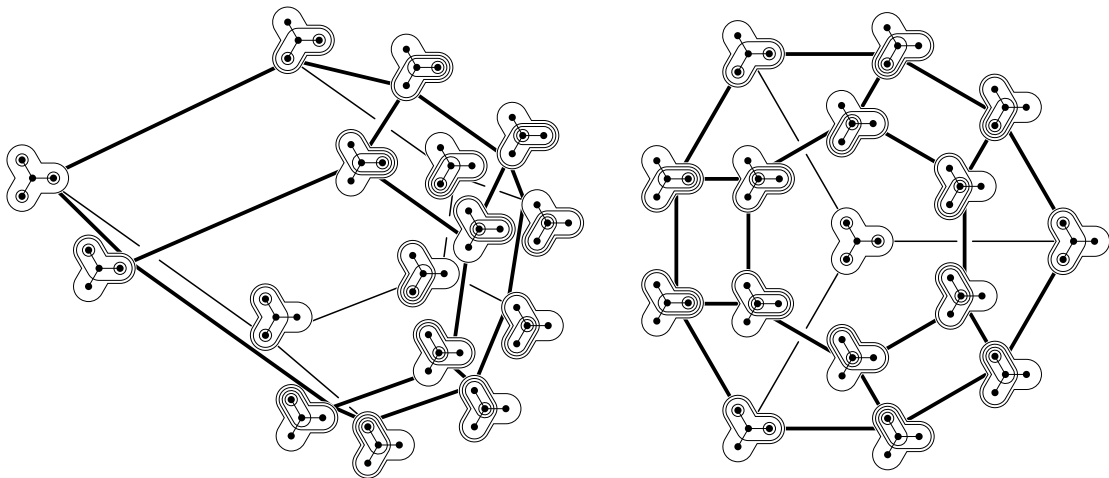
Figure 6.12 – Two polytopal realizations of the 3-dimensional stellohedron: their normal fans are the nested fan (left) and a compatibility fan (right).
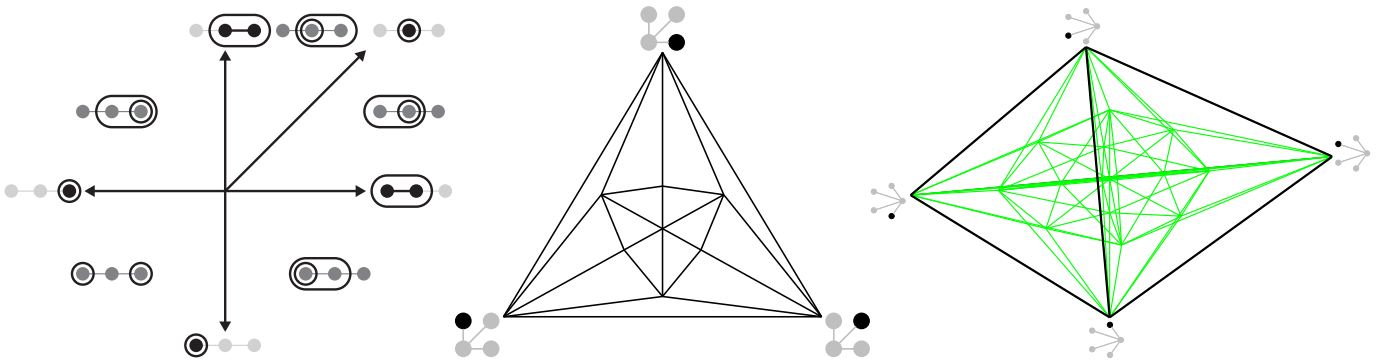
Figure 6.13 – The compatibility fans $\mathcal{D}(X_{n+1}, T^\circ)$ for the star X_{n+1} and the initial tubing $T^\circ = \{\{\ell_1\}, \ldots, \{\ell_n\}\}$ formed by its leaves (for $n \in \{2, 3, 4\}$).

vertex $*$ and some leaves (but not all). The compatibility degree of such a tube t containing $*$ with a tube $\{\ell_i\}$ is 0 if $\ell_i \in t$ and 1 if $\ell_i \notin t$. The compatibility vector $\mathbf{d}(T^\circ, t)$ of t with respect to T° is thus given by the characteristic vector of the leaves of X_{n+1} not contained in t. Moreover, two tubes $t, t' \notin T^\circ$ are compatible if and only if they are nested (since they both contain the vertex $*$). Therefore, the compatibility fan $\mathcal{D}(X_{n+1}, T^\circ)$ is obtained from the coordinate hyperplane fan by a barycentric subdivision of the positive orthant. Examples in dimension 2, 3 and 4 are gathered in Figure 6.13.

Remark 6.28 (Dual compatibility fan)**.** Observe that the compatibility degree of any tube of X_{n+1} with any leaf of X_{n+1} belongs to $\{-1, 0, 1\}$. Therefore, $\mathbf{d}(T^\circ, t) = \mathbf{d}^*(t, T^\circ)$ for any tube t, so that the compatibility and dual compatibility fans with respect to the initial tubing T° coincide. This does not hold for arbitrary initial tubings on X_{n+1}, see Remark 6.20 and Figure 6.7 (right).

Remark 6.29 (Linear dependences)**.** In the special case discussed in this section, all linear dependences between compatibility vectors of tubes involved in a flip are inclusion-exclusion dependences as in the beginning of the proof of Theorem 6.10 in Section 6.5.3. The coefficients of the flipped tubes thus always equal 1 while those of the forced tubes (not in the initial tubing T°) always equal -1.

Remark 6.30. The stellohedron $\mathsf{Asso}(X_{n+1})$ is also the secondary polytopes [San15] of two concentric copies of an $(n-1)$-dimensional simplex. See Figure 6.14.
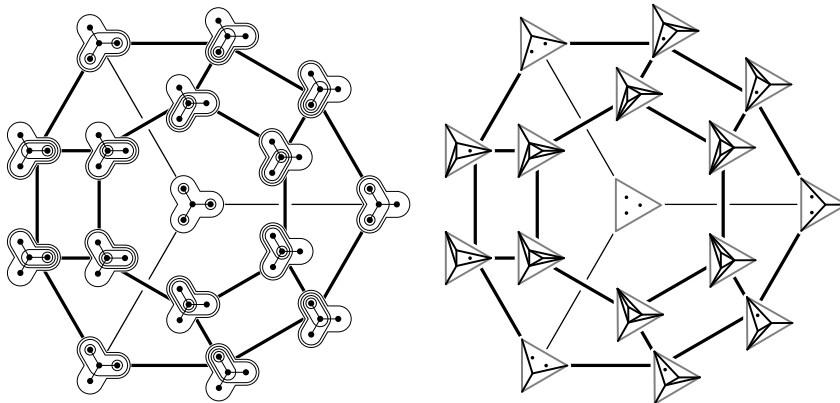
Figure 6.14 – The stellohedron (left) is a secondary polytope (right).

6.4 Further topics

In this section, we discuss several further topics in connection to compatibility fans. Note that we only state the results for compatibility fans, but similar statements hold for dual compatibility fans. Section 6.4.1 studies the behavior of the compatibility fans with respect to products and links. In Section 6.4.2, we show that most compatibility fans are not linearly isomorphic, which requires a description of all nested complex isomorphisms. Section 6.4.3 discusses the question of the realization of our compatibility fans as normal fans of convex polytopes. In Section 6.4.4, we extend our construction to design nested complexes [DHV11]. Finally, we discuss in Section 6.4.5 the connection of this chapter to LP-algebras [LP16a, LP16b].

6.4.1 Products and restrictions

In all examples that we discussed earlier, we only considered connected graphs. Compatibility fans for disconnected graphs can be reconstructed from those for connected graphs by the following statement, whose proof is left to the reader.

Proposition 6.31. *If* G *has connected components* $G_1, \ldots, G_k$, *then the nested complex* $\mathcal{N}(G)$ *is the join of the nested complexes* $\mathcal{N}(G_1), \ldots, \mathcal{N}(G_k)$. *Moreover, for any maximal tubings* $\mathsf{T}_1^\circ, \ldots, \mathsf{T}_k^\circ$ *on* $G_1, \ldots, G_k$ *respectively, the compatibility fan* $\mathcal{D}(G, \mathsf{T}^\circ)$ *with respect to the maximal tubing* $\mathsf{T}^\circ := \mathsf{T}_1^\circ \cup \cdots \cup \mathsf{T}_k^\circ$ *on* G *is the product of the compatibility fans* $\mathcal{D}(G_1, \mathsf{T}_1^\circ), \ldots, \mathcal{D}(G_k, \mathsf{T}_k^\circ)$:

$$\mathcal{D}(G, \mathsf{T}^\circ) = \mathcal{D}(G_1, \mathsf{T}_1^\circ) \times \cdots \times \mathcal{D}(G_k, \mathsf{T}_k^\circ) = \{C_1 \times \cdots \times C_k \mid C_i \in \mathcal{D}(G_i, \mathsf{T}_i^\circ) \text{ for all } i \in [k]\}.$$

Figure 6.15 (right) illustrates Proposition 6.31 with the compatibility fan of a graph formed by two paths. Compatibility fans of paths are discussed in Section 6.3.2. Besides all compatibility vectors, the cones of three different tubings are represented in Figure 6.15 (right).
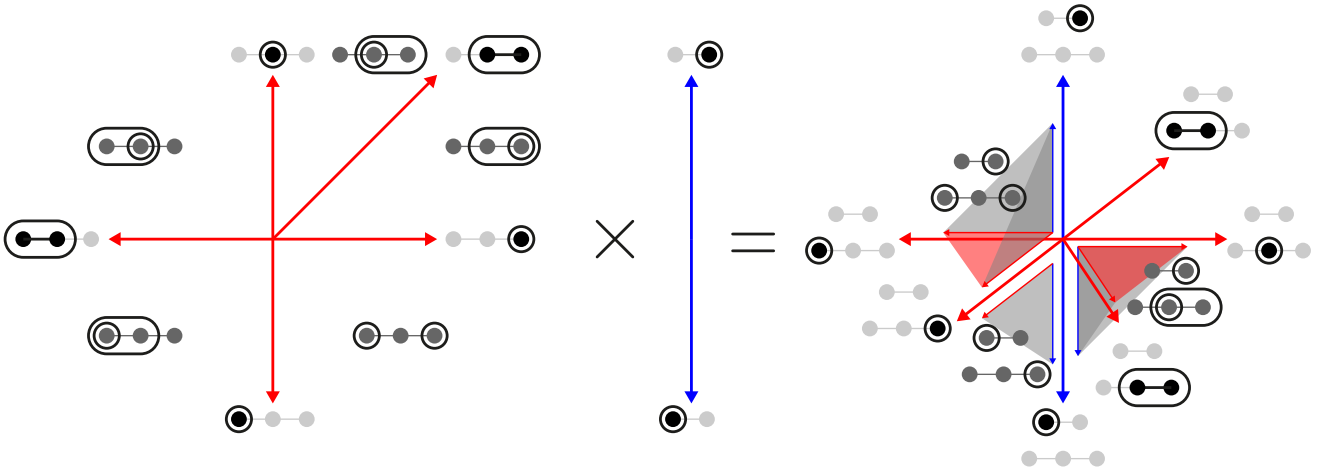
Figure 6.15 – The compatibility fan of a disconnected graph is the product (right) of the compatibility fans of its connected components (left and middle).

As observed in [CD06], all links of graphical nested complexes are joins of graphical nested complexes. The following statement asserts that the compatibility fans reflect this property on coordinate hyperplanes. To be more precise, for a tube t° of G, we denote by $G[\mathsf{t}^\circ]$ the restriction of G to t° and by $G \star \mathsf{t}^\circ$ the *reconnected complement* of t° in G, *i.e.* the graph with vertex set $V \smallsetminus \mathsf{t}^\circ$ and edge set $\left\{ e \in \binom{V \smallsetminus \mathsf{t}^\circ}{2} \mid e \text{ or } e \cup \mathsf{t}^\circ \text{ is connected in } G \right\}$.
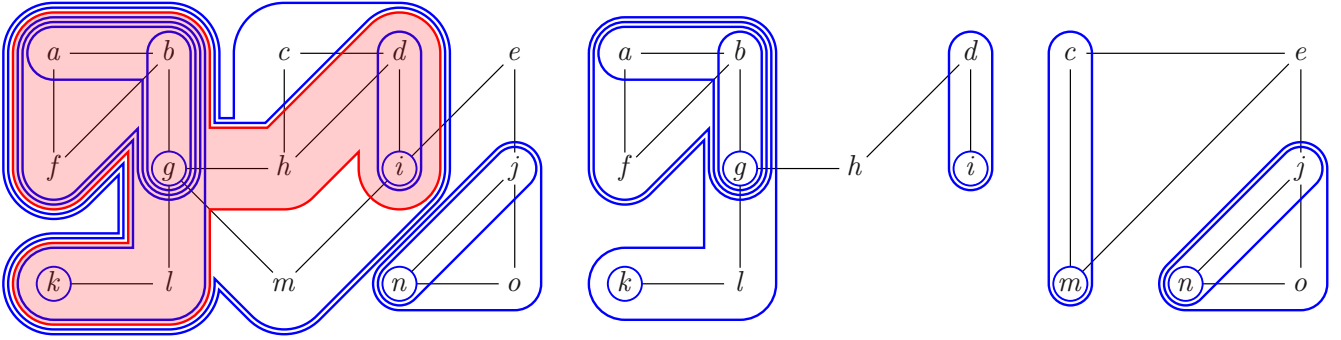
Figure 6.16 – The red tube $t_{ex}^{\circ} = \{a, b, d, f, g, h, i, k, l\}$ in the maximal tubing T° (left) yields a maximal tubing $T_{ex}^{\circ}[t_{ex}^{\circ}]$ on the restriction $G_{ex}[t_{ex}^{\circ}]$ (middle) and a maximal tubing $T_{ex}^{\circ} \star t_{ex}^{\circ}$ on the reconnected complement $G_{ex} \star t_{ex}^{\circ}$ (right).

A maximal tubing T° on G containing t° induces maximal tubings $T^{\circ}[t^{\circ}] := \{t \mid t \in T^{\circ}, t \subsetneq t^{\circ}\}$ on the restriction $G[t^{\circ}]$ and $T^{\circ} \star t^{\circ} := \{t \smallsetminus t^{\circ} \mid t \in T^{\circ}, t \not\subset t^{\circ}\}$ on the reconnected complement $G \star t^{\circ}$. See Figure 6.16.

Proposition 6.32. *The link of a tube* t° *in the nested complex* $\mathcal{N}(G)$ *is isomorphic to the join of the nested complexes* $\mathcal{N}(G[t^{\circ}])$ *and* $\mathcal{N}(G \star t^{\circ})$. *Moreover, for an initial maximal tubing* T° *containing* t°, *the intersection of the compatibility fan* $\mathcal{D}(G, T^{\circ})$ *with the coordinate hyperplane orthogonal to* $e_{t^{\circ}}$ *is the product of the compatibility fans* $\mathcal{D}(G[t^{\circ}], T^{\circ}[t^{\circ}])$ *and* $\mathcal{D}(G \star t^{\circ}, T^{\circ} \star t^{\circ})$.

This statement follows from Lemmas 6.63 and 6.64 and Theorem 6.10, proved in Section 6.5.

6.4.2   Many compatibility fans

In this section, we show that we obtained many distinct compatibility fans. Following [CSZ15], we classify compatibility fans up to linear isomorphisms: two fans $\mathcal{F}, \mathcal{F}'$ of $\mathbb{R}^n$ are linearly isomorphic if there exists an invertible linear map which sends the cones of $\mathcal{F}$ to the cones of $\mathcal{F}'$. Observe already that if two compatibility fans $\mathcal{D}(G, T^{\circ})$ and $\mathcal{D}(G', T'^{\circ})$ are linearly isomorphic, then the two nested complexes $\mathcal{N}(G)$ and $\mathcal{N}(G')$ are (combinatorially) isomorphic, meaning that there is a bijection Φ from the tubes of G to the tubes of G' which preserves the compatibility. The converse does not always hold: a nested complex isomorphism can preserve compatibility without preserving the compatibility degree. However, we prove below that the nested complex isomorphisms are so constrained that they all either preserve the compatibility degree and thus induce linear isomorphisms between compatibility fans, or exchange the compatibility and dual compatibility degrees and thus induce linear isomorphisms between compatibility and dual compatibility fans.

In the sequel, we describe all nested complex isomorphisms. Observe first that an isomorphism ϕ between two graphs G and G' automatically induces an isomorphism Φ between the nested complexes $\mathcal{N}(G)$ and $\mathcal{N}(G')$ defined by $\Phi(t) := \{\phi(v) \mid v \in t\}$ for all tubes t on G. We say that such a nested complex isomorphism Φ is *trivial*. Trivial isomorphisms clearly preserve compatibility degrees: $(\Phi(t) \| \Phi(t')) = (t \| t')$ for any tubes t, t' on G. We are interested in nontrivial nested complex isomorphisms. We first want to underline two relevant examples.

t	[1]	[2]	[3]	[4]	[5]	[6]	[1,2]	[2,3]	[3,4]	[4,5]	[5,6]	[1,3]	[2,4]	[3,5]	[4,6]	[1,4]	[2,5]	[3,6]	[1,5]	[2,6]
↻ t	[2,6]	[1]	[2]	[3]	[4]	[5]	[3,6]	[1,2]	[2,3]	[3,4]	[4,5]	[4,6]	[1,3]	[2,4]	[3,5]	[5,6]	[1,4]	[2,5]	[6]	[1,5]
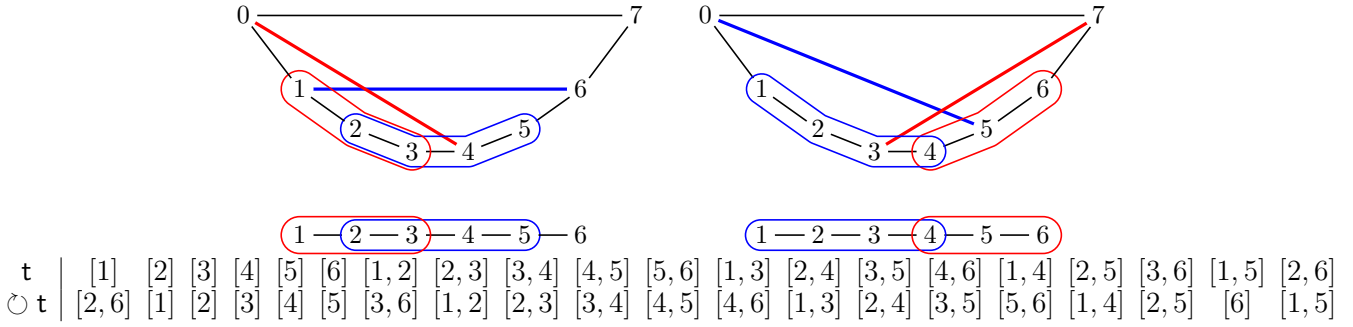
Figure 6.17 – The 1-vertex clockwise rotation of the $(n + 3)$-gon induces a nontrivial automorphism $\circlearrowleft$ of the nested complex $\mathcal{N}(\mathrm{P}_{n+1})$.

Example 6.33. The reader can check that:

(i) The complementation $\mathsf{t} \mapsto \mathrm{V} \smallsetminus \mathsf{t}$ is a nontrivial automorphism of the nested complex $\mathcal{N}(\mathrm{K}_{n+1})$ of the complete graph K_{n+1}. It dualizes the compatibility degree: $(\mathrm{V} \smallsetminus \mathsf{t} \,\|\, \mathrm{V} \smallsetminus \mathsf{t}') = (\mathsf{t}' \,\|\, \mathsf{t})$ for any tubes t, t' of K_{n+1}.

(ii) The map $\circlearrowleft$ defined for $1 \le j \le k \le n + 1$ by

$$\circlearrowleft [j, k] := \begin{cases} [k + 1, n + 1] & \text{if } j = 1, \\ [j - 1, k - 1] & \text{if } j > 1, \end{cases}$$

is a nontrivial automorphism of the nested complex $\mathcal{N}(\mathrm{P}_{n+1})$ of the path P_{n+1}. Indeed, up to conjugation by the bijection $\delta \mapsto \mathsf{t}_\delta$ of Section 6.3.2, the map $\circlearrowleft$ coincides with the (combinatorial) 1-vertex clockwise rotation of the $(n + 3)$-gon Q_{n+3}. See Figure 6.17.

Therefore, $\circlearrowleft$ has order $n + 3$, and its iterated powers are explicitly described by

$$\circlearrowleft^p [j, k] := \begin{cases} [j - p, k - p] & \text{if } 0 \le p < j, \\ [k - p + 2, n + j - p + 1] & \text{if } j \le p < k + 2, \\ [n + p + j - 2k - 1, n + p - k - 1] & \text{if } k + 2 \le p < n + 3. \end{cases}$$

In fact, it is shown in [CSZ15, Lemma 2.2] that the automorphism group of the nested complex $\mathcal{N}(\mathrm{P}_{n+1})$ is the dihedral group generated by the nontrivial automorphism $\circlearrowleft$ (the rotation of the $(n + 3)$-gon Q_{n+3}) and the automorphism $\leftrightarrow: [j, k] \mapsto [n + 2 - k, n + 2 - j]$ induced by the graph automorphism $j \mapsto n + 2 - j$ of P_{n+1} (the vertical reflection of the $(n + 3)$-gon Q_{n+3}). Note that since the compatibility degree on P_{n+1} is in $\{-1, 0, 1\}$, any nested complex automorphism preserves the compatibility degree (and also dualizes it since it is symmetric).

We now generalize both cases of Example 6.33. For $\underline{n} := \{n_1, \ldots, n_\ell\} \in \mathbb{N}^\ell$ with $n + 1 = \sum_{i \in [\ell]} (n_i + 1)$, the *spider* $\mathfrak{X}_{\underline{n}}$ is the graph with vertices $\left\{ v_j^i \mid i \in [\ell], 0 \le j \le n_i \right\}$ and edges $\left\{ \{v_{j-1}^i, v_j^i\} \mid i \in [\ell], j \in [n_i] \right\} \cup \left\{ \{v_0^i, v_0^{i'}\} \mid i \ne i' \in [\ell] \right\}$. For $0 \le j \le k \le n_i$, we denote by $[v_j^i, v_k^i]$ the path between v_j^i and v_k^i in $\mathfrak{X}_{\underline{n}}$. Informally, the spider $\mathfrak{X}_{\underline{n}}$ consists in ℓ paths $[v_1^i, v_{n_i}^i]$ called *legs* of the spider, each attached to a vertex v_0^i of a clique called *body* of the spider. See Figure 6.18. Note that spiders are sometimes called sunlike graphs in the literature.

We now define a nontrivial automorphism Ω of the nested complex $\mathcal{N}(\mathfrak{X}_{\underline{n}})$ of the spider $\mathfrak{X}_{\underline{n}}$. We distinguish two kinds of tubes of $\mathcal{N}(\mathfrak{X}_{\underline{n}})$:

Leg tubes A tube t disjoint from the body is included in a leg. The map Ω sends t into its image by the transformation which cuts the leg containing t and glues it back to the body by its other endpoint. Formally, for $i \in [\ell]$ and $1 \le j \le k \le n_i$,

$$\Omega([v_j^i, v_k^i]) := [v_{n_i+1-k}^i, v_{n_i+1-j}^i].$$

Note that Ω sends a leg tube t to a leg tube $\Omega(t)$ with $|\Omega(t)| = |t|$.

Body tubes A tube t intersecting the body is the union of segments $[v_0^i, v_{k_i}^i]$, with $-1 \le k_i \le n_i$ (with the convention that $[v_0^i, v_{-1}^i] = \varnothing$). We then define

$$\Omega(\bigcup_{i \in [\ell]} [v_0^i, v_{k_i}^i]) := \bigcup_{i \in [\ell]} [v_0^i, v_{n_i-1-k_i}^i].$$

Note that Ω sends a body tube t to a body tube $\Omega(t)$ with $|\Omega(t)| = |V| - |t|$.

Figure 6.18 illustrates the map Ω on different tubes of the spider $\mathfrak{X}_{\{0,3,2,3,0,3,2,3\}}$. Observe that Ω indeed generalizes both nontrivial nested complex automorphisms of Example 6.33:

(i) The complete graph K_{n+1} is the spider $\mathfrak{X}_{\{0\}^{n+1}}$ whose legs are all empty. The automorphism Ω of $\mathcal{N}(\mathfrak{X}_{\{0\}^{n+1}})$ specializes to the complementation $t \mapsto V \smallsetminus t$ on $\mathcal{N}(K_{n+1})$.

(ii) The path P_{n+1} is a degenerate spider whose body can be chosen at different places. Indeed, the path P_{n+1} coincides with the spider $\mathfrak{X}^1 := \mathfrak{X}_{\{n\}}$ with body $\{1\}$ and the single leg $[2, n+1]$, and the automorphism Ω of $\mathcal{N}(\mathfrak{X}^1)$ is the composition of the rotation automorphism $\circlearrowright$ with the vertical reflection automorphism $\leftrightarrow$. Similarly, for any $2 \le p \le n+1$, the path P_{n+1} coincides with the spider $\mathfrak{X}^p := \mathfrak{X}_{\{p-2,n+1-p\}}$ with body $\{p-1, p\}$ and legs $[1, p-2]$ and $[p+1, n+1]$, and the automorphism Ω of $\mathcal{N}(\mathfrak{X}^p)$ is the composition of $\circlearrowright^p$ with $\leftrightarrow$. Finally, the path P_{n+1} coincides with the spider $\mathfrak{X}^{n+2} := \mathfrak{X}_{\{n\}}$ with body $\{n+1\}$ and the single leg $[n]$, and the automorphism Ω of $\mathcal{N}(\mathfrak{X}^{n+2})$ is the composition of $\circlearrowright^{n+2}$ with $\leftrightarrow$.

This actually suggests an alternative description of Ω on arbitrary spiders $\mathfrak{X}_{\underline{n}}$. Namely, Ω is equivalently described by the following steps: shift all leg tubes towards the body, complement all body tubes, delete all edges $\{\{v_0^i, v_0^{i'}\} \mid i \ne i' \in [\ell]\}$ of the body, replace them by the clique $\{\{v_{n_i}^i, v_{n_{i'}}^{i'}\} \mid i \ne i' \in [\ell]\}$ on the feets of the spider, and finally apply the trivial isomorphism from the resulting spider back to the initial spider. Our original presentation of Ω will nevertheless be easier to handle in the proofs. The following statement is proved in Section 6.5.5.

Proposition 6.34. *The map Ω is a nontrivial involutive automorphism of the nested complex $\mathcal{N}(\mathfrak{X}_{\underline{n}})$ of the spider $\mathfrak{X}_{\underline{n}}$ dualizing the compatibility degree:* $(\Omega(t) \| \Omega(t')) = (t' \| t)$.

Remark 6.35. It follows from Proposition 6.34 that all dual compatibility fans of a spider $\mathfrak{X}_{\underline{n}}$ are also compatibility fans of $\mathfrak{X}_{\underline{n}}$: we have $\mathcal{D}^*(\mathfrak{X}_{\underline{n}}, T^\circ) = \mathcal{D}(\mathfrak{X}_{\underline{n}}, \Omega(T^\circ))$ for any maximal tubing T° on $\mathfrak{X}_{\underline{n}}$. Note that we already used this observation for complete graphs in Remark 6.26.

In fact, these nontrivial automorphisms of the nested complexes of the spiders are essentially the only nontrivial nested complex isomorphisms. The following statements are proved in Section 6.5.5.
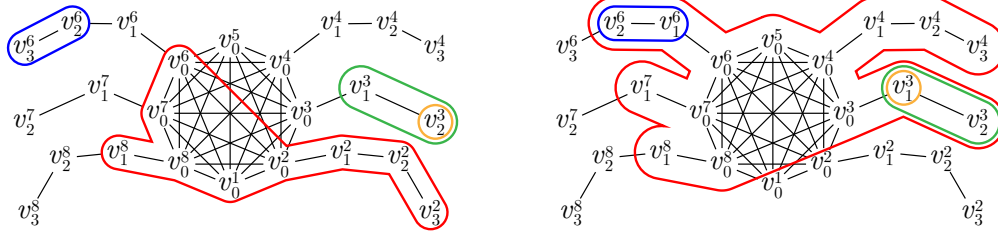
Figure 6.18 – The spider $\mathfrak{X}_{\{0,3,2,3,0,3,2,3\}}$ and examples of the action of the nontrivial nested complex isomorphism Ω: the tubing T on the left is sent to the tubing $\Omega(\mathsf{T})$ on the right.

Proposition 6.36. *A nested complex isomorphism* $\Phi : \mathcal{N}(\mathrm{G}) \to \mathcal{N}(\mathrm{G}')$ *restricts to nested complex isomorphisms* $\mathcal{N}(\mathrm{H}) \to \mathcal{N}(\mathrm{H}')$ *between maximal connected subgraphs* H *of* G *and* H' *of* G'.

Theorem 6.37. *Let* G *and* G' *be two connected graphs and* $\Phi : \mathcal{N}(\mathrm{G}) \to \mathcal{N}(\mathrm{G}')$ *be a nontrivial nested complex isomorphism. Then* G *and* G' *are spiders and there exists a graph isomorphism* $\psi : \mathrm{G} \to \mathrm{G}'$ *which induces a nested complex isomorphism* $\Psi : \mathcal{N}(\mathrm{G}) \to \mathcal{N}(\mathrm{G}')$ *(defined by* $\Psi(\mathsf{t}) := \{\psi(v) \mid v \in \mathsf{t}\}$*) such that the composition* $\Psi^{-1} \circ \Phi$ *coincides with the nontrivial nested complex automorphism* Ω *on* $\mathcal{N}(\mathrm{G})$.

Corollary 6.38. *For connected graphs* G, G', *any nested complex isomorphism* $\Phi : \mathcal{N}(\mathrm{G}) \to \mathcal{N}(\mathrm{G}')$ *either preserves or dualizes the compatibility degree: either* $(\Phi(\mathsf{t}) \| \Phi(\mathsf{t}')) = (\mathsf{t} \| \mathsf{t}')$ *for all* t, t' *of* G, *or* $(\Phi(\mathsf{t}) \| \Phi(\mathsf{t}')) = (\mathsf{t}' \| \mathsf{t})$ *for all* t, t' *of* G.

To finish our classification of primal and dual compatibility fans up to linear isomorphisms, it remains to understand when the primal and the dual compatibility fans of G with respect to the same initial maximal tubing are linearly isomorphic. For example, we already observed that

(i) $\mathcal{D}(\mathrm{P}_{n+1}, \mathsf{T}^\circ) = \mathcal{D}^*(\mathrm{P}_{n+1}, \mathsf{T}^\circ)$ for any initial tubing T° on a path P_{n+1}, see Remark 6.18,

(ii) $\mathcal{D}(\mathrm{X}_{n+1}, \mathsf{T}^\circ) = \mathcal{D}^*(\mathrm{X}_{n+1}, \mathsf{T}^\circ)$ for the initial tubing $\mathsf{T}^\circ := \{\{\ell_1\}, \dots, \{\ell_n\}\}$ of the star X_{n+1} whose tubes are the n leaves, see Remark 6.28.

These examples extend to subdivisions of stars. Namely, for $\underline{n} := \{n_1, \dots, n_\ell\} \in \mathbb{N}^\ell$ with $n = \sum_{i \in [\ell]}(n_i + 1)$, the *octopus* $\mathcal{X}_{\underline{n}}$ is the graph with vertices $\{*\} \cup \{v_j^i \mid i \in [\ell], 0 \leq j \leq n_i\}$ and edges $\{\{v_{j-1}^i, v_j^i\} \mid i \in [\ell], j \in [n_i]\} \cup \{\{*, v_0^i\} \mid i \in [\ell]\}$. Informally, the octopus $\mathcal{X}_{\underline{n}}$ consists in ℓ paths $[v_0^i, v_{n_i}^i]$ called *legs*, each attached to a *head* $*$. These graphs are often called starlike graphs in the literature, we use the term octopus to stay in the wildlife lexical field. Note that the path P_{n+1} is a degenerate octopus where the head can be chosen at any vertex. As for stars, a tube of an octopus $\mathcal{X}_{\underline{n}}$ that does not contain its head $*$ is either compatible or exchangeable with any other tube of $\mathcal{X}_{\underline{n}}$. Therefore, if T° is a maximal tubing on $\mathcal{X}_{\underline{n}}$ whose tubes do not contain the head $*$, then the compatibility fan $\mathcal{D}(\mathcal{X}_{\underline{n}}, \mathsf{T}^\circ)$ and the dual compatibility fan $\mathcal{D}^*(\mathcal{X}_{\underline{n}}, \mathsf{T}^\circ)$ coincide. The following lemma states that this only happens in this situation.

Lemma 6.39. *Let* G *be a connected graph and* T° *be an initial maximal tubing on* G. *If* $\mathcal{D}(\mathrm{G}, \mathsf{T}^\circ)$ *and* $\mathcal{D}^*(\mathrm{G}, \mathsf{T}^\circ)$ *are linearly isomorphic, then* G *is an octopus whose head is contained in no tube of* T°.

We finally obtain our classification of primal and dual compatibility fans. We first focus on primal compatibility fans and then conclude with both primal and dual compatibility fans together.

Corollary 6.40. *The number of linear isomorphism classes of compatibility fans of a connected graph* G *is:*

(i) *the number of triangulations of the regular* $(n+3)$*-gon up to the action of the dihedral group if* $\mathrm{G} = \mathrm{P}_{n+1}$ *is a path,*

(ii) *the number of orbits of maximal tubings on* G *under graph automorphisms of* G *otherwise.*

Corollary 6.41. *The number of linear isomorphism classes of primal and dual compatibility fans of a connected graph* G *is:*

(i) *the number of triangulations of the regular* $(n+3)$*-gon up to the action of the dihedral group if* $\mathrm{G} = \mathrm{P}_{n+1}$ *is a path,*

(ii) *the number of* G*-automorphism orbits of maximal tubings on* G *if* G *is a spider but not a path,*

(iii) *the number of* G*-automorphism orbits of maximal tubings on* G*, counted twice if not rooted at* $*$*, if* G *is an octopus with head* $*$ *but not a path,*

(iv) *twice the number of* G*-automorphism orbits of maximal tubings on* G *otherwise.*

Remark 6.42. Not only we obtain many nonisomorphic complete simplicial fan realizations for graphical nested complexes (as stated in Corollary 6.40), but these realizations cannot be derived from the existing geometric constructions for graph associahedra. Indeed, all previous polytopal realizations of graph associahedra can be obtained by successive face truncations of a simplex [CD06] or of a cube [Vol10, DFRS15]. Not all compatibility fans can be constructed in this way. For example, the leftmost compatibility fan of Figure 6.3 is not linearly isomorphic to the normal fan of a polytope obtained by face truncations of the 3-dimensional simplex or cube.

6.4.3 Polytopality

In this section, we briefly discuss the polytopality of our compatibility fans for graphical nested complexes. A complete polyhedral fan is said to be *polytopal* (or *regular*) if it is the normal fan of a polytope. It is well known that not all complete polyhedral fans (even simplicial) are polytopal. Examples are easily constructed from nonregular triangulations, see *e.g.* the discussion in [DRS10, Chapter 2].

Polytopality of cluster fans. The polytopality of cluster fans has been studied since the foundations of finite type cluster algebras. For compatibility fans, polytopality was shown for particular initial clusters by F. Chapoton, S. Fomin and A. Zelevinsky [CFZ02] and in type A by F. Santos [CSZ15, Section 5].

Theorem 6.43 ([CFZ02, CSZ15])**.** *The* $\mathbf{d}$*-vector fan (or compatibility fan) is polytopal for*

- *any initial cluster in any type* A *cluster algebra [CSZ15, Section 5], and*

- *the bipartite initial cluster in any finite type cluster algebra [CFZ02].*

The polytopality of g-vector fans was studied by C. Hohlweg, C. Lange and H. Thomas in [HLT11]. Recent alternative proofs were also given by S. Stella [Ste13] and V. Pilaud and C. Stump [PS15a].

Theorem 6.44 ([HLT11, Ste13, PS15a])**.** *The $\mathbf{g}$-vector fan (or Cambrian fan) is polytopal for any acyclic initial cluster in any finite type cluster algebra.*

All these results rely on the characterization of polytopality for complete simplicial fans given by Proposition 3.9.

Polytopality of compatibility fans. We have seen in Section 6.1.1 that the nested fan is the normal fan of the graph associahedron of [CD06, Dev09, Pos09, Zel06]. For the compatibility fan, the question of the polytopality remains open:

Conjecture 6.45. *All primal and dual compatibility fans of graphical nested complexes are polytopal.*

To settle this conjecture, our hope again rely on Proposition 3.9. Besides finding an explicit function ω on the compatibility vectors of the tubes of a graph, our main issue is that we do not control the details of the linear dependence between the compatibility vectors of the tubes involved in a flip. See the proof of Theorem 6.10 in Section 6.5.3.

To support Conjecture 6.45, we have studied the polytopality of the compatibility fans of the specific families of graphs discussed in Section 6.3. We show in Section 6.5.6 that Conjecture 6.45 holds for paths and cycles.

Theorem 6.46. *All compatibility and dual compatibility fans of paths and cycles are polytopal.*

Note that the case of paths is covered by the results of [CSZ15, Section 5] presented in Theorem 6.43. For cycles, the result was unknown except for the bipartite initial tubing by the results of [CFZ02] on type B and C cluster algebras. Via the correspondences given in Propositions 6.16 and 6.21, Theorem 6.46 translates to the following relevant property of $\mathbf{d}$-vector fans.

Corollary 6.47. *In types A, B and C cluster algebras, the $\mathbf{d}$-vector fan with respect to any initial cluster (acyclic or not) is polytopal.*

We were not able to settle Conjecture 6.45 for arbitrary graphs. We believe that this question is worth investigating. As already mentioned, it requires a better understanding of all linear dependences between the compatibility vectors of the tubes involved in a flip. In another direction, we checked empirically that all 3-dimensional compatibility and dual compatibility fans of Section 6.3.1 and Figure 6.4 are polytopal. Using the characterization given in Proposition 3.9, it boils down to check the feasibility of (many) linear programs.

Finally, as a curiosity and to conclude this polytopality section on a recreative note, we provide a polytopal realization of the compatibility fan for the star X_{n+1} with respect to the initial tubing $\mathsf{T}^{\circ} := \{\{\ell_1\}, \ldots, \{\ell_n\}\}$ whose tubes are the n leaves of X_{n+1}. We first observe that this fan is linearly isomorphic to the fan $\mathcal{G}(\mathrm{G})$ of Theorem 6.1. Therefore, it can be realized by an affine transformation of the graph associahedra constructed in Theorem 6.3. Here, we prefer to give a direct construction with integer coordinates. We provide both the vertex and the facet descriptions of this realization. On the one hand, for each maximal tubing T on X_{n+1} we define a point $\mathbf{x}(\mathsf{T}) \in \mathbb{R}^n$ whose ith coordinate is the cardinality of the inclusion minimal tube of $\mathsf{T} \cup \{V\}$ containing the leaf ℓ_i minus 1. The set $\{\mathbf{x}(\mathsf{T}) \mid \mathsf{T} \text{ maximal tubing on } X_{n+1}\}$ is the orbit under permutation coordinates of the set $\{\sum_{i>k} i\, \mathbf{e}_i \mid 0 \le k \le n\}$. On the other hand, for a tube t of X_{n+1} containing the central vertex $*$, we observed earlier that the compatibility vector of t with respect to T° is the characteristic vector of the leaves of X_{n+1} not contained in t. Let $f(k) := \sum_{j=k}^{n} j = \frac{1}{2}(n+k)(n+1-k)$ and define a half-space $\mathbf{H}^{\ge}(\mathsf{t})$ of $\mathbb{R}^n$ by

$$\mathbf{H}^{\ge}(\mathsf{t}) := \left\{ \mathbf{x} \in \mathbb{R}^n \;\middle|\; \langle \mathbf{d}(\mathsf{T}^{\circ}, \mathsf{t}) | \mathbf{x} \rangle \le f(|\mathsf{t}|) \right\} = \left\{ \mathbf{x} \in \mathbb{R}^n \;\middle|\; \sum_{\substack{i \in [n] \\ \ell_i \in \mathsf{t}}} x_i \le f(|\mathsf{t}|) \right\}.$$
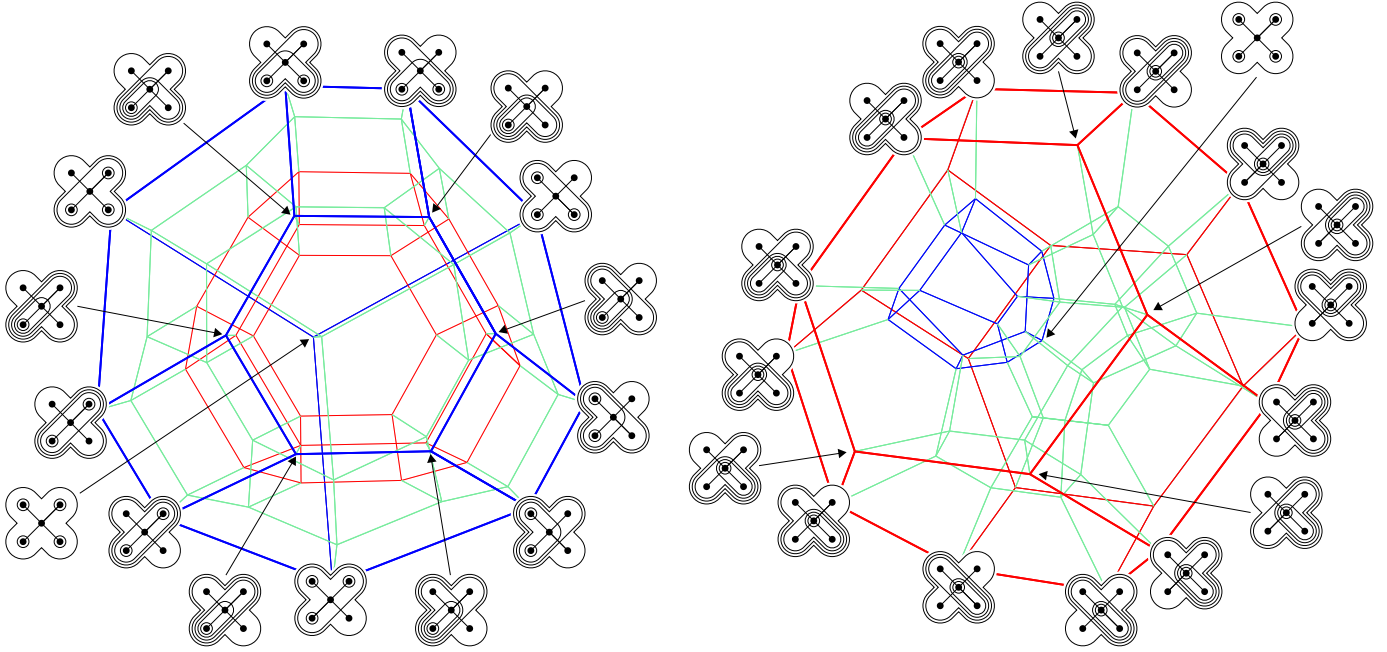
Figure 6.19 – Two Schlegel diagrams for the 4-dimensional stellohedron defined in Proposition 6.48. The red facet corresponds to all tubings containing the tube $\{*\}$ while the blue facet corresponds to all tubings containing the tube $\{\ell\}$, where ℓ is the bottom left leaf of X_5.

Finally, for the tubes of the initial tubing T°, we define

$$\mathbf{H}^{\geq}(\{\ell_i\}) := \{\mathbf{x} \in \mathbb{R}^n \mid \langle \mathbf{d}(\mathsf{T}^\circ, \{\ell_i\}) | \mathbf{x} \rangle \leq 0\} = \{\mathbf{x} \in \mathbb{R}^n \mid x_i \geq 0\}\,.$$

Proposition 6.48. *The compatibility fan $\mathcal{D}(X_{n+1}, \mathsf{T}^\circ)$ with respect to the initial tubing $\mathsf{T}^\circ := \{\{\ell_1\}, \ldots, \{\ell_n\}\}$, whose tubes are the n leaves of X_{n+1}, is the normal fan of the n-dimensional simple polytope defined equivalently as*

- *the convex hull of the points $\mathbf{x}(\mathsf{T})$ for all maximal tubings T on X_{n+1}, or*

- *the intersection of the half-spaces $\mathbf{H}^{\geq}(\mathsf{t})$ for all tubes t of X_{n+1}.*

The proof of this statement is given in Section 6.5.6. As an illustration, the 3-dimensional stellohedron defined in Proposition 6.48 is represented in Figure 6.12 (right). Figure 6.19 represents two Schlegel diagrams (see [Zie95, Lecture 5] for definition) for the 4-dimensional stellohedron defined in Proposition 6.48. In both pictures, we have distinguished two particular facets:

- The red facet corresponds to all tubings containing the tube $\{*\}$. Since the reconnected complement of $\{*\}$ in X_5 is the complete graph K_4, it has the combinatorics of the permutahedron. In fact, by definition of our polytopal realization, this facet is the classical permutahedron, obtained as the convex hull of the orbit of $\sum_{i \in [4]} i\,\mathbf{e}_i$ under permutation of the coordinates.
- The blue facet corresponds to all tubings containing the tube $\{\ell\}$, where ℓ is the bottom left leaf of X_5. This facet contains the initial tubing T° at the back. Note that there are 4 isometric facets to this blue facet, corresponding to the four leaves of X_5. This is visible in Figure 6.19 (right).

The blue (resp. red) facet is the projection facet on the left (resp. right) picture.

Remark 6.49. To conclude, observe that we could have replaced the function f in the definition of the half-spaces $\mathbf{H}^{\geq}(\mathsf{t})$ by any concave function. This follows from Proposition 3.9 since the linear dependence between the compatibility vectors of the tubes of $\mathsf{T} \cup \mathsf{T}'$ is given for any adjacent maximal tubings T, T' on X_{n+1} distinct from T° such that $\mathsf{T} \smallsetminus \{\mathsf{t}\} = \mathsf{T}' \smallsetminus \{\mathsf{t}'\}$ by

$$\mathbf{d}(\mathsf{T}^{\circ}, \mathsf{t}) + \mathbf{d}(\mathsf{T}^{\circ}, \mathsf{t}') = \mathbf{d}(\mathsf{T}^{\circ}, \underline{\mathsf{t}}) + \mathbf{d}(\mathsf{T}^{\circ}, \bar{\mathsf{t}})$$

where $\bar{\mathsf{t}} := \mathsf{t} \cap \mathsf{t}'$ and $\underline{\mathsf{t}} := \mathsf{t} \cap \mathsf{t}'$ (which are tubes of X_{n+1}). Details are left to the reader.

6.4.4 Design nested complex

Generalizing graphical nested complexes, S. Devadoss, T. Heath and C. Vipismakul introduced design nested complexes in [DHV11, Section 5]. To define these complexes, one considers *design tubes* of G, which are of two types:

- the *round tubes* are usual tubes of G (including the connecting components of G),

- the *square tubes* are just single nodes of G.

We denote by $v^{\square}$ the square tube containing v, and still denote round tubes as sets. Two design tubes are *compatible* if

- they are both round tubes and they are either nested, or disjoint and nonadjacent,

- or at least one of them is a square tube and they are not nested.

The *design nested complex* of G is the simplicial complex $\mathcal{N}^{\square}(G)$ of sets of pairwise compatible design tubes of G. Examples are given in Figure 6.20. As we mentioned in Section 4.4.2, the definition of design nested complexes can easily be extended to arbitrary building sets, but we do not need it here. By definition, the nested complex $\mathcal{N}(G)$ is (isomorphic to) the subcomplex of the design nested complex $\mathcal{N}^{\square}(G)$ involving none of the square tubes, or equivalently containing all improper round tubes.

For a design tube t of G, set

$$\mathbf{g}^{\square}(\mathsf{t}) := \begin{cases} \sum_{v \in \mathsf{t}} \mathbf{e}_v & \text{if } \mathsf{t} \text{ is a round tube,} \\ -\mathbf{e}_v & \text{if } \mathsf{t} \text{ is the square tube } \{v\}. \end{cases}$$

For a tubing T on G, define $\mathbf{g}^{\square}(\mathsf{T}) := \{\mathbf{g}^{\square}(\mathsf{t}) \mid \mathsf{t} \in \mathsf{T}\}$. These vectors again support a complete simplicial fan realization of the design nested complex $\mathcal{N}^{\square}(G)$.

Theorem 6.50 ([DHV11])**.** *For any graph* G*, the collection of cones*

$$\mathcal{G}^{\square}(G) := \{\mathbb{R}_{\geq 0}\, \mathbf{g}^{\square}(\mathsf{T}) \mid \mathsf{T} \text{ tubing on } G\}$$

is a complete simplicial fan of $\mathbb{R}^{V}$*, called* design nested fan *of* G*, which realizes* $\mathcal{N}^{\square}(G)$*.*

By definition, the $\mathbf{g}^{\square}$ vector of a round tube t is just the characteristic vector of t. Therefore, the nonnegative part of the design nested fan $\mathcal{G}^{\square}(G)$ projects to the nested fan $\mathcal{G}(G)$ defined in Section 6.1.1. Using ideas similar to the construction of the graph associahedra $\mathrm{Asso}(G)$ realizing $\mathcal{G}(G)$, S. L. Devadoss, T. Heath and C. Vipismakul prove that $\mathcal{G}^{\square}(G)$ is as well polytopal.

Theorem 6.51 ([DHV11])**.** *The design nested fan is the normal fan of a polytope obtained from the cube by iterated face truncations.*
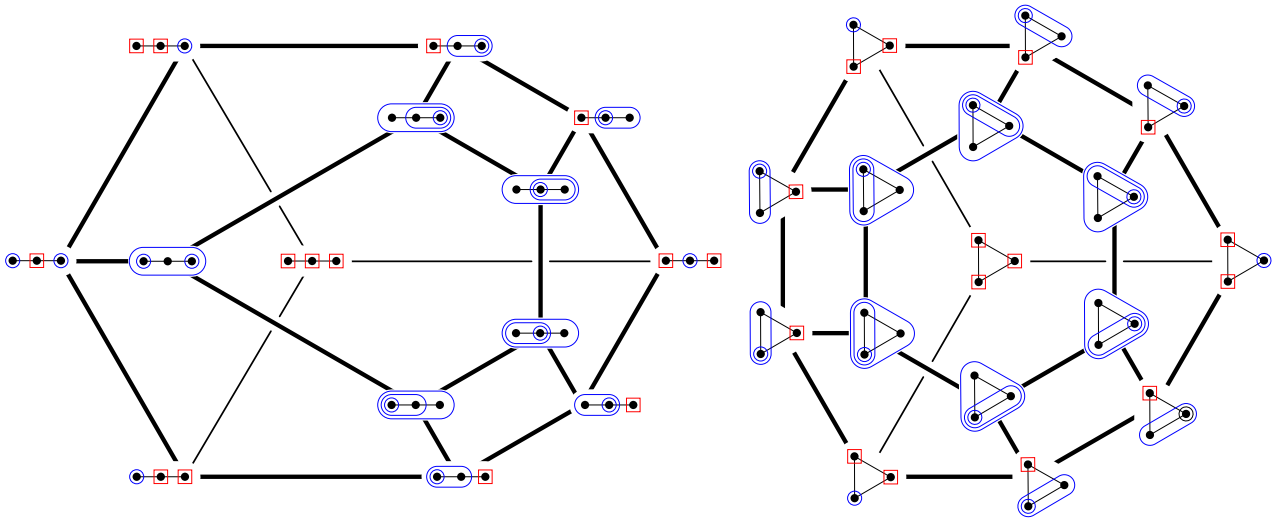
Figure 6.20 – Two design graph associahedra: the design P_3-associahedron (left) and the design K_3-associahedron (right). For readability, round tubes are colored blue while square tubes are colored red.

We denote this polytope by $\mathsf{Asso}^\square(G)$ and call it *design graph associahedron* (although it is called *graph cubeahedron* in [DHV11]). Observe that the face of $\mathsf{Asso}^\square(G)$ corresponding to the tubing formed by the connected components of G coincides with the graph associahedron $\mathsf{Asso}(G)$. Figure 6.20 illustrates the design P_3-associahedron and the design K_3-associahedron. In this figure, the attentive reader should recognize different standard graph associahedra: on the one hand, the front 2-dimensional faces of $\mathsf{Asso}^\square(P_3)$ and $\mathsf{Asso}^\square(K_3)$ are respectively $\mathsf{Asso}(P_3)$ and $\mathsf{Asso}(K_3)$, and on the other hand, the design graph associahedra $\mathsf{Asso}^\square(P_3)$ and $\mathsf{Asso}^\square(K_3)$ themselves turn out to coincide respectively with $\mathsf{Asso}(P_4)$ and $\mathsf{Asso}(X_4)$ (see Example 6.54). Starting from dimension 4, most design graph associahedra are not standard graph associahedra (see Proposition 6.56). Figures 6.21 and 6.22 represent two Schlegel diagrams (see [Zie95, Lecture 5] for definition) for the 4-dimensional design cycle associahedron $\mathsf{Asso}^\square(O_4)$ and design star associahedron $\mathsf{Asso}^\square(X_4)$.

This section aims at showing that our compatibility fan construction extends to the design nested complex. That is, we produce a complete simplicial fan realizing the design nested complex from any initial maximal design tubing. Interestingly, we will see in Remark 6.61 that the compatibility fan associated to the specific maximal design tubing consisting of all square tubes coincides with the design nested fan. This provides a relevant connection between our construction and the classical constructions [CD06, FS05, Dev09, Zel06] for graph associahedra.

Observe that a square tube is compatible with all design tubes not containing it and exchangeable with all design tubes containing it. Definition 6.5 of compatibility degree thus naturally extends on all pairs of design tubes as follows.

Definition 6.52. For two design tubes t, t' of G, the *compatibility degree* of t with t' is

$$
(t \parallel t') = \begin{cases} -1 & \text{if } t = t', \\ 1 & \text{if } t \text{ and } t' \text{ are nested and exactly one is square}, \\ |\{\text{neighbors of } t \text{ in } t' \smallsetminus t\}| & \text{if } t \text{ and } t' \text{ are round and } t \nsubseteq t', \\ 0 & \text{otherwise}. \end{cases}
$$

By construction, this compatibility degree still satisfies the conclusions of Proposi-
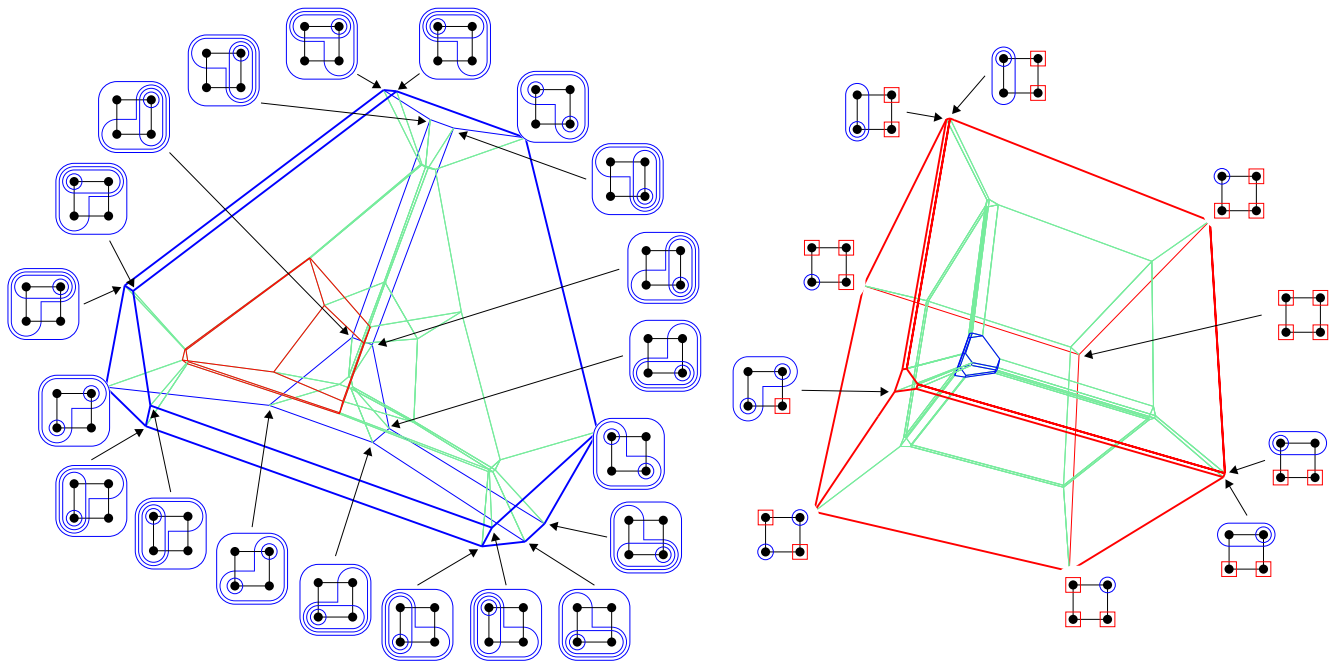
Figure 6.21 – Two Schlegel diagrams for the 4-dimensional design cycle associahedron. The blue facet corresponds to all round tubings while the red facet corresponds to all tubings containing the bottom right square tube of O_4.
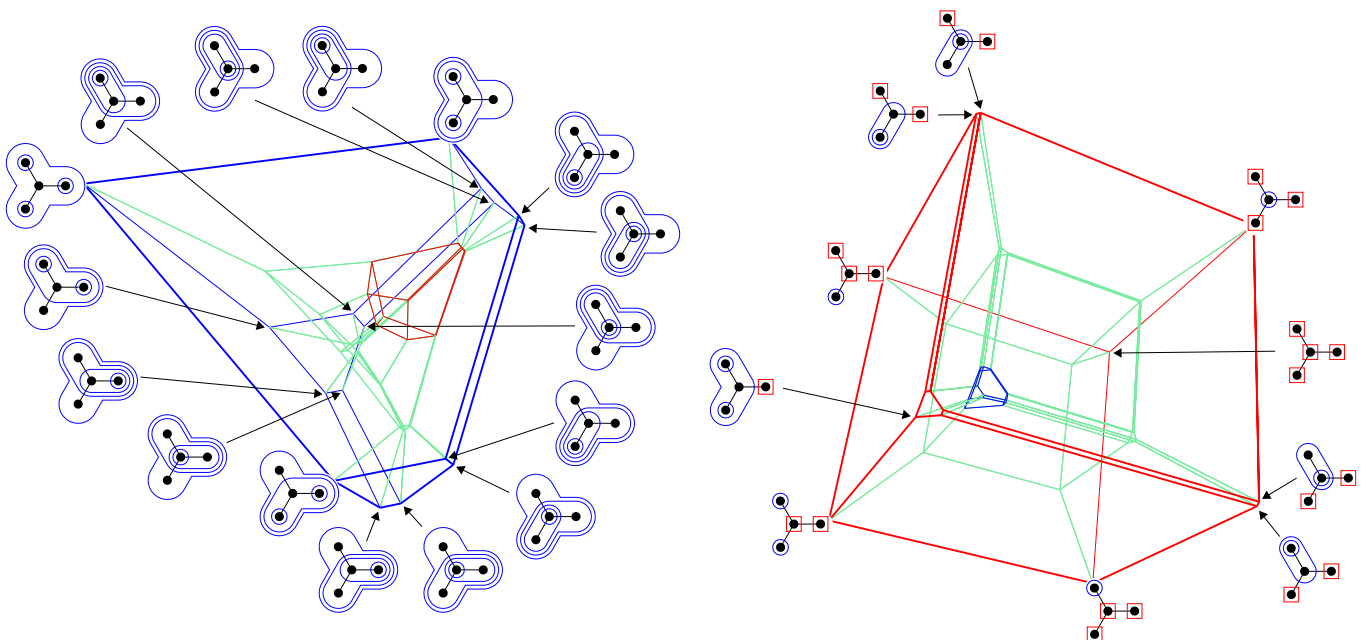
Figure 6.22 – Two Schlegel diagrams for the 4-dimensional design star associahedron. The blue facet corresponds to all round tubings while the red facet corresponds to all tubings containing the right square tube of X_4.
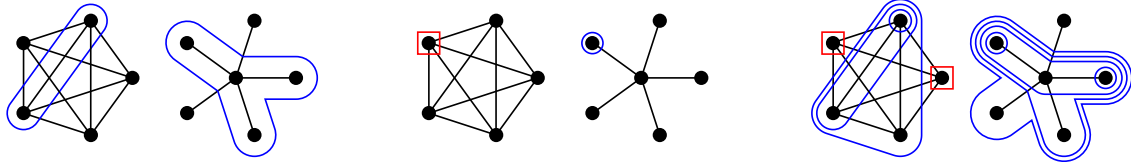
Figure 6.23 – An isomorphism from the design nested complex of a complete graph with 5 vertices (left) to the nested complex of a star with 6 vertices (right).
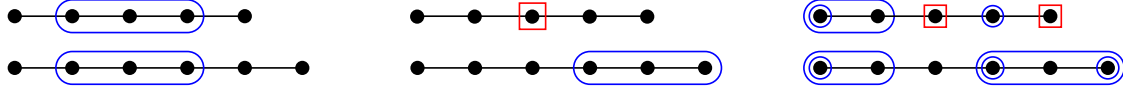
Figure 6.24 – An isomorphism from the design nested complex of a path with 5 vertices (top) to the nested complex of a path with 6 vertices (bottom).

tion 6.7 and thus measures the incompatibility between design tubes. We then define as usual the *compatibility vector* of a design tube t of G with respect to an initial maximal design tubing $\mathsf{T}^\circ := \{\mathsf{t}_1^\circ, \ldots, \mathsf{t}_n^\circ\}$ as the vector $\mathbf{d}(\mathsf{T}^\circ, \mathsf{t}) := [(\mathsf{t}_1^\circ \,\|\, \mathsf{t}), \ldots, (\mathsf{t}_n^\circ \,\|\, \mathsf{t})]$ and the *compatibility matrix* of a design tubing $\mathsf{T} := \{\mathsf{t}_1, \ldots, \mathsf{t}_m\}$ on G with respect to T° as the matrix $\mathbf{d}(\mathsf{T}^\circ, \mathsf{T}) := [(\mathsf{t}_i^\circ \,\|\, \mathsf{t}_j)]_{i \in [n], j \in [m]}$. We extend Theorem 6.10 in the following statement, whose proof is sketched in Section 6.5.7.

Theorem 6.53. *For any graph* G *and any maximal design tubing* T° *on* G*, the collection of cones*

$$\mathcal{D}^\square(\mathrm{G}, \mathsf{T}^\circ) := \{\mathbb{R}_{\geq 0}\, \mathbf{d}(\mathsf{T}^\circ, \mathsf{T}) \mid \mathsf{T} \text{ design tubing on } \mathrm{G}\}$$

is a complete simplicial fan which realizes the design nested complex $\mathcal{N}^\square(\mathrm{G})$*. We call it the* design compatibility fan *of* G *with respect to* T°*.*

Using the same duality trick as in the proof of Theorem 6.14, the reader can obtain as well dual design compatibility fans.

Concerning isomorphisms, we have similar results as in Section 6.4.2. Notice first that the conclusions of Proposition 6.36 still hold for design nested complexes. We can thus restrict our discussion to design nested complexes of connected graphs. We first compare design and standard nested complexes, starting with the following examples.

Example 6.54. The reader can check that:

(i) The design nested complex $\mathcal{N}^\square(\mathrm{K}_n)$ is isomorphic to the standard nested complex $\mathcal{N}(\mathrm{X}_{n+1})$. A natural isomorphism sends a square tube $v^\square$ of K_n to the tube $\{v\}$ of X_{n+1}, and a round tube t of K_n to the tube $\{*\} \cup ([n] \smallsetminus \mathsf{t})$ of X_{n+1} (where $*$ is the central vertex). See Figure 6.23.

(ii) The design nested complex $\mathcal{N}^\square(\mathrm{P}_n)$ is isomorphic to the standard nested complex $\mathcal{N}(\mathrm{P}_{n+1})$. A natural isomorphism sends a square tube $v^\square$ of P_n to the tube $\{v+1, \ldots, n+1\}$ of P_{n+1}, and a round tube t of P_n to the tube t of P_{n+1}. See Figure 6.24. We denote this isomorphism by $\Pi : \mathcal{N}^\square(\mathrm{P}_n) \to \mathcal{N}(\mathrm{P}_{n+1})$.

We now generalize both cases of Example 6.54. Consider the spiders and octopuses defined in Section 6.4.2: for $\underline{n} := \{n_1, \ldots, n_\ell\} \in \mathbb{N}^\ell$ with $n = \sum_{i \in [\ell]}(n_i + 1)$,

• the spider $\mathfrak{X}_{\underline{n}}$ has ℓ *legs* $[v_1^i, v_{n_i}^i]$ attached to its *body* (the complete graph on $\{v_0^i\}_{i \in [\ell]}$),

• the octopus $\mathcal{X}_{\underline{n}}$ has ℓ *legs* $[v_0^i, v_{n_i}^i]$ attached to its *head* (the single vertex $*$).

We define an isomorphism $\bar{\Omega}$ from the design nested complex $\mathcal{N}^\square(\mathfrak{X}_{\underline{n}})$ of the spider $\mathfrak{X}_{\underline{n}}$ to the nested complex $\mathcal{N}(\mathcal{X}_{\underline{n}})$ of the octopus $\mathcal{X}_{\underline{n}}$. We distinguish three kinds of tubes of $\mathcal{N}^\square(\mathfrak{X}_{\underline{n}})$:
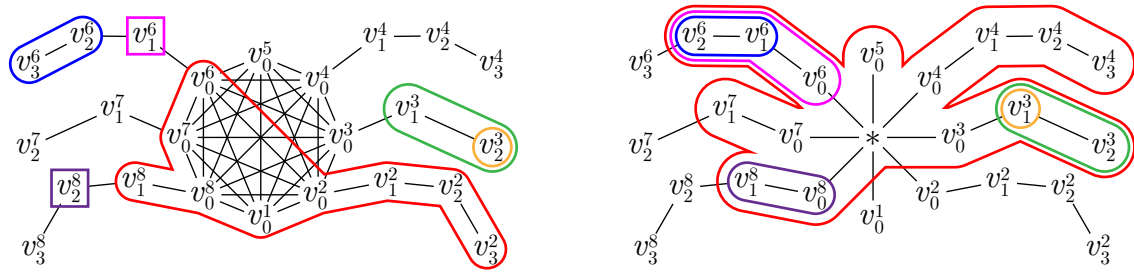
Figure 6.25 – An isomorphism from the design nested complex of the spider $\mathfrak{X}_{\{0,3,2,3,0,3,2,3\}}$ (left) to the nested complex of the octopus $\mathcal{X}_{\{0,3,2,3,0,3,2,3\}}$ (right).

Square tubes for $i \in [\ell]$ and $j \in [0, n_i]$, $\quad \bar{\Omega}(v_j^{i^\square}) := [v_0^i, v_{n_i-j}^i]$,

Leg tubes for $i \in [\ell]$ and $1 \leq j \leq k \leq n_i$, $\quad \bar{\Omega}([v_j^i, v_k^i]) := [v_{n_i+1-k}^i, v_{n_i+1-j}^i]$,

Body tubes for $-1 \leq k_i \leq n_i$ ($i \in [\ell]$), $\quad \bar{\Omega}(\bigcup_{i\in[\ell]} [v_0^i, v_{k_i}^i]) := \{*\} \cup \bigcup_{i\in[\ell]} [v_0^i, v_{n_i-1-k_i}^i]$.

Figure 6.25 illustrates the map $\bar{\Omega}$ on different tubes of the spider $\mathfrak{X}_{\{0,3,2,3,0,3,2,3\}}$. Observe that $\bar{\Omega}$ indeed generalizes both isomorphisms of Example 6.54:

(i) As $K_n = \mathfrak{X}_{\{0\}^n}$ and $X_{n+1} = \mathcal{X}_{\{0\}^n}$, the isomorphism $\bar{\Omega} : \mathcal{N}^\square(\mathfrak{X}_{\{0\}^n}) \to \mathcal{N}(\mathcal{X}_{\{0\}^n})$ coincides with the isomorphism of Example 6.54 (i).

(ii) As $P_n = \mathfrak{X}_{\{n\}}$ and $P_{n+1} = \mathcal{X}_{\{n\}}$, the isomorphism $\bar{\Omega} : \mathcal{N}^\square(\mathfrak{X}_{\{n\}}) \to \mathcal{N}(\mathcal{X}_{\{n\}})$ coincides with the isomorphism Π of Example 6.54 (ii) up to the automorphisms $\circlearrowright$ and $\leftrightarrow$ of the nested complex $\mathcal{N}(\mathcal{X}_{\{n\}})$ described in Example 6.33 (ii). More precisely if we consider the leftmost vertex of P_n as the body of $\mathfrak{X}_{\{n\}}$ and the leftmost vertex of P_{n+1} as the head of $\mathcal{X}_{\{n\}}$, then one can check that $\circlearrowright \circ \bar{\Omega} = \leftrightarrow \circ \Pi$.

The proof of the following statement is similar to that of Proposition 6.34 and therefore left to the reader.

Proposition 6.55. *The map $\bar{\Omega}$ is an isomorphism from the design nested complex $\mathcal{N}^\square(\mathfrak{X}_{\underline{n}})$ of the spider $\mathfrak{X}_{\underline{n}}$ to the nested complex $\mathcal{N}(\mathcal{X}_{\underline{n}})$ of the octopus $\mathcal{X}_{\underline{n}}$ which dualizes the compatibility degree:* $(\bar{\Omega}(\mathsf{t}) \| \bar{\Omega}(\mathsf{t}')) = (\mathsf{t}' \| \mathsf{t})$.

The following proposition, proved in Section 6.5.8, states that $\bar{\Omega}$ is essentially the only isomorphism between design and standard nested complexes.

Proposition 6.56. *Let $\bar{G}$ and G be two connected graphs and $\Phi : \mathcal{N}^\square(\bar{G}) \to \mathcal{N}(G)$ be a simplicial complex isomorphism. Then $\bar{G}$ is a spider $\mathfrak{X}_{\underline{n}}$ while G is an octopus $\mathcal{X}_{\underline{n}}$ and Φ coincides with $\bar{\Omega}$ up to composition with a nested complex automorphism of $\mathcal{N}(G)$ (described in Theorem 6.37).*

We now classify combinatorial isomorphisms of design nested complexes. As in the case of standard nested complexes, any graph isomorphism $\phi : G \to G'$ induces a *trivial* design nested complex isomorphism $\Phi : \mathcal{N}^\square(G) \to \mathcal{N}^\square(G')$, defined on round tubes by $\Psi(\mathsf{t}) := \{\psi(v) \mid v \in \mathsf{t}\}$ and on square tubes by $\Psi(v^\square) := \psi(v)^\square$, which preserves compatibility degrees. We again focus on nontrivial design nested complex isomorphisms. We first underline two examples.
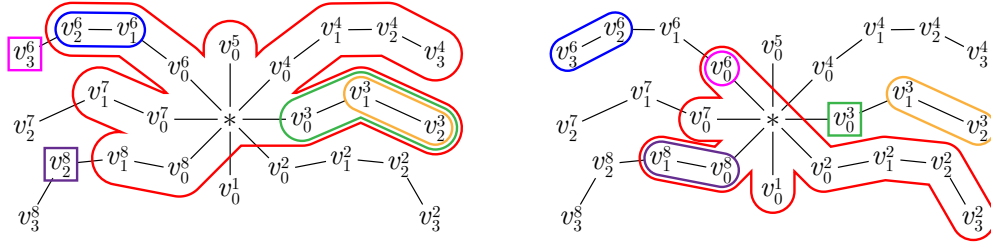
Figure 6.26 – The octopus $\mathfrak{X}_{\{0,3,2,3,0,3,2,3\}}$ and examples of the action of the nontrivial design nested complex isomorphism $\Omega^\square$: the design tubing T on the left is sent to the design tubing $\Omega^\square(\mathsf{T})$ on the right.

Example 6.57. The reader can check that:

(i) For the star X_n with central vertex $*$, the map which preserves the square tube $*^\square$, exchanges the square tube $v^\square$ with the round tube $\{v\}$, and exchanges any other round tube t with the round tube $([n] \smallsetminus \mathsf{t}) \cup \{*\}$, is a nontrivial design nested complex automorphism of $\mathcal{N}^\square(\mathrm{X}_n)$.

(ii) For $p \in [n+3]$, the conjugation $\Pi \circ \circlearrowright^p \circ \Pi^{-1}$ of the automorphism $\circlearrowright^p : \mathcal{N}(\mathrm{P}_{n+1}) \to \mathcal{N}(\mathrm{P}_{n+1})$ of Example 6.33 (ii) by the isomorphism $\Pi : \mathcal{N}^\square(\mathrm{P}_n) \to \mathcal{N}(\mathrm{P}_{n+1})$ of Example 6.54 (ii) is a nontrivial design nested complex automorphism of $\mathcal{N}^\square(\mathrm{P}_n)$.

Note that these two automorphisms send some square tubes to round tubes and thus are nontrivial.

We now describe a generalization of both cases of Example 6.57. Namely, we define an automorphism $\Omega^\square$ of the design nested complex $\mathcal{N}^\square(\mathcal{X}_{\underline{n}})$ of the octopus $\mathcal{X}_{\underline{n}}$ for any $\underline{n} := \{n_1, \ldots, n_\ell\} \in \mathbb{N}^\ell$ with $n = \sum_{i \in [\ell]}(n_i + 1)$ as follows:

Square tubes for $i \in [\ell]$ and $j \in [0, n_i]$, $\qquad \Omega^\square(v_j^{i\,\square}) := [v_0^i, v_{n_i-j}^i]$ $\quad$ and $\quad$ $\Omega^\square(*^\square) := *^\square$,

Leg tubes for $i \in [\ell]$ and $0 \le k \le n_i$, $\qquad \Omega^\square\big([v_0^i, v_k^i]\big) := v_{n_i-k}^i{}^\square$,
$\qquad\qquad$ for $i \in [\ell]$ and $1 \le j \le k \le n_i$, $\quad \Omega^\square\big([v_j^i, v_k^i]\big) := [v_{n_i+1-k}^i, v_{n_i+1-j}^i]$,

Head tubes for $-1 \le k_i \le n_i$ ($i \in [\ell]$), $\quad \Omega^\square\big(\{*\} \cup \bigcup_{i \in [\ell]} [v_0^i, v_{k_i}^i]\big) := \{*\} \cup \bigcup_{i \in [\ell]} [v_0^i, v_{n_i-1-k_i}^i]$.

Figure 6.26 illustrates the map $\Omega^\square$ on different tubes of the octopus $\mathcal{X}_{\{0,3,2,3,0,3,2,3\}}$. The reader is invited to check that $\Omega^\square$ indeed generalizes the nontrivial automorphisms of Example 6.57. The following statement is also left to the reader. The proof is similar to that of Proposition 6.34.

Proposition 6.58. *The map $\Omega^\square$ is a nontrivial involutive automorphism of the design nested complex $\mathcal{N}(\mathcal{X}_{\underline{n}})$ which dualizes the compatibility degree: $(\Omega^\square(\mathsf{t}) \,\|\, \Omega^\square(\mathsf{t}')) = (\mathsf{t}' \,\|\, \mathsf{t})$.*

The following theorem, proved in Section 6.5.8, states that $\Omega^\square$ is essentially the only nontrivial design nested complex isomorphism.

Theorem 6.59. *Let G and G' be two connected graphs and $\Phi : \mathcal{N}^\square(\mathrm{G}) \to \mathcal{N}^\square(\mathrm{G}')$ be a nontrivial design nested complex isomorphism. Then G and G' are octopuses and there exists a graph isomorphism $\psi : \mathrm{G} \to \mathrm{G}'$ which induces a design nested complex isomorphism $\Psi : \mathcal{N}^\square(\mathrm{G}) \to \mathcal{N}^\square(\mathrm{G}')$ (defined by $\Psi(\mathsf{t}) := \{\psi(v) \mid v \in \mathsf{t}\}$ and $\Psi(v^\square) := \psi(v)^\square$) such that the composition $\Psi^{-1} \circ \Phi$ coincides with the nontrivial design nested complex automorphism $\Omega^\square$ on $\mathcal{N}^\square(\mathrm{G})$.*

We conclude that we get many design compatibility fans (up to linear isomorphism).

Corollary 6.60. *If a connected graph* G *is not an octopus, then the number of linear isomorphism classes of primal (resp. dual) design compatibility fans of* G *is the number of orbits of maximal design tubings on* G *under graph automorphisms of* G.

Finally, as for the compatibility fan, we do not know in general whether the design compatibility fan is or not polytopal. Nevertheless, we know it for the following initial tubing.

Remark 6.61. Consider the maximal tubing $\mathsf{T}^\square$ of a graph G consisting of all square tubes of G. By definition of the compatibility degree with square tubes, the compatibility vector of a square tube $\{v\}$ is just $-\mathrm{e}_v$ while the compatibility vector of a round tube t with respect to $\mathsf{T}^\square$ is just the characteristic vector of t. Therefore, the design compatibility fan $\mathcal{D}^\square(\mathrm{G}, \mathsf{T}^\square)$ coincides with the design nested fan $\mathcal{G}^\square(\mathrm{G})$. It follows that $\mathcal{D}^\square(\mathrm{G}, \mathsf{T}^\square)$ is the normal fan of the design graph associahedron $\mathsf{Asso}^\square(\mathrm{G})$ for any graph G. In fact, as the linear dependencies among the compatibility vectors with respect to the initial tubing $\mathsf{T}^\square$ are simply described, a direct computation shows that the map ω defined by $\omega(\mathsf{t}) = 3^{|\mathrm{V}|}|\mathsf{t}| - 3^{|\mathsf{t}|}$ for a round tube and $\omega(v^\square) = C$ for a sufficiently large constant C provides a suitable weight function for Condition (2) of Proposition 3.9.

6.4.5 Laurent Phenomenon algebras

To conclude, we discuss our construction with respect to the framework of LP-algebras presented in Section 4.4. We mentioned there that graph associahedra happen to be examples of cluster complexes of some LP-algebras so as the existence of **d**-vectors. In view of the relatively bad properties of **d**-vectors in LP-algebra mentioned in Section 4.4.3, the denominator vectors in the linear LP-algebra $\mathcal{A}(\mathrm{G})$ associated to a graph G in [LP16b] cannot always coincide with our compatibility vectors on tubes of G. But despite all these difficulties, we hope that the study of the linear LP-algebras arising from (design) nested complexes of graphs will yield progresses towards an answer to Question 4.16. Since nonisomorphic LP-algebra may have isomorphic cluster complexes (see again Section 4.4.2), another simpler question would be to look for other LP-algebras whose denominators interpret our compatibility degrees.

Question 6.62. For which graph G does there exist a LP-algebra whose cluster complex is isomorphic to the nested complex $\mathsf{Asso}(\mathrm{G})$ (resp. to the design nested complex $\mathsf{Asso}^\square(\mathrm{G})$) and whose denominators are given by the (primal or dual) compatibility degrees defined in this chapter?

6.5 Proofs

This section contains the proofs of our results. Some of them require additional technical steps, which motivated us to put them apart. We also hope that the many examples treated in Section 6.3 help the reader's intuition throughout these proofs.

6.5.1 Compatibility degree (Proposition 6.7)

We start with the proof that our graphical compatibility degree encodes compatibility and exchangeability between tubes. We show the three points of Proposition 6.7:

- $(\mathsf{t} \,\|\, \mathsf{t}') < 0 \iff (\mathsf{t}' \,\|\, \mathsf{t}) < 0 \iff \mathsf{t} = \mathsf{t}'$.
This is immediate from the definition since the compatibility degree between two distinct tubes is either a cardinal or 0.

- $(t \,\|\, t') = 0 \iff (t' \,\|\, t) = 0 \iff$ t and t' are compatible.

Consider two distinct tubes t, t' of G. If they are compatible, then either $t \subseteq t'$, or $t' \subseteq t$, or t and t' are nonadjacent. In the first case, $(t \,\|\, t') = 0$ by the last line of Definition 6.5 of the compatibility degree. In the last two cases, $(t \,\|\, t') = |\{\text{neighbors of t in } t' \smallsetminus t\}| = |\varnothing| = 0$. Conversely, if $(t \,\|\, t') = 0$, then either t has no neighbor in t', or $t' \subseteq t$, or $t \subseteq t'$, so that the two tubes are compatible.

- $(t \,\|\, t') = 1 = (t' \,\|\, t) \iff$ t and t' are exchangeable.

The $\Leftarrow$ part follows from the explicit flip description in Proposition 5.2. Indeed, assume that t and t' are exchangeable, let $\bar{t} := t \cup t'$, and let T, T' be two adjacent maximal tubings on G such that $T \smallsetminus \{t\} = T' \smallsetminus \{t'\}$. Since t' is the connected component of $G[\bar{t} \smallsetminus \lambda(t, T)]$ containing $\lambda(\bar{t}, T)$, the root $\lambda(\bar{t}, T)$ is the unique neighbor of t in $t' \smallsetminus t$. Therefore, $(t \,\|\, t') = 1$, and $(t' \,\|\, t) = 1$ by symmetry.

Assume conversely that $(t \,\|\, t') = 1 = (t' \,\|\, t)$. Since $(t' \,\|\, t) = 1$, there exists a unique neighbor r of t' in $t \smallsetminus t'$. Similarly, there exists a unique neighbor r' of t in $t' \smallsetminus t$. We want to find two adjacent maximal tubings T, T' on G such that $T \smallsetminus \{t\} = T' \smallsetminus \{t'\}$. We start with the forced tubes (see the end of Section 6.2.1): we define $\bar{t} := t \cup t'$ and we let $s_1, \dots, s_\ell$ be the connected components of $\bar{t} \smallsetminus \{r, r'\}$. We choose an arbitrary maximal tubing S_i on $G[s_i]$ for each i, and an arbitrary maximal tubing S on G containing $\bar{t}$. The set of tubes

$$R := \{\bar{t}, s_1, \dots, s_\ell\} \,\sqcup\, S_1 \sqcup \cdots \sqcup S_\ell \,\sqcup\, \{s \mid s \in S, s \not\subseteq \bar{t}\}.$$

is clearly a tubing, and is compatible with both t and t'. We now compute the cardinality of R. Observe first that $|S| = |V| - |\kappa(G)|$ so that $|\{s \mid s \in S, s \not\subseteq \bar{t}\}| = |V| - |\kappa(G)| - |\bar{t}|$ since $\bar{t}$ is a tube of G. Moreover, $|S_i| = |s_i| - 1$ since s_i is a tube, and $\sum_i |s_i| = |\bigcup_i s_i| = |\bar{t} \smallsetminus \{r, r'\}| = |\bar{t}| - 2$. We conclude that

$$|R| = (1 + \ell) + (|\bar{t}| - 2 - \ell) + (|V| - |\kappa(G)| - |\bar{t}|) = |V| - |\kappa(G)| - 1$$

Therefore, R is a ridge of the nested complex $\mathcal{N}(G)$, so that $T := R \cup \{t\}$ and $T' := R \cup \{t'\}$ are maximal tubings related by the flip of t into t'. ∎

6.5.2   Restriction on coordinate hyperplanes (Proposition 6.32)

We now state two lemmas needed in the proofs of Theorem 6.10. They have essentially the same content as Proposition 6.32, except that they focus on compatibility vectors (rays) and not on the other cones of the compatibility fan since Theorem 6.10 is not proved yet. In particular, they will imply Proposition 6.32 once Theorem 6.10 will be established.

Remember that for a tube t° of G, we denote by $G[t^\circ]$ the restriction of G to t° and by $G \star t^\circ$ the reconnected complement of t° in G, defined as the graph with vertex set $V \smallsetminus t^\circ$ and edge set $\{e \in \binom{V \smallsetminus t^\circ}{2} \mid e \text{ or } e \cup t^\circ \text{ is connected in } G\}$.

Lemma 6.63 ([CD06]). *For a tube* t° *of* G*, the map*

$$s \longmapsto \widetilde{s} := \begin{cases} s & \text{if } s \subsetneq t^\circ \\ s \smallsetminus t^\circ & \text{if } s \supsetneq t^\circ \text{ or } s \cap t^\circ = \varnothing \end{cases}$$

sending the tubes of G *compatible with* t° *to the tubes of* $\widetilde{G} := G[t^\circ] \sqcup G \star t^\circ$ *defines an isomorphism between the link of* t° *in the nested complex* $\mathcal{N}(G)$ *and the nested complex* $\mathcal{N}(\widetilde{G})$.

We denote by $\widetilde{T} := \{\widetilde{t} \mid t \in T\}$ the image of a tubing T on G. This map actually preserves the compatibility degrees between tubes and the compatibility vectors.

Lemma 6.64. *Let* t° *be a tube of* G. *The map* $s \mapsto \widetilde{s}$ *between the link of* t° *in the nested complex* $\mathcal{N}(G)$ *and the nested complex* $\mathcal{N}(\widetilde{G})$ *of the graph* $\widetilde{G} := G[t^\circ] \sqcup G^\star t^\circ$ *defined in Lemma 6.63 preserves the compatibility degree:* $(t \,\|\, t') = (\widetilde{t} \,\|\, \widetilde{t}')$ *for any tubes* t, t' *of* G *compatible with* t°. *Therefore, for any maximal tubing* T° *on* G *containing* t° *and any tube* t *of* G *compatible with* t°, *the compatibility vector* $\mathbf{d}(\widetilde{T}^\circ, \widetilde{t})$ *is obtained from the compatibility vector* $\mathbf{d}(T^\circ, t)$ *by deletion of its vanishing* t°-*coordinate.*

Proof. If t and t' are compatible, so are $\widetilde{t}$ and $\widetilde{t}'$ by Lemma 6.63, thus the result follows from Proposition 6.7. We can therefore assume that t and t' are incompatible, so as $\widetilde{t}$ and $\widetilde{t}'$. Therefore, the compatibility degrees $(t \,\|\, t')$ and $(\widetilde{t} \,\|\, \widetilde{t}')$ actually count neighbors. However, it follows immediately from the definitions of the graph $\widetilde{G}$ and of the map $s \mapsto \widetilde{s}$ that the neighbors of t in $t' \smallsetminus t$ are precisely the neighbors of $\widetilde{t}$ in $\widetilde{t}' \smallsetminus \widetilde{t}$. This proves the equality between the compatibility degrees. The equality between the compatibility vectors follows coordinate by coordinate. ∎

6.5.3 Compatibility fan (Theorem 6.10)

In order to show that the cones of the compatibility matrices of all tubings on G form a complete simplicial fan, we need the following refinement.

Theorem 6.65. *For any graph* G *and any maximal tubing* T° *on* G, *the compatibility vectors with respect to* T° *have the following properties.*

Span Property *For any tube* u *of* G, *the span of* $\{\mathbf{d}(T^\circ, s) \mid s \in T, s \subseteq u\}$, *for a maximal tubing* T *on* G *containing* u, *is independent of* T.

Flip Property *For any two adjacent maximal tubings* T, T' *on* G *with* $T \smallsetminus \{t\} = T' \smallsetminus \{t'\}$, *there exists a linear dependence*

$$\alpha\, \mathbf{d}(T^\circ, t) + \alpha'\, \mathbf{d}(T^\circ, t') + \sum_{s \in T \cap T'} \beta_s\, \mathbf{d}(T^\circ, s) = 0$$

between the compatibility vectors of $T \cup T'$ *with respect to* T° *which is:*

Separating *the hyperplane spanned by* $\{\mathbf{d}(T^\circ, s) \mid s \in T \cap T'\}$ *separates* $\mathbf{d}(T^\circ, t)$ *and* $\mathbf{d}(T^\circ, t')$, *i.e. the coefficients* α *and* α' *have the same sign different from* 0.

Local *the dependence is supported by tubes included in* $\bar{t}$, *i.e.* $\beta_s = 0$ *for all* $s \not\subseteq \bar{t}$.

Theorem 6.10 follows from the **Separating Flip Property** and the characterization of complete simplicial fans in Proposition 3.7. The **Span Property** and **Local Flip Property** are not required to get Theorem 6.10 but we use them to obtain the proof of the **Separating Flip Property**. Observe also that we do not need to prove that the linear dependence between the compatibility vectors of $T \cup T'$ is unique: it is a consequence of Proposition 3.7 once we know the **Separating Flip Property**.

Before entering details, let us sketch the general idea of the proof of Theorem 6.65. We seek for a linear dependence between the compatibility vectors of the tubes of $T \cup T'$ with respect to the initial tubing T°, that is, for a linear relation satisfied by their compatibility degrees with any tube of T°. There are simple combinatorial relations between the compatibility degrees of the tubes of $T \cup T'$ with all tubes of T° not contained in $\bar{t}$. Our strategy is to start from such a relation and adapt it iteratively such that it holds for the other tubes of T° as well. This transformation is done in two steps:

- We first deal with the tubes of T° contained in $\bar{t}$ and maximal for this property. They determine the coefficients of the linear dependence on the forced tubes

- For the remaining tubes of T°, we need to make successive corrections to the linear dependence. We first get an explicit linear dependence assuming that $\mathsf{T} \cap \mathsf{T}'$ contains certain suitable tubes included in $\bar{\mathsf{t}}$. We then use inductively the **Span Property** and the **Local Flip Property** to get an implicit linear dependence in general.

The key of the proof is that our transformation increases the set of tubes of T° for which the relation between the compatibility degrees of the tubes of $\mathsf{T} \cup \mathsf{T}'$ is valid.

   We now start the formal proof. We proceed by induction on the dimension of the nested complex $\mathcal{N}(\mathrm{G})$. It is immediate when this dimension is 0. We now consider an arbitrary graph G and assume that we have shown Theorem 6.65 and thus Corollary 6.12 for any graph H such that $\dim(\mathcal{N}(\mathrm{H})) < \dim(\mathcal{N}(\mathrm{G}))$. Given a exchangeable pair of tubes t, t' of G, our first objective is to exhibit **separating** and **local** linear dependences for some adjacent maximal tubings T, T' on G such that $\mathsf{T} \smallsetminus \{\mathsf{t}\} = \mathsf{T}' \smallsetminus \{\mathsf{t}'\}$. We will show later the **Span Property** and use it to prove that the linear dependence is **separating** and **local** for all adjacent maximal tubings T, T' on G such that $\mathsf{T} \smallsetminus \{\mathsf{t}\} = \mathsf{T}' \smallsetminus \{\mathsf{t}'\}$.

Lemma 6.66. *For any two exchangeable tubes* t, t' *of* G, *there exist adjacent maximal tubings* T, T' *on* G *such that* $\mathsf{T} \smallsetminus \{\mathsf{t}\} = \mathsf{T}' \smallsetminus \{\mathsf{t}'\}$ *and a linear dependence between the compatibility vectors of the tubes of* $\mathsf{T} \cup \mathsf{T}'$ *which is both* **separating** *and* **local**.

Proof. We fix some notations for the forced tubes of the exchangeable pair $\{\mathsf{t}, \mathsf{t}'\}$. First recall that since t and t' are exchangeable, the tube t (resp. t') has a single neighbor in $\mathsf{t}' \smallsetminus \mathsf{t}$ (resp. in $\mathsf{t} \smallsetminus \mathsf{t}'$) that we denote by r (resp. r'). We set $\bar{\mathsf{t}} := \mathsf{t} \cup \mathsf{t}'$, and we denote by $\underline{\mathsf{t}}_1, \ldots, \underline{\mathsf{t}}_k$ the connected components of $\mathrm{G}[\mathsf{t} \cap \mathsf{t}']$, by $\mathsf{a}_1, \ldots, \mathsf{a}_\ell$ the connected components of $\mathrm{G}[\mathsf{t} \smallsetminus (\mathsf{t}' \cup \{r\})]$, and by $\mathsf{a}'_1, \ldots, \mathsf{a}'_{\ell'}$ the connected components of $\mathrm{G}[\mathsf{t}' \smallsetminus (\mathsf{t} \cup \{r'\})]$. Although it is not a tube, we set $\underline{\mathsf{t}} := \bigsqcup_{i \in [k]} \underline{\mathsf{t}}_i$ and we abuse notation to write $(\mathsf{t}^\circ \,\|\, \underline{\mathsf{t}})$ for $\sum_{i \in [k]} (\mathsf{t}^\circ \,\|\, \underline{\mathsf{t}}_i)$ and similarly $\mathbf{d}(\mathsf{T}^\circ, \underline{\mathsf{t}})$ for $\sum_{i \in [k]} \mathbf{d}(\mathsf{T}^\circ, \underline{\mathsf{t}}_i)$. We will use in the same way the notations a and a'.

   We need to distinguish different cases, for which the linear dependences are slightly different, while the proofs are essentially identical. To simplify the discussion, we assume in Cases (A), (B) and (C) below that $\mathsf{t}, \mathsf{t}' \notin \mathsf{T}^\circ$ and that no tube of T° is compatible with both t and t'. At the end of the proof, Cases (D) and (E) show how to restrict to these hypotheses.

(A) A first relation. Consider a tube t° of T° not contained in $\bar{\mathsf{t}}$. We claim that

$$(\mathsf{t}^\circ \,\|\, \mathsf{t}) + (\mathsf{t}^\circ \,\|\, \mathsf{t}') = (\mathsf{t}^\circ \,\|\, \bar{\mathsf{t}}) + (\mathsf{t}^\circ \,\|\, \underline{\mathsf{t}}).$$

Indeed, since $\mathsf{t}^\circ \not\subseteq \bar{\mathsf{t}}$, these four compatibility degrees actually count neighbors of t°. The formula thus follows from inclusion-exclusion principle since $\bar{\mathsf{t}} = \mathsf{t} \cup \mathsf{t}'$ and $\underline{\mathsf{t}} = \mathsf{t} \cap \mathsf{t}'$.

   There are other tubes of T° satisfying this relation. Indeed, consider a tube t° in T° included in $\bar{\mathsf{t}}$ which contains r but does not contain nor is adjacent to r'. Then $\mathsf{t}^\circ \subsetneq \mathsf{t} \subsetneq \bar{\mathsf{t}}$ so that $(\mathsf{t}^\circ \,\|\, \mathsf{t}) = (\mathsf{t}^\circ \,\|\, \bar{\mathsf{t}}) = 0$. Moreover, t° is incompatible with t' and all $\underline{\mathsf{t}}_1, \ldots, \underline{\mathsf{t}}_k$. Since r' is not adjacent to t°, all neighbors of t° in $\mathsf{t}' \smallsetminus \mathsf{t}^\circ$ are in $\underline{\mathsf{t}} \smallsetminus \mathsf{t}^\circ$. Therefore $(\mathsf{t}^\circ \,\|\, \mathsf{t}') = (\mathsf{t}^\circ \,\|\, \underline{\mathsf{t}})$. The relation follows. Similarly, the relation follows if t° contains r' and does not contain nor is adjacent to r.

   If all tubes of T° included in $\bar{\mathsf{t}}$ satisfy the previous conditions, we have obtained a **separating** and **local** linear dependence:

$$\mathbf{d}(\mathsf{T}^\circ, \mathsf{t}) + \mathbf{d}(\mathsf{T}^\circ, \mathsf{t}') = \mathbf{d}(\mathsf{T}^\circ, \underline{\mathsf{t}}) + \mathbf{d}(\mathsf{T}^\circ, \bar{\mathsf{t}}). \tag{6.1}$$

This linear dependence would be valid for any adjacent maximal tubings T, T' on G such that $\mathsf{T} \smallsetminus \{\mathsf{t}\} = \mathsf{T}' \smallsetminus \{\mathsf{t}'\}$ since the tube $\bar{\mathsf{t}}$ and the tubes $\underline{\mathsf{t}}$ are forced in any such pair. Unfortunately, these conditions do not always hold for all tubes of T°. In this case,

we will therefore adapt the linear dependence (6.1) to cover all possible configurations for the tubes of T°.

(B) No tube of T° contained in $\bar{\mathsf{t}}$ contains both r and r'. Except if the linear dependence (6.1) is valid, there must exist w.l.o.g. a tube $\mathsf{t}^\circ \in \mathsf{T}^\circ$ contained in $\bar{\mathsf{t}}$, containing r and adjacent to r'. Choose t° maximal for these properties. Since we have assumed that no tube of T° is compatible with both t and t', all tubes of T° included in t° contain r. These tubes thus form a nested chain $\mathsf{t}^\circ = \mathsf{t}_0^\circ \supsetneq \mathsf{t}_1^\circ \supsetneq \cdots \supsetneq \mathsf{t}_p^\circ = \{r\}$. For $i \in [p]$, define $\mathsf{t}_i^\star$ to be the connected component of $G[\mathsf{t}_{i-1}^\circ \smallsetminus \{r\}]$ containing the singleton $\mathsf{t}_{i-1}^\circ \smallsetminus \mathsf{t}_i^\circ$.

Set
$$\alpha := (\mathsf{t}^\circ \,\|\, \mathsf{a}) + (\mathsf{t}^\circ \,\|\, \mathsf{t}') \qquad \text{and} \qquad \alpha' := (\mathsf{t}^\circ \,\|\, \underline{\mathsf{t}}) + (\mathsf{t}^\circ \,\|\, \mathsf{a}),$$

and define inductively $\beta_1, \ldots, \beta_p$ by

$$\beta_i = \alpha'\,(\mathsf{t}_i^\circ \,\|\, \mathsf{t}') - \alpha\,(\mathsf{t}_i^\circ \,\|\, \underline{\mathsf{t}}) - (\alpha - \alpha')(\mathsf{t}_i^\circ \,\|\, \mathsf{a}) - \sum_{j \in [i-1]} \beta_j\,(\mathsf{t}_i^\circ \,\|\, \mathsf{t}_j^\star).$$

We claim that

$$\alpha\,\mathbf{d}(\mathsf{T}^\circ, \mathsf{t}) + \alpha'\,\mathbf{d}(\mathsf{T}^\circ, \mathsf{t}') = \alpha\,\mathbf{d}(\mathsf{T}^\circ, \underline{\mathsf{t}}) + \alpha'\,\mathbf{d}(\mathsf{T}^\circ, \bar{\mathsf{t}}) + (\alpha - \alpha')\,\mathbf{d}(\mathsf{T}^\circ, \mathsf{a}) + \sum_{i \in [p]} \beta_i\,\mathbf{d}(\mathsf{T}^\circ, \mathsf{t}_i^\star). \quad \textbf{(6.2)}$$

To prove it, we check this linear dependence coordinate by coordinate.

Observe first that $(\mathsf{t}_i^\circ \,\|\, \mathsf{t}) = (\mathsf{t}_i^\circ \,\|\, \bar{\mathsf{t}}) = 0$ for all $0 \le i \le p$ since $\mathsf{t}_i^\circ \subsetneq \mathsf{t} \subseteq \bar{\mathsf{t}}$. Moreover, for all $i < j$, we have by definition $\mathsf{t}_j^\star \subsetneq \mathsf{t}_i^\circ$, so that $(\mathsf{t}_i^\circ \,\|\, \mathsf{t}_j^\star) = 0$. Finally, we have $(\mathsf{t}_i^\circ \,\|\, \mathsf{t}_i^\star) = 1$ since t_i° and $\mathsf{t}_i^\star$ are incompatible and the only neighbor of t_i° in $\mathsf{t}_i^\star \smallsetminus \mathsf{t}_i^\circ$ is the singleton $\mathsf{t}_{i-1}^\circ \smallsetminus \mathsf{t}_i^\circ$. Therefore, Relation (6.2) holds for t° by definition of α and α' and for t_i° by definition of β_i.

Consider now a tube s° of T° not included in t°. Suppose that s° is included in $\bar{\mathsf{t}}$. Then s° contains precisely one of r and r' (it cannot contain both by assumption (B), and it cannot avoid both as it would be compatible with both t and t'). If s° contains r, it contains t° and therefore equals t° by maximality of the latter. Otherwise, s° contains r', thus is adjacent to t°, thus contains it (by compatibility), and thus contains r, a contradiction. We therefore obtained that s° is not included in $\bar{\mathsf{t}}$, so that all compatibility degrees $(\mathsf{s}^\circ \,\|\, \mathsf{t})$, $(\mathsf{s}^\circ \,\|\, \bar{\mathsf{t}})$, $(\mathsf{s}^\circ \,\|\, \underline{\mathsf{t}})$ and $(\mathsf{s}^\circ \,\|\, \mathsf{a})$ actually count neighbors of s°. Observe now that r cannot be adjacent to s° (except if it belongs to s°), since r belongs to t° which is compatible with s°. Therefore, we have

$$(\mathsf{s}^\circ \,\|\, \mathsf{t}) = (\mathsf{s}^\circ \,\|\, \underline{\mathsf{t}}) + (\mathsf{s}^\circ \,\|\, \mathsf{a}) \qquad \text{and} \qquad (\mathsf{s}^\circ \,\|\, \mathsf{t}') = (\mathsf{s}^\circ \,\|\, \bar{\mathsf{t}}) - (\mathsf{s}^\circ \,\|\, \mathsf{a}),$$

since $\mathsf{t} = \underline{\mathsf{t}} \sqcup \mathsf{a} \sqcup \{r\}$ and $\mathsf{t}' = \bar{\mathsf{t}} \smallsetminus \mathsf{a} \smallsetminus \{r\}$. Finally, since any $\mathsf{t}_i^\star$ is contained in t°, it is compatible with s°, so that $(\mathsf{s}^\circ \,\|\, \mathsf{t}_i^\star) = 0$ by Proposition 6.7. Combining these equalities, we obtain that Relation (6.2) holds for any $\mathsf{s}^\circ \in \mathsf{T}^\circ$.

We found a linear dependence between the compatibility vectors, with respect to the initial tubing T°, of the tubes $\{\mathsf{t}, \mathsf{t}', \bar{\mathsf{t}}\} \cup \underline{\mathsf{t}} \cup \mathsf{a} \cup \{\mathsf{t}_i^\star \mid i \in [p]\}$. Any two of these tubes, except t and t', are compatible:

- the forced tubes are pairwise compatible;

- each $\mathsf{t}_i^\star$ is a connected component of $\mathsf{t}_i^\circ \smallsetminus \{r\}$, thus is contained in $\bar{\mathsf{t}} \smallsetminus \{r, r'\}$, and thus is compatible with the connected components of $\bar{\mathsf{t}} \smallsetminus \{r, r'\}$ (*i.e.* all forced tubes);

- for $\mathsf{t}_i^\circ \supseteq \mathsf{t}_j^\circ$, any connected component of $\mathsf{t}_j^\circ \smallsetminus \{r\}$ is contained in a connected component of $\mathsf{t}_i^\circ \smallsetminus \{r\}$ and thus is compatible with all connected components of $\mathsf{t}_i^\circ \smallsetminus \{r\}$. In particular $\mathsf{t}_i^\star$ and $\mathsf{t}_j^\star$ are compatible.

Therefore, there exist adjacent maximal tubings T, T' on G such that $\mathsf{T} \smallsetminus \{\mathsf{t}\} = \mathsf{T}' \smallsetminus \{\mathsf{t}'\}$ and $\mathsf{T} \cup \mathsf{T}' \supseteq \{\mathsf{t}, \mathsf{t}', \bar{\mathsf{t}}\} \cup \underline{\mathsf{t}} \cup \mathsf{a} \cup \{\mathsf{t}_i^\star \mid i \in [p]\}$. For this choice of T, T', we thus obtained a **separating** and **local** linear dependence (6.2) between the compatibility vectors of the tubes of $\mathsf{T} \cup \mathsf{T}'$.

(C) A tube of T° contained in $\bar{\mathsf{t}}$ contains both r and r'. There are again two cases.

(C.1) No tube of T° contained in $\bar{\mathsf{t}}$ contains r and is adjacent to r' or conversely. There must exist a tube $\mathsf{t}^\circ \in \mathsf{T}^\circ$ included in t and containing r. Choose t° maximal for these properties. With the same arguments as in Case (B), the tubes of T° included in t° form a nested chain $\mathsf{t}^\circ = \mathsf{t}_0^\circ \supsetneq \mathsf{t}_1^\circ \supsetneq \cdots \supsetneq \mathsf{t}_p^\circ = \{r\}$. For $i \in [p]$, define $\mathsf{t}_i^\star$ to be the connected component of $\mathsf{G}[\mathsf{t}_{i-1}^\circ \smallsetminus \{r\}]$ containing the singleton $\mathsf{t}_{i-1}^\circ \smallsetminus \mathsf{t}_i^\circ$. We define the tube t'°, the chain $\mathsf{t}'^\circ = \mathsf{t}_0'^\circ \supsetneq \mathsf{t}_1'^\circ \supsetneq \cdots \supsetneq \mathsf{t}_{p'}'^\circ = \{r'\}$ and the tubes $\mathsf{t}_i'^\star$ for $i \in [p']$ similarly.

Consider now the inclusion minimal tube $\bar{\mathsf{t}}^\circ$ of T° contained in $\bar{\mathsf{t}}$ and containing both r and r'. Since we assumed that no tube of T° is compatible with both t and t', we have $\bar{\mathsf{t}}^\circ = \mathsf{t}^\circ \sqcup \mathsf{t}'^\circ \sqcup \{\bar{r}\}$ where $\bar{r} \in \underline{\mathsf{t}}$. Let $\bar{\mathsf{t}}^\star$ be the connected component of $\mathsf{G}[\bar{\mathsf{t}}^\circ \smallsetminus \{r, r'\}]$ containing $\bar{r}$.

Set
$$\alpha := (\mathsf{t}'^\circ \,\|\, \underline{\mathsf{t}}) + (\mathsf{t}'^\circ \,\|\, \mathsf{a}') \qquad \text{and} \qquad \alpha' := (\mathsf{t}^\circ \,\|\, \underline{\mathsf{t}}) + (\mathsf{t}^\circ \,\|\, \mathsf{a}),$$
and define inductively $\beta_1, \ldots, \beta_p$ and $\beta_1', \ldots, \beta_{p'}'$ by

$$\beta_i = \alpha' \, (\mathsf{t}_i^\circ \,\|\, \mathsf{t}') - (\alpha + \alpha') \, (\mathsf{t}_i^\circ \,\|\, \underline{\mathsf{t}}) - \alpha \, (\mathsf{t}_i^\circ \,\|\, \mathsf{a}) + \alpha \alpha' \, (\mathsf{t}_i^\circ \,\|\, \bar{\mathsf{t}}^\star) - \sum_{j \in [i-1]} \beta_j \, (\mathsf{t}_i^\circ \,\|\, \mathsf{t}_j^\star),$$

$$\beta_i' = \alpha \, (\mathsf{t}_i'^\circ \,\|\, \mathsf{t}) - (\alpha + \alpha') \, (\mathsf{t}_i'^\circ \,\|\, \underline{\mathsf{t}}) - \alpha' \, (\mathsf{t}_i'^\circ \,\|\, \mathsf{a}') + \alpha \alpha' \, (\mathsf{t}_i'^\circ \,\|\, \bar{\mathsf{t}}^\star) - \sum_{j \in [i-1]} \beta_j' \, (\mathsf{t}_i'^\circ \,\|\, \mathsf{t}_j'^\star).$$

We claim that

$$\alpha \, \mathbf{d}(\mathsf{T}^\circ, \mathsf{t}) + \alpha' \, \mathbf{d}(\mathsf{T}^\circ, \mathsf{t}') = (\alpha + \alpha') \, \mathbf{d}(\mathsf{T}^\circ, \underline{\mathsf{t}}) + \alpha \, \mathbf{d}(\mathsf{T}^\circ, \mathsf{a}) + \alpha' \, \mathbf{d}(\mathsf{T}^\circ, \mathsf{a}') - \alpha \alpha' \, \mathbf{d}(\mathsf{T}^\circ, \bar{\mathsf{t}}^\star)$$

(6.3)

$$+ \sum_{i \in [p]} \beta_i \, \mathbf{d}(\mathsf{T}^\circ, \mathsf{t}_i^\star) + \sum_{i \in [p']} \beta_i' \, \mathbf{d}(\mathsf{T}^\circ, \mathsf{t}_i'^\star).$$

To prove it, we check this linear dependence coordinate by coordinate.

We start with t° and t'°. We have $(\mathsf{t}^\circ \,\|\, \mathsf{t}) = 0$ since $\mathsf{t}^\circ \subsetneq \mathsf{t}$. Moreover, $(\mathsf{t}^\circ \,\|\, \bar{\mathsf{t}}^\star) = |\{\bar{r}\}| = 1$. Finally, we have by definition $\mathsf{t}_j^\star \subsetneq \mathsf{t}^\circ$ so that $(\mathsf{t}^\circ \,\|\, \mathsf{t}_j^\star) = 0$ for all $j \in [p]$. Combining these equalities, Relation (6.3) follows for t° from the definition of α and α'. The argument is identical for t'°.

We now consider the tubes t_i° and $\mathsf{t}_i'^\circ$. Observe first that $(\mathsf{t}_i^\circ \,\|\, \mathsf{t}) = 0$ for all $0 \leq i \leq p$ since $\mathsf{t}_i^\circ \subsetneq \mathsf{t}$. Moreover, for all $i < j$, we have by definition $\mathsf{t}_j^\star \subsetneq \mathsf{t}_i^\circ$, so that $(\mathsf{t}_i^\circ \,\|\, \mathsf{t}_j^\star) = 0$. In addition, we have $(\mathsf{t}_i^\circ \,\|\, \mathsf{t}_j'^\star) = 0$ for all $i \in [p]$ and $j \in [p']$ since t_i° and $\mathsf{t}_j'^\star$ are compatible. Finally, we have $(\mathsf{t}_i^\circ \,\|\, \mathsf{t}_i^\star) = 1$ since t_i° and $\mathsf{t}_i^\star$ are incompatible and the only neighbor of t_i° in $\mathsf{t}_i^\star \smallsetminus \mathsf{t}_i^\circ$ is the singleton $\mathsf{t}_{i-1}^\circ \smallsetminus \mathsf{t}_i^\circ$. Therefore, Relation (6.3) holds for t_i° by definition of β_i. The argument is identical for $\mathsf{t}_i'^\circ$.

Finally, we consider a tube s° of T° not strictly contained in $\bar{\mathsf{t}}^\circ$. With similar arguments as in Case (B), the compatibility degrees $(\mathsf{s}^\circ \,\|\, \mathsf{t})$, $(\mathsf{s}^\circ \,\|\, \mathsf{t}')$, $(\mathsf{s}^\circ \,\|\, \underline{\mathsf{t}})$, $(\mathsf{s}^\circ \,\|\, \mathsf{a})$ and $(\mathsf{s}^\circ \,\|\, \mathsf{a}')$ actually count neighbors of s°, and (by assumption C) satisfy

$$(\mathsf{s}^\circ \,\|\, \mathsf{t}) = (\mathsf{s}^\circ \,\|\, \underline{\mathsf{t}}) + (\mathsf{s}^\circ \,\|\, \mathsf{a}) \qquad \text{and} \qquad (\mathsf{s}^\circ \,\|\, \mathsf{t}') = (\mathsf{s}^\circ \,\|\, \underline{\mathsf{t}}) + (\mathsf{s}^\circ \,\|\, \mathsf{a}').$$

Moreover, since all $\mathsf{t}_i^\star$, $\mathsf{t}_i'^\star$ and $\bar{\mathsf{t}}^\star$ are contained in $\bar{\mathsf{t}}^\circ$, they are all compatible with s°, so that $(\mathsf{s}^\circ \,\|\, \mathsf{t}_i^\star) = (\mathsf{s}^\circ \,\|\, \mathsf{t}_i'^\star) = (\mathsf{s}^\circ \,\|\, \bar{\mathsf{t}}^\star) = 0$ by Proposition 6.7. Combining these equalities, we obtain that Relation (6.3) holds for any $\mathsf{s}^\circ \in \mathsf{T}^\circ$.

With the same arguments as in Case (B), there exist adjacent maximal tubings T, T' on G such that $\mathsf{T} \smallsetminus \{\mathsf{t}\} = \mathsf{T}' \smallsetminus \{\mathsf{t}'\}$ and $\mathsf{T} \cup \mathsf{T}' \supseteq \{\mathsf{t}, \mathsf{t}', \bar{\mathsf{t}}^\star\} \cup \underline{\mathsf{t}} \cup \mathsf{a} \cup \mathsf{a}' \cup \{\mathsf{t}_i^\star \mid i \in [p]\} \cup \{\mathsf{t}_i'^\star \mid i \in [p]\}$. For this choice of T, T', we thus obtained a **separating** and **local** linear dependence (6.3) between the compatibility vectors of the tubes of $\mathsf{T} \cup \mathsf{T}'$.

(C.2) A tube of T° contained in $\bar{\mathsf{t}}$ contains r and is adjacent to r' or conversely. W.l.o.g., consider an inclusion maximal tube $\mathsf{t}^\circ \in \mathsf{T}^\circ$ contained in $\bar{\mathsf{t}}$, containing r and adjacent to r'. Since we have assumed that no tube of T° is compatible with both t and t', all tubes of T° included in t° contain r. These tubes thus form a nested chain $\mathsf{t}^\circ = \mathsf{t}_0^\circ \supsetneq \mathsf{t}_1^\circ \supsetneq \cdots \supsetneq \mathsf{t}_p^\circ = \{r\}$. For $i \in [p]$, define $\mathsf{t}_i^\star$ to be the connected component of $G[\mathsf{t}_{i-1}^\circ \smallsetminus \{r\}]$ containing the singleton $\mathsf{t}_{i-1}^\circ \smallsetminus \mathsf{t}_i^\circ$.

Set
$$\alpha := (\mathsf{t}^\circ \,\|\, \mathsf{t}') - (\mathsf{t}^\circ \,\|\, \underline{\mathsf{t}}) = |\{r'\}| = 1 \qquad \text{and} \qquad \alpha' := (\mathsf{t}^\circ \,\|\, \underline{\mathsf{t}}) + (\mathsf{t}^\circ \,\|\, \mathsf{a}),$$

and define inductively $\beta_1, \ldots, \beta_p$ by

$$\beta_i = \alpha' \, (\mathsf{t}_i^\circ \,\|\, \mathsf{t}') - (1 + \alpha') \, (\mathsf{t}_i^\circ \,\|\, \underline{\mathsf{t}}) - (\mathsf{t}_i^\circ \,\|\, \mathsf{a}) - \sum_{j \in [i-1]} \beta_j \, (\mathsf{t}_i^\circ \,\|\, \mathsf{t}_j^\star).$$

We claim that

$$\mathbf{d}(\mathsf{T}^\circ, \mathsf{t}) + \alpha' \, \mathbf{d}(\mathsf{T}^\circ, \mathsf{t}') = (1 + \alpha') \, \mathbf{d}(\mathsf{T}^\circ, \underline{\mathsf{t}}) + \mathbf{d}(\mathsf{T}^\circ, \mathsf{a}) + \alpha' \, \mathbf{d}(\mathsf{T}^\circ, \mathsf{a}') + \sum_{i \in [p]} \beta_i \, \mathbf{d}(\mathsf{T}^\circ, \mathsf{t}_i^\star). \quad \textbf{(6.4)}$$

To prove it, we check this linear dependence coordinate by coordinate.

Observe first that $(\mathsf{t}_i^\circ \,\|\, \mathsf{t}) = 0$ for all $0 \le i \le p$ since $\mathsf{t}_i^\circ \subsetneq \mathsf{t}$. Moreover, for all $i < j$, we have by definition $\mathsf{t}_j^\star \subsetneq \mathsf{t}_i^\circ$, so that $(\mathsf{t}_i^\circ \,\|\, \mathsf{t}_j^\star) = 0$. Finally, we have $(\mathsf{t}_i^\circ \,\|\, \mathsf{t}_i^\star) = 1$ since t_i° and $\mathsf{t}_i^\star$ are incompatible and the only neighbor of t_i° in $\mathsf{t}_i^\star \smallsetminus \mathsf{t}_i^\circ$ is the singleton $\mathsf{t}_{i-1}^\circ \smallsetminus \mathsf{t}_i^\circ$. Therefore, Relation (6.2) holds for t° by definition of α and α' and for t_i° by definition of β_i.

Consider now a tube s° of T° not strictly contained in t°. With similar arguments as in Case (B), the compatibility degrees $(\mathsf{s}^\circ \,\|\, \mathsf{t})$, $(\mathsf{s}^\circ \,\|\, \mathsf{t}')$, $(\mathsf{s}^\circ \,\|\, \underline{\mathsf{t}})$, $(\mathsf{s}^\circ \,\|\, \mathsf{a})$ and $(\mathsf{s}^\circ \,\|\, \mathsf{a}')$ actually count neighbors of s°, and (by assumption C) satisfy

$$(\mathsf{s}^\circ \,\|\, \mathsf{t}) = (\mathsf{s}^\circ \,\|\, \underline{\mathsf{t}}) + (\mathsf{s}^\circ \,\|\, \mathsf{a}) \qquad \text{and} \qquad (\mathsf{s}^\circ \,\|\, \mathsf{t}') = (\mathsf{s}^\circ \,\|\, \underline{\mathsf{t}}) + (\mathsf{s}^\circ \,\|\, \mathsf{a}').$$

Moreover, since all $\mathsf{t}_i^\star$ are contained in t°, they are all compatible with s°, so that $(\mathsf{s}^\circ \,\|\, \mathsf{t}_i^\star) = 0$ by Proposition 6.7. Combining these equalities, we obtain that Relation (6.3) holds for any $\mathsf{s}^\circ \in \mathsf{T}^\circ$.

With the same arguments as in Case (B), there exist adjacent maximal tubings T, T' on G such that $\mathsf{T} \smallsetminus \{\mathsf{t}\} = \mathsf{T}' \smallsetminus \{\mathsf{t}'\}$ and $\mathsf{T} \cup \mathsf{T}' \supseteq \{\mathsf{t}, \mathsf{t}'\} \cup \underline{\mathsf{t}} \cup \mathsf{a} \cup \mathsf{a}' \cup \{\mathsf{t}_i^\star \mid i \in [p]\}$. For this choice of T, T', we thus obtained a **separating** and **local** linear dependence (6.4) between the compatibility vectors of the tubes of $\mathsf{T} \cup \mathsf{T}'$.

We assumed in Cases (A), (B) and (C) above that $\mathsf{t}, \mathsf{t}' \notin \mathsf{T}^\circ$ and that no tube of T° is compatible with both t and t'. The remaining two cases show how to force this assumption.

(D) A tube t° of T° is compatible with both t and t'. We treat this case by induction on the number of tubes of T° compatible with both t and t'. By Lemma 6.64, the compatibility vectors with respect to T° of the tubes of G compatible with t° correspond to the compatibility vectors of the tubes of $\widetilde{G} := G[\mathsf{t}^\circ] \sqcup G^\star \mathsf{t}^\circ$ with respect to the maximal tubing $\widetilde{\mathsf{T}}^\circ$. Since there are strictly less tubes of $\widetilde{\mathsf{T}}^\circ$ compatible with both $\widetilde{\mathsf{t}}$ and $\widetilde{\mathsf{t}}'$ than tubes of T° compatible with both t and t', the induction hypothesis ensures that there exist adjacent maximal tubings $\widetilde{\mathsf{T}}, \widetilde{\mathsf{T}}'$ on $\widetilde{G}$ such that $\widetilde{\mathsf{T}} \smallsetminus \{\widetilde{\mathsf{t}}\} = \widetilde{\mathsf{T}}' \smallsetminus \{\widetilde{\mathsf{t}}'\}$ and a **separating** and **local** linear dependence between the compatibility vectors of $\widetilde{\mathsf{T}} \cup \widetilde{\mathsf{T}}'$ with respect

to $\widetilde{\mathsf{T}}^\circ$. By Lemma 6.63, the sets $\mathsf{T} := \{\mathsf{t}^\circ\} \cup \{\mathsf{s} \mid \widetilde{\mathsf{s}} \in \widetilde{\mathsf{T}}\}$ and $\mathsf{T}' := \{\mathsf{t}^\circ\} \cup \{\mathsf{s}' \mid \widetilde{\mathsf{s}}' \in \widetilde{\mathsf{T}}'\}$ are tubings on G (since t° is compatible with all preimages of tubes of $\widetilde{G}$) and they are maximal by cardinality. Moreover, Lemma 6.64 ensures that the linear dependence between the compatibility vectors of the tubes of $\mathsf{T} \cup \mathsf{T}'$ with respect to T° coincides with the linear dependence between the compatibility vectors of the tubes of $\widetilde{\mathsf{T}} \cup \widetilde{\mathsf{T}}'$ with respect to $\widetilde{\mathsf{T}}^\circ$. The linear dependence clearly remains **separating** and **local**, which concludes when there is a tube $\mathsf{t}^\circ \in \mathsf{T}^\circ$ compatible with both t and t'.

(E) t **or** t' **belongs to** T°**.** We can assume w.l.o.g. that $\mathsf{t} = \mathsf{t}^\circ$ belongs to T°. Consider any two adjacent maximal tubings T, T' on G such that $\mathsf{T} \smallsetminus \{\mathsf{t}\} = \mathsf{T}' \smallsetminus \{\mathsf{t}'\}$. Since any tube s in $\mathsf{T} \cap \mathsf{T}'$ is compatible with $\mathsf{t} = \mathsf{t}^\circ$, the t°-coordinate of the compatibility vector $\mathbf{d}(\mathsf{T}^\circ, \mathsf{s})$ vanishes. The same happens for the vector $\mathbf{v} := \mathbf{d}(\mathsf{T}^\circ, \mathsf{t}) + \mathbf{d}(\mathsf{T}^\circ, \mathsf{t}')$ since $(\mathsf{t}^\circ \| \mathsf{t}) = -1$ (as $\mathsf{t} = \mathsf{t}^\circ$) while $(\mathsf{t}^\circ \| \mathsf{t}') = 1$ (by Proposition 6.7). The set of vectors $\{\mathbf{v}\} \cup \{\mathbf{d}(\mathsf{T}^\circ, \mathsf{s}) \mid \mathsf{s} \in \mathsf{T} \cap \mathsf{T}'\}$ has cardinality $|\mathsf{T}^\circ|$ but is contained in the hyperplane of $\mathbb{R}^{\mathsf{T}^\circ}$ orthogonal to $\mathbf{e}_{\mathsf{t}^\circ}$. Therefore, there is a linear dependence between these vectors, which translates into a linear dependence between the compatibility vectors of the tubes of $\mathsf{T} \cup \mathsf{T}'$ with the same coefficient on $\mathbf{d}(\mathsf{T}^\circ, \mathsf{t})$ and $\mathbf{d}(\mathsf{T}^\circ, \mathsf{t}')$. This coefficient cannot vanish: otherwise, we would have a linear dependence on the compatibility vectors of $\widetilde{\mathsf{T}}$ with respect to $\widetilde{\mathsf{T}}^\circ$. Since $\widetilde{\mathsf{T}}$ is a maximal tubing on $\widetilde{G}$, and $\dim(\mathcal{N}(\widetilde{G})) = \dim(\mathcal{N}(G)) - 1$, this would contradict Corollary 6.12 and thus the induction hypothesis for $\widetilde{G}$. This linear dependence is therefore **separating**. It is automatically **local** if $\bar{\mathsf{t}} = V$ (all tubes are then subsets of $\bar{\mathsf{t}}$). Otherwise, we prove that it is **local** by restriction. There are two cases.

(E.1) A tube $\bar{\mathsf{t}}^\circ$ of T° contains $\mathsf{t} \cup \{r'\}$ and is contained in $\bar{\mathsf{t}}$. Consider the restricted graph $\hat{G} = G[\mathsf{t} \cup \{r'\}]$. Any tube s of G included in t is also a tube of $\hat{G}$. Therefore, the set $\hat{\mathsf{T}} := \{\mathsf{s} \mid \mathsf{s} \in \mathsf{T}, \mathsf{s} \subseteq \mathsf{t}\}$ is a tubing on $\hat{G}$ for any tubing T containing t. Define also the tube $\hat{\mathsf{t}}' := \mathsf{t}' \smallsetminus \mathsf{a}'$ of $\hat{G}$. The existence of $\bar{\mathsf{t}}^\circ$ implies that $(\mathsf{s}^\circ \| \mathsf{t}') = (\mathsf{s}^\circ \| \mathsf{a}')$ for any $\mathsf{s}^\circ \in \mathsf{T}^\circ$ not included in t. It follows that the compatibility vector $\mathbf{d}(\hat{\mathsf{T}}^\circ, \hat{\mathsf{t}}')$ is the restriction of $\mathbf{d}(\mathsf{T}^\circ, \mathsf{t}') - \mathbf{d}(\mathsf{T}^\circ, \mathsf{a}')$ to the coordinates indexed by $\hat{\mathsf{T}}^\circ$. Similarly, for any tube $\mathsf{s} \in \mathsf{T}$ contained in t, the compatibility vector $\mathbf{d}(\hat{\mathsf{T}}^\circ, \mathsf{s})$ is the restriction of $\mathbf{d}(\mathsf{T}^\circ, \mathsf{s})$ to the coordinates indexed by $\hat{\mathsf{T}}^\circ$. This shows that the linear dependence on $\{\mathbf{d}(\hat{\mathsf{T}}^\circ, \mathsf{s}) \mid \mathsf{s} \in \hat{\mathsf{T}} \cup \hat{\mathsf{T}}'\}$ provides a linear dependence on $\{\mathbf{d}(\mathsf{T}^\circ, \mathsf{s}) \mid \mathsf{s} \in \mathsf{T} \cup \mathsf{T}', \mathsf{s} \subseteq \mathsf{t}\} \cup \{\mathbf{d}(\mathsf{T}^\circ, \mathsf{t}') - \mathbf{d}(\mathsf{T}^\circ, \mathsf{a}')\}$. The resulting linear dependence on $\{\mathbf{d}(\mathsf{T}^\circ, \mathsf{s}) \mid \mathsf{s} \in \mathsf{T} \cup \mathsf{T}'\}$ is **local**.

(E.2) No tube of T° contains $\mathsf{t} \cup \{r'\}$ and is contained in $\bar{\mathsf{t}}$. The proof is identical to Case (E.1), replacing $\mathbf{d}(\mathsf{T}^\circ, \mathsf{t}') - \mathbf{d}(\mathsf{T}^\circ, \mathsf{a}')$ by $\mathbf{d}(\mathsf{T}^\circ, \mathsf{t}') - \mathbf{d}(\mathsf{T}^\circ, \bar{\mathsf{t}})$. ∎

We can now prove the **Span Property**.

Lemma 6.67. *For any tube u of G, the span of $\{\mathbf{d}(\mathsf{T}^\circ, \mathsf{s}) \mid \mathsf{s} \in \mathsf{T}, \mathsf{s} \subseteq \mathsf{u}\}$, for a maximal tubing T on G containing u, is independent of T.*

Proof. We proceed by induction on the size of u. The result is immediate if u is a singleton. Consider now two adjacent maximal tubings T, T' on G containing u such that $\mathsf{T} \smallsetminus \{\mathsf{t}\} = \mathsf{T}' \smallsetminus \{\mathsf{t}'\}$. Assume first that t and t' are contained in u. By Lemma 6.66, there exist adjacent maximal tubings S, S' on G containing u such that $\mathsf{S} \smallsetminus \{\mathsf{t}\} = \mathsf{S}' \smallsetminus \{\mathsf{t}'\}$ and a linear dependence between the compatibility vectors of the tubes of $\mathsf{S} \cup \mathsf{S}'$ with respect to T° which is both **separating** and **local**. By definition, this implies that there exist $\alpha > 0$ and $\alpha' > 0$ such that the vector $\alpha\, \mathbf{d}(\mathsf{T}^\circ, \mathsf{t}) + \alpha'\, \mathbf{d}(\mathsf{T}^\circ, \mathsf{t}')$ belongs to $\mathrm{vect}(\{\mathbf{d}(\mathsf{T}^\circ, \mathsf{s}) \mid \mathsf{s} \in \mathsf{S} \cap \mathsf{S}', \mathsf{s} \subseteq \bar{\mathsf{t}}\})$. However,

$$\{\mathsf{s} \in \mathsf{S} \cap \mathsf{S}' \mid \mathsf{s} \subseteq \bar{\mathsf{t}}\} = \{\bar{\mathsf{t}}\} \cup \{\mathsf{s} \in \mathsf{S} \cap \mathsf{S}' \mid \mathsf{s} \subseteq \underline{\mathsf{t}}\} \cup \{\mathsf{s} \in \mathsf{S} \cap \mathsf{S}' \mid \mathsf{s} \subseteq \mathsf{a}\} \cup \{\mathsf{s} \in \mathsf{S} \cap \mathsf{S}' \mid \mathsf{s} \subseteq \mathsf{a}'\}.$$

By induction hypothesis applied to each tube of $\underline{t}$, we have

$$\text{vect}(\{\mathbf{d}(\mathsf{T}^\circ, \mathsf{s}) \mid \mathsf{s} \in \mathsf{S} \cap \mathsf{S}', \mathsf{s} \subseteq \underline{t}\})$$

$$
\begin{aligned}
&= \text{vect}(\{\mathbf{d}(\mathsf{T}^\circ, \mathsf{s}) \mid \mathsf{s} \in \mathsf{S}, \mathsf{s} \subseteq \underline{t}\}) && \text{(as } \mathsf{S} \smallsetminus (\mathsf{S} \cap \mathsf{S}') = \mathsf{t} \not\subseteq \underline{t}) \\
&= \text{vect}(\{\mathbf{d}(\mathsf{T}^\circ, \mathsf{s}) \mid \mathsf{s} \in \mathsf{T}, \mathsf{s} \subseteq \underline{t}\}) && \text{(induction hypothesis)} \\
&= \text{vect}(\{\mathbf{d}(\mathsf{T}^\circ, \mathsf{s}) \mid \mathsf{s} \in \mathsf{T} \cap \mathsf{T}', \mathsf{s} \subseteq \underline{t}\}) && \text{(as } \mathsf{T} \smallsetminus (\mathsf{T} \cap \mathsf{T}') = \mathsf{t} \not\subseteq \underline{t})
\end{aligned}
$$

and similarly replacing $\underline{t}$ by a or a'. It follows that the vector $\alpha\,\mathbf{d}(\mathsf{T}^\circ, \mathsf{t}) + \alpha'\,\mathbf{d}(\mathsf{T}^\circ, \mathsf{t}')$ also belongs to $\text{vect}(\{\mathbf{d}(\mathsf{T}^\circ, \mathsf{s}) \mid \mathsf{s} \in \mathsf{T} \cap \mathsf{T}', \mathsf{s} \subseteq \mathsf{u}\})$. Since $\alpha \neq 0$, this implies that the vector $\mathbf{d}(\mathsf{T}^\circ, \mathsf{t})$ belongs to $\text{vect}(\{\mathbf{d}(\mathsf{T}^\circ, \mathsf{s}) \mid \mathsf{s} \in \mathsf{T}', \mathsf{s} \subseteq \mathsf{u}\})$. Similarly, the vector $\mathbf{d}(\mathsf{T}^\circ, \mathsf{t}')$ belongs to $\text{vect}(\{\mathbf{d}(\mathsf{T}^\circ, \mathsf{s}) \mid \mathsf{s} \in \mathsf{T}, \mathsf{s} \subseteq \mathsf{u}\})$. We therefore obtained that

$$\text{vect}(\{\mathbf{d}(\mathsf{T}^\circ, \mathsf{s}) \mid \mathsf{s} \in \mathsf{T}, \mathsf{s} \subseteq \mathsf{u}\}) = \text{vect}(\{\mathbf{d}(\mathsf{T}^\circ, \mathsf{s}) \mid \mathsf{s} \in \mathsf{T}', \mathsf{s} \subseteq \mathsf{u}\}).$$

This also clearly holds when t and t' are not contained in u. This concludes the proof since the graph of flips on the maximal tubings on G containing u is connected. ∎

We can finally conclude the proof of Theorem 6.65 using both Lemmas 6.66 and 6.67.

Proof of Theorem 6.65. The **Span Property** is proved in Lemma 6.67. It only remains to show the **Flip Property** for arbitrary adjacent maximal tubings. Consider two adjacent maximal tubings T, T' on G with $\mathsf{T} \smallsetminus \{\mathsf{t}\} = \mathsf{T}' \smallsetminus \{\mathsf{t}'\}$. By Lemma 6.66, there exist adjacent maximal tubings S, S' on G such that $\mathsf{S} \smallsetminus \{\mathsf{t}\} = \mathsf{S}' \smallsetminus \{\mathsf{t}'\}$ and a linear dependence between the compatibility vectors of the tubes of $\mathsf{S} \cup \mathsf{S}'$ with respect to T° which is both **separating** and **local**. By definition, this implies that there exist $\alpha > 0$ and $\alpha' > 0$ such that the vector $\alpha\,\mathbf{d}(\mathsf{T}^\circ, \mathsf{t}) + \alpha'\,\mathbf{d}(\mathsf{T}^\circ, \mathsf{t}')$ belongs to $\text{vect}(\{\mathbf{d}(\mathsf{T}^\circ, \mathsf{s}) \mid \mathsf{s} \in \mathsf{S} \cap \mathsf{S}', \mathsf{s} \subseteq \bar{\mathsf{t}}\})$. Lemma 6.67 applied to $\underline{t}$ ensures that

$$\text{vect}(\{\mathbf{d}(\mathsf{T}^\circ, \mathsf{s}) \mid \mathsf{s} \in \mathsf{T} \cap \mathsf{T}', \mathsf{s} \subseteq \underline{t}\}) = \text{vect}(\{\mathbf{d}(\mathsf{T}^\circ, \mathsf{s}) \mid \mathsf{s} \in \mathsf{S} \cap \mathsf{S}', \mathsf{s} \subseteq \underline{t}\}).$$

and similarly replacing $\underline{t}$ by a or a'. We thus conclude that

$$\text{vect}(\{\mathbf{d}(\mathsf{T}^\circ, \mathsf{s}) \mid \mathsf{s} \in \mathsf{T} \cap \mathsf{T}', \mathsf{s} \subseteq \bar{\mathsf{t}}\}) = \text{vect}(\{\mathbf{d}(\mathsf{T}^\circ, \mathsf{s}) \mid \mathsf{s} \in \mathsf{S} \cap \mathsf{S}', \mathsf{s} \subseteq \bar{\mathsf{t}}\})$$

contains the vector $\alpha\,\mathbf{d}(\mathsf{T}^\circ, \mathsf{t}) + \alpha'\,\mathbf{d}(\mathsf{T}^\circ, \mathsf{t}')$ with $\alpha > 0$ and $\alpha' > 0$. In other words, we obtained a **separating** and **local** linear dependence on $\{\mathbf{d}(\mathsf{T}^\circ, \mathsf{s}) \mid \mathsf{s} \in \mathsf{T} \cup \mathsf{T}'\}$. ∎

6.5.4 Dual compatibility fan (Theorem 6.14)

The fact that dual compatibility vectors support a complete simplicial fan realizing the nested complex is a direct consequence of Theorem 6.10, using the following duality trick. Observe first that given $n + 1$ column vectors $\{u, v, w_1, \ldots, w_{n-1}\}$ in $\mathbb{R}^n$, the hyperplane spanned by $\{w_1, \ldots, w_{n-1}\}$ separates u and v if and only if

$$\det([u|w_1|\ldots|w_{n-1}]) \cdot \det([v|w_1|\ldots|w_{n-1}]) < 0.$$

Theorem 6.10 shows this condition for primal compatibility matrices and we need to show it for dual compatibility matrices. For this, we notice that the primal and dual compatibility matrices are related by

$$\mathbf{d}^*(\mathsf{T}, \mathsf{T}^\circ) := [(\mathsf{t}_j \,\|\, \mathsf{t}_i^\circ)]_{i,j \in [n]} = [(\mathsf{t}_i \,\|\, \mathsf{t}_j^\circ)]_{i,j \in [n]}^t =: \mathbf{d}(\mathsf{T}, \mathsf{T}^\circ)^t, \tag{6.5}$$

where M^t denotes the transpose of the matrix M. Consider now two pairs of adjacent maximal tubings $\mathsf{T}^\circ, \mathsf{T}^{\circ\prime}$ and T, T' on G. The **Separation Flip Property** of Theorem 6.10, applied to the initial tubing T, implies that $\det(\mathbf{d}(\mathsf{T}, \mathsf{T}^\circ)) \cdot \det(\mathbf{d}(\mathsf{T}, \mathsf{T}^{\circ\prime})) < 0$.

Similarly, for the initial tubing T', we obtain that $\det(\mathbf{d}(\mathsf{T}', \mathsf{T}^\circ)) \cdot \det(\mathbf{d}(\mathsf{T}', \mathsf{T}^{\circ\prime})) < 0$. Multiplying these two inequalities, we get

$$\Big(\det(\mathbf{d}(\mathsf{T}, \mathsf{T}^\circ)) \cdot \det(\mathbf{d}(\mathsf{T}', \mathsf{T}^\circ))\Big) \cdot \Big(\det(\mathbf{d}(\mathsf{T}, \mathsf{T}^{\circ\prime})) \cdot \det(\mathbf{d}(\mathsf{T}', \mathsf{T}^{\circ\prime}))\Big) > 0.$$

Since the transposition preserves the determinant, we obtain by Equation 6.5 that

$$\Big(\det(\mathbf{d}^*(\mathsf{T}, \mathsf{T}^\circ)) \cdot \det(\mathbf{d}^*(\mathsf{T}', \mathsf{T}^\circ))\Big) \cdot \Big(\det(\mathbf{d}^*(\mathsf{T}, \mathsf{T}^{\circ\prime})) \cdot \det(\mathbf{d}^*(\mathsf{T}', \mathsf{T}^{\circ\prime}))\Big) > 0.$$

This implies that $\det(\mathbf{d}^*(\mathsf{T}, \mathsf{T}^\circ)) \cdot \det(\mathbf{d}^*(\mathsf{T}', \mathsf{T}^\circ))$ and $\det(\mathbf{d}^*(\mathsf{T}, \mathsf{T}^{\circ\prime})) \cdot \det(\mathbf{d}^*(\mathsf{T}', \mathsf{T}^{\circ\prime}))$ have the same sign. Since we know that $\det(\mathbf{d}^*(\mathsf{T}, \mathsf{T}^\circ)) \cdot \det(\mathbf{d}^*(\mathsf{T}', \mathsf{T}^\circ)) < 0$ for $\mathsf{T}^\circ = \mathsf{T}$, we obtain by repeated flips in T° that $\det(\mathbf{d}^*(\mathsf{T}, \mathsf{T}^\circ)) \cdot \det(\mathbf{d}^*(\mathsf{T}', \mathsf{T}^\circ)) < 0$ for any initial tubing T° and pair of adjacent maximal tubings T, T' on G. This shows the **Separation Flip Property** for dual compatibility vectors. We conclude again by Proposition 3.7. ∎

Remark 6.68. Observe that this proof does not provide us with any explicit linear dependence between dual compatibility vectors. In particular, we do not know whether the following analogue properties of Theorem 6.65 hold:

Dual Span Property For any tube u of G, the span of $\{\mathbf{d}^*(\mathsf{t}, \mathsf{T}^\circ) \mid \mathsf{t} \in \mathsf{T}, \mathsf{t} \not\subset \mathsf{u}\}$, for a maximal tubing T on G containing u, is independent of T.

Dual Local Flip Property For any two maximal tubings T, T' with $\mathsf{T} \smallsetminus \{\mathsf{t}\} = \mathsf{T}' \smallsetminus \{\mathsf{t}'\}$, the unique linear dependence between the dual compatibility vectors of $\mathsf{T} \cup \mathsf{T}'$ with respect to T° is supported by tubes not strictly included in a connected component of $\underline{\mathsf{t}} = \mathsf{t} \cap \mathsf{t}'$.

6.5.5   Nested complex isomorphisms (Proposition 6.34, Proposition 6.36 and Theorem 6.37)

We prove various results on nested complex isomorphisms presented in Section 6.4.2. We first show that the map Ω on the tubes of a spider $\mathfrak{X}_{\underline{n}}$ defines a nested complex automorphism that dualizes the compatibility degree.

Proof of Proposition 6.34. First, Ω clearly sends tubes of $\mathfrak{X}_{\underline{n}}$ to tubes of $\mathfrak{X}_{\underline{n}}$. We just have to show that $(\Omega(\mathsf{t}) \,\|\, \Omega(\mathsf{t}')) = (\mathsf{t}' \,\|\, \mathsf{t})$ for any two tubes t, t' of $\mathfrak{X}_{\underline{n}}$, and Proposition 6.7 will imply that Ω is a nested complex automorphism. This follows from the definition of Ω and the fact that

$$\left([v_j^i, v_k^i] \,\Big\|\, [v_{j'}^{i'}, v_{k'}^{i'}] \right) = \delta_{i=i'} \cdot \left(\delta_{j < j' \le k+1 < k'+1} + \delta_{j' < j \le k'+1 < k+1} \right),$$

$$\left([v_j^i, v_k^i] \,\Big\|\, \bigcup_{h \in \ell} [v_0^h, v_{k_h}^h] \right) = \delta_{j \le k_i+1 \le k},$$

$$\text{and} \quad \left(\bigcup_{i \in \ell} [v_0^i, v_{k_i}^i] \,\Big\|\, \bigcup_{i \in \ell} [v_0^i, v_{k'_i}^i] \right) = |\{i \in [\ell] \mid k_i < k'_i\}| \cdot \delta_{\exists i \in [\ell],\, k_i > k'_i}. \quad\blacksquare$$

Our objective is to show that these maps Ω on spiders are essentially the only nontrivial nested complex isomorphisms. We fix an isomorphism Φ between two nested complexes $\mathcal{N}(\mathrm{G})$ and $\mathcal{N}(\mathrm{G}')$. We first show that Φ preserves connected components in the following sense.

Lemma 6.69. *Two tubes t and t' of G belong to the same connected component of G if and only if their images $\Phi(\mathsf{t})$ and $\Phi(\mathsf{t}')$ belong to the same connected component of G'.*

Proof. Observe first that two tubes from distinct connected components are automatically compatible. Assume now that t and t' are in the same connected component of G. If t and t' are incompatible, then $\Phi(t)$ and $\Phi(t')$ are also incompatible and therefore in the same connected component of G'. If t and t' are compatible, then there exists a tube t'' incompatible with both t and t':

- if $t \cap t' = \varnothing$, consider a path from a neighbor of t to a neighbor of t' in $G[V \smallsetminus (t \cup t')]$;

- if $t \subseteq t'$, consider a path from a neighbor of t to a neighbor of t' in $G[V \smallsetminus t]$.

We obtain that $\Phi(t'')$ is incompatible with both $\Phi(t)$ and $\Phi(t')$, so that they all belong to the same connected component of G'. This proves one direction. For the other direction, the same arguments can be applied to Φ^{-1}. ∎

Consequently, the nested complex $\mathcal{N}(G)$ records the sizes of the connected components of the graph G. We define the *connected size partition* of G as the partition $\lambda(G) := |V_1|, |V_2|, \ldots, |V_\kappa|$ of $|V|$, where $V_1, \ldots, V_\kappa$ are the connected components of G ordered such that $|V_i| \geq |V_{i+1}|$.

Corollary 6.70. *Two graphs whose nested complexes are isomorphic have the same connected size partitions:* $\mathcal{N}(G) \simeq \mathcal{N}(G') \implies \lambda(G) = \lambda(G')$. *In particular, they have the same number of vertices.*

Proof. Consider a maximal tubing T on G and decompose it into subtubings $T_1, \ldots, T_\kappa$ on the connected components $V_1, \ldots, V_\kappa$ of G. Their images $\Phi(T_1), \ldots, \Phi(T_\kappa)$ decompose the maximal tubing $\Phi(T)$. Moreover, Lemma 6.69 ensures that two tubes $\Phi(t) \in \Phi(T_i)$ and $\Phi(t') \in \Phi(T_{i'})$ belong to the same connected component of G' if and only if $i = i'$. We therefore obtain that

$$\lambda(G) = \{|V_1|, \ldots, |V_\kappa|\} = \{|T_1| + 1, \ldots, |T_\kappa| + 1\} = \{|\Phi(T_1)| + 1, \ldots, |\Phi(T_\kappa)| + 1\} = \lambda(G').$$
∎

Proposition 6.36 is another immediate consequence of Lemma 6.69: since it sends all tubes in a connected component H of G to tubes in the same connected component H' of G', the map Φ induces a nested complex isomorphism between $\mathcal{N}(H)$ and $\mathcal{N}(H')$. From now on, we assume without loss of generality that G is connected. Our next step is a crucial structural property of Φ.

Lemma 6.71. *For any nested complex isomorphism* $\Phi : \mathcal{N}(G) \to \mathcal{N}(G')$ *and any tube* t *of* G, *either* $|\Phi(t)| = |t|$ *or* $|\Phi(t)| = |V| - |t|$.

Proof. By Lemma 6.63, the link of a tube t in $\mathcal{N}(G)$ is isomorphic to the nested complex $\mathcal{N}(G[t] \sqcup G^\star t)$ of the union of the restriction $G[t]$ with the reconnected complement $G^\star t$. The former has $|t|$ vertices while the latter has $|V| - |t|$ vertices. Since Φ induces an isomorphism from the link of t in $\mathcal{N}(G)$ to the link of $\Phi(t)$ in $\mathcal{N}(G')$, the result follows from Corollary 6.70. ∎

We say that Φ *maintains* the tube t if $|\Phi(t)| = |t|$ and that Φ *swaps* the tube t if $|\Phi(t)| = |V| - |t|$.

Proposition 6.72. *If it maintains all tubes of* G, *then* Φ *is the trivial nested complex isomorphism induced by the graph isomorphism* $\psi : G \to G'$ *defined by* $\Phi(\{v\}) = \{\psi(v)\}$.

Proof. Two vertices v and w of G are adjacent if and only if the two tubes $\{v\}$ and $\{w\}$ are incompatible. Since Φ preserves the compatibility relation, this shows that v and w are adjacent if and only if $\psi(v)$ and $\psi(w)$ are, *i.e.* that ψ defines a graph isomorphism. Let Ψ denote the nested complex isomorphism induced by ψ, *i.e.* defined by $\Psi(t) := \{\psi(v) \mid v \in t\}$.

We prove by induction on $|\mathsf{t}|$ that $\Phi(\mathsf{t}) = \Psi(\mathsf{t})$ for any tube t on G. It holds for singletons. For the induction step, consider an arbitrary tube t of G. Let $v \in V \smallsetminus \mathsf{t}$ be a neighbor of t. Since $\{v\}$ and t are incompatible, so are $\Phi(\{v\}) = \{\psi(v)\}$ and $\Phi(\mathsf{t})$, and thus $\psi(v)$ is a neighbor of $\Phi(\mathsf{t})$. Let $w \in V$ be such that $\psi(w)$ is a neighbor of $\psi(v)$ in $\Phi(\mathsf{t})$. If $w \notin \mathsf{t}$ then it is incompatible with $\mathsf{t} \cup \{v\}$, and thus $\Phi(\{w\}) = \{\psi(w)\}$ is incompatible with $\Phi(\mathsf{t} \cup \{v\})$. Therefore, $\Phi(\mathsf{t} \cup \{v\})$ is adjacent to and does not contain $\psi(w)$ which is in $\Phi(\mathsf{t})$. Since $|\Phi(\mathsf{t} \cup \{v\})| = |\mathsf{t}| + 1 = |\Phi(\mathsf{t})| + 1$, this implies that $\Phi(\mathsf{t} \cup \{v\})$ is incompatible with $\Phi(\mathsf{t})$, a contradiction. Therefore, we know that $w \in \mathsf{t}$. Let $\mathsf{t}_1, \dots, \mathsf{t}_k$ denote the connected components of $G[\mathsf{t} \smallsetminus \{w\}]$. By induction hypothesis, $\Phi(\mathsf{t}_i) = \Psi(\mathsf{t}_i)$ for all $i \in [k]$. Moreover, since $\Phi(\mathsf{t}_i)$ is compatible with $\Phi(\mathsf{t})$ and adjacent to $\psi(w) \in \Phi(\mathsf{t})$, it is included in $\Phi(\mathsf{t})$. So we obtain $\Psi(\mathsf{t}) = \{\psi(w)\} \cup \Psi(\mathsf{t}_1) \cup \cdots \cup \Psi(\mathsf{t}_k) \subseteq \Phi(\mathsf{t})$ and thus $\Phi(\mathsf{t}) = \Psi(\mathsf{t})$ as $|\Phi(\mathsf{t})| = |\mathsf{t}| = |\Psi(\mathsf{t})|$. ∎

Lemma 6.73. *If Φ does not maintain a tube t of G (i.e. $|\Phi(\mathsf{t})| \neq |\mathsf{t}|$), then*
  (i) *Φ swaps any tube of G containing t,*
 (ii) *Φ maintains any tube of G disjoint from and nonadjacent to t, and*
(iii) *Φ swaps at least one singleton included in t.*

Proof. Consider a tube s of G strictly containing t. The link of $\{\mathsf{s}, \mathsf{t}\}$ in $\mathcal{N}(G)$ is isomorphic to the nested complex of the union of the graphs $G[\mathsf{t}]$, $(G^{\star}\mathsf{t})[\mathsf{s} \smallsetminus \mathsf{t}]$, and $G^{\star}\mathsf{s}$ with $|\mathsf{t}|$, $|\mathsf{s}| - |\mathsf{t}|$ and $|V| - |\mathsf{s}|$ vertices respectively. Therefore, Corollary 6.70 ensures that the link of $\{\Phi(\mathsf{s}), \Phi(\mathsf{t})\}$ in $\mathcal{N}(G')$ is isomorphic to the nested complex of a graph with three connected components with $|\mathsf{t}|$, $|\mathsf{s}| - |\mathsf{t}|$ and $|V| - |\mathsf{s}|$ vertices respectively. If $\Phi(\mathsf{s})$ is not contained in $\Phi(\mathsf{t})$, then the link of $\{\Phi(\mathsf{s}), \Phi(\mathsf{t})\}$ in $\mathcal{N}(G')$ would be isomorphic to the nested complex of a graph with one connected component $G'[\Phi(\mathsf{t})]$ having $|\Phi(\mathsf{t})|$ vertices. We reach a contradiction as $|\Phi(\mathsf{t})| = |V| - |\mathsf{t}|$ is neither $|\mathsf{t}|$ (by assumption on t), nor $|V| - |\mathsf{s}|$ (since $|\mathsf{s}| > |\mathsf{t}|$), nor $|\mathsf{s}| - |\mathsf{t}|$ (since $|\mathsf{s}| < |V|$). Therefore, $\Phi(\mathsf{s})$ is contained in $\Phi(\mathsf{t})$ and the link of $\{\Phi(\mathsf{s}), \Phi(\mathsf{t})\}$ in $\mathcal{N}(G')$ is isomorphic to the union of the graphs $G[\Phi(\mathsf{s})]$, $(G^{\star}\Phi(\mathsf{s}))[\Phi(\mathsf{t}) \smallsetminus \Phi(\mathsf{s})]$, and $G^{\star}\Phi(\mathsf{t})$ with $|\Phi(\mathsf{s})|$, $|\Phi(\mathsf{t})| - |\Phi(\mathsf{s})|$ and $|V| - |\Phi(\mathsf{t})|$ vertices respectively. If $|\Phi(\mathsf{s})| \neq |V| - |\mathsf{s}|$, then it forces $|\Phi(\mathsf{s})| = |\mathsf{s}| - |\mathsf{t}| = |\mathsf{s}|$, a contradiction. This proves (i).

Consider now a tube s of G disjoint from and nonadjacent to t. Note that $|\mathsf{s}| + |\mathsf{t}| < |V|$ as there is at least a vertex separing them. The link of $\{\mathsf{s}, \mathsf{t}\}$ in $\mathcal{N}(G)$ is isomorphic to the nested complex of the union of the graphs $G[\mathsf{s}]$, $G[\mathsf{t}]$, and $(G^{\star}\mathsf{s})^{\star}\mathsf{t}$ with $|\mathsf{s}|$, $|\mathsf{t}|$ and $|V| - |\mathsf{s}| - |\mathsf{t}|$ vertices respectively. Again, Corollary 6.70 ensures that the link of $\{\Phi(\mathsf{s}), \Phi(\mathsf{t})\}$ in $\mathcal{N}(G')$ is isomorphic to the nested complex of a graph with three connected components with $|\mathsf{s}|$, $|\mathsf{t}|$ and $|V| - |\mathsf{s}| - |\mathsf{t}|$ vertices respectively. If $\Phi(\mathsf{s})$ is not contained in $\Phi(\mathsf{t})$, then the link of $\{\Phi(\mathsf{s}), \Phi(\mathsf{t})\}$ in $\mathcal{N}(G')$ would be isomorphic to the nested complex of a graph with one connected component $G'[\Phi(\mathsf{t})]$ having $|\Phi(\mathsf{t})|$ vertices. We reach a contradiction as $|\Phi(\mathsf{t})| = |V| - |\mathsf{t}|$ is neither $|\mathsf{t}|$ (by assumption on t), nor $|\mathsf{s}|$ (since $|\mathsf{s}| + |\mathsf{t}| < |V|$), nor $|V| - |\mathsf{s}| - |\mathsf{t}|$ (since $|\mathsf{s}| > 0$). Therefore, $\Phi(\mathsf{s})$ is contained in $\Phi(\mathsf{t})$ and the link of $\{\Phi(\mathsf{s}), \Phi(\mathsf{t})\}$ in $\mathcal{N}(G')$ is isomorphic to the union of the graphs $G[\Phi(\mathsf{s})]$, $(G^{\star}\Phi(\mathsf{s}))[\Phi(\mathsf{t}) \smallsetminus \Phi(\mathsf{s})]$, and $G^{\star}\Phi(\mathsf{t})$ with $|\Phi(\mathsf{s})|$, $|\Phi(\mathsf{t})| - |\Phi(\mathsf{s})|$ and $|V| - |\Phi(\mathsf{t})|$ vertices respectively. If $|\Phi(\mathsf{s})| \neq |\mathsf{s}|$, then it forces $|\Phi(\mathsf{s})| = |V| - |\mathsf{s}| - |\mathsf{t}| = |V| - |\mathsf{s}|$, a contradiction. This proves (ii).

Finally, to prove (iii) we can assume that t is not a singleton. Thus $\Phi(\mathsf{t})$ is not an inclusion maximal tube. Let t' be a tube of G such that $\Phi(\mathsf{t}')$ is a maximal tube of G' containing $\Phi(\mathsf{t})$. Since Φ^{-1} swaps $\Phi(\mathsf{t})$ and $\Phi(\mathsf{t}')$ contains $\Phi(\mathsf{t})$, Φ^{-1} also swaps $\Phi(\mathsf{t}')$ by (i). Thus, t' is a singleton swapped by Φ and contained in t. ∎

Lemma 6.74. *Denote by $M := \{v \in V \mid |\Phi(\{v\})| = 1\}$ the set of vertices maintained by Φ and by $S := \{v \in V \mid |\Phi(\{v\})|) = |V| - 1\}$ the set of vertices swapped by Φ. Then*
  (i) *S forms a clique of G,*
 (ii) *any vertex in M has at most one neighbor in S, and*
(iii) *any vertex in S has at most one neighbor in M.*

Proof. Let $s, s' \in S$. Since $|\Phi(\{s\})| = |\Phi(\{s'\})| = |V| - 1$, the tubes $\Phi(\{s\})$ and $\Phi(\{s'\})$ are incompatible. Therefore $\{s\}$ and $\{s'\}$ are incompatible, so that s and s' are neighbors. The set S thus forms a clique.

To prove (ii) and (iii), assume that some vertices $m \in M$ and $s \in S$ are neighbors. The tubes $\{m\}$ and $\{s\}$ are thus incompatible, so that $\Phi(\{m\})$ and $\Phi(\{s\})$ are also incompatible. Since $|\Phi(\{m\})| = 1$ while $|\Phi(\{s\})| = |V| - 1$, this implies that $\Phi(\{s\}) = V' \smallsetminus \Phi(\{m\})$. It follows that m cannot have another neighbor swapped by Φ and s cannot have another neighbor maintained by Φ. ∎

We are now ready to prove that any nontrivial nested complex isomorphism coincides, up to composition with a trivial nested complex isomorphism, with the isomorphism Ω on a spider.

Proof of Theorem 6.37. The proof works by induction on the number $|V|$ of vertices of G. It is clear when $|V| \leq 2$. For the induction step, assume that the result holds for all graphs on less than $|V|$ vertices and consider a nontrivial nested complex isomorphism $\Phi : \mathcal{N}(G) \to \mathcal{N}(G')$. Then Φ does not maintain all tubes of G by Proposition 6.72, and thus swaps at least one singleton $\{s\}$ by Lemma 6.73 (iii). Let s' denote the vertex of G' such that $\Phi(\{s\}) = V' \smallsetminus \{s'\}$.

The map Φ induces a nested complex isomorphism between the link of $\{s\}$ in $\mathcal{N}(G)$ and the link of $\Phi(\{s\})$ in $\mathcal{N}(G')$. The former is isomorphic to the nested complex of the reconnected complement $\widetilde{G} := G^\star \{s\}$ while the latter is isomorphic to the nested complex of the restriction $\widetilde{G}' := G'[\Phi(\{s\})]$. Let $\widetilde{\Phi} : \tilde{t} \mapsto \Phi(t)$ denote the resulting nested complex isomorphism between $\mathcal{N}(\widetilde{G})$ and $\mathcal{N}(\widetilde{G}')$. This isomorphism $\widetilde{\Phi}$ is nontrivial: by Lemma 6.73, Φ swaps any tube t containing $\{s\}$, so that $\widetilde{\Phi}$ swaps the tube $t \smallsetminus \{s\}$. It follows by induction hypothesis that $\widetilde{G}$ and $\widetilde{G}'$ are spiders and that there exists a graph isomorphism $\widetilde{\psi} : \widetilde{G} \to \widetilde{G}'$ inducing a trivial nested complex isomorphism $\widetilde{\Psi} : \mathcal{N}(\widetilde{G}) \to \mathcal{N}(\widetilde{G}')$ such that $\widetilde{\Psi}^{-1} \circ \widetilde{\Phi} =: \widetilde{\Omega}$ is the automorphism of $\mathcal{N}(\widetilde{G})$ described in Section 6.4.2. In other words, we can label by $\widetilde{v}_j^i$ the vertices of the spider $\widetilde{G}$ and by $\widetilde{v}_j'^i$ the vertices of the spider $\widetilde{G}'$, with $i \in [\widetilde{\ell}]$ and $0 \leq j \leq \widetilde{n}_i$, such that

$$\widetilde{\Phi}([\widetilde{v}_j^i, \widetilde{v}_k^i]) = [\widetilde{v}_{n_i+1-k}'^i, \widetilde{v}_{n_i+1-j}'^i] \quad \text{and} \quad \widetilde{\Phi}\Big(\bigcup_{i \in [\widetilde{\ell}]} [\widetilde{v}_0^i, \widetilde{v}_{k_i}^i] \Big) = \bigcup_{i \in [\widetilde{\ell}]} [\widetilde{v}_0'^i, \widetilde{v}_{n_i-1-k_i}'^i]. \quad (6.6)$$

We now claim that G and G' are both spiders. To prove it, we distinguish two cases:

Body case all neighbors of s in G are swapped by Φ. Then they form a clique in G (by Lemma 6.74 (i)), so that G is the spider $\widetilde{G}$ where we add one more body vertex s with no attached leg. Moreover, s' is necessarily swapped by Φ^{-1} (otherwise $\Phi^{-1}(\{s'\})$ would be a neighbor of s maintained by Φ). We conclude by symmetry that G' is the spider $\widetilde{G}'$ where we add one more body vertex s' with no attached leg.

Leg case s has a neighbor m maintained by Φ. It is unique by Lemma 6.74 (iii) and not connected to any other vertex swapped by Φ by Lemma 6.74 (ii). Therefore, G is the spider $\widetilde{G}$ where we replace the edges connecting m to all other body vertices of $\widetilde{G}$ by a new body vertex s with an edge to m. Moreover, s' is necessarily maintained by Φ^{-1} (otherwise $\Phi^{-1}(\{s'\})$ should be $V \smallsetminus \{s\}$ which is not connected). We conclude that G' is the spider $\widetilde{G}'$ where we add one additional leg vertex s' to the free endpoint of a leg.

We now label by v_j^i the vertices of G according to the labels $\widetilde{v}_j^i$ of $\widetilde{G}$ and by $v_j'^i$ the vertices of G' according to the labels $\widetilde{v}_j'^i$ of $\widetilde{G}'$. We follow the two cases above:

Body case We set $\ell := \widetilde{\ell}+1$, $n_i := \widetilde{n}_i$ for $i \in [\widetilde{\ell}]$ and $n_\ell = 0$. For any $i \in [\widetilde{\ell}]$ and $0 \leq j \leq n_i$, we label by v_j^i the vertex of G corresponding to the vertex labeled by $\widetilde{v}_j^i$ in $\widetilde{G}$, and similarly we label by $v_j'^i$ the vertex of G' corresponding to the vertex labeled by $\widetilde{v}_j'^i$ in $\widetilde{G}'$. Finally, we label s by v_0^ℓ and s' by $v_0'^\ell$.

Leg case Assume that the neighbor of s maintained by Φ corresponds to the vertex labeled by $\widetilde{v}_0^a$ in $\widetilde{G}$. Then the neighbor of s' corresponds to the vertex labeled by $\widetilde{v}_{n_a}'^a$ in $\widetilde{G}'$. We set $\ell := \widetilde{\ell}$, $n_i := \widetilde{n}_i$ for $i \in [\ell] \smallsetminus \{a\}$ and $n_a := \widetilde{n}_a + 1$. For any $i \in [\ell]$ and $0 \leq j \leq \widetilde{n}_i$, we label by v_j^i if $i \neq a$ and v_{j+1}^i if $i = a$ the vertex of G corresponding to the vertex labeled by $\widetilde{v}_j^i$ in $\widetilde{G}$ and by $v_j'^i$ the vertex of G' corresponding to the vertex labeled by $\widetilde{v}_j'^i$ in $\widetilde{G}'$. Finally, we label s by v_0^a and s' by $v_{n_a}'^a$.

By our previous description of the two graphs G and G', these labels are indeed valid labels for the vertices of a spider, meaning that the edge set of G is indeed given by $\{\{v_{j-1}^i, v_j^i\} \mid i \in [\ell], j \in [n_i]\} \cup \{\{v_0^i, v_0^{i'}\} \mid i \neq i' \in [\ell]\}$, and similarly for G'. We moreover claim that Φ is given by

$$\Phi([v_j^i, v_k^i]) = [v_{n_i+1-k}^i, v_{n_i+1-j}^i] \qquad \text{and} \qquad \Phi(\bigcup_{i \in [\ell]} [v_0^i, v_{k_i}^i]) = \bigcup_{i \in [\ell]} [v_0^i, v_{n_i-1-k_i}^i]. \quad (6.7)$$

It is immediate for all tubes compatible with $\{s\} = \{v_0^a\}$ as it is easily transported from (6.6). We thus only have to check it for the tubes of G adjacent to $s = v_0^a$ and not containing it. Observe first that $\Phi([v_1^a, v_k^a])$ is a tube with k vertices (by Lemma 6.73 (iii)), containing $s' = v_{n_a}'^a$ since it has to be incompatible with $\Phi(\{s\}) = V' \smallsetminus \{s'\}$. Therefore, $\Phi([v_1^a, v_k^a]) = [v_{n_a+1-k}^a, v_{n_a}^a]$. Consider now a tube $\mathsf{t} = \bigcup_{i \in [\ell]} [v_0^i, v_{k_i}^i]$, not containing $s = v_0^a$ (*i.e.* with $k_a = -1$). Since the nested tubes t and $\mathsf{t} \cup \{s\}$ are both swapped, we have $\Phi(\mathsf{t}) = \Phi(\mathsf{t} \cup \{s\}) \cup \{s'\}$. Since $\Phi(\mathsf{t} \cup \{s\})$ is given by Equation (6.7), so is $\Phi(\mathsf{t})$. This concludes the proof that Φ is given by Equation (6.7), so that it coincides with Ω up to the graph automorphism defined by $v_j^i \mapsto v_j'^i$. ∎

We now prove that if the primal and dual compatibility fans of G with respect to the same initial maximal tubing T° are linearly isomorphic, then G is an octopus whose head is contained in no tube of T°.

Proof of Lemma 6.39. Consider a graph G and an initial tubing T° on G such that the fans $\mathcal{D}(G, \mathsf{T}^\circ)$ and $\mathcal{D}^*(G, \mathsf{T}^\circ)$ are linearly isomorphic. Notice that they both contain precisely n pairs of opposite rays, given by the vectors $\mathbf{e}_i$ of the canonical basis and their opposites $-\mathbf{e}_i$. Therefore, the fans $\mathcal{D}(G, \mathsf{T}^\circ)$ and $\mathcal{D}^*(G, \mathsf{T}^\circ)$ have the same rays, which implies that the compatibility vector $\mathbf{d}(\mathsf{T}^\circ, \mathsf{t})$ and dual compatibility vector $\mathbf{d}^*(\mathsf{t}, \mathsf{T}^\circ)$ are collinear for any tube t of G. In other words, we have $(\mathsf{t}_1^\circ \| \mathsf{t})(\mathsf{t} \| \mathsf{t}_2^\circ) = (\mathsf{t} \| \mathsf{t}_1^\circ)(\mathsf{t}_2^\circ \| \mathsf{t})$ for all tubes t of G and $\mathsf{t}_1^\circ, \mathsf{t}_2^\circ \in \mathsf{T}^\circ$.

We now prove by induction that this condition implies that G is an octopus whose head is contained in no tube of T°. The result is clear when $|V| \leq 3$. Consider thus a connected graph G on more than 4 vertices and a maximal tubing T° on G with root u (*i.e.* u is the only vertex of V contained in no proper tube of T°). The graph $G[V \smallsetminus \{u\}]$ has connected components $G_1, \dots, G_k$ and T° induces a maximal tubing T_i° on each component G_i. We know that G_1 is an octopus whose head v is contained in no tube of T°. Otherwise, by induction hypothesis, we could find three tubes $\mathsf{t}, \mathsf{t}_1^\circ, \mathsf{t}_2^\circ$ of G_1 such that $(\mathsf{t}_1^\circ \| \mathsf{t})(\mathsf{t} \| \mathsf{t}_2^\circ) \neq (\mathsf{t} \| \mathsf{t}_1^\circ)(\mathsf{t}_2^\circ \| \mathsf{t})$, which would contradict our assumption on T° since $\mathsf{t}, \mathsf{t}_1^\circ, \mathsf{t}_2^\circ$ are also tubes of G. Assume that G_1 is not a path, there are four cases:

- Suppose that v is the unique vertex of G_1 adjacent to u. Let $\mathsf{t} = \{u, v\}$, $\mathsf{t}_1^\circ = G_1$ and t_2° be a leg of G_1. Then $(\mathsf{t} \| \mathsf{t}_1^\circ) \geq 2$ and $(\mathsf{t}_1^\circ \| \mathsf{t}) = (\mathsf{t} \| \mathsf{t}_2^\circ) = (\mathsf{t}_2^\circ \| \mathsf{t}) = 1$.

- Suppose that u is adjacent to v and at least another vertex w of G_1. Let $\mathsf{t} = \{u\}$, $\mathsf{t}_1^\circ = \mathrm{G}_1$ and t_2° be the leg of G_1 containing w. Then $(\mathsf{t}_1^\circ \,\|\, \mathsf{t}) = (\mathsf{t}_2^\circ \,\|\, \mathsf{t}) = 1$ and $(\mathsf{t} \,\|\, \mathsf{t}_2^\circ) < (\mathsf{t} \,\|\, \mathsf{t}_1^\circ)$.

- Suppose that u is adjacent to at least two legs of G_1. Let $\mathsf{t} = \{u\}$, $\mathsf{t}_1^\circ = \mathrm{G}_1$ and t_2° be a leg of G_1 adjacent to u. Then $(\mathsf{t}_1^\circ \,\|\, \mathsf{t}) = (\mathsf{t}_2^\circ \,\|\, \mathsf{t}) = 1$ and $(\mathsf{t} \,\|\, \mathsf{t}_2^\circ) < (\mathsf{t} \,\|\, \mathsf{t}_1^\circ)$.

- Suppose that u is adjacent to a single leg H of $\mathrm{G}_1 \smallsetminus \{v\}$ but not to v. Let $\mathsf{t} = \{u, v\} \cup \mathrm{H}$, $\mathsf{t}_1^\circ = \mathrm{G}_1$ and t_2° be a leg of G_1 distinct from H. Then $(\mathsf{t} \,\|\, \mathsf{t}_1^\circ) \geq 2$ and $(\mathsf{t}_1^\circ \,\|\, \mathsf{t}) = (\mathsf{t} \,\|\, \mathsf{t}_2^\circ) = (\mathsf{t}_2^\circ \,\|\, \mathsf{t}) = 1$.

In all cases, we have $(\mathsf{t}_1^\circ \,\|\, \mathsf{t})(\mathsf{t} \,\|\, \mathsf{t}_2^\circ) \neq (\mathsf{t} \,\|\, \mathsf{t}_1^\circ)(\mathsf{t}_2^\circ \,\|\, \mathsf{t})$, contradicting our assumption on T°. Thus, G_1 is a path. A similar case analysis shows that G_1 is attached to u only by one of its endpoints. By symmetry, all components $\mathrm{G}_1, \ldots, \mathrm{G}_k$ of $\mathrm{G} \smallsetminus \{u\}$ are paths attached to u only by an endpoint, and G is an octopus whose head is contained in no tube of T°. ∎

Proof of Corollaries 6.40 and 6.41. Consider the compatibility fans on all maximal tubings on G. Two maximal tubings related by a graph automorphism of G clearly produce the same primal and dual compatibility fans. Reciprocally, consider two compatibility fans $\mathcal{D}(\mathrm{G}, \mathsf{T}_1^\circ)$ and $\mathcal{D}(\mathrm{G}, \mathsf{T}_2^\circ)$ of the graph G. As already observed in the introduction of Section 6.4.2, a linear isomorphism between $\mathcal{D}(\mathrm{G}, \mathsf{T}_1^\circ)$ and $\mathcal{D}(\mathrm{G}, \mathsf{T}_2^\circ)$ induces a nested complex automorphism Φ of $\mathcal{N}(\mathrm{G})$. If Φ is not trivial, then Theorem 6.37 ensures that G is a spider and Φ dualizes the compatibility degree. Therefore, G is an octopus by Lemma 6.39. This concludes the proof of Corollary 6.40 since the path is the only graph which is simultaneously a spider and an octopus. The proof of Corollary 6.41 follows the same lines, distinguishing the cases of spiders and octopuses. ∎

6.5.6 Polytopality of compatibility fans (Theorem 6.46 and Proposition 6.48)

This section provides the proof of the polytopality results presented in Section 6.4.3. Using a similar method as [CSZ15, Section 5] based on Proposition 3.9, we first prove that all compatibility and dual compatibility fans of paths and cycles are polytopal.

Proof of Theorem 6.46. We use the characterization of polytopality of complete simplicial fans given in Proposition 3.9. For this, we need to understand better the linear dependences on compatibility vectors for paths and cycles.

We specialize the notations introduced in the beginning of the proof of Lemma 6.66 to the setting of paths and cycles. Let t and t' be the exchanged tubes, let r (resp. r') be the unique neighbor of t (resp. t') in $\mathsf{t}' \smallsetminus \mathsf{t}$ (resp. in $\mathsf{t} \smallsetminus \mathsf{t}'$), and let $\underline{\mathsf{t}}_1, \ldots, \underline{\mathsf{t}}_k$ be the connected components of $\mathrm{G}[\mathsf{t} \cap \mathsf{t}']$ (where G is a path or a cycle). We then consider

$$\bar{\mathsf{t}} := \mathsf{t} \cup \mathsf{t}', \qquad \underline{\mathsf{t}} := \bigsqcup_{i \in [k]} \underline{\mathsf{t}}_i, \qquad \mathsf{a} := \mathsf{t} \smallsetminus (\mathsf{t}' \cup \{r\}) \qquad \text{and} \qquad \mathsf{a}' = \mathsf{t}' \smallsetminus (\mathsf{t} \cup \{r'\}).$$

Consider first the case of the path. When $(\mathsf{T} \cup \mathsf{T}') \cap \mathsf{T}^\circ = \varnothing$, the linear dependences can only be of the form

$$\mathbf{d}(\mathsf{T}^\circ, \mathsf{t}) + \mathbf{d}(\mathsf{T}^\circ, \mathsf{t}') = \mathbf{d}(\mathsf{T}^\circ, \bar{\mathsf{t}}) + \mathbf{d}(\mathsf{T}^\circ, \underline{\mathsf{t}}),$$
$$\mathbf{d}(\mathsf{T}^\circ, \mathsf{t}) + \mathbf{d}(\mathsf{T}^\circ, \mathsf{t}') = \mathbf{d}(\mathsf{T}^\circ, \mathsf{a}) + \mathbf{d}(\mathsf{T}^\circ, \mathsf{a}'),$$
$$2\,\mathbf{d}(\mathsf{T}^\circ, \mathsf{t}) + \mathbf{d}(\mathsf{T}^\circ, \mathsf{t}') = \mathbf{d}(\mathsf{T}^\circ, \bar{\mathsf{t}}) + \mathbf{d}(\mathsf{T}^\circ, \mathsf{a}),$$
$$2\,\mathbf{d}(\mathsf{T}^\circ, \mathsf{t}) + \mathbf{d}(\mathsf{T}^\circ, \mathsf{t}') = \mathbf{d}(\mathsf{T}^\circ, \underline{\mathsf{t}}) + \mathbf{d}(\mathsf{T}^\circ, \mathsf{a}'),$$

up to exchanging simultaneously t with t' and a with a'. If $T \cap T'$ contains a tube $t^\circ \in T^\circ$, then the compatibility degree of all tubes of $(T \cup T') \smallsetminus \{t^\circ\}$ with t° vanishes, so that the tube t° cannot appear in the linear dependence. When $t, t' \notin T^\circ$ but $(T \cap T') \cap T^\circ \neq \varnothing$, the relations are thus obtained from the ones above by deleting terms in their right hand sides. The dependences when t or t' belong to T° will be treated separately.

We now define a height function ω on tubes on P_{n+1} by

$$\omega(t) = \begin{cases} f(|t|) & \text{if } t \notin T^\circ, \\ \Omega & \text{otherwise,} \end{cases}$$

where $f : \mathbb{R} \to \mathbb{R}_{>0}$ is any strictly concave increasing positive function and $\Omega \in \mathbb{R}$ is a large enough constant. When $(T \cup T') \cap T^\circ = \varnothing$, we obtain by definition of $\bar{t}$, $\underline{t}$, a and a', and using that f is concave and increasing, that

$$\omega(t) + \omega(t') > \omega(\bar{t}) + \omega(\underline{t}),$$
$$\omega(t) + \omega(t') > \omega(a) + \omega(a'),$$
$$2\,\omega(t) + \omega(t') > \omega(\bar{t}) + \omega(a),$$
$$2\,\omega(t) + \omega(t') > \omega(\underline{t}) + \omega(a').$$

Moreover, the inequalities still hold when we delete terms in their right hand sides since ω is positive. Therefore, ω satisfies Condition (2) of Proposition 3.9 when we do not flip an initial tube. Finally, initial tubes only appear in the left hand sides of linear dependences, so choosing $\omega(t^\circ) = \Omega$ large enough ensures that ω satisfies Condition (2) of Proposition 3.9 for any flip. Observe that this is essentially the same proof as in [CSZ15, Section 5].

We now adapt this proof for the cycle O_{n+1}. Clearly, the dependences described above for the path also appear for the cycle (as cycles contain paths). Beside those, when $(T \cup T') \cap T^\circ = \varnothing$, a straightforward case analysis shows that the linear dependences can only be of the form

$$\mathbf{d}(T^\circ, t) + \mathbf{d}(T^\circ, t') = 2\,\mathbf{d}(T^\circ, \underline{t}_1), \qquad \text{where } \underline{t}_1 \in \underline{t}.$$

Again, no tube of T° can appear in their right hand sides of the linear dependences. Therefore, when $t, t' \notin T^\circ$ but $(T \cap T') \cap T^\circ \neq \varnothing$, the linear dependences are obtained from the generic ones above by deleting terms in their right hand sides. The dependences when t or t' belong to T° will again be treated separately.

We choose the same height function ω as before. For the same reasons, the linear dependences for the path are again transformed to strict inequalities on ω. Moreover, as $t_1 \subseteq t \cap t'$ and f is increasing, we have

$$\omega(t) + \omega(t') > 2\,\omega(\underline{t}_1).$$

We conclude as before by choosing Ω large enough that ω satisfies the Condition (2) of Proposition 3.9 for any flip.

Finally, for dual compatibility vectors, a straightforward case analysis shows that the linear dependences are all of the form

$$\mathbf{d}^*(t, T^\circ) + \mathbf{d}^*(t', T^\circ) = \mathbf{d}^*(\bar{t}, T^\circ) + \mathbf{d}^*(\underline{t}, T^\circ),$$
$$\mathbf{d}^*(t, T^\circ) + \mathbf{d}^*(t', T^\circ) = \mathbf{d}^*(a, T^\circ) + \mathbf{d}^*(a', T^\circ),$$
$$2\,\mathbf{d}^*(t, T^\circ) + \mathbf{d}^*(t', T^\circ) = \mathbf{d}^*(\bar{t}, T^\circ) + \mathbf{d}^*(a, T^\circ),$$
$$2\,\mathbf{d}^*(t, T^\circ) + \mathbf{d}^*(t', T^\circ) = \mathbf{d}^*(\underline{t}, T^\circ) + \mathbf{d}^*(a', T^\circ),$$

when none of t, t' and t̄ have n vertices. We can also have the linear dependences

$$\mathbf{d}^*(\mathsf{t}, \mathsf{T}^\circ) + \mathbf{d}^*(\mathsf{t}', \mathsf{T}^\circ) = 2\,\mathbf{d}^*(\bar{\mathsf{t}}, \mathsf{T}^\circ) + \mathbf{d}^*(\underline{\mathsf{t}}, \mathsf{T}^\circ),$$
$$2\,\mathbf{d}^*(\mathsf{t}, \mathsf{T}^\circ) + \mathbf{d}^*(\mathsf{t}', \mathsf{T}^\circ) = 2\,\mathbf{d}^*(\bar{\mathsf{t}}, \mathsf{T}^\circ) + \mathbf{d}^*(\mathsf{a}, \mathsf{T}^\circ),$$

when $|\bar{\mathsf{t}}| = n$ and

$$\mathbf{d}^*(\mathsf{t}, \mathsf{T}^\circ) + \mathbf{d}^*(\mathsf{t}', \mathsf{T}^\circ) = \mathbf{d}^*(\underline{\mathsf{t}}_1, \mathsf{T}^\circ), \qquad \text{where } \underline{\mathsf{t}}_1 \in \underline{\mathsf{t}},$$

when $|\mathsf{t}| = |\mathsf{t}'| = n$. Again, no tube of T° can appear in the right hand sides of the linear dependences. Therefore, when $\mathsf{t}, \mathsf{t}' \notin \mathsf{T}^\circ$ but $(\mathsf{T} \cap \mathsf{T}') \cap \mathsf{T}^\circ \neq \varnothing$, the linear dependences are obtained from the generic ones above by deleting terms in their right hand sides.

We now define a height function ω on tubes on O_{n+1} by

$$\omega(\mathsf{t}) = \begin{cases} f(|\mathsf{t}|) & \text{if } \mathsf{t} \notin \mathsf{T}^\circ \text{ and } |\mathsf{t}| \neq n, \\ \dfrac{f(|\mathsf{t}|)}{2} & \text{if } \mathsf{t} \notin \mathsf{T}^\circ \text{ and } |\mathsf{t}| = n, \\ \Omega & \text{otherwise,} \end{cases}$$

where $f : \mathbb{R} \to \mathbb{R}_{>0}$ is any strictly concave increasing positive function and $\Omega \in \mathbb{R}$ is a large enough constant. By definition of $\bar{\mathsf{t}}$, $\underline{\mathsf{t}}$, a and a', and using that f is concave and increasing, we obtain that ω satisfies a strict inequality for each linear dependence above. We conclude as before by choosing Ω large enough that ω satisfies the Condition (2) of Proposition 3.9 for any flip. ∎

Our last proof concerns the polytopality of the compatibility fan for the star, for which we have presented a candidate in Section 6.4.3.

Proof of Proposition 6.48. We just have to show that for any tube t and any maximal tubing T on X_{n+1}, the point $\mathbf{x}(\mathsf{T})$ belongs to the half-space $\mathbf{H}^\geq(\mathsf{t})$ and to the boundary of this half-space if and only if $\mathsf{t} \in \mathsf{T}$.

Consider first a tube t not in T°. Let $\underline{\mathsf{t}}$ denote the inclusion minimal tube of $\mathsf{T} \cup \mathsf{V}$ containing the central vertex $*$. Then the other tubes of T are all leaves of X_{n+1} contained in $\underline{\mathsf{t}}$ and a nested chain of tubes $\underline{\mathsf{t}} = \mathsf{t}_{|\underline{\mathsf{t}}|} \subsetneq \mathsf{t}_{|\underline{\mathsf{t}}|+1} \subsetneq \cdots \subsetneq \mathsf{t}_{n+1} = \mathsf{V}$ of X_{n+1}. Therefore, we have $\mathbf{x}(\mathsf{T})_i = 0$ if $\{\ell_i\} \subseteq \underline{\mathsf{t}}$ and $\mathbf{x}(\mathsf{T})_i = j-1$ if $\{\ell_i\} = \mathsf{t}_j \smallsetminus \mathsf{t}_{j-1}$. We conclude that

$$\langle \mathbf{d}(\mathsf{T}^\circ, \mathsf{t}) | \mathbf{x}(\mathsf{T}) \rangle = \sum_{\substack{i \in [n] \\ \ell_i \in \mathsf{t}}} \mathbf{x}(\mathsf{t})_i = \sum_{\substack{|\underline{\mathsf{t}}| \leq j \leq n+1 \\ \mathsf{t}_j \smallsetminus \mathsf{t}_{j-1} \nsubseteq \mathsf{t}}} (j-1) \leq \sum_{j=|\mathsf{t}|}^n j = f(|\mathsf{t}|),$$

with equality if and only if $\mathsf{t}_j \smallsetminus \mathsf{t}_{j-1} \nsubseteq \mathsf{t}$ for all $|\mathsf{t}| \leq j \leq n+1$, *i.e.* if and only if $\mathsf{t} = \mathsf{t}_{|\mathsf{t}|}$. Finally, for any $i \in [n]$, we have $\langle \mathbf{d}(\mathsf{T}^\circ, \{\ell_i\}) | \mathbf{x}(\mathsf{T}) \rangle = -\mathbf{x}(\mathsf{T})_i \leq 0$, with equality if and only if the inclusion minimal tube of $\mathsf{T} \cup \mathsf{V}$ containing i is $\{\ell_i\}$, *i.e.* if and only if $\{\ell_i\} \in \mathsf{T}$. ∎

6.5.7 Design compatibility fan (Theorem 6.53)

The proof of Theorem 6.53 still relies on Proposition 3.7, that is on the understanding of the linear dependences of the compatibility vectors of the tubes involved in a flip. We now need to distinguish two kinds of flips: we call *round flips* those exchanging two round tubes, and *square flips* those exchanging a square to a round tube.

We claim that Theorem 6.65 still holds for round flips. Indeed, a coordinate-wise verification shows that the linear dependences exhibited in Section 6.5.3 still hold for initial maximal design tubings: the arguments are identical for coordinates corresponding to round tubes and straightforward for coordinates corresponding to square tubes.

It thus remains to show the **Separating Flip Property** for square flips. It turns out that the proof for square flips is much easier as the linear dependences only involve compatibility vectors of forced tubes. Using the duality trick presented in Section 6.5.4 and the fact that any two maximal design tubings are connected by a sequence of square flips, it is equivalent to prove the **Separating Flip Property** for the primal or for the dual compatibility fan. In the sequel, we prefer to work with the dual compatibility vectors.

Fix an initial maximal design tubing T° on a graph G. Consider a round tube t exchangeable with a square tube $v^\square$, that is v is contained in t. The forced tubes of this square flip (*i.e.* the tubes contained in all flips exchanging t and $v^\square$) are the following:

- the square tubes $w_1{}^\square, \ldots w_k{}^\square$ for the neighbors $w_1, \ldots, w_k$ of t in G,

- the round tubes $\mathsf{a}_1, \ldots, \mathsf{a}_\ell$ given by the connected components of $\mathrm{G}[\mathsf{t} \smallsetminus \{v\}]$.

Let p be number of w_i's which are roots of initial round tubes in T° and let q be the number of a_i's containing an initial square tube of T°. Suppose that

- the w_i's are ordered such that $w_1, \ldots, w_p$ are roots of tubes $\mathsf{t}_1^\circ, \ldots, \mathsf{t}_p^\circ$ in T° with $\mathsf{t}_i^\circ \not\supseteq \mathsf{t}_j^\circ$ for $1 \leq i < j \leq p$, while $w_{p+1}{}^\square, \ldots, w_k{}^\square$ are square tubes of T°,

- the a_i's are ordered such that $\mathsf{a}_1, \ldots, \mathsf{a}_q$ contain an initial square tube of T° while $\mathsf{a}_{q+1}, \ldots, \mathsf{a}_\ell$ do not.

With these notations, the reader can check that if $p = 0$ and $q > 0$, then the dual compatibility vectors of these forced tubes satisfy the dependence

$$\mathbf{d}^*(\mathsf{t}, \mathsf{T}^\circ) = \sum_{j \in [q]} \left(\mathbf{d}^*(\mathsf{a}_j, \mathsf{T}^\circ) - \mathbf{d}^*(v^\square, \mathsf{T}^\circ) \right) \tag{6.8}$$

We now adapt this linear dependence to case when $p \geq 0$ and $q > 0$. We claim that

$$\mathbf{d}^*(\mathsf{t}, \mathsf{T}^\circ) = \sum_{j \in [q]} \left(\mathbf{d}^*(\mathsf{a}_j, \mathsf{T}^\circ) - \mathbf{d}^*(v^\square, \mathsf{T}^\circ) \right) + \sum_{i \in [p]} \beta_i \, \mathbf{d}^*(w_i{}^\square, \mathsf{T}^\circ)$$

where the coefficients $\beta_1, \ldots, \beta_p$ are recursively defined by

$$\beta_i = (\mathsf{t} \,\|\, \mathsf{t}_i^\circ) - \left(\sum_{j \in [q]} \left((\mathsf{a}_j \,\|\, \mathsf{t}_i^\circ) - (v^\square \,\|\, \mathsf{t}_i^\circ) \right) + \sum_{r \in [i-1]} \beta_r \left(w_r{}^\square \,\|\, \mathsf{t}_i^\circ \right) \right). \tag{6.9}$$

To prove it, we check this linear dependence coordinate by coordinate. It boils down to Equation (6.8) for initial tubes contained in t. It is also clear for the initial square tubes not contained in t as all dual compatibility degrees involved in (6.9) vanish. Moreover, the coefficients $\beta_1, \ldots, \beta_p$ are defined in order to compensate for the default of the initial tubes $\mathsf{t}_1^\circ, \ldots, \mathsf{t}_p^\circ$ in Equation (6.8). Finally, we proceed by induction for the remaining initial tubes of T°, that is the initial round tubes not contained in t and whose root is not one of the w_i's. Namely, since $q > 0$ and thanks to our special ordering on the w_i's, the coordinate corresponding to such a tube in all terms of Equality (6.9) is a linear combination of the coordinates corresponding to its predecessors in the spine of T° (*i.e.* the inclusion poset on round tubes of T°).

Finally, we still have to check the case where $q = 0$, meaning where t is contained in an initial round tube of T°. We denote by t° the inclusion minimal initial round tube of T° containing t and by z° its root in T°. We then have to distinguish whether or not $z^\circ = v$:

- If $z^\circ = v$, call $w_1, \ldots, w_r$ ($r \geq 1$) the neighbors of t that also belong to t°. We then claim that the following linear dependence holds:

$$\mathbf{d}^*(\mathsf{t}, \mathsf{T}^\circ) + r\, \mathbf{d}^*(v^\square, \mathsf{T}^\circ) = \sum_{i \in [r]} \mathbf{d}^*(w_i^\square, \mathsf{T}^\circ).$$

Indeed an initial tube s° of T° either contains t and thus all the vertices $v, w_1, \ldots, w_r$, or does not contain v so that the equality holds by counting the vertices $w_1, \ldots, w_r$ in s°.

- If $z^\circ \neq v$, then z° belongs to one of the tubes $\mathsf{a}_1, \ldots, \mathsf{a}_\ell$, say a_1. Let $w_1, \ldots, w_r$ be the neighbors of t contained in t° that are also neighbors of a_1, and $w_{r+1}, \ldots, w_s$ be the other neighbors of t contained in t°. Observe that $s \geq 1$ since $\mathsf{t} \subset \mathsf{t}^\circ$. One can then check that the linear dependence we look for is

$$(s - r + 1)\, \mathbf{d}^*(\mathsf{t}, \mathsf{T}^\circ) = s\left(\mathbf{d}^*(\mathsf{a}_1, \mathsf{T}^\circ) - \mathbf{d}^*(v^\square, \mathsf{T}^\circ) - \sum_{i=r+1}^{s} \mathbf{d}^*(w_i^\square, \mathsf{T}^\circ)\right) + (s - r + 1)\sum_{i=1}^{s} \mathbf{d}^*(w_i^\square, \mathsf{T}^\circ).$$

It clearly holds for tubes not contained in t° and for t° itself. Consider thus an initial round tube s° of T° contained in t°. Since $z^\circ \in \mathsf{a}_1$, s° cannot contain a_1. Thus the first term of the right hand side vanishes for s°, while $(\mathsf{t} \,\|\, \mathsf{s}^\circ) = \sum_{i \in [s]} (w_i^\square \,\|\, \mathsf{s}^\circ)$, concluding the proof. ∎

6.5.8 Design nested complex isomorphisms (Proposition 6.56 and Theorem 6.59)

We now prove our characterization of the design nested complex isomorphisms announced in Section 6.4.4. In both proofs, we will use the following description of links in design nested complexes, similar to that of [CD06] for links in nested complexes. We leave this proof to the reader.

Lemma 6.75. *The link of a tube t in the design nested complex $\mathcal{N}^\square(\mathrm{G})$ is isomorphic,*

- *for a square tube $\mathsf{t} = v^\square$, to the join $\mathcal{N}^\square(\mathrm{G}_1) * \cdots * \mathcal{N}^\square(\mathrm{G}_\ell)$ of the design nested complexes of the connected components $\mathrm{G}_1, \ldots, \mathrm{G}_\ell$ of $\mathrm{G}[\mathrm{V} \smallsetminus \{v\}]$.*

- *for a round tube t, to the join of the nested complex $\mathcal{N}(\mathrm{G}[\mathsf{t}])$ of the restriction of G to t with the design nested complex $\mathcal{N}^\square(\mathrm{G}^\star \mathsf{t})$ of the reconnected complement of t in G.*

Before proving Proposition 6.56 and Theorem 6.59, we need a technical result.

Lemma 6.76. *Let $\bar{\mathrm{G}}$ and G be connected graphs with vertex sets $\bar{\mathrm{V}}$ and V respectively. Let Φ be an isomorphism from the design nested complex $\mathcal{N}^\square(\bar{\mathrm{G}})$ of $\bar{\mathrm{G}}$ to the design (resp. standard) nested complex $\mathcal{N}^\square(\mathrm{G})$ (resp. $\mathcal{N}(\mathrm{G})$) of G. If there exists a vertex $v \in \mathrm{V}$ such that all tubes of G incompatible with $\Phi(\bar{\mathrm{V}})$ are round tubes containing v, then $\bar{\mathrm{G}}$ and G are paths.*

Proof. Since Φ is an isomorphism, it induces a bijection between the design tubes of $\bar{\mathrm{G}}$ incompatible with $\bar{\mathrm{V}}$ and the tubes of G incompatible with $\Phi(\bar{\mathrm{V}})$. The former are precisely the square tubes of $\bar{\mathrm{G}}$ (by definition of the compatibility of design tubes) while the later are some round tubes of G containing v (by assumption). Since all the square tubes of $\bar{\mathrm{G}}$ are compatible, it follows that their images by Φ are nested in G. Let $\bar{u}, \bar{v} \in \bar{\mathrm{V}}$ be the only vertices such that $|\Phi(\bar{u}^\square)| = 1$ and $|\Phi(\bar{v}^\square)| = |\mathrm{V}| - 1$. For any other vertex $\bar{w} \in \bar{\mathrm{V}}$, the link of the tube $\Phi(\bar{w}^\square)$ is the join of two nontrivial design or standard nested complexes by Lemma 6.75. Since Φ is an isomorphism, so is the link of the square tube $\bar{w}^\square$, so that $\bar{w}$ disconnects $\bar{\mathrm{G}}$ again by Lemma 6.75. We conclude that all but two vertices of $\bar{\mathrm{G}}$ disconnect $\bar{\mathrm{G}}$, which implies that $\bar{\mathrm{G}}$ is a path. In order to show that G is also a path, we now distinguish two situations:

(i) Suppose first that Φ is an isomorphism from the design nested complex $\mathcal{N}^\square(\bar{G})$ of $\bar{G}$ to the standard nested complex $\mathcal{N}(G)$ of G. Then the composition of Φ^{-1} with the isomorphism Π of Example 6.54 (ii) is an isomorphism between the standard nested complex $\mathcal{N}(G)$ of G and the standard nested complex of a path, which implies by Theorem 6.37 that G itself is a path.

(ii) Suppose now that Φ is an isomorphism from the design nested complex $\mathcal{N}^\square(\bar{G})$ of $\bar{G}$ to the design nested complex $\mathcal{N}^\square(G)$ of G. Using Lemma 6.75 and a similar argument as in the proof of Lemma 6.69, the image $\Phi(\bar{V})$ of $\bar{V}$ is either a square tube $v^\square$ of G, or a singleton round tube $\{v\}$ of G, or the round tube V of G. The last two cases are discarded by our assumption since the square tube $v^\square$ is incompatible with $\{v\}$ and with V. Therefore, we obtain that $\Phi(\bar{V}) = v^\square$ and the tubes of G incompatible with $\Phi(\bar{V}) = v^\square$ are exactly the round tubes containing v. So the square tubes of $\bar{G}$ are in bijection with the tubes of G containing v. Since $|\bar{V}| = |V|$ (dimensions of isomorphic simplicial complexes), an immediate induction shows that G is a path.   ■

We are now ready to prove our classification of design nested complex isomorphisms.

Proof of Proposition 6.56. We show the result by induction on $|\bar{V}|$, the cases $|\bar{V}| \leq 2$ being trivial. Assume that $|\bar{V}| \geq 3$ and consider an isomorphism $\Phi : \mathcal{N}^\square(\bar{G}) \to \mathcal{N}(G)$.
    We first consider the image $\Phi(\bar{V})$ of the round tube $\bar{V}$ of $\bar{G}$. It is either a singleton, or the complement of a singleton. Otherwise, its link would be the join of two nontrivial complexes by Lemma 6.75, which yields a contradiction using a similar argument as in the proof of Lemma 6.69. We claim that we can assume that $\Phi(\bar{V})$ is a singleton adjacent to at least two vertices in G. Indeed,

- if $\Phi(\bar{V}) = V \smallsetminus \{v\}$, then all tubes incompatible with $\Phi(\bar{V}) = V \smallsetminus \{v\}$ contain v,

- if $\Phi(\bar{V}) = \{v\}$ where v has a unique neighbor w in G, then all tubes incompatible with $\Phi(\bar{V}) = \{v\}$ contain w,

In both cases, Lemma 6.76 ensures that $\bar{G}$ and G are paths, and we can compose Φ with a rotation $\circlearrowright^p$ to ensure that $\Phi(\bar{V})$ is a singleton adjacent to at least two vertices in G.
    We now consider a vertex $\bar{w} \in \bar{V}$ which does not disconnect $\bar{G}$ (such a vertex always exists). By Lemma 6.75, the link of the square tube $\bar{w}^\square$ is not the join of two nontrivial nested complexes. Since Φ is an isomorphism, so is the link of $\Phi(\bar{w}^\square)$, so that $\Phi(\bar{w}^\square)$ is either a singleton or the complement of a singleton again by Lemma 6.75. Moreover, since $\bar{w}^\square$ is incompatible with $\bar{V}$ and Φ is an isomorphism, $\Phi(\bar{w}^\square)$ is incompatible with $\Phi(\bar{V}) = \{v\}$. Therefore, $\Phi(\bar{w}^\square)$ is either a singleton $\{w\}$ adjacent to $\{v\}$, or the complement $V \smallsetminus \{v\}$ of the singleton $\{v\}$. Now, since $\bar{V}$ contains at least two vertices $\bar{w}, \bar{w}'$ which do not disconnect G and since $\Phi(\bar{w}^\square) \neq \Phi(\bar{w}'^\square)$, we can assume that $\Phi(\bar{w}^\square)$ is a singleton $\{w\}$ adjacent to $\{v\}$. It implies that Φ induces an isomorphism from the design nested complex $\mathcal{N}^\square(\bar{G}[\bar{V} \smallsetminus \{\bar{w}\}])$ to the nested complex $\mathcal{N}(G^\star\{w\})$ of the reconnected complement of the tube $\{w\}$ in G. The induction hypothesis implies that

- the graph $\bar{G}[\bar{V} \smallsetminus \{\bar{w}\}]$ is isomorphic to the spider $\mathfrak{X}_{\underline{n}}$ and the graph $G^\star\{w\}$ is isomorphic to the octopus $\mathcal{X}_{\underline{n}}$ (with head denoted v), for some $\underline{n} = \{n_1, \ldots, n_\ell\} \in \mathbb{N}^\ell$.
- the image $\Phi(\bar{V} \smallsetminus \{\bar{w}\})$ of $\bar{V} \smallsetminus \{\bar{w}\}$ is the pair $\{v, w\}$ containing the central vertex of $G^\star\{w\}$,
- the description of the images of the tubes of $\bar{G}$ not containing $\bar{w}$ is given by $\bar{\Omega}$, in particular $\Phi(\bar{w}'^\square)$ is a singleton adjacent to v in $G^\star\{w\}$. As $\Phi(\bar{w}'^\square)$ cannot be an edge in G, it has to be a singleton $\{w'\}$ in G, nonadjacent to w for compatibility.

Since $G^\star\{w\}$ is an octopus with head v, it follows by definition of the reconnected complement that G is either an octopus with head v or an octopus with head v with an additional edge of the form $\{v, v_i^1\}$ for a certain $i \in [\ell]$. We can now apply the same reasoning to $\bar{w}'$ and since $\Phi(\bar{w}^\square)$ and $\Phi(\bar{w}'^\square)$ are nonadjacent singletons in G, we conclude that G is an octopus. Since $\Phi(\bar{V}) = \{v\}$, the graph $\bar{G}$ is a spider and the reader can check that the restriction of Φ to the link of $\bar{V}$ in the design nested complex $\mathcal{N}^\square(\bar{G})$ is the nontrivial isomorphism $\Omega : \mathcal{N}(\bar{G}) \to \mathcal{N}(G^\star\{v\})$ defined in Section 6.4.2. It follows that Φ coincides with $\bar{\Omega}$. ∎

Proof of Theorem 6.59. If G is the path P_n, then its design nested complex $\mathcal{N}^\square(G)$ is isomorphic to the nested complex $\mathcal{N}(P_{n+1})$ by Example 6.54 (ii). Therefore, the design nested complex $\mathcal{N}^\square(G')$ is also isomorphic to the nested complex $\mathcal{N}(P_{n+1})$, which implies that G' is the path P_n by Proposition 6.56. We can therefore assume that G and G' are not paths.

Let V and V' denote the vertex sets of G and G'. By Lemma 6.75, the link of V in $\mathcal{N}^\square(G)$ is the nested complex $\mathcal{N}(G)$. With a similar argument as in the proof of Lemma 6.69, it follows that its image $\Phi(V)$ is either a square tube of G', or a singleton round tube of G', or the round tube V' of G'. We treat these situations separately.

if $\Phi(V) = v'^\square$ All tubes of G' incompatible with $\Phi(V) = v'^\square$ are round tubes containing v'. Thus by Lemma 6.76, the graphs G and G' are paths, which we already excluded.

if $\Phi(V) = V'$ By Lemma 6.75, Φ induces a nontrivial nested complex isomorphism Ψ from $\mathcal{N}(G)$ to $\mathcal{N}(G')$. It follows from Theorem 6.37 that G and G' are isomorphic spiders and Ψ coincides with the nontrivial nested complex isomorphism Ω described in Section 6.4.2. It thus suffices to show that the nested complex isomorphism Ω cannot be extended to design nested complexes. For this observe first that such an extension would send square tubes to square tubes. Now consider a singleton $\{v\}$ of G swapped by Ω. This singleton $\{v\}$ is incompatible with the square tube $v^\square$ and compatible with all other square tubes of G. Yet its image is incompatible with more than one square tube, a contradiction.

if $\Phi(V) = \{v'\}$ The link of $\{v'\}$ in the design nested complex $\mathcal{N}^\square(G')$ is a design nested complex isomorphic to the nested complex $\mathcal{N}(G)$. By Proposition 6.56, we obtain that G is an octopus and $\Phi^{-1}(V')$ is the singleton containing its central vertex. Since $\Phi^{-1}(V') \neq V$, the same argument applies to Φ^{-1} and shows that G' is also an octopus with the same legs as G. Moreover Proposition 6.56 describes the images of round tubes of G by Φ and of round tubes of G' by Φ^{-1}, which together forces Φ to coincide with the map $\Omega^\square$. ∎

PART III

SUBWORD COMPLEXES AND ACCORDION COMPLEXES

7

Context and motivations

7.1 Introduction

The main concern of this second part is the study of *subword complexes* introduced by A. Knutson and E. Miller [KM04, KM05]. Similarly to nested complexes and graph associahedra, they are related to cluster algebras, as generalized associahedra are very natural instances of subword complexes. The main issue though is that no geometric realization is known in general for them, in spite of several attempts (see Section 10.1.1). Moreover the (type A) associahedron and, as a byproduct, the cyclohedron (type B associahedron) are the only serious combinatorial connections between (type A) subword complexes and nested complexes so far. Therefore this part is oriented toward two natural ideas. First study potential geometric properties of subword complexes; second look for common properties shared by subword complexes and nested complexes.

As mentioned, the first problem is hard in general and has resisted to investigations for about a decade. A tentative and say "semi-fruitful" approach is proposed in Chapter 10. A problem a bit easier, and going simultaneously in both directions, is to find a d-vector-like construction for flag subword complexes (we discuss it in Section 7.4). Yet the combinatorial models for subword complexes are too poor so far to describe linear dependences along the flips. It is from this lack that our interest came to *accordion complexes*, when F. Chapoton made us notice that some subword complexes appear as instances of them. Their combinatorics is described by dissections and is thus much more tractable than subword complexes'. Chapters 8 and 9 answer specific questions about accordion complexes, among which we propose a d-vector construction.

In the rest of this chapter, we present subword complexes in Section 7.2 and discuss the class of *root-independent* subword complexes in Section 7.3.

In Chapter 8, we define accordion complexes and settle two enumerative conjectures of F. Chapoton. In particular the *serpent nest conjecture* is to appear in [Man17b].

In Chapter 9 we give geometric realizations of accordion complexes both as fans and polytopes, using g-vector and d-vector-like constructions inspired from cluster algebras. The results of this chapter are gathered in an article to appear [MP17b].

Finally we present in Chapter 10 the family of *multiassociahedra* and give a construction for some 2-associahedra, based on combinatorial transformations on subword complexes. We delay this chapter to the end as it is more experimental than the rest of the thesis. The result presented there can be found in [Man17a].

7.2   Subword complexes

Subword complexes were introduced by A. Knutson and E. Miller in [KM04, KM05]. We refer the reader to the same papers for the original motivations. The definition in [KM04] describes a family of simplicial complexes for each (not necessarily finite) Coxeter group. For our concerns, we only need the definition of *type A spherical subword complexes*, that we however abbreviate to *subword complexes* from now on.

We denote the symmetric group of permutations of $[n+1]$ by $\mathfrak{S}_{n+1}$, and by S the set of simple transpositions $s_i := (i \;\; i+1)$ (for $i \leq n$), that we consider as an alphabet. To avoid confusion, a simple transposition will be referred to with an italic letter s_i when considered as an element of $\mathfrak{S}_{n+1}$, and with a sans serif letter s_i when considered as a letter in S. Since simple transpositions generate $\mathfrak{S}_{n+1}$, any permutation $\pi \in \mathfrak{S}_{n+1}$ can be written as a product $\pi = s_{i_1} \cdots s_{i_\ell}$. The word $\mathsf{s}_{i_1} \ldots \mathsf{s}_{i_\ell}$ is then called an *expression* of the permutation π. It is a *reduced expression* of π if ℓ is smallest possible among all expressions, in which case ℓ is called the *length* of π. We denote by $w_\circ := [n+1, n, \ldots, 1]$ the unique longest element in $\mathfrak{S}_{n+1}$, also referred to as the *maximal permutation*.

Given a word $\mathsf{Q} = \mathsf{q}_1 \ldots \mathsf{q}_p$ in S^*, a *subword* of Q is a subsequence $\mathsf{q}_{i_1} \ldots \mathsf{q}_{i_r}$ (with $1 \leq i_1 < \cdots < i_r \leq p$) of its letters. A *factor* of Q is a subword of Q consisting in consecutive letters and a *prefix* (resp. *suffix*) of Q is a factor containing its first (resp. last) letter. For any set $J \subseteq [p]$, we denote by Q_J the subword of Q consisting in the letters with index in J. Let Q be a word containing a reduced expression of $w_\circ$ as a subword. Following [KM04], we define the *subword complex* of Q as the simplicial complex

$$\mathcal{S}(\mathsf{Q}) := \{ J \subseteq [p] \mid \mathsf{Q}_{[p] \smallsetminus J} \text{ contains a reduced expression of } w_\circ \text{ as a subword} \}.$$

We always consider a letter q_r in a word Q as both data of its *position* r in Q and of the actual letter s_i in the alphabet S such that $\mathsf{q}_r = \mathsf{s}_i$. We identify the *vertices* of the subword complex $\mathcal{S}(\mathsf{Q})$ to the letters of Q whose position is contained in a facet of the complex and denote their set by $\mathcal{V}_\mathsf{Q}$. Observe that the vertices of $\mathcal{S}(\mathsf{Q})$ are the letters of Q which are not contained in all reduced expressions of $w_\circ$ contained in Q. The other letters of the word Q are the *nonvertices* of $\mathcal{S}(\mathsf{Q})$. A convenient way to think about a subword complex $\mathcal{S}(\mathsf{Q})$ consists in encoding the underlying word $\mathsf{Q} = \mathsf{q}_1 \ldots \mathsf{q}_p$ with a set of segments $\mathcal{N}_\mathsf{Q} := \{ \mathbf{I}_r \mid r \in [p] \}$ called its corresponding *sorting network* (we follow the presentation of [PP12, PS12]). Each letter $\mathsf{q}_r = \mathsf{s}_i$ ($r \in [p], i \in [n]$) is represented by a vertical segment $\mathbf{I}_r$ whose extremities are the points (r, i) and $(r, i+1)$ in the plane. As we are interested in combinatorics, we consider the sorting network up to horizontal moves of its segments such that no two of them ever touch each other (see Figure 7.1 left). With this "relaxed" definition, the order on the abscissa of the segments is not well-defined any more, so that the sorting network $\mathcal{N}_\mathsf{Q}$ does not determine the word Q.
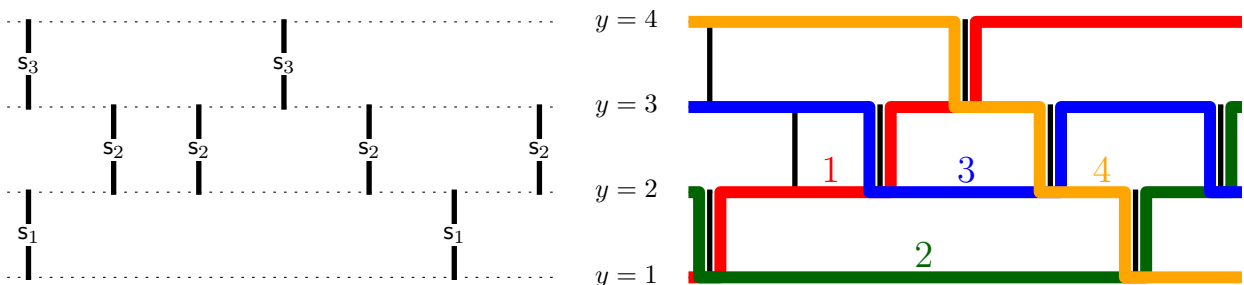
Figure 7.1 – The sorting network $\mathcal{N}_\mathsf{Q}$ (or $n = 3$) of the word $\mathsf{Q} = \mathsf{s}_1\mathsf{s}_3\mathsf{s}_2\mathsf{s}_2\mathsf{s}_3\mathsf{s}_2\mathsf{s}_1\mathsf{s}_2 = \mathsf{q}_1\mathsf{q}_2\mathsf{q}_3\mathsf{q}_4\mathsf{q}_5\mathsf{q}_6\mathsf{q}_7\mathsf{q}_8$ (left) and the pseudo-line arrangement $\mathcal{A}$ corresponding to the facet $\{\mathsf{q}_2, \mathsf{q}_3\}$ of the subword complex $\mathcal{S}(\mathsf{Q})$ (right). The subword complex $\mathcal{S}(\mathsf{Q})$ is root-independent since the contact graph of $\mathcal{A}$ is a path with edges $\{1, 3\}$ and $\{3, 4\}$.

Asso(1) :   Asso(2) :   Asso(3) :
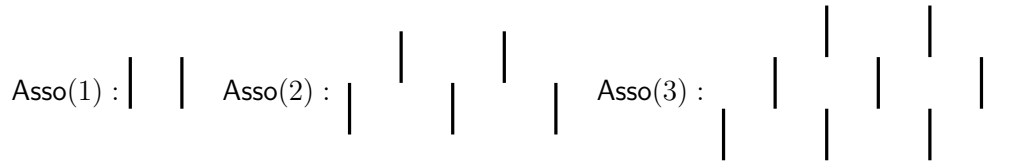
Figure 7.2 – Sorting networks of subword complexes isomorphic to the simplicial asso-ciahedron of dimension 1 (left), of dimension 2 (middle) and of dimension 3 (right).

However it still fully describes the combinatorics of the subword complex $\mathcal{S}(\mathsf{Q})$. Indeed since s_i and s_j commute when $|i - j| \geq 2$, if Q' is obtained from Q by replacing a factor $\mathsf{s}_i\mathsf{s}_j$ by $\mathsf{s}_j\mathsf{s}_i$, then the subword complexes $\mathcal{S}(\mathsf{Q})$ and $\mathcal{S}(\mathsf{Q}')$ are clearly isomorphic.

Sorting networks give us a way to visualize the facets in subword complexes: a *pseudo-line* on $\mathcal{N}_\mathsf{Q}$ is an abscissa-increasing curve included in the union of the segments in $\mathcal{N}_\mathsf{Q}$ together with the lines of equations $y = i$ ($i \in [n + 1]$). A *pseudo-line arrangement* on $\mathcal{N}_\mathsf{Q}$ is a set $\mathcal{A}$ of $n + 1$ pseudo-lines on $\mathcal{N}_\mathsf{Q}$ labeled form 1 to $n + 1$ such that

- the pseudo-line labeled i stays on the line of equation $y = i$ when abscissa go to $-\infty$ and on the line of equation $y = n + 2 - i$ when abscissa go to $+\infty$, and
- the intersection of any two pseudo-lines in $\mathcal{A}$ is exactly one of the segments in $\mathcal{N}_\mathsf{Q}$.

Given a pseudo-line arrangement $\mathcal{A}$, the *contacts* of $\mathcal{A}$ are the letters of Q represented by the segments in $\mathcal{N}_\mathsf{Q}$ whose interior intersects no pseudo-line of $\mathcal{A}$. The facets of the subword complex $\mathcal{S}(\mathsf{Q})$ are then identified with the sets of contacts of all pseudo-line arrangements on $\mathcal{N}_\mathsf{Q}$ (see Figure 7.1 right, and [PP12, PS12] for details).

As mentioned in Section 7.1, the simplicial associahedron is an instance of subword complex. Figure 7.2 illustrates the sorting networks of subword complexes isomorphic to the first associahedra. A more complete and general description of the correspon-dence is given in Theorem 10.5 and illustrated in Figure 10.5.

Spherical subword complexes [KM04] are conjectured to have polytopal realizations. A way to attack this problem consists in restricting the study to well-chosen families. This idea relies on the fact that subword complexes are closed under links: on the corresponding networks, taking the link of a face just consists in forgetting the corre-sponding segments. This yields that some subfamilies of subword complexes are "uni-versal", in the sense that finding realizations as fans or polytopes for them is enough to obtain realizations for any subword complex. This was already observed in [PS12, Corollary 5.8] and [CLS14, Corollary 2.16] for the family of *multiassociahedra* discussed in Chapter 10, which admit other combinatorial models than sorting networks.

7.3 Root-independent subword complexes

If no geometric realization is known in general for subword complexes, there is a class of them realized by *brick polytopes*, introduced by V. Pilaud and F. Santos in [PS12] for type A spherical subword complexes, and later extended by V. Pilaud and C. Stump to arbitrary spherical subword complexes [PS15a]. The subword complexes in this class are called *root-independent* in [PS15a].They are interesting in our context because they seem to fully describe all flag subword complexes, and therefore are the only ones for which a $\mathbf{d}$-vector approach makes sense (see Section 3.2.3).

Let $\mathsf{Q} = \mathsf{q}_1 \ldots \mathsf{q}_p$ be a word in S^*, let $\{\mathsf{q}_{r_1}, \ldots, \mathsf{q}_{r_\ell}\}$ be a facet of the subword com-plex $\mathcal{S}(\mathsf{Q})$ represented by a pseudo-line arrangement $\mathcal{A}$ on $\mathcal{N}_\mathsf{Q}$. Following [PS12], we de-fine the *contact graph* of $\mathcal{A}$ as the multigraph whose vertices are the pseudo-lines in $\mathcal{A}$, and with one edge for each contact q_{r_i} of $\mathcal{A}$, relating the two pseudo-lines of $\mathcal{A}$ that con-tain the endpoints of the segment $\mathbf{I}_{r_i}$. The subword complex $\mathcal{S}(\mathsf{Q})$ is *root-independent* if the contact graph of one (equivalently any) pseudo-line arrangement on $\mathcal{N}_\mathsf{Q}$ is a forest.

Theorem 7.1 ([PS12, Theorem 3.26],[PS15a, Theorems 1.1 and 4.8]). *Root-independent subword complexes can be realized as boundary complexes of convex polytopes.*

7.4   Towards a d-vector construction

As we mentioned, root-independent subword complexes seem to essentially describe those subword complexes that are flag. Following the same lines as in the proof of Lemma 10.10, where we show that two vertices of a subword complex are either *compatible* (they belong to a common face), or *exchangeable* (they are exchanged along a ridge of the complex), or both, one could expect to prove the following conjecture.

Conjecture 7.2. *Flag subword complexes are exactly those subword complexes that decompose into joins of root-independent subword complexes.*

Since d-vectors are well-behaved with respect to joins, finding a best possible d-vector construction for subword complexes boils down, up to Conjecture 7.2, to find suitable d-vectors in root-independent subword complexes.

In [CP15, Definition 2.15], C. Ceballos and V. Pilaud rephrased the compatibility degree of cluster complexes to the subword complexes context. Their definition naturally extends to arbitrary subword complexes and thus provides natural candidate d-vectors for any root-independent subword complex. However the definition is so far hard to deal with and only allows to derive few properties of Proposition G. Namely let $Q = q_1 \ldots q_p$ be a word such that $\mathcal{S}(Q)$ is root-independent. The *compatibility degree* $(. \| .)$ on the vertices of $\mathcal{S}(Q)$, defined as in [CP15, Definition 2.15], has the following properties.

1. For any vertex $q_r \in \mathcal{V}_Q$, we have $(q_r \| q_r) = -1$.

2. If two vertices $q_r, q_t \in \mathcal{V}_Q$ are compatible, then $(q_r \| q_t) = (q_t \| q_r) = 0$.

3. If two vertices $q_r, q_t \in \mathcal{V}_Q$ are exchangeable, then $(q_r \| q_t) = (q_t \| q_r) = 1$.

For general (not only in type A) spherical subword complexes, it is not even known whether $(q_r \| q_t)$ is nonnegative if $r \neq t$. Moreover the reverse implications of (2) and (3) are not known either. Nevertheless we can prove all these properties in our context (namely in type A), using similar argument as in the proof of Lemma 10.10. Finally computational experiments indicate that the d-vectors defined from this compatibility degree support fans realizing root-independent subword complexes, at least in type A, attesting that the definition is promising.

8

Combinatorial properties of accordion complexes

8.1 Introduction

In this chapter and in Chapter 9, we concentrate on specific properties of accordion complexes defined by A. Garver and T. McConville [GM16]. We underline the connections with flag subword complexes in Section 8.4.

8.1.1 Motivations

Y. Baryshnikov introduced in [Bar01] the simplicial complex of crossing-free subsets of the set of diagonals of a polygon that are in some sense compatible with a reference quadrangulation $Q_\circ$. Although the precise definition of compatibility is a bit technical in [Bar01], it turns out that a diagonal is compatible with $Q_\circ$ if and only if it crosses a connected subset of diagonals of $Q_\circ$ that we call *accordion* of $Q_\circ$. We thus call Y. Baryshnikov's simplicial complex the *accordion complex* $\mathcal{AC}(Q_\circ)$. For instance, this complex coincides with the classical associahedron when all the diagonals of the reference quadrangulation $Q_\circ$ have a common endpoint. A polytopal realization of $\mathcal{AC}(Q_\circ)$ was announced in [Bar01], but the proof was never published as far as we know. Revisiting some combinatorial and algebraic properties of $\mathcal{AC}(Q_\circ)$, F. Chapoton [Cha16] raised three explicit challenges: first prove that the dual graph of $\mathcal{AC}(Q_\circ)$, endowed with a certain orientation, has a lattice structure extending the Tamari and Cambrian lattices [MHPS12, Rea06]; second construct geometric realizations of $\mathcal{AC}(Q_\circ)$ as fans and polytopes generalizing the known constructions of the associahedron; third show enumerative properties of the faces of $\mathcal{AC}(Q_\circ)$, in particular a bijection between the facets of $\mathcal{AC}(Q_\circ)$ and other combinatorial objects called *serpent nests*.

In [GM16], A. Garver and T. McConville defined and studied the accordion complex $\mathcal{AC}(D_\circ)$ of any reference dissection $D_\circ$ (our presentation slightly differs from theirs as they use a compatibility condition on the dual tree of the dissection $D_\circ$, but the simplicial complex is the same). In this context, they settled F. Chapoton's lattice question, using lattice quotients of a lattice of biclosed sets. In Chapter 9, geometric realizations (as fans and convex polytopes) of $\mathcal{AC}(D_\circ)$ are given for any reference dissection $D_\circ$, providing in particular an answer to F. Chapoton's geometric question. This chapter settles some of F. Chapoton's enumerative questions [Cha16]. In particular we prove the serpent nest conjecture, in the general context of accordion complexes.

135

8.1.2   Overview

The chapter is organized as follows. Section 8.2 introduces the accordion complex and accordion lattice of a dissection $D_\circ$. We essentially follow the definitions and arguments of A. Garver and T. McConville [GM16], except that we prefer to work on the dissection $D_\circ$ rather than on its dual graph. We present in Section 8.3 bijective proofs of enumerative conjectures stated in [Cha16]. This includes a bijection between *serpent nests* and maximal $D_\circ$-accordion dissections of a reference dissection $D_\circ$. Finally we make some quick link between accordion complexes and root-independent subword complexes in Section 8.4.

8.2   The accordion complex and the accordion lattice

In this section, we define the accordion complex $\mathcal{AC}(D_\circ)$ of a dissection $D_\circ$, show that it is a pseudo-manifold, and define an orientation of its dual graph. Our definitions and proofs are essentially translations of the arguments of A. Garver and T. McConville [GM16] given in terms of the dual tree of the dissection $D_\circ$. However our presentation in terms of dissections is more convenient for our latter purposes.

8.2.1   The accordion complex

Let $\mathcal{P}$ be a convex polygon. Here by a *diagonal* of $\mathcal{P}$, we mean either an internal diagonal or an external diagonal (a boundary edge) of $\mathcal{P}$, but a *dissection* D of $\mathcal{P}$ is still a set of noncrossing *internal* diagonals of $\mathcal{P}$. The *cells* of D are the closures of the connected components of $\mathcal{P}$ minus the diagonals of D. We denote by $\bar{D}$ the dissection D together with all boundary edges of $\mathcal{P}$. An *accordion* of D is a subset of $\bar{D}$ which contains either no or two consecutive diagonals in each cell of D. A *subaccordion* of D is a subset of D formed by the diagonals between two given internal diagonals in an accordion of D. A *zigzag* of D is a subset $\{\delta_0, \dots, \delta_{p+1}\}$ of D where δ_i shares distinct endpoints with and separates δ_{i-1} and δ_{i+1} for any $i \in [p]$. The *zigzag* of an accordion A is the subset of the diagonals of A which disconnect A. Note that we include boundary edges of $\mathcal{P}$ in the accordions of D, but not in the subaccordions nor in the zigzags of D. See Figure 8.1.

We consider $2n$ points on the unit circle labeled clockwise by $1_\circ$, $2_\bullet$, $3_\circ$, $4_\bullet$, ..., $(2n-1)_\circ$, $(2n)_\bullet$. We say that $1_\circ, \dots, (2n-1)_\circ$ are the *hollow vertices* while $2_\bullet, \dots, (2n)_\bullet$ are the *solid vertices*. The *hollow polygon* is the convex hull $\mathcal{P}_\circ$ of $1_\circ, \dots, (2n-1)_\circ$ while the *solid polygon* is the convex hull $\mathcal{P}_\bullet$ of $2_\bullet, \dots, (2n)_\bullet$. We simultaneously consider *hollow diagonals* $\delta_\circ$ (with two hollow vertices) and *solid diagonals* $\delta_\bullet$ (with two solid vertices), but we never consider diagonals with one hollow vertex and one solid vertex. Similarly, we consider *hollow dissections* $D_\circ$ (with only hollow diagonals) and *solid dissections* $D_\bullet$ (with only solid diagonals), but never mix hollow and solid diagonals in a dissection. To help distinguishing them, hollow vertices and diagonals appear red while solid vertices and diagonals appear blue in all pictures.
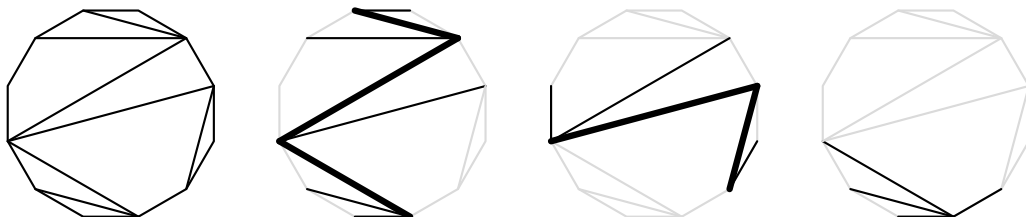
Figure 8.1 – A dissection (left) and three accordions with bold zigzags (middle and right).
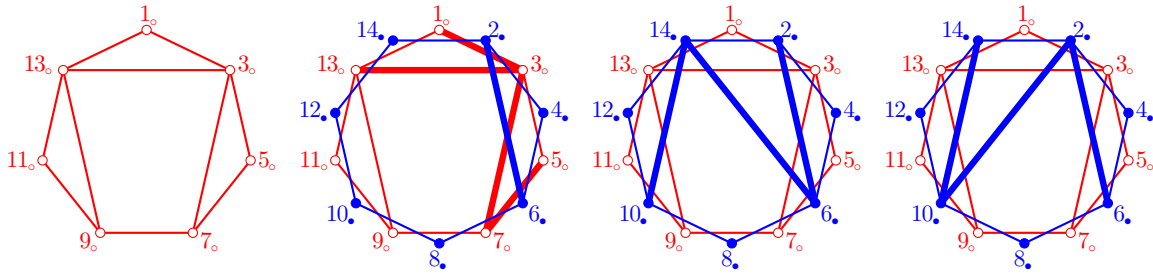
Figure 8.2 – A hollow dissection $D_\circ^{ex}$, a solid $D_\circ^{ex}$-accordion diagonal whose corresponding hollow accordion is bold, and two maximal solid $D_\circ^{ex}$-accordion dissections.

We fix an arbitrary reference hollow dissection $D_\circ$. A solid diagonal $\delta_\bullet$ is a $D_\circ$-*accordion diagonal* if the hollow diagonals of $\bar{D}_\circ$ crossed by $\delta_\bullet$ form an accordion of $D_\circ$. In other words, $\delta_\bullet$ cannot enter and exit a cell of $D_\circ$ using two nonincident diagonals. For example, note that for any hollow diagonal $(i_\circ, j_\circ) \in \bar{D}_\circ$, the solid diagonals $((i-1)_\bullet, (j-1)_\bullet)$ and $((i+1)_\bullet, (j+1)_\bullet)$ are $D_\circ$-accordion diagonals (labels are considered modulo $2n$). In particular, all boundary edges of the solid polygon are $D_\circ$-accordion diagonals. A $D_\circ$-*accordion dissection* is a set of pairwise noncrossing internal $D_\circ$-accordion diagonals. We call *accordion complex* of $D_\circ$ the simplicial complex $\mathcal{AC}(D_\circ)$ of $D_\circ$-accordion dissections.

Example 8.1. Consider the reference dissection $D_\circ^{ex}$ of Figure 8.2 (left). Examples of maximal $D_\circ^{ex}$-accordion dissections are given in Figure 8.2 (right). The accordion complex of $D_\circ^{ex}$ is illustrated in Figure 8.3 (left).

Remark 8.2. Special reference hollow dissections $D_\circ$ give rise to special accordion complexes $\mathcal{AC}(D_\circ)$:
 (i) If $D_\circ$ is the empty dissection with the whole hollow polygon as unique cell, then the $D_\circ$-accordion complex $\mathcal{AC}(D_\circ)$ is reduced to the empty $D_\circ$-accordion dissection.
 (ii) If $D_\circ$ has a unique diagonal, then the accordion complex $\mathcal{AC}(D_\circ)$ is a segment.
 (iii) For any hollow triangulation $T_\circ$, all solid diagonals are $T_\circ$-accordions, so that the $T_\circ$-accordion complex $\mathcal{AC}(T_\circ)$ is the simplicial associahedron.
 (iv) For any hollow quadrangulation $Q_\circ$, a solid diagonal is a $Q_\circ$-accordion if and only if it never crosses two opposite edges of a quadrangle of $Q_\circ$, so that the accordion complex $\mathcal{AC}(Q_\circ)$ is the Stokes complex defined by Y. Baryshnikov [Bar01] and studied by F. Chapoton [Cha16].
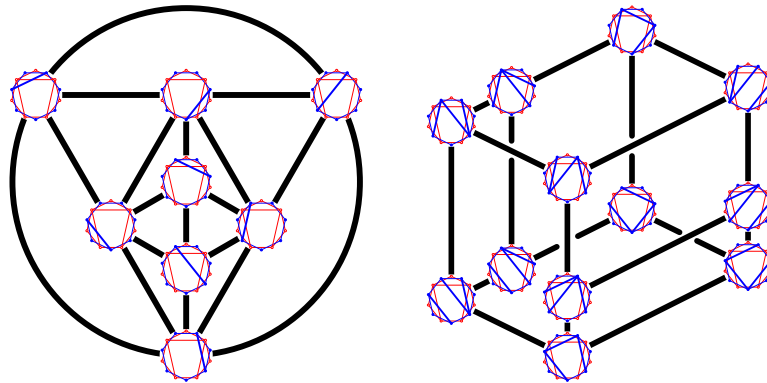
Figure 8.3 – The accordion complex of $D_\circ^{ex}$ (left) and the $D_\circ^{ex}$-accordion lattice (right), oriented from bottom to top, for the reference hollow dissection $D_\circ^{ex}$ of Figure 8.2 (left).

Remark 8.3. Following the original definition of the noncrossing complex of A. Garver and T. McConville [GM16], the accordion complex could equivalently be defined in terms of the dual tree $D_\circ^\star$ of $D_\circ$ (with one node in each cell of D and one edge connecting two adjacent cells). For example, a diagonal $(u_\bullet, v_\bullet)$ is a $D_\circ$-accordion diagonal if and only if any two consecutive edges of the (unique) path between $u_\bullet$ and $v_\bullet$ in $D_\circ^\star$ belong to the boundary of a face of the complement of $D_\circ^\star$ in the unit disk. The **g**-, **c**- and **d**-vectors defined in Section 9.2.1 could as well be defined in terms of $D_\circ^\star$.

8.2.2   Links in accordion complexes

Let us quickly deal with links in accordion complexes. As we will see in Section 8.3.1, the following descriptions are the main tools to prove the serpent nest conjecture.

Remark 8.4. Assume that $D_\circ$ has a cell $C_\circ$ containing p boundary edges of the hollow polygon $\mathcal{P}_\circ$. Let $C_\circ^1, \ldots, C_\circ^p$ denote the p (possibly empty) connected components of the hollow polygon minus $C_\circ$. For $i \in [p]$, let $D_\circ^i$ denote the dissection formed by the cell $C_\circ$ together with the cells of $D_\circ$ in $C_\circ^i$. Since no $D_\circ$-accordion can contain internal diagonals crossing diagonals of distinct dissections $D_\circ^i$ and $D_\circ^j$ (with $i \neq j$), the accordion complex of $D_\circ$ decomposes as the join: $\mathcal{AC}(D_\circ) = \mathcal{AC}(D_\circ^1) * \cdots * \mathcal{AC}(D_\circ^p)$. In particular, we have the following reductions:
  (i) If a nontriangular cell of $D_\circ$ has two consecutive boundary edges $\gamma_\circ, \delta_\circ$ of the hollow polygon, then contracting $\gamma_\circ$ and $\delta_\circ$ to a single boundary edge preserves the accordion complex of $D_\circ$.
  (ii) If a cell of $D_\circ$ has two nonconsecutive boundary edges of the hollow polygon, then the accordion complex of $D_\circ$ is a join of smaller accordion complexes.
In all the examples of this chapter, we therefore only consider dissections where any cell of $D_\circ$ has at most two boundary edges and that two boundary edges in a common cell of $D_\circ$ are consecutive. All our constructions work in general, but are just obtained as joins of the nondegenerate situation.

Remark 8.5. The links in an accordion complex are joins of accordion complexes. Namely, consider a $D_\circ$-accordion dissection $D_\bullet$ with cells $C_\bullet^1, \ldots, C_\bullet^p$. Let $D_\circ^i$ denote the hollow dissection obtained from $D_\circ$ by contracting all hollow (internal and external) diagonals which do not cross an edge of $C_\bullet^i$. Then the link of $D_\bullet$ in $\mathcal{AC}(D_\circ)$ is clearly isomorphic to the join $\mathcal{AC}(D_\circ^1) * \cdots * \mathcal{AC}(D_\circ^p)$.

Following F. Chapoton [Cha16], we define a *bridge* in $D_\circ$ as a cell of $D_\circ$ containing two nonconsecutive external diagonals of $D_\circ$. Remark 8.4 states that if $D_\circ$ contains a bridge, the accordion complex $\mathcal{AC}(D_\circ)$ is the join of smaller complexes.

Proposition 8.6. *The accordion complex $\mathcal{AC}(D_\circ)$ decomposes into a join of other simplicial complexes if and only if it contains a bridge.*

Observe that by Remarks 8.4 and 8.5, accordion complexes form a class of complexes closed by links, so that if $\mathcal{AC}(D_\circ)$ decomposes into a join of other simplicial complexes, then all these complexes are themselves accordion complexes.

Proof. A quick induction on the number of cells of $D_\circ$ shows that if it contains no bridge, then for any two $D_\circ$-accordion diagonals $\delta_\bullet$ and $\delta_\bullet'$, there is a sequence of $D_\circ$-accordion (internal) diagonals $\delta_\bullet = \delta_\bullet^1, \ldots, \delta_\bullet^\ell = \delta_\bullet'$ such that $\delta_\bullet^i$ and $\delta_\bullet^{i+1}$ cross for $i \in [\ell - 1]$. In particular if $\mathcal{AC}(D_\circ)$ decomposes into a join of other nonempty simplicial complexes, the diagonals $\delta_\bullet^i$ and $\delta_\bullet^{i+1}$ have to belong to the same one, as they are vertices of $\mathcal{AC}(D_\circ)$ not forming an edge of the complex. By transitivity $\delta_\bullet$ and $\delta_\bullet'$ also belong to the same complex. As it is true for any pair of $D_\circ$-accordion diagonals, all diagonals are the vertices of a same term in the decomposition of $\mathcal{AC}(D_\circ)$ as a join, a contradiction.   ∎

8.2.3 Pseudo-manifold

We now prove that the accordion complex $\mathcal{AC}(D_\circ)$ is a pseudo-manifold. We follow here the arguments of A. Garver and T. McConville [GM16] (except that they work on the dual tree of the dissection $D_\circ$). A much more concise but less instructive proof of the pseudo-manifold property will be derived from geometric considerations in Remark 9.43.

Recall that we denote by $\bar{D}_\circ$ the set formed by $D_\circ$ together with all boundary edges of the hollow polygon. An *angle $u_\circ v_\circ w_\circ$* of $\bar{D}_\circ$ is a pair $\{(u_\circ, v_\circ), (v_\circ, w_\circ)\}$ of two consecutive diagonals of $\bar{D}_\circ$ around a common vertex $v_\circ$, called *apex* (that is, no diagonal of $D_\circ$ crosses the diagonal $u_\circ w_\circ$). Note that $\bar{D}_\circ$ has $2|D_\circ| + n = 2|\bar{D}_\circ| - n$ angles. We say that a solid vertex $p_\bullet$ belongs to a hollow angle $u_\circ v_\circ w_\circ$ if it lies in the cone generated by the diagonals $(v_\circ, u_\circ)$ and $(v_\circ, w_\circ)$ of the angle. The key observation is the following.

Lemma 8.7. *Let $D_\bullet$ be a maximal $D_\circ$-accordion dissection, and let $p_\bullet, q_\bullet, r_\bullet, s_\bullet$ denote four consecutive vertices around a cell $C_\bullet$ of $D_\bullet$ (with possibly $p_\bullet = s_\bullet$ if $C_\bullet$ is a triangle). Then $p_\bullet$ and $s_\bullet$ belong to the same angle of the accordion of $\bar{D}_\circ$ crossed by $(q_\bullet, r_\bullet)$.*

Proof. Let $A_\circ$ be the accordion of $\bar{D}_\circ$ crossed by $(q_\bullet, r_\bullet)$. Assume that $p_\bullet$ and $s_\bullet$ belong to distinct angles of $A_\circ$. Then they are separated by a diagonal $\varepsilon_\circ$ of $A_\circ$. Therefore, there are two boundary edges $(q_\bullet, r_\bullet)$ and $(u_\bullet, v_\bullet)$ of $C_\bullet$ with distinct vertices such that the hollow diagonal $\varepsilon_\circ$ separates the vertices $q_\bullet, u_\bullet$ from the vertices $r_\bullet, v_\bullet$. Let $\gamma_\circ^1, \ldots, \gamma_\circ^i = \varepsilon_\circ, \ldots, \gamma_\circ^a$ (resp. $\delta_\circ^1, \ldots, \delta_\circ^j = \varepsilon_\circ, \ldots, \delta_\circ^b$) denote the diagonals of $D_\circ$ crossed by $(q_\bullet, r_\bullet)$ from $q_\bullet$ to $r_\bullet$ (resp. crossed by $(u_\bullet, v_\bullet)$ from $u_\bullet$ to $v_\bullet$). Then the hollow diagonals $\gamma_\circ^1, \ldots, \gamma_\circ^i = \varepsilon_\circ = \delta_\circ^j, \ldots, \delta_\circ^b$ which are crossed by $(q_\bullet, v_\bullet)$ also form an accordion. It follows that $D_\bullet$ is not maximal as we can still include $(q_\bullet, v_\bullet)$. ∎

Consider an angle $u_\circ v_\circ w_\circ$ of $\bar{D}_\circ$. In any maximal $D_\circ$-accordion dissection $D_\bullet$, the set $X_\bullet$ of diagonals of $\bar{D}_\bullet$ crossing both $(u_\circ, v_\circ)$ and $(v_\circ, w_\circ)$ is nonempty (it contains the boundary edge $((v-1)_\bullet, (v+1)_\bullet)$) and totally ordered (as the diagonals of $D_\bullet$ do not cross). We say that the angle $u_\circ v_\circ w_\circ$ is *closed* by the farthest diagonal of $X_\bullet$ from $v_\circ$ in the dissection $\bar{D}_\bullet$. Note that each angle of $\bar{D}_\circ$ is closed by precisely one diagonal of $\bar{D}_\bullet$. The following lemma is stated in [GM16] in terms of the dual tree $D_\circ^\star$ of the dissection $D_\circ$.

Lemma 8.8 ([GM16]). *In any maximal $D_\circ$-accordion dissection, each internal diagonal closes two angles of $\bar{D}_\circ$ (one apex on each side) and each boundary edge of the solid polygon closes one angle of $\bar{D}_\circ$. The accordion complex $\mathcal{AC}(D_\circ)$ is thus pure of dimension $|D_\circ|$.*

Proof. The first sentence is a consequence of Lemma 8.7: for any four consecutive vertices $p_\bullet, q_\bullet, r_\bullet, s_\bullet$ in a cell of $\bar{D}_\bullet$, the diagonal $(q_\bullet, r_\bullet)$ closes the unique angle of the accordion of $\bar{D}_\circ$ crossed by $(q_\bullet, r_\bullet)$ that contains the vertices $p_\bullet$ and $s_\bullet$. Therefore, $(q_\bullet, r_\bullet)$ closes precisely two angles (resp. one angle) of $D_\circ$ if it is an internal (resp. external) solid diagonal. We obtain by double-counting that $2|D_\circ| + n = |\{\text{angles of } \bar{D}_\circ\}| = 2|D_\bullet| + n$ and thus $|D_\bullet| = |D_\circ|$ for any maximal $D_\circ$-accordion dissection $D_\bullet$. ∎

We can now prove that the accordion complex of $D_\circ$ is thin (any internal diagonal of a maximal $D_\circ$-accordion dissection can be flipped into a unique other one to form a new maximal $D_\circ$-accordion dissection). The following statement is illustrated in Figure 8.4.

Lemma 8.9 ([GM16]). *Let $D_\bullet$ be a maximal $D_\circ$-accordion dissection and $\delta_\bullet$ be a diagonal of $D_\bullet$. Let $u_\circ$ and $v_\circ$ be the apices of the angles of $D_\circ$ closed by $\delta_\bullet$, let $\mu_\bullet$ and $\nu_\bullet$ denote the edges of the cells of $D_\bullet$ incident to $\delta_\bullet$ which separate $\delta_\bullet$ from $u_\circ$ and $v_\circ$ respectively, and let $Q_\bullet$ denote the quadrilateral defined by the four vertices of $\mu_\bullet$ and $\nu_\bullet$. Note that $\delta_\bullet$ is a diagonal of $Q_\bullet$, and let $\delta_\bullet'$ denote the other diagonal. Then $D_\bullet' := D_\bullet \triangle \{\delta_\bullet, \delta_\bullet'\}$ is a maximal $D_\circ$-accordion dissection, and $D_\bullet$ and $D_\bullet'$ are the only maximal $D_\circ$-accordion dissections containing $D_\bullet \smallsetminus \{\delta_\bullet\}$. In other words, the accordion complex $\mathcal{AC}(D_\circ)$ is thin.*
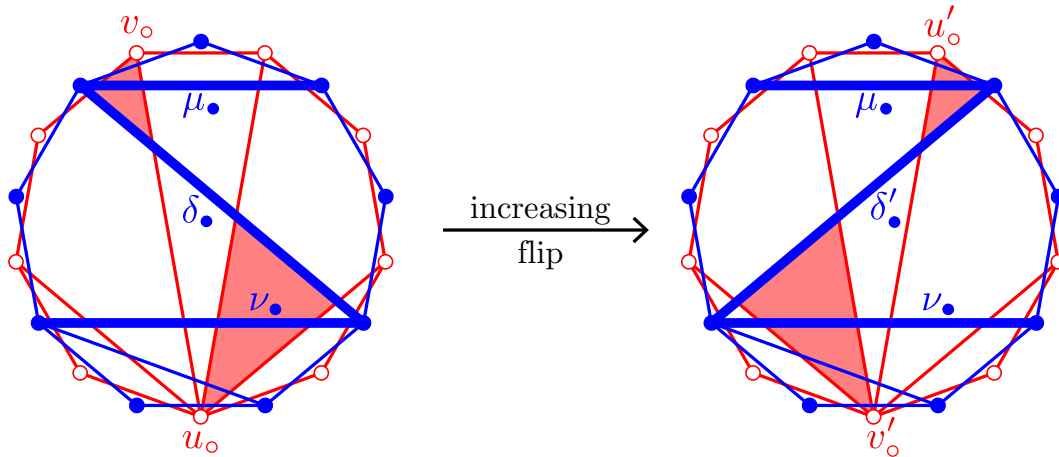
Figure 8.4 – Two maximal $D_\circ$-accordion dissections $D_\bullet$ (left) and $D'_\bullet$ (right) related by the flip of $\delta_\bullet$ to $\delta'_\bullet$. The angles of $D_\circ$ closed by $\delta_\bullet$ and $\delta'_\bullet$ are shaded. The flip is oriented from $D_\bullet$ to $D'_\bullet$.

Proof. We first observe that $\delta'_\bullet$ is a $D_\circ$-accordion diagonal, since the edges of $\bar{D}_\circ$ crossed by $\delta'_\bullet$ are obtained by merging three subaccordions of $D_\circ$: the subaccordion formed by the diagonals of $\bar{D}_\circ$ crossed by $\mu_\bullet$ but not $\delta_\bullet$ nor $\nu_\bullet$, the subaccordion formed by the diagonals of $\bar{D}_\circ$ crossed by $\delta_\bullet$, $\mu_\bullet$ and $\nu_\bullet$, and the subaccordion formed by the diagonals of $\bar{D}_\circ$ crossed by $\nu_\bullet$ but not $\delta_\bullet$ nor $\mu_\bullet$. Moreover, $\delta_\bullet$ and $\delta'_\bullet$ are the only $D_\circ$-accordion diagonals compatible with $D_\bullet \smallsetminus \{\delta_\bullet\}$. Indeed, any other such diagonal would cross $\delta_\bullet$ and $\delta'_\bullet$ (by maximality of $D_\bullet$ and $D'_\bullet$), and thus also the subaccordion $A_\circ$ of $D_\circ$ crossed by $\delta_\bullet$ and $\delta'_\bullet$ (because it cannot cross μ and ν). But it would then improperly intersect the two cells of $D_\circ$ containing precisely one diagonal of $A_\circ$.   ∎

The $D_\circ$-*accordion flip graph* is the dual graph $\mathcal{AFG}(D_\circ)$ of the accordion complex of $D_\circ$: its vertices are the maximal $D_\circ$-accordion dissections, and its edges are the *flips* between them, that is the pairs $\{D_\bullet, D'_\bullet\}$ of maximal $D_\circ$-accordion dissections with $D_\bullet \smallsetminus \{\delta_\bullet\} = D'_\bullet \smallsetminus \{\delta'_\bullet\}$. See Figure 8.3 (right).

8.2.4   The accordion lattice

We now define a natural orientation on the $D_\circ$-accordion flip graph. We use the notations of Lemma 8.9, where $D_\bullet \smallsetminus \{\delta_\bullet\} = D'_\bullet \smallsetminus \{\delta'_\bullet\}$ and $\delta_\bullet, \delta'_\bullet$ are the two diagonals of the quadrilateral defined by $\mu_\bullet, \nu_\bullet$. Observe that one of the path $\mu_\bullet \delta_\bullet \nu_\bullet$ and $\mu_\bullet \delta'_\bullet \nu_\bullet$ forms a Σ while the other forms a Z, see Figure 8.4 (right). We then orient the flip from the dissection containing the Σ to that containing the Z. Figure 8.3 (right) illustrates a $D_\circ$-accordion oriented flip graph (where the graph is oriented from bottom to top).

A. Garver and T. McConville introduced a natural closure on sets of $D_\circ$-subaccordions, and showed that the inclusion poset of biclosed sets of $D_\circ$-subaccordions is a well-behaved lattice (namely, semidistributive, congruence-uniform and polygonal). Then, they introduced a lattice congruence map from biclosed sets of $D_\circ$-subaccordions to maximal $D_\circ$-accordion dissections, which imply the following statement.

Theorem 8.10 ([GM16])**.** *The $D_\circ$-accordion oriented flip graph is the Hasse diagram of a lattice, that we call the $D_\circ$-accordion lattice and denote by $\mathcal{AL}(D_\circ)$.*

The $D_\circ$-accordion oriented flip graph is thus connected and acyclic. It has a unique source $D_\bullet^- := \{((i-1)_\bullet, (j-1)_\bullet) \,|\, (i_\circ, j_\circ) \in D_\circ\}$ obtained by rotating $D_\circ$ counterclockwise, and a unique sink $D_\bullet^+ := \{((i+1)_\bullet, (j+1)_\bullet) \,|\, (i_\circ, j_\circ) \in D_\circ\}$ obtained by rotating $D_\circ$ clockwise.

Remark 8.11. Following Remark 8.2, note that special reference hollow dissections $D_\circ$ give rise to special accordion lattices $\mathcal{AL}(D_\circ)$, as it was already observed in [GM16]:

⋄ For a *comb triangulation* $T_\circ$ (where all internal diagonals are incident to a common vertex), the $T_\circ$-accordion lattice $\mathcal{AL}(T_\circ)$ is the Tamari lattice [Tam51, MHPS12].

⋄ More generally, for any *accordion triangulation* $A_\circ$ (with no interior triangle), the $A_\circ$-accordion lattice $\mathcal{AL}(A_\circ)$ is a type A Cambrian lattice defined by N. Reading [Rea06].

⋄ For an arbitrary triangulation $T_\circ$, the $T_\circ$-accordion oriented flip graph $\mathcal{AFG}(A_\circ)$ is the poset originally defined by T. Brüstle, G. Dupont and M. Pérotin [BDP14].

⋄ For a quadrangulation $Q_\circ$, the $Q_\circ$-accordion lattice $\mathcal{AL}(Q_\circ)$ is the Stokes poset on $Q_\circ$-compatible quadrangulations studied by F.Chapoton [Cha16].

Remark 8.12. Following Remark 8.4, assume that $D_\circ$ has a cell containing p boundary edges of the hollow polygon, and consider the dissections $D_\circ^1, \ldots, D_\circ^p$ as in Remark 8.4. Then the $D_\circ$-accordion lattice is the Cartesian product of the $D_\circ^i$-accordion lattices: $\mathcal{AL}(D_\circ) = \mathcal{AL}(D_\circ^1) \times \cdots \times \mathcal{AL}(D_\circ^p)$. In particular, if two consecutive boundary edges of the hollow polygon belong to the same nontriangular cell of $D_\circ$, then contracting them to a single boundary edge preserves the $D_\circ$-accordion lattice. This shows in particular that the $D_\circ$-accordion lattice of a ribbon dissection $D_\circ$ is a Cambrian lattice, as conjectured for quadrangulations in [Cha16] and proved in [BMP17].

Remark 8.13. Call *cell-sequence* of a dissection the sequence whose i-th entry is its number of $(i + 2)$-cells. For example, the cell-sequence of the dissection of Figure 8.2 (left) is $3, 1, 0^\infty$ and this of any $(p+2)$-angulation of a $(pm+2)$-gon is $0^p, m, 0^\infty$. Observe that the flip preserves the cell-sequence so that all maximal $D_\circ$-accordion dissections have the same cell-sequence as $D_\circ$.

We conclude this section with a reciprocity result on accordion dissections.

Proposition 8.14. *Let $D_\circ$ be a hollow dissection and $D_\bullet$ be a solid dissection. Then $D_\bullet$ is a maximal $D_\circ$-accordion dissection if and only if $D_\circ$ is a maximal $D_\bullet$-accordion dissection.*

Proof. Since $D_\bullet^+ := \{((i-1)_\bullet, (j-1)_\bullet) \mid (i_\circ, j_\circ) \in D_\circ\}$ is a $D_\circ$-accordion dissection, we already know that $D_\circ$ is a $D_\bullet^-$-accordion dissection. Observe now in Figure 8.4 that if $D_\bullet$ and $D_\bullet'$ are maximal $D_\circ$-accordion dissections connected by a flip, then $D_\circ$ is a $D_\bullet$-accordion dissection if and only if it is a $D_\bullet'$-accordion dissection. Indeed, if $\delta_\bullet$ belongs to the zigzag of the $D_\bullet$-accordion $A_\bullet$ of a hollow diagonal $\delta_\circ$, then $\delta_\circ$ crosses both $\mu_\bullet$ and $\nu_\bullet$, so that it also crosses $\delta_\bullet'$, and thus the $D_\bullet'$-accordion $A_\bullet \triangle \{\delta_\bullet, \delta_\bullet'\}$. Since the $D_\circ$-accordion flip graph is connected, we obtain that $D_\circ$ is a $D_\bullet$-accordion dissection for any maximal $D_\circ$-accordion dissection $D_\bullet$. It is maximal since all maximal $D_\circ$-accordion dissections have $|D_\circ|$ diagonals. The equivalence follows by symmetry. ∎

8.3 Enumerative questions

We are now interested in conjectures stated by F. Chapoton in [Cha16] in the context of Stokes complexes, namely the accordion complexes of quadrangulations. We prove these conjectures for arbitrary reference dissections. Before this we need some precisions on the labels of the (hollow and solid) vertices. They are meant modulo $2n$, so as the results of algebraic operations on them. However we denote hollow and solid diagonals by (u, v) with $u, v \in [2n]$ and $u < v$, and consider them as elements of the Cartesian product $[2n] \times [2n] =: [2n]^2$. Moreover for arbitrary vertices represented by residues modulo $2n$, we mean by $u < v < w$ that u, v and w are positioned in this order in clockwise cyclic order. In this chapter, we abuse notations and keep denoting cyclic intervals by $[u, v] := \{w \mid u \leq w \leq v\}$, and cyclic hollow (resp. solid) intervals by $[u_\circ, v_\circ]_\circ$ (resp. $[u_\bullet, v_\bullet]_\bullet$). Finally it will be convenient for us to denote by $\mathcal{P}$ the polygon whose vertices are all (hollow or solid) vertices.

8.3.1   The serpent nest conjecture

We first focus on objects called *serpent nests* in [Cha16]. Recall that we denote by $D_\circ^\star$ the dual tree of a reference hollow dissection $D_\circ$, whose vertices are the cells of $D_\circ$ and whose edges are the pairs of cells of $D_\circ$ that share a common diagonal of $D_\circ$. From now on we identify the edges of $D_\circ^\star$ with the diagonals of $D_\circ$ in the natural way. A *serpent* of $D_\circ$ is an nonempty undirected dual path S in $D_\circ^\star$ whose edges (considered as hollow diagonals of $D_\circ$) form a subaccordion of $D_\circ$. Informally S is a path in $D_\circ$ going through cells of $D_\circ$ by incident diagonals. The edges of S not disconnecting it as a path (its "end edges") are its *final edges* (see Figure 8.5 left for an illustration).
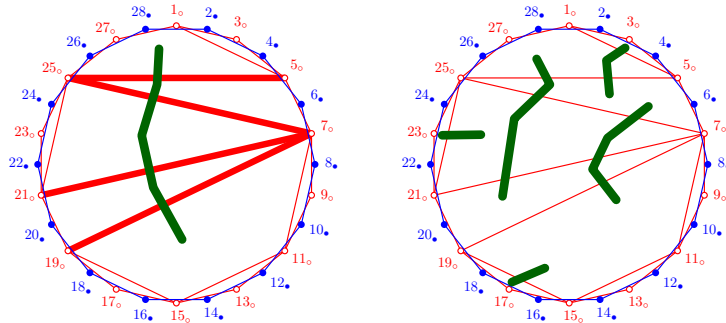
Figure 8.5 – A serpent S with final edges $(5_\circ, 25_\circ)$ and $(7_\circ, 19_\circ)$ in a hollow dissection $D_\circ$, with the subaccordion crossed by S being bold (left), and a serpent nest in $D_\circ$ (right).

Two serpents S_1, S_2 are *incompatible* if they intersect, so that $S_1 \cap S_2$ is a serpent whose final edges are diagonals $(u_\circ^h, v_\circ^h)$ and $(u_\circ^t, v_\circ^t)$ of $D_\circ$ with $u_\circ^h < v_\circ^h \le u_\circ^t < v_\circ^t$, and if they satisfy either of the following conditions, where S_1 and S_2 may be exchanged, so as $(u_\circ^h, v_\circ^h)$ and $(u_\circ^t, v_\circ^t)$.

1. The serpents S_1 and S_2 have a common final edge (Figure 8.6 left).

2. The serpents S_1 and S_2 "cross". Formally S_1 simultaneously contains two diagonals incident to $u_\circ^h$ and two diagonals incident to $u_\circ^t$, and S_2 simultaneously contains two diagonals incident to $v_\circ^h$ and two diagonals incident to $v_\circ^t$ (Figure 8.6 middle left).

3. The diagonal $(u_\circ^h, v_\circ^h)$ is a final edge of the serpent S_2, and the serpent S_1 simultaneously contains two diagonals of $D_\circ$ incident to $u_\circ^h$ (resp. $v_\circ^h$) and two diagonals of $D_\circ$ incident to $u_\circ^t$ (resp. $v_\circ^t$) (Figure 8.6 middle right).

4. The diagonal $(u_\circ^h, v_\circ^h)$ is a final edge of S_1, the diagonal $(u_\circ^t, v_\circ^t)$ is a final edge of S_2, S_1 contains two diagonals incident to $u_\circ^t$ (resp. $v_\circ^t$), and S_2 contains two diagonals incident to $v_\circ^h$ (resp. $u_\circ^t$) (Figure 8.6 right).

Serpents S_1 and S_2 are *compatible* if they are not incompatible and a *serpent nest* of $D_\circ$ is a (potentially empty) set of pairwise compatible serpents (see Figures 8.5 right).
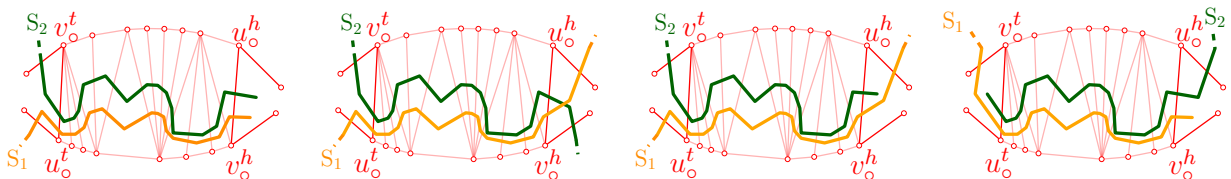
Figure 8.6 – Pairs of serpents S_1 (yellow) and S_2 (green) incompatible because of Condition 1 (left), Condition 2 (middle left), Condition 3 (middle right) or Condition 4 (right).
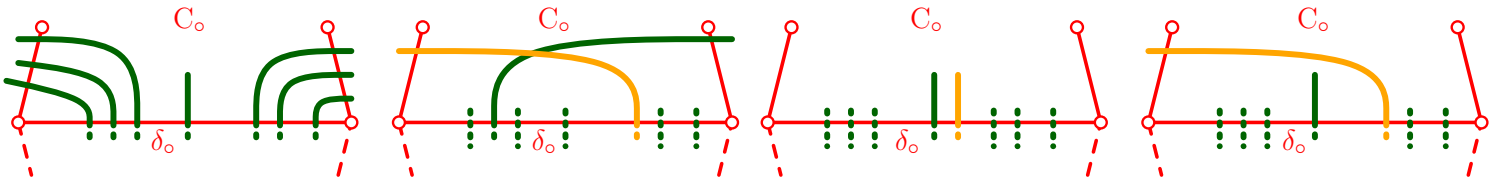
Figure 8.7 – A valid serpent nest pattern at an internal diagonal $\delta_\circ$ of a cell $C_\circ$ in a hollow dissection (left) and the three obstructions to valid patterns (middle and right).

Informally a set of serpents is a serpent nest if all its serpents can be simultaneously drawn as pairwise noncrossing dual paths in $D_\circ$ (Figure 8.6 middle left), with the additional conditions that no two of them "end up in the same cell by entering it through a same diagonal of $D_\circ$" (Figure 8.6 left) and that no serpent "goes over the head of another serpent" (Figure 8.6 middle right and right). To see that this description is indeed equivalent to the actual definition, observe that a serpent nest induces a unique valid[1] local pattern at each side of each internal diagonal of $D_\circ$, which immediately describes how to suitably draw all serpents. Figure 8.7 (left) illustrates what such a local valid pattern typically looks like while Figure 8.7 (middle and right) describes the forbidden local patterns. The following statement confirms a prediction in the introduction of [Cha16].

Theorem 8.15. *For any hollow dissection $D_\circ$, there is a bijection between the serpent nests of $D_\circ$ and the maximal $D_\circ$-accordion dissections.*

We need the following observation to prove Theorem 8.15.

Lemma 8.16. *Let $D_\circ$ be a hollow dissection, let $C_\circ$ be a triangular cell of $D_\circ$ which is a leaf of $D_\circ^\star$, whose unique internal diagonal of $D_\circ$ is $(1_\circ, 5_\circ)$. For any maximal $D_\circ$-accordion dissection $D_\bullet$, there exists a unique solid vertex $x_\bullet > 4_\bullet$ such that both solid (internal or external) diagonals $(2_\bullet, x_\bullet)$ and $(4_\bullet, x_\bullet)$ belong to $\bar{D}_\bullet$.*

Proof. For any two solid vertices $4_\bullet < x_\bullet < x'_\bullet$, the solid diagonals $(2_\bullet, x_\bullet)$ and $(4_\bullet, x'_\bullet)$ cross, which settles the uniqueness part. Let $x_\bullet$ be the smallest element in $[6_\bullet, (2n)_\bullet]_\bullet$ such that $(2_\bullet, x_\bullet)$ is a (internal or external) diagonal of $\bar{D}_\bullet$. Then observe that the solid diagonal $(4_\bullet, x_\bullet)$ crosses no diagonal of $D_\bullet$. Indeed such a diagonal should be of the form $(2_\bullet, y_\bullet)$ with $y_\bullet < x_\bullet$, contradicting the minimality of $x_\bullet$. Moreover, the diagonal $(4_\bullet, x_\bullet)$ crosses the same set of hollow diagonals as $(2_\bullet, x_\bullet)$ but with the external diagonal $(1_\circ, 3_\circ)$ replaced by $(3_\circ, 5_\circ)$, so that it is a $D_\circ$-accordion solid diagonal. This concludes the proof since then $(4_\bullet, x_\bullet) \in D_\bullet$ by maximality of $D_\bullet$. ∎

The assumptions in Lemma 8.16 do not introduce any real restriction on the number of vertices of $C_\circ$ nor on its unique internal diagonal. Indeed Remark 8.4 allows us to assume that $C_\circ$ is triangular as soon as it is a dual leaf, and we may rotate the labels of the vertices of the polygon $\mathcal{P}$ in order that the internal diagonal of $C_\circ$ is $(1_\circ, 5_\circ)$. We thus keep these assumptions in the proof of Theorem 8.15. It consists in an induction relying on Lemma 8.16 and the description of links in accordion complexes given in Remark 8.5. Informally we decompose any maximal $D_\circ$-accordion dissection $D_\bullet$ into two parts, according to its distinguished vertex $x_\bullet$ given by Lemma 8.16 (Figure 8.8 left and middle left), and find a corresponding serpent nest inductively in each of them (Figure 8.8 middle right). One must then remark that the two serpent nests in these two parts can be "unfolded" and gathered into a valid serpent nest N of $D_\circ$ (nonbold serpents in Figure 8.8 right). We then add a last serpent to N, whose final edges are $(1_\circ, 5_\circ)$ and the farthest possible diagonal of the "zigzag crossed by both $(2_\bullet, x_\bullet)$ and $(4_\bullet, x_\bullet)$" such that the new serpent (bold in Figure 8.8 right) does not create a validity obstruction in the local patterns inherited from N.

---

[1]Informally a pattern "avoiding" Conditions 1, 2 , 3 and 4.
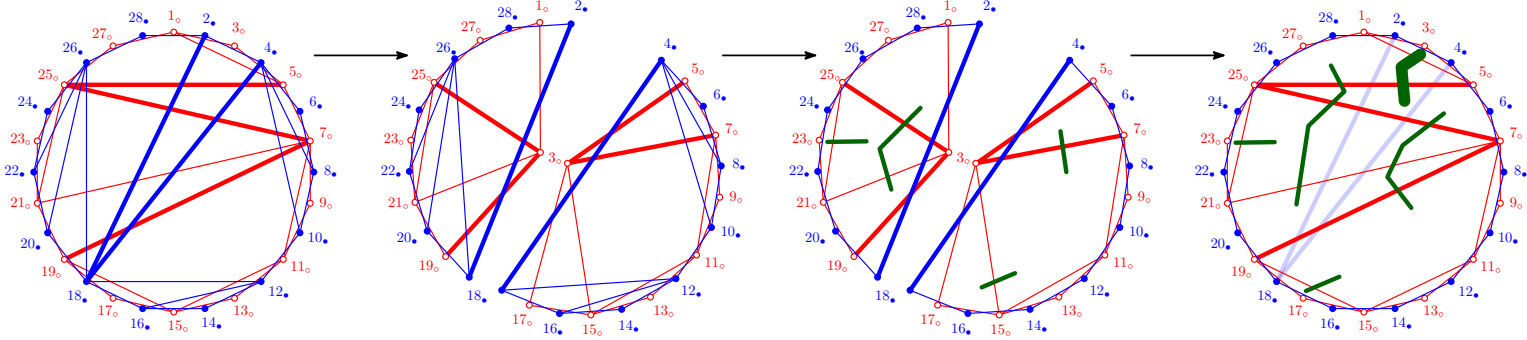
Figure 8.8 – A hollow dissection $D_\circ$ and a maximal $D_\circ$-accordion dissection $D_\bullet$ (left), and the serpent nest $\Phi_{D_\circ}(D_\bullet)$ of $D_\circ$ defined in the proof of Theorem 8.15 (right). Here the solid vertex $x_\bullet$ given by Lemma 8.16 is $18_\bullet$ and the zigzag $Z_\circ$ defined in the proof of Theorem 8.15 contains 3 diagonals (appearing bold). The bijection Φ is applied inductively in each part of the link of $\{(2_\bullet, 18_\bullet), (4_\bullet, 18_\bullet)\}$ in $\mathcal{AC}(D_\circ)$ to obtain serpent nests whose serpents do not cross the diagonals $(2_\bullet, 18_\bullet)$ and $(4_\bullet, 18_\bullet)$ (middle). All these serpents are "unfolded" into a valid serpent nest in $D_\circ$ (right), to which a (bold) serpent "lying between the diagonals $(2_\bullet, 18_\bullet)$ and $(4_\bullet, 18_\bullet)$" is added. The final edges of this additional serpent are $(1_\circ, 5_\circ)$ and $(5_\circ, 25_\circ)$, which is the farthest diagonal of $Z_\circ$ after which it can end in order to be compatible with the serpents inductively obtained.

Proof of Theorem 8.15. The proof is by induction on the number of diagonals in $D_\circ$. If $D_\circ$ is empty, then the unique $D_\circ$-accordion dissection is the empty set and the unique serpent nest in $D_\circ$ is also the empty set. Now as previously explained, we can assume for the induction step that $D_\circ$ contains the diagonal $(1_\circ, 5_\circ)$ (since its dual tree has a leaf). Let $\mathcal{AC}^{\max}(D_\circ)$ be the set of maximal $D_\circ$-accordion dissections and $\mathcal{SN}(D_\circ)$ be the set of serpent nests of $D_\circ$. We define bijections $\Phi_{D_\circ} : \mathcal{AC}^{\max}(D_\circ) \to \mathcal{SN}(D_\circ)$ and $\Psi_{D_\circ} : \mathcal{SN}(D_\circ) \to \mathcal{AC}^{\max}(D_\circ)$ that are reverse to each other as follows.

Let $D_\bullet \in \mathcal{AC}^{\max}(D_\circ)$ and let $x_\bullet$ be the solid vertex, given by Lemma 8.16, such that $\{(2_\bullet, x_\bullet), (4_\bullet, x_\bullet)\} \subseteq D_\bullet$. Let $D_\circ^{>x\bullet}$ (resp $D_\circ^{<x\bullet}$) be the hollow dissection obtained by contracting all diagonals of $D_\circ$ with both endpoints in $[3_\circ, (x-1)_\circ]_\circ$ (resp. $[(x+1)_\circ, 3_\circ]_\circ$) into a single vertex $c_\circ^1$ (resp. $c_\circ^2$). Let $D_\bullet^{>x\bullet} \in \mathcal{AC}^{\max}(D_\circ^{>x\bullet})$ (resp. $D_\bullet^{<x\bullet} \in \mathcal{AC}^{\max}(D_\circ^{<x\bullet})$) be the dissection obtained by keeping only the diagonals of $D_\bullet$ with both endpoints in $[x_\bullet, 2_\bullet]_\bullet$ (resp. $[4_\bullet, x_\bullet]_\bullet$). Since they have less diagonals than $D_\circ$, we can apply the induction hypothesis to both dissections $D_\circ^{>x\bullet}$ and $D_\circ^{<x\bullet}$ in order to obtain two bijections $\Phi_{D_\circ^{>x\bullet}} : \mathcal{AC}^{\max}(D_\circ^{>x\bullet}) \to \mathcal{SN}(D_\circ^{>x\bullet})$ and $\Phi_{D_\circ^{<x\bullet}} : \mathcal{AC}^{\max}(D_\circ^{<x\bullet}) \to \mathcal{SN}(D_\circ^{<x\bullet})$, whose respective reverse functions we denote by $\Psi_{D_\circ^{>x\bullet}} : \mathcal{SN}(D_\circ^{>x\bullet}) \to \mathcal{AC}^{\max}(D_\circ^{>x\bullet})$ and $\Psi_{D_\circ^{<x\bullet}} : \mathcal{SN}(D_\circ^{<x\bullet}) \to \mathcal{AC}^{\max}(D_\circ^{<x\bullet})$. We then define

$$N_1 := \Phi_{D_\circ^{>x\bullet}}(D_\bullet^{>x\bullet}) \qquad \text{and} \qquad N_2 := \Phi_{D_\circ^{<x\bullet}}(D_\bullet^{<x\bullet}).$$

Observe that a cell of $D_\circ$ different from $(1_\circ, 3_\circ, 5_\circ)$ either contains at least two vertices in $[3_\circ, (x-1)_\circ]_\circ$ and at most one in $[(x+1)_\circ, 3_\circ]_\circ$ or conversely, as both diagonals $(2_\bullet, x_\bullet)$ and $(4_\bullet, x_\bullet)$ cross accordions of $D_\circ$. The cells of $D_\circ$ are thus naturally partitioned and identified into the cells of $D_\circ^{>x\bullet}$ and $D_\circ^{<x\bullet}$. Moreover a subaccordion of $D_\circ^{>x\bullet}$ (resp. $D_\circ^{<x\bullet}$) naturally extends to a subaccordion of $D_\circ$ by replacing its diagonals $(a_\circ^1, c_\circ^1)$ (resp. $(a_\circ^2, c_\circ^2)$) by the set of all diagonals of the accordion crossed by $(2_\bullet, x_\bullet)$ with $a_\circ^1$ (resp. $a_\circ^2$) as an endpoint. So serpents in $D_\circ^{>x\bullet}$ (resp. $D_\circ^{<x\bullet}$) are also naturally identified to some serpents in $D_\circ$. It is moreover clear that compatible serpents in $D_\circ^{>x\bullet}$ (resp. $D_\circ^{<x\bullet}$) extend to compatible serpents in $D_\circ$, and that any serpent in $D_\circ^{>x\bullet}$ extends to a serpent in $D_\circ$ that is compatible with any serpent obtained by extending a serpent

of $D_\circ^{<x\bullet}$. We therefore abuse notations and still denote by $N_1 \sqcup N_2$ the corresponding serpent nests in $D_\circ$. We first settle two degenerate cases.

◇ If $x_\bullet = (2n)_\bullet$, then we define $\Phi_{D_\circ}(D_\bullet) = N_1 \sqcup N_2$.

◇ If $x_\bullet = 6_\bullet$, then we define $\Phi_{D_\circ}(D_\bullet) = N_1 \sqcup N_2 \sqcup \{S\}$ where S is the serpent of $D_\circ$ whose single edge corresponds to $(1_\circ, 5_\circ)$. It is clear that this serpent is compatible with all those in $N_1 \sqcup N_2$ since it does not share any common edge with them.

We are left with the case where both solid diagonals $(2_\bullet, x_\bullet)$ and $(4_\bullet, x_\bullet)$ are internal. Let $Z_\circ = \{\delta_\circ^1, \ldots \delta_\circ^\ell\}$ denote the zigzag of the accordion crossed by $(2_\bullet, x_\bullet)$, where the diagonal $(1_\circ, 5_\circ)$ is considered as a boundary edge (and therefore not in $Z_\circ$), and such that $\delta_\circ^i$ is incident to $\delta_\circ^{i-1}$ and $\delta_\circ^{i+1}$ for $i \in [2, \ell - 1]$. As we already dealt with the cases where $x_\bullet \in \{6_\bullet, (2n)_\bullet\}$, the zigzag $Z_\circ$ is not empty, and we can assume by symmetry that $5_\circ$ is an endpoint of $\delta_\circ^1$. Let S be the serpent of $D_\circ$ with final edges $(1_\circ, 5_\circ)$ and the diagonal $\delta_\circ^{i_{\max}}$, where $i_{\max}$ is the maximal index in $[\ell]$ such that S is compatible with all serpents in $N_1 \sqcup N_2$. It is well-defined since

◇ all dual paths in $D_\circ$ with final edges $(1_\circ, 5_\circ)$ and $\delta_\circ^i$ ($i \in [\ell]$) are serpents of $D_\circ$, and

◇ the serpent with final edges $(1_\circ, 5_\circ)$ and $\delta_\circ^1$ is compatible with all serpents in $N_1 \sqcup N_2$, by a quick case analysis.

We finally define
$$\Phi_{D_\circ}(D_\bullet) := N_1 \sqcup N_2 \sqcup \{S\}.$$

To show that $\Phi_{D_\circ}$ is a bijection, we define its reverse bijection $\Psi_{D_\circ}$. For this, we only need to show how to determine, given a serpent nest N of $D_\circ$, the distinguished vertex $x_\bullet$ of the maximal $D_\circ$-accordion dissection $\Psi_{D_\circ}(N)$ that we want to define. This vertex $x_\bullet$ should be chosen such that the serpents in N then separate on each sides of the diagonals $(2_\bullet, x_\bullet)$ and $(4_\bullet, x_\bullet)$, in order for us to conclude the proof using the reverse bijections $\Psi_{D_\circ^{>x\bullet}} : \mathcal{SN}(D_\circ^{>x\bullet}) \to \mathcal{AC}^{\max}(D_\circ^{>x\bullet})$ and $\Psi_{D_\circ^{<x\bullet}} : \mathcal{SN}(D_\circ^{<x\bullet}) \to \mathcal{AC}^{\max}(D_\circ^{<x\bullet})$. The way we determine the vertex $x_\bullet$ is illustrated in Figure 8.9.

The two "degenerate" cases where N either contains no serpent containing $(1_\circ, 5_\circ)$ or the serpent whose unique edge is $(1_\circ, 5_\circ)$ are easily settled, as we also dealt with them separately when defining $\Phi_{D_\circ}$. Suppose that N contains a serpent S with final edges $(1_\circ, 5_\circ)$ and a hollow diagonal $\delta_\circ$. As $(1_\circ, 5_\circ)$ is incident to a dual leaf, there is no other serpent than S in N that contains it, since otherwise it would fulfill Condition 1 together with S. We now inductively define a sequence of hollow diagonals $(\gamma_\circ^i)_{i \geq 1}$, such that for $i \geq 1$, the dual path from $(1_\circ, 5_\circ)$ to $\gamma_\circ^i$ is a serpent, that we denote by S_i. In what follows, we denote by $u_\circ^i$ the endpoint of $\gamma_\circ^i$ contained in another edge of S_i.

◇ Let $C_\circ^1$ be the cell which is the endpoint (as dual node in $D_\circ^\star$) of S (as dual path in $D_\circ^\star$) incident to $\delta_\circ$. We let $u_\circ^1$ be the endpoint of $\delta_\circ$ not contained in another edge of S and $\gamma_\circ^1$ be the diagonal of $C_\circ^1$ incident to $\delta_\circ$ at $u_\circ^1$. The edges of S_1 are then the edges of S together with $\gamma_\circ^1$, so that $\gamma_\circ^1$ and $u_\circ^1$ satisfy the required property.

◇ For $i > 1$, we consider the cell $C_\circ^i$ which is the endpoint (as dual node in $D_\circ^\star$) of S_{i-1} (as dual path in $D_\circ^\star$) incident to $\gamma_\circ^{i-1}$. Let $\lambda_\circ^i$ be the other diagonal of $C_\circ^i$ containing $u_\circ^{i-1}$. The dual path with final edges $(1_\circ, 5_\circ)$ and $\lambda_\circ^i$ is then a serpent, that we denote by S_{i-1}^+. We distinguish two cases.

(i) If S_{i-1}^+ is compatible with all serpents of $N \setminus \{S\}$ not containing $\lambda_\circ^i$, then we define $\gamma_\circ^i := \lambda_\circ^i$ and $u_\circ^i := u_\circ^{i-1}$.

(ii) If a serpent in $N \setminus \{S\}$ not containing $\lambda_\circ^i$ is incompatible with S_{i-1}^+, then we let $\gamma_\circ^i$ be the diagonal of $C_\circ^i$ incident to $\gamma_\circ^{i-1}$ different from $\lambda_\circ^i$, which fulfills the required condition. Observe that in this case we necessarily have $u_\circ^i \neq u_\circ^{i-1}$.
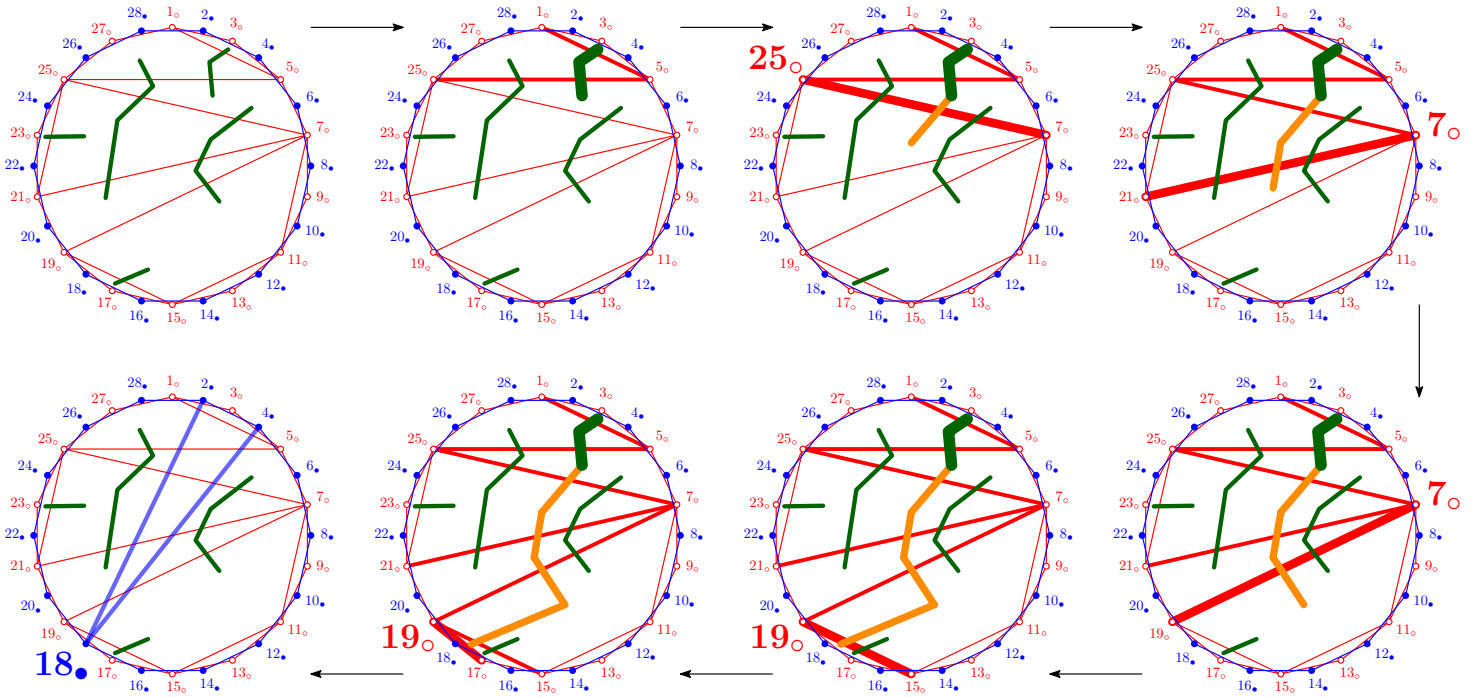
Figure 8.9 – Illustration of the algorithm used to determine the image $\Psi_{D_\circ}(N)$ of a serpent nest N of a hollow dissection $D_\circ$ (top left). In the successive pictures, the diagonals γ_i's appear bold, the currently defined one being double bold. At the end of the process, we are left with a vertex $x_\bullet$ ($18_\bullet$ here) which allows to suitably separate the serpents of N at each sides of the diagonals $(2_\bullet, 18_\bullet)$ and $(4_\bullet, 18_\bullet)$ (bottom left).

Observe that any serpent S_i ($i \geq 1$) is compatible with all serpents of $N \smallsetminus \{S\}$ not containing $\lambda_\circ^i$. This is clear for serpents S_i obtained from Case (i), and it follows from straightforward case analyses for S_1 and for serpents S_i obtained from Case (ii). The sequence $(\gamma_\circ^i)_{i \geq 1}$ cannot be infinite for there are finitely many hollow diagonals in $D_\circ$. It thus stops when the new diagonal $\gamma_\circ^j$ (for some $j \geq 1$) that we want to define is an external hollow diagonal $((x-1)_\circ, (x+1)_\circ)$ for some $x_\bullet \in [2_\bullet, (2n)_\bullet]_\bullet$. In fact it is immediate that $x_\bullet \in [8_\bullet, (2n-2)_\bullet]_\bullet$. Notice that the solid diagonal $(2_\bullet, x_\bullet)$ crosses an accordion whose diagonals are those of S_{j-1} (with $S_0 = S$ by convention) together with the external hollow diagonals $(1_\circ, 3_\circ)$ and $((x-1)_\circ, (x+1)_\circ)$. Moreover the vertices of the zigzag of $(2_\bullet, x_\bullet)$ are some vertices of edges of the serpent S together with the vertices in $\{u_\circ^i \mid i \geq 0\}$, that we denote $\{u_\circ^{i_1}, \ldots, u_\circ^{i_p}\}$ without repetition. Observe finally that the compatibility conditions on S_j imply that any serpent of $N \smallsetminus \{S\}$ can be obtained by extending either a serpent of $D_\circ^{>x_\bullet}$ or of $D_\circ^{<x_\bullet}$ to $D_\circ$. Therefore $N \smallsetminus \{S\}$ splits into two serpent nests N_1 and N_2 in the hollow dissections $D_\circ^{>x_\bullet}$ and $D_\circ^{<x_\bullet}$ obtained from $x_\bullet$. Let

$$\Psi_{D_\circ}(N) := \Psi_{D_\circ^{>x_\bullet}}(N_1) \sqcup \Psi_{D_\circ^{<x_\bullet}}(N_2) \sqcup \{(2_\bullet, x_\bullet), (4_\bullet, x_\bullet)\}.$$

It remains to check that $\Psi_{D_\circ} \circ \Phi_{D_\circ}$ is the identity function on $\mathcal{AC}^{\max}(D_\circ)$. It is clear, from the definition in Cases (i) and (ii), that if $u_\circ^i \neq u_\circ^{i-1}$ for some $2 \leq i \leq j$, then the serpent S_{i-1} is incompatible with at least one serpent in $N \smallsetminus \{S\}$. Thus S is the only serpent, among all serpents S_i for $i \in \{0, i_1, \ldots, i_p\}$, that is compatible with all serpents in $N \smallsetminus \{S\}$ and whose final edge different from $(1_\circ, 5_\circ)$ belongs to the zigzag of $(2_\bullet, x_\bullet)$ (where $(1_\circ, 5_\circ)$ is considered as a boundary edge). This concludes the proof since it implies that the vertex $x_\bullet$ given by Lemma 8.16 is the same for $D_\bullet$ and $\Psi_{D_\circ} \circ \Phi_{D_\circ}(D_\bullet)$. ∎

8.3.2 Twists and F-triangle

To prove our second enumerative result, we need a few more definitions. We call *rotations* (resp. *mirror symmetries*) the functions $i \mapsto \alpha + i$ (resp. $i \mapsto \alpha - i$), for some $\alpha \in 2\mathbb{N}$, on both hollow and solid vertices of $\mathcal{P}$. These functions extend to diagonals and sets of diagonals. Rotations and mirror symmetries send hollow (resp. solid) dissections to hollow (resp. solid) dissections and induce isomorphisms of accordion complexes. Finally we will call *minimal* (resp. *maximal*) *solid* diagonals of $\mathcal{AC}(D_\circ)$ the diagonals in $D_\bullet^- = \{((i-1)_\bullet, (j-1)_\bullet) \,|\, (i_\circ, j_\circ) \in D_\circ\}$ (resp. $D_\bullet^+ = \{((i+1)_\bullet, (j+1)_\bullet) \,|\, (i_\circ, j_\circ) \in D_\circ\}$). Rotations (resp. mirror symmetries) clearly send minimal solid diagonals to minimal (resp. maximal) solid diagonals (see Figure 8.10 for mirror symmetries).

We now define the *twist* operation on dissections as follows. Let $D_\circ$ be any hollow dissection and $e_\circ$ be a (internal or external) diagonal of $\bar{D}_\circ$. Up to a canonical clockwise rotation, we can assume that the endpoints of $e_\circ$ are $1_\circ$ and $j_\circ \geq 3_\circ$. For any hollow diagonal $\delta_\circ = (k_\circ, \ell_\circ)$ (with $1_\circ \leq k_\circ < \ell_\circ \leq (2n)_\circ$) of $D_\circ$, we define

$$\mathrm{tw}^{e_\circ}(\delta_\circ) := \begin{cases} ((j-k+1)_\circ, (j-\ell+1)_\circ) \text{ if } \ell_\circ \leq j_\circ, \\ (k_\circ, \ell_\circ) \text{ otherwise.} \end{cases}$$

The hollow dissection $\mathrm{tw}^{e_\circ}(D_\circ) := \{\mathrm{tw}^{e_\circ}(\delta_\circ) \,|\, \delta_\circ \in D_\circ\}$ is *obtained by twisting* $D_\circ$ *along* $e_\circ$. Informally, it consists in "cutting $D_\circ$ along $e_\circ$, reflecting one of the two resulting parts, and gluing it back to the preserved part along $e_\circ$" (see Figure 8.11 for an illustration).

Remark 8.17. Observe that there are two degenerate situations when twisting a dissection along a diagonal, namely when this diagonal is an external one.
  ◇ If $e_\circ = (1_\circ, 3_\circ)$, then $\mathrm{tw}^{e_\circ}(D_\circ) = D_\circ$.
  ◇ If $e_\circ = (1_\circ, (2n-1)_\circ)$, then $\mathrm{tw}^{e_\circ}(D_\circ)$ is the image of $D_\circ$ by the mirror symmetry $i \mapsto -i$ (see Figure 8.10).

We are interested in the properties of $\mathcal{AC}(D_\circ)$ preserved by the twist operation. Originally, F. Chapoton asked whether the two complexes $\mathcal{AC}(D_\circ)$ and $\mathcal{AC}(\mathrm{tw}^{e_\circ}(D_\circ))$ were isomorphic. One can computationally check that the pair of reference hollow dissections of Figure 8.11 is *the* minimal (in terms of the number of diagonals) counterexample to such statement in full generality. F. Chapoton conjectures that it however holds, provided that the dissection $D_\circ$ and the diagonal $e_\circ$ fulfill additional conditions [Cha16, Conjecture 2.7]. We prove this conjecture in the following statement.
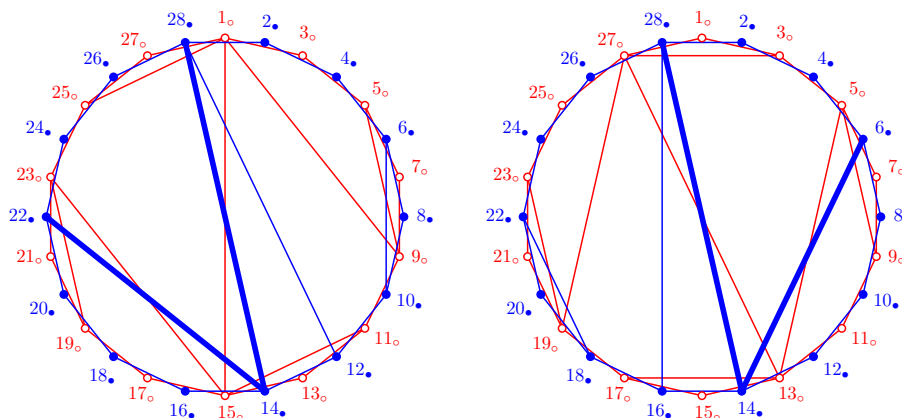
Figure 8.10 – The isomorphism between the accordion complexes of a hollow dissection $D_\circ$ (left) and its image $\Phi(D_\circ)$ by the mirror symmetry $\Phi : i \mapsto -i$ (right). This isomorphism sends minimal $D_\circ$-accordion solid diagonals (bold in the left picture) to maximal $\Phi(D_\circ)$-accordion solid diagonals (bold in the right picture).
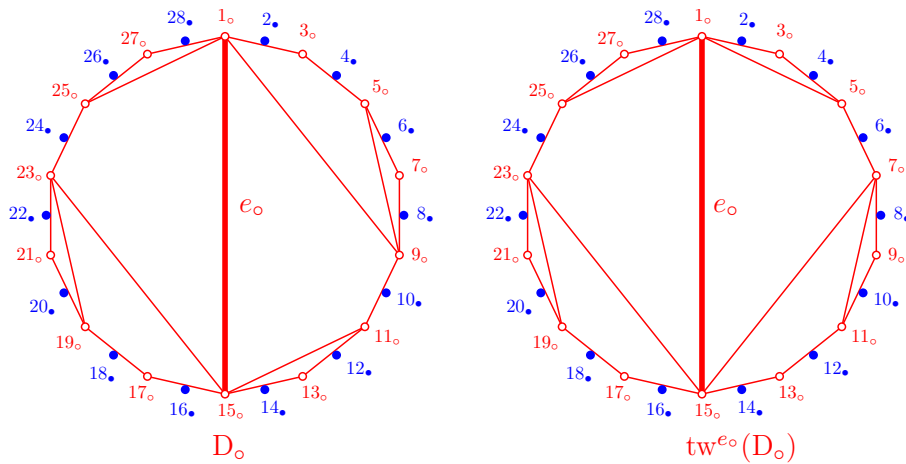
Figure 8.11 – A pair of hollow dissections $(\mathrm{D}_\circ, \mathrm{tw}^{e_\circ}(\mathrm{D}_\circ))$ related by a twist along the diagonal $e_\circ = (1_\circ, 15_\circ)$. The left part is preserved while the right part is reflected. The accordion complexes $\mathcal{AC}(\mathrm{D}_\circ)$ and $\mathcal{AC}(\mathrm{tw}^{e_\circ}(\mathrm{D}_\circ))$ are not isomorphic.

Proposition 8.18. *Let $\mathrm{D}_\circ$ be a hollow dissection and let $e_\circ$ be any (internal or external) diagonal of $\bar{\mathrm{D}}_\circ$. Suppose that the dual tree of one of the two hollow dissections obtained by cutting $\mathrm{D}_\circ$ at $e_\circ$ is a path and that $e_\circ$ is contained in a cell that is an endpoint of this path. Then the two accordion complexes $\mathcal{AC}(\mathrm{D}_\circ)$ and $\mathcal{AC}(\mathrm{tw}^{e_\circ}(\mathrm{D}_\circ))$ are isomorphic.*

Proof. We already noticed that the complexes of two hollow dissections obtained from each other by a mirror symmetry are isomorphic. This allows to choose "which side of $e_\circ$ is twisted" in the proof. Let $j_\circ$ be a hollow vertex such that $e_\circ = (1_\circ, j_\circ)$ (up to relabeling). As we saw, we only need to do the proof in the case where the dual tree of the dissection $\mathrm{D}'_\circ$ induced by $\mathrm{D}_\circ$ on the hollow vertices $1_\circ, 3_\circ, \ldots, j_\circ$ is a path and the hollow diagonals $(1_\circ, 3_\circ)$ and $(1_\circ, j_\circ)$ belong to a common cell of $\mathrm{D}'_\circ$. We can moreover assume that any cell of the dissection $\mathrm{D}'_\circ$ is adjacent to its two neighbors by incident edges, for otherwise the complex would decompose into a join of smaller complexes and we could conclude by induction on the number of cells of $\mathrm{D}_\circ$. Therefore the internal diagonals of $\mathrm{D}'_\circ$ form an accordion and Remark 8.4 allows us to assume that $\mathrm{D}'_\circ$ is in fact an accordion triangulation. In this situation one easily sees that the two complexes $\mathcal{AC}(\mathrm{D}_\circ)$ and $\mathcal{AC}(\mathrm{tw}^{e_\circ}(\mathrm{D}_\circ))$ are equal. Indeed a solid diagonal $\delta_\bullet$ is a $\mathrm{D}_\circ$ accordion if and only if it crosses an accordion of $\mathrm{D}_\circ \smallsetminus \mathrm{D}'_\circ$, which moreover contains $e_\circ$ if $\delta_\bullet$ crosses $e_\circ$. This description concludes the proof as it is independent of the shape of the dual path of $\mathrm{D}'_\circ$.   ∎

If the twist operation need not preserve accordion complexes, we wonder whether it satisfies some weaker properties, as for instance preserving their *f-vectors* (the vectors whose entries are the number of faces in each dimension). We define the following refined statistic, introduced in [Cha16]. For a hollow dissection $\mathrm{D}_\circ$ and to integers r and d, let $F_r^d(\mathrm{D}_\circ)$ denote the number of $\mathrm{D}_\circ$-accordion dissections with d diagonals, among which exactly r belong to $\mathrm{D}_\bullet^-$. Observe that $\sum_{0 \leq r \leq d} F_r^d(\mathrm{D}_\circ)$ is the d-th entry of the f-vector of the accordion complex $\mathcal{AC}(\mathrm{D}_\circ)$. Following F. Chapoton [Cha16], we call *F-triangle* of $\mathrm{D}_\circ$ the triangle of numbers $(F_r^d(\mathrm{D}_\circ))_{0 \leq r \leq d}$.

The following statement is the generalization of Conjecture 2.6 in [Cha16].

Theorem 8.19. *For any hollow dissection $\mathrm{D}_\circ$ and any (internal or external) diagonal $e_\circ$ of $\bar{\mathrm{D}}_\circ$, the hollow dissections $\mathrm{D}_\circ$ and $\mathrm{tw}^{e_\circ}(\mathrm{D}_\circ)$ have the same F-triangle.*

As F-triangles refine f-vectors, Theorem 8.19 directly implies the following result.

Corollary 8.20. *For any hollow dissection* $D_\circ$ *and any (internal or external) diagonal* $e_\circ$ *of* $\bar{D}_\circ$, *the accordion complexes* $\mathcal{AC}(D_\circ)$ *and* $\mathcal{AC}(\mathrm{tw}^{e_\circ}(D_\circ))$ *have the same f-vector.*

To prove Theorem 8.19 , we need some notations. For a subset $S_\circ \subseteq D_\circ$, we denote by $S_\bullet^- := \{((i-1)_\bullet, (j-1)_\bullet) \,|\, (i_\circ, j_\circ) \in S_\circ\}$ (resp. $S_\bullet^+ := \{((i+1)_\bullet, (j+1)_\bullet) \,|\, (i_\circ, j_\circ) \in S_\circ\}$) the corresponding subset in $D_\bullet^-$ (resp. $D_\bullet^+$). We also denote by $\mathrm{tw}^{e_\circ}(S_\circ) := \{\mathrm{tw}^{e_\circ}(\delta_\circ) \,|\, \delta_\circ \in S_\circ\}$ the set of diagonals (of $\mathrm{tw}^{e_\circ}(D_\circ)$) obtained by twisting $S_\circ$ along $e_\circ$ and by $\mathrm{tw}^{e_\circ}(S_\bullet)^-$ (resp. $\mathrm{tw}^{e_\circ}(S_\bullet)^+$) the corresponding set in $\mathrm{tw}^{e_\circ}(D_\bullet)^-$ (resp. $\mathrm{tw}^{e_\circ}(D_\bullet)^+$). We now fix an integer $d \geq 0$ and define, for any $D_\circ$-accordion dissection $S_\bullet$, the quantity

$$F_{S_\bullet}(D_\circ) := \#\left(D_\circ\text{-accordion dissections } D_\bullet \text{ such that } |D_\bullet| = d \text{ and } S_\bullet \subseteq D_\bullet\right).$$

The proof of Theorem 8.19 relies on the following intermediary statement.

Lemma 8.21. *Let* $D_\circ$ *be any hollow dissection and* $e_\circ$ *be any (internal or external) diagonal of* $\bar{D}_\circ$. *For any subset* $S_\circ$ *of (internal) diagonals of* $D_\circ$, *there holds*

$$F_{S_\bullet^-}(D_\circ) = F_{\mathrm{tw}^{e_\circ}(S_\bullet)^+}(\mathrm{tw}^{e_\circ}(D_\circ)).$$

We show Lemma 8.21 bijectively. If $e_\circ = (1_\circ, (2n-1)_\circ)$, then the twist along $e_\circ$ is the mirror symmetry $\Phi : i \mapsto -i$ and the result is a given by the basic properties of mirror symmetries (see Figure 8.10 again). Before giving the actual proof of Lemma 8.21, we informally describe the bijection that we use in the other "degenerate" case, where the twist induces the identity on $D_\circ$. This shall prepare the reader's intuition as the bijection that we define in the generic case "interpolates" between the "degenerate" ones.

Suppose that $e_\circ = (1_\circ, 3_\circ)$, so that $\mathrm{tw}^{e_\circ}(D_\circ) = D_\circ$, and let $D_\bullet$ be a $D_\circ$-accordion dissection with d diagonals containing a set $S_\bullet^-$, for a certain $S_\circ \subseteq D_\circ$. We associate to $D_\bullet$ the $D_\circ$-accordion dissection $\Psi(D_\bullet)$ defined as follows. Consider separately the dissections induced by $D_\bullet$ in all cells of the solid dissection $\bar{S}_\bullet^-$. Let $C_\bullet$ be one of these cells. We denote by $(i_\bullet^1, j_\bullet^1), \dots, (i_\bullet^r, j_\bullet^r)$ the boundary diagonals of $C_\bullet$ that are in $S_\bullet^-$. Let $\phi_{C_\bullet}$ be the function on the vertices of $C_\bullet$ sending a solid vertex $v_\bullet$ to itself if it does not belong to $\{j_\bullet^1, \dots, j_\bullet^r\}$ and to the solid vertex $(i^\ell + 2)_\bullet$ if $v_\bullet = j_\bullet^\ell$. Then $\Psi(D_\bullet)$ contains all solid diagonals $(\phi_{C_\bullet}(i_\bullet), \phi_{C_\bullet}(j_\bullet))$, for all solid diagonals $(i_\bullet, j_\bullet)$ of $D_\bullet$ contained in any cell $C_\bullet$ of the dissection $\bar{S}_\bullet^-$, together with $S_\bullet^+$. More visually, the dissection $\Psi(D_\bullet)$ is obtained by letting simultaneously, at the neighborhood of each diagonal $\delta_\bullet^-$ in $S_\bullet^-$, each "semi-diagonal" of $D_\bullet$ in a cell bounded by $\delta_\bullet^-$ and which crosses $\delta_\bullet^+$ "slide along the corresponding reference hollow diagonal $\delta_\circ$ and attach itself, at the opposite extremity of $\delta_\circ$, on the corresponding endpoint of $\delta_\bullet^+$" (Figure 8.12 illustrates this local transformation). The function Ψ is then a bijection between the $D_\circ$-accordion dissections with d diagonals containing $S_\bullet^-$ and the $D_\circ$-accordion dissections with d diagonals containing $S_\bullet^+$ (see Figure 8.13 for an illustration).

The proof of Lemma 8.21 essentially consists in two steps:

$\diamond$ apply the "degenerate" bijections respectively to the twisted and the nontwisted parts of $D_\circ$, forgetting the potential diagonals of $D_\bullet \smallsetminus S_\bullet^-$ that cross $e_\circ$ between two diagonals of $S_\bullet^-$ also crossing $e_\circ$, and

$\diamond$ insert the forgotten diagonals of $D_\bullet \smallsetminus S_\bullet^-$ after the first operation in the natural way "preserving the shape of the union of subaccordions initially formed by them".

The reason why our first step is well-defined is that the "degenerate" operations on the twisted and nontwisted parts agree on the "common frontier" of these parts. For the second step, observe that the two "degenerate" operations both work pointwise in each cell, and that all initially forgotten diagonals lie in a common cell of the dissection formed by the remaining ones. Therefore the vertices on which we reproduce the mentioned "union of subaccordions" are naturally identified with some endpoints of the
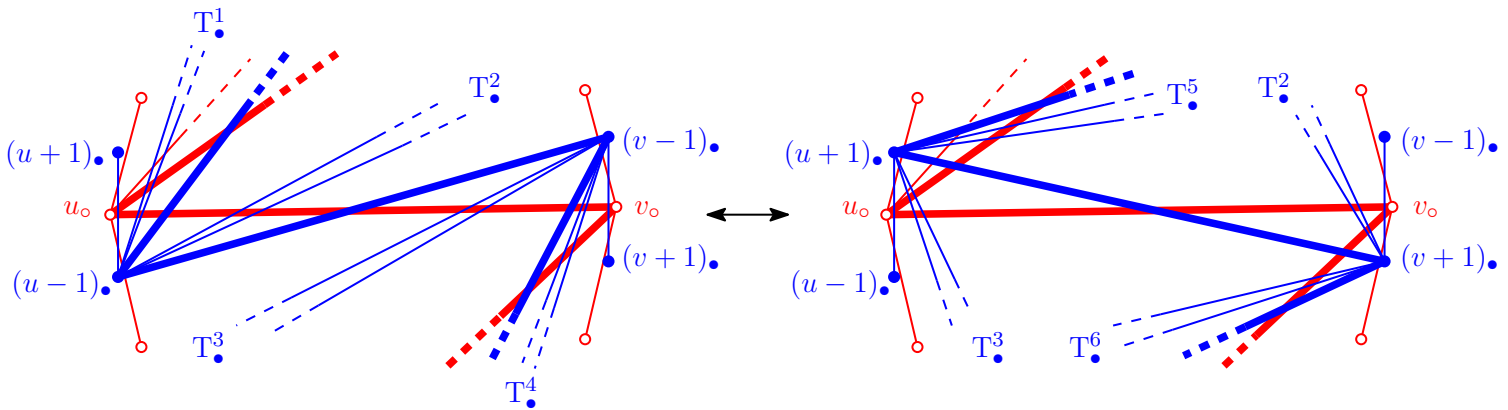
Figure 8.12 – The local transformation on "semi-diagonals" to show Lemma 8.21 when $e_\circ = (1_\circ, 3_\circ)$. Both pictures illustrate the neighborhood of a diagonal $(u_\circ, v_\circ)$ in a hollow dissection $D_\circ$ with a distinguished subset of diagonals $S_\circ$ containing $(u_\circ, v_\circ)$, and potentially other diagonals incident to $u_\circ$ or $v_\circ$. The diagonals of $S_\circ$ that appear in the neighborhood of $(u_\circ, v_\circ)$ are bold red. In the left picture, we represent the diagonals of a $D_\circ$-accordion dissection $D_\bullet$ containing $S_\bullet^-$, with the diagonals of $S_\bullet^-$ bold blue. In the right picture, we represent the diagonals of the dissection $\Psi(D_\bullet)$, where Ψ is defined with respect to $S_\circ$. The diagonals of $\Psi(D_\bullet) \cap S_\bullet^+$ are bold blue. In both pictures, the sets $T_\bullet^i$ ($i \in [6]$) are disjoint and contain the other endpoints of the nonbold solid diagonals that appear. The transformation Ψ lets the diagonals with endpoints in $T_\bullet^1 \sqcup T_\bullet^4$ disappear of the neighborhood of $(u_\circ, v_\circ)$. Those with endpoints in $T_\bullet^5 \sqcup T_\bullet^6$ appear from the same transformation applied at the neighborhood of other diagonals in $S_\circ$.

$\{(14_\bullet, 28_\bullet), (24_\bullet, 28_\bullet)\} \subseteq D_\bullet$ $\{(2_\bullet, 16_\bullet), (2_\bullet, 26_\bullet)\} \subseteq \Psi(D_\bullet)$
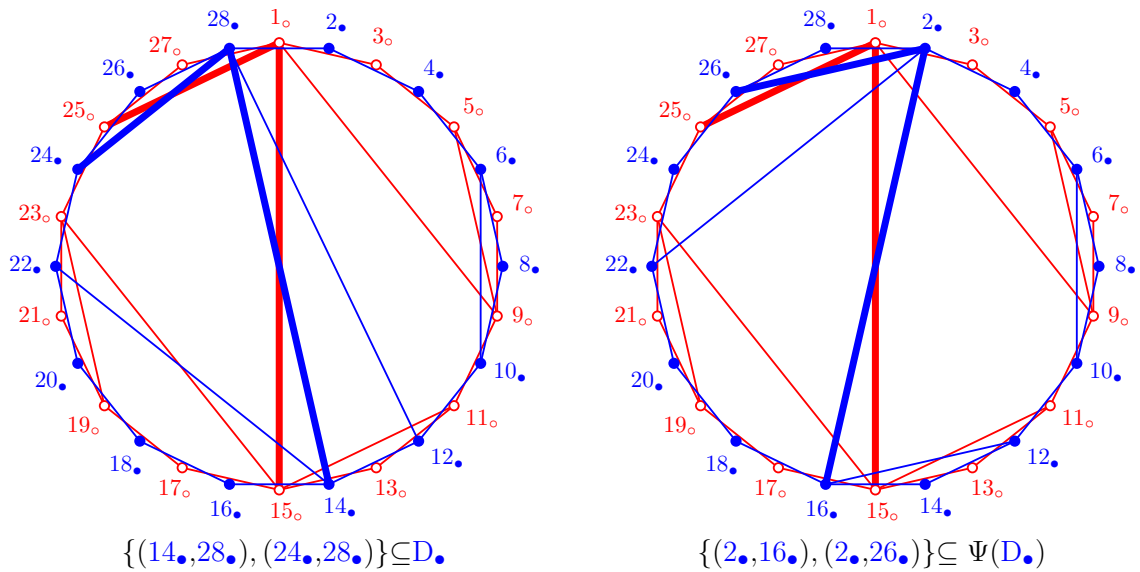
Figure 8.13 – A hollow dissection $D_\circ$, with a distinguished set $S_\circ = \{(1_\circ, 15_\circ), (1_\circ, 25_\circ)\}$ of (bold) diagonals. The bijection Ψ defined with respect to $S_\circ$ sends the $D_\circ$-accordion dissection $D_\bullet$ with 5 diagonals and containing $S_\bullet^- = \{(14_\bullet, 28_\bullet), (24_\bullet, 28_\bullet)\}$ (left) to the $D_\circ$-accordion dissection $\Psi(D_\bullet)$ with 5 diagonals and containing $S_\bullet^+ = \{(2_\bullet, 16_\bullet), (2_\bullet, 26_\bullet)\}$ (right). Notice that $D_\bullet$ also contains the diagonal $(14_\bullet, 22_\bullet)$ which is in $D_\bullet^-$, but that $\Psi(D_\bullet)$ does not contain $(16_\bullet, 24_\bullet)$. Conversely observe that $\Psi(D_\bullet)$ contains the diagonal $(12_\bullet, 16_\bullet)$ which is in $D_\bullet^+$ while $D_\bullet$ does not contain the corresponding diagonal $(10_\bullet, 14_\bullet)$ of $D_\bullet^-$. This is because Ψ is specifically defined with respect to the set $S_\circ$.

$\{(8_\bullet, 28_\bullet), (24_\bullet, 28_\bullet), (14_\bullet, 22_\bullet)\} \subseteq D_\bullet$ $\{(2_\bullet, 26_\bullet), (8_\bullet, 16_\bullet), (16_\bullet, 24_\bullet)\} \subseteq \Psi_{\Gamma_\circ}(D_\bullet)$
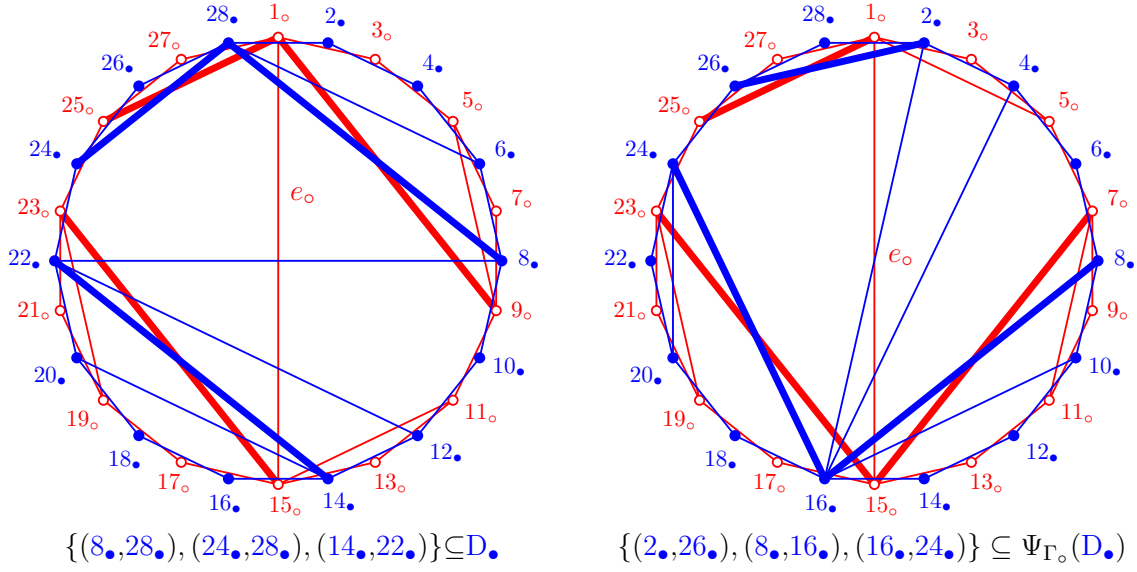
Figure 8.14 – A hollow dissection $D_\circ$ containing the diagonal $e_\circ = (1_\circ, 15_\circ)$ and the distinguished (bold) subset $S_\circ = \{(1_\circ, 9_\circ), (1_\circ, 25_\circ), (15_\circ, 23_\circ)\}$, together with a $D_\circ$-accordion dissections $D_\bullet$ containing the (bold) set $S_\bullet^- = \{(8_\bullet, 28_\bullet), (24_\bullet, 28_\bullet), (14_\bullet, 22_\bullet)\}$ (left); and the hollow dissection $\mathrm{tw}^{e_\circ}(D_\circ)$ together with the $\mathrm{tw}^{e_\circ}(D_\circ)$-accordion dissection $\Psi_{\Gamma_\circ}(D_\bullet)$ defined in the proof of Lemma 8.21 (right). The solid dissection $\Psi_{\Gamma_\circ}(D_\bullet)$ has $7 = |D_\bullet|$ diagonals and contains the (bold) set $\mathrm{tw}^{e_\circ}(S_\bullet)^+ = \{(2_\bullet, 26_\bullet), (8_\bullet, 16_\bullet), (16_\bullet, 24_\bullet)\}$.

initially forgotten diagonals. Our bijection is self-reverse, up to conjugation with a mirror symmetry. This can be checked on Figure 8.14, which illustrates this bijection in the generic case where the twist is done along an internal diagonal of $D_\circ$.

For the proof of Lemma 8.21, we recall that two diagonals cross if and only if they satisfy a (purely combinatorial) condition on the cyclic ordering of their vertices. All case analyses omitted in the proof rely on this description.

Proof of Lemma 8.21. Let $j_\circ$ be the hollow vertex such that $e_\circ = (1_\circ, j_\circ)$ and $S_\circ \subseteq D_\circ$ be a subset of hollow diagonals of $D_\circ$. We denote by $\Gamma_\circ$ the triple $(D_\circ, e_\circ, S_\circ)$ and define a bijection $\Psi_{\Gamma_\circ}$ between the $D_\circ$-accordion dissections with d diagonals containing $S_\bullet^-$ and the $\mathrm{tw}^{e_\circ}(D_\circ)$-accordion dissections with d diagonals containing $\mathrm{tw}^{e_\circ}(S_\bullet)^+$ as follows.

Let $D_\bullet$ be a $D_\circ$-accordion dissection with d diagonals containing $S_\bullet^-$. Let $x_\bullet$ (resp. $y_\bullet$) be the greatest vertex in $[2_\bullet, (j-1)_\bullet]_\bullet$ (resp. in $[(j+1)_\bullet, (2n)_\bullet]_\bullet$) such that $(x_\bullet, (2n)_\bullet) \in S_\bullet^- \cup \{(2_\bullet, (2n)_\bullet)\}$ (resp. $((j-1)_\bullet, y_\bullet) \in S_\bullet^- \cup \{((j-1)_\bullet, (j+1)_\bullet)\}$). We then define

$$D_\bullet^{\mathrm{rev}} := (D_\bullet \smallsetminus S_\bullet^-) \bigcap \left([2_\bullet, (j-1)_\bullet]_\bullet^2 \bigcup [2_\bullet, x_\bullet]_\bullet \times \{(2n)_\bullet\} \right),$$

$$D_\bullet^{\mathrm{id}} := (D_\bullet \smallsetminus S_\bullet^-) \bigcap \left([(j+1)_\bullet, (2n)_\bullet]_\bullet^2 \bigcup \{(j-1)_\bullet\} \times [(j+1)_\bullet, y_\bullet]_\bullet \right), \text{ and}$$

$$D_\bullet^{\mathrm{cr}} := D_\bullet \smallsetminus \left(S_\bullet^- \cup D_\bullet^{\mathrm{rev}} \cup D_\bullet^{\mathrm{id}} \right)$$

so that $D_\bullet = S_\bullet^- \sqcup D_\bullet^{\mathrm{rev}} \sqcup D_\bullet^{\mathrm{id}} \sqcup D_\bullet^{\mathrm{cr}}$. We define $\Psi_{\Gamma_\circ}$ separately on each of these sets of diagonals, starting with

$$\Psi_{\Gamma_\circ}(S_\bullet^-) := \mathrm{tw}^{e_\circ}(S_\bullet)^+ \quad \text{and} \quad \Psi_{\Gamma_\circ}(D_\bullet^{\mathrm{rev}}) := \{((j-\ell+1)_\bullet, (j-k+1)_\bullet) \mid (k_\bullet, \ell_\bullet) \in D_\bullet^{\mathrm{rev}}\}.$$

Let now

$$L_{\Gamma_\circ}^{\mathrm{id}}(D_\bullet) := \{[k_\bullet^1, \{\ell_\bullet^{1,1}, \dots, \ell_\bullet^{1,i_1}\}], \dots, [k_\bullet^r, \{\ell_\bullet^{r,1}, \dots, \ell_\bullet^{r,i_r}\}]\} \tag{8.1}$$

and

$$R^{\mathrm{id}}_{\Gamma_\circ}(\mathrm{D}_\bullet) := \{[q^1_\bullet, \{p^{1,1}_\bullet, \ldots, p^{1,j_1}_\bullet\}], \ldots, [q^s_\bullet, \{p^{1,1}_\bullet, \ldots, p^{1,j_s}_\bullet\}]\} \tag{8.2}$$

be the two *lexicographic descriptions* of the diagonals of $S^-_\bullet \cap [(j-1)_\bullet, (2n)_\bullet]^2_\bullet$ by their smallest and greatest endpoints respectively. Namely we require

  ◇ that $k^t_\bullet < \ell^{t,i}_\bullet$ for $t \in [r]$ and $i \in [i_t]$,

  ◇ that $\ell^{t,\alpha}_\bullet < \ell^{t,\beta}_\bullet$ for $t \in [r]$ and $1 \le \alpha < \beta \le i_t$,

  ◇ that $p^{t,j}_\bullet < q^t_\bullet$ for $t \in [s]$ and $j \in [j_t]$,

  ◇ that $p^{t,\alpha}_\bullet < p^{t,\beta}_\bullet$ for $t \in [s]$ and $1 \le \alpha < \beta \le j_t$ and

  ◇ that $S^-_\bullet \cap [(j-1)_\bullet, (2n)_\bullet]^2_\bullet = \{(k^t_\bullet, \ell^{t,i}_\bullet) \,|\, t \in [r], i \in [i_t]\} = \{(p^{t,j}_\bullet, q^t_\bullet) \,|\, t \in [s], j \in [j_t]\}$.

For a diagonal $(a_\bullet, b_\bullet)$ (with $a_\bullet < b_\bullet$) in $\mathrm{D}^{\mathrm{id}}_\bullet$, let $\varphi^{\mathrm{id}}(a_\bullet, b_\bullet) := (\phi^{0,\mathrm{id}}(a_\bullet), \phi^{1,\mathrm{id}}(b_\bullet))$ where

$$\phi^{0,\mathrm{id}}(a_\bullet) := \begin{cases} (p^{t,1}+2)_\bullet & \text{if } a_\bullet = q^t_\bullet \text{ and } q^t_\bullet \notin \{k^\alpha_\bullet \,|\, \alpha \in [r]\}, \\ (p^{t,1}+2)_\bullet & \text{if } a_\bullet = q^t_\bullet = k^\alpha_\bullet \text{ and } \ell^{\alpha,i_\alpha}_\bullet < b_\bullet, \\ (\ell^{t,i}+2)_\bullet & \text{if } a_\bullet = k^t_\bullet \text{ and } \ell^{t,i-1}_\bullet < b_\bullet < \ell^{t,i}_\bullet \text{ (with the convention } \ell^{t,0}_\bullet = k^t_\bullet), \\ a_\bullet & \text{otherwise} \end{cases}$$

and

$$\phi^{1,\mathrm{id}}(b_\bullet) := \begin{cases} (p^{t,i}+2)_\bullet & \text{if } b_\bullet = q^t_\bullet \text{ and } p^{t,i-1}_\bullet < a_\bullet < p^{t,i}_\bullet \text{ (with the convention } p^{t,0}_\bullet = 2_\bullet), \\ b_\bullet & \text{otherwise.} \end{cases}$$

A case analysis shows that the pairs $(\phi^{0,\mathrm{id}}(a_\bullet), \phi^{1,\mathrm{id}}(b_\bullet))$ for $(a_\bullet, b_\bullet) \in \mathrm{D}^{\mathrm{id}}_\bullet$ are distinct noncrossing internal solid diagonals with endpoints in $\{2_\bullet\} \cup [(j+1)_\bullet, (2n)_\bullet]_\bullet$. We let

$$\Psi_{\Gamma_\circ}(\mathrm{D}^{\mathrm{id}}_\bullet) := \{\varphi^{\mathrm{id}}(a_\bullet, b_\bullet) \,|\, (a_\bullet, b_\bullet) \in \mathrm{D}^{\mathrm{id}}_\bullet\}.$$

Finally let $x_\bullet = u^0_\bullet < \cdots < u^{\lambda+1}_\bullet = (j-1)_\bullet$ and $y_\bullet = v^{\eta+1}_\bullet < \cdots < v^0_\bullet = (2n)_\bullet$ be the vertices such that $\{u^i_\bullet \,|\, i \in [\lambda]\} \cup \{v^i_\bullet \,|\, i \in [\eta]\}$ are the endpoints of diagonals in $\mathrm{D}^{\mathrm{cr}}_\bullet$. The dissection $\mathrm{D}^{\mathrm{cr}}_\bullet$ is characterized by these endpoints together with the numbers c^α and d^β of its diagonals respectively incident to $u^\alpha_\bullet$ and $v^\beta_\bullet$ for all $\alpha \in [0, \lambda+1]$ and $\beta \in [0, \eta+1]$. For $i \in [0, \eta+1]$ let

$$\phi^{\mathrm{cr}}(v^i_\bullet) := \begin{cases} (p^{t,1}+2)_\bullet & \text{if } v^i_\bullet = q^t_\bullet, \\ v^i_\bullet & \text{otherwise.} \end{cases}$$

Then we define $\Psi_\Gamma(\mathrm{D}^{\mathrm{cr}}_\bullet)$ to be the dissection containing c^α diagonals incident to $(j+1-u^{\lambda+1-\alpha})_\bullet$ and d^β diagonals incident to $\phi^{\mathrm{cr}}(v^\beta_\bullet)$ for all $\alpha \in [0, \lambda+1]$ and $\beta \in [0, \eta+1]$.

We finally set

$$\Psi_{\Gamma_\circ}(\mathrm{D}_\bullet) := \Psi_{\Gamma_\circ}(\mathrm{S}^-_\bullet) \cup \Psi_{\Gamma_\circ}(\mathrm{D}^{\mathrm{rev}}_\bullet) \cup \Psi_{\Gamma_\circ}(\mathrm{D}^{\mathrm{id}}_\bullet) \cup \Psi_{\Gamma_\circ}(\mathrm{D}^{\mathrm{cr}}_\bullet).$$

Observe that the way we defined $\Psi_{\Gamma_\circ}(\mathrm{D}_\bullet)$ induces a natural function from the diagonals of $\mathrm{D}_\bullet$ onto those of $\Psi_{\Gamma_\circ}(\mathrm{D}_\bullet)$. A case analysis shows that the four sets that we use to define $\Psi_{\Gamma_\circ}(\mathrm{D}_\bullet)$ are disjoint dissections, and that diagonals between two of them also do not cross, so that $\Psi_{\Gamma_\circ}(\mathrm{D}_\bullet)$ is a dissection. Moreover the function from the diagonals of $\mathrm{D}_\bullet$ onto those of $\Psi_{\Gamma_\circ}(\mathrm{D}_\bullet)$ is clearly into on each of these four sets, so that $\Psi_{\Gamma_\circ}(\mathrm{D}_\bullet)$ has d diagonals and contains $\mathrm{tw}^{e_\circ}(\mathrm{S}_\bullet)^+$. Therefore, we only need to show that any diagonal of $\Psi_{\Gamma_\circ}(\mathrm{D}_\bullet)$ is a $\mathrm{tw}^{e_\circ}(\mathrm{D}_\bullet)$-accordion to conclude that $\Psi_{\Gamma_\circ}$ is well-defined. It is trivial for $\Psi_{\Gamma_\circ}(\mathrm{S}^-_\bullet)$ and easily settled for diagonals in $\Psi_{\Gamma_\circ}(\mathrm{D}^{\mathrm{rev}}_\bullet)$ and $\Psi_{\Gamma_\circ}(\mathrm{D}^{\mathrm{id}}_\bullet)$, by two straightforward case analyses. Observe finally that the diagonals of $\Psi_{\Gamma_\circ}(\mathrm{D}^{\mathrm{cr}}_\bullet)$ cross accordions

obtained by gluing together (along their common diagonal $e_\circ$) "halves" of accordions, that are obtained by applying either a mirror symmetry or an operation similar to this applied to $D_\bullet^{\mathrm{id}}$ to the diagonals of $D_\bullet^{\mathrm{cr}}$.

Let $\Phi : i \mapsto j + 1 - i$. We define the triple $\bar{\Gamma}_\circ := (\Phi(\mathrm{tw}^{e_\circ}(D_\circ)), e_\circ, \Phi(\mathrm{tw}^{e_\circ}(S_\circ)))$ and claim that $\Phi \circ \Psi_{\bar{\Gamma}_\circ} \circ \Phi$ is the reverse function $\Psi_{\Gamma_\circ}^{-1}$. This can be shown separately by case analyses on each set $D_\bullet^{\mathrm{rev}}, D_\bullet^{\mathrm{id}}$ and $D_\bullet^{\mathrm{cr}}$, remarking that $\Phi(\Psi_{\Gamma_\circ}(D_\bullet^{\mathrm{rev}})) = \Phi(\Psi_{\Gamma_\circ}(D_\bullet))^{\mathrm{rev}}$, that $\Phi(\Psi_{\Gamma_\circ}(D_\bullet^{\mathrm{id}})) = \Phi(\Psi_{\Gamma_\circ}(D_\bullet))^{\mathrm{id}}$ and that $\Phi(\Psi_{\Gamma_\circ}(D_\bullet^{\mathrm{cr}})) = \Phi(\Psi_{\Gamma_\circ}(D_\bullet))^{\mathrm{cr}}$. The claim is clear for $D_\bullet^{\mathrm{rev}}$ and $D_\bullet^{\mathrm{cr}}$, and the argument for the set $D_\bullet^{\mathrm{id}}$ is based on the observation that the sets defined in Equations (8.1) and (8.2) in this case are respectively given by

$$L_{\bar{\Gamma}_\circ}^{\mathrm{id}}(\Phi(\Psi_{\Gamma_\circ}(D_\bullet))) = \rho \circ \Phi(R_{\bar{\Gamma}_\circ}^{\mathrm{id}}(D_\bullet)) \quad \text{and} \quad R_{\bar{\Gamma}_\circ}^{\mathrm{id}}(\Phi(\Psi_{\Gamma_\circ}(D_\bullet))) = \rho \circ \Phi(L_{\bar{\Gamma}_\circ}^{\mathrm{id}}(D_\bullet))$$

where ρ denotes the rotation $i \mapsto i - 2$. ∎

Theorem 8.19 follows from Lemma 8.21 and inclusion-exclusion principle. For a hollow dissection $D_\circ$ and a set $S_\bullet^-$ of minimal $D_\circ$-accordion diagonals, we define

$$F_{S_\bullet^-}^=(D_\circ) := \# \left(D_\circ\text{-accordion dissections } D_\bullet \text{ such that } |D_\bullet| = d \text{ and } D_\bullet \cap D_\bullet^- = S_\bullet^- \right).$$

Proof of Theorem 8.19. For $S_\circ \subseteq D_\circ$, we can apply Lemma 8.21 to the diagonal $(1_\circ, 3_\circ)$ of any hollow dissection $D_\circ$. We obtain by Remark 8.17 that

$$F_{S_\bullet^-}(D_\circ) = F_{S_\bullet^+}(D_\circ).$$

As twisting along a diagonal is self-reverse, applying Lemma 8.21 to $\mathrm{tw}^{e_\circ}(D_\circ)$ thus yields

$$F_{S_\bullet^+}(D_\circ) = F_{\mathrm{tw}^{e_\circ}(S_\bullet)^-}(\mathrm{tw}^{e_\circ}(D_\circ)),$$

so that

$$F_{S_\bullet^-}(D_\circ) = F_{\mathrm{tw}^{e_\circ}(S_\bullet)^-}(\mathrm{tw}^{e_\circ}(D_\circ)). \tag{8.3}$$

Now by inclusion-exclusion principle, we have that

$$F_{S_\bullet^-}^=(D_\circ) = \sum_{\substack{S_\circ \subseteq S_\circ' \subseteq D_\circ \\ |S_\circ' \smallsetminus S_\circ| = k}} (-1)^k \, F_{S_\bullet'^-}(D_\circ).$$

Applying this equation also to $\mathrm{tw}^{e_\circ}(D_\circ)$, we obtain by Equation (8.3) that

$$F_{S_\bullet^-}^=(D_\circ) = F_{\mathrm{tw}^{e_\circ}(S_\bullet)^-}^=(\mathrm{tw}^{e_\circ}(D_\circ)). \tag{8.4}$$

Notice then that for any integer r, we have

$$F_r^d(D_\circ) = \sum_{\substack{S_\circ \subseteq D_\circ \\ |S_\circ| = r}} F_{S_\bullet^-}^=(D_\circ) \quad \text{and} \quad F_r^d(\mathrm{tw}^{e_\circ}(D_\circ)) = \sum_{\substack{S_\circ \subseteq D_\circ \\ |S_\circ| = r}} F_{\mathrm{tw}^{e_\circ}(S_\bullet)^-}^=(D_\circ).$$

By Equation (8.4), this finally implies that

$$F_r^d(D_\circ) = F_r^d(\mathrm{tw}^{e_\circ}(D_\circ)). \quad ∎$$

8.4   Connections with subword complexes

As mentioned in Chapter 7, our original motivation for looking at accordion complexes is a question of F. Chapoton, who asked whether *Stokes complexes* (accordion complexes of reference quadrangulations) were subword complexes. It first seemed to be the case for an important subfamily, but it appears now quite clearly that the intersection is not as big as we initially expected. We would now be interested in a simple characterization of this intersection. We conclude this chapter with a few connections.

We originally expected accordion complexes of quadrangulations without interior quadrangle to be root-independent subword complexes (see Section 7.4). It is the case in small dimensions. On the other hand one can computationally check that the accordion complex of the unique quadrangulation Q_{int} of an 12-gon with an interior quadrangle is not a subword complex, so that neither is any quadrangulation with an interior quadrangle. Indeed the accordion complex $\mathcal{AC}(Q_{\mathrm{int}})$ is the join of a face in any accordion complex $\mathcal{AC}(Q)$ of such a quadrangulation Q, while root-independent subword complexes are closed by joins. Our first experiments thus initially indicated a new combinatorial representation for a subfamily of flag subword complexes. Another relevant support for this idea was the fact that the only class of quadrangulations not encoding subword complexes would in addition have been the only one for which the d-vector construction of Section 9.3 does not work. However we have now strong evidences that the accordion complex of the quadrangulation of Figure 8.15 is not isomorphic to any subword complex, for the following reasons.

As explained in Chapter 10, there are natural operations on words whose effects induced on the corresponding subword complexes are stellar subdivisions and reverse stellar subdivisions of edges (see Theorem 10.9 due to M. Gorsky [Gor14]). So it is tempting to look for analogous operations on dissections that induce analogous effects on the corresponding accordion complexes. We expect the two operations on quadrangulations informally illustrated in Figure 8.16 to be the only ones with this property. Observe that none of them can be applied to the quadrangulation of Figure 8.15.

Conjecture 8.22. *If a quadrangulation $Q_\circ$ is obtained from another one Q, whose dual tree is a path, by a sequence of successive operations described in Figure 8.16, then the accordion complex $\mathcal{AC}(Q_\circ)$ is isomorphic to a root-independent subword complex.*

In view of Theorem 9.33, a proof of Conjecture 8.22 would provide us with new serious insights towards a d-vector construction for root-independent subword complexes.
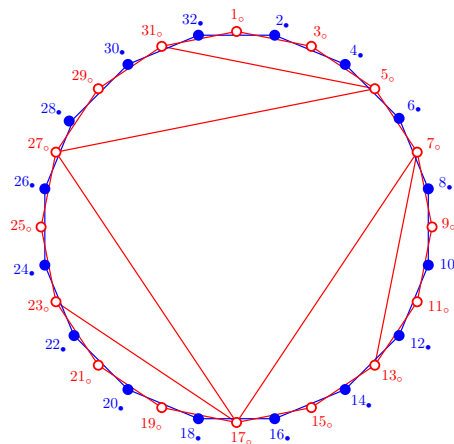
Figure 8.15 – A quadrangulation $Q_\circ$ without interior quadrangle for which we conjecture that $\mathcal{AC}(Q_\circ)$ is not isomorphic to a flag subword complex.
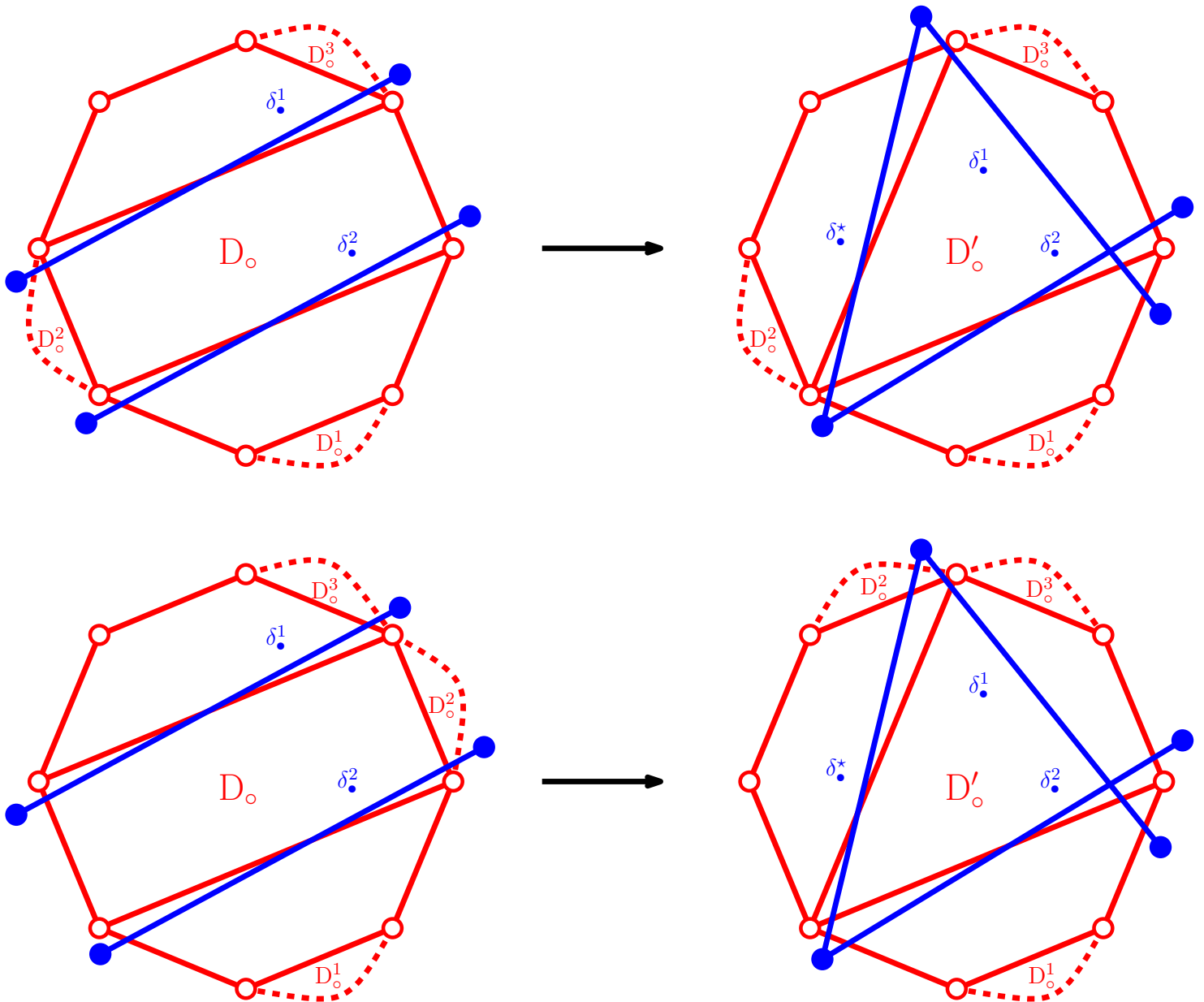
Figure 8.16 – Two operations on hollow quadrangulations inducing stellar subdivisions on the corresponding accordion complexes. For both operations the complex $\mathcal{AC}(D'_\circ)$ is isomorphic to the stellar subdivision of the edge $\{\delta^1_\bullet, \delta^2_\bullet\}$ in $\mathcal{AC}(D_\circ)$, where the introduced subdivision vertex is identified to the diagonal $\delta^\star_\bullet$.

9

Geometric realizations of accordion complexes

9.1 Introduction

9.1.1 Motivations

In this chapter, we settle the geometric challenge of F. Chapoton on accordion complexes studied in Chapter 8, namely we provide polytopal and fan realizations for them. The original reasons that lead us to look at these complexes are discussed in Sections 7.1 and the interest that they have by themselves is given in Section 8.1.1. We present three methods to realize accordion complexes, based on constructions of the associahedron.

Our first construction generalizes the g-vector fan. It belongs to a series of constructions of associahedra initiated by S. Shnider and S. Sternberg [SS93], popularised by J.-L. Loday [Lod04], and developed by C. Hohlweg, C. Lange and H. Thomas [HL07, HLT11] using works of N. Reading and D. Speyer [Rea06, Rea07, RS09]. It was revisited by S. Stella [Ste13] and by V. Pilaud, F. Santos, and C. Stump [PS12, PS15a]. It was extended by C. Hohlweg, V. Pilaud, and S. Stella [HPS16] to construct an associahedron parametrized by any initial triangulation. We extend to accordion complexes the g-vectors and c-vectors, defined in the context of cluster algebras by S. Fomin and A. Zelevinski [FZ07], and show that the g-vectors with respect to a dissection $D_\circ$ support a complete simplicial fan realizing the accordion complex $\mathcal{AC}(D_\circ)$. It is the normal fan of a polytope obtained by deleting facets of the Minkowski sum of all c-vectors.

Our second method generalizes the d-vector fan. For any dissection $D_\circ$, we associate to each diagonal a d-vector which records the crossings of this diagonal with those of $D_\bullet^-$. The d-vectors then support a complete simplicial fan realizing $\mathcal{AC}(D_\circ)$ if and only if $D_\circ$ contains no even interior cell. The polytopality of the resulting fan is known for initial triangulations [CSZ15], but remains open in general.

Finally, our third method is based on projections of associahedra. Namely, for any dissection $D_\circ$ and triangulation $T_\circ$ such that $D_\circ \subseteq T_\circ$, the accordion complex $\mathcal{AC}(D_\circ)$ is a subcomplex of the simplicial associahedron $\mathcal{AC}(T_\circ)$ and the g-vector fan realizing $\mathcal{AC}(D_\circ)$ can be obtained as a section of the classical g-vector fan of $T_\circ$ by a coordinate subspace. Therefore, the accordion complex $\mathcal{AC}(D_\circ)$ is realized by a projection of an associahedron realized in [HPS16]. This leads to more concise proofs of combinatorial properties of accordion complexes, and to natural conjectures on cluster algebras, subcomplexes of cluster complexes, and sections of the g-vector fan.

9.1.2   Overview

The chapter is organized as follows. Section 9.2 is devoted to the generalization of the g-vector fan and the associahedra of [HL07, HPS16]. Section 9.3 discusses the generalization of the construction of the d-vector fan and associahedra of [FZ03a, CSZ15]. Finally, Section 9.4 shows that the accordion complex is realized by a projection of a well-chosen associahedron and presents related conjectures on cluster algebras.

9.2   The g-vector fan

In this Section, we construct accordiohedra using g- and c-vectors. Our construction is in the same spirit as the Cambrian fans of N. Reading and D. Speyer [Rea06, Rea07, RS09] and their polytopal realizations by C. Hohlweg, C. Lange and H. Thomas [HL07, HLT11], recently extended in [HPS16] to any initial triangulation, acyclic or not. A different approach to the g-vector fan together with an alternative polytopal realization will be presented in Section 9.4.

9.2.1   g- and c-vectors

Consider a hollow dissection $D_\circ$ and a solid dissection $D_\bullet$ that are maximal accordion dissection of each other (see Proposition 8.14), and let $\delta_\circ \in D_\circ$ and $\delta_\bullet \in D_\bullet$. When $\delta_\circ$ crosses $\delta_\bullet$, we let $\mu_\circ$ and $\nu_\circ$ be the other diagonals of $\bar{D}_\circ$ crossed by $\delta_\bullet$ in the two cells of $D_\circ$ containing $\delta_\circ$. We say that $\delta_\bullet$ *slaloms* on $\delta_\circ$ if $\mu_\circ\delta_\circ\nu_\circ$ forms a path, and we define $\varepsilon_\circ(\delta_\circ \in D_\circ \mid \delta_\bullet)$ to be 1, -1, or 0 depending on whether $\mu_\circ\delta_\circ\nu_\circ$ forms a Z, a Ƨ, or a V. Similarly we let $\mu_\bullet$ and $\nu_\bullet$ be the other diagonals of $\bar{D}_\bullet$ crossed by $\delta_\circ$ in the two cells of $D_\bullet$ containing $\delta_\bullet$, we say that $\delta_\circ$ slaloms on $\delta_\bullet$ if $\mu_\bullet\delta_\bullet\nu_\bullet$ forms a path, and we define $\varepsilon_\bullet(\delta_\circ \mid \delta_\bullet \in D_\bullet)$ to be 1, -1, or 0 depending on whether $\mu_\bullet\delta_\bullet\nu_\bullet$ forms a Ƨ, a Z, or a V. Note that the sign convention for $\varepsilon_\circ(\delta_\circ \in D_\circ \mid \delta_\bullet)$ and $\varepsilon_\bullet(\delta_\circ \mid \delta_\bullet \in D_\bullet)$ is opposite: the reciprocity already observed in Proposition 8.14 naturally reverses the orientation. More informally, we exchange the role of hollow and solid dissections by looking at the picture from the opposite side of the blackboard, which of course reverses the orientation. Finally, if $\delta_\circ$ and $\delta_\bullet$ do not cross, then we let $\varepsilon_\circ(\delta_\circ \in D_\circ \mid \delta_\bullet) = \varepsilon_\bullet(\delta_\circ \mid \delta_\bullet \in D_\bullet) = 0$.

Let $(\mathbf{e}_{\delta_\circ})_{\delta_\circ\in D_\circ}$ denote the canonical basis of $\mathbb{R}^{D_\circ}$. As in [HPS16], we define the following vectors:

(i) the g-*vector* of $\delta_\bullet$ with respect to $D_\circ$ is $\mathbf{g}(D_\circ \mid \delta_\bullet) := \sum_{\delta_\circ\in D_\circ} \varepsilon_\circ(\delta_\circ \in D_\circ \mid \delta_\bullet)\,\mathbf{e}_{\delta_\circ}$. We also define $\mathbf{g}(D_\circ \mid D_\bullet) := \{\mathbf{g}(D_\circ \mid \delta_\bullet) \mid \delta_\bullet \in D_\bullet\}$.

(ii) the c-*vector* of $\delta_\bullet \in D_\bullet$ with respect to $D_\circ$ is $\mathbf{c}(D_\circ \mid \delta_\bullet \in D_\bullet) := \sum_{\delta_\circ\in D_\circ} \varepsilon_\bullet(\delta_\circ \mid \delta_\bullet \in D_\bullet)\,\mathbf{e}_{\delta_\circ}$. We denote by $\mathbf{c}(D_\circ \mid D_\bullet) := \{\mathbf{c}(D_\circ \mid \delta_\bullet \in D_\bullet) \mid \delta_\bullet \in D_\bullet\}$ the set of c-vectors of the diagonals of $D_\bullet$ and by $\mathbf{C}(D_\circ) := \bigcup_{D_\bullet} \mathbf{c}(D_\circ \mid D_\bullet)$ the set of all c-vectors with respect to $D_\circ$.

Example 9.1. Consider the hollow dissection $D_\circ^{\mathrm{ex}} = \{(3_\circ, 7_\circ), (3_\circ, 13_\circ), (9_\circ, 13_\circ)\}$ and the rightmost solid dissection $D_\bullet^{\mathrm{ex}} = \{(2_\bullet, 6_\bullet), (2_\bullet, 10_\bullet), (10_\bullet, 14_\bullet)\}$ of Figure 8.2. Then we have for example

    ⋄ $\varepsilon_\circ\big((3_\circ, 13_\circ) \in D_\circ^{\mathrm{ex}} \mid (2_\bullet, 10_\bullet)\big) = 1$ since the path $1_\circ - 3_\circ - 13_\circ - 9_\circ$ forms a Z,

    ⋄ $\varepsilon_\circ\big((9_\circ, 13_\circ) \in D_\circ^{\mathrm{ex}} \mid (2_\bullet, 10_\bullet)\big) = -1$ since the path $3_\circ - 13_\circ - 9_\circ - 11_\circ$ forms a Ƨ, and

    ⋄ $\varepsilon_\circ\big((3_\circ, 13_\circ) \in D_\circ^{\mathrm{ex}} \mid (2_\bullet, 6_\bullet)\big) = 0$ since $3_\circ$ connects $1_\circ, 13_\circ, 7_\circ$ as a V.

Moreover, we have

$$\mathbf{g}\big(D_\circ^{ex}\,|\,(2_\bullet,6_\bullet)\big) = \mathbf{e}_{(3_\circ,7_\circ)}, \qquad\qquad \mathbf{c}\big(D_\circ^{ex}\,|\,(2_\bullet,6_\bullet) \in D_\bullet^{ex}\big) = \mathbf{e}_{(3_\circ,7_\circ)},$$
$$\mathbf{g}\big(D_\circ^{ex}\,|\,(2_\bullet,10_\bullet)\big) = \mathbf{e}_{(3_\circ,13_\circ)} - \mathbf{e}_{(9_\circ,13_\circ)}, \quad \mathbf{c}\big(D_\circ^{ex}\,|\,(2_\bullet,10_\bullet) \in D_\bullet^{ex}\big) = \mathbf{e}_{(3_\circ,13_\circ)},$$
$$\mathbf{g}\big(D_\circ^{ex}\,|\,(10_\bullet,14_\bullet)\big) = -\mathbf{e}_{(9_\circ,13_\circ)}, \qquad \mathbf{c}\big(D_\circ^{ex}\,|\,(10_\bullet,14_\bullet) \in D_\bullet^{ex}\big) = -\mathbf{e}_{(3_\circ,13_\circ)} - \mathbf{e}_{(9_\circ,13_\circ)}.$$

Example 9.2. For any hollow diagonal $(i_\circ, j_\circ) \in D_\circ$, we have

$$\mathbf{g}\big(D_\circ\,|\,((i-1)_\bullet,(j-1)_\bullet)\big) = -\mathbf{e}_{(i_\circ,j_\circ)}, \qquad \mathbf{c}\big(D_\circ\,|\,((i-1)_\bullet,(j-1)_\bullet) \in D_\bullet^-\big) = -\mathbf{e}_{(i_\circ,j_\circ)},$$
$$\mathbf{g}\big(D_\circ\,|\,((i+1)_\bullet,(j+1)_\bullet)\big) = \mathbf{e}_{(i_\circ,j_\circ)}, \qquad \mathbf{c}\big(D_\circ\,|\,((i+1)_\bullet,(j+1)_\bullet) \in D_\bullet^+\big) = \mathbf{e}_{(i_\circ,j_\circ)}.$$

Remark 9.3. For a hollow triangulation $T_\circ$, our definitions of $\mathbf{g}$- and $\mathbf{c}$-vectors coincide with the shear coordinates of S. Fomin and D. Thurston [FT12] (defined in the much more general context of triangulations and laminations on marked surfaces).

Remark 9.4. Consider the quiver $Q(D_\circ)$ of the reference dissection $D_\circ$, with one node on each internal diagonal of $D_\circ$ and one arrow between two diagonals counterclockwise consecutive around a cell of $D_\circ$. Let $W(D_\circ)$ be the reflection group with Dynkin diagram $Q(D_\circ)$. Then all $\mathbf{g}$-vectors of the $D_\circ$-accordion diagonals are weights of $W(D_\circ)$ and all $\mathbf{c}$-vectors of $\mathbf{C}(D_\circ)$ are roots of $W(D_\circ)$.

Remark 9.5. Informally, the $\mathbf{g}$- and $\mathbf{c}$-vectors can be interpreted as follows:

(i) The $\mathbf{g}$-vector $\mathbf{g}(D_\circ\,|\,\delta_\bullet)$ has coordinate 1 and -1 alternating along the zigzag of the accordion crossed by $\delta_\bullet$ in $D_\circ$, and coordinate 0 on all other diagonals of $D_\circ$.

(ii) The $\mathbf{c}$-vector $\mathbf{c}(D_\circ\,|\,\delta_\bullet \in D_\bullet)$ is, up to a sign, the characteristic vector of the diagonals of the subaccordion of $D_\circ$ crossed by both $\mu_\bullet$ and $\nu_\bullet$ of Lemma 8.9 (see Figure 8.4). Thus, any $\mathbf{c}$-vector is either *positive* (only nonnegative coordinates) or *negative* (only nonpositive coordinates).

In fact, the $\mathbf{g}$-vectors are clearly in bijection with the accordions and with the zigzags in $D_\circ$. In contrast, many $\delta_\bullet \in D_\bullet$ produce the same $\mathbf{c}$-vector $\mathbf{c}(D_\circ\,|\,\delta_\bullet \in D_\bullet)$. For example, if two dissections $D_\bullet, D_\bullet'$ contain $\delta_\bullet$ and have the same cells incident to $\delta_\bullet$, then $\mathbf{c}(D_\circ\,|\,\delta_\bullet \in D_\bullet) = \mathbf{c}(D_\circ\,|\,\delta_\bullet \in D_\bullet')$. The set of $\mathbf{c}$-vectors $\mathbf{C}(D_\circ)$ without repetitions can be understood as follows.

Lemma 9.6. *There are bijections between:*

◇ *the negative (resp. positive) $\mathbf{c}$-vectors of $\mathbf{C}(D_\circ)$,*

◇ *the subaccordions of $D_\circ$,*

◇ *the $D_\circ$-accordion diagonals not in $D_\bullet^- := \{((i-1)_\bullet,(j-1)_\bullet)\,|\,(i_\circ,j_\circ) \in D_\circ\}$ (resp. not in $D_\bullet^+ := \{((i+1)_\bullet,(j+1)_\bullet)\,|\,(i_\circ,j_\circ) \in D_\circ\}$).*

Proof. By Remark 9.5 (ii), the support of any $\mathbf{c}$-vector is a subaccordion of $D_\circ$. Reciprocally, let $A_\circ$ be a subaccordion of $D_\circ$, let $C_\circ$ and $C_\circ'$ denote the two cells of $D_\circ$ containing exactly one diagonal of $A_\circ$, and let $p_\circ, q_\circ, r_\circ, s_\circ$ (resp. $p_\circ', q_\circ', r_\circ', s_\circ'$) denote the four consecutive vertices in clockwise order around $C_\circ$ (resp. around $C_\circ'$) such that $(q_\circ, r_\circ)$ (resp. $(q_\circ', r_\circ')$) is the diagonal of $A_\circ$ in $C_\circ$ (resp. in $C_\circ'$). Let $\delta_\bullet := ((s-1)_\bullet,(s'-1)_\bullet)$, $\mu_\bullet := ((p+1)_\bullet,(s'-1)_\bullet)$ and $\nu_\bullet := ((p'+1)_\bullet,(s-1)_\bullet)$ and consider any $D_\circ$-accordion dissection $D_\bullet$ containing $\{\mu_\bullet, \delta_\bullet, \nu_\bullet\}$. Then $A_\circ$ is precisely the support of the negative $\mathbf{c}$-vector $\mathbf{c}(D_\circ\,|\,\delta_\bullet \in D_\bullet)$. Finally, we have associated to the subaccordion $A_\circ$ of $D_\circ$ a $D_\circ$-diagonal $\delta_\bullet = ((s-1)_\bullet,(s'-1)_\bullet)$ which cannot be in $D_\bullet^-$ as otherwise $(s_\circ, s_\circ')$ would cross $(q_\circ, r_\circ)$. Reciprocally, $A_\circ$ is precisely the set of diagonals of $D_\circ$ crossed by $\delta_\bullet$ and not incident to $s_\circ$ or $s_\circ'$. ∎

The g-vectors and c-vectors are connected in the following two statements, inspired and motivated by a classical analogy in cluster algebra theory.

Proposition 9.7. *For any maximal* $D_\circ$*-accordion dissection* $D_\bullet$*, the set of* g*-vectors* $\mathbf{g}(D_\circ \,|\, D_\bullet)$ *and the set of* c*-vectors* $\mathbf{c}(D_\circ \,|\, D_\bullet)$ *form dual bases.*

Proof. For solid diagonals $\gamma_\bullet, \delta_\bullet$ of $D_\bullet$, we compute $\langle \mathbf{g}(D_\circ \,|\, \gamma_\bullet) | \mathbf{c}(D_\circ \,|\, \delta_\bullet \in D_\bullet) \rangle$. By Remark 9.5 (i), the g-vector $\mathbf{g}(D_\circ \,|\, \gamma_\bullet)$ has coordinate ± 1 alternating along the zigzag $Z_\circ$ of the accordion crossed by $\gamma_\bullet$ in $D_\circ$, and coordinate 0 on all other diagonals of $D_\circ$. Moreover, by Remark 9.5 (ii), the c-vector $\mathbf{c}(D_\circ \,|\, \delta_\bullet \in D_\bullet)$ has coordinate ± 1 on the diagonals of $D_\circ$ which slalom on $\delta_\bullet$ in $D_\bullet$, and coordinate 0 on all other diagonals of $D_\circ$. We thus need to understand how the diagonals of $Z_\circ$ slalom on $\delta_\bullet$ in $D_\bullet$. Observe that there is an even (resp. odd) number of hollow diagonals of $Z_\circ$ that slalom on $\delta_\bullet$ when $\delta_\bullet \neq \gamma_\bullet$ (resp. when $\delta_\bullet = \gamma_\bullet$). Moreover, since they are noncrossing, all hollow diagonals of $Z_\circ$ slaloming on $\delta_\bullet$ do it the same way (either all as a Σ or all as a Z). Finally, when $\gamma_\bullet = \delta_\bullet$, consider the first hollow diagonal $\delta_\circ$ of the zigzag $Z_\circ$ which slaloms on $\delta_\bullet$. Then $\delta_\circ$ slaloms on $\delta_\bullet$ in the opposite way as $\delta_\bullet$ slaloms on $\delta_\circ$. This shows that

$$\langle \mathbf{g}(D_\circ \,|\, \gamma_\bullet) | \mathbf{c}(D_\circ \,|\, \delta_\bullet \in D_\bullet) \rangle = \sum_{\delta_\circ \in D_\circ} \varepsilon_\circ(\delta_\circ \in D_\circ \,|\, \gamma_\bullet) \cdot \varepsilon_\bullet(\delta_\circ \,|\, \delta_\bullet \in D_\bullet) = \mathbb{1}_{\gamma = \delta},$$

since we sum an even number of alternating ± 1 when $\gamma_\bullet \neq \delta_\bullet$, and an odd number of alternating ± 1 starting by a 1 when $\gamma_\bullet \neq \delta_\bullet$. In other words, $\mathbf{g}(D_\circ \,|\, D_\bullet)$ and $\mathbf{c}(D_\circ \,|\, D_\bullet)$ form dual bases.   ∎

Proposition 9.8. *Let* $D_\circ$ *be a hollow dissection and* $D_\bullet$ *be a solid dissection such that* $D_\circ$ *and* $D_\bullet$ *are maximal accordion dissection of each other (see Proposition 8.14). Then*

$$\mathbf{g}(D_\circ \,|\, D_\bullet) = -\mathbf{c}(D_\bullet \,|\, D_\circ)^t \qquad and \qquad \mathbf{c}(D_\circ \,|\, D_\bullet) = -\mathbf{g}(D_\bullet \,|\, D_\circ)^t,$$

where we consider the sets of g*-vectors* $\mathbf{g}(D_\circ \,|\, D_\bullet)$ *and* c*-vectors* $\mathbf{c}(D_\circ \,|\, D_\bullet)$ *as matrices in* $\mathbb{R}^{D_\circ \times D_\bullet}$*, and* M^t *denotes the transpose of a matrix* M*.*

Proof. We immediately derive from the definitions that for any $\delta_\circ \in D_\circ$ and $\delta_\bullet \in D_\bullet$,

$$\mathbf{g}(D_\circ \,|\, D_\bullet)_{(\delta_\circ, \delta_\bullet)} = \varepsilon_\circ(\delta_\circ \in D_\circ \,|\, \delta_\bullet) = -\varepsilon_\bullet(\delta_\bullet \,|\, \delta_\circ \in D_\circ) = -\mathbf{c}(D_\bullet \,|\, D_\circ)_{(\delta_\bullet, \delta_\circ)},$$

which shows $\mathbf{g}(D_\circ \,|\, D_\bullet) = -\mathbf{c}(D_\bullet \,|\, D_\circ)^t$. The other equality follows by exchanging $D_\circ$ and $D_\bullet$.   ∎

Corollary 9.9. *For any maximal* $D_\circ$*-accordion dissection* $D_\bullet$*, we have the following* sign coherence*:*

   (i) for any $\delta_\bullet \in D_\bullet$, all coordinates of the c*-vector* $\mathbf{c}(D_\circ \,|\, \delta_\bullet \in D_\bullet)$ *have the same sign,*

   (ii) for any $\delta_\circ \in D_\circ$, the $\delta_\circ$-coordinate of all g*-vectors* $\mathbf{g}(D_\circ \,|\, \delta_\bullet)$ *for $\delta_\bullet \in D_\bullet$ have the same sign.*

Proof. Point (i) is Remark 9.5 (ii), and Point (ii) follows by Proposition 9.8.   ∎

9.2.2   c-vector fan and $D_\circ$-zonotope

Call *c-vector fan* of $D_\circ$ the complete polyhedral fan $\mathcal{F}^{\mathbf{c}}(D_\circ)$ defined by the arrangement of the linear hyperplanes orthogonal to the c-vectors of $\mathbf{C}(D_\circ)$. Be careful: contrarily to the g- and d-vector fans defined later, the c-vectors are not the rays of $\mathcal{F}^{\mathbf{c}}(D_\circ)$ but the normal vectors of the hyperplanes supporting the facets of $\mathcal{F}^{\mathbf{c}}(D_\circ)$.

We call $D_\circ$-*zonotope* the Minkowski sum $\mathsf{Zono}(D_\circ)$ of all $\mathbf{c}$-vectors:

$$\mathsf{Zono}(D_\circ) := \sum_{\mathbf{c} \in \mathbf{C}(D_\circ)} \mathbf{c}.$$

The normal fan of the $D_\circ$-zonotope $\mathsf{Zono}(D_\circ)$ is the $\mathbf{c}$-vector fan $\mathcal{F}^{\mathbf{c}}(D_\circ)$. Note that the $\mathbf{c}$-vector fan is not always simplicial, and thus the $D_\circ$-zonotope $\mathsf{Zono}(D_\circ)$ is not always simple. See Figure 9.2.

Example 9.10. Consider an accordion dissection $A_\circ = \{\delta_\circ^1, \ldots, \delta_\circ^{|A_\circ|}\}$, with diagonals labeled such that $\delta_\circ^k$ and $\delta_\circ^{k+1}$ belong to the same cell of $A_\circ$ for all k. Identifying $\mathbf{e}_{\delta_\circ^k}$ to the simple root $\mathbf{f}_k - \mathbf{f}_{k+1}$ of type $A_{|A_\circ|}$, the $\mathbf{c}$-vectors of $\mathbf{C}(A_\circ)$ are all roots $\pm(\mathbf{f}_i - \mathbf{f}_j) = \pm\sum_{i \le k \le j} \mathbf{e}_{\delta_\circ^k}$ of type type $A_{|A_\circ|}$. Therefore, the $\mathbf{c}$-vector fan is the type A_n Coxeter fan and the $A_\circ$-zonotope is the permutahedron $\mathsf{Perm}(|A_\circ|) := \mathrm{conv}\left\{\sum_{i \in [|A_\circ|+1]} \sigma(i)\,\mathbf{f}_i \;\middle|\; \sigma \in \mathfrak{S}_{|A_\circ|+1}\right\}$.

The vertices of $\mathsf{Zono}(D_\circ)$ correspond to separable subsets of $\mathbf{C}(D_\circ)$. Although we could work out all facets of $\mathsf{Zono}(D_\circ)$, we will only need the following inequalities.

Proposition 9.11. *For any $D_\circ$-accordion diagonal $\gamma_\bullet$, the $D_\circ$-zonotope $\mathsf{Zono}(D_\circ)$ has a facet defined by the inequality*

$$\langle \mathbf{g}(D_\circ \,|\, \gamma_\bullet)|\mathbf{x}\rangle \le \omega(D_\circ \,|\, \gamma_\bullet),$$

*where $\omega(D_\circ \,|\, \gamma_\bullet)$ is the $D_\circ$-*height* of $\gamma_\bullet$, i.e. the number of $D_\circ$-accordion diagonals that cross $\gamma_\bullet$.*

Proof. Let $\omega(D_\circ \,|\, \gamma_\bullet)$ denote the maximum of $\langle \mathbf{g}(D_\circ \,|\, \gamma_\bullet)|\mathbf{x}\rangle$ over $\mathsf{Zono}(D_\circ)$. As $\mathsf{Zono}(D_\circ)$ is the Minkowski sum of all $\mathbf{c}$-vectors, we have

$$\omega(D_\circ \,|\, \gamma_\bullet) = \sum_{\substack{\mathbf{c} \in \mathbf{C}(D_\circ) \\ \langle \mathbf{g}(D_\circ \,|\, \gamma_\bullet)|\mathbf{c}\rangle > 0}} \langle \mathbf{g}(D_\circ \,|\, \gamma_\bullet)|\mathbf{c}\rangle.$$

By Remark 9.5, we have $\langle \mathbf{g}(D_\circ \,|\, \gamma_\bullet)|\mathbf{c}\rangle \in \{-1, 0, 1\}$ for any $\mathbf{c} \in \mathbf{C}(D_\circ)$. We thus just need to count the distinct $\mathbf{c}$-vectors $\mathbf{c}$ such that $\langle \mathbf{g}(D_\circ \,|\, \gamma_\bullet)|\mathbf{c}\rangle > 0$. It turns out that it is more convenient and equivalent (since $\mathbf{C}(D_\circ) = -\mathbf{C}(D_\circ)$) to count the distinct $\mathbf{c}$-vectors $\mathbf{c}$ such that $\langle \mathbf{g}(D_\circ \,|\, \gamma_\bullet)|\mathbf{c}\rangle < 0$. For that, let $Z_\circ$ denote the zigzag of the accordion crossed by $\gamma_\bullet$ in $D_\circ$, and decompose $Z_\circ = Z_\circ^- \sqcup Z_\circ^+$ such that $\mathbf{g}(D_\circ \,|\, \gamma_\bullet) = \mathbb{1}_{Z_\circ^+} - \mathbb{1}_{Z_\circ^-}$ (where $\mathbb{1}_{X_\circ} := \sum_{\delta_\circ \in X_\circ} \mathbf{e}_{\delta_\circ}$ for $X_\circ \subseteq D_\circ$). Let $\delta_\bullet$ be a $D_\circ$-accordion diagonal. Let $A_\circ^-$ (resp. $A_\circ^+$) denote the accordion crossed by $\delta_\bullet = u_\bullet v_\bullet$ in $D_\circ$ and not incident to $(u+1)_\circ$ or $(v+1)_\circ$ (resp. to $(u-1)_\circ$ or $(v-1)_\circ$). Recall from Lemma 9.6 that the negative (resp. positive) $\mathbf{c}$-vectors of $\mathbf{C}(D_\circ)$ are given by $\mathbf{c}^-(\delta_\bullet) := -\mathbb{1}_{A_\circ^-}$ (resp. $\mathbf{c}^+(\delta_\bullet) := \mathbb{1}_{A_\circ^+}$) for all $D_\circ$-accordion diagonal $\delta_\bullet$ not in $D_\bullet^-$ (resp. $D_\bullet^+$). We let the reader check that:

◇ If $\gamma_\bullet$ and $\delta_\bullet$ do not cross and have no common endpoint, both $|Z_\circ \cap A_\circ^-|$ and $|Z_\circ \cap A_\circ^+|$ are even. Thus $\langle \mathbf{g}(D_\circ \,|\, \gamma_\bullet)|\mathbf{c}^-(\delta_\bullet)\rangle = \langle \mathbf{g}(D_\circ \,|\, \gamma_\bullet)|\mathbf{c}^+(\delta_\bullet)\rangle = 0$.

◇ If $\gamma_\bullet$ and $\delta_\bullet$ have a common endpoint, and $\gamma_\bullet\delta_\bullet$ form a counterclockwise angle, then $|Z_\circ \cap A_\circ^-|$ is even while $Z_\circ \cap A_\circ^+$ is empty or starts and ends in $Z_\circ^+$. Thus $\langle \mathbf{g}(D_\circ \,|\, \gamma_\bullet)|\mathbf{c}^-(\delta_\bullet)\rangle = 0$ while $\langle \mathbf{g}(D_\circ \,|\, \gamma_\bullet)|\mathbf{c}^+(\delta_\bullet)\rangle \ge 0$. The situation is similar if $\gamma_\bullet\delta_\bullet$ form a clockwise angle.

◇ If $\gamma_\bullet$ and $\delta_\bullet$ cross, $Z_\circ \cap A_\circ^-$ and $Z_\circ \cap A_\circ^+$ are empty or start and end both in $Z_\circ^-$ or both in $Z_\circ^+$. Thus, either $\langle \mathbf{g}(D_\circ \,|\, \gamma_\bullet)|\mathbf{c}^-(\delta_\bullet)\rangle < 0$ and $\langle \mathbf{g}(D_\circ \,|\, \gamma_\bullet)|\mathbf{c}^+(\delta_\bullet)\rangle \ge 0$ or conversely.

We conclude from this case analysis that

$$\omega(\mathrm{D}_\circ \,|\, \gamma_\bullet) = |\,\{\mathbf{c} \in \mathbf{C}(\mathrm{D}_\circ) \mid \langle \mathbf{g}(\mathrm{D}_\circ \,|\, \gamma_\bullet)|\mathbf{c}\rangle < 0\}\,| = |\{\mathrm{D}_\circ\text{-accordion diagonals crossing } \gamma_\bullet\}|.$$

Finally, the inequality $\langle \mathbf{g}(\mathrm{D}_\circ \,|\, \gamma_\bullet)|\mathbf{x}\rangle \leq \omega(\mathrm{D}_\circ \,|\, \gamma_\bullet)$ defines a priori a face $F(\gamma_\bullet)$ of the zonotope $\mathrm{Zono}(\mathrm{D}_\circ)$. This face $F(\gamma_\bullet)$ is the Minkowski sum of the $\mathbf{c}$-vectors of $\mathbf{C}(\mathrm{D}_\circ)$ orthogonal to $\mathbf{g}(\mathrm{D}_\circ \,|\, \gamma_\bullet)$. Proposition 9.7 ensures that any $\mathrm{D}_\circ$-accordion dissection $\mathrm{D}_\bullet$ containing $\gamma_\bullet$ already provides $|\mathrm{D}_\bullet| - 1$ linearly independent such $\mathbf{c}$-vectors $\mathbf{c}(\mathrm{D}_\circ \,|\, \delta_\bullet \in \mathrm{D}_\bullet)$ for $\delta_\bullet \in \mathrm{D}_\bullet \smallsetminus \{\gamma_\bullet\}$. We obtain that $F(\gamma_\bullet)$ has dimension $|\mathrm{D}_\bullet| - 1 = |\mathrm{D}_\circ| - 1$ and is therefore a facet of the zonotope $\mathrm{Zono}(\mathrm{D}_\circ)$. ∎

Let the half-space and the hyperplane associated to a $\mathrm{D}_\circ$-accordion diagonal $\gamma_\bullet$ be

$$\mathbf{H}^{\leq}(\mathrm{D}_\circ \,|\, \gamma_\bullet) := \big\{\mathbf{x} \in \mathbb{R}^{\mathrm{D}_\circ} \mid \langle \mathbf{g}(\mathrm{D}_\circ \,|\, \gamma_\bullet)|\mathbf{x}\rangle \leq \omega(\mathrm{D}_\circ \,|\, \gamma_\bullet)\big\},$$

$$\text{and} \qquad \mathbf{H}^{=}(\mathrm{D}_\circ \,|\, \gamma_\bullet) := \big\{\mathbf{x} \in \mathbb{R}^{\mathrm{D}_\circ} \mid \langle \mathbf{g}(\mathrm{D}_\circ \,|\, \gamma_\bullet)|\mathbf{x}\rangle = \omega(\mathrm{D}_\circ \,|\, \gamma_\bullet)\big\} \text{ respectively.}$$

9.2.3   g-**vector fan and** $\mathrm{D}_\circ$-**accordiohedron**

In this section, we give a geometric realization of the accordion complex of $\mathrm{D}_\circ$. We start by realizing this simplicial complex as a complete simplicial fan in $\mathbb{R}^{\mathrm{D}_\circ}$. We denote by $\mathbb{R}_{\geq 0}\mathbf{R}$ the positive span of a set $\mathbf{R}$ of vectors in $\mathbb{R}^{\mathrm{D}_\circ}$.

Theorem 9.12. *The collection of cones*

$$\mathcal{F}^{\mathbf{g}}(\mathrm{D}_\circ) := \big\{\mathbb{R}_{\geq 0}\mathbf{g}(\mathrm{D}_\circ \,|\, \mathrm{D}_\bullet) \mid \mathrm{D}_\bullet \text{ any } \mathrm{D}_\circ\text{-accordion dissection}\big\}$$

forms a complete simplicial fan, that we call the g-vector fan *of* $\mathrm{D}_\circ$.

The proof still uses the characterization of complete simplicial fans of Proposition 3.7. We will provide an alternative proof in Remark 9.43 based on sections of Cambrian fans.

Proof. Observe first that $\mathbb{R}_{\geq 0}\mathbf{g}(\mathrm{D}_\circ \,|\, \mathrm{D}_\bullet^-)$ is the only cone of $\mathcal{F}^{\mathbf{g}}(\mathrm{D}_\circ)$ which intersects the interior of the positive orthant. Consider now two adjacent maximal $\mathrm{D}_\circ$-accordion dissections $\mathrm{D}_\bullet, \mathrm{D}_\bullet'$. Let $\delta_\bullet \in \mathrm{D}_\bullet$ and $\delta_\bullet' \in \mathrm{D}_\bullet'$ be such that $\mathrm{D}_\bullet \smallsetminus \{\delta_\bullet\} = \mathrm{D}_\bullet' \smallsetminus \{\delta_\bullet'\}$, and let $\mu_\bullet$ and $\nu_\bullet$ be the other diagonals of Figure 8.4 as defined in Lemma 8.9 (describing the flips in $\mathcal{AC}(\mathrm{D}_\circ)$). Note that a diagonal of $\mathrm{D}_\circ$ crosses none of (resp. one of, resp. both) the diagonals $\delta_\bullet, \delta_\bullet'$ if and only if it crosses none of (resp. one of, resp. both) the diagonals $\mu_\bullet, \nu_\bullet$. The same holds for a Z or a Σ of $\mathrm{D}_\circ$. Therefore, we have the linear dependence $\mathbf{g}(\mathrm{D}_\circ \,|\, \delta_\bullet) + \mathbf{g}(\mathrm{D}_\circ \,|\, \delta_\bullet') = \mathbf{g}(\mathrm{D}_\circ \,|\, \mu_\bullet) + \mathbf{g}(\mathrm{D}_\circ \,|\, \mu_\bullet)$. This shows that $\mathcal{F}^{\mathbf{g}}(\mathrm{D}_\circ)$ satisfies the two conditions of Proposition 3.7, and thus concludes the proof. ∎

Remark 9.13. Let $\mathrm{D}_\bullet, \mathrm{D}_\bullet'$, with $\mathrm{D}_\bullet \smallsetminus \{\delta_\bullet\} = \mathrm{D}_\bullet' \smallsetminus \{\delta_\bullet'\}$, be two adjacent maximal $\mathrm{D}_\circ$-accordion dissections. The linear dependence $\mathbf{g}(\mathrm{D}_\circ \,|\, \delta_\bullet) + \mathbf{g}(\mathrm{D}_\circ \,|\, \delta_\bullet') = \mathbf{g}(\mathrm{D}_\circ \,|\, \mu_\bullet) + \mathbf{g}(\mathrm{D}_\circ \,|\, \mu_\bullet)$ shows that $\det\big(\mathbf{g}(\mathrm{D}_\circ \,|\, \mathrm{D}_\bullet)\big) = -\det\big(\mathbf{g}(\mathrm{D}_\circ \,|\, \mathrm{D}_\bullet')\big)$. Since the cone $\mathbb{R}_{\geq 0}\mathbf{g}(\mathrm{D}_\circ \,|\, \mathrm{D}_\bullet^-)$ is generated by the coordinate vectors (see Example 9.2), we obtain that $\det\big(\mathbf{g}(\mathrm{D}_\circ \,|\, \mathrm{D}_\bullet)\big) = \pm 1$ for all $\mathrm{D}_\circ$-accordion dissection $\mathrm{D}_\bullet$, so that the g-vector fan $\mathcal{F}^{\mathbf{g}}(\mathrm{D}_\circ)$ is always *smooth*.

Remark 9.14. By Proposition 9.7, any nonmaximal cone of $\mathcal{F}^{\mathbf{g}}(\mathrm{D}_\circ)$ is supported by an hyperplane orthogonal to a $\mathbf{c}$-vector of $\mathbf{C}(\mathrm{D}_\circ)$. The g-vector fan $\mathcal{F}^{\mathbf{g}}(\mathrm{D}_\circ)$ thus coarsens the $\mathbf{c}$-vector fan $\mathcal{F}^{\mathbf{c}}(\mathrm{D}_\circ)$.

Remark 9.15. Following Remark 8.2, we observe that special reference dissections give rise to the following relevant fans:
   ◇ For an accordion triangulation $\mathrm{A}_\circ$ (*i.e.* with no interior triangle), the g-vector fan $\mathcal{F}^{\mathbf{g}}(\mathrm{A}_\circ)$ coincides with the type A Cambrian fan of N. Reading and D. Speyer [RS09].
   ◇ For any triangulation $\mathrm{T}_\circ$ (with or without interior triangle), the g-vector fan $\mathcal{F}^{\mathbf{g}}(\mathrm{T}_\circ)$ was recently constructed in [HPS16].
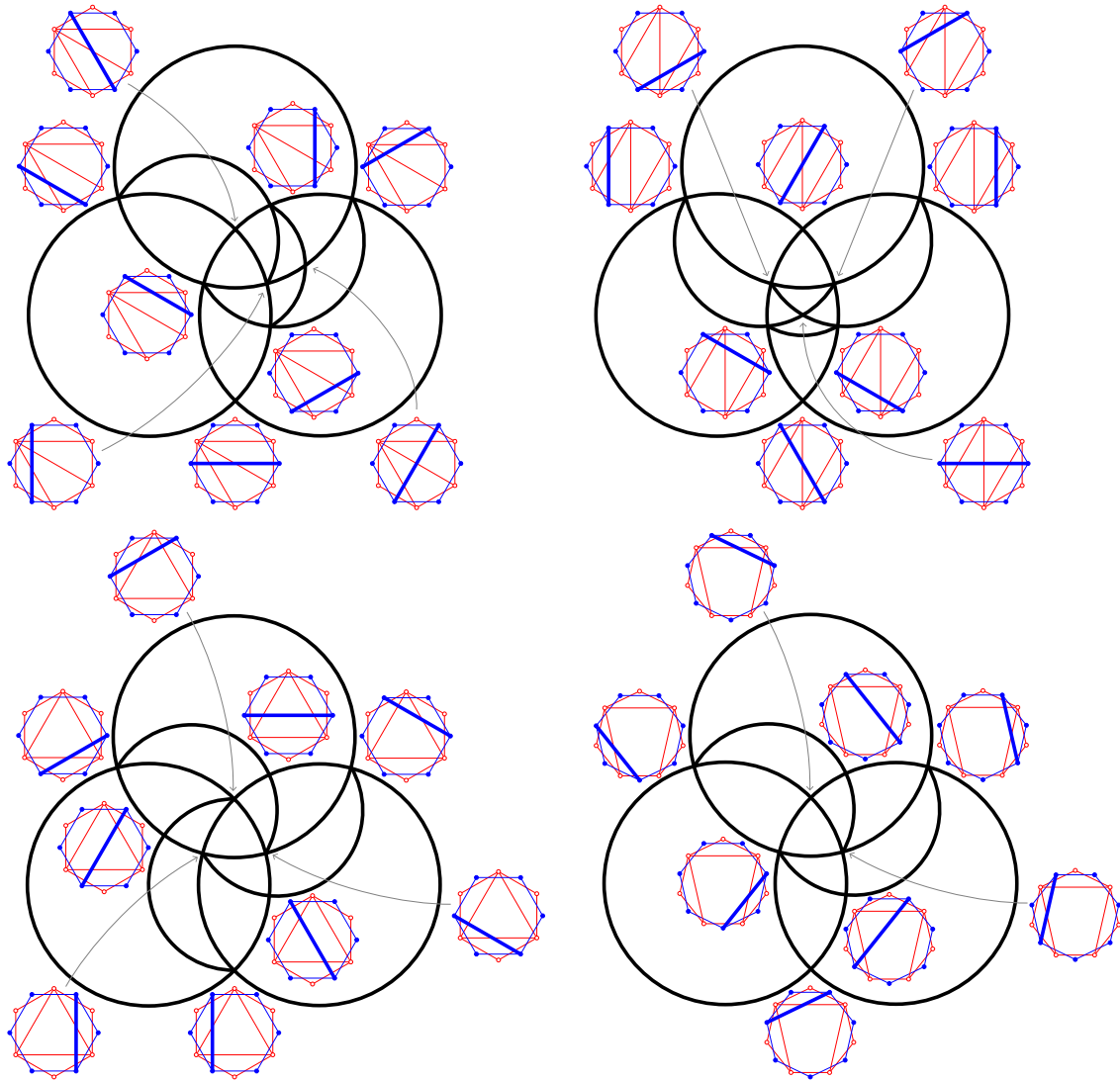
Figure 9.1 – Stereographic projections of the g-vector fans $\mathcal{F}^{\mathbf{g}}(D_\circ)$ for various reference hollow dissections $D_\circ$. See Figure 9.4 for alternative simplicial fan realizations of these accordion complexes.

Example 9.16. Figure 9.1 illustrates the g-vector fans $\mathcal{F}^{\mathbf{d}}(D_\circ)$ for various reference dissections $D_\circ$: the fan, the snake, and the cyclic triangulation of the hexagon, and a dissection of the heptagon. More precisely, we have represented the stereographic projection of the fans from the point $[\, 1, 1, 1 \,]$. Therefore, the external face of the projection corresponds to the $D_\circ$-accordion dissection $D_\bullet^-$. We have labeled all vertices of the projection (*i.e.* the rays of the fan) by the corresponding $D_\circ$-accordion diagonals.

We now provide a first polytopal realization of the g-vector fan $\mathcal{F}^{\mathbf{g}}(D_\circ)$ (see also Section 9.4). This fan has a maximal cone for each maximal $D_\circ$-accordion dissection and a ray for each $D_\circ$-accordion diagonal. For a maximal $D_\circ$-accordion dissection $D_\bullet$, we define a point $\mathbf{p}\big(D_\circ \,|\, D_\bullet\big) \in \mathbb{R}^{D_\circ}$ by

$$\mathbf{p}\big(D_\circ \,|\, D_\bullet\big) \coloneqq \sum_{\delta_\bullet \in D_\bullet} \omega\big(D_\circ \,|\, \delta_\bullet\big) \cdot \mathbf{c}\big(D_\circ \,|\, \delta_\bullet \in D_\bullet\big),$$

where $\omega(D_\circ \,|\, \delta_\bullet)$ still denotes the $D_\circ$-*height* of $\delta_\bullet$ defined as the number of $D_\circ$-accordion diagonals that cross $\delta_\bullet$. We will need the following lemmas in the proof of Theorem 9.19.

Lemma 9.17. *For any maximal $D_\circ$-accordion dissection $D_\bullet$, the point $\mathbf{p}(D_\circ \,|\, D_\bullet)$ is the intersection of the hyperplanes $\mathbf{H}^=(D_\circ \,|\, \delta_\bullet)$ for $\delta_\bullet \in D_\bullet$.*

Proof. Since $\mathbf{g}(D_\circ \,|\, D_\bullet)$ and $\mathbf{c}(D_\circ \,|\, D_\bullet)$ form dual bases by Proposition 9.7, we have for any $\gamma_\bullet \in D_\bullet$:

$$
\begin{aligned}
\langle \mathbf{g}(D_\circ \,|\, \gamma_\bullet) | \mathbf{p}(D_\circ \,|\, D_\bullet) \rangle \ &= \textstyle\sum_{\delta_\bullet \in D_\bullet} \omega(D_\circ \,|\, \delta_\bullet) \cdot \langle \mathbf{g}(D_\circ \,|\, \gamma_\bullet) | \mathbf{c}(D_\circ \,|\, \delta_\bullet \in D_\bullet) \rangle \\
&= \textstyle\sum_{\delta_\bullet \in D_\bullet} \omega(D_\circ \,|\, \delta_\bullet) \cdot \mathbb{1}_{\gamma_\bullet = \delta_\bullet} \ = \ \omega(D_\circ \,|\, \gamma_\bullet). \quad \blacksquare
\end{aligned}
$$

Lemma 9.18. *If $D_\bullet, D_\bullet'$ are two adjacent maximal $D_\circ$-accordion dissections, and $\delta_\bullet \in D_\bullet$ and $\delta_\bullet' \in D_\bullet'$ are such that $D_\bullet \smallsetminus \{\delta_\bullet\} = D_\bullet' \smallsetminus \{\delta_\bullet'\}$, then*

$$
\mathbf{c}(D_\circ \,|\, \delta_\bullet \in D_\bullet) = -\mathbf{c}(D_\circ \,|\, \delta_\bullet' \in D_\bullet') \quad \text{and} \quad \mathbf{p}(D_\circ \,|\, D_\bullet') - \mathbf{p}(D_\circ \,|\, D_\bullet) \in \mathbb{Z}_{<0} \cdot \mathbf{c}(D_\circ \,|\, \delta_\bullet \in D_\bullet).
$$

Proof. Let $D_\bullet, D_\bullet'$ be two adjacent maximal $D_\circ$-accordion dissections, let $\delta_\bullet \in D_\bullet$ and $\delta_\bullet' \in D_\bullet'$ be such that $D_\bullet \smallsetminus \{\delta_\bullet\} = D_\bullet' \smallsetminus \{\delta_\bullet'\}$, and let $\mu_\bullet$ and $\nu_\bullet$ be the other diagonals of Figure 8.4 as defined in Lemma 8.9. A quick case analysis then shows that

$$
\mathbf{c}(D_\circ \,|\, \gamma_\bullet \in D_\bullet') = \begin{cases} \mathbf{c}(D_\circ \,|\, \gamma_\bullet \in D_\bullet) & \text{for all diagonal } \gamma_\bullet \in D_\bullet \smallsetminus \{\delta_\bullet, \mu_\bullet, \nu_\bullet\}, \\ -\mathbf{c}(D_\circ \,|\, \delta_\bullet \in D_\bullet) & \text{if } \gamma_\bullet = \delta_\bullet', \\ \mathbf{c}(D_\circ \,|\, \gamma_\bullet \in D_\bullet) + \mathbf{c}(D_\circ \,|\, \delta_\bullet \in D_\bullet) & \text{if } \gamma_\bullet \in \{\mu_\bullet, \nu_\bullet\}. \end{cases}
$$

Summing the contribution of all $\mathbf{c}$-vectors with their coefficients $\omega(D_\circ \,|\, \gamma_\bullet)$, we obtain

$$
\mathbf{p}(D_\circ \,|\, D_\bullet') - \mathbf{p}(D_\circ \,|\, D_\bullet) = \big(\omega(D_\circ \,|\, \mu_\bullet) + \omega(D_\circ \,|\, \nu_\bullet) - \omega(D_\circ \,|\, \delta_\bullet) - \omega(D_\circ \,|\, \delta_\bullet')\big) \cdot \mathbf{c}(D_\circ \,|\, \delta_\bullet \in D_\bullet).
$$

Finally, note that any diagonal of $\mathcal{P}_\bullet$ that crosses one of (resp. both) the diagonals $\mu_\bullet, \nu_\bullet'$ also crosses one of (resp. both) the diagonals $\delta_\bullet, \delta_\bullet'$. Moreover, $\delta_\bullet$ and $\delta_\bullet'$ cross each other but do not cross $\mu_\bullet$ and $\nu_\bullet$. It follows that $\omega(D_\circ \,|\, \mu_\bullet) + \omega(D_\circ \,|\, \nu_\bullet) - \omega(D_\circ \,|\, \delta_\bullet) - \omega(D_\circ \,|\, \delta_\bullet') \leq -2 < 0$. $\qquad\blacksquare$

Theorem 9.19. *The two sets given by*

$\diamond$ *the convex hull of the points $\mathbf{p}(D_\circ \,|\, D_\bullet)$ for all maximal $D_\circ$-accordion dissection $D_\bullet$,*

$\diamond$ *the intersection of the half-spaces $\mathbf{H}^\leq(D_\circ \,|\, \gamma_\bullet)$ for all $D_\circ$-accordion diagonals $\gamma_\bullet$,*

define the same polytope, that we call $D_\circ$-accordiohedron and denote by $\mathsf{Acco}(D_\circ)$. Its normal fan is the $\mathbf{g}$-vector fan $\mathcal{F}^{\mathbf{g}}(D_\circ)$. Thus, $\mathsf{Acco}(D_\circ)$ is a polytopal realization of the accordion complex of $D_\circ$.

The proof of Theorem 9.19 is based on the following characterization of polytopal realizations of complete simplicial fan, proven for instance in [HLT11, Theorem 4.1].

Theorem 9.20 ([HLT11, Theorem 4.1])**.** *Given a complete simplicial fan $\mathcal{F}$ in $\mathbb{R}^d$, consider for each ray $\mathbf{r}$ of $\mathcal{F}$ a half-space $\mathbf{H}_{\mathbf{r}}^\leq$ of $\mathbb{R}^d$ containing the origin and defined by a hyperplane $\mathbf{H}_{\mathbf{r}}^=$ orthogonal to $\mathbf{r}$. For each maximal cone C of $\mathcal{F}$, let $\mathbf{a}(C) \in \mathbb{R}^d$ be the intersection of the hyperplanes $\mathbf{H}_{\mathbf{r}}^=$ for $\mathbf{r} \in C$. Then the following assertions are equivalent:*

(i) The vector $\mathbf{a}(C') - \mathbf{a}(C)$ points from C to C' for any two adjacent maximal cones C, C' of $\mathcal{F}$.

(ii) The polytopes

$$\operatorname{conv}\left\{\mathbf{a}(C) \mid C \text{ maximal cone of } \mathcal{F}\right\} \quad \text{and} \quad \bigcap_{\mathbf{r} \text{ ray of } \mathcal{F}} \mathbf{H}_{\mathbf{r}}^{\leq}$$

coincide and their normal fan is $\mathcal{F}$.

Proof of Theorem 9.19. The $\mathbf{g}$-vector fan $\mathcal{F}^{\mathbf{g}}(D_\circ)$ has a ray $\mathbf{g}(D_\circ \mid \delta_\bullet)$ for each $D_\circ$-accordion diagonal $\delta_\bullet$ and a maximal cone $C(D_\bullet) = \mathbb{R}_{\geq 0}\mathbf{g}(D_\circ \mid D_\bullet)$ for each maximal $D_\circ$-accordion dissection $D_\bullet$. Consider the half-spaces $\mathbf{H}^{\leq}(D_\circ \mid \gamma_\bullet)$ for all $D_\circ$-accordion diagonals $\delta_\bullet$. Lemma 9.17 ensures that the point $\mathbf{a}(C(D_\bullet))$ coincides with $\mathbf{p}(D_\circ \mid D_\bullet)$ for each maximal $D_\circ$-accordion dissection $D_\bullet$. Finally, Lemma 9.18 shows that the conditions of application of Theorem 9.20 are fulfilled. ∎

Remark 9.21. Following Remark 8.2, observe that special reference hollow dissections give rise to the following relevant polytopes, illustrated in Figure 9.2:
- ◇ For a fan triangulation $T_\circ$, the $T_\circ$-accordiohedron $\mathsf{Acco}(T_\circ)$ is the classical associahedron constructed by S. Shnider and S. Sternberg [SS93] and J.-L. Loday [Lod04].
- ◇ The $A_\circ$-associahedra $\mathsf{Acco}(A_\circ)$ for all accordion triangulations $A_\circ$ are precisely the associahedra constructed by C. Hohlweg and C. Lange in [HL07].
- ◇ For a triangulation $T_\circ$ with an interior triangle, the $T_\circ$-accordiohedron $\mathsf{Acco}(T_\circ)$ was recently constructed in [HPS16]. For example, for the triangulation of the hexagon with an interior triangle, this associahedron appeared as a mysterious realization in [CSZ15].
- ◇ For a quadrangulation $Q_\circ$, the $Q_\circ$-accordiohedron $\mathsf{Acco}(Q_\circ)$ is a realization of the Stokes polytope announced by S. Baryshnikov [Bar01] and discussed by F. Chapoton in [Cha16].

9.2.4 Some properties of $\mathsf{Acco}(D_\circ)$

We conclude this section by pointing out some relevant combinatorial and geometric properties and observations on the $D_\circ$-accordiohedron.

Proposition 9.22. *The graph of the $D_\circ$-accordiohedron $\mathsf{Acco}(D_\circ)$ linearly oriented in the direction $-\mathbb{1} := -\sum_{\delta_\circ \in D_\circ} \mathbf{e}_{\delta_\circ}$ is the Hasse diagram of the accordion lattice $\mathcal{AL}(D_\circ)$.*

Proof. Consider two adjacent maximal $D_\circ$-accordion dissections $D_\bullet, D'_\bullet$ such that the flip from $D_\bullet$ to $D'_\bullet$ is increasing. Let $\delta_\bullet \in D_\bullet$ and $\delta'_\bullet \in D'_\bullet$ be such that $D_\bullet \smallsetminus \{\delta_\bullet\} = D'_\bullet \smallsetminus \{\delta'_\bullet\}$. As observed in Remark 9.5 (ii), the $\mathbf{c}$-vector $\mathbf{c}(D_\circ \mid \delta_\bullet \in D_\bullet)$ is the characteristic vector $\mathbb{1}_{A_\circ}$ of the set $A_\circ$ of diagonals of $D_\circ$ crossed by both $\delta_\bullet$ and $\delta'_\bullet$. Applying Lemma 9.18, we therefore obtain that

$$\langle -\mathbb{1} \mid \mathbf{p}(D_\circ \mid D'_\bullet) - \mathbf{p}(D_\circ \mid D_\bullet)\rangle = \langle -\mathbb{1} \mid \lambda \cdot \mathbf{c}(D_\circ \mid \delta_\bullet \in D_\bullet)\rangle = \lambda \cdot \langle -\mathbb{1} \mid \mathbb{1}_{A_\circ}\rangle = -\lambda \cdot |A_\circ|,$$

for some $\lambda \in \mathbb{Z}_{<0}$. The edge $[\mathbf{p}(D_\circ \mid D_\bullet), \mathbf{p}(D_\circ \mid D'_\bullet)]$ is therefore indeed oriented from its vertex $\mathbf{p}(D_\circ \mid D_\bullet)$ to its vertex $\mathbf{p}(D_\circ \mid D'_\bullet)$ by the linear functional $-\mathbb{1}$. ∎

Remark 9.23. Since the $\mathbf{c}$-vector fan $\mathcal{F}^{\mathbf{c}}(D_\circ)$ refines the $\mathbf{g}$-vector fan $\mathcal{F}^{\mathbf{g}}(D_\circ)$, there is a natural projection π from the vertices of the $D_\circ$-zonotope $\mathsf{Zono}(D_\circ)$ to that of the $D_\circ$-accordiohedron $\mathsf{Acco}(D_\circ)$. In analogy to the acyclic case, one could hope to obtain the accordion lattice as a lattice quotient through this projection. However, the transitive closure of the graph of the $D_\circ$-zonotope $\mathsf{Zono}(D_\circ)$ oriented in the direction $-\mathbb{1}$ is not a lattice in general (the first counter-example is the dissection with a central square surrounded by 4 triangles). As shown in [GM16], the right objects are not the separable subsets of $\mathbf{c}$-vectors (*i.e.* the vertices of $\mathsf{Zono}(D_\circ)$) but the biclosed subsets of $\mathbf{c}$-vectors.
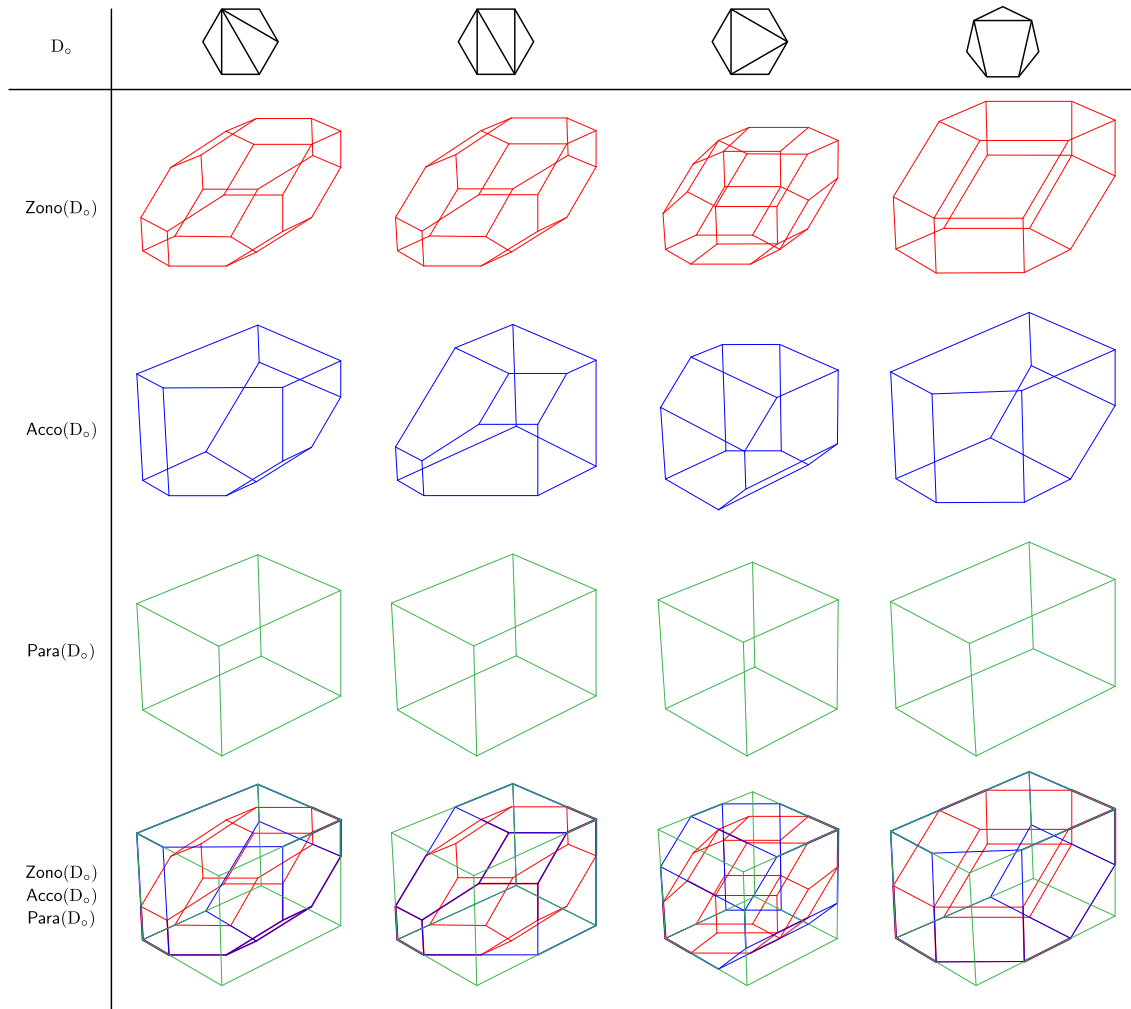
Figure 9.2 – The zonotope $\mathsf{Zono}(D_\circ)$, $D_\circ$-accordiohedron $\mathsf{Acco}(D_\circ)$ and parallelepiped $\mathsf{Para}(D_\circ)$ for different reference dissections $D_\circ$. The first column is J.-L. Loday's associahedron [Lod04], the second column is one of C. Hohlweg and C. Lange's associahedra [HL07], the third column appeared in a discussion in C. Ceballos, F. Santos and G. Ziegler's survey on associahedra [CSZ15, Figure 3] and was explained in C. Hohlweg, V. Pilaud and S. Stella's recent paper [HPS16], and the last column is a Stokes complex discussed by F. Chapoton in [Cha16] and illustrated in Figure 8.3.

Proposition 9.24. *The accordiohedron* $\mathsf{Acco}(D_\circ)$ *has precisely* $|D_\circ|$ *pairs of parallel facets.*

Proof. Two facets of $\mathsf{Acco}(D_\circ)$ are parallel if and only if the corresponding g-vectors are opposite. We therefore want to prove that the pairs of opposite coordinate vectors are the only pairs of opposite g-vectors. Assume that there exist two hollow diagonals $\delta_\circ, \delta_\circ' \in D_\circ$ and two solid $D_\circ$-diagonals $\delta_\bullet, \delta_\bullet'$ such that $\mathbf{g}(D_\circ \,|\, \delta_\bullet)$ and $\mathbf{g}(D_\circ \,|\, \delta_\bullet')$ have nonzero opposite coordinate both on $\delta_\circ$ and $\delta_\circ'$. Then both $\delta_\bullet$ and $\delta_\bullet'$ cross both $\delta_\circ$ and $\delta_\circ'$. This implies that they both slalom on $\delta_\circ$ (and on $\delta_\circ'$) in the same way, a contradiction. ∎

Consider the $D_\circ$-*parallelepiped*

$$\mathsf{Para}(D_\circ) := \left\{ \mathbf{x} \in \mathbb{R}^{D_\circ} \,\middle|\, |\langle \mathbf{e}_{\delta_\circ} | \mathbf{x} \rangle| \leq \omega(D_\circ \,|\, (i_\bullet, j_\bullet)) \text{ for all } \delta_\circ = (i_\circ, j_\circ) \in D_\circ \right\}$$

defined by the inequalities of the $D_\circ$-zonotope $\mathsf{Zono}(D_\circ)$ corresponding to the positive and negative basis vectors. Our next statement follows from Proposition 9.24 and is illustrated in Figure 9.2.

Corollary 9.25. *For any* $D_\circ$, *we have matriochka polytopes.*

$$\mathsf{Zono}(D_\circ) \subseteq \mathsf{Acco}(D_\circ) \subseteq \mathsf{Para}(D_\circ).$$

Each polytope in this chain is obtained by deleting facets from the previous one.

Consider now an isometry σ of the plane that preserves the hollow polygon $\mathcal{P}_\circ$ and the solid polygon $\mathcal{P}_\bullet$. For any diagonals and dissections $\delta_\bullet \in D_\bullet$ and $\delta_\circ \in D_\circ$, we have

$\diamond$ $\delta_\bullet$ is a $D_\circ$-accordion diagonal $\iff$ $\sigma(\delta_\bullet)$ is a $\sigma(D_\circ)$-accordion diagonal,

$\diamond$ $D_\bullet$ is a $D_\circ$-accordion dissection $\iff$ $\sigma(D_\bullet)$ is a $\sigma(D_\circ)$-accordion dissection,

$\diamond$ if $\Sigma : \mathbb{R}^{D_\circ} \to \mathbb{R}^{\sigma(D_\circ)}$ denotes the isometry defined by $\big(\Sigma(\mathbf{x})\big)_{\sigma(\delta_\circ)} := \varepsilon(\sigma) \cdot \mathbf{x}_{\delta_\circ}$, (where $\varepsilon(\sigma) = 1$ if σ is direct and -1 if σ is indirect), then we have

$$\mathbf{g}\big(\sigma(D_\circ) \,|\, \sigma(\delta_\bullet)\big) = \Sigma\big(\mathbf{g}(D_\circ \,|\, \delta_\bullet)\big), \qquad \mathbf{c}\big(\sigma(D_\circ) \,|\, \sigma(\delta_\bullet) \in \sigma(D_\bullet)\big) = \Sigma\big(\mathbf{c}(D_\circ \,|\, \delta_\bullet \in D_\bullet)\big),$$
$$\omega\big(\sigma(D_\circ) \,|\, \sigma(\delta_\bullet)\big) = \omega(D_\circ \,|\, \delta_\bullet), \qquad \text{and} \qquad \mathbf{p}\big(\sigma(D_\circ) \,|\, \sigma(D_\bullet)\big) = \Sigma\big(\mathbf{p}(D_\circ \,|\, D_\bullet)\big).$$

This immediately implies the following statement.

Proposition 9.26. *Any* $\mathcal{P}_\circ$*-preserving isometry* $\sigma : \mathbb{R}^2 \to \mathbb{R}^2$ *induces an isometry* $\Sigma : \mathbb{R}^{D_\circ} \to \mathbb{R}^{\sigma(D_\circ)}$ *with* $\Sigma(\mathsf{Zono}(D_\circ)) = \mathsf{Zono}(\sigma(D_\circ))$, $\Sigma(\mathsf{Acco}(D_\circ)) = \mathsf{Acco}(\sigma(D_\circ))$ *and* $\Sigma(\mathsf{Para}(D_\circ)) = \mathsf{Para}(\sigma(D_\circ))$.

We say that a dissection D is σ-*invariant* when $\sigma(D) = D$. Assume now that σ is a rotation and $D_\circ$ is σ-invariant. We call σ-*invariant accordion complex* of $D_\circ$ the simplicial complex $\mathcal{AC}^\sigma(D_\circ)$ whose vertices are the crossing-free σ-orbits of $D_\circ$-accordion diagonals, and whose faces are sets of such orbits whose union is crossing-free. In other words, the faces of $\mathcal{AC}^\sigma(D_\circ)$ are σ-invariant $D_\circ$-accordion dissections, seen as sets of σ-orbits of diagonals.

Lemma 9.27. *The* σ-*invariant accordion complex* $\mathcal{AC}^\sigma(D_\circ)$ *is a pseudo-manifold.*

Proof. Assume first that σ is the central symmetry. In this case, there are two possible types of orbits: the long $D_\circ$-accordion diagonals and the centrally symmetric pairs of $D_\circ$-accordion diagonals. One can check that any facet of $\mathcal{AC}^\sigma(D_\circ)$ has a long diagonal if and only if $D_\circ$ has, and has as many centrally symmetric pairs of diagonals as $D_\circ$. Finally, any orbit in any facet of $\mathcal{AC}^\sigma(D_\circ)$ can be flipped: long diagonals can already be

flipped in $\mathcal{AC}(\mathrm{D_o})$, and a centrally symmetric pair of diagonals can be flipped by flipping one after the other its two diagonals in $\mathcal{AC}(\mathrm{D_o})$.

Finally, the general statement follows from this special case. Indeed, if σ is not a central symmetry, let $\mathrm{C_o}$ denote the cell of $\mathrm{D_o}$ containing the center of $\mathcal{P_o}$, let u_o be a vertex of $\mathrm{C_o}$, let $\underline{\mathrm{D}}_o$ be the set of diagonals of $\mathrm{D_o}$ whose endpoints are between u_o and $\sigma(u_o)$, and let ρ be the central symmetry around the middle of $u_o\sigma(u_o)$. Then $\mathcal{AC}^\sigma(\mathrm{D_o})$ is isomorphic to $\mathcal{AC}^\rho(\underline{\mathrm{D}}_o \cup \rho(\underline{\mathrm{D}}_o))$. ∎

Let $\Sigma : \mathbb{R}^{\mathrm{D_o}} \to \mathbb{R}^{\sigma(\mathrm{D_o})}$ denote the isometry defined by $\big(\Sigma(\mathbf{x})\big)_{\sigma(\delta_o)} := \mathbf{x}_{\delta_o}$ and $\mathrm{Fix}(\Sigma)$ denote the linear subspace of fixed points of Σ. According to the previous discussion, a maximal $\mathrm{D_o}$-accordion dissection $\mathrm{D_\bullet}$ is σ-invariant if and only if $\mathbf{p}(\mathrm{D_o}\,|\,\mathrm{D_\bullet}) \in \mathrm{Fix}(\Sigma)$. We obtain the following statement.

Proposition 9.28. *For a σ-invariant dissection $\mathrm{D_o}$, the polytope $\mathsf{Acco}^\sigma(\mathrm{D_o})$ defined equivalently as*

  ◇ *the convex hull of $\mathbf{p}(\mathrm{D_o}\,|\,\mathrm{D_\bullet})$ for all σ-invariant maximal $\mathrm{D_o}$-accordion dissections $\mathrm{D_\bullet}$,*

  ◇ *the intersection of the $\mathrm{D_o}$-accordiohedron $\mathsf{Acco}(\mathrm{D_o})$ with the fixed space $\mathrm{Fix}(\Sigma)$,*

is a polytopal realization of the σ-invariant accordion complex $\mathcal{AC}^\sigma(\mathrm{D_o})$.

Proof. We let $P := \mathrm{conv}\,\{\mathbf{p}(\mathrm{D_o}\,|\,\mathrm{D_\bullet}) \mid \sigma\text{-invariant maximal }\mathrm{D_o}\text{-accordion dissections }\mathrm{D_\bullet}\}$ and $Q := \mathsf{Acco}(\mathrm{D_o}) \cap \mathrm{Fix}(\Sigma)$. The inclusion $P \subseteq Q$ is clear since $\mathrm{D_\bullet}$ is σ-invariant if and only if $\mathbf{p}(\mathrm{D_o}\,|\,\mathrm{D_\bullet}) \in \mathrm{Fix}(\Sigma)$. We now prove the reverse inclusion. For that, consider an arbitrary σ-invariant maximal $\mathrm{D_o}$-accordion dissection $\mathrm{D_\bullet}$. Its corresponding point $\mathbf{p}(\mathrm{D_o}\,|\,\mathrm{D_\bullet})$ is a common vertex P and Q. Moreover, any edge e of Q incident to $\mathbf{p}(\mathrm{D_o}\,|\,\mathrm{D_\bullet})$ is the intersection of $\mathrm{Fix}(\Sigma)$ with a face F of $\mathsf{Acco}(\mathrm{D_o})$ that corresponds to a σ-invariant $\mathrm{D_o}$-dissection. Since $\mathcal{AC}^\sigma(\mathrm{D_o})$ is a pseudo-manifold, this dissection can be refined into another maximal $\mathrm{D_o}$-accordion dissection $\mathrm{D}'_\bullet$. The point $\mathbf{p}(\mathrm{D_o}\,|\,\mathrm{D}'_\bullet)$ belongs to F and to $\mathrm{Fix}(\Sigma)$ and thus to e. We conclude that if v is a common vertex of P and Q, then so are all neighbors of v in the graph of Q. Propagating this property, we obtain that all vertices of Q are also vertices of Q, so that $P = Q$. Finally, we proved that the graph of $P = Q$ is the flip graph of $\mathcal{AC}^\sigma(\mathrm{D_o})$. Since P and Q are simple, this proves that the boundary complex of $P = Q$ is $\mathcal{AC}^\sigma(\mathrm{D_o})$. ∎

9.3   The d-vector fan

In this section, we discuss the generalization to the accordion complex of $\mathrm{D_o}$ of another classical geometric realization of the associahedron coming from the theory of cluster algebras [FZ02, FZ03a, CFZ02, CSZ15]. Namely, we define compatibility vectors in analogy with the denominator vectors of cluster variables, and we characterize the reference dissections $\mathrm{D_o}$ for which these vectors support a complete simplicial fan realizing the accordion complex of $\mathrm{D_o}$.

9.3.1   d-vectors

Fix a dissection $\mathrm{D_o}$ of the hollow n-gon. For a hollow diagonal $\delta_o = (i_o, j_o)$ and a solid diagonal $\delta_\bullet$, we denote by

$$(\delta_o \,|\, \delta_\bullet) := \begin{cases} -1 & \text{if } \delta_\bullet = ((i-1)_\bullet, (j-1)_\bullet), \\ 0 & \text{if } \delta_\bullet \text{ and } ((i-1)_\bullet, (j-1)_\bullet) \text{ do not cross}, \\ 1 & \text{if } \delta_\bullet \text{ and } ((i-1)_\bullet, (j-1)_\bullet) \text{ cross}. \end{cases}$$

For any $D_\circ$-accordion diagonal $\delta_\bullet$, the **d-*vector*** of $\delta_\bullet$ with respect to $D_\circ$ is the vector

$$\mathbf{d}(D_\circ \,|\, \delta_\bullet) = \sum_{\delta_\circ \in D_\circ} (\delta_\circ \,|\, \delta_\bullet)\, \mathbf{e}_{\delta_\circ}.$$

In other words, our d-vector $\mathbf{d}(D_\circ \,|\, \delta_\bullet)$ records the compatibility of the diagonal $\delta_\bullet$ with the dissection $D_\bullet^-$. For a $D_\circ$-accordion dissection $D_\bullet$, we define

$$\mathbf{d}(D_\circ \,|\, D_\bullet) := \{\mathbf{d}(D_\circ \,|\, \delta_\bullet) \,|\, \delta_\bullet \in D_\bullet\}.$$

Example 9.29. Consider the hollow dissection $D_\circ^{\mathrm{ex}} = \{(3_\circ, 7_\circ), (3_\circ, 13_\circ), (9_\circ, 13_\circ)\}$ and the (right) solid dissection $D_\bullet^{\mathrm{ex}} = \{(2_\bullet, 6_\bullet), (2_\bullet, 10_\bullet), (10_\bullet, 14_\bullet)\}$ of Figure 8.2. The d-vectors of the diagonals of $D_\bullet^{\mathrm{ex}}$ are

$$\mathbf{d}(D_\circ^{\mathrm{ex}} \,|\, (2_\bullet, 6_\bullet)) = -\mathbf{e}_{(3_\circ, 7_\circ)}, \mathbf{d}(D_\circ^{\mathrm{ex}} \,|\, (2_\bullet, 10_\bullet)) = \mathbf{e}_{(9_\circ, 13_\circ)}, \text{ and } \mathbf{d}(D_\circ^{\mathrm{ex}} \,|\, (10_\bullet, 14_\bullet)) = \mathbf{e}_{(3_\circ, 13_\circ)} + \mathbf{e}_{(9_\circ, 13_\circ)}.$$

Remark 9.30. By definition, the d-vectors of $D_\bullet^- = \{((i-1)_\bullet, (j-1)_\bullet) \,|\, (i_\circ, j_\circ) \in D_\circ\}$ are given by the opposite coordinate vectors $\mathbf{d}(D_\circ \,|\, D_\bullet^-) = \{-\mathbf{e}_{\delta_\circ} \,|\, \delta_\circ \in D_\circ\}$.

9.3.2 d-**vector fan**

We now consider the set of cones

$$\{\mathbb{R}_{\geq 0}\mathbf{d}(D_\circ \,|\, D_\bullet) \,|\, D_\bullet \text{ any } D_\circ\text{-accordion dissection}\}$$

generated by the d-vectors of the $D_\circ$-accordion dissections. We want to characterize the reference hollow dissections $D_\circ$ for which these cones form a complete simplicial fan realizing the accordion complex of $D_\circ$. We start with a negative result.

Remark 9.31. Assume that the reference hollow dissection $D_\circ$ contains an *even interior cell* $C_\circ$, with an even number of edges which are all internal diagonals of $D_\circ$. Denote its vertices by $i_\circ^1, \dots, i_\circ^{2p}$ (in counterclockwise order) and its edges $\delta_\circ^k := (i_\circ^k, i_\circ^{k+1})$ for $k \in [2p]$ (where $i^{2p+1} = i^1$ by convention). Denote by $D_\circ^k$ the set of diagonals of $D_\circ$ separated from $C_\circ$ by $\delta_\circ^k$ (including $\delta_\circ^k$ itself), and let $D_\bullet^k := \left\{((i-1)_\bullet, (j-1)_\bullet) \,\middle|\, (i_\circ, j_\circ) \in D_\circ^k\right\}$. Consider the solid diagonals $\delta_\bullet^k := ((i^k+1)_\bullet, (i^{k+1}+1)_\bullet)$ for $k \in [2p]$. Observe that $\delta_\bullet^k$ only crosses diagonals of $D_\bullet^{k-1}$ and $D_\bullet^k$, and that $\delta_\bullet^k$ and $\delta_\bullet^{k+1}$ cross precisely the same diagonals of $D_\bullet^k$. Since the cell is even, it ensures that the d-vectors of the diagonals $\delta_\bullet^k$ for $k \in [2p]$ satisfy the linear dependence

$$\sum_{\substack{k \in [2p] \\ k \text{ even}}} \mathbf{d}(D_\circ \,|\, \delta_\bullet^k) = \sum_{\substack{k \in [2p] \\ k \text{ odd}}} \mathbf{d}(D_\circ \,|\, \delta_\bullet^k).$$

However, as already mentioned in Section 8.2.4, the diagonals $\delta_\bullet^k$ for $k \in [2p]$ all belong to the $D_\circ$-accordion dissection $D_\bullet^+ := \{((i+1)_\bullet, (j+1)_\bullet) \,|\, i_\circ j_\circ \in D_\circ\}$. Therefore, the cone $\mathbb{R}_{\geq 0}\mathbf{d}(D_\circ \,|\, D_\bullet^+)$ is degenerate, so that the d-vectors cannot realize the accordion complex of $D_\circ$.

Example 9.32. Consider the reference dissection $D_\circ := \{(1_\circ, 5_\circ), (5_\circ, 9_\circ), (9_\circ, 13_\circ), (13_\circ, 1_\circ)\}$ in a hollow octagon. It has an interior square cell $1_\circ 5_\circ 9_\circ 13_\circ$ and we have

$$\mathbf{d}(D_\circ \,|\, (2_\bullet, 6_\bullet)) = \mathbf{e}_{(1_\circ, 5_\circ)} + \mathbf{e}_{(5_\circ, 9_\circ)} \qquad \mathbf{d}(D_\circ \,|\, (6_\bullet, 10_\bullet)) = \mathbf{e}_{(5_\circ, 9_\circ)} + \mathbf{e}_{(9_\circ, 13_\circ)}$$
$$\mathbf{d}(D_\circ \,|\, (10_\bullet, 14_\bullet)) = \mathbf{e}_{(9_\circ, 13_\circ)} + \mathbf{e}_{(13_\circ, 1_\circ)} \qquad \mathbf{d}(D_\circ \,|\, (14_\bullet, 2_\bullet)) = \mathbf{e}_{(13_\circ, 1_\circ)} + \mathbf{e}_{(1_\circ, 5_\circ)}$$

so that there is a linear dependence

$$\mathbf{d}(D_\circ \,|\, (2_\bullet, 6_\bullet)) + \mathbf{d}(D_\circ \,|\, (10_\bullet, 14_\bullet)) = \mathbf{d}(D_\circ \,|\, (6_\bullet, 10_\bullet)) + \mathbf{d}(D_\circ \,|\, (14_\bullet, 2_\bullet))$$

among the d-vectors of the $D_\circ$-accordion dissection $D_\bullet^+ = \{(2_\bullet, 6_\bullet), (6_\bullet, 10_\bullet), (10_\bullet, 14_\bullet), (14_\bullet, 2_\bullet)\}$.

On the negative side, even interior cells are crippling for the $\mathbf{d}$-vector fan. The positive side is that even interior cells are the only obstructions to our construction.

Theorem 9.33. *The collection of cones*

$$\mathcal{F}^{\mathbf{d}}(D_\circ) := \{\mathbb{R}_{\geq 0}\mathbf{d}(D_\circ \,|\, D_\bullet) \mid D_\bullet \text{ any } D_\circ\text{-accordion dissection}\}$$

forms a complete simplicial fan, that we call the d-vector fan *of* $D_\circ$*, if and only if* $D_\circ$ *contains no even interior cell.*

Proof. We still use the characterization of complete simplicial fans in Proposition 3.7. Observe first that $\mathbf{d}(D_\circ \,|\, D_\bullet^-) = (\mathbb{R}_{\leq 0})^{D_\circ}$ is the only cone of $\mathcal{F}^{\mathbf{d}}(D_\circ)$ intersecting the open negative orthant $(\mathbb{R}_{>0})^{D_\circ}$. Therefore, $\mathcal{F}^{\mathbf{d}}(D_\circ)$ fulfills Condition (1) of Proposition 3.7.

To check Condition (2), consider two adjacent maximal $D_\circ$-accordion dissections $D_\bullet$ and $D_\bullet'$ and let $\delta_\bullet \in D_\bullet$ and $\delta_\bullet' \in D_\bullet'$ be such that $D_\bullet \smallsetminus \{\delta_\bullet\} = D_\bullet' \smallsetminus \{\delta_\bullet'\}$. Let $\mu_\bullet$ and $\nu_\bullet$ be the diagonals of $\bar{D}_\bullet \cap \bar{D}_\bullet'$ as defined in Lemma 8.9. In other words, $\mu_\bullet$ and $\nu_\bullet$ are incident to both $\delta_\bullet$ and $\delta_\bullet'$, and they are crossed by the hollow diagonal which intersect $\delta_\bullet$ and $\delta_\bullet'$. Let $\gamma_\circ = (i_\circ, j_\circ)$ be such a hollow diagonal crossing $\delta_\bullet, \delta_\bullet', \mu_\bullet$ and $\nu_\bullet$, and let $\gamma_\bullet = ((i-1)_\bullet, (j-1)_\bullet)$. We now distinguish three cases:

$\diamond$ Assume that $\gamma_\bullet$ still crosses $\mu_\bullet$ and $\nu_\bullet$. In this case, any diagonal of $D_\bullet^-$ crossing both (resp. either) $\delta_\bullet$ and (resp. or) $\delta_\bullet'$ also crosses both (resp. either) $\mu_\bullet$ and (resp. or) $\nu_\bullet$. See Figure 9.3 (left). Therefore, the $\mathbf{d}$-vectors of $D_\bullet \cup D_\bullet'$ satisfy the linear dependence

$$\mathbf{d}(D_\circ \,|\, \delta_\bullet) + \mathbf{d}(D_\circ \,|\, \delta_\bullet') = \mathbf{d}(D_\circ \,|\, \mu_\bullet) + \mathbf{d}(D_\circ \,|\, \nu_\bullet).$$

$\diamond$ Assume that $\gamma_\bullet$ crosses neither $\mu_\bullet$ nor $\nu_\bullet$. Then $\gamma_\bullet$ is incident to both $\mu_\bullet$ and $\nu_\bullet$, and therefore is either $\delta_\bullet$ or $\delta_\bullet'$, say $\gamma_\bullet = \delta_\bullet$. Then $\mathbf{d}(\gamma_\circ \,|\, \delta_\bullet) = -1$ while $\mathbf{d}(\gamma_\circ \,|\, \delta_\bullet') = 1$ (since $\delta_\bullet'$ crosses $\delta_\bullet = \gamma_\bullet$), so that $\mathbf{d}(\gamma_\circ \,|\, \delta_\bullet) + \mathbf{d}(\gamma_\circ \,|\, \delta_\bullet') = 0$. Moreover $\mathbf{d}(\gamma_\circ \,|\, \delta_\bullet') = 0$ for any diagonal $\varepsilon_\bullet \in D_\bullet \cap D_\bullet'$ since $\delta_\bullet = \gamma_\bullet$ cannot cross $\varepsilon_\bullet$ as they both belongs to $D_\bullet$. Therefore, the set $\{\mathbf{d}(D_\circ \,|\, \delta_\bullet) + \mathbf{d}(D_\circ \,|\, \delta_\bullet)\} \cup \mathbf{d}(D_\circ \,|\, D_\bullet \cap D_\bullet')$ contains $|D_\circ|$ vectors of $\mathbb{R}^{D_\circ}$ whose $\gamma_\circ$-coordinate all vanish, so that it admits a linear dependence.

$\diamond$ Otherwise, we can assume that $\gamma_\bullet$ crosses $\mu_\bullet$ but not $\nu_\bullet$. Then $\gamma_\bullet$ has a common endpoint with $\nu_\bullet$ and $\delta_\bullet$ (or $\delta_\bullet'$, but we then permute notations). Changing our initial choice of $\gamma_\circ$, we can assume that no diagonal of $D_\bullet^-$ separates $\gamma_\bullet$ from $\delta_\bullet$. We now denote clockwise
  – by $\nu_\bullet =: \lambda_\bullet^0, \lambda_\bullet^1, \ldots, \lambda_\bullet^\ell := \delta_\bullet$ the edges of the cell $C_\bullet$ of $D_\bullet$ containing $\nu_\bullet$ and $\delta_\bullet$,
  – by $\gamma_\bullet =: \lambda_\bullet^0, \gamma_\bullet^1, \ldots, \gamma_\bullet^k$ the edges of the cell $C_\bullet^-$ of $D_\bullet^-$ containing $\gamma_\bullet$ and crossed by $\nu_\bullet$.

These notations are illustrated on Figure 9.3. We still distinguish two subcases as in Figure 9.3:
  – If $\gamma_\bullet^i$ crosses $\lambda_\bullet^i$ for all i as in Figure 9.3 (middle), then $\ell = k$ and we have the linear dependence

$$2\mathbf{d}(D_\circ \,|\, \delta_\bullet) + \mathbf{d}(D_\circ \,|\, \delta_\bullet') = \mathbf{d}(D_\circ \,|\, \mu_\bullet) + \sum_{i \in [\ell-1]} (-1)^{(i-1)} \mathbf{d}(D_\circ \,|\, \lambda_\bullet^i).$$

  It is essential here that $\ell = k$ is even. This is guaranteed by the assumption that $D_\circ$ (and thus $D_\bullet^-$) has no even interior cell, since $C_\bullet^-$ is an interior cell of $D_\bullet^-$ of size k.
  – Otherwise, we are in a situation similar to Figure 9.3 (right). Consider the index $m := \{i \in [\min(\ell, k)] \mid \gamma_\bullet^i \text{ crosses } \lambda_\bullet^i\}$, and we have the linear dependence

$$\mathbf{d}(D_\circ \,|\, \delta_\bullet) + \mathbf{d}(D_\circ \,|\, \delta_\bullet') = \mathbf{d}(D_\circ \,|\, \mu_\bullet) + \sum_{i \in [m]} (-1)^{(i-1)} \mathbf{d}(D_\circ \,|\, \lambda_\bullet^i). \qquad \blacksquare$$
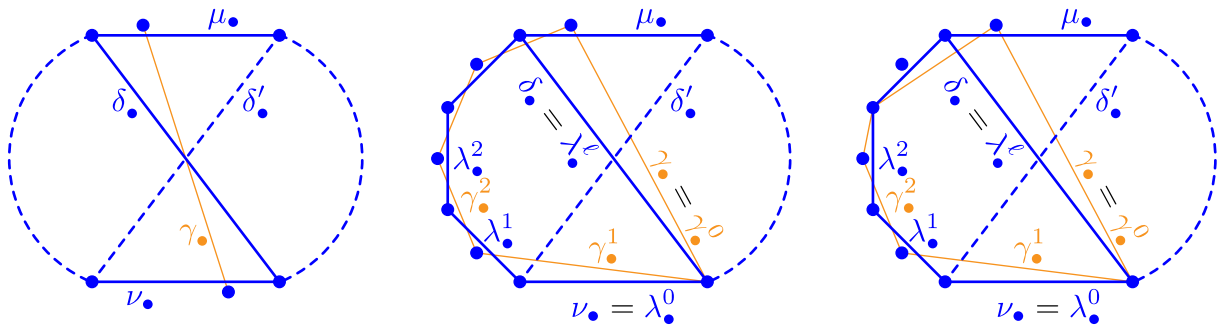
Figure 9.3 – Illustration of the notations and cases in the proof of Theorem 9.33.

Remark 9.34. Following Remark 8.2, we observe that special reference dissections give rise to the following relevant fans:

⋄ For a snake triangulation $\Sigma_\circ$, the **d**-vector fan $\mathcal{F}^{\mathbf{d}}(\Sigma_\circ)$ coincides with the type A cluster fan of S. Fomin and A. Zelevinsky [FZ03a].

⋄ For any triangulation $T_\circ$, the **d**-vector fan $\mathcal{F}^{\mathbf{d}}(T_\circ)$ was already constructed in [CSZ15].

⋄ For a quadrangulation $Q_\circ$ with no interior quadrangle (equivalently, with no cross), we obtain a realization of the Stokes complexes studied in [Bar01, Cha16].

Figure 9.4 illustrates the **d**-vector fans $\mathcal{F}^{\mathbf{d}}(D_\circ)$ for the same reference dissections $D_\circ$ as in Figure 9.1. More precisely, we have represented the stereographic projection of the fans from the point $[-1, -1, -1]$. Therefore, the external face of the projection corresponds to the $D_\circ$-accordion dissection $D_\bullet^-$. We have labeled all vertices of the projection (that is the rays of the fan) by the corresponding $D_\circ$-accordion diagonals.

Remark 9.35. To prove that the **d**-fan $\mathcal{F}^{\mathbf{d}}(D_\circ)$ is polytopal, we would need to find suitable hyperplanes orthogonal to their rays in order to apply Theorem 9.20. For the **g**-vector fan, these hyperplanes were defined using the height function $\omega(D_\circ \mid \delta_\bullet)$. It would be natural to use the same height function for the **d**-vector fan as well. Unfortunately, we can only prove Condition (i) of Theorem 9.20 when $D_\circ$ is a triangulation (see also [CSZ15]).

Remark 9.36. Our **d**-vectors records the compatibility with the dissection $D_\bullet^-$. A priori, we could compute compatibility vectors with respect to any other maximal $D_\circ$-accordion dissection $D_\bullet^{\text{ini}}$. Experiments suggest that the **d**-vector construction provides a complete simplicial fan as soon as either $D_\circ$ or $D_\bullet^{\text{ini}}$ contain no even interior cell. We checked it for reference quadrangulations with at most 5 diagonals.

9.4 Sections and projections

Recall that for a fan $\mathcal{F}$ of $\mathbb{R}^d$ and a linear subspace V of $\mathbb{R}^d$, the *section* of $\mathcal{F}$ by V is the fan $\mathcal{F}|_V := \{C \cap V \mid C \in \mathcal{F}\}$. For a polytope $P \subseteq \mathbb{R}^d$ and a projection $\pi : \mathbb{R}^d \to V$, the normal fan of the projected polytope $\pi(P)$ is the section of the normal fan of P by V [Zie95, Lemma 7.11]. We now consider sections of the **g**- and **d**-vector fans by coordinate subspaces. For two dissections $D_\circ \subset D_\circ'$, we naturally identify $\mathbb{R}^{D_\circ}$ with the subspace spanned by $\{\mathbf{e}_{\delta_\circ} \mid \delta_\circ \in D_\circ\}$ in $\mathbb{R}^{D_\circ'}$.
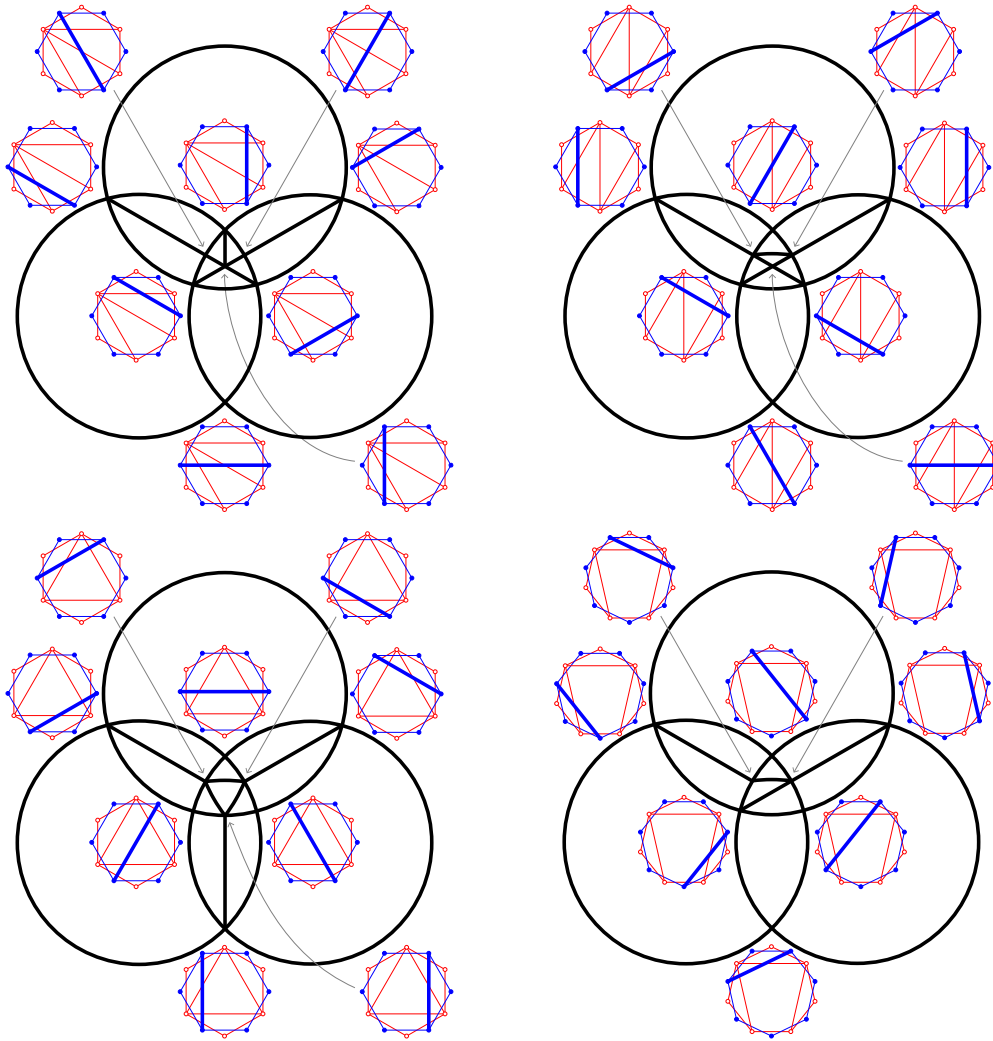
Figure 9.4 – Stereographic projections of the $\mathbf{d}$-vector fans $\mathcal{F}^{\mathbf{d}}(\mathrm{D}_{\circ})$ for various reference hollow dissections $\mathrm{D}_{\circ}$. See Figure 9.1 for alternative simplicial fan realizations of these accordion complexes.

9.4.1   Coordinate sections of the $\mathbf{d}$-vector fan

We start by sections of the $\mathbf{d}$-vector fan which are not very surprising. The following lemma is immediate from the definition of $\mathbf{d}$-vectors.

Lemma 9.37. *For dissections $\mathrm{D}_{\circ} \subset \mathrm{D}_{\circ}'$ and a $\mathrm{D}_{\circ}'$-accordion diagonal $\delta_{\bullet}$, we have $\mathbf{d}(\mathrm{D}_{\circ} \,|\, \delta_{\bullet}) \in \mathbb{R}^{\mathrm{D}_{\circ}}$ if and only if $\delta_{\bullet}$ does not cross any diagonal of $\mathrm{D}_{\bullet}^{-} = \{((i-1)_{\bullet}, (j-1)_{\bullet}) \,|\, (i_{\circ}, j_{\circ}) \in \mathrm{D}_{\circ}\}$.*

Corollary 9.38. *For two dissections $\mathrm{D}_{\circ} \subset \mathrm{D}_{\circ}'$, the section of the $\mathbf{d}$-vector fan $\mathcal{F}^{\mathbf{d}}(\mathrm{D}_{\circ}')$ by $\mathbb{R}^{\mathrm{D}_{\circ}}$ has the combinatorics of the link of the dissection $\mathrm{D}_{\bullet}^{-}$ in the accordion complex $\mathcal{AC}(\mathrm{D}_{\circ}')$, thus of a join of smaller accordion complexes (see Remark 8.5).*

9.4.2   Coordinate sections of the $\mathbf{g}$-vector fan

More relevant are the sections of the $\mathbf{g}$-vector fan. They provide an alternative approach to polytopal realizations of the accordion complex based projected associahedra. This approach relies on the following crucial observation.
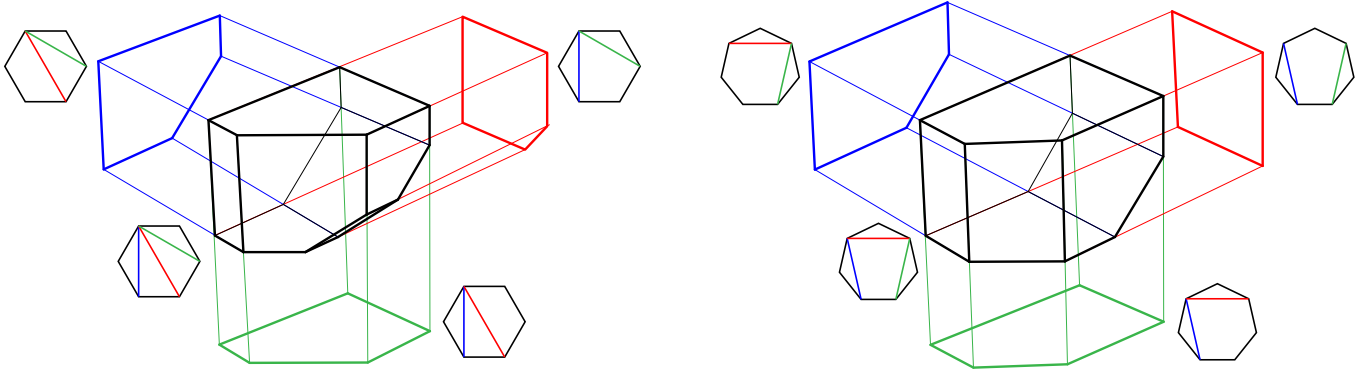
Figure 9.5 – Projecting accordiohedra on coordinate planes yields smaller accordiohedra.

Lemma 9.39. *Consider two dissections* $D_\circ \subset D'_\circ$, *and a* $D'_\circ$*-accordion diagonal* $\delta_\bullet$. *Then we have* $\mathbf{g}(D'_\circ \,|\, \delta_\bullet) \in \mathbb{R}^{D_\circ}$ *if and only if* $\delta_\bullet$ *is a* $D_\circ$*-accordion diagonal. Moreover, in this case, the* $\mathbf{g}$*-vectors* $\mathbf{g}(D_\circ \,|\, \delta_\bullet)$ *and* $\mathbf{g}(D'_\circ \,|\, \delta_\bullet)$ *coincide.*

Proof. Let $\delta_\circ \in D'_\circ \smallsetminus D_\circ$. By definition, $\delta_\bullet$ slaloms on $\delta_\circ$ if and only if $\mathbf{g}(D_\circ \,|\, \delta_\bullet)_{\delta_\circ} = \varepsilon_\circ(\delta_\circ \in D_\bullet \,|\, \delta_\bullet) \neq 0$. Therefore, $\delta_\bullet$ is a $D_\circ$-accordion diagonal if and only if it slaloms on none of the diagonals of $D'_\circ \smallsetminus D_\circ$, *i.e.* if and only if $\mathbf{g}(D'_\circ \,|\, \delta_\bullet)_{\delta_\circ} = 0$ for all $\delta_\circ \in D'_\circ \smallsetminus D_\circ$. ∎

Based on this lemma, we obtain in the following statement an alternative realization on the **g**-vector fan, which is illustrated on Figure 9.5.

Theorem 9.40. *Consider two dissections* $D_\circ \subset D'_\circ$. *Then the* $\mathbf{g}$*-vector fan* $\mathcal{F}^{\mathbf{g}}(D_\circ)$ *is given by* $\mathcal{F}^{\mathbf{g}}(D_\circ) = \{C \in \mathcal{F}^{\mathbf{g}}(D'_\circ) \,|\, C \subset \mathbb{R}^{D_\circ}\}$ *and coincides with the section of the* $\mathbf{g}$*-vector fan* $\mathcal{F}^{\mathbf{g}}(D'_\circ)$ *by* $\mathbb{R}^{D_\circ}$. *Thus* $\mathcal{F}^{\mathbf{g}}(D_\circ)$ *is realized by the orthogonal projection of the* $D'_\circ$*-accordiohedron* $\mathsf{Acco}(D'_\circ)$ *on* $\mathbb{R}^{D_\circ}$, *which is equivalently described by:*
  ◇ *the convex hull of the points* $\sum_{\delta_\bullet \in D_\bullet} \omega(D'_\circ \,|\, \delta_\bullet) \cdot \mathbf{c}(D_\circ \,|\, \delta_\bullet \in D_\bullet)$ *for all* $D_\circ$*-accordion dissections* $D_\bullet$,
  ◇ *the intersection of the half-spaces* $\left\{ \mathbf{x} \in \mathbb{R}^{D_\circ} \,\middle|\, \langle \mathbf{g}(D_\circ \,|\, \gamma_\bullet) | \mathbf{x} \rangle \leq \omega(D'_\circ \,|\, \delta_\circ) \right\}$ *for all* $D_\circ$*-accordion diagonals* $\gamma_\bullet$.

Proof. Lemma 9.39 immediately implies that $\mathcal{F}^{\mathbf{g}}(D_\circ) = \left\{ C \in \mathcal{F}^{\mathbf{g}}(D'_\circ) \,\middle|\, C \subset \mathbb{R}^{D_\circ} \right\}$. A priori, it is a subfan of the section $\mathcal{F}^{\mathbf{g}}(D'_\circ)\big|_{\mathbb{R}^{D_\circ}} = \left\{ C \cap \mathbb{R}^{D_\circ} \,\middle|\, C \in \mathcal{F}^{\mathbf{g}}(D'_\circ) \right\}$. However, since $\mathcal{F}^{\mathbf{g}}(D_\circ)$ is already a complete simplicial fan of $\mathbb{R}^{D_\circ}$, it coincides with $\mathcal{F}^{\mathbf{g}}(D'_\circ)\big|_{\mathbb{R}^{D_\circ}}$. Since $\mathcal{F}^{\mathbf{g}}(D'_\circ)$ is the normal fan of $\mathsf{Acco}(D'_\circ)$, this shows that $\mathcal{F}^{\mathbf{g}}(D_\circ) = \mathcal{F}^{\mathbf{g}}(D'_\circ)\big|_{\mathbb{R}^{D_\circ}}$ is the normal fan of the orthogonal projection of $\mathsf{Acco}(D'_\circ)$ on $\mathbb{R}^{D_\circ}$ [Zie95, Lemma 7.11].

To conclude, we prove the given vertex and facet descriptions of this projection. Since $\mathcal{F}^{\mathbf{g}}(D_\circ) = \mathcal{F}^{\mathbf{g}}(D'_\circ)\big|_{\mathbb{R}^{D_\circ}}$, the inequalities of the projection of $\mathsf{Acco}(D'_\circ)$ on $\mathbb{R}^{D_\circ}$ are just the inequalities of $\mathsf{Acco}(D'_\circ)$ whose normal vectors are in $\mathbb{R}^{D_\circ}$. The vertex description follow from the inequality description using the same argument as in Lemma 9.17. ∎

Remark 9.41. The projection of the accordiohedron $\mathsf{Acco}(D'_\circ)$ on $\mathbb{R}^{D_\circ}$ differs from the accordiohedron $\mathsf{Acco}(D_\circ)$: they have both $\mathcal{F}^{\mathbf{g}}(D_\circ)$ as normal fan, but their precise geometry is different.

Corollary 9.42. *For any hollow dissection* $D_\circ$, *the* $\mathbf{g}$*-vector fan* $\mathcal{F}^{\mathbf{g}}(D_\circ)$ *is realized by a projection of an associahedron of [HPS16].*

Proof. Apply Corollary 9.40 to any triangulation $T_\circ$ that refines $D_\circ$. ∎

Remark 9.43. Approaching accordion complexes as coordinate sections of g-vector fans actually provides more concise (but also less instructive) proofs for Sections 8.2.3 and 9.2.3. Namely, consider any dissection $D_\circ$ and let $T_\circ$ be a triangulation that refines $D_\circ$. For the triangulation $T_\circ$, it is known that the normal fan of the associahedron $\mathsf{Asso}(T_\circ)$ (*i.e.* the g-vector fan $\mathcal{F}^{\mathbf{g}}(T_\circ)$) refines the fan defined by the coordinate hyperplane arrangement. This implies that the section $\mathcal{F}^{\mathbf{g}}(T_\circ)|_{\mathbb{R}^{D_\circ}}$ actually coincides with $\{C \in \mathcal{F}^{\mathbf{g}}(T_\circ) \,|\, C \subset \mathbb{R}^{D_\circ}\}$ and gives an alternative concise proof that the collection of cones $\{C \in \mathcal{F}^{\mathbf{g}}(T_\circ) \,|\, C \subset \mathbb{R}^{D_\circ}\}$ forms a complete simplicial fan. Moreover, this fan has the same combinatorics as the accordion complex $\mathcal{AC}(D_\circ)$ by Lemma 9.39. We conclude directly that $\mathcal{AC}(D_\circ)$ is a pseudo-manifold realized by the fan $\{C \in \mathcal{F}^{\mathbf{g}}(T_\circ) \,|\, C \subset \mathbb{R}^{D_\circ}\}$ and by the orthogonal projection of the associahedron $\mathsf{Asso}(T_\circ)$ on $\mathbb{R}^{D_\circ}$.

9.4.3   Cluster algebra analogues

The perspective on accordion complexes developed in this section also opens the door to generalizations on arbitrary cluster algebras (finite type or not). Namely, consider an arbitrary cluster $X_\circ = (x_\circ^1, \dots, x_\circ^m)$ in an arbitrary cluster algebra $\mathcal{A}$. For any cluster variable $y \in \mathcal{A}$, we denote by $\mathbf{g}(X_\circ \,|\, y) \in \mathbb{R}^m$ and $\mathbf{d}(X_\circ \,|\, y) \in \mathbb{R}^m$ the $\mathbf{g}$- and $\mathbf{d}$-vectors of y computed with respect to $X_\circ$, see [FZ02, FZ07]. Fix a nonempty proper subset I of $[m]$. We consider two natural subcomplexes of the cluster complex of $\mathcal{A}$:

  ◇ the subcomplex $\Delta^{\mathbf{d}}(X_\circ, I)$ induced by the variables y with $\mathbf{d}(X_\circ \,|\, y)_i = 0$ for $i \in I$,
  ◇ the subcomplex $\Delta^{\mathbf{g}}(X_\circ, I)$ induced by the variables y with $\mathbf{g}(X_\circ \,|\, y)_i = 0$ for $i \in I$.

It is well-known that the subcomplex $\Delta^{\mathbf{d}}(X_\circ, I)$ is the cluster complex obtained by freezing all variables x_i for $i \in I$. For example in type A, it is a join of simplicial associahedra and it can therefore be realized by a product of smaller simplicial associahedra. In contrast, we are not aware of the subcomplex $\Delta^{\mathbf{g}}(X_\circ, I)$ being investigated.

Example 9.44. Let $T_\circ$ be a triangulation, with internal diagonals labeled by $1, \dots, m$. Consider the corresponding type A_m cluster $X_\circ$. Then for any nonempty proper subset I of $[m]$, the subcomplex $\Delta^{\mathbf{g}}(X_\circ, I)$ is isomorphic to the $D_\circ$ accordion complex, where $D_\circ$ is the dissection obtained by deleting in $T_\circ$ the diagonals labeled by I.

   This example should extend to cluster algebras on surfaces [FT12]. Motivated by the results of this chapter and preliminary computational investigations, we point out some observations and questions on arbitrary cluster algebras. First, consider the subset $\{C \in \mathcal{F}^{\mathbf{g}}(X_\circ) \,|\, C \subseteq \mathbb{R}^{[m] \smallsetminus I}\}$ of the g-vector fan of $X_\circ$. Since it is a downward-closed subset of cones of a fan, it provides a simplicial fan realization of $\Delta^{\mathbf{g}}(X_\circ, I)$. Is it always also the section of $\mathcal{F}^{\mathbf{g}}(X_\circ)$ by $\mathbb{R}^{[m] \smallsetminus I}$?

   Assume now that $\mathcal{A}$ is a finite type cluster algebra, and $X_\circ$ is an acyclic seed. The g-vector fan $\mathcal{F}^{\mathbf{g}}(X_\circ)$ is then a Cambrian fan of N. Reading and D. Speyer [RS09], and it is realized by a generalized associahedron $\mathsf{Asso}(X_\circ)$ of C. Hohlweg, C. Lange and H. Thomas [HLT11]. Similar arguments as in Remark 9.43 indeed show that the set of cones $\{C \in \mathcal{F}^{\mathbf{g}}(X_\circ) \,|\, C \subseteq \mathbb{R}^{[m] \smallsetminus I}\}$ is a section of $\mathcal{F}^{\mathbf{g}}(X_\circ)$ by $\mathbb{R}^{[m] \smallsetminus I}$ in this case. Therefore, the orthogonal projection of $\mathsf{Asso}(X_\circ)$ on $\mathbb{R}^{[m] \smallsetminus I}$ is a realization of $\Delta^{\mathbf{g}}(X_\circ, I)$. Is there an analogue for an arbitrary seed $X_\circ$ (acyclic or not)?

   Finally, when oriented in the suitable direction v (the sum of the positive roots, or equivalently of the fundamental weights), the graph of the generalized associahedron $\mathsf{Asso}(X_\circ)$ is the Hasse diagram of a Cambrian lattice [Rea06]. One can similarly orient the graph of the projection of $\mathsf{Asso}(X_\circ)$ on $\mathbb{R}^{[m] \smallsetminus I}$ in the direction of the projection of v on $\mathbb{R}^{[m] \smallsetminus I}$. Is the resulting graph the Hasse diagram of a lattice? The results of [GM16] and that of the present chapter show that this property holds in type A. We also computationally verified the statement in types B_4, B_5, D_4 and D_5.

Fan realizing
some 2-associahedra

10.1 Introduction

10.1.1 Motivations

In this last chapter, we develop a new approach towards geometric realizations of *multi-associahedra*. As mentioned in Section 7.2, they form a universal subfamily of subword complexes admitting another combinatorial model, namely *multitriangulations*.

For integers k and n, we consider a convex polygon $\mathcal{P}$ with $n+2k+1$ vertices and call a *k-triangulation* (or *multitriangulation* for unspecified k) of $\mathcal{P}$ any inclusion maximal set of diagonals such that no $k+1$ of them mutually cross (see Figure 10.1). As any diagonal with at most $k-1$ vertices of $\mathcal{P}$ on one side belongs to any k-triangulation, we only consider the other diagonals, called *k-relevant diagonals*, as part of a k-triangulation. The *k-associahedron* $\mathbf{\Delta}_{k,n}$ (or *multiassociahedron* for unspecified k) is then the simplicial complex whose facets are the k-triangulations of $\mathcal{P}$. It was introduced by V. Capoyleas and J. Pach in [CP92] where multitriangulations were studied as geometric graphs, after which the complex itself was independently shown to be pure by T. Nakamigawa [Nak00], and A. W. M. Dress, J. H. Koolen and V. Moulton [DKM02]. It was also proved to be a piecewise linear sphere of dimension $(kn-1)$ in an unpublished paper of J. Jonsson [Jon03]. Many structural aspects of multitriangulations, in particular their decomposition into *stars*, were then studied by V. Pilaud and F. Santos [PS09] in order to approach several open problems. Among them V. Pilaud and F. Santos recall a question asked by J. Jonsson [Jon05] about geometric realizations of multiassociahedra.

Question 10.1. Are multiassociahedra boundary complexes of some convex polytopes?

Some instances of multiassociahedra turn out to be classical in polytope theory and therefore give a positive answer to this question in the following cases (see [PS09]).
- For $n=0$, the complex $\mathbf{\Delta}_{k,0}$ is reduced to a single point (the empty set).
- For $n=1$, the complex $\mathbf{\Delta}_{k,1}$ is the boundary of a k-simplex.
- For $n=2$, the complex $\mathbf{\Delta}_{k,2}$ is the boundary complex of a cyclic polytope.
- For $k=1$, the complex $\mathbf{\Delta}_{1,n}$ is the (classical) associahedron $\mathsf{Asso}(n)$, as 1-triangulations are just usual triangulations.

Apart from these classical realizations, a first oriented matroid theory approach allowed J. Bokowski and V. Pilaud to realize $\mathbf{\Delta}_{2,3}$ as a convex polytope in [BP09]. Using
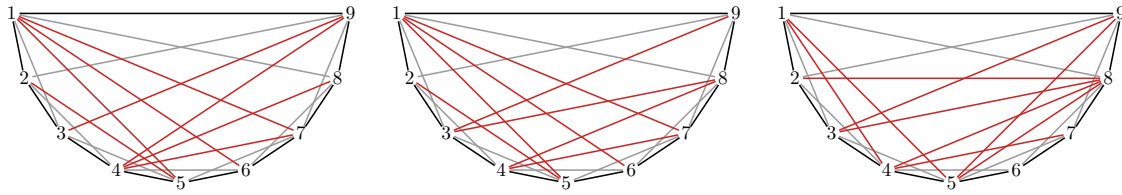
Figure 10.1 – Three 2-triangulations of a 9-gon (2-relevant diagonals appear red).

the framework of *sorting networks* as introduced by V. Pilaud and M. Pocchiola [PP12], V. Pilaud and F. Santos then constructed brick polytopes in [PS12] as an attempt to realize multiassociahedra, and more generally type A spherical subword complexes. If these objects turned out to be interesting by themselves, none of them realized more multiassociahedra. That multiassociahedra appear as instances of subword complexes was observed by V. Pilaud and M. Pocchiola [PP12] and by C. Stump [Stu11] (see Theorem 10.5). C. Ceballos, J.-P. Labbé and C. Stump extended multiassociahedra to *multi cluster complexes* in any Coxeter type and developed combinatorial tools for subword complexes in [CLS14]. Finally N. Bergeron, C. Ceballos and J.-P. Labbé used Gale duality in [BCL15] to realize as fans all complexes $\mathbf{\Delta}_{k,3}$ for $k \in \mathbb{N}$, so as $\mathbf{\Delta}_{2,4}$ and $\mathbf{\Delta}_{3,4}$.

Using recently discovered operations on subword complexes, we provide the first fan realizations of the complexes $\mathbf{\Delta}_{2,n}$ for $n \in \{5, 6, 7, 8\}$ and conjectural rays for any complex $\mathbf{\Delta}_{2,n}$ for $n \in \mathbb{N}$ (Question 10.3). All computations involved in this work were done with the software Sagemath [Dev15] (with available source code[1]). We consider a convex $(n+5)$-gon with vertices cyclically labeled from 1 to $n+5$ and denote the diagonal between $i \in [n + 5]$ and $j \geq i$ by (i, j). We denote by $(\mathbf{e}_1, \dots, \mathbf{e}_n, \mathbf{f}_1, \dots, \mathbf{f}_n)$ the canonical basis of $\mathbb{R}^{2n}$ and associate to each 2-relevant diagonal (i, j) a vector $\mathbf{v}_{(i,j)}$ in $\mathbb{R}^{2n}$ as follows (see Theorem 10.5 and Figure 10.5, and Figure 10.14).

a) $\mathbf{v}_{(1,4)} = \mathbf{e}_n - \mathbf{f}_n$ and $\mathbf{v}_{(1,j+4)} = (2n + 2 - j)(\mathbf{e}_j - \mathbf{e}_{j+1}) + \mathbf{e}_n + \mathbf{f}_j - \mathbf{f}_n$ for $j \in [n - 1]$;

b) $\mathbf{v}_{(2,j+4)} = \mathbf{e}_j + (2n + 2 - j)(\mathbf{e}_j - \mathbf{e}_{j+1}) + \mathbf{f}_j$ for $j \in [n - 1]$ and $\mathbf{v}_{(2,n+4)} = \mathbf{e}_n + \mathbf{f}_n$;

c) $\mathbf{v}_{(3,j+5)} = -\mathbf{e}_j$ for $j \in [n]$;

d) $\mathbf{v}_{(4,j+6)} = \mathbf{e}_j + (2n + 2 - j)(\mathbf{e}_j - \mathbf{e}_{j+1}) - \mathbf{f}_j$ for $j \in [n - 1]$;

e) $\mathbf{v}_{(i+4,i+j+6)} = j\,\mathbf{e}_i - (j-1)(\mathbf{e}_{i+j} + \mathbf{e}_{i+j+1}) + (2n + 4 - i)(\mathbf{e}_{i+j} - \mathbf{e}_{i+1}) + \mathbf{f}_i - \mathbf{f}_{i+j}$ for $i \in [n-2]$ and $j \in [n - i - 1]$.

Theorem 10.2. *The vectors* $\mathbf{v}_{(i,j)}$ *are the rays of a complete simplicial fan in* $\mathbb{R}^{2n}$ *which realizes the multiassociahedron* $\mathbf{\Delta}_{2,n}$ *for* $n \in [8]$.

Question 10.3. *Are the vectors* $\mathbf{v}_{(i,j)}$ *the rays of a complete simplicial fan in* $\mathbb{R}^{2n}$ *which realizes the multiassociahedron* $\mathbf{\Delta}_{2,n}$ *for any* $n \geq 1$?

10.1.2 Overview

Theorem 10.2 is the main result of this chapter and was checked computationally using the characterization of complete simplicial fans of Proposition 3.7. The rest of the chapter will therefore mostly be a report on the heuristic process leading to the candidate rays. We describe in Section 10.2 complementary notions on simplicial complexes, polyhedral geometry and subword complexes that we need for our presentation. In particular we state Theorem 10.5 describing the identification of multiassociahedra to some subword complexes. In Section 10.3 we obtain by a new method the realization of the associahedron by J.-L. Loday [Lod04]. This method is the starting point of our heuristic construction of 2-associahedra as fans, which is presented in Section 10.4. Finally we briefly discuss some further aspects of our work in Section 10.5.

---

[1] https://arxiv.org/abs/1608.08491

10.2 Preliminaries

Our work relies on the interpretation of multiassociahedra as subword complexes (Theorem 10.5 in Section 10.2.3). Our main tools will be combinatorial operations on them studied by M. Gorsky in [Gor13, Gor14], that we try to translate geometrically. We present the complementary notions that we need on simplicial complexes, polyhedral geometry and subword complexes in Sections 10.2.1, 10.2.2 and 10.2.3 respectively. The operations on subword complexes due to M. Gorsky are described in Section 10.2.4.

10.2.1 Simplicial complexes

Recall that given two complexes $\mathcal{C}_1$ and $\mathcal{C}_2$, the *join* of $\mathcal{C}_1$ and $\mathcal{C}_2$ is the complex

$$\mathcal{C}_1 * \mathcal{C}_2 := \{f \sqcup f' \mid f \in \mathcal{C}_1, f' \in \mathcal{C}_2\}$$

where the complexes $\mathcal{C}_1$ and $\mathcal{C}_2$ are considered with disjoint sets of vertices and $\sqcup$ denotes the disjoint union. The *suspension* of a complex $\mathcal{C}$ is the join of $\mathcal{C}$ with a complex consisting in two singletons, called *suspension vertices*. Given a vertex x of $\mathcal{C}$, the *one-point-suspension* of $\mathcal{C}$ with respect to x is the complex

$$\mathrm{ops}_{\mathcal{C}}(x) := \big(\mathrm{del}_{\mathcal{C}}(x) * \{x_0, x_1\} \big) \cup \big(\mathrm{lk}_{\mathcal{C}}(x) * x_0 x_1 \big)$$

where x_0 and x_1 are two new vertices, also called *suspension vertices* in $\mathrm{ops}_{\mathcal{C}}(x)$. This operation extends the usual suspension: in the particular case where the vertex x is only contained in the face $\{x\}$ of $\mathcal{C}$, then we consider by convention that the right part of the union is empty and the left part is just the suspension of the complex where the disconnected vertex x has been forgotten. So the suspension of a complex is obtained by adding an artificial disconnected vertex to it and taking the one-point-suspension with respect to this vertex. Figure 10.2 illustrates the one-point-suspension operation on two complexes. We finally recall that for a complex $\mathcal{C}$ and a face f of $\mathcal{C}$, the *stellar subdivision* of the face f in $\mathcal{C}$ is the complex

$$\mathrm{stell}_{\mathcal{C}}(f) := \mathrm{del}_{\mathcal{C}}(f) \cup \{f' \cup \{a\} \mid f \not\subseteq f' \in \mathrm{st}_{\mathcal{C}}(f)\} = \mathrm{del}_{\mathcal{C} \cup \mathrm{st}_{\mathcal{C}}(f) * \{a\}}(f)$$

where a is a new vertex, called *subdivision vertex* (see Figure 10.3 for examples).
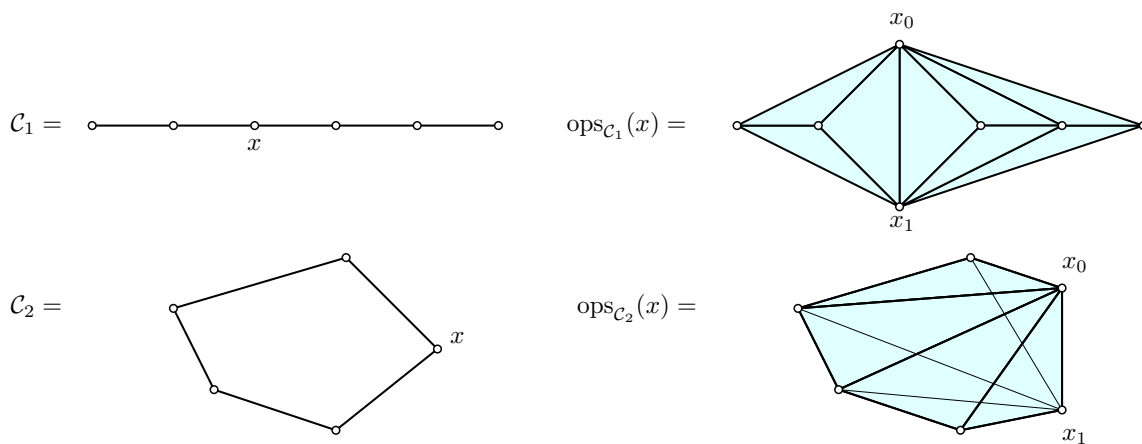
Figure 10.2 – Two 1-dimensional complexes $\mathcal{C}_1$ and $\mathcal{C}_2$ (left) and their one-point-suspensions $\mathrm{ops}_{\mathcal{C}_1}(x)$ and $\mathrm{ops}_{\mathcal{C}_2}(x)$ with respect to a given vertex x (right).
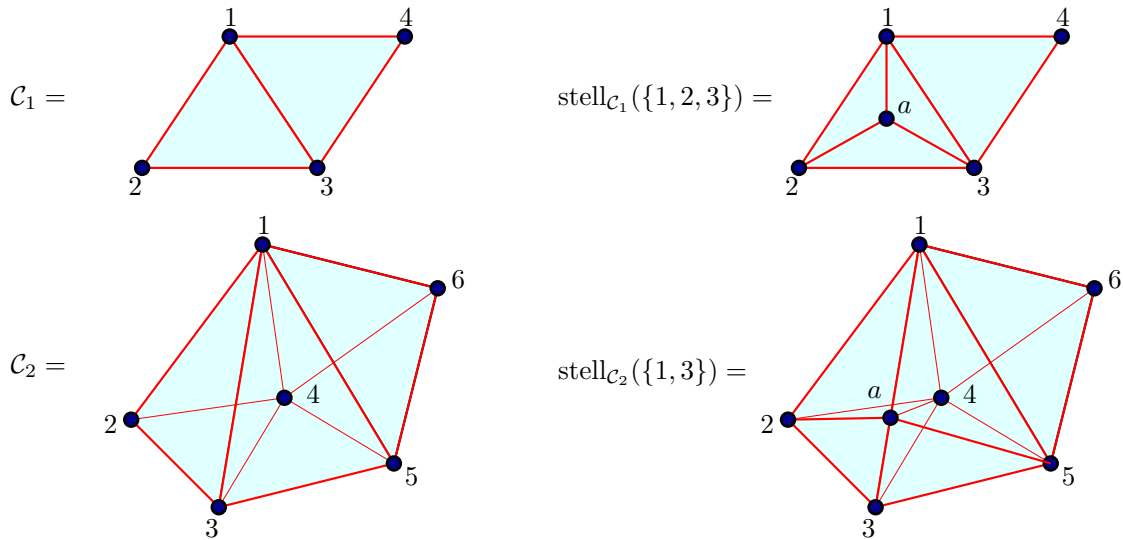
Figure 10.3 – A 2-dimensional complex $\mathcal{C}_1 = \{\{1,2,3\},\{1,3,4\}\}$ (top left) and the stellar subdivision of the facet $\{1,2,3\}$ in it (top right), and a 3-dimensional complex $\mathcal{C}_2 = \{\{1,2,3,4\},\{1,3,4,5\},\{1,4,5,6\}\}$ (bottom left) and the stellar subdivision of the edge $\{1,3\}$ in it (bottom right).

10.2.2   Polyhedral geometry

We recall that given a simplicial fan $\mathcal{F}$, we denote by $\mathcal{C}_{\mathcal{F}}$ the abstract simplicial complex whose vertices are the rays of $\mathcal{F}$ and whose faces are the subsets of rays generating the cones of $\mathcal{F}$. In this chapter we will use the following realizability results on the operations defined in Section 10.2.1.

Lemma 10.4 (folklore). *One-point-suspensions and stellar subdivisions of simplicial complexes realizable as polytopes (resp. complete simplicial fans, resp. spheres) still are realizable as simplicial polytopes (resp. complete simplicial fans, resp. spheres).*

Lemma 10.4 is classical and its proof is left to the reader. We only describe the actual transformation on the rays of a complete simplicial fan allowing to realize as well the stellar subdivisions and the one-point-suspensions of the corresponding complex. We will indeed need them to derive the coordinates of Question 10.3. Let $\mathcal{F}$ be a complete simplicial fan in $\mathbb{R}^n$ and let R be a set of vectors in $\mathbb{R}^n$ such that for each ray ρ of $\mathcal{F}$ there is exactly one vector $\mathbf{v} \in R$ such that $\rho = \mathbb{R}_{\geq 0}\mathbf{v}$. The vertex set of the simplicial complex $\mathcal{C}_{\mathcal{F}}$ associated to the fan $\mathcal{F}$ can then naturally be identified with the set R. Let $f = \{\mathbf{v}_1, \ldots, \mathbf{v}_\ell\}$ be a face of the complex $\mathcal{C}_{\mathcal{F}}$. Then the complex $\mathrm{stell}_{\mathcal{C}_{\mathcal{F}}}(f)$ can be realized as a complete simplicial fan by adding a ray to the fan $\mathcal{F}$, generated by any vector of the form $\alpha_1\mathbf{v}_1 + \cdots + \alpha_\ell\mathbf{v}_\ell$ with $\alpha_1 > 0, \ldots, \alpha_\ell > 0$. This new ray corresponds to the subdivision vertex of the stellar subdivision. The generic choice consists to set all α_i's equal to 1 (see Figure 10.4). Let $\mathbf{v}$ be a vector in R, then the complex $\mathrm{ops}_{\mathcal{C}_{\mathcal{F}}}(\mathbf{v})$ is of dimension one more than the complex $\mathcal{C}_{\mathcal{F}}$. We consider the vector space $\mathbb{R}^{n+1} := \mathbb{R}^n \oplus \mathbb{R}\mathbf{e}_{n+1}$ and associate to a vector $\mathbf{v}' \in R \smallsetminus \{\mathbf{v}\}$ the vector $\mathbf{v}' \oplus \mathbf{0}$. The suspensions vertices obtained from $\mathbf{v}$ are associated to two vectors $\mathbf{v} \oplus \alpha\mathbf{e}_{n+1}$ and $\mathbf{v} \oplus \beta\mathbf{e}_{n+1}$, with $\alpha\beta < 0$. The generic choice for us will be $\alpha = -1$ and $\beta = 1$. The set of rays that we obtain in $\mathbb{R}^{n+1}$ then supports a complete simplicial fan realizing $\mathrm{ops}_{\mathcal{C}_{\mathcal{F}}}(\mathbf{v})$ (see Figure 10.4). In the particular case of a suspension, one can artificially add the zero vector $\mathbf{0}$ to the set R and choose $\mathbf{v} = \mathbf{0}$ in the previous construction (see Figure 10.4). The previous descriptions give valid coordinates but certainly not all of them. Yet these realizations are easy to implement and they will be enough for our purposes.
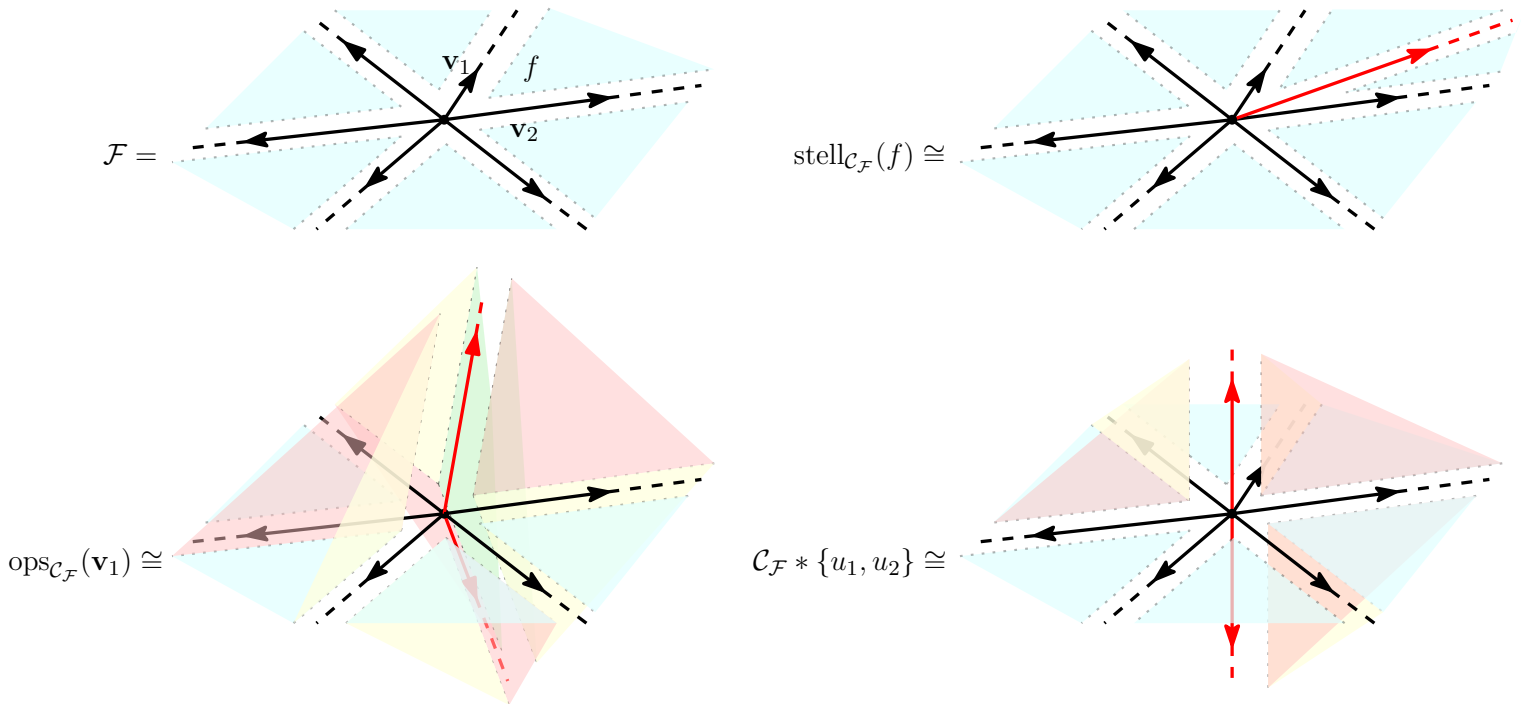
Figure 10.4 – A complete 2-dimensional simplicial fan $\mathcal{F}$ with a distinguished face $f = \mathbb{R}_{\geq 0}\{\mathbf{v}_1, \mathbf{v}_2\}$ (top left), a complete 2-dimensional simplicial fan realizing the complex $\mathrm{stell}_{\mathcal{C}_{\mathcal{F}}}(f)$ (top right), a complete 3-dimensional simplicial fan realizing the complex $\mathrm{ops}_{\mathcal{C}_{\mathcal{F}}}(\mathbf{v}_1)$ (bottom left), and a complete 3-dimensional simplicial fan realizing the suspension of the complex $\mathcal{C}_{\mathcal{F}}$ (bottom right). The new fans are obtained by the generic transformations on $\mathcal{F}$ described after Lemma 10.4.

10.2.3 Subword complexes

Recall that, for $n \geq 1$, we denote by S the set of simple transpositions $s_i := (i \; i+1)$ (for $i \leq n$), that we consider as an alphabet. To avoid confusion, a simple transposition is referred to with an italic letter s_i when considered as an element of the symmetric group $\mathfrak{S}_{n+1}$, and with a sans serif letter s_i when considered as a letter in the alphabet S. Finally we recall the definition of the *subword complex* $\mathcal{S}(\mathsf{Q})$ of a word $\mathsf{Q} = \mathsf{q}_1 \ldots \mathsf{q}_p$ in S^* given in Section 7.2.

$$\mathcal{S}(\mathsf{Q}) := \big\{ J \subseteq [p] \,\big|\, \mathsf{Q}_{[p] \smallsetminus J} \text{ contains a reduced expression of } w_\circ \text{ as a subword} \big\}.$$

Let $\mathsf{c} := \mathsf{s}_1 \ldots \mathsf{s}_n$, the c-*sorted expression* of $w_\circ$ (see [Rea06]) is the word

$$\mathsf{w}_\circ(\mathsf{c}) := \prod_{i=1}^{n} \left(\prod_{j=1}^{n+1-i} \mathsf{s}_j \right) \tag{10.1}$$

where the product symbol denotes the concatenation on words in increasing order of indexes, that is $\mathsf{w}_\circ(\mathsf{c}) = \mathsf{s}_1 \mathsf{s}_2 \ldots \mathsf{s}_n \; \mathsf{s}_1 \ldots \mathsf{s}_{n-1} \; \ldots \; \mathsf{s}_1 \mathsf{s}_2 \; \mathsf{s}_1$. We will also use the notation $\mathsf{c}[i] := \mathsf{s}_1 \ldots \mathsf{s}_i$, so that $\mathsf{w}_\circ(\mathsf{c}) = \prod_{i=1}^{n} \mathsf{c}[n+1-i]$. The c-sorted expression $\mathsf{w}_\circ(\mathsf{c})$ is a reduced expression of $w_\circ$. It will be convenient to consider smaller symmetric groups $\mathfrak{S}_p$ (with $p \leq n+1$) as embedded in $\mathfrak{S}_{n+1}$ and still denote by $\mathsf{w}_\circ(\mathsf{c}[p])$ the c-sorted expression of their longest element. The following statement describes how multiassociahedra arise as instances of subword complexes.
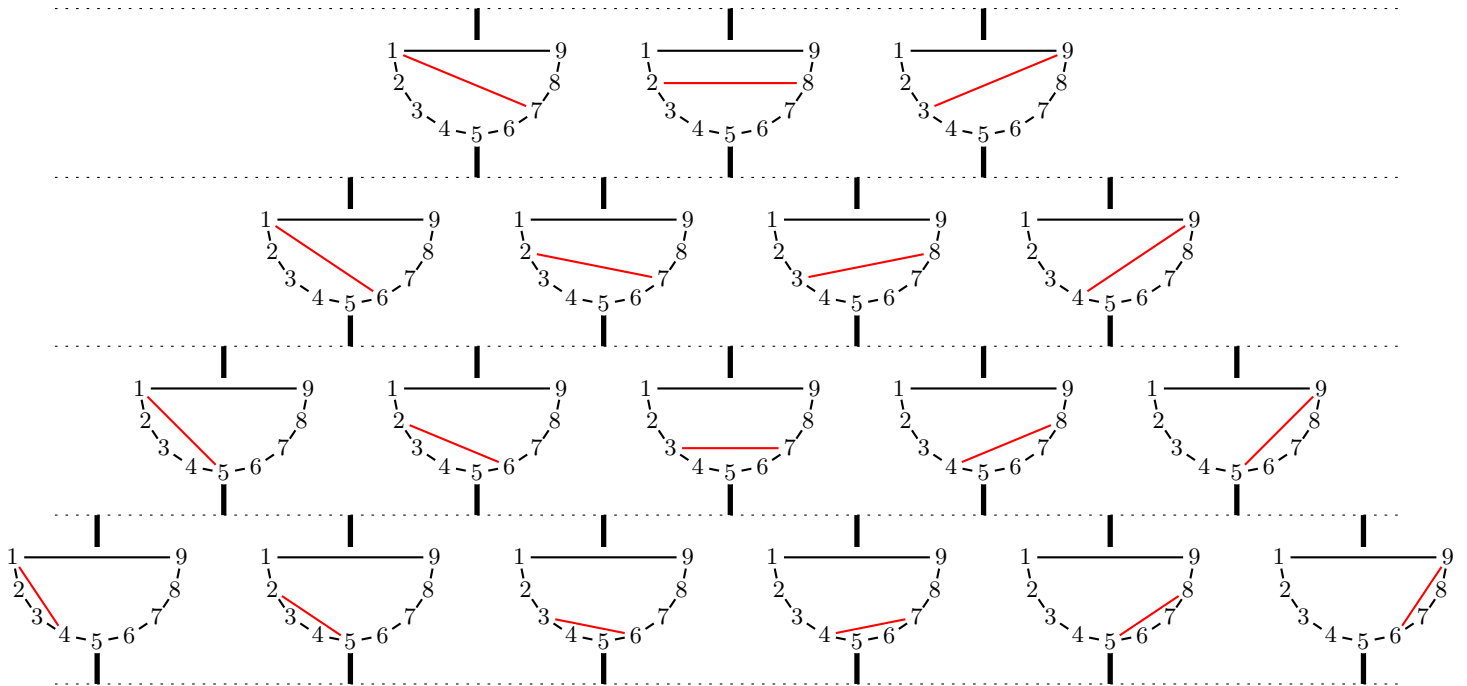
Figure 10.5 – The identification of Theorem 10.5, for $n = 4$ and $k = 2$, between the 2-relevant diagonals (of length at least 2) of a convex polygon with 9 vertices and the letters of the word $\mathsf{c}^2\mathsf{w}_\circ(\mathsf{c})$ seen on the corresponding sorting network.

Theorem 10.5 ([PP12, Stu11])**.** *For $k \geq 0$ and $n \geq 1$, the multiassociahedron $\Delta_{k,n}$ is isomorphic to the subword complex $\mathcal{S}(\mathsf{c}^k\mathsf{w}_\circ(\mathsf{c}))$. Given a convex polygon $\mathcal{P}_{n+2k+1}$ with $n + 2k + 1$ vertices cyclically labeled from 1 to $n + 2k + 1$, an isomorphism between the complexes $\Delta_{k,n}$ and $\mathcal{S}(\mathsf{c}^k\mathsf{w}_\circ(\mathsf{c}))$ is given by the following identification of the k-relevant diagonals of $\mathcal{P}_{n+2k+1}$ with the letters of $\mathsf{c}^k\mathsf{w}_\circ(\mathsf{c})$.*
  - *for $i \leq k$ and $j \in [n]$, the diagonal $(i, i+j+k)$ is associated to the letter at position $(i-1)n + j$ in the word $\mathsf{c}^k\mathsf{w}_\circ(\mathsf{c})$, namely its i-th letter s_j;*
  - *for $i + k \geq k + 1$ and $j \in [n + 1 - i]$, the diagonal $(i + k, i + j + 2k)$ is associated to the letter in position $(k + i - 1)n - (i - 1)(i - 2)/2 + j$ in the word $\mathsf{c}^k\mathsf{w}_\circ(\mathsf{c})$, namely the letter s_j whose indices are i and j in the factor $\mathsf{w}_\circ(\mathsf{c})$ of the word $\mathsf{c}^k\mathsf{w}_\circ(\mathsf{c})$, seen as the product in Equation (10.1).*

The identification given in Theorem 10.5 is illustrated in Figure 10.5. Multiassociahedra form a universal family, as discussed in Section 7.2. So giving geometric realizations for them is equivalent to giving geometric realizations for any subword complex.

We conclude this section with useful properties of subword complexes. Let $\mathsf{Q} = \mathsf{s}_{i_1} \ldots \mathsf{s}_{i_\ell}$ be a word, the *rotated word* of Q is the word $\mathsf{Q}^\circlearrowleft := \mathsf{s}_{n+1-i_\ell}\mathsf{s}_{i_1} \ldots \mathsf{s}_{i_{\ell-1}}$.

Theorem 10.6 (rotation map [CLS14])**.** *For any word Q, the subword complexes $\mathcal{S}(\mathsf{Q})$ and $\mathcal{S}(\mathsf{Q}^\circlearrowleft)$ are isomorphic. An isomorphism is obtained by identifying all letters in the common factor of Q and $\mathsf{Q}^\circlearrowleft$, and the two letters by which they differ.*

Let Q^{-1} denote the mirror image of a word Q and Q^{-i} the concatenation of i copies of Q^{-1}. Theorems 10.5 and 10.6 imply that the multiassociahedron is isomorphic to all complexes of the form $\mathcal{S}(\mathsf{c}^{k-i}\mathsf{w}_\circ(\mathsf{c})\mathsf{c}^{-i})$ (for $i \in [k]$). Finally basic properties of sorting networks imply that any subword complex $\mathcal{S}(\mathsf{Q})$ is isomorphic to $\mathcal{S}(\mathsf{Q}^{-1})$ with identification of the vertices given by the mirror symmetry (see [PP12, PS12]).

10.2.4 Operations on subword complexes

We now focus on three natural operations on subword complexes. A word Q is *obtained by a commutation move* from a word Q' if there exist two words $U_1, U_2 \in S^*$ and $i, j \in [n]$ such that $|i - j| \geq 2$ and $Q = U_1\, s_i s_j\, U_2$ and $Q' = U_1\, s_j s_i\, U_2$. As mentioned in Section 10.2.3 the subword complexes $\mathcal{S}(Q)$ and $\mathcal{S}(Q')$ are then isomorphic since s_i and s_j commute in the symmetric group $\mathfrak{S}_{n+1}$. We also consider two operations studied by M. Gorsky in [Gor13, Gor14], which are our main combinatorial tools.

- A word Q is *obtained by a 0-Hecke move* from a word Q' if there exist words $U_1, U_2 \in S^*$ and $i \in [n]$ such that $Q = U_1\, s_i\, U_2$ and $Q' = U_1\, s_i^2\, U_2$. In this case Q' is *obtained by a reverse 0-Hecke move* from Q. Alternatively we will also say that Q' is *obtained by doubling a letter* in Q.
- A word Q is *obtained by a braid move* from a word Q' if there exist words $U_1, U_2 \in S^*$ and $i, j \in [n]$, with $|i - j| = 1$, such that $Q = U_1\, s_i s_j s_i\, U_2$ and $Q' = U_1\, s_j s_i s_j\, U_2$.

Remark 10.7. Commutation and braid moves are natural operations to consider since the corresponding relations $s_i s_j = s_j s_i$ for $|i - j| \geq 2$, and $s_i s_j s_i = s_j s_i s_j$ for $|i - j| = 1$, hold in the symmetric group $\mathfrak{S}_{n+1}$, and can be completed into a presentation of $\mathfrak{S}_{n+1}$ by adding the relations $s_i^2 = \mathrm{Id}$ for $i \in [n]$. Here the corresponding operation on words is replaced by $s_i^2 = s_i$, which is in fact the last relation in the classical presentation of the 0-Hecke algebra of the symmetric group $\mathfrak{S}_{n+1}$, hence the name of the corresponding transformation. M. Gorsky calls these moves *nil-Hecke moves* in [Gor13] but the corresponding relation in the nil-Hecke algebra would be $s_i^2 = 0$.

We say that we *apply a braid* (resp. *0-Hecke*, resp. *commutation*) *move* to a subword complex $\mathcal{S}(Q)$ when we consider the subword complex $\mathcal{S}(Q')$, where Q and Q' are related by the same operation. The combinatorial effect of these operations on the subword complex $\mathcal{S}(Q)$ depend on the vertex status of the letters implied in the transformation (see Figure 10.6) and were described by M. Gorsky as follows.

Theorem 10.8 ([Gor13])**.** *Suppose that a word $Q' = U_1\, q'_r q'_{r+1}\, U_2$ is obtained from a word $Q = U_1\, q_r\, U_2$ by doubling the letter q_r. If q_r is a vertex of the subword complex $\mathcal{S}(Q)$, then the subword complex $\mathcal{S}(Q')$ is isomorphic to the one-point-suspension $\mathrm{ops}_{\mathcal{S}(Q)}(q_r)$ of $\mathcal{S}(Q)$ with respect to q_r. Otherwise $\mathcal{S}(Q')$ is isomorphic to the suspension of $\mathcal{S}(Q)$. The suspension vertices in $\mathcal{S}(Q')$ are q'_r and q'_{r+1}.*

0-Hecke move   Braid move
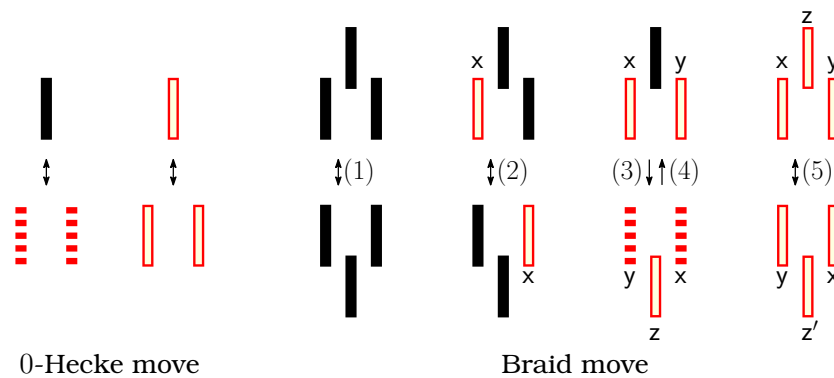
Figure 10.6 – The evolution of the vertex status of letters implied in 0-Hecke and braid moves, seen on the corresponding part of the sorting network $\mathcal{N}_Q$. Two red dashed segments denote vertices not belonging to a common edge while empty red segment denote vertices in all faces not forbidden by dashed segments. Black plain segments represent nonvertices. The letters x, y, z and z' give the identifications of the exchanged letters by a braid move in the topological realizations of the corresponding complexes. The numbers for braid moves correspond to the different Cases in Theorem 10.9.

$$xzy = q_r q_{r+1} q_{r+2} \leftrightarrow q'_r q'_{r+1} q'_{r+2} = yz'x$$
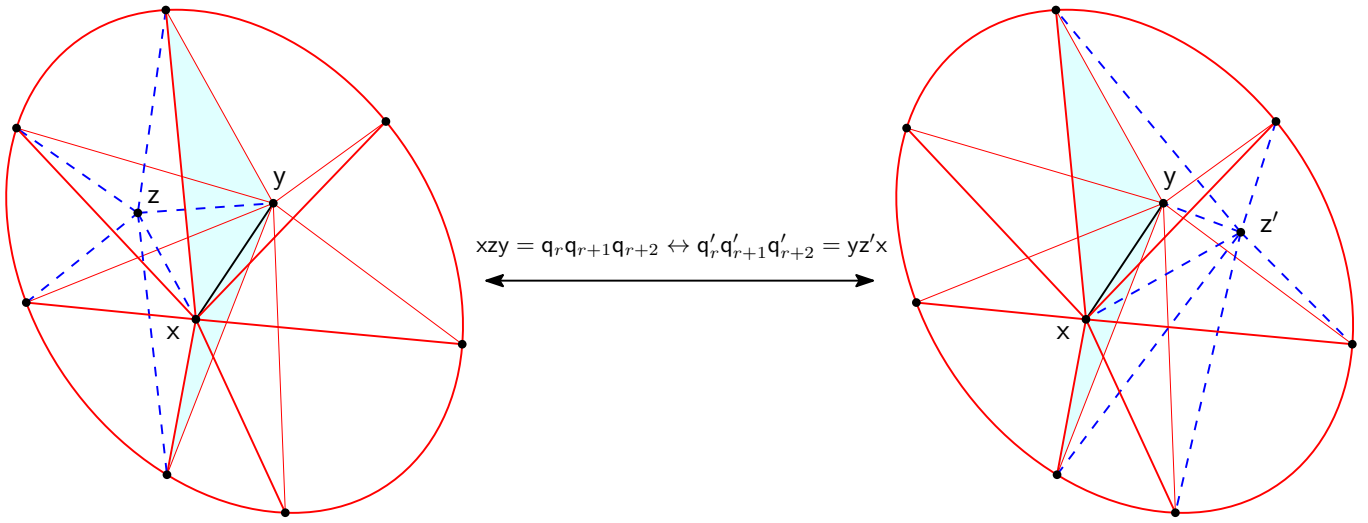
Figure 10.7 – The effect of a braid move in Case (5) of Theorem 10.9, seen as a local transformation on the topological realization of a 3-dimensional subword complex $\mathcal{S}(Q)$. Only the parts of the complex affected by the transformation are depicted, namely the star $\mathrm{st}_{\mathcal{S}(Q)}(q_{r+1})$ of the vertex q_{r+1} in $\mathcal{S}(Q)$ and the star $\mathrm{st}_{\mathcal{S}(Q)}(q_r q_{r+2})$ of the edge $q_r q_{r+2}$ in $\mathcal{S}(Q)$. As in Figure 10.6, the letters x, y, z and z' describe the identifications of the exchanged letters in the topological realizations of the two subword complexes.

Theorem 10.9 ([Gor14])**.** *Suppose that a word* $Q' = U_1 q'_r q'_{r+1} q'_{r+2} U_2$ *is obtained from a word* $Q = U_1 q_r q_{r+1} q_{r+2} U_2$ *by applying a braid move.*
1. *If none of the letters* q_r, q_{r+1} *and* q_{r+2} *is a vertex of* $\mathcal{S}(Q)$*, then* $\mathcal{S}(Q)$ *and* $\mathcal{S}(Q')$ *have the same vertices and are isomorphic.*
2. *If exactly one of the letters* q_r, q_{r+1} *and* q_{r+2} *is a vertex of* $\mathcal{S}(Q)$*, then it is either* q_r *or* q_{r+2}*, say* q_r *without loss of generality*[2]*. In this case* $\mathcal{S}(Q)$ *and* $\mathcal{S}(Q')$ *are isomorphic and an isomorphism is given by identifying their common vertices and identifying* q_r *to* q'_{r+2}*. In particular* q'_r *and* q'_{r+1} *are nonvertices in* $\mathcal{S}(Q')$*.*
3. *If exactly two of the letters* q_r, q_{r+1} *and* q_{r+2} *are vertices of* $\mathcal{S}(Q)$*, then these letters are* q_r *and* q_{r+2}*. If moreover* $q_r q_{r+2}$ *is an edge of the complex* $\mathcal{S}(Q)$*, then the complex* $\mathcal{S}(Q')$ *is isomorphic to the stellar subdivision* $\mathrm{stell}_{\mathcal{S}(Q)}(q_r q_{r+2})$ *of the edge* $q_r q_{r+2}$ *in* $\mathcal{S}(Q)$*. In* $\mathcal{S}(Q')$*, the subdivision vertex is* q'_{r+1}*, the vertex* q'_r *(resp.* q'_{r+2}*) is identified to the vertex* q_{r+2} *(resp.* q_r*) of* $\mathcal{S}(Q)$*, and all common vertices are identified.*
4. *If all letters* q_r, q_{r+1} *and* q_{r+2} *are vertices of* $\mathcal{S}(Q)$ *but do not all belong to a common facet, and if* $q_r q_{r+1}$ *is an edge of the subword complex* $\mathcal{S}(Q)$*, then the roles of* $\mathcal{S}(Q)$ *and* $\mathcal{S}(Q')$ *are exchanged in the previous case. That is* $\mathcal{S}(Q)$ *is obtained from* $\mathcal{S}(Q')$ *by applying a stellar subdivision of the edge* $q'_r q'_{r+2}$*.*
5. *If all letters* q_r, q_{r+1} *and* q_{r+2} *are vertices of* $\mathcal{S}(Q)$ *and belong to a common facet, then it is also the case for* q'_r, q'_{r+1} *and* q'_{r+2} *in* $\mathcal{S}(Q)$*, and the two stellar subdivisions* $\mathrm{stell}_{\mathcal{S}(Q)}(q_r q_{r+2})$ *and* $\mathrm{stell}_{\mathcal{S}(Q')}(q'_r q'_{r+2})$ *are isomorphic. The vertex* q_r *(resp.* q_{r+2}*) of the complex* $\mathrm{stell}_{\mathcal{S}(Q)}(q_r q_{r+2})$ *is identified to the vertex* q'_{r+2} *(resp.* q'_r*) of the complex* $\mathrm{stell}_{\mathcal{S}(Q')}(q'_r q'_{r+2})$*, the subdivisions vertex in* $\mathrm{stell}_{\mathcal{S}(Q)}(q_r q_{r+2})$ *(resp.* $\mathrm{stell}_{\mathcal{S}(Q')}(q'_r q'_{r+2})$*) is identified to* q'_{r+1} *(resp.* q_{r+1}*) and all common vertices are identified.*

Theorem 10.9 does not seem to cover all possible cases because of the additional condition that the edge $q_r q_{r+2}$ (resp $q_r q_{r+1}$) exists in Case (3) (resp. (4)). The following statement implies that this condition is in fact always satisfied[3].

---

[2]Since $\mathcal{S}(Q)$ and $\mathcal{S}(Q^{-1})$ are isomorphic.
[3]Lemma 10.10 is true for type A subword complexes, but needs not be in other types.

Lemma 10.10. *Any two vertices of a subword complex $\mathcal{S}(\mathsf{Q})$ either form an edge of $\mathcal{S}(\mathsf{Q})$, or belong to adjacent facets of $\mathcal{S}(\mathsf{Q})$, or have these two properties simultaneously.*

Proof. The *word property* (see *e.g.* [BB05, Theorem 3.3.1]) asserts that any expression containing a reduced expression of $w_\circ$ can be transformed into a reduced expression of $w_\circ$ by a sequence of braid moves and simplifications $s^2 = \mathrm{Id}$. This allows to prove the result by induction on the length of such a sequence. The property is clear when Q is already a reduced expression of $w_\circ$ since the complex is then empty. Now for any word Q strictly containing a reduced expression of $w_\circ$, we can applying the induction hypothesis and Theorems 10.8 and 10.9 to the sequence provided by the word property. The induction hypothesis is indeed preserved by reverse one-point-suspension and basic arguments on sorting networks (see [PP12, PS12]) imply, by a quick case analysis, that it is also preserved by braid moves. ∎

Finally it is standard to check that the letters q_r and q_{r+2} (resp. q_{r+1}) are not exchangeable in Case (3) (resp (4)) of Theorem 10.9 (see [PP12, PS12]), so that $\mathsf{q}_r\mathsf{q}_{r+2}$ (resp $\mathsf{q}_r\mathsf{q}_{r+1}$) is in fact automatically an edge of the complex. Figure 10.6 sums up all cases of Theorems 10.8 and 10.9 more visually than with their actual descriptions.

The effects of 0-Hecke and braid moves are already illustrated on the complex itself in Figures 10.2 and 10.3, except for Case (5) of Theorem 10.9. Indeed we have described a relation between the subword complexes $\mathcal{S}(\mathsf{Q})$ and $\mathcal{S}(\mathsf{Q}')$, but not in terms of "transforming $\mathcal{S}(\mathsf{Q})$ into $\mathcal{S}(\mathsf{Q}')$". In this case $\mathcal{S}(\mathsf{Q}')$ is obtained from $\mathcal{S}(\mathsf{Q})$ by a stellar subdivision of the edge $\mathsf{q}_r\mathsf{q}_{r+2}$ with subdivision vertex q'_{r+1}, followed by a reverse stellar subdivision of the same edge where the disappearing vertex is q_{r+1}. This can somehow be geometrically interpreted as "moving" the vertex q_{r+1} "from one side" of the edge $\mathsf{q}_r\mathsf{q}_{r+2}$ "to the other side" and relabeling it q'_{r+1} (see Figure 10.7). Reverse stellar subdivision is bad behaved with respect to geometry, and we present in the next sections a tentative construction of 2-associahedra based on commutation moves, 0-Hecke moves and braid moves avoiding Case (4) of Theorem 10.9, and as much as possible Case (5) of Theorem 10.9. The key is that the effect induced by moves on the complex both only depends on vertex status of the implied letters, and is topologically local.

10.3 Loday associahedron by suspensions and stellar subdivisions

We keep the product notation $\prod_{j=\mu}^{\nu}\mathsf{Q}_j$ to denote the concatenation of a sequence of words $(\mathsf{Q}_j)_{\mu\leq j\leq\nu}$, with the convention that empty products represent the empty word. We will use the notation $\mathsf{c}[\mu,\nu] = \prod_{j=\mu}^{\nu}\mathsf{s}_j$ for $1 \leq \mu \leq \nu \leq n$. Recall that with this notation, we have $\mathsf{c}[\mu] = \mathsf{c}[1,\mu]$ for $\mu \in \mathbb{N}$ and $w_\circ(\mathsf{c}) = \prod_{i=1}^{n}\mathsf{c}[n+1-i]$. Moreover in any word, we will from now on denote the positions of the letters of a distinguished factor $w_\circ(\mathsf{c})$ by the corresponding pair (i,j) of indices in the double product formula $w_\circ(\mathsf{c}) \overset{\text{Eq (10.1)}}{=} \prod_{i=1}^{n}\prod_{j=1}^{n+1-i}\mathsf{s}_j$. A word Q can be *moved to* a word Q' if Q can be transformed into Q' by applying a sequence of commutation, 0-Hecke, reverse 0-Hecke and braid moves. If Q can be moved to Q' using only commutations moves, then Q and Q' are *equivalent under commutation* (or simply *equivalent*) and we use the notation $\mathsf{Q} \sim \mathsf{Q}'$. Recall that then, the subword complexes $\mathcal{S}(\mathsf{Q})$ and $\mathcal{S}(\mathsf{Q}')$ are isomorphic.

Lemma 10.11. *For $\ell \in [n]$, the c-sorted word $w_\circ(\mathsf{c})$ can be moved to the word $w_\circ(\mathsf{c})\mathsf{s}_\ell$ by doubling its letter s_1 at position $(\ell,1)$ (that is its ℓ-th letter s_1) and applying a sequence of $\ell - 1$ braid moves interlaced with some commutation moves.*

Proof. For $k \in [\ell-1]$, we can let the second letter s_k of the word $\mathsf{s}_k\mathsf{c}[k+1,\ell]\mathsf{c}[k,\ell-1]$ commute as much as possible to the left to obtain that it is equivalent to the word $\mathsf{s}_k\mathsf{s}_{k+1}\mathsf{s}_k\mathsf{c}[k+2,\ell]\mathsf{c}[k+1,\ell-1]$. We can then apply a braid move on the prefix $\mathsf{s}_k\mathsf{s}_{k+1}\mathsf{s}_k$ of this last word to obtain the word $\mathsf{s}_{k+1}\mathsf{s}_k\mathsf{s}_{k+1}\mathsf{c}[k+2,\ell]\mathsf{c}[k+1,\ell-1]$. Therefore a straightforward

induction on k shows that the word $\mathsf{s}_1\mathsf{c}[\ell]\mathsf{c}[\ell-1]$ can be moved to the word $\mathsf{c}[\ell]\mathsf{c}[\ell-1]\mathsf{s}_\ell$ applying $\ell-1$ braid moves interlaced with some commutation moves. Multiplying both words by $\mathsf{w}_\circ(\mathsf{c}[\ell-2])$ on the right, the identity $\mathsf{w}_\circ(\mathsf{c}[\ell]) = \mathsf{c}[\ell]\mathsf{c}[\ell-1]\mathsf{w}_\circ(\mathsf{c}[\ell-2])$ yields that the word $\mathsf{s}_1\mathsf{w}_\circ(\mathsf{c}[\ell])$ can be moved to the word $\mathsf{c}[\ell]\mathsf{c}[\ell-1]\mathsf{s}_\ell\mathsf{w}_\circ(\mathsf{c}[\ell-2])$ by a sequence of $\ell-1$ braid moves interlaced with some commutation moves. Since the letter s_ℓ commutes to all letters of the word $\mathsf{w}_\circ(\mathsf{c}[\ell-2])$, we obtain by the same identity that the word $\mathsf{s}_1\mathsf{w}_\circ(\mathsf{c}[\ell])$ can be moved to the word $\mathsf{w}_\circ(\mathsf{c}[\ell])\mathsf{s}_\ell$ by a sequence of $\ell-1$ braid moves interlaced with some commutation moves. This is the result for $\ell = n$ since the word $\mathsf{s}_1\mathsf{w}_\circ(\mathsf{c}[\ell])$ is obtained from the word $\mathsf{w}_\circ(\mathsf{c}[\ell])$ by doubling its first letter s_1. Since any word $\mathsf{w}_\circ(\mathsf{c}[\ell])$ (for $\ell \in [n]$) is a suffix of the word $\mathsf{w}_\circ(\mathsf{c}[n])$, the result for any $\ell \in [n]$ finally follows by multiplying on the left by the suitable prefix. ∎

Applying Lemma 10.11 repeatedly, we obtain the following more specific statement.

Corollary 10.12 (fattening a triangle). *The c-sorted word $\mathsf{w}_\circ(\mathsf{c})$ can be moved to the word $\mathsf{w}_\circ(\mathsf{c})\mathsf{c}^{-1} = \mathsf{w}_\circ(\mathsf{c})\,\mathsf{s}_n\,\mathsf{s}_{n-1}\,\ldots\,\mathsf{s}_1$ by doubling all its letters s_1 and applying a sequence of $n(n-1)/2$ braid moves interlaced with some commutation moves.*

Proof. We check by induction on $n \geq 1$ that all the letters s_1 in the word $\mathsf{w}_\circ(\mathsf{c})$ can be doubled at first before applying the other moves of Lemma 10.11. The word $\mathsf{s}_1\mathsf{w}_\circ(\mathsf{c})$ can be obtained from the word $\mathsf{w}_\circ(\mathsf{c})$ by doubling its first letter s_1. We apply the induction hypothesis to the suffix $\mathsf{w}_\circ(\mathsf{c}[n-1])$ of the word $\mathsf{s}_1\mathsf{w}_\circ(\mathsf{c}) = \mathsf{s}_1\mathsf{c}\,\mathsf{w}_\circ(\mathsf{c}[n-1])$ to find a sequence of moves starting by doubling all the letters s_1 in this factor and transforming the word $\mathsf{s}_1\mathsf{w}_\circ(\mathsf{c})$ into the word $\mathsf{s}_1\mathsf{w}_\circ(\mathsf{c})(\mathsf{c}[n-1])^{-1}$. We finally apply Lemma 10.11 to the prefix $\mathsf{s}_1\mathsf{w}_\circ(\mathsf{c})$ of this last word, omitting the initial doubling, into moving it to the word $\mathsf{s}_1\mathsf{w}_\circ(\mathsf{c})\mathsf{s}_n$. Since $\mathsf{c}^{-1} = \mathsf{s}_n(\mathsf{c}[n-1])^{-1}$, we are done. ∎

We will now refer to a distinguished factor $\mathsf{w}_\circ(\mathsf{c})$ in a word $\mathsf{Q} = \mathsf{U}_1\,\mathsf{w}_\circ(\mathsf{c})\,\mathsf{U}_2$ as a *triangle* in Q, because of the shape of the corresponding sorting network. We say that we *fatten a triangle in* Q when we consider a word $\mathsf{Q}' = \mathsf{U}_1\,\mathsf{w}_\circ(\mathsf{c})\mathsf{c}^{-1}\,\mathsf{U}_2$ obtained from Q by applying the sequence of moves of Corollary 10.12 to its distinguished triangle. Let $\mathsf{Q} = \mathsf{Q}_1,\ldots,\mathsf{Q}_\ell = \mathsf{Q}'$ be the successive words obtained in this sequence of moves, where we write $\mathsf{Q}_k = \mathsf{U}_1\mathsf{T}_k\mathsf{U}_2$ for $k \in [\ell]$. Notice that $\mathsf{T}_1 = \mathsf{w}_\circ(\mathsf{c})$ and $\mathsf{T}_\ell = \mathsf{w}_\circ(\mathsf{c})\mathsf{c}^{-1}$. The operation of fattening a triangle comes together with a natural correspondence between the letters in the word Q and those in the word Q'. The letters in the common factors U_1 and U_2 are indeed naturally identified, and the letters of the middle factor $\mathsf{w}_\circ(\mathsf{c})\mathsf{c}^{-1}$ of Q' can be associated to these of the middle factor $\mathsf{w}_\circ(\mathsf{c})$ of Q using the following labeling rules along moves.
- The letters in the distinguished factor $\mathsf{w}_\circ(\mathsf{c})$ of the word Q are labeled with their position (given by a pair of indices) in $\mathsf{w}_\circ(\mathsf{c})$ (see Figure 10.8 left).
- After doubling a letter s_1 at position $(i,1)$ in a distinguished factor T_k of a word Q_k, for some $k \in [\ell-1]$, we label the two resulting letters s_1 in Q_{k+1} with $(i,1)$ and $(i,1)'$. Indeed Theorem 10.8 asserts that the new subword complex $\mathcal{S}(\mathsf{Q}_{k+1})$ is somehow the same as the previous subword complex $\mathcal{S}(\mathsf{Q}_k)$, but with two copies of its initial letters s_1 (see Figure 10.8 middle).
- After a braid move on a factor $\mathsf{q}_r\mathsf{q}_{r+1}\mathsf{q}_{r+2}$ of a word Q_k ($k \in [\ell-1]$) producing a factor $\mathsf{q}'_r\mathsf{q}'_{r+1}\mathsf{q}'_{r+2}$ in the word Q_{k+1}, we label the letter q'_r (resp. q'_{r+1}, resp. q'_{r+2}) in the word Q_{k+1} with the same label as that of the letter q_{r+2} (resp. q_{r+1}, resp. q_r) in the word Q_k (see Figure 10.8 right). This corresponds to the identifications suggested by Theorem 10.9 (see Figure 10.6).

Notice that even if there are cases in Theorem 10.9, the identification between the letters implied in a braid move always follows ours, independently of their vertex status (see Figure 10.6). The letters q_r and q'_{r+2} (resp q_{r+2} and q'_r) are indeed always identified, and in each case the letter q'_{r+1} is obtained by some transformation of the letter q_{r+1}. Figure 10.9 illustrates the labeling evolution rules on an example.
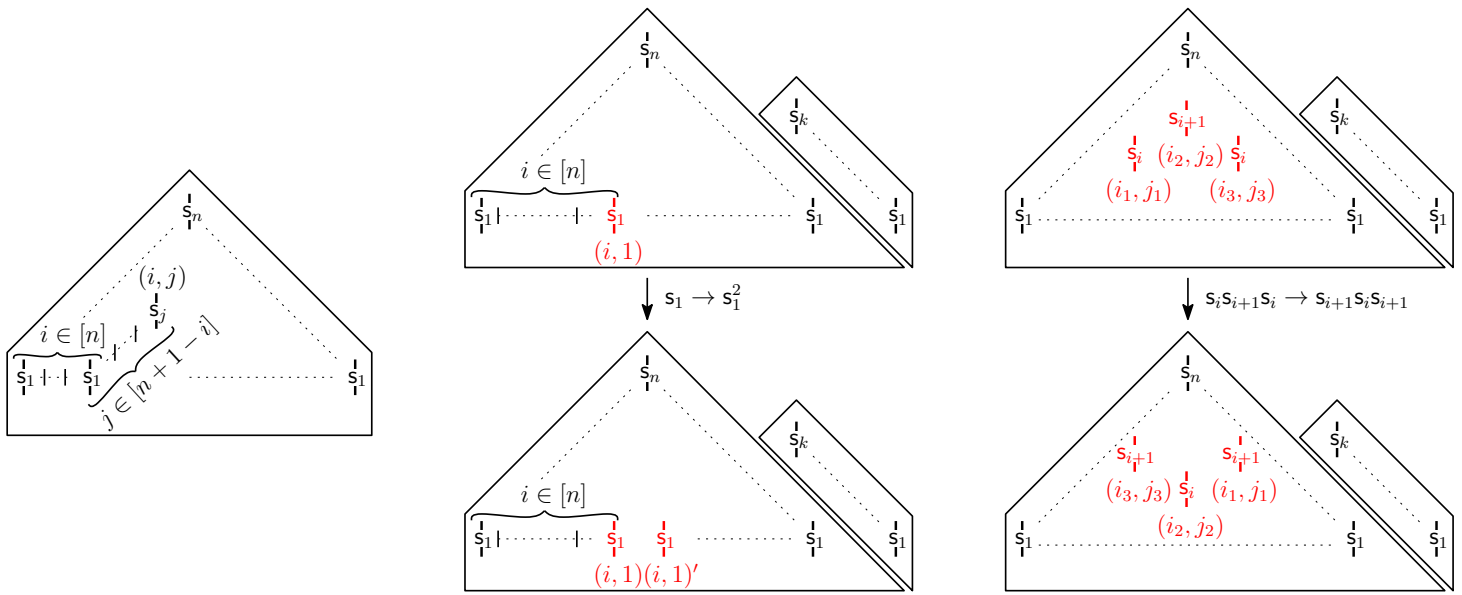
Figure 10.8 – The evolution of the labels of the letters in a sequence of moves to fatten a triangle $\mathsf{w}_\circ(\mathsf{c})$, seen on the corresponding sorting networks. The initial letters of the triangle $\mathsf{w}_\circ(\mathsf{c})$ are labeled with their position (i, j) (with $i \in [n]$, $j \in [n+1-j]$) (left). After doubling a letter s_1 labeled $(i, 1)$ (top middle), the two new letters s_1 are labeled $(i, 1)$ and $(i, 1)'$ (bottom middle). The letters obtained by braid moves are labeled following the identification in Theorem 10.9 (right).
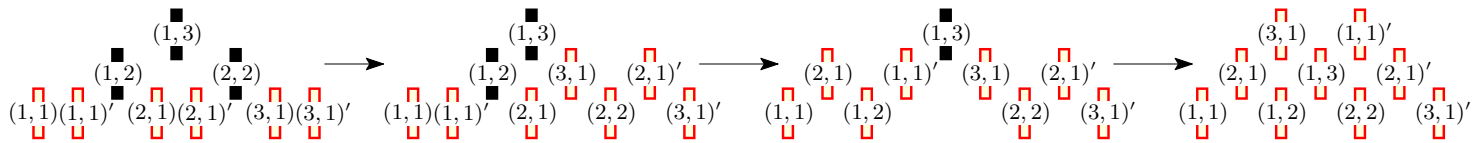
Figure 10.9 – The evolution of the vertex status and labels of the letters along a sequence to fatten a triangle $\mathsf{s}_1\mathsf{s}_2\mathsf{s}_3\mathsf{s}_1\mathsf{s}_2\mathsf{s}_1$, seen on the sorting networks of the words in the sequence. After doubling all letters s_1, one obtains successively the words $\mathsf{s}_1\mathsf{s}_1\mathsf{s}_2\mathsf{s}_3\mathsf{s}_1\mathsf{s}_2\mathsf{s}_1\mathsf{s}_2\mathsf{s}_1$, $\mathsf{s}_1\mathsf{s}_2\mathsf{s}_1\mathsf{s}_2\mathsf{s}_3\mathsf{s}_2\mathsf{s}_1\mathsf{s}_2\mathsf{s}_1$ and $\mathsf{s}_1\mathsf{s}_2\mathsf{s}_3\mathsf{s}_1\mathsf{s}_2\mathsf{s}_3\mathsf{s}_1\mathsf{s}_2\mathsf{s}_1$ by applying three braid moves and several commutation moves. The red empty (resp. black plain) segments denote vertices (resp. nonvertices) of the current subword complex.

Lemma 10.13. *Let* $\mathsf{Q} = \mathsf{U}_1\mathsf{w}_\circ(\mathsf{c})\mathsf{U}_2$ *be a word with a distinguished triangle and let* $\mathsf{Q} = \mathsf{Q}_1, \ldots, \mathsf{Q}_\ell$ *(with* $\mathsf{Q}_k = \mathsf{U}_1\mathsf{T}_k\mathsf{U}_2$ *for* $k \in [\ell]$*) be a fattening sequence of this triangle.*

- *The labels of the letters of* $\mathsf{T}_\ell = \mathsf{w}_\circ(\mathsf{c})\mathsf{c}^{-1} = \mathsf{c}\mathsf{w}_\circ(\mathsf{c}[n-1])\mathsf{c}^{-1}$, *obtained by the identification rules, are these of Figure 10.10. Namely the letter at position* $i \in [n]$ *in the* c *prefix is labeled* $(i, 1)$, *the letter indexed* (i, j) *(with* $i \in [n-1]$, $j \in [n-i]$*) in the factor* $\mathsf{w}_\circ(\mathsf{c}[n-1]) = \prod_{1 \le i \le n-1} \prod_{1 \le j \le n-i} \mathsf{s}_j$ *is labeled* $(i, j+1)$ *and the letter in position* $i \in [n]$ *in the* c^{-1} *suffix is labeled* $(n-i+1, 1)'$.
- *If the word* Q_k *(for* $k \in [\ell]$*) contains a factor* $\mathsf{q}_r\mathsf{q}_{r+1}\mathsf{q}_{r+2}$ *implied in a braid move, then the labels of* $\mathsf{q}_r, \mathsf{q}_{r+1}$ *and* q_{r+2} *in* Q_k *are* $(i, 1)', (i, j+1)$ *and* $(i+j, 1)$ *respectively for some* $i \in [n-1], j \in [n-i+1]$. *Moreover* $\mathsf{q}_r\mathsf{q}_{r+2}$ *is an edge of the subword complex* $\mathcal{S}(\mathsf{Q}_k)$, *and* q_{r+1} *is a vertex of* $\mathcal{S}(\mathsf{Q}_k)$ *if and only if the letter with label* $(i, j+1)$ *in* T_1 *is a vertex of* $\mathcal{S}(\mathsf{Q})$.

Lemma 10.13 translates obvious phenomena that can be observed on the example in Figure 10.9. The proof is an easy but technical refinement of the proofs of Lemma 10.11 and Corollary 10.12. We only give a sketch of it and leave the details to the reader.
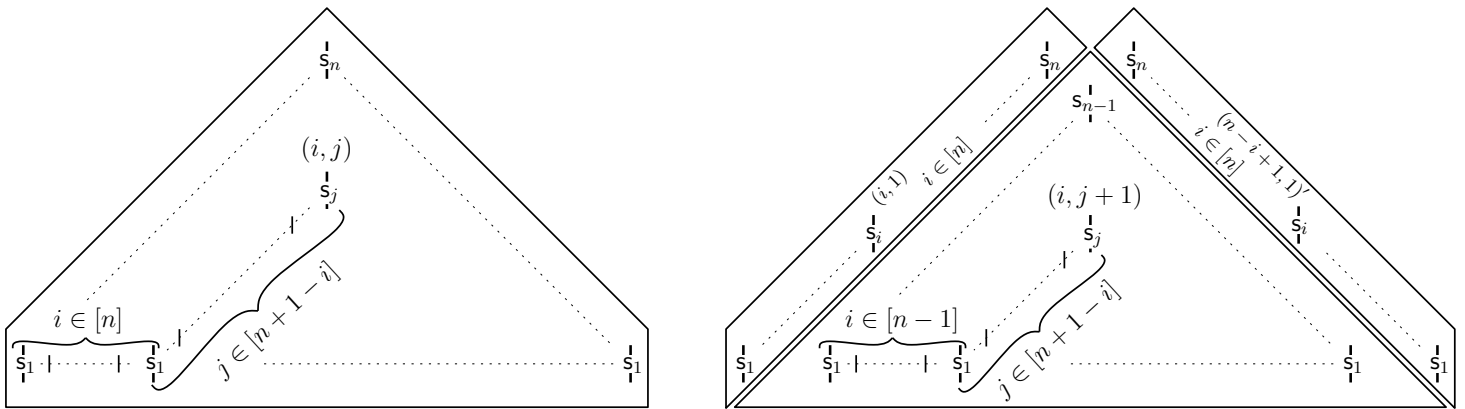
Figure 10.10 – The identification pattern of the letters of a word $w_\circ(c)c^{-1}$ (right) obtained by fattening a triangle $w_\circ(c)$ (left) by following the labeling rules. The pattern is given by the labeling on the sorting networks of the two words.

Proof (sketch). The proof is by induction on $n \geq 1$, the case $n = 1$ being trivial. Given a triangle $w_\circ(c) = cw_\circ(c[n-1])$ in a word Q, we first fatten its subfactor $w_\circ(c[n-1])$ into transforming $w_\circ(c)$ into the factor $cw_\circ(c[n-1])(c(n-1))^{-1}$. In this last factor, the labels of the letters in the prefix c are still the initial ones, while the labels of the other letters are described by the induction hypothesis. Moreover, the vertex status of the letters in the prefix c is the same as in the word Q since the effect of reverse 0-Hecke and braid moves is local, by Theorems 10.8 and 10.9. To move the factor $cw_\circ(c[n-1])(c[n-1])^{-1} = w_\circ(c)(c(n-1))^{-1}$ to the factor $w_\circ(c)c^{-1}$, we apply Lemma 10.11 to its $w_\circ(c)$ prefix in order to insert a new letter s_n. It is then straightforward to adapt the induction in the proof of Lemma 10.11 into keeping track of the labels and vertex status of the letters in the final factor $w_\circ(c)c^{-1}$, so as of the prescribed edges. The key point for the induction step is that doubling the first letter s_1 creates an edge between any of the two resulting letters and any other vertex q of the current subword complex (by Theorem 10.8), and that this edge is never affected by the stellar subdivisions and reverse stellar subdivisions corresponding to the braid moves (by Theorem 10.9) which do not imply both letters. ∎

Observe that Lemma 10.13 implies that all the braid moves implied in a fattening sequence either induce Case (3) or Case (5) of Theorem 10.9. Therefore Lemma 10.13 yields a new construction for the classical associahedron, choosing the word Q to be simply a triangle $Q = w_\circ(c)$. Indeed no letter is a vertex in $\mathcal{S}(Q) = \{\varnothing\}$, and so no letter with label $(i, j+1)$ (for $i \in [n-1], j \in [n-i+1]$) is a vertex in the subword complex $\mathcal{S}(Q')$, where the Q' is obtained from the word Q by doubling all its s_1 letters. Since those letters are nonvertices in the subword complex $\mathcal{S}(Q)$, all corresponding reverse 0-Hecke moves induce suspensions by Theorem 10.8 so that the subword complex $\mathcal{S}(Q')$ is isomorphic to the boundary complex of the n-dimensional *cross-polytope*. Finally Lemma 10.13 implies that all braid moves in the fattening sequence induce stellar subdivisions of edges, by Theorem 10.9. We obtain by Lemma 10.4 a construction of the classical associahedron by successive stellar subdivisions of edges of the cross-polytope.

Corollary 10.14. *The simplicial n-associahedron can be obtained by successive stellar subdivisions of edges of the n-dimensional cross-polytope. Equivalently its polar dual can be obtained by successive truncations of codimension-2 faces of the n-dimensional cube.*

This is a special case of a result by V. Volodin [Vol10] stating that any flag nestohedron can be obtained by successive such truncations of a cube. The last figure in [Vol10] depicts a 3-dimensional associahedron geometrically equivalent to the realization by J.-L. Loday [Lod04] (see Figure 2.5 left). Corollary 10.14 shows that the realization by
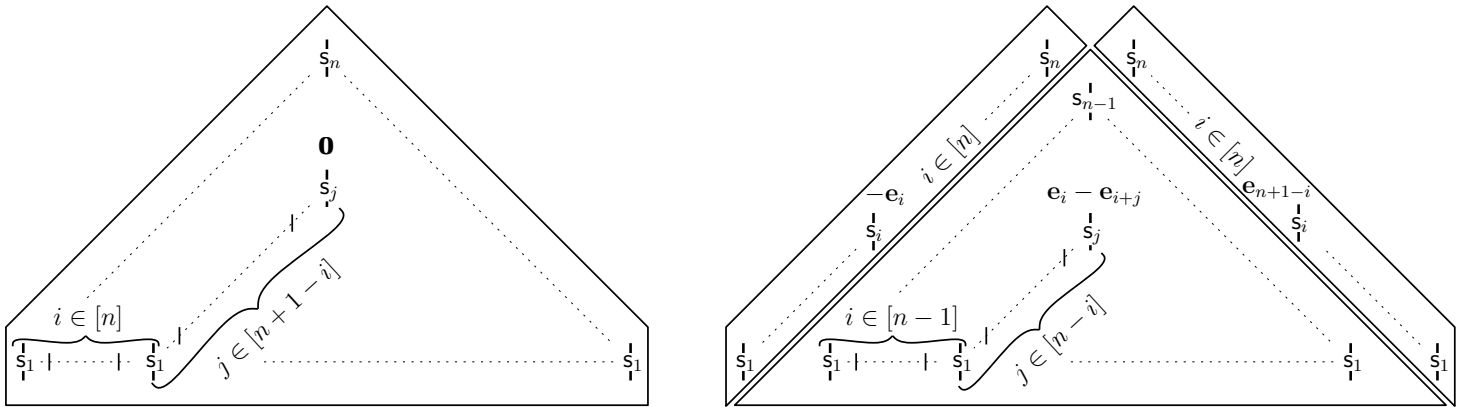
Figure 10.11 – The pattern of coordinates obtained for the associahedron (right) after fattening a triangle (left). The obtained rays are these of the realization of the associahedron by J.-L. Loday [Lod04] (see Figures 2.5 left and 2.6 left).

J.-L. Loday can be obtained that way in all dimensions. Indeed while following the sequence $Q = Q_1, \ldots, Q_\ell$ to fatten the triangle, we can apply the generic transformations described after Lemma 10.4 to realize the successive suspensions and stellar subdivisions of edges of the current subword complex. We first associate to each letter of the word Q the zero vector $\mathbf{0}$ in $\mathbb{R}^0$, and we take the convention that when applying a reverse 0-Hecke move to a letter $\mathsf{q} = \mathsf{s}_1$ labeled $(i, 1)$ in the word Q_r, and associated to a ray $\mathbf{v}$ in the current fan realizing $\mathcal{S}(Q_r)$ (say of dimension $d \in \mathbb{N}$), the resulting letters labeled $(i, 1)$ and $(i, 1)'$ are respectively associated to the vectors $\mathbf{v} \oplus (-\mathbf{f})$ and $\mathbf{v} \oplus \mathbf{f}$ in the new fan realizing the suspension $\mathcal{S}(Q_{r+1}) \cong \mathcal{S}(Q_r) * \{u_1, u_2\}$, where $\mathbb{R}^{d+1} = \mathbb{R}^d \oplus \mathbb{R}\,\mathbf{f}$. After fattening the triangle, we therefore obtain the pattern of coordinates of Figure 10.11 which provides rays supporting a complete simplicial fan realizing the associahedron. The reader can refer to [PS12] to check that this fan is isomorphic to the normal fan of the realization of the associahedron as a convex polytope by J.-L Loday [Lod04].

10.4 The construction continued to 2-associahedra

10.4.1 Heuristic construction

Cases (1), (2) and (4) of Theorem 10.9 are always avoided by the braid moves of a fattening sequence, by Lemma 10.13. But we need a geometric transformation implementing the topological effect induced by Case (5), similar to these after Lemma 10.4. Consider a braid move changing a factor $\mathsf{q}_r\mathsf{q}_{r+1}\mathsf{q}_{r+2}$ of a word Q to a factor $\mathsf{q}'_r\mathsf{q}'_{r+1}\mathsf{q}'_{r+2}$ of a word Q'. Suppose that the subword complex $\mathcal{S}(Q)$ is realized by a fan $\mathcal{F}_Q$ in which the vertices $\mathsf{q}_r, \mathsf{q}_{r+1}$ and q_{r+2} of $\mathcal{S}(Q)$ are associated to rays generated by vectors $\mathbf{v}_r, \mathbf{v}_{r+1}$ and $\mathbf{v}_{r+2}$ respectively, that we identify to the rays themselves. Recall that we described the topological effect in Case (5) of Theorem 10.9 as "moving the vertex q_{r+1} from one side of the edge $\mathsf{q}_r\mathsf{q}_{r+2}$ to the other" (see Figure 10.7). In fan words, it heuristically means that the cone $\mathbb{R}_{\geq 0}\{\mathbf{v}_r, \mathbf{v}_{r+2}\}$ should separate the ray $\mathbf{v}_{r+1}$, associated to q_{r+1} in the fan $\mathcal{F}_Q$, and the ray $\mathbf{v}'_{r+1}$ associated to q'_{r+1} in a potential fan realizing the subword complex $\mathcal{S}(Q')$. This intuitive description can be geometrically translated as follows.
  - take any vector $\mathbf{v}$ in the interior of the cone $\mathbb{R}_{\geq 0}\{\mathbf{v}_r, \mathbf{v}_{r+2}\}$, that is $\mathbf{v}$ can be written in the form $\alpha\,\mathbf{v}_r + \beta\,\mathbf{v}_{r+2}$ for some $\alpha, \beta > 0$;
  - move $\mathbf{v}_{r+1}$ in the direction of $\mathbf{v}$ in order to cross the cone $\mathbb{R}_{\geq 0}\{\mathbf{v}_r, \mathbf{v}_{r+2}\}$.

For the last point, the ray $\mathbf{v}_{r+1}$ should be moved "not to far" from $\mathbf{v}$ in order to ensure it to cross the cone $\mathbb{R}_{\geq 0}\{\mathbf{v}_r, \mathbf{v}_{r+2}\}$, but no other cone of the fan. Since the direction
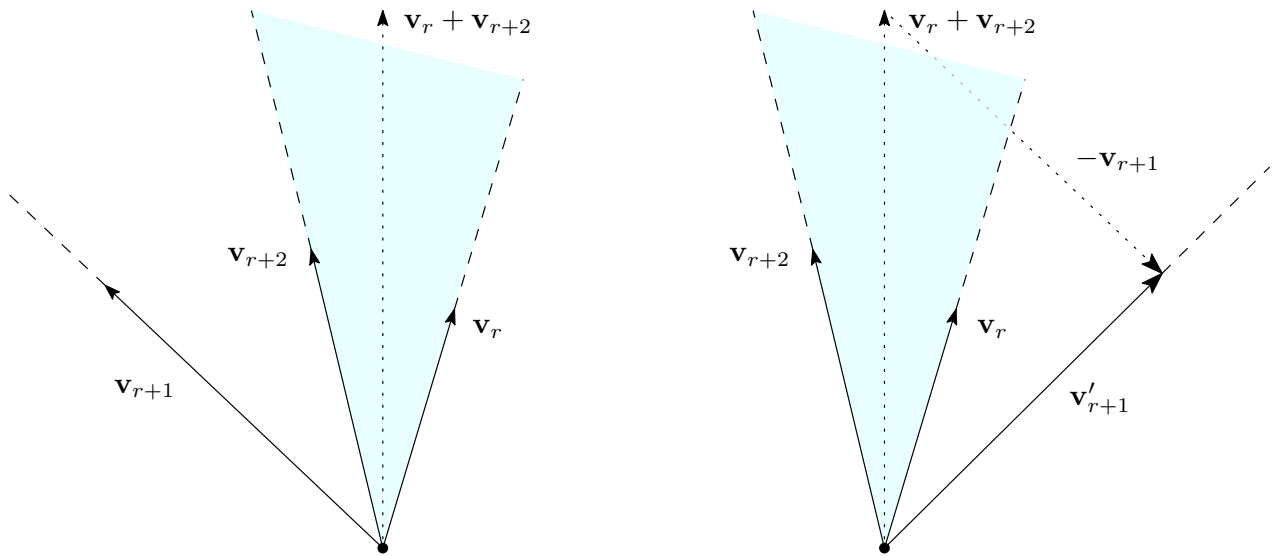
Figure 10.12 – The geometric transformation on the rays of a complete simplicial fan corresponding to a braid move in Case (5) of Theorem 10.9. In this figure only the relevant rays and cones are represented. The dotted vectors are represented in order to help understanding the figure but they are not rays of the fan.

from $\mathbf{v}_{r+1}$ to $\mathbf{v}$ is $\mathbf{v} - \mathbf{v}_{r+1}$, our intuitive description suggests to replace the ray $\mathbf{v}_{r+1}$ by the ray $\mathbf{v}'_{r+1} := \mathbf{v} + \varepsilon(\mathbf{v} - \mathbf{v}_{r+1})$, with $\varepsilon > 0$ small enough. As we are interested in rays, we can consider their generators up to rescaling and therefore replace the ray generated by $\mathbf{v}_{r+1}$ by the ray generated by $\mathbf{v}'_{r+1} := \mathbf{v} - \varepsilon\,\mathbf{v}_{r+1}$. In other words, any vector of the form $\alpha\,\mathbf{v}_r + \beta\,\mathbf{v}_{r+2} - \varepsilon\,\mathbf{v}_{r+1}$ with $\alpha, \beta, \varepsilon > 0$ and ε small enough would be a legitimate candidate for $\mathbf{v}'_{r+1}$. We generically choose $\alpha = 1, \beta = 1$ and $\varepsilon = 1$ (see Figure 10.12 for an illustration). Finally, following the identifications between the letters of Q and Q', the letter q'_r (resp. q'_{r+2}) is associated to the ray $\mathbf{v}_{r+2}$ (resp. $\mathbf{v}_r$).

In the sequel, we will consider vectors $\mathbf{v}_\mathsf{q} \in \mathbb{R}^d$ associated to the letters q of some words Q (with $d = \dim(\mathcal{S}(\mathsf{Q})) + 1$), that we will then abusively call the *rays* of the subword complex $\mathcal{S}(\mathsf{Q})$, even if the rays in $\{\mathbf{v}_\mathsf{q} \mid \mathsf{q}$ is a letter in $\mathsf{Q}\}$ may not support a complete simplicial fan realizing $\mathcal{S}(\mathsf{Q})$. If they do, we say that these rays are *realizing* for $\mathcal{S}(\mathsf{Q})$. We only require that nonvertices are associated to the zero vector $\mathbf{0}$. The previous description allows to derive a general heuristic formula for the rays obtained after a fattening sequence. Notice that we already gave after Lemma 10.4 some transformations on rays associated to one-point-suspensions and stellar subdivisions, that correspond to the effect of moves described in Theorem 10.8 and Case (3) of Theorem 10.9. Observe that the transformation that we defined for Case (5) of Theorem 10.9 is in fact also valid for Case (3), since we impose that nonvertices are associated to the zero vector. So given a word $\mathsf{Q} = \mathsf{U}_1 \mathsf{w}_\circ(\mathsf{c}) \mathsf{U}_2$ containing a distinguished triangle, and to which letters some rays are associated, we can use Lemma 10.13 and the transformations corresponding to moves to derive rays associated to the letters of a word $\mathsf{Q}' = \mathsf{U}_1 \mathsf{w}_\circ(\mathsf{c}) \mathsf{c}^{-1} \mathsf{U}_2$ obtained by fattening the distinguished triangle of Q. The rays corresponding to the letters of the word Q span a vector space isomorphic to $\mathbb{R}^d$ (with $d = \dim(\mathcal{S}(\mathsf{Q})) + 1$), and we consider a basis $\mathbf{f}_1, \ldots, \mathbf{f}_n$ of $\mathbb{R}^n$ in direct sum with this vector space, so that each reverse 0-Hecke move of a fattening sequence lets a coordinate corresponding to one of the $\mathbf{f}_i$ appear in the rays of the current subword complex. The resulting pattern for the rays of the letters in the factor $\mathsf{w}_\circ(\mathsf{c}) \mathsf{c}^{-1}$ of the word Q' is presented in Figure 10.13.

The pattern of Figure 10.13 gives an algorithmic way to produce candidates rays for a fan realization of the subword complex $\mathcal{S}(\mathsf{Q}')$ whenever we already know that the
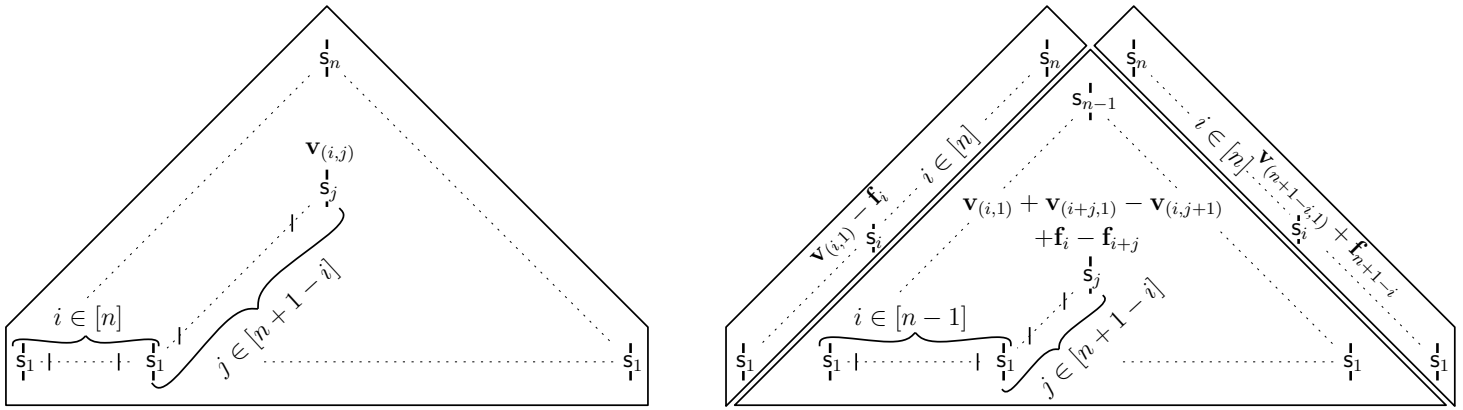
Figure 10.13 – The sorting network of a triangle in a word Q, in which the letter in position (i,j) is labeled with its associated ray $\mathbf{v}_{(i,j)} \in \mathbb{R}^d$, for $d = \dim(\mathcal{S}(Q))-1$ (left) and the sorting network of the factor $\mathsf{w}_\circ(\mathsf{c})\mathsf{c}^{-1}$ in the word Q' obtained from Q by fattening the triangle (right). The letters in this factor are again labeled with their associated ray, obtained from these in the initial triangle following the geometric transformations along the fattening sequence.

$s_1 : [-1$	0	0	0	0	0	0	$0\ ]$
$s_2 : [\ 0$	-1	0	0	0	0	0	$0\ ]$
$s_3 : [\ 0$	0	-1	0	0	0	0	$0\ ]$
$s_4 : [\ 0$	0	0	-1	0	0	0	$0\ ]$
$s_1 : [\ 1$	-1	0	0	-1	0	0	$0\ ]$
$s_2 : [\ 0$	1	-1	0	0	-1	0	$0\ ]$
$s_3 : [\ 0$	0	1	-1	0	0	-1	$0\ ]$
$s_4 : [\ 0$	0	0	1	0	0	0	$-1]$
$s_1 : [\ 0$	0	0	0	1	-1	0	$0\ ]$
$s_2 : [\ 0$	-1	1	0	1	0	-1	$0\ ]$
$s_3 : [\ 0$	-1	0	1	1	0	0	$-1]$
$s_4 : [\ 1$	-1	0	0	1	0	0	$0\ ]$
$s_1 : [\ 0$	0	0	0	0	1	-1	$0\ ]$
$s_2 : [\ 0$	0	-1	1	0	1	0	$-1]$
$s_3 : [\ 0$	1	-1	0	0	1	0	$0\ ]$
$s_1 : [\ 0$	0	0	0	0	0	1	$-1]$
$s_2 : [\ 0$	0	1	-1	0	0	1	$0\ ]$
$s_1 : [\ 0$	0	0	1	0	0	0	$1\ ]$

Table 10.1 – The coordinates of the rays associated to the letters of the word $\mathsf{c}^2\mathsf{w}_\circ(\mathsf{c})$ obtained by fattening twice a triangle for $n = 4$. These first candidate rays yet do not support a complete simplicial fan realizing the 2-associahedron $\Delta_{2,4}$.

set of rays we started with for the subword complex $\mathcal{S}(Q)$ support a complete simplicial fan realizing it. For 2-associahedra, we only need to fatten twice a triangle. Indeed, the word $\mathsf{w}_\circ(\mathsf{c})$ can be fattened into the word $\mathsf{w}_\circ(\mathsf{c})\mathsf{c}^{-1}$, which is equivalent to the word $\mathsf{cw}_\circ(\mathsf{c})$, in which we can fatten the suffix triangle into obtaining the word $\mathsf{cw}_\circ(\mathsf{c})\mathsf{c}^{-1}$, which is equivalent to $\mathsf{c}^2\mathsf{w}_\circ(\mathsf{c})$. The resulting rays for the subword complex $\mathcal{S}(\mathsf{c}^2\mathsf{w}_\circ(\mathsf{c}))$ are illustrated in Table 10.1 for $n = 4$.

We now wonder whether the rays we obtained support a complete simplicial fan realizing the subword complexes $\mathcal{S}(\mathsf{c}^2\mathsf{w}_\circ(\mathsf{c}))$, and if not "how close" it is to be so. For this we consider the set $\mathcal{F}_n$ of all cones generated by any set of rays which corresponds to a face of the subword complex $\mathcal{S}(\mathsf{c}^2\mathsf{w}_\circ(\mathsf{c}))$. We recall that a ridge of the subword complex $\mathcal{S}(\mathsf{c}^2\mathsf{w}_\circ(\mathsf{c}))$ is a face which is the intersection of exactly two facets. We will

n	1	2	3	4	5	6	7	8
dimension of $\mathbf{\Delta}_{2,n}$	1	3	5	7	9	11	13	15
#bad ridges	**0**	**0**	**0**	**0**	**0**	**0**	**0**	**0**
# degenerate ridges	0	0	11	282	5,058	78,904	1,144,499	15,909,182
# ridges	3	28	252	2,376	23,595	245,388	2,654,652	29,695,328
ratio (%)	0	0	4.37	11.87	21.44	32.15	43.11	53.57
# degenerate cones	0	0	2	48	782	10,992	143,838	1,811,972
# cones	3	14	84	594	4,719	40,898	379,236	3,711,916
ratio (%)	0	0	2.38	8.08	16.57	26.88	37.93	48.82
minimal dimension	2	4	5	6	7	8	9	10

Table 10.2 – The statistics for the sets of cones $\mathcal{F}_n$.

abusively refer to the cones of $\mathcal{F}_n$ corresponding to facets (resp. ridges) of the subword complex $\mathcal{S}(\mathsf{c}^2\mathsf{w}_\circ(\mathsf{c}))$ as to the *facets* (resp. *ridges*) of $\mathcal{F}_n$. The rays of $\mathcal{F}_n$ lie in $\mathbb{R}^{2n}$ and any ridge is contained in two facets, each generated by $2n$ vectors, that differ by a single generator. Therefore a ridge R defines exactly $2n + 1$ rays, and thus at least one linear dependence between them. If the rays associated to the ridge R are link by a single (up to rescaling) linear dependence not satisfying Condition (2) of Proposition 3.7, we say that R is a *bad ridge* of $\mathcal{F}_n$. If the space of linear dependences on the rays defined by R has dimension greater than 1, we say that R is a *degenerate ridge* of $\mathcal{F}_n$. In this case at least one of the facets containing the ridge R is not full dimensional. We call such a facet a *degenerate cone* of $\mathcal{F}_n$. Proposition 3.7 suggests to look at the following statistics on the set of cones $\mathcal{F}_n$.

- The rate of bad ridges in $\mathcal{F}_n$, which sort of measures "nontractable issues".
- The rates of degenerate cones and ridges in $\mathcal{F}_n$, which describe the "global degeneracy" in $\mathcal{F}_n$. Since the dual graph of the complex $\mathcal{S}(\mathsf{c}^2\mathsf{w}_\circ(\mathsf{c}))$ is regular, they also give the number of pairs of adjacent degenerate cones.
- The minimal dimension of a facet in $\mathcal{F}_n$, which measures "local degeneracy".

We gather these statistics in Table 10.2 for $n \leq 8$.

Observation 10.15. *The empirical data suggest that fattening twice a triangle produce rays that do not realize the 2-associahedron, but "only" up to degeneracies. Indeed the process does not seem to let bad ridges appear. Yet the indicators for degeneracy are high, so that the rays we obtain should not be perturbed easily into realizing ones.*

10.4.2 Degrees of freedom

In view of Observation 10.15, we need a less naive construction to obtain realizing rays for 2-associahedra. We derive it from making the one presented in Section 10.4.1 less generic. Indeed we always used "generic" coefficients in the geometric translations for the different topological effects of the braid moves. But as we notice after Lemma 10.4 and at the beginning of Section 10.4.1, we may let some of them vary for the new rays of the letters implied in a reverse 0-Hecke move or in a braid move. This belongs to the following many degrees of freedom that we could consider for the construction.

coefficients for reverse 0-Hecke moves For any reverse 0-Hecke move, we can turn the ray $\mathbf{v}$ of the doubled letter into $\mathbf{v} \oplus \alpha\,\mathbf{f}$ and $\mathbf{v} \oplus \beta\,\mathbf{f}$, for any α and β satisfying $\alpha\beta < 0$, to realize the corresponding one-point-suspension. The construction of Section 10.4.1 generically keeps $\alpha = -1$ and $\beta = 1$.

coefficients for braid moves According to Lemma 10.13, a braid move in a fattening sequence always implies a factor $\mathsf{q}_r\mathsf{q}_{r+1}\mathsf{q}_{r+2}$ with letters $\mathsf{q}_r, \mathsf{q}_{r+1}$ and q_{r+2} respectively labeled $(i,1)', (i,j+1)$ and $(i+j,1)$ (for $i \in [n-1], j \in [n-i]$). We denote the

respective rays associated to these letters $\mathbf{v}_r$, $\mathbf{v}_{r+1}$ and $\mathbf{v}_{r+2}$, and by $\mathsf{q}'_r\mathsf{q}'_{r+1}\mathsf{q}'_{r+2}$ the factor by which $\mathsf{q}_r\mathsf{q}_{r+1}\mathsf{q}_{r+2}$ is replaced by the braid move. We chose in Section 10.4.1 to associate the letter q'_{r+1} to any ray of the form $\alpha\,\mathbf{v}_r + \beta\,\mathbf{v}_{r+2} - \varepsilon\,\mathbf{v}_{r+1}$ with $\alpha > 0, \beta > 0, \varepsilon > 0$ and ε small enough. In our construction of Section 10.4.1, we fatten twice a triangle. The first fattening sequence only contains braid move inducing stellar subdivisions while the second one only contains braid move inducing Case (5) of Theorem 10.9. In the first case there is in fact only two choices of coefficients since the ray associated to the letter q_{r+1} is the zero vector. We will denote by $\lambda_{(i,j)}$ and $\rho_{(i,j)}$ the respective coefficients of $\mathbf{v}_r$ and $\mathbf{v}_{r+2}$ in the first fattening sequence, and by $\alpha_{(i,j)}, \beta_{(i,j)}$ and $\varepsilon_{(i,j)}$ the respective coefficients of $\mathbf{v}_r, \mathbf{v}_{r+1}$ and $\mathbf{v}_{r+2}$ in the second fattening sequence of the construction. Since the effect of braid moves are local, we can *a priori* choose all these coefficients independently whereas the initial construction of Section 10.4.1 generically set $\lambda_{(i,j)} = \rho_{(i,j)} = \alpha_{(i,j)} = \beta_{(i,j)} = \varepsilon_{(i,j)} = 1$.

choice of the triangle We did not insist on the triangle that we fatten in the construction. There is indeed only one choice for the initial word, which is itself a triangle, but the second fattening sequence is applied to the suffix triangle of the word $\mathsf{cw}_\circ(\mathsf{c})$. This word can be moved to the word $\mathsf{w}_\circ(\mathsf{c})\mathsf{c}^{-1}$ by commutation moves so that we could also apply the second fattening sequence to the prefix triangle of this new word. It is easy to check that the two sets of rays obtained by both methods are linearly equivalent. Yet we can use the rotation map described in Theorem 10.6 to obtain other nonequivalent constructions. Denoting by $\mathsf{Q}^{\circlearrowright k}$ the word obtained by applying k times the rotation map to a word Q, we see that any word of the form $(\mathsf{cw}_\circ(\mathsf{c}))^{\circlearrowright k.n}$, for $k \in \mathbb{N}$, can be moved back to $\mathsf{cw}_\circ(\mathsf{c})$ by commutation moves. Therefore we could choose a lot of triangles to fatten (in fact $n+1$) instead of always taking the suffix one without applying any rotation to the current word, as in the construction of Section 10.4.1.

starting associahedron Finally we observe that we could start from any realizing rays for the subword complex $\mathcal{S}(\mathsf{cw}_\circ(\mathsf{c}))$ to apply the second fattening sequence of the construction. In view of the numerous fan realizations for the usual associahedron, this is a wide additional degree of freedom.

We did not test exhaustively all the possibilities allowed by these multiple degrees of freedom. Since the initial motivation of this project was to realize as fans one of the first unrealized multiassociahedra $\mathbf{\Delta}_{2,5}$ and $\mathbf{\Delta}_{4,4}$, we mostly made some kind of "depth first search testing" in that direction. Therefore we will not mention all combinations that failed out and concentrate on this that actually provided results. It turns out that letting the coefficients $\lambda_{(i,j)}$ and $\rho_{(i,j)}$ vary was somehow successful. So from now on we will denote by $\mathcal{F}_n(\lambda_{(i,j)}, \rho_{(i,j)})$ the set of cones obtained by fattening twice a suffix triangle of an initial triangle, where the first fattening is done with coefficients $\lambda_{(i,j)}$ and $\rho_{(i,j)}$, and the second one with coefficients $\alpha_{(i,j)} = \beta_{(i,j)} = \varepsilon_{(i,j)} = 1$. The choice $\lambda_{(i,j)} = 5$ and $\rho_{(i,j)} = 3$ was the best one among these not letting the coefficients depend on the position of the corresponding letter. Table 10.3 gathers the statistics for the set of cones $\mathcal{F}_n(5,3)$ for $n \leq 8$. Observe that the rates of degenerate ridges and cones decreases by a factor of about 2 with this simple change in the coefficients. In particular we obtain new realizing rays for the 2-associahedron $\mathbf{\Delta}_{2,3}$ (see Table 10.4). We came out with such coefficients mostly because we observed that having $\lambda_{(i,j)}$ and $\rho_{(i,j)}$ relatively prime helped reducing degeneracies. Finally it turns out that letting them be moreover linear in (i,j) yielded us the best results, namely when letting $\lambda_{(i,j)} = 2n + 4 - i - j$ and $\rho_{(i,j)} = \lambda_{(i,j)} - 1$. The statistics of the sets of cones $\mathcal{F}_n(2n+4-i-j, 2n+3-i-j)$, for $n \leq 8$, are gathered in Table 10.5 .

n	1	2	3	4	5	6	7	8
dimension of $\Delta_{2,n}$	1	3	5	7	9	11	13	15
#bad ridges	**0**	**0**	**0**	**0**	**0**	**0**	**0**	**0**
# degenerate ridges	0	0	0	78	2,216	43,298	724,546	11,150,457
# ridges	3	28	252	2,376	23,595	245,388	2,654,652	29,695,328
ratio (%)	0	0	0	3.28	9.39	17.63	27.29	37.55
# degenerate cones	0	0	0	12	320	5,742	87,714	1,233,154
# cones	3	14	84	594	4,719	40,898	379,236	3,711,916
ratio (%)	0	0	0	2.02	6.78	14.04	23.13	33.22
minimal dimension	2	4	6	7	8	9	10	11

Table 10.3 – The statistics for the sets of cones $\mathcal{F}_n(5,3)$.

$$
\begin{array}{ll}
\mathsf{s}_1: & [-1 \quad 0 \quad 0 \quad 0 \quad 0 \quad 0 \ ] \\
\mathsf{s}_2: & [\ 0 \quad -1 \quad 0 \quad 0 \quad 0 \quad 0 \ ] \\
\mathsf{s}_3: & [\ 0 \quad 0 \quad -1 \quad 0 \quad 0 \quad 0 \ ] \\
\mathsf{s}_1: & [\ 5 \quad -3 \quad 0 \quad -1 \quad 0 \quad 0 \ ] \\
\mathsf{s}_2: & [\ 0 \quad 5 \quad -3 \quad 0 \quad -1 \quad 0 \ ] \\
\mathsf{s}_3: & [\ 0 \quad 0 \quad 1 \quad 0 \quad 0 \quad -1 \ ] \\
\mathsf{s}_1: & [\ 0 \quad 2 \quad 0 \quad 1 \quad -1 \quad 0 \ ] \\
\mathsf{s}_2: & [\ 4 \quad -3 \quad 1 \quad 1 \quad 0 \quad -1 \ ] \\
\mathsf{s}_3: & [\ 5 \quad -3 \quad 0 \quad 1 \quad 0 \quad 0 \ ] \\
\mathsf{s}_1: & [\ 0 \quad 4 \quad -2 \quad 0 \quad 1 \quad -1 \ ] \\
\mathsf{s}_2: & [\ 0 \quad 5 \quad -3 \quad 0 \quad 1 \quad 0 \ ] \\
\mathsf{s}_1: & [\ 0 \quad 0 \quad 1 \quad 0 \quad 0 \quad 1 \ ]
\end{array}
$$

Table 10.4 – The rays supporting the set of cones $\mathcal{F}_3(5,3)$, associated to each letter of the word $\mathsf{c}^2\mathsf{w}_\circ(\mathsf{c})$ for $n = 3$. These rays are realizing, that is the set of cones $\mathcal{F}_3(5,3)$ is a complete simplicial fan realizing the 2-associahedron $\Delta_{2,3}$.

n	1	2	3	4	5	6	7	8
dimension of $\Delta_{2,n}$	1	3	5	7	9	11	13	15
#bad ridges	**0**	**0**	**0**	**0**	**0**	**0**	**0**	**20**
# degenerate ridges	0	0	0	39	1,122	22,317	381,533	6,026,814
# ridges	3	28	252	2,376	23,595	245,388	2,654,652	29,695,328
ratio (%)	0	0	0	1.64	4.76	9.09	14.37	20.30
# degenerate cones	0	0	0	6	160	2,904	45,173	650,734
# cones	3	14	84	594	4,719	40,898	379,236	3,711,916
ratio (%)	0	0	0	1.01	3.39	7.10	11.91	17.53
minimal dimension	2	4	6	7	8	9	10	11

Table 10.5 – The statistics for the sets of cones $\mathcal{F}_n(2n + 4 - i - j, 2n + 3 - i - j)$. With this choice of coefficients, some bad ridges appear in the construction for $n = 8$.

Observation 10.16. *It is possible to let the coefficients $\lambda_{(i,j)}$ and $\rho_{(i,j)}$ vary in order to still obtain sets of cones $\mathcal{F}_n(\lambda_{(i,j)}, \rho_{(i,j)})$ with degeneracies but almost no bad ridges. Moreover some choices let the degeneracy indicator decrease remarkably. Indeed the choice $\lambda_{(i,j)} = 2n + 4 - i - j$ and $\rho_{(i,j)} = 2n + 3 - i - j$ again decreases by a factor of about 2 these indicators by comparison to the choice $\lambda_{(i,j)} = 5$ and $\rho_{(i,j)} = 3$.*

10.4.3 Perturbations

As a particular case of Observation 10.16, we noticed that $\mathcal{F}_5(14 - i - j, 13 - i - j)$ seemed really close of realizing the 2-associahedron $\mathbf{\Delta}_{2,5}$. So we stopped our experiments on the coefficients $\lambda_{(i,j)}$ and $\rho_{(i,j)}$ and tried to perturb the rays randomly with the hope of killing the last remaining degeneracies. Again there is some freedom in this idea of "perturbing" the rays. Indeed we tried to add a random and small enough term to each of their coordinate, unsuccessfully. But then, applying the perturbations to the coefficients $\lambda_{(i,j)}$ and $\rho_{(i,j)}$ themselves finally gave us realizing rays for the 2-associahedron $\mathbf{\Delta}_{2,5}$ (see Table 10.6). Of course not all perturbations terms that appear in these rays are necessary. So working on the coordinates in Table 10.6, we found the simpler ones in Table 10.7. Notice that these rays now have integer coordinates between -10 and 10. Moreover the number of perturbation terms is now reduced to 3.

Observing the pattern formed on the sorting network of the word $c^2 w_5(c)$ by these perturbation terms, we derived the conjectural pattern for realizing rays for any 2-associahedron of Figure 10.14, and described in Section 10.1. There we stated Question 10.3 as a question rather than as a conjecture, because of the 20 bad ridges appearing with our choice of coefficients for $n = 8$. This is *a priori* not a problem since the number of perturbations grows quadratically with n and our candidate pattern of rays is still realizing for $n = 8$. Moreover the other tries we made seemed to indicate that more random integer perturbations failed realizing 2-associahedra before $n = 6$. Yet these bad ridges may grow quickly with n and let our pattern finally fail being realizing for all n. But we still obtain realizations for some 2-associahedra with integer coordinates between $-(2n + 1)$ and $(2n + 2)$, for $n \leq 8$.

Theorem 10.17. *The rays of the pattern in Figure 10.14 support a complete simplicial fan in $\mathbb{R}^{2n}$ which realizes the multiassociahedron $\mathbf{\Delta}_{2,n}$ for $n \in [8]$.*

s_1: [-1	0	0	0	0	0	0	0	0	0]
s_2: [0	-1	0	0	0	0	0	0	0	0]
s_3: [0	0	-1	0	0	0	0	0	0	0]
s_4: [0	0	0	-1	0	0	0	0	0	0]
s_5: [0	0	0	0	-1	0	0	0	0	0]
s_1: [11.995220082449654	-11.002018603888557	0	0	0	-1	0	0	0	0]
s_2: [0	10.998025890846899	-10.000386365505443	0	0	0	-1	0	0	0]
s_3: [0	0	9.995777402249201	-8.998111068535287	0	0	0	-1	0	0]
s_4: [0	0	0	9.00229715779829	-8.001163693705028	0	0	0	-1	0]
s_5: [0	0	0	0	1	0	0	0	0	-1]
s_1: [0.9957828222479908	-0.003992713041657936	-0.0014994963267600525	0	0	1	-1	0	0	0]
s_2: [1.9999160791264572	-11.002018603888557	9.995777402249201	-0.0030142895687461646	0	1	0	-1	0	0]
s_3: [2.9965399682572844	-11.002018603888557	0	9.00229715779829	-0.0040464541747882166	1	0	0	-1	0]
s_4: [10.995220082449654	-11.002018603888557	0	0	1	1	0	0	0	-1]
s_5: [11.995220082449654	-11.002018603888557	0	0	0	1	0	0	0	0]
s_1: [0	0.9936127652497042	-0.004608963256242049	0.0012209718570073136	0	0	1	-1	0	0]
s_2: [0	2.001435184525553	-10.000386365505443	9.00229715779829	-0.0008415764775513424	0	1	0	-1	0]
s_3: [0	9.998025890846899	-10.000386365505443	0	1.0	0	1	0	0	-1]
s_4: [0	10.998025890846899	-10.000386365505443	0	0	0	1	0	0	0]
s_1: [0	0	0.9945133005526081	0.004186089263003012	0.0007304432600054866	0	0	1	-1	0]
s_2: [0	0	8.995777402249201	-8.998111068535287	1	0	0	1	0	-1]
s_3: [0	0	9.995777402249201	-8.998111068535287	0	0	0	1	0	0]
s_1: [0	0	0	8.00229715779829	-7.001163693705028	0	0	0	1	-1]
s_2: [0	0	0	9.00229715779829	-8.001163693705028	0	0	0	1	0]
s_1: [0	0	0	0	1	0	0	0	0	1]

Table 10.6 – Realizing rays of the 2-associahedron $\mathbf{\Delta}_{2,5}$, associated to each letter of the word $c^2 w_\circ(c)$ for $n = 5$. These rays were obtained by fattening twice the suffix triangle of an initial triangle with coefficients $\lambda_{(i,j)} = 14 - i - j + \varepsilon^\ell_{(i,j)}$ and $\rho_{(i,j)} = 13 - i - j + \varepsilon^r_{(i,j)}$, where $\varepsilon^\ell_{(i,j)}$ and $\varepsilon^r_{(i,j)}$ were uniform independent random variables in $[-0.001, 0.001]$ for $i \in [4]$ and $j \in [5 - i]$.

$s_1:[\,-1$	0	0	0	0	0	0	0	0	$0\,]$
$s_2:[\,0$	-1	0	0	0	0	0	0	0	$0\,]$
$s_3:[\,0$	0	-1	0	0	0	0	0	0	$0\,]$
$s_4:[\,0$	0	0	-1	0	0	0	0	0	$0\,]$
$s_5:[\,0$	0	0	0	-1	0	0	0	0	$0\,]$
$s_1:[\,12$	-11	0	0	0	-1	0	0	0	$0\,]$
$s_2:[\,0$	11	-10	0	0	0	-1	0	0	$0\,]$
$s_3:[\,0$	0	10	-9	0	0	0	-1	0	$0\,]$
$s_4:[\,0$	0	0	9	-8	0	0	0	-1	$0\,]$
$s_5:[\,0$	0	0	0	1	0	0	0	0	$-1\,]$
$s_1:[\,1$	0	0	0	0	1	-1	0	0	$0\,]$
$s_2:[\,2$	-11	10	$\boxed{-1}$	0	1	0	-1	0	$0\,]$
$s_3:[\,3$	-11	0	9	$\boxed{-2}$	1	0	0	-1	$0\,]$
$s_4:[\,11$	-11	0	0	1	1	0	0	0	$-1\,]$
$s_5:[\,12$	-11	0	0	0	1	0	0	0	$0\,]$
$s_1:[\,0$	1	0	0	0	0	1	-1	0	$0\,]$
$s_2:[\,0$	2	-10	9	$\boxed{-1}$	0	1	0	-1	$0\,]$
$s_3:[\,0$	10	-10	0	1	0	1	0	0	$-1\,]$
$s_4:[\,0$	11	-10	0	0	0	1	0	0	$0\,]$
$s_1:[\,0$	0	1	0	0	0	0	1	-1	$0\,]$
$s_2:[\,0$	0	9	-9	1	0	0	1	0	$-1\,]$
$s_3:[\,0$	0	10	-9	0	0	0	1	0	$0\,]$
$s_1:[\,0$	0	0	8	-7	0	0	0	1	$-1\,]$
$s_2:[\,0$	0	0	9	-8	0	0	0	1	$0\,]$
$s_1:[\,0$	0	0	0	1	0	0	0	0	$1\,]$

Table 10.7 – Realizing rays of the 2-associahedron $\mathbf{\Delta}_{2,5}$, associated to each letter of the word $\mathsf{c}^2\mathsf{w}_\circ(\mathsf{c})$ for $n=5$. These rays were obtained by working on the coordinates of these in Table 10.6. The perturbation terms, that is the coordinates that are different from these obtained by fattening twice a suffix triangle in an initial triangle with coefficients $\lambda_{(i,j)}=14-i-j$ and $\rho_{(i,j)}=13-i-j$, appear boxed and red. In the nonperturbed set of rays, all the corresponding terms are equal to zero. Observe finally that all perturbation terms are negative integers.
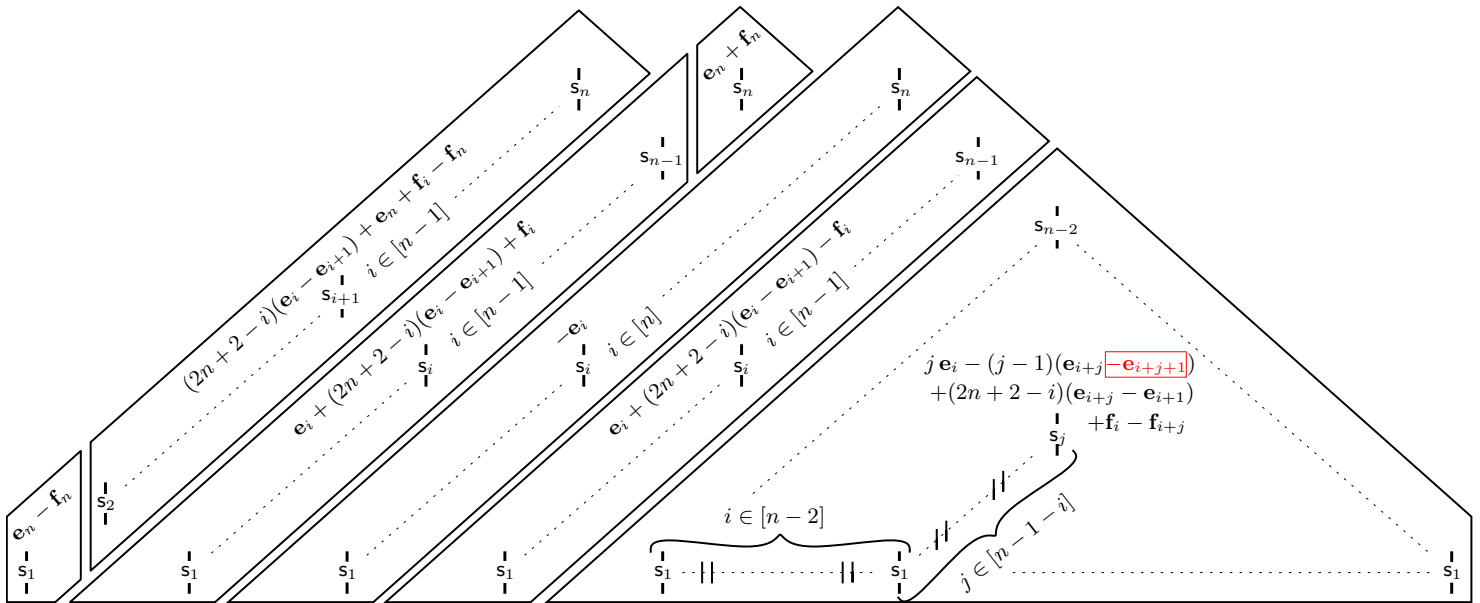
Figure 10.14 – The candidate pattern for integer rays supporting a fan realizing 2-associahedra. We denote the n first vectors of the canonical basis of $\mathbb{R}^{2n}$ by $(\mathbf{e}_i)_{i\in[n]}$ and the n last ones by $(\mathbf{f}_i)_{i\in[n]}$. The perturbation terms appear boxed and red. They are negative and replace zero coordinates of the nonperturbed construction. This pattern is the one we obtain after applying $2n$ times the rotation map to the underlying word $\mathsf{c}^2\mathsf{w}_\circ(\mathsf{c})$ to have a better presentation.

10.5 Discussion

10.5.1 Polytopality

Unfortunately none of the new fans we produce happens to be the normal fan of a polytope. Not even in the case of the 2-associahedron $\Delta_{2,3}$ which is known to have a polytopal realization by J. Bokowski and V. Pilaud [BP09], although our transformations are intuitively chosen to fit with geometric constraints. This confirms[4] that the way from combinatorics to geometry is very tight and how hard it is to handle with in the case of multiassociahedra.

10.5.2 Further k's

The few tries we made towards more general k than 2 did not work successfully and quickly produced sets of cones with many bad ridges, in contrast with Section 10.4.1. We tried to fatten three times a triangle, which produced really bad objects, and then tried to fatten a triangle starting from the valid rays we had obtained after perturbing, which was not better. But our experiments lack exhaustive tries and the main issue with our method somehow comes from the fact that we have too many and too wide degrees of freedom to apply it.

---

[4]If ever it was still needed...

Hamiltonicity of graph associahedra

In this appendix, we prove that the flip graph $\mathcal{F}(G)$ is Hamiltonian for any graph G with at least 2 edges. This extends the result of H. Steinhaus [Ste64], S. Johnson [Joh63], and H. Trotter [Tro62] for the permutahedron, and of J. Lucas [Luc87] for the associahedron (see also [HN99]). For all the proof, it is more convenient to work with spines than with tubings. We invite the reader to remind Sections 5.2.2 and 5.2.3, were spines were defines as the Hasse diagrams of the inclusion posets of tubings, with nodes labeled by sets of the form $\lambda(t, T)$. We first sketch the strategy of our proof.

A.1 Strategy

For any vertex v of G, we denote by $\mathcal{F}_v(G)$ the graph of flips on all spines on G where v is a root. We call *fixed-root subgraphs* of $\mathcal{F}(G)$ the subgraphs $\mathcal{F}_v(G)$ for $v \in V$. Note that the fixed-root subgraph $\mathcal{F}_v(G)$ is isomorphic to the flip graph $\mathcal{F}(G[\hat{v}])$, where $G[\hat{v}]$ is the subgraph of G induced by $\hat{v} := V \smallsetminus \{v\}$.

We now distinguish two extreme types of flips. Consider two maximal tubings T, T' on G and tubes $t \in T$ and $t' \in T'$ such that $\bar{T} := T \smallsetminus \{t\} = T' \smallsetminus \{t'\}$. Let S, S' and $\bar{S}$ denote the corresponding spines and $\{v\} = \lambda(t, T)$ and $\{v'\} = \lambda(t', T')$. We say that the flip $\bar{T}$ (or equivalently $\bar{S}$) is

(i) a *short flip* if both t and t' are singletons, that is, if $\{v, v'\}$ is a leaf of $\bar{S}$;

(ii) a *long flip* if t and t' are maximal proper tubes in T and T', that is, if $\{v, v'\}$ is a root of $\bar{S}$.

Note that in a short flip, the vertices v, v' are necessarily adjacent in G. In the short flip $\bar{S}$, we call *short leaf* the leaf labeled by $\{v, v'\}$ of $\bar{S}$, *short root* the root of the tree of $\bar{S}$ containing the short leaf, and *short child* the child w of the short root on the path to the short leaf. If the short leaf is already a child of the short root, then it coincides with the short child. Moreover, the short root, short child and short leaf all coincide if they form an isolated edge of G. In the long flip $\bar{S}$, we call *long root* the root labeled by $\{v, v'\}$.

We define a *bridge* to be a square B in the flip graph $\mathcal{F}(G)$ formed by two short and two long flips. We say that these two short (resp. long) flips are *parallel*, and we borrow the terms long root and short leaf for the bridge B. Figure A.1 illustrates the notions of bridge, long flips and short flips.

In terms of spines, a bridge can equivalently be defined as a spine B of G where all labels are singletons, except the label $\{r, r'\}$ of a root and the label $\{s, s'\}$ of a leaf. We denote by B$[r]$ the short flip of B where r is a root, by B$[s]$ the long flip of B where s is a leaf, and by B$[rs]$ the maximal spine on G refining both B$[r]$ and B$[s]$, *i.e.* where r is a root and s a leaf. The flips B$[r']$ and B$[s']$ as well as the maximal spines B$[r's]$, B$[rs']$, and B$[r's']$ are defined similarly. These notations are summarized below
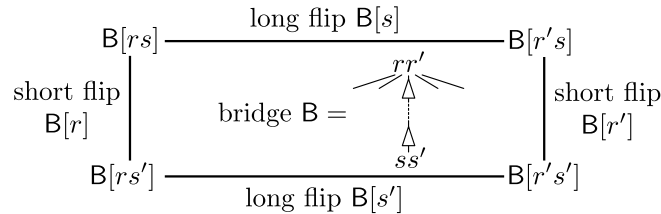
To obtain a Hamiltonian cycle $\mathcal{H}$ of the flip graph $\mathcal{F}(G)$, we proceed as follows. The idea is to construct by induction a Hamiltonian cycle $\mathcal{H}_{\hat{v}}$ of each flip graph $\mathcal{F}(G[\hat{v}])$, which is isomorphic to a Hamiltonian cycle $\mathcal{H}_v$ in each fixed-root subgraph $\mathcal{F}_v(G)$. We then select an ordering $v_1, \ldots, v_{n+1}$ of V, such that two consecutive Hamiltonian cycles $\mathcal{H}_{v_i}$ and $\mathcal{H}_{v_{i+1}}$ meet the parallel short flips of a bridge B$_i$ for all $i \in [n]$. The Hamiltonian cycle of $\mathcal{F}(G)$ is then obtained from the union of the cycles $\mathcal{H}_{v_1}, \ldots, \mathcal{H}_{v_{n+1}}$ by exchanging the short flips with the long flips of all bridges B$_1, \ldots, B_n$, as illustrated in Figure A.2.

Of course, this description is a simplified and naive approach. The difficulty lies in that, given the Hamiltonian cycles $\mathcal{H}_v$ of the fixed-root subgraphs $\mathcal{F}_v(G)$, the existence of a suitable ordering $v_1, \ldots, v_{n+1}$ of V and of the bridges B$_1, \ldots, B_n$ connecting the consecutive Hamiltonian cycles $\mathcal{H}_{v_i}$ and $\mathcal{H}_{v_{i+1}}$ is not guaranteed. To overpass this
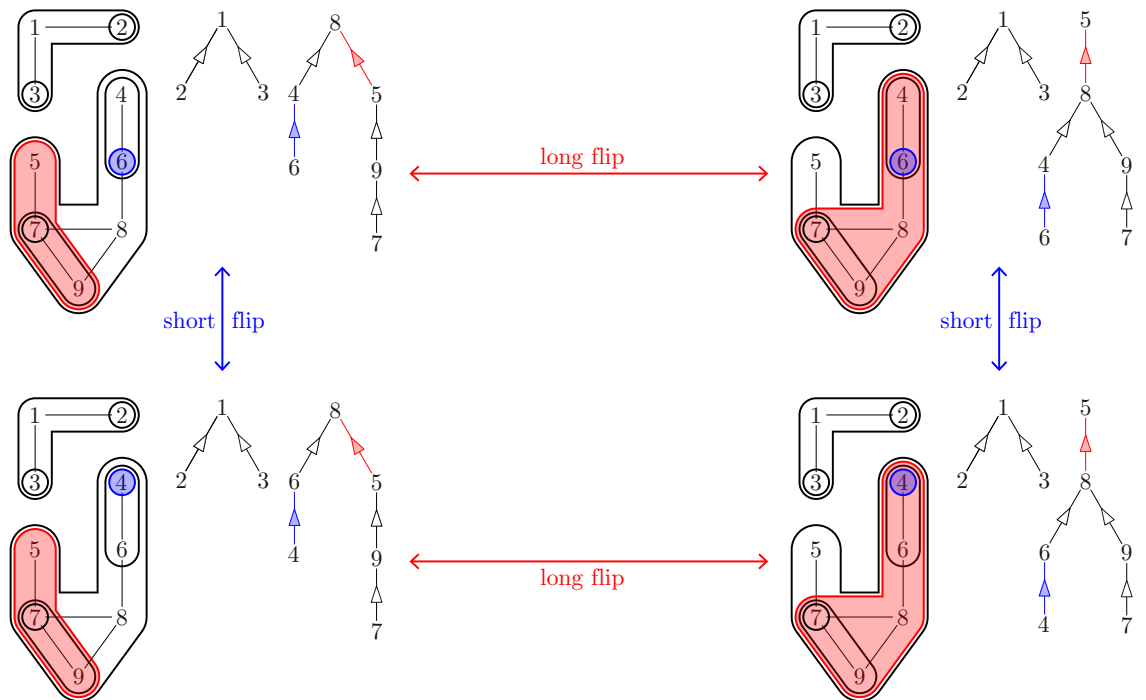
Figure A.1 – A bridge, with two long flips (horizontal, red) and two short flips (vertical, blue).
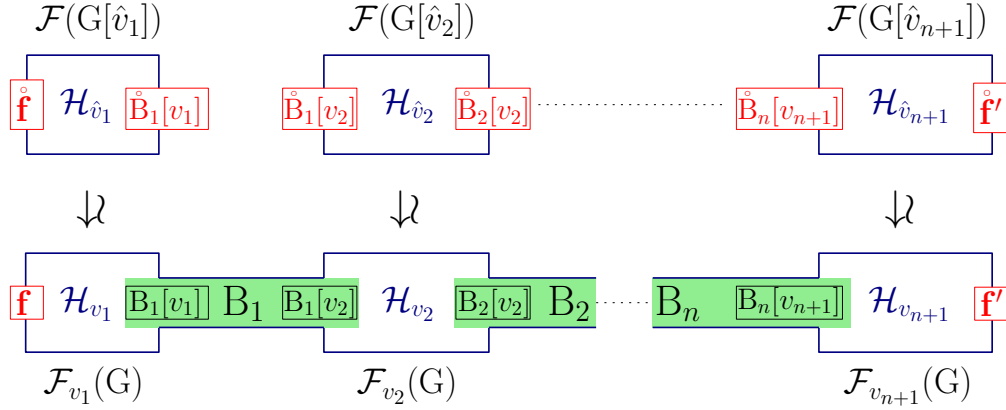
Figure A.2 – The strategy for the proof of the hamiltonicity of the flip graph $\mathcal{F}(\mathrm{G})$. The circles above the short flips in the flip graphs $\mathcal{F}(\mathrm{G}[\hat{v}_i])$ on top indicate that they are obtained by deleting the root v_i in the corresponding short flip of the fixed-root subgraph $\mathcal{F}_{v_i}(\mathrm{G})$ on bottom. See also Theorem A.1.

issue, we need to impose the presence of two forced short flips in each Hamiltonian cycle $\mathcal{H}_v$. We include this condition in the induction hypothesis and prove the following sharper version of Theorem 5.1.

Theorem A.1. *For any graph* G*, any pair of short flips of* $\mathcal{F}(\mathrm{G})$ *with distinct short roots is contained in a Hamiltonian cycle of the flip graph* $\mathcal{F}(\mathrm{G})$*.*

Note that for any graph G with at least 2 edges, the flip graph $\mathcal{F}(\mathrm{G})$ always contains two short flips with distinct short roots. Theorem 5.1 thus follows from the formulation of Theorem A.1.

The issue in our inductive approach is that the fixed-root subgraphs of $\mathcal{F}(\mathrm{G})$ do not always contain two edges, and therefore cannot be treated by Theorem A.1. Indeed, it can happen that:

- $\mathrm{G}[\hat{v}]$ has a single edge and thus the fixed-root subgraph $\mathcal{F}_v(\mathrm{G}) \sim \mathcal{F}(\mathrm{G}[\hat{v}])$ is reduced to a single (short) flip. This case can still be treated with the same strategy: we consider this single flip $\mathcal{F}_v(\mathrm{G})$ as a degenerate Hamiltonian cycle and we can concatenate two bridges containing this short flip.

- $\mathrm{G}[\hat{v}]$ has no edge and thus the fixed-root subgraph $\mathcal{F}_v(\mathrm{G}) \sim \mathcal{F}(\mathrm{G}[\hat{v}])$ is a point. This is the case when G is a star with central vertex v together with some isolated vertices. We need to make a special and independent treatment for this particular case. See Section A.4.

A.2 Disconnected graphs

We first show how to restrict the proof to connected graphs using some basic results on products of cycles. We need the following lemmas.

Lemma A.2. *For any two cycles* $\mathcal{H}, \mathcal{H}'$ *and any two edges* e, e' *of* $\mathcal{H} \times \mathcal{H}'$*, there exists a Hamiltonian cycle of* $\mathcal{H} \times \mathcal{H}'$ *containing both* e *and* e'*.*

Proof. The idea is illustrated in Figure A.3. The precise proof is left to the reader. ∎

Lemma A.3. *For any cycle* $\mathcal{H}$*, any isolated edge* $e_\circ$ *and any two edges* e, e' *of* $\mathcal{H} \times e_\circ$*, there exists a Hamiltonian cycle containing both* e *and* e'*, as soon as one of the following conditions hold:*
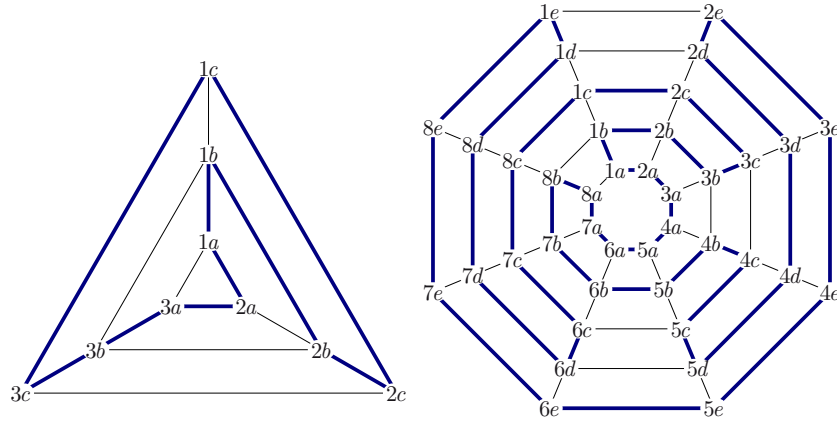
Figure A.3 – An idea for the proof of Lemma A.2. Any pair of edges is contained in a Hamiltonian cycle similar to those. The pictures represent Cartesian products of the cycle $\mathcal{H}$ with the path obtained by deleting one edge in $\mathcal{H}'$.

  1. *the edges e, e' are not both of the form $\{v\} \times e_\circ$ with $v \in \mathcal{H}$;*

  2. *$e = \{v\} \times e_\circ$ and $e' = \{v'\} \times e_\circ$ where $\{v, v'\}$ is an edge de $\mathcal{H}$;*

  3. *$\mathcal{H}$ has an even number of edges.*

Proof. The idea is illustrated in Figure A.4. The precise proof is left to the reader.   ∎
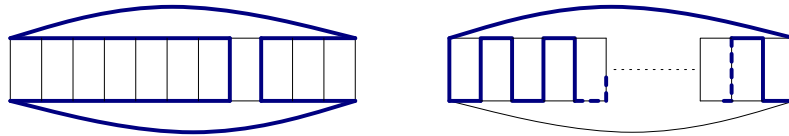
Figure A.4 – An idea for the proof of Lemma A.3. The right picture only works for even cycles.

Corollary A.4. *If two graphs G, G' both have the property that any pair of short flips of their flip graph with distinct short roots is contained in a Hamiltonian cycle of their flip graph, then $G \sqcup G'$ fulfills the same property.*

Proof. We have seen that the flip graph of the disjoint union of two graphs G_1 and G_2 is the product of their flip graphs $\mathcal{F}(G_1)$ and $\mathcal{F}(G_2)$. The statement thus follows from the previous lemmas.   ∎

A.3 Generic proof

We now present an inductive proof of Theorem A.1. Corollary A.4 allows us to restrict to the case where G is connected. For technical reasons, the stars and the graphs with at most 6 vertices will be treated separately. We thus assume here that G is not a star and has at least 7 vertices, which ensures that any fixed root subgraph of the flip graph $\mathcal{F}(G)$ has at least one short flip. Fix two short flips $\mathbf{f}, \mathbf{f}'$ of $\mathcal{F}(G)$ with distinct short roots v_1, v_{n+1} respectively.

   We follow the strategy described in Section A.1 and illustrated in Figure A.2. To apply Theorem A.1 by induction on $G[\hat{v}_i]$, the short flips $B_{i-1}[v_i]$ and $B_i[v_i]$ should have distinct short children. This forbids certain positions for v_{i+1} in $B_{i-1}[v_i]$ illustrated in

Figure A.5, and motivates the following definition. We say that a vertex w and a short flip $\mathbf{g}$ with root v are *in conflict* if either of the following happens:

(A) $\{w\}$ is the short child of $\mathbf{g}$ and all other children of v in $\mathbf{g}$ are isolated in $G[\hat{v}]$;

(B) the graph $G[\hat{v}]$ has at least three edges, the graph $G \smallsetminus \{v, w\}$ has exactly one edge which is the short leaf of $\mathbf{g}$;

(C) the graph $G[\hat{v}]$ has exactly two edges, the graph $G \smallsetminus \{v, w\}$ has exactly one edge which is the short leaf of $\mathbf{g}$, and w is a child of v.

It is immediate that a short flip is in conflict with at most one vertex. Observe also that if w is in the short leaf of $\mathbf{g}$, then w and $\mathbf{g}$ cannot be in conflict.

(A) (B) (C)
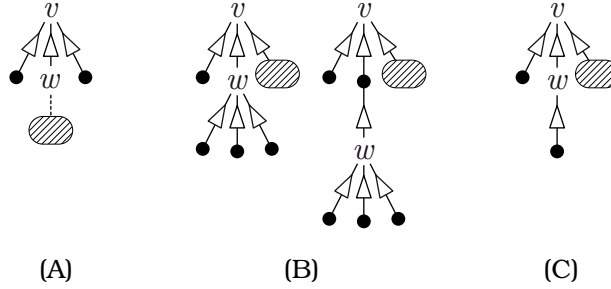
Figure A.5 – Short flips in conflict with vertex w. The short leaf is shaded. The second short flip of Case (B) is in conflict with w only if the connected component of $G[\hat{v}]$ containing w is a star with central vertex w.

We now show how we order the vertices $v_1, \dots, v_{n+1}$ such that for each $i \in [n]$ there exists a bridge B_i connecting the fixed-root subgraphs $\mathcal{F}_{v_i}(G)$ and $\mathcal{F}_{v_{i+1}}(G)$.

Lemma A.5. *There exists an ordering $v_1, \dots, v_{n+1}$ of the vertices of G (provided $|V| \geq 7$) satisfying the following properties:*

- *v_2 and $\mathbf{f}$ are not in conflict, and v_n and $\mathbf{f}'$ are not in conflict, and*

- *for any $i \in [n]$, the graph G contains an edge disjoint from $\{v_i, v_{i+1}\}$.*

Proof. Let a and a' denote the vertices in conflict with $\mathbf{f}$ and $\mathbf{f}'$ if any. Let D denote the set of *totally disconnecting pairs* of G, *i.e.* of pairs $\{x, y\}$ such that $G \smallsetminus \{x, y\}$ has no edge. We want to show that there exists an ordering on the vertices of G in which neither $\{v_1, a\}$ nor $\{a', v_{n+1}\}$, nor any pair of D are consecutive. For this, we prove that if G has at least 5 vertices and is not a star (*i.e.* all edges contain a central vertex), then $|D| \leq 2$ and the pairs in D are not disjoint.

Suppose by contradiction that D contains two disjoint pairs $\{x_1, y_1\}$ and $\{x_2, y_2\}$. Then any edge of G intersects both pairs, so that x_1, x_2, y_1, y_2 are the only vertices in G (by connectivity), contradicting that G has at least 5 vertices. Suppose now that D contains three pairwise distinct pairs $\{x, y_1\}$, $\{x, y_2\}$ and $\{x, y_3\}$. Then any edge of G contains x since it cannot contain y_1, y_2 and y_3 together. It follows that G is a star with central vertex x.

Since $|D| \leq 2$, at most 4 pairs of vertices of G cannot be consecutive in our ordering. It is thus clear that if there are enough other vertices, we can find a suitable ordering. In fact, it turns out that it is already possible as soon as G has 7 vertices. It is easy to prove by a boring case analysis. We just treat the worst case below.

Assume that $D = \{\{x, y\}, \{x, z\}\}$ where $x, y, z \notin \{v_1, v_{n+1}\}$ and that x is in conflict with both short flips $\mathbf{f}$ and $\mathbf{f}'$. Since $|V| \geq 7$, there exist two distinct vertices $u, v \notin \{v_1, v_{n+1}, x, y, z\}$ and we set $v_2 = z, v_3 = y, v_4 = u, v_5 = x, v_6 = v$ and choose any ordering for the remaining vertices. This order satisfies the requested conditions. ∎

Remark A.6. In fact, using similar arguments, one can easily check that the result of Lemma A.5 holds in the following situations:

- $|V| = 6$, and either $|D| \leq 1$ or $D = \{\{x, y\}, \{x, z\}\}$ where x is not in conflict with both $\mathbf{f}, \mathbf{f}'$.
- $|V| = 5$, and either $D = \varnothing$ or $D = \{\{x, y\}\}$ where neither x nor y is in conflict with both $\mathbf{f}, \mathbf{f}'$.
- $|V| = 5$, and $D = \{\{x, y\}, \{x, z\}\}$ and $|\{x, y, z\} \cap \{v_1, v_5\}| = 2$.
- $|V| = 5$, and $D = \{\{x, y\}, \{x, z\}\}$ and $|\{x, y, z\} \cap \{v_1, v_5\}| = 1$ and neither of x, y, z is in conflict with any of $\mathbf{f}$ and $\mathbf{f}'$.

Given such an ordering $v_1, \ldots, v_{n+1}$, we choose bridges $\mathsf{B}_1, \ldots, \mathsf{B}_n$ connecting the fixed-root subgraphs $\mathcal{F}_{v_1}(\mathrm{G}), \ldots, \mathcal{F}_{v_{n+1}}(\mathrm{G})$. We start with the choice of B_1.

Lemma A.7. *There exists a bridge* B_1 *with root* $\{v_1, v_2\}$ *such that*

- *if* $\mathcal{F}_{v_1}(\mathrm{G})$ *is a square, the short flips* $\mathbf{f}$ *and* $\mathsf{B}_1[v_1]$ *are distinct,*

- *if* $\mathcal{F}_{v_1}(\mathrm{G})$ *is not reduced to a single flip nor to a square, the short flips* $\mathbf{f}$ *and* $\mathsf{B}_1[v_1]$ *have distinct short children,*

- $\mathsf{B}_1[v_2]$ *and* v_3 *are not in conflict, and*

- *the singleton* $\{v_3\}$ *is a child of* v_2 *in* $\mathsf{B}_1[v_2]$ *only if* v_3 *is isolated in* $\mathrm{G} \smallsetminus \{v_1, v_2\}$.

Proof. The proof is an intricate case analysis. In each case, we will provide a suitable choice for B_1, but the verification that this bridge exists and satisfies the conditions of the statement is immediate and left to the reader. We denote by κ the connected component of $\mathrm{G}[\hat{v}_1]$ containing v_2. The following cases cover all possibilities:

♠ $\kappa = \{v_2\}$:

♡ $\mathrm{G} \smallsetminus \{v_1, v_2\}$ has only one edge: the fixed root subgraph $\mathcal{F}_{v_1}(\mathrm{G})$ is reduced to the short flip $\mathbf{f}$ and the bridge obtained by contracting $\{v_1, v_2\}$ in $\mathbf{f}$ suits for B_1.

♡ $\mathrm{G} \smallsetminus \{v_1, v_2\}$ has at least two edges: we choose for B_1 any bridge with root $\{v_1, v_2\}$ and with a short child different from that of $\mathbf{f}$.

♠ $\kappa \neq \{v_2\}$, so that κ has at least one edge:

♡ $\mathrm{G}[\hat{v}_1] \smallsetminus \kappa$ has no edge: Condition (A) on $\mathbf{f}$ and v_2 ensures that v_2 is not the short child of $\mathbf{f}$. Since the short leaf of $\mathbf{f}$ has to be in κ, the short children of $\mathbf{f}$ and $\mathsf{B}_1[v_1]$ will automatically be different.

◇ $v_3 \notin \kappa$: any bridge with root $\{v_1, v_2\}$ suits for B_1.

◇ $v_3 \in \kappa$:

♣ v_3 is isolated in $\kappa \smallsetminus \{v_2\}$: any bridge with root $\{v_1, v_2\}$ suits for B_1.

♣ v_3 is not isolated in $\kappa \smallsetminus \{v_2\}$: we choose for B_1 a bridge with root $\{v_1, v_2\}$ and whose short leaf contains v_3.

♡ $\mathrm{G}[\hat{v}_1] \smallsetminus \kappa$ has precisely one edge e:

◇ e is not the short leaf of $\mathbf{f}$: we choose for B_1 any bridge with root $\{v_1, v_2\}$, short leaf e and in which $\{v_3\}$ is a child of the root only if it is isolated in $\mathrm{G} \smallsetminus \{v_1, v_2\}$.

◇ e is the short leaf of $\mathbf{f}$:

♣ κ is a single edge: we choose for B_1 the bridge obtained by contracting $\{v_1, v_2\}$ in the short flip opposite to $\mathbf{f}$ in the square $\mathcal{F}_{v_1}(\mathrm{G})$ (which suits by Condition (C)).

♣ κ has at least two edges: Condition (B) ensures that $\kappa \smallsetminus \{v_2\}$ has at least one edge.

◦ $v_3 \notin \kappa$: any bridge with root $\{v_1, v_2\}$ and short leaf in κ suits for B_1.
◦ $v_3 \in \kappa$:
  ⋆ v_3 is isolated in $\kappa \smallsetminus \{v_2\}$: any bridge with root $\{v_1, v_2\}$ and short leaf in κ suits.
  ⋆ v_3 is not isolated in $\kappa \smallsetminus \{v_2\}$: we choose for B_1 a bridge with root $\{v_1, v_2\}$ and whose short leaf contains v_3.

♡ $\mathrm{G}[\hat{v}_1] \smallsetminus \kappa$ has at least two edges:
  ◇ $\mathrm{G}[\hat{v}_1] \smallsetminus \kappa$ has only one nontrivial connected component: we choose for B_1 a bridge with root $\{v_1, v_2\}$, with short leaf containing the nonisolated child of v_1 in $\mathbf{f}$ which is not in κ, and in which $\{v_3\}$ is a child of the root only if it is either isolated in $\mathrm{G} \smallsetminus \{v_1, v_2\}$ or the short child of $\mathsf{B}_1[v_1]$.
  ◇ $\mathrm{G}[\hat{v}_1] \smallsetminus \kappa$ has at least two nontrivial connected components: we choose for B_1 a bridge with root $\{v_1, v_2\}$, with short leaf in a connected component of $\mathrm{G}[\hat{v}_1] \smallsetminus \kappa$ not containing the short leaf of $\mathbf{f}$, and in which $\{v_3\}$ is a child of the root only if it is either isolated in $\mathrm{G} \smallsetminus \{v_1, v_2\}$ or the short child of $\mathsf{B}_1[v_1]$. ∎

The choice of B_n is similar to that of B_1, replacing v_1, v_2, v_3 and $\mathbf{f}$ by v_{n+1}, v_n, v_{n-1} and $\mathbf{f}'$ respectively. For choosing the other bridges $\mathsf{B}_2, \ldots, \mathsf{B}_{n-1}$, we first observe the existence of certain special vertices in G.

We say that a vertex distinct from v_1 and v_{n+1} which disconnects at most one vertex is an *almost leaf* of G. Observe that G contains at least one almost leaf: Consider a spanning tree T of G. If T is a path from v_1 to v_{n+1}, the neighbor of v_1 in T is an almost leaf of G. Otherwise, any leaf of T distinct from v_1 and v_{n+1} is an almost leaf of G.

Choose an almost leaf v_i of G which disconnects no vertex if possible, and any almost leaf otherwise. We sequentially construct the bridges $\mathsf{B}_2, \ldots, \mathsf{B}_{i-1}$: once B_j is constructed, we choose B_{j+1} using Lemma A.7 where we replace v_1, v_2, v_3 and $\mathbf{f}$ by $v_{j+1}, v_{j+2}, v_{j+3}$ and $\mathsf{B}_j[v_{j+1}]$. Similarly, we choose the bridges $\mathsf{B}_{n-1}, \ldots, \mathsf{B}_{i+1}$: once B_{j+1} is constructed, we choose B_j using Lemma A.7 where we replace v_1, v_2, v_3 and $\mathbf{f}$ by v_{j+1}, v_j, v_{j-1} and $\mathsf{B}_{j+1}[v_{j+1}]$. Note that the conditions on B_1 required in Lemma A.7 ensure that the hypothesizes in Lemma A.5 can be propagated.

It remains to properly choose the last bridge B_i. This is done by the following statement.

Lemma A.8. *Let $\mathbf{g}, \mathbf{h}$ be two short flips on G with distinct roots v, w respectively. Assume that*

 (i) $\mathrm{G} \smallsetminus \{v, w\}$ *has at least one edge;*

 (ii) $\mathbf{g}$ *and w are not in conflict, and $\mathbf{h}$ and v are not in conflict;*

 (iii) $\{v\}$ *is a child of w in $\mathbf{h}$ only if v is isolated in $\mathrm{G}[\hat{w}]$;*

 (iv) v *disconnects at most one vertex of G and this vertex is not w.*

Then there exists a bridge B with root $\{v, w\}$ such that $\mathbf{g}$ and $\mathsf{B}[v]$ are distinct if $\mathcal{F}_v[\mathrm{G}]$ is not reduced to a single flip and have distinct short children if $\mathcal{F}_v[\mathrm{G}]$ is not a square, and similarly for $\mathbf{h}$ and $\mathsf{B}[w]$.

Proof. Condition (iv) implies that $\{w\}$ is the short child of $\mathsf{B}[v]$ for any bridge B with root $\{v, w\}$. In contrast, Condition (iv) and Condition (A) for $\mathbf{g}$ and w ensure that $\{w\}$ is not the short child of $\mathbf{g}$. Therefore, the conclusion of the lemma holds for $\mathbf{g}$ and $\mathsf{B}[v]$, for any bridge B with root $\{v, w\}$. The difficulty is to choose B in order to satisfy the conclusion for $\mathbf{h}$ and $\mathsf{B}[w]$. For this, we distinguish various cases, in a similar manner as in Lemma A.7. Again, we provide in each case a suitable choice for B, but the verification that this bridge exists and satisfies the conditions of the statement is immediate and left to the reader.

♠ $G \smallsetminus \{v, w\}$ has exactly one edge e: this edge e has to be the short leaf of any bridge with root $\{v, w\}$, thus Condition (A) for $\mathbf{h}$ and v ensures that e is isolated in $G[\hat{w}]$.

   ♡ e is the short leaf of $\mathbf{h}$: Condition (B) for $\mathbf{h}$ and v ensures that $\mathcal{F}_w(G)$ is either a single flip or a square (because v disconnects at most one vertex from G).

      ◇ $\mathcal{F}_w(G)$ is a single flip: B is obtained by contracting $\{v, w\}$ in $\mathbf{h}$.
      ◇ $\mathcal{F}_w(G)$ is a square: Condition (C) for $\mathbf{h}$ and v ensures that v is not a child of w in $\mathbf{h}$ and B is obtained by contracting $\{v, w\}$ in the short flip opposite to $\mathbf{h}$ in the square $\mathcal{F}_w(G)$.

   ♡ e is not the short leaf of $\mathbf{h}$: we choose for B any bridge with root $\{v, w\}$ and short leaf e.

♠ $G \smallsetminus \{v, w\}$ has at least two edges:

   ♡ the short leaf and the short child of $\mathbf{h}$ coincide: any bridge with root $\{v, w\}$ and a short leaf distinct from that of $\mathbf{h}$ suits for B.

   ♡ the short leaf and the short child of $\mathbf{h}$ are distinct: we choose for B a bridge with root $\{v, w\}$ whose short leaf contains the short child of $\mathbf{h}$. ■

We have now chosen the order on the vertices $v_1, \dots, v_{n+1}$ and chosen for each $i \in [n]$ a bridge B_i connecting the fixed-root subgraphs $\mathcal{F}_{v_i}(G)$ and $\mathcal{F}_{v_{i+1}}(G)$. Our choice forces the short flips $B_{i-1}[v_i]$ and $B_i[v_i]$ (as well as the short flips $\mathbf{f}$ and $B_1[v_1]$ and the short flips $B_n[v_{n+1}]$ and $\mathbf{f}'$) to be distinct if $\mathcal{F}_{v_i}[G]$ is not reduced to a single flip and have distinct short children if $\mathcal{F}_{v_i}[G]$ is not a square. We then construct a Hamiltonian cycle $\mathcal{H}_i$ in each fixed-root subgraph $\mathcal{F}_{v_i}(G)$ such that $\mathcal{H}_1$ contains the short flips $\mathbf{f}$ and $B_1[v_1]$, $\mathcal{H}_{n+1}$ contains the short flips $B_n[v_{n+1}]$ and $\mathbf{f}'$, and $\mathcal{H}_i$ contains the short flips $B_{i-1}[v_i]$ and $B_i[v_i]$ for all $2 \le i \le n$. Note that

   • when $\mathcal{F}_{v_i}(G)$ is reduced to a single flip, we just set $\mathcal{H}_i = \mathcal{F}_{v_i}(G)$ and consider it as a degenerate Hamiltonian cycle;

   • when $\mathcal{F}_{v_i}(G)$ is a square, it is already a cyle;

   • otherwise, we apply Theorem A.1 by induction to $G[\hat{v}_i]$ and obtain the Hamiltonian cycle $\mathcal{H}_i$. The theorem applies since the short flips $B_{i-1}[v_i]$ and $B_i[v_i]$ have distinct short children, so that the corresponding short flips in $\mathcal{F}(G[\hat{v}_i])$ have distinct short roots.

Finally, we obtain a Hamiltonian cycle of $\mathcal{F}(G)$ containing $\mathbf{f}$ and $\mathbf{f}'$ by gluing the cycles $\mathcal{H}_1, \dots, \mathcal{H}_{n+1}$ together using the bridges $B_1, \dots, B_n$ as explained in Section A.1. This is possible since the short flips $B_{i-1}[v_i]$ and $B_i[v_i]$ both belong to the Hamiltonian cycle $\mathcal{H}_i$, and are distinct when $\mathcal{F}_{v_i}(G)$ is not reduced to a single flip. This concludes the proof for all generic cases. The remaining of the paper deals with the special cases of stars and graphs with at most 6 vertices.

A.4 Stars

We now treat the particular case of stars. Consider a ground set V where a vertex $*$ is distinguished. The *star* on V is the tree X_V where all vertices of $V \smallsetminus \{*\}$ are leaves connected to $*$. The flip graph $\mathcal{F}(X_V)$ has two kinds of fixed-root subgraphs:

   • $\mathcal{F}_*(X_V)$ is reduced to a single spine ⊛ with root $*$ and n leaves;

   • for any other vertex $v \in V \smallsetminus \{*\}$, the fixed-root subgraph $\mathcal{F}_v(X_V)$ is isomorphic to the flip graph $\mathcal{F}(X_{\hat{v}})$ of the star $X_{\hat{v}}$, where $*$ is still the distinguished vertex in $\hat{v} = V \smallsetminus \{v\}$. For a spine $S \in \mathcal{F}_v(X_V)$, we denote by $\mathring{S}$ the unique subspine of S, and we write in column $S = \overset{v}{\mathring{S}}$.

To find a Hamiltonian cycle passing through forced short flips and through the spine ⊛ we need to refine again the induction hypothesis of Theorem A.1 as follows.

Proposition A.9. *Assume that $|V| \geq 3$, and fix two short flips $\mathbf{f}, \mathbf{f}'$ of $\mathcal{F}(X_V)$ with distinct roots $r \neq r'$ and a long flip $\mathbf{g}$ of $\mathcal{F}(X_V)$ with root $\{r'', *\}$. Then the flip graph $\mathcal{F}(X_V)$ has a Hamiltonian cycle containing $\mathbf{f}, \mathbf{f}', \mathbf{g}$.*

Proof. The proof works by induction on $|V|$. If $|V| = 3$, then X_V is a 3-path and its flip graph is a pentagon. The case $|V| = 4$ is solved by Figure A.6 up to relabeling of V. Namely, whatever triple $\mathbf{f}, \mathbf{f}', \mathbf{g}$ is imposed, there is a permutation of the leaves of $X_{\{1,2,3,*\}}$ which sends the Hamiltonian cycle of Figure A.6 to a Hamiltonian cycle passing through $\mathbf{f}, \mathbf{f}', \mathbf{g}$. Assume now that $|V| \geq 5$. We distinguish two cases.

Case 1:. $r'' \in \{r, r'\}$, say for instance $r'' = r$. Let w' denote the child of r' in the short flip $\mathbf{f}'$. Let $v_1, \ldots, v_{n-2}$ be an arbitrary ordering of $V \smallsetminus \{*, r, r'\}$ such that $v_1 \neq w'$ (this is possible since $|V| \geq 5$), and $B_1, \ldots, B_{n-2}$ any bridges such that the root of B_i is $\{v_{i-1}, v_i\}$ (where we set $v_0 = r'$). We now choose inductively a Hamiltonian cycle $\mathcal{H}_{\hat{v}}$ in each flip graph $\mathcal{F}(X_{\hat{v}})$ for all $v \in V \smallsetminus \{*\}$ as follows.

  (i) In $\mathcal{F}(X_{\hat{r}})$, we choose a cycle $\mathcal{H}_{\hat{r}}$ containing the short flip $\mathring{\mathbf{f}}$ and the long flip $\circledast \leftrightarrow \overset{r'}{\circledast}$.

 (ii) In $\mathcal{F}(X_{\hat{r}'})$, we choose a cycle $\mathcal{H}_{\hat{r}'}$ containing the short flips $\mathring{\mathbf{f}}'$ and $\mathring{B}_1[r']$ and the long flip $\circledast \leftrightarrow \overset{r}{\circledast}$.

(iii) In $\mathcal{F}(X_{\hat{v}_i})$ for $i \in [n-3]$, we choose a cycle $\mathcal{H}_{\hat{v}_i}$ containing the short flips $\mathring{B}_i[v_i]$ and $\mathring{B}_{i+1}[v_i]$.

 (iv) In $\mathcal{F}(X_{\hat{v}_{n-2}})$, we choose a cycle $\mathcal{H}_{\hat{v}_{n-2}}$ containing the short flip $\mathring{B}_{n-2}[v_{n-2}]$.

Note that these Hamiltonian cycles exist by induction hypothesis. Indeed, the short flips $\mathring{B}_i[v_i]$ and $\mathring{B}_{i+1}[v_i]$ have distinct roots v_{i-1} and v_{i+1}. The only delicate case is thus Point (ii): the short flips $\mathring{\mathbf{f}}'$ and $\mathring{B}_1[r']$ have distinct roots since we forced v_1 to be different from w'. Each Hamiltonian cycle $\mathcal{H}_{\hat{v}}$ on $\mathcal{F}(X_{\hat{v}})$ induces a Hamiltonian cycle $\mathcal{H}_v$ on $\mathcal{F}_v(X_V)$ (just add v at the root in all spines). From these Hamiltonian cycles, we construct a Hamiltonian cycle for $\mathcal{F}(X_V)$ as illustrated in Figure A.7. We join $\mathcal{H}_r$ with $\mathcal{H}_{r'}$ by deleting the flips $\overset{r}{\circledast} \leftrightarrow \overset{r}{\underset{\circledast}{r'}}$ and $\overset{r'}{\circledast} \leftrightarrow \overset{r'}{\underset{\circledast}{r}}$ while inserting the long flips $\overset{r}{\circledast} \leftrightarrow \circledast \leftrightarrow \overset{r'}{\circledast}$
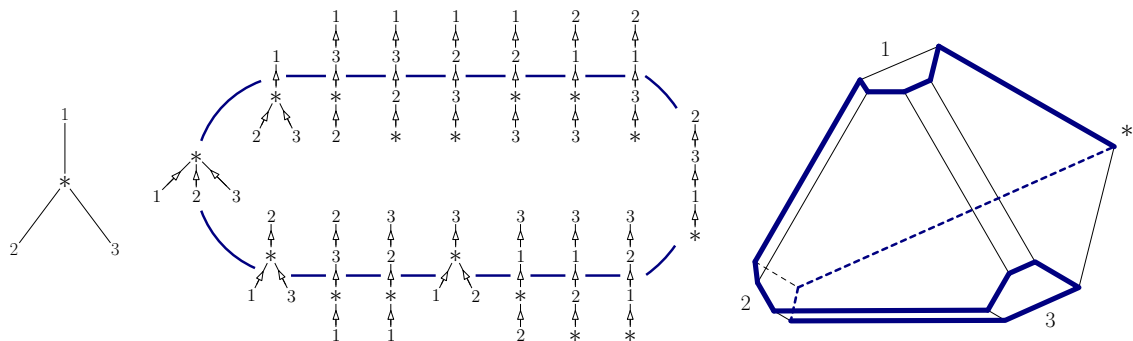

Figure A.6 – A Hamiltonian cycle in the flip graph $\mathcal{F}(X_{\{1,2,3,*\}})$. Up to permutations of the leaves $\{1, 2, 3\}$, this cycle contains all possible triples $\mathbf{f}, \mathbf{f}', \mathbf{g}$ considered in Proposition A.9.

and $\overset{r}{\underset{\circledast}{r'}} \leftrightarrow \overset{r'}{\underset{\circledast}{r}}$. Finally, we use the bridges $B_1, \ldots, B_{n-2}$ to connect the resulting cycle to the cycles $\mathcal{H}_{v_1}, \ldots, \mathcal{H}_{v_{n-2}}$ by exchanging their short flips with their long flips.
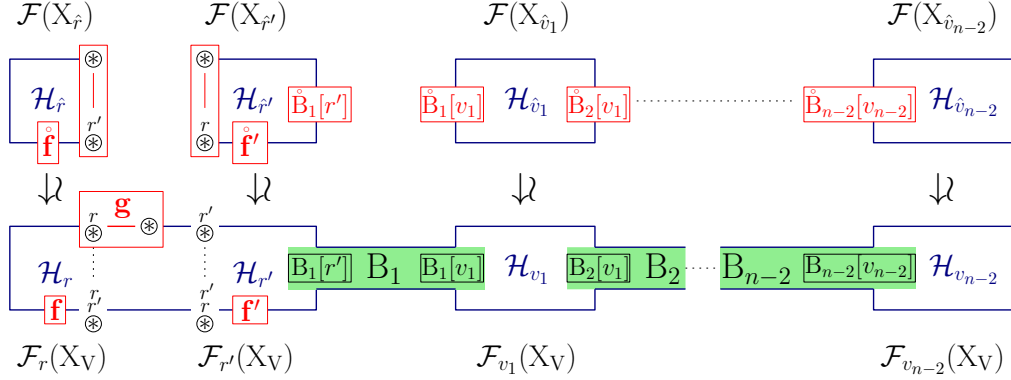

Figure A.7 – Construction of a Hamiltonian cycle in $\mathcal{F}(X_V)$ when $r'' = r$.

Case 2:. $r'' \notin \{r, r'\}$. Let $v_1, \ldots, v_{n-3}$ be an arbitrary ordering of $V \smallsetminus \{*, r, r', r''\}$, and $B_1, \ldots, B_{n-3}$ any bridges such that the root of B_i is $\{v_{i-1}, v_i\}$ (where we set $v_0 = r''$). We now choose inductively a Hamiltonian cycle $\mathcal{H}_{\hat{v}}$ in each flip graph $\mathcal{F}(X_{\hat{v}})$ for all $v \in V \smallsetminus \{*, r'\}$ as follows.

(i) In $\mathcal{F}(X_{\hat{r}})$, we choose a cycle $\mathcal{H}_{\hat{r}}$ containing the short flip $\mathring{f}$ and the long flip $\circledast \leftrightarrow \overset{r''}{\circledast}$.

(ii) In $\mathcal{F}(X_{\hat{r}''})$, we choose a cycle $\mathcal{H}_{\hat{r}''}$ containing a short flip $\mathring{h}$ with root r', the short flip $\mathring{B}_1[r'']$ and the long flip $\circledast \leftrightarrow \overset{r}{\circledast}$.

(iii) In $\mathcal{F}(X_{\hat{v}_i})$ for $i \in [n-4]$, we choose a cycle $\mathcal{H}_{\hat{v}_i}$ containing the short flips $\mathring{B}_i[v_i]$ and $\mathring{B}_{i+1}[v_i]$.

(iv) In $\mathcal{F}(X_{\hat{v}_{n-3}})$, we choose a cycle $\mathcal{H}_{\hat{v}_{n-3}}$ containing the short flip $\mathring{B}_{n-3}[v_{n-3}]$ and a short flip $\mathring{k}$ with root r'.
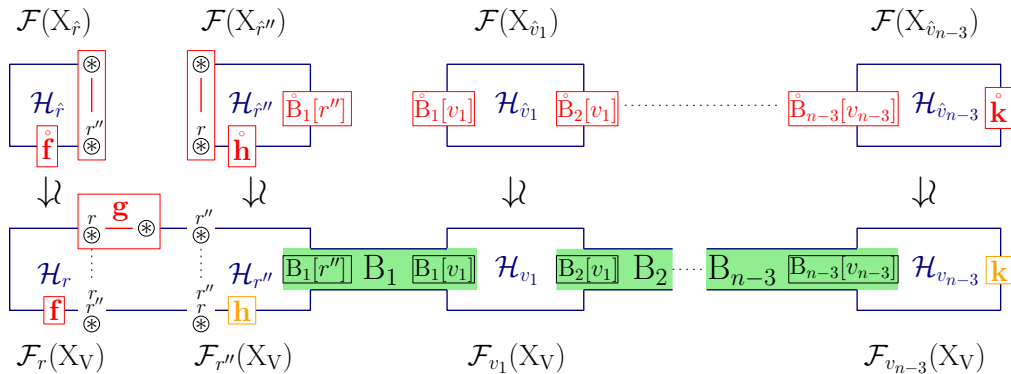
Figure A.8 – Construction of a Hamiltonian cycle in $\mathcal{F}(X_V)$ when $r'' \notin \{r, r'\}$.

Each Hamiltonian cycle $\mathcal{H}_{\hat{v}}$ on $\mathcal{F}(X_{\hat{v}})$ induces a Hamiltonian cycle $\mathcal{H}_v$ on $\mathcal{F}_v(X_V)$ (just add v at the root in all spines). From these Hamiltonian cycles, we construct the cycle illustrated in Figure A.8. We still have to enlarge this cycle to cover $\mathcal{F}_{r'}(X_V)$. Let $\mathbf{h}'$

and $\mathbf{k}'$ denote the short flips in $\mathcal{F}_{r'}(X_V)$ parallel to the short flips $\mathbf{h}$ and $\mathbf{k}$ respectively. Since $r'' \neq v_{n-3}$, the root w' of $\mathbf{f}'$ cannot coincide with both. Assume for example that $w' \neq r''$. By induction, we can then find a Hamiltonian cycle $\mathcal{H}_{\hat{r}'}$ of $\mathcal{F}(X_{\hat{r}'})$ containing both $\mathring{\mathbf{f}}'$ and $\mathring{\mathbf{h}}'$. This cycle induces a Hamiltonian cycle $\mathcal{H}_{r'}$ of $\mathcal{F}_{r'}(X_V)$ passing through $\mathbf{f}'$ and $\mathbf{h}'$. We can then connect this cycle to the cycle of Figure A.8 by exchanging the parallel short flips $\mathbf{h}$ and $\mathbf{h}'$ by the corresponding parallel long flips. In the situation when $w' = r''$, we have $w' \neq v_{n-3}$ and we argue similarly by attaching $\mathcal{F}_{r'}(X_V)$ to $\mathbf{k}$ instead of $\mathbf{h}$. ∎

A.5 Graph with at most 6 vertices

Again we will focus on connected graphs because of Corollary A.4. The analysis for graphs with at most 3 vertices is immediate. We now treat separately the graphs with $4, 5$ and 6 vertices, which are not stars (stars have been treated in the previous section).

A.5.1 Graphs with 4 vertices

We consider all possible connected graphs on 4 vertices and exhibit explicit Hamiltonian cycles of their flip graphs. To do so, we could draw a cycle of spines as in Figure A.6 (middle). Instead, we rather draw the Hamiltonian cycle on the flip graph $\mathcal{F}(G)$ represented as the 1-skeleton of the graph associahedron $\mathsf{Asso}(G)$ as in Figure A.6 (right). Let us remind from [CD06] that the graph associahedron $\mathsf{Asso}(G)$ is obtained from the standard simplex $\triangle_V := \mathrm{conv}\{e_v \mid v \in V\}$ (where $(e_v)_{v \in V}$ denotes the canonical basis of $\mathbb{R}^V$) by successive truncations of the faces $\triangle_{V \smallsetminus t} = \mathrm{conv}\{e_v \mid v \in V \smallsetminus t\}$ for the tubes t of G, in decreasing order of dimension. Each tube t of G corresponds to a facet F_t of $\mathsf{Asso}(G)$, and each maximal tubing T corresponds to the vertex of $\mathsf{Asso}(G)$ which belongs to all facets F_t for $t \in T$. In Figure A.9 (right), we label the positions of the vertices of $\triangle_V$ before the truncations. The fixed-root subgraphs appear as the 1-skeleta of the four shaded faces of G, and the bridges are the five thin parallelograms (the short flips correspond to their short sides, and the long flips correspond to their long sides).
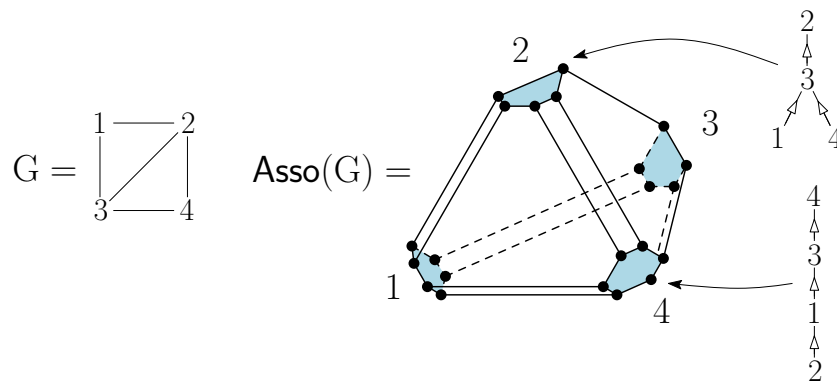

Figure A.9 – Correspondence between vertices of $\mathsf{Asso}(G)$ and spines on G.

Using these conventions, Figure A.10 represents Hamiltonian cycles for the flip graphs on all connected graphs on 4 vertices (the 4-star was already treated in Figure A.6). The Hamiltonian cycles, together with their orbits under the action of the isomorphism group of the corresponding graph, prove the following statements, which imply Theorem A.1 for all graphs on 4 vertices.

Proposition A.10. *(a) For any graph* G *on at most* 4 *vertices, any pair of short flips (even with the same root) is contained in a Hamiltonian cycle of* $\mathcal{F}(G)$.
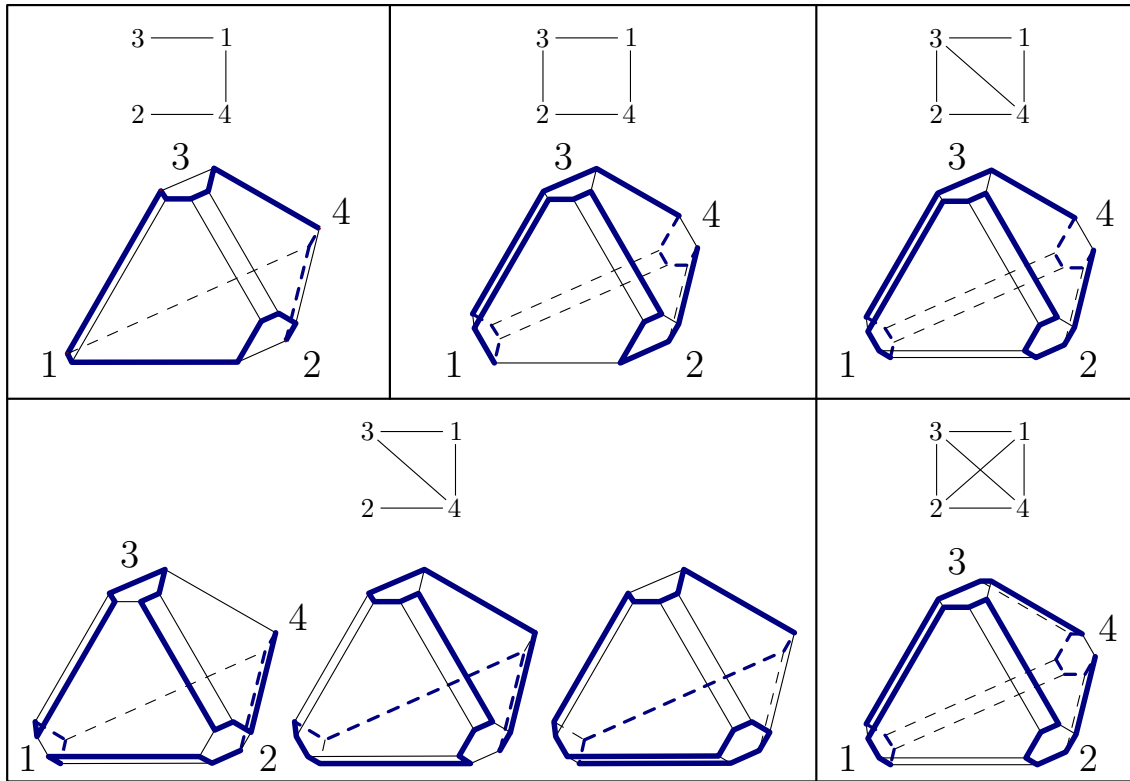
Figure A.10 – Hamiltonian cycles showing Proposition A.10. Each vertex of the graph associahedra corresponds to a spine as explained in Figure A.9.

(b) For the stars on 3 and 4 vertices, each triple consisting of two short flips (even with the same root) and one long flip as in Proposition A.9 is contained in a Hamiltonian cycle of $\mathcal{F}(G)$.

(c) For the classical 3-dimensional (path) associahedron, there exists a Hamiltonian cycle containing simultaneously all short flips.

(d) For all connected graphs on 4 vertices, there is a Hamiltonian cycle of $\mathcal{F}(G)$ containing at least one short flip in each fixed-root subgraph. We can even preserve this property if we impose the Hamiltonian cycle to pass through one distinguished short flip.

A.5.2 Graphs with 5 vertices

Graphs on 5 vertices are treated by a case analysis. As in the proof of Lemma A.5, we will denote by D the set of totally disconnecting pairs of G, *i.e.* pairs $\{x, y\}$ of vertices of G such that $G \smallsetminus \{x, y\}$ has no edge. Recall from the proof of Lemma A.5 that D has at most two elements and that they are not disjoint.

Consider now a graph G on 5 vertices. According to Remark A.6, the proof of Section A.3 applies in various configurations. We treat here the remaining cases. As we observed in Proposition A.10 (a) that for any connected graph G on at most 4 vertices, any pair of short flips (even with the same root) is contained in a Hamiltonian cycle of $\mathcal{F}(G)$, we can ignore Condition (A) in the definition of conflict. We therefore say that a vertex w and a short flip **g** with root v are *in conflict* if $G \smallsetminus \{v, w\}$ has a single edge which is the short leaf of **g**, and w is a child of v. With this definition, there is only one bridge connecting $\mathcal{F}_v(G)$ and $\mathcal{F}_w(G)$, but we cannot use it if we want the short flip **g** to

belong to the Hamiltonian cycle. One can check that the conclusions of Lemmas A.7 and A.8 still hold in this situation.

We first suppose that $D = \{\{x, y\}\}$ is a singleton and that either x or y is in conflict with both $\mathbf{f}$ and $\mathbf{f}'$. Checking all connected graphs on five vertices, we see that this situation can only happen for the following graphs:

$$G_1 = \quad G_2 = \quad G_3 = \quad G_4 = \quad .$$
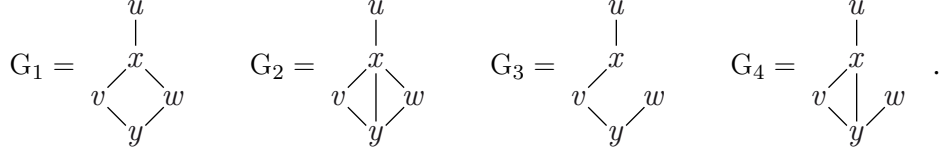
For each one, we explain how to prove Theorem A.1.

$G = G_1$ The only possible conflicts are between x and a short flip with root v or w. Thus, up to isomorphism of the graph, the only instance of Theorem A.1 fitting to the configuration we are looking at is given by
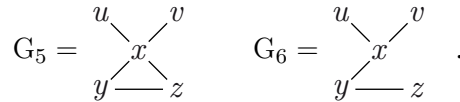
$$\mathbf{f} = \qquad \text{and} \qquad \mathbf{f}' = \quad .$$
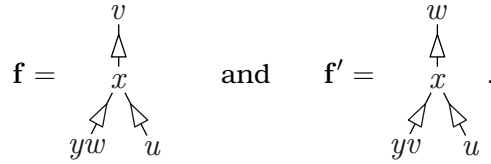
Observe that there exist bridges $\mathsf{B}_v, \mathsf{B}_u, \mathsf{B}_y$ with respective roots $\{w, v\}, \{w, u\}, \{w, y\}$ and a bridge B with root $\{u, x\}$. Notice that the fixed root subgraph $\mathcal{F}_w(G_1)$ is isomorphic to the classical (path) associahedron so that Proposition A.10 (c) ensures that there exists a Hamiltonian cycle $\mathcal{H}_w$ of the flip graph $\mathcal{F}_w(G_1)$ containing all the short flips $\mathbf{f}, \mathsf{B}_v[w], \mathsf{B}_u[w], \mathsf{B}_y[w]$. Moreover Proposition A.10 (a) ensures that there exists a Hamiltonian cycle $\mathcal{H}_y$ (resp. $\mathcal{H}_x$) of the flip graph $\mathcal{F}_y(G_1)$ (resp. $\mathcal{F}_x(G_1)$) containing the short flip $\mathsf{B}_y[y]$ (resp. $\mathsf{B}[x]$). Proposition A.10 (a) again gives us a Hamiltonian cycle $\mathcal{H}_u$ (resp. $\mathcal{H}_v$) of the flip graph $\mathcal{F}_u(G_1)$ (resp. $\mathcal{F}_v(G_1)$) containing the two short flips $\mathsf{B}_u[u]$ and $\mathsf{B}[u]$ (resp. $\mathbf{f}'$ and $\mathsf{B}_v[v]$). Note that the short flips of the bridges are all distinct since u, v and w do no disconnect the graph. Gluing all the Hamiltonian cycles of the fixed root subgraphs along the bridges as explained in Section A.1 gives a Hamiltonian cycle of $\mathcal{F}(G_1)$ containing $\mathbf{f}$ and $\mathbf{f}'$.

$G = G_2$ The only possible conflicts are between x and a short flip with root v or w. Thus, up to isomorphism of the graph, the only instance of Theorem A.1 fitting to the configuration we are looking at is given by

$$\mathbf{f} = \qquad \text{and} \qquad \mathbf{f}' = \quad .$$
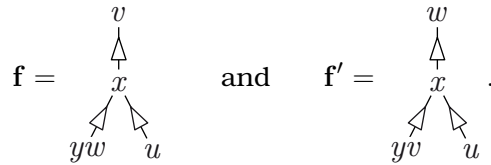
Observe that there exists a bridge B with root $\{u, x\}$. Notice that the fixed root subgraph $\mathcal{F}_w(G_1)$ is isomorphic to the graph associahedron of a connected graph on 4 vertices so that Proposition A.10 (d) ensures that there exists a Hamiltonian cycle $\mathcal{H}_w$ of the flip graph $\mathcal{F}_w(G_2)$ containing the short flip $\mathbf{f}$ and three short flips $\mathsf{B}_v[w], \mathsf{B}_u[w], \mathsf{B}_y[w]$ of some bridges $\mathsf{B}_v, \mathsf{B}_u, \mathsf{B}_y$ whose respective roots are $\{w, v\}, \{w, u\}, \{w, y\}$. Moreover Proposition A.10 (a) ensures that there exists a Hamiltonian cycle $\mathcal{H}_y$ (resp. $\mathcal{H}_x$) of the flip graph $\mathcal{F}_y(G_2)$ (resp. $\mathcal{F}_x(G_2)$) containing the short flip $\mathsf{B}_y[y]$ (resp. $\mathsf{B}[x]$). Proposition A.10 (a) again gives us a Hamiltonian cycle $\mathcal{H}_u$ (resp. $\mathcal{H}_v$) of the flip graph $\mathcal{F}_u(G_2)$ (resp. $\mathcal{F}_v(G_2)$) containing the two

short flips $B_u[u]$ and $B[u]$ (resp. $\mathbf{f}'$ and $B_v[v]$). Note that the short flips of the bridges are all distinct since u, v and w do no disconnect the graph. Gluing all the Hamiltonian cycles of the fixed root subgraphs along the bridges as explained in Section A.1 gives a Hamiltonian cycle of $\mathcal{F}(G_2)$ containing $\mathbf{f}$ and $\mathbf{f}'$.

$G = G_3$ The analysis is identical to the case $G = G_1$.

$G = G_4$ The analysis is identical to the case $G = G_2$.

We now suppose that G has 5 vertices and that $D = \{\{x, y\}, \{x, z\}\}$. Since all edges either contain x or both y and z, G is one of the following graphs:

$$G_5 = \quad \begin{matrix} u & & v \\ & \diagdown\!\!\!\diagup x & \\ y & \!\!\!\!\rule{1cm}{0.4pt}\!\!\!\! & z \end{matrix} \qquad\qquad G_6 = \quad \begin{matrix} u & & v \\ & \diagdown x \!\!\diagup & \\ y & \!\!\!\!\rule{1cm}{0.4pt}\!\!\!\! & z \end{matrix} \quad .$$

We note that in both of them, the only possible conflicts are between x and short flips with root either u or v. Indeed, $\{x, u\}$ and $\{x, v\}$ are the only pairs of vertices disjoint from exactly one edge, and the fixed-root subgraphs $\mathcal{F}_x(G_5)$ and $\mathcal{F}_x(G_6)$ are reduced to single flips. Using Remark A.6, we can restrict to the cases in which $x \notin \{v_1, v_5\}$. Again we treat separately the two graphs:

$G = G_5$ Notice that the fixed-root subgraphs $\mathcal{F}_y(G_5)$ and $\mathcal{F}_z(G_5)$ both are isomorphic to the flip graph of a star on 4 vertices with central vertex x. So given a short flip $\mathbf{h}$ (resp. $\mathbf{k}$) with roots y (resp. z), Proposition A.9 provides us with a Hamiltonian cycle $\mathcal{H}_y$ (resp. $\mathcal{H}_z$) of $\mathcal{F}_y(G_5)$ (resp. $\mathcal{F}_z(G_5)$) containing $\mathbf{h}$ (resp. $\mathbf{k}$) and the flip of $\mathcal{F}_y(G_5)$ (resp. $\mathcal{F}_z(G_5)$) corresponding to the long flip of $\mathcal{F}(G_5[\hat{y}])$ (resp. $\mathcal{F}(G_5[\hat{y}])$) with root $\{x, z\}$ (resp. $\{x, y\}$). Then gluing together the cycles $\mathcal{H}_y$ and $\mathcal{H}_z$ and the fixed-root subgraph $\mathcal{F}_x(G_5)$ as in Figure A.11 gives a tool to deal with the remaining configurations, always with the strategy of gluing Hamiltonian cycles of the fixed-root subgraphs along bridges.
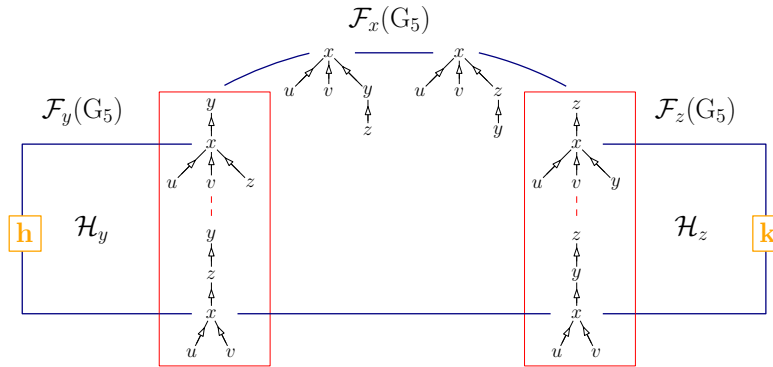

Figure A.11 – How to glue together the flip graphs $\mathcal{F}_y(G_5), \mathcal{F}_x(G_5)$ and $\mathcal{F}_z(G_5)$.

$G = G_6$ Observe that both fixed-root subgraphs $\mathcal{F}_u(G_6)$ and $\mathcal{F}_v(G_6)$ are isomorphic to the classical (path) associahedron. Thus as soon as one of the short flips $\mathbf{f}$ and $\mathbf{f}'$ is not in conflict with x, one can find an arrangement of the vertices in the same way as when we treated the graph G_2 and G_4 (without the intermediary of the vertex u) which always makes our strategy work. We thus only need to deal with the case where x is in conflict with both $\mathbf{f}$ and $\mathbf{f}'$, which corresponds to a single instance of Theorem A.1, checked by hand in Figure A.12.
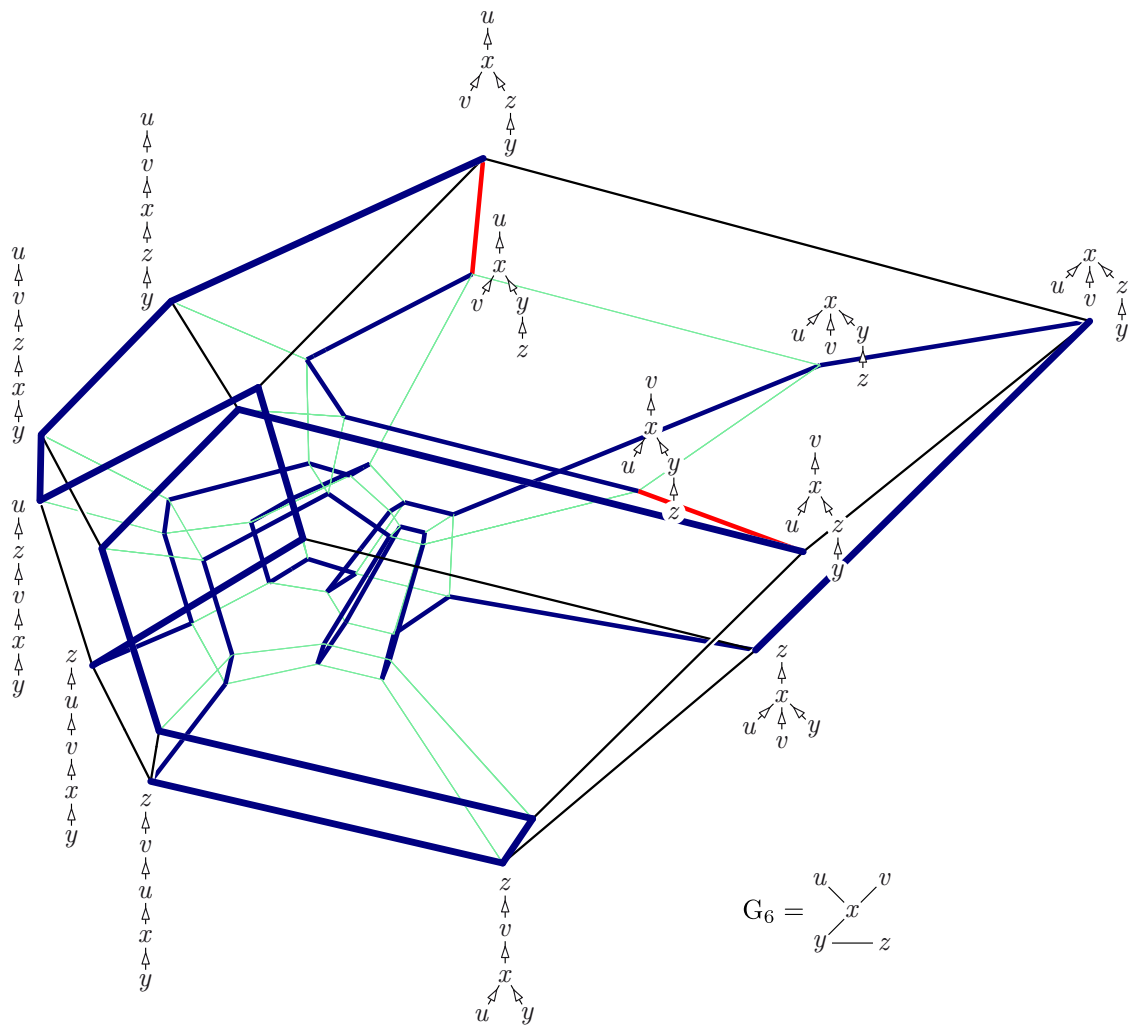
Figure A.12 – The flip graph $\mathcal{F}(G_6)$ represented as the 1-skeleton of the graph associahedron $\mathsf{Asso}(G_6)$, visualized by its Schlegel diagram. The (blue) Hamiltonian cycle passes through the only two short flips in conflict with x (in red).

A.5.3 Graphs with 6 vertices

To finish, we need to deal with the case where G has 6 vertices, $D = \{\{x, y\}, \{x, z\}\}$ and x is in conflict with both f and f'. Again G can only be one of the two following graphs:

The graph G_7 is treated exactly as G_5, using Remark A.6 instead of Proposition A.10 to restrict the number of cases to analyze. In the case of G_8, there is again a single difficult instance which can be treated by hand (since the graph associahedron $\mathsf{Asso}(G_8)$ has 236 vertices, we do not include here the resulting picture).

Bibliography

[Bar01]   Yuliy Baryshnikov. On Stokes sets. In *New developments in singularity theory (Cambridge, 2000)*, volume 21 of *NATO Sci. Ser. II Math. Phys. Chem.*, pages 65–86. Kluwer Acad. Publ., Dordrecht, 2001.

[BB05]   Anders Björner and Francesco Brenti. *Combinatorics of Coxeter groups*, volume 231 of *Grad. Texts in Math.* Springer-Verlag, Berlin Heidelberg, 2005.

[BCL15]   Nantel Bergeron, Cesar Ceballos, and Jean-Philippe Labbé. Fan realizations of type A subword complexes and multi-associahedra of rank 3. *Discrete Comput. Geom.*, 54(1):195–231, 2015.

[BDP14]   Thomas Brüstle, Grégoire Dupont, and Matthieu Pérotin. On maximal green sequences. *Int. Math. Res. Not. IMRN*, (16):4547–4586, 2014.

[Ber58]   Claude Berge. *Théorie des graphes et ses applications*, volume 2 of *Collection Universitaire de Mathématiques*. Dunod, second edition, 1958.

[BFS90]   Louis J. Billera, Paul Filliman, and Bernd Sturmfels. Constructions and complexity of secondary polytopes. *Adv. Math.*, 83(2):155–179, 1990.

[BFZ05]   Arkady Berenstein, Sergey Fomin, and Andrei Zelevinsky. Cluster algebras. III. Upper bounds and double Bruhat cells. *Duke Math. J.*, 126(1):1–52, 2005.

[BHLT09]   Nantel Bergeron, Christophe Hohlweg, Carsten Lange, and Hugh Thomas. Isometry classes of generalized associahedra. *Sém. Lothar. Combin.*, 61A:Art. B61Aa, 13, 2009.

[BM87]   Roswitha Blind and Peter Mani-Levistka. On puzzles and polytope isomorphisms. *Aequationes Math.*, 34(2):287–297, 1987.

[BMP17]   Amir-Hossein Bateni, Thibault Manneville, and Vincent Pilaud. A note on quadrangulations and Stokes complexes. to appear in the proceedings of Eurocomb 2017, *Electron. Notes Discrete Math.*, 2017.

[BP80]   Louis J. Billera and J. Scott Provan. Decompositions of simplicial complexes related to diameters of convex polyhedra. *Math. Oper. Res.*, 5(4):576–594, 1980.

[BP09]   Jürgen Bokowski and Vincent Pilaud. On symmetric realizations of the
           simplicial complex of 3-crossing-free sets of diagonals of the octagon. In
           *Proceedings of the 21st Canadian Conference on Computational Geometry
           (CCCG2009)*, pages 41–44, 2009.

[BP15]   Victor M. Buchstaber and Taras E. Panov. *Toric Topology*, volume 204 of
           Math. Surveys Monogr. Amer. Math. Soc., 2015.

[BW97]   Anders Björner and Michelle L. Wachs. Shellable nonpure complexes and
           posets II. *Trans. Amer. Math. Soc.*, 349(10):3945–3975, 1997.

[CD06]   Michael P. Carr and Satyan L. Devadoss. Coxeter complexes and graph-
           associahedra. *Topology Appl.*, 153(12):2155–2168, 2006.

[CFZ02]   Frédéric Chapoton, Sergey Fomin, and Andrei Zelevinsky. Polytopal realiza-
           tions of generalized associahedra. *Canad. Math. Bull.*, 45(4):537–566, 2002.

[Cha00]   Frédéric Chapoton. Algèbres de Hopf des permutahèdres, associahèdres et
           hypercubes. *Adv. Math.*, 150(2):264–275, 2000.

[Cha16]   Frédéric Chapoton. Stokes posets and serpent nests. *Discrete Math. Theor.
           Comput. Sci.*, 18(3), 2016.

[CLS14]   Cesar Ceballos, Jean-Philippe Labbé, and Christian Stump. Subword com-
           plexes, cluster complexes and generalized multi-associahedra. *J. Alge-
           braic Combin.*, 39(1):17–51, 2014.

[CP92]   Vasilis Capoyleas and János Pach. A Turán-type problem on chords of a
           convex polygon. *J. Combin. Theory Ser. B*, 56(1):9–15, 1992.

[CP15]   Cesar Ceballos and Vincent Pilaud. Denominator vectors and compatibility
           degrees in cluster algebras of finite types. *Trans. Amer. Math. Soc.*, 367:1421–
           1439, 2015.

[CP16]   Cesar Ceballos and Vincent Pilaud. The diameter of type D associahedra and
           the non-leaving-face property. *European J. Combin.*, 51:109–124, 2016.

[CP17]   Grégory Chatel and Vincent Pilaud. Cambrian Hopf algebras. *Adv. Math.*,
           311:598–633, 2017.

[CSZ15]   Cesar Ceballos, Francisco Santos, and Günter M. Ziegler. Many non-
           equivalent realizations of the associahedron. *Combinatorica*, 35(5):513–551,
           2015.

[Deh10]   Patrick Dehornoy. On the rotation distance between binary trees. *Adv.
           Math.*, 223(4):1316–1355, 2010.

[Dev09]   Satyan L. Devadoss. A realization of graph associahedra. *Discrete Math.*,
           309(1):271–276, 2009.

[Dev15]   The Sage Developers. *SageMath, the Sage Mathematics Software System (Ver-
           sion 6.8.beta2)*, 2015. sagemath.org.

[DFRS15]   Satyan L. Devadoss, Stefan Forcey, Stephen Reisdorf, and Patrick Showers.
           Convex polytopes from nested posets. *European J. Combin.*, 43:229–248,
           2015.

[DHV11]   Satyan L. Devadoss, Timothy Heath, and Wasin Vipismakul. Deformations of
           bordered surfaces and convex polytopes. *Notices Amer. Math. Soc.*, 58(4):530–
           541, 2011.

[Die10]   Reinhard Diestel. *Graph Theory*, volume 173 of *Grad. Texts in Math.* Springer-Verlag, Berlin Heidelberg, 4 edition, 2010.

[DKM02]   Andreas. W. M. Dress, Jacobus H. Koolen, and Vincent Moulton. On line arrangements in the hyperbolic plane. *European J. Combin.*, 23(5):549–557, 2002.

[DP95]   Conrado De Concini and Claudio Procesi. Wonderful models of subspace arrangements. *Selecta Math. (N.S.)*, 1(3):459–494, 1995.

[DRS10]   Jesús A. De Loera, Jörg Rambau, and Francisco Santos. *Triangulations – Structures for Algorithms and Applications*, volume 25 of *Algorithms Comput. Math.* Springer-Verlag, Berlin Heidelberg, 2010.

[Ewa96]   Günter Ewald. *Combinatorial Convexity and Algebraic Geometry*, volume 168 of *Grad. Texts in Math.* Springer-Verlag, New York, 1996.

[FK04]   Eva Maria Feichtner and Dmitry N. Kozlov. Incidence combinatorics of resolutions. *Selecta. Math. (N.S.)*, 10:37–60, 2004.

[FM94]   William E. Fulton and Robert MacPherson. A compactification of configuration spaces. *Ann. of Math. (2)*, 139:183–225, 1994.

[FM04]   Eva Maria Feichtner and Irene Müller. On the topology of nested set complexes. *Proc. Amer. Math. Soc.*, 133(4):999–1006, 2004.

[FS05]   Eva Maria Feichtner and Bernd Sturmfels. Matroid polytopes, nested sets and Bergman fans. *Portugal. Math. (N.S.)*, 62(4):437–468, 2005.

[FT12]   Sergey Fomin and Dylan Thurston. Cluster algebras and triangulated surfaces. part ii: Lambda lengths. Preprint, arXiv:1210.5569, 2012.

[FZ02]   Sergey Fomin and Andrei Zelevinsky. Cluster algebras. I. Foundations. *J. Amer. Math. Soc.*, 15(2):497–529 (electronic), 2002.

[FZ03a]   Sergey Fomin and Andrei Zelevinsky. Cluster algebras. II. Finite type classification. *Invent. Math.*, 154(1):63–121, 2003.

[FZ03b]   Sergey Fomin and Andrei Zelevinsky. Y-systems and generalized associahedra. *Ann. of Math. (2)*, 158(3):977–1018, 2003.

[FZ04]   Sergey Fomin and Andrei Zelevinsky. Cluster algebras: Notes for the CDM-03 conference. In *Current Developments in Mathematics, 2003*, pages 1–34, Cambridge, MA, 2004. International Press of Boston, Inc.

[FZ07]   Sergey Fomin and Andrei Zelevinsky. Cluster algebras. IV. Coefficients. *Compositio Math.*, 143(1):112–164, 2007.

[GKZ08]   Israel Gelfand, Mikhail M. Kapranov, and Andrei Zelevinsky. *Discriminants, resultants and multidimensional determinants.* Mod. Birkhäuser Class. Birkhäuser Boston, Inc., 2008. Reprint of the 1994 edition.

[GM07]   Bernd Gärtner and Jiři Matoušek. *Understanding and Using Linear Programming.* Universitext. Springer-Verlag, Berlin Heidelberg, first edition, 2007.

[GM16]   Alexander Garver and Thomas McConville. Oriented flip graphs and non-crossing tree partitions. Preprint, arXiv:1604.06009, 2016.

[Gor13]   Mikhail Gorsky. Subword complexes and nil-Hecke moves. *Modeling and analysis of information systems*, 20(6):121–128, 2013.

[Gor14]   Mikhail Gorsky. Subword complexes and edge subdivisions. In *Proceedings of the Steklov Institute of Mathematics*, volume 286, pages 114–127, 2014.

[Hai84]   Mark Haiman. Constructing the associahedron. Unpublished manuscript, 11 pages, available at http://www.math.berkeley.edu/~mhaiman/ftp/assoc/manuscript.pdf, 1984.

[Hat02]   Allen Hatcher. *Algebraic Topology*. Cambridge University Press, 2002. https://www.math.cornell.edu/~hatcher/AT/AT.pdf.

[HL07]   Christophe Hohlweg and Carsten Lange. Realizations of the associahedron and cyclohedron. *Discrete Comput. Geom.*, 37(4):517–543, 2007.

[HLR10]   Christophe Hohlweg, Jonathan Lortie, and Annie Raymond. The centers of gravity of the associahedron and of the permutahedron are the same. *Electron. J. Combin.*, 17(1):Research Paper 72, 14, 2010.

[HLT11]   Christophe Hohlweg, Carsten Lange, and Hugh Thomas. Permutahedra and generalized associahedra. *Adv. Math.*, 226(1):608–640, 2011.

[HN99]   Ferran Hurtado and Marc Noy. Graph of triangulations of a convex polygon and tree of triangulations. *Comput. Geom.*, 13(3):179–188, 1999.

[HNT05]   Florent Hivert, Jean-Christophe Novelli, and Jean-Yves Thibon. The algebra of binary search trees. *Theoret. Comput. Sci.*, 339(1):129–165, 2005.

[Hoh12]   Christophe Hohlweg. Permutahedra and associahedra. In Folkert Müller-Hoissen, Jean Marcel Pallo, and Jim Stasheff, editors, *Associahedra, Tamari Lattices and Related Structures – Tamari Memorial Festschrift*, volume 299 of *Progr. Math.*, pages 129–159. Birkhäuser, Basel, 2012.

[HPS16]   Christophe Hohlweg, Vincent Pilaud, and Salvatore Stella. Polytopal realizations of finite type g-vector fans. Preprint, arXiv:1703.09551, 2016.

[Hum90]   James E. Humphreys. *Reflection Groups and Coxeter Groups*, volume 29 of *Cambridge Stud. Adv. Math.* Cambridge University Press, 1990.

[Joh63]   Selmer M. Johnson. Generation of permutations by adjacent transposition. *Math. Comp.*, 17:282–285, 1963.

[Jon03]   Jakob Jonsson. Generalized triangulations of the n-gon. An abstract was included in "Topological and Geometric Combinatorics, April 2003", Mathematisches Forschungsinstitut Oberwolfach, Report No. 16, 2003.

[Jon05]   Jakob Jonsson. Generalized triangulations and diagonal-free subsets of stack polyominoes. *J. Combin. Theory Ser. A*, 112:117–142, 2005.

[Kal88]   Gil Kalai. A very simple way to tell a simple polytope from its graph. *J. Combin. Theory Ser. A*, 49(2):381–383, 1988.

[Kel13]   Bernhard Keller. Cluster algebras and derived categories. In *Derived Categories in Algebraic Geometry – Tokyo 2011*, EMS Ser. Congr. Rep., pages 123–183. Eur. Math. Soc., 2013.

[KM04]   Allen Knutson and Ezra Miller. Subword complexes in Coxeter groups. *Adv. Math.*, 184(1):161–176, 2004.

[KM05]   Allen Knutson and Ezra Miller. Gröbner geometry of Schubert polynomials. *Ann. of Math. (2)*, 161(3):1245–1318, 2005.

[Knu98]   Donald E. Knuth. *The art of computer programming – Vol 3: Sorting and searching.* Addison Wesley Longman Publishing Co., Inc., Redwood City, CA, second edition, 1998.

[Lam15]   Lisa Lamberti. Combinatorial model for the cluster categories of type E. *J. Algebraic Combin.*, 441, 2015.

[Lee89]   Carl W. Lee. The associahedron and triangulations of the n-gon. *European J. Combin.*, 10(6):551–560, 1989.

[LN16]   Frank H. Lutz and Eran Nevo. Stellar theory for flag complexes. *Math. Scand.*, 118:70–82, 2016.

[Lod04]   Jean-Louis Loday. Realization of the Stasheff polytope. *Arch. Math. (Basel)*, 83(3):267–278, 2004.

[LP13]   Carsten Lange and Vincent Pilaud. Associahedra via spines. *Preprint, arXiv:1307.4391, to appear in Combinatorica*, 2013.

[LP16a]   Thomas Lam and Pavlo Pylyavskyy. Laurent phenomenon algebras. *Camb. J. Math.*, 4(1):121–162, 2016.

[LP16b]   Thomas Lam and Pavlo Pylyavskyy. Linear Laurent phenomenon algebras. *Int. Math. Res. Not. IMRN*, 2016(10):3163–3203, 2016.

[LR98]   Jean-Louis Loday and María O. Ronco. Hopf algebra of the planar binary trees. *Adv. Math.*, 139(2):293–309, 1998.

[Luc87]   Joan M. Lucas. The rotation graph of binary trees is Hamiltonian. *J. Algorithms*, 8(4):503–535, 1987.

[Man17a]   Thibault Manneville. Fan realizations for some 2-associahera. *Preprint, arXiv:1608.08491, to appear in Experiment. Math.*, 2017.

[Man17b]   Thibault Manneville. The serpent nest conjecture on accordion complexes. Preprint, arXiv:1704.01534, 2017.

[Mat01]   Jiři Matoušek. *Lectures on Discrete Geometry*, volume 212 of *Grad. Texts in Math.* Springer-Verlag, New York, 2001.

[MHPS12]   Folkert Müller-Hoissen, Jean Marcel Pallo, and Jim Stasheff, editors. *Associahedra, Tamari Lattices and Related Structures – Tamari Memorial Festschrift*, volume 299 of *Prog. Math.* Birkhäuser, Basel, 2012.

[MP15]   Thibault Manneville and Vincent Pilaud. Graph properties of graph associahedra. *Sém. Lothar. Combin.*, 73:B73d, 2015.

[MP17a]   Thibault Manneville and Vincent Pilaud. Compatibility fans for graphical nested complexes. *J. Combin. Theory Ser. A*, 150:36–107, 2017.

[MP17b]   Thibault Manneville and Vincent Pilaud. Geometric realizations of accordion complexes. Preprint, arXiv:1703.09953, 2017.

[Nak00]   Tomoki Nakamigawa. A generalization of diagonal flips in a convex polygon. *Theoret. Comput. Sci.*, 235(2):271–282, 2000.

[OEI10]   The On-Line Encyclopedia of Integer Sequences, 2010. Published electronically at oeis.org.

[Pil13]   Vincent Pilaud. Signed tree associahedra. Preprint, arXiv:1309.5222, 2013.

[Pos09]   Alexander Postnikov.   Permutohedra, associahedra,   and beyond.
          Int. Math. Res. Not. IMRN, 2009(6):1026–1106, 2009.

[Pou14]   Lionel Pournin. The diameter of associahedra. *Adv. Math.*, 259:13–42, 2014.

[Pou17]   Lionel Pournin. The asymptotic diameter of cyclohedra. *Israel J. Math.*,
          219(2):609–635, 2017.

[PP12]   Vincent Pilaud and Michel Pocchiola. Multitriangulations, pseudotriangu-
          lations and primitive sorting networks. *Discrete Comput. Geom.*, 48(1):142–
          191, 2012.

[PS09]   Vincent Pilaud and Francisco Santos. Multitriangulations as complexes of
          star polygons. *Discrete Comput. Geom.*, 41(2):284–317, 2009.

[PS12]   Vincent Pilaud and Francisco Santos. The brick polytope of a sorting net-
          work. *European J. Combin.*, 33(4):632–662, 2012.

[PS15a]   Vincent Pilaud and Christian Stump. Brick polytopes of spherical subword
          complexes and generalized associahedra. *Adv. Math.*, 276:1–61, 2015.

[PS15b]   Vincent Pilaud and Christian Stump. Vertex barycenter of generalized asso-
          ciahedra. *Proc. Amer. Math. Soc.*, 143(6):2623–2636, 2015.

[Rea04]   Nathan Reading. Lattice congruences of the weak order. *Order*, 21(4):315–
          344 (2005), 2004.

[Rea06]   Nathan Reading. Cambrian lattices. *Adv. Math.*, 205(2):313–353, 2006.

[Rea07]   Nathan Reading. Sortable elements and Cambrian lattices. *Algebra Univer-
          salis*, 56(3-4):411–437, 2007.

[Rea14]   Nathan Reading. Universal geometric cluster algebras. *Math. Z.*, 277(1-
          2):499–547, 2014.

[RS09]   Nathan Reading and David E. Speyer. Cambrian fans. *J. Eur. Math. Soc.*,
          11(2):407–447, 2009.

[RSS03]   Günter Rote, Francisco Santos, and Ileana Streinu. Expansive motions and
          the polytope of pointed pseudo-triangulations. In *Discrete and computational
          geometry*, volume 25 of *Algorithms Combin.*, pages 699–736. Springer, Berlin
          Heidelberg, 2003.

[San13]   Francisco Santos. Recent progress on the combinatorial diameter of polyto-
          pes and simplicial complexes. *TOP*, 21(3):426–460, 2013.

[San15]   Francisco Santos, 2015. Personal communication, Oberwolfach workshop
          on Geometric and Algebraic Combinatorics.

[SS93]   Steve Shnider and Shlomo Sternberg. *Quantum groups – From coalgebras
          to Drinfeld algebras*. Ser. Math. Phys. International Press of Boston, Inc.,
          Cambridge, MA, 1993.

[SS97]   Steve Shnider and Jim Stasheff. From operads to "physically" inspired
          theories. In *Operads: Proceedings of Renaissance Conferences (Hartfort,
          CT/Luminy, 1995)*, volume 202 of *Contemp. Math.*, pages 53–81. Amer. Math.
          Soc., 1997. Appendix B by Steve Shnider and Jim Stasheff for a corrected
          polytope construction.

[Sta63]   Jim Stasheff. Homotopy associativity of H-spaces I, II. *Trans. Amer. Math. Soc.*, 108(2):293–312, 1963.

[Sta97]   Richard P. Stanley. *Enumerative Combinatorics, Volume I*, volume 49 of *Cambridge Stud. Adv. Math.* Cambridge University Press, second edition, 1997. http://www-math.mit.edu/~rstan/ec/ec1.pdf.

[Sta01]   Richard P. Stanley. *Enumerative Combinatorics, Volume II*, volume 62 of *Cambridge Stud. Adv. Math.* Cambridge University Press, 2001.

[Sta13]   Richard P. Stanley. *Algebraic Combinatorics – Walks, Trees, Tableaux, and More.* Undergrad. Texts Math. Springer-Verlag, New York, 2013. http://www-math.mit.edu/~rstan/algcomb/.

[Ste64]   Hugo Steinhaus. *One hundred problems in elementary mathematics.* Basic Books Inc. Publishers, 1964. With a foreword by Martin Gardner.

[Ste13]   Salvatore Stella. Polyhedral models for generalized associahedra via Coxeter elements. *J. Algebraic Combin.*, 38(1):121–158, 2013.

[STT88]   Daniel D. Sleator, Robert E. Tarjan, and William P. Thurston. Rotation distance, triangulations, and hyperbolic geometry. *J. Amer. Math. Soc.*, 1(3):647–681, 1988.

[Stu11]   Christian Stump. A new perspective on k-triangulations. *J. Combin. Theory Ser. A*, 118(6):1794–1800, 2011.

[Tam51]   Dov Tamari. *Monoïdes préordonnés et chaînes de Malcev.* PhD thesis, Université Paris Sorbonne, 1951.

[Tro62]   Hale. F. Trotter. Algorithm 115: Perm. *Commun. ACM*, 5(8):434–435, 1962.

[Vol10]   Vadim Volodin. Cubical realizations of flag nestohedra and a proof of Gal's conjecture for them. *Russian Math. Surveys*, 65(1):188–190, 2010. The mentioned pictures appear only in the arXiv version "Cubical realizations of flag nestohedra and Gal's conjecture" at arXiv:0912.5478.

[Zel06]   Andrei Zelevinsky. Nested complexes and their polyhedral realizations. *Pure Appl. Math. Q.*, 2(3):655–671, 2006.

[Zie95]   Günter M. Ziegler. *Lectures on polytopes*, volume 152 of *Grad. Texts in Math.* Springer, New York, 1995.

Titre : Généralisations géométriques et combinatoires de l'associaèdre

Mots-clefs : associaèdre, éventail, algèbres amassées, graphe, polytope, triangulation

Résumé : L'associaèdre se situe à l'interface de plusieurs domaines mathématiques. Combinatoirement, il s'agit du complexe simplicial des dissections d'un polygone convexe (ensembles de diagonales ne se croisant pas deux à deux). Géométriquement, il s'agit d'un polytope dont les sommets et les arêtes encodent le graphe dual du complexe des dissections. Enfin l'associaèdre décrit la structure combinatoire qui définit la présentation par générateurs et relations de certaines algèbres, dites « amassées ». Du fait de son omniprésence, de nouvelles familles généralisant cet objet sont régulièrement découvertes. Cependant elles n'ont souvent que de faibles interactions. Leurs études respectives présentent de notre point de vue deux enjeux majeurs : chercher à les relier en se basant sur les propriétés connues de l'associaèdre ; et chercher pour chacune des cadres combinatoire, géométrique et algébrique dans le même esprit.

Dans cette thèse, nous traitons le lien entre combinatoire et géométrie pour certaines de ces généralisations : les associaèdres de graphes, les complexes de sous-mots et les complexes d'accordéons. Nous suivons un fil rouge consistant à adapter, à ces trois familles, une méthode de construction des associaèdres comme éventails (ensembles de cônes polyédraux), dite méthode des d-vecteurs et issue de la théorie des algèbres amassées. De manière plus large, notre problématique principale consiste à réaliser, c'est-à-dire plonger géométriquement dans un espace vectoriel, des complexes abstraits. Nous obtenons trois familles de nouvelles réalisations, ainsi qu'une quatrième encore conjecturale dont les premières instances constituent déjà des avancées significatives.

Enfin, en sus des résultats géométriques, nous démontrons des propriétés combinatoires spécifiques à chaque complexe simplicial abordé.

Title: Geometric and combinatorial generalizations of the associahedron

Keywords: associahedron, fan, cluster algebras, graph, polytope, triangulation

Abstract: The associahedron is at the interface between several mathematical fields. Combinatorially, it is the simplicial complex of dissections of a convex polygon (sets of mutually noncrossing diagonals). Geometrically, it is a polytope whose vertices and edges encode the dual graph of the complex of dissections. Finally the associahedron describes the combinatorial structure defining a presentation by generators and relations of certain algebras, called "cluster algebras". Because of its ubiquity, we regularly come up with new families generalizing this object. However there often are only few interactions between them. From our perspective, there are two main issues when studying them: looking for relations on the basis of known properties of the associahedron; and, for each, looking for combinatorial, geometric and algebraic frameworks in the same spirit.

In this thesis, we deal with the link between combinatorics and geometry for some of these generalizations: graph associahedra, subword complexes and accordion complexes. We follow a guidelight consisting in adapting, to these three families, a method for constructing associahedra as fans (sets of polyhedral cones), called the d-vector method and coming from cluster algebra theory. More generally, our main concern is to realize, that is geometrically embed in a vector space, abstract complexes. We obtain three new families of generalizations, and a fourth conjectural one whose first instances already constitute significant advances.

Finally in addition to the geometric results, we prove combinatorial properties specific to each encountered simplicial complex.